BEHAVIOR OF COMPACTED COLLAPSIBLE SOILS SUBJECTED TO WATER INFILTRATION

水浸による締固め崩壊性土の挙動

by

Feng Yi
易　鋒

A Dissertation in The Department of Civil Engineering
Presented in Partial Fulfillment of the Requirements for
Degree of **Doctor of Engineering**

University of Tokyo

September, 1991

BEHAVIOR OF COMPACTED COLLAPSIBLE SOILS SUBJECTED TO WATER INFILTRATION

水浸による締固め崩壊性土の挙動

by

Feng Yi
易　鋒

A
Dissertation
in
The Department
of
Civil Engineering

Presented in Partial Fulfillment of the
Requirements for Degree of
Doctor of Engineering

University of Tokyo
September, 1991

ABSTRACT

The wetting-induced volume change of compacted collapsible soils and their strength and deformation characteristics under monotonic and cyclic loading conditions when subjected to water infiltration were presented in this study. In order to obtain representative test results, the experimental investigation was carried out on five types of materials: a mixture of commercially available *Toyoura sand* and *kaolinite* in proportion of 1:0.15 in weight, and two silty and two clayey sands sampled from manufactured fills. The *scanning electron microscope* analysis verified that the mixture can represent the nature of natural soil if it is mixed at a certain moisture content and dried before the preparation of the samples. The strength and deformation characteristics were studied using *simple shear test apparatus* under plane strain and constant volume conditions or plane strain and drained conditions, depending on the purposes, while the volume collapse caused by soaking was investigated using conventional *consolidmeter*. The insufficiency of work and the importance of the investigation on the effect of wetting and collapsibility on strength and deformation properties of collapsible soils have been emphasized through a comprehensive review of the state-of-the-art studies on collapsible soils and relevant case histories.

Prior to the experiments, a detailed analysis of the stress state and stress changes in plane strain and constant volume conditions was made. The analysis showed that the measured vertical stress is the vertical effective stress caused by external load while the reduction in the vertical stress is equivalent to the increase in *excess pore pressure*.

The collapsibility of the aforementioned materials was initially investigated. The experimental investigation was concentrated on the effect of molding water content, as-compacted dry density and overburden pressure as well as the types of materials on the collapsibility of soils. The test results demonstrated that, under constant overburden pressure, there existed a critical value of molding water content at which the magnitude of collapse was maximum. This tendency decreased as the increase in as-compacted dry density. Up to a certain value of as-compacted dry density, the wetting-induced volume change increased with the decrease in dry density. It also revealed that under identical state of molding water content and as-compacted dry density, there was a value of overburden pressure which yielded the maximum value of collapse, and under constant

overburden pressure, the volume decrease caused by water infiltration decreased as the dry density at which a sample was prepared by compaction increased. The existence of the upper limit of dry density and degree of saturation at which no collapse will occur had been validated in the tests.

On the basis of the test results mentioned above, the strength and deformation behaviors have been studied under monotonic and cyclic loading conditions. Two series of tests namely with or without wetting and with different history of collapse were performed. For wetted tests, samples were tested under plane strain and constant volume conditions, while for unwetted tests, samples were tested under drained and volume changeable conditions. It was discovered that it is possible for liquefaction to occur in wetted collapsible soils. It was also noted that the monotonic shearing resistance of samples decreased significantly upon soaking even though the wetted samples had higher dry density before the application of shear load. The reduction was as great as 83.3% (at σ_{v0}=98kPa). An important fact was that the reduction of monotonic shear resistance showed as the reduction of either the cohesive intercept or the angle of shearing resistance, or both. As for the effect of collapse history, the results demonstrated that both the monotonic and cyclic shear resistance of the test samples having experienced larger amount of collapse was smaller compared to that of the samples which have undergone smaller degree of hydraulic collapse, even though the density and saturation ratio of the samples were almost identical before shearing. Thus, it may be mentioned that fine-containing sands with high potential to hydraulic collapse were in an unstable condition susceptible to monotonic and cyclic softening, if they were in a state wetted by water invasion.

The investigation on deformation characteristics indicated that, for most of the materials tested, the shape of the shear stress and shear strain curves under monotonic loading condition changed from strain hardening to strain softening as the samples were wetted. However, the test results demonstrated that under cyclic loading condition, the shape of the skeleton curves was independent of collapse history, and could be well predicted by hyperbolic model. No matter what type of loads was applied, the secant shear modulus (stiffness) decreased due to wetting or due to different history of hydraulic collapse. In case of monotonic loading condition, the reduction of secant shear modulus increased with shear strain. Under cyclic loading condition, the reduction increased rapidly at shear strain less than about 2% beyond which the reduction was almost constant and was in a range of 10~23% due to different collapse history.

For different types of tested materials, the test results demonstrated that both

hydraulic collapse behavior and strength loss caused by wetting or different collapse history were affected by the properties of materials, *e.g.*, the clay content, grain size distribution, mineralogy of clay components, *etc.* There existed a critical value of clay content at which the magnitude of collapse and loss of shear strength were maximum.

In order to illustrate the effect of degree of saturation on shear strength, a series of samples having different molding saturation ratios were tested under monotonic loading condition. The results demonstrated that the monotonic shear resistance decreased greatly with the increase in saturation ratio up to a certain value beyond which value the change of strength was relatively gent. Based on the experimental observation that the volumetric compressibility, the secant shear modulus, the cohesive intercept and angle of shearing resistance changed with initial degree of saturation or wetting, a *general principle of effective stress* was proposed, which was equivalent to the *classical principle of effective stress* at saturation ratio of 100%. An explanation of the phenomenon of hydraulic collapse as well as hydraulic swelling had been given based on the general principle of effective stress, which proved that the general principle of effective stress can explain both phenomena perfectly.

The scanning electron microscope (SEM) analysis showed that the strength difference caused by different collapse history was the result of the difference in microstructure. It was further suggested that the soil must always be compacted at moisture content higher than the *line of optimum*. The SEM results also verified that the governing factors of hydraulic collapse were the low saturation ratio and the loose structures. The two factors are inseparable. Collapse may not occur if any one of the two factors does not hold.

論 文 要 旨

本研究においては，水浸した時の締固め崩壊性土の体積変化と単調と繰り返し載荷条件下の強度と変形特性にていて述べた．実験結果を得るために五つの試料について実験的な調査をした．五つの試料は一般によく使用する豊浦砂とカオリナイトを重量比で１：０．１５に調整したものと人工的な盛土から採取した二つのシルト質砂と二つの粘土質砂である．走査電子顕微鏡により，自然状態の土構造は砂とカオリナイトをある含水比で混合し，乾燥させた後の状態と同じ状態になりうることを示した．

崩壊性土の強度や変形特性に関する水浸とコラプスの影響の研究が重要であるにもかかわらず不足していることを崩壊性土ついての現状の包括的な要約と実列を通して特に示した．単純せんたん試験装置を用いて強度と変形特性を研究し，慣用的な圧密試験装置を使って水侵によるコラプスの体積変化を調べた．実験に先立って，平面ひずみと体積一定条件における応力状態と応力変化の詳細な解析を行った．その解析により計測された垂直応力は外的荷重による垂直有効応力であり，垂直応力の減少は過剰間隙水圧の増加に等しいことを示した．

コラプス現象は，その問題の基本と考えられるので，先ず最初に前述した試料のコラプス性について調べた．実験的な研究は，崩壊性土の締固め時の含水比，予め締固められた時の乾燥密度，それに上載圧に関するものに要約される．試験結果により次に示すようなことが明らかになった．

1. 締固め時の含水比，予め締固められた時の乾燥密度が同一の状態下において最大のコラプスを生じる上載圧が存在する．

2. 一定の上載圧の下では水の浸透によって生じる体積の減少は，締め固めにより準備された試料の乾燥密度の増加に伴い減少する傾向にある．

3. 一定の上載圧の下で最大のコラプスが生じる時の締固め時の含水比にも臨界的な値が存在し，この傾向は，予め締固められた時の乾燥密度が低いほど強くなる．そして，予め締め固められたときの乾燥密度がある値まで水浸により生じた体積変化は飽和度が小さいほど増加する．

4. 一定の上載圧の下でコラプスが生じない乾燥密度と飽和度が存在する．

以上の試験結果をもとに水浸したもの·無水浸のもの，コラプス履歴の異なるもの，締固め時の飽和度の異なるものの三つのシリーズの試験を単純載荷と繰り返し載荷の条件下で実施した．その結果，単純載荷と繰り返し載荷のせん断抵抗は，たとえせん断荷重をかける前に水浸した試料がより大きな乾燥密度であったも明かに減少することが判明した．その減少率は単調載荷時（σ_{v0}=98 kPa ）において 74%，繰り返し載荷時（繰り返し回数 10 回）で 46%であった．重要なことは，単調載荷時のせん断抵抗の減少は $\tau-\sigma_{v0}$ 関係における切片と傾きの一方か，両方の減少として示されることである．されに単調載荷時のせん断抵抗はある値まで（初期）飽和度の増加に伴って大きく減少し，ある値を越えると強度変化が相対的ゆるやかとなることを示した．コラプスの履歴の影響としては，これらの試料の単調載荷と繰り返し載荷時のせん断抵抗は，たとえ試料の密度と飽和度がせん断前において同じであっても，水浸によるコラプスの程度が小さいな試料に比べてコラプスの程度が大きいものほど小さくなることを示した．このことは，細粒分を含む水浸によるコラプスの高いポテンシャルをもった砂は，水の侵入によって湿った状態にある時，単調載荷と繰り返し載荷による軟化を受けやすい不安定な状態にあると言える．

変形特性についての研究としては，次のようなことを示した．

1. 試験を実施たほとんどの試料について，単調載荷条件ではせん断応力とせん断ひずみ曲線の形状は，試料を水浸させるとひずみ硬化からひずみ軟化へと変化する．

2. 繰り返し載荷条件において骨格曲線の形状は，水浸やコラプス履歴とは独立してお

り，双曲線モデルにより予測できる．

3. いかなるタイプの載荷であろうと割線せん断定数は水浸か水浸による異なるコラプス履歴により減少する．

4. 単調載荷条件において割線せん断定数の差は，せん断ひずみとともに増加する．

5. 繰り返し載荷条件において割線せん断定数の減少は，せん断ひずみが約2%以下では急激に増加し，このひずみ以上は，水浸か水浸による異なるコラプス履歴により，それぞれ10%－40%と10%－23%の範囲ではほとんど一定となる．

異なる種類の試験試料において，水浸によるコラプスの挙動と水浸や異なるコラプス履歴により生じた強度低下は，材料特性に影響されることを示した．材料特性とは，例えば粘土分，粒度分布，粘土分の中の鉱物成分などである．そして，コラプスが最大となりせん断強度が最大となるある粘土分混入率がある．

体積の圧縮性，割線せん断定数，強度曲線における勾配の切片と傾きが初期飽和度によって変化するという実験の観察に基づき，広義の有効応力の原理を提案する．そして，それは飽和度が100%の時の古典的な有効応力原理となりうるものである．膨張と同様に水浸によるコラプスの現象の説明は，広義の有効応力の原理に基づいてなされきた．そして，それは広義の有効応力の原理が両方の現象を完全に説明しうることを証明した．

走査電子顕微鏡解析により異なるコラプス履歴により生じた強度の相違は微視構造の相違であることを示した．それは，さらに言えば常には最適含水線よりも大きな含水比において締め固めるべきであるということである．走査電子顕微鏡解析により水浸によるコラプスを左右する要因は低い飽和度であって土構造のマクロポアではないが，後者の要因もコラプスの大きさに重要であることを示した．

ACKNOWLEDGMENT

I am indebted to many people for their assistance in the course of my research work. I wish to express my deepest and sincere gratitude to my advisor Prof. Kenji Ishihara for his valuable support and guidance throughout the course of this study. I am very grateful for his careful reading of the draft of this dissertation. His comments and discussions lead me to clarify many of my ideas. It is a pleasure to study under his direction.

I am deeply grateful to Prof. Ikuo Towhata for his advice and helpful suggestions. Thanks are also due to Prof. F. Tatsuoka, Prof. F. Yamazaki and Prof. H. Horii for their discussions and serving as members of the thesis committee.

I gratefully acknowledge the staffs of the Geotechnical Engineering laboratory: Ms. A. Herano, Ms. N. Karasuda, Ms. M. Yamamoto and the former staffs Mr. Y. Yoshida, Mrs. S. Aizawa for their continuous assistance. I am particularly grateful for the assistance of Mr. K. Harada, Mr. M. Murata and Mr. H. Miura in carrying out the laboratory experiments. Mr. K. Harada had been very helpful with his skill in translation. I am deeply grateful to Mr. Y. Huang for his constructive criticisms and valuable discussions, to Mr. R. Verdügo for providing me with valuable experimental data that have been obtained at University of La Serena, Chile, and to my roommate Ms. S. Zlatović for the talking and for offering me many stamps. My special thanks are due to Mr. R. Orense for reviewing the draft manuscript.

I would also like to thank Mr. M. Adachi, chief of Electron Microscopy Laboratory, and Mr. H. Kaneda, research associate of Department of Source Development, for their help and friendship in carrying out the Scanning Electron Microscopy analysis and mineral component analysis, respectively.

Here, I would like to give my acknowledgment to Dr. Wen-shao Wang, my former advisor of master degree, for his direction leading me working in this field and for his help giving to me.

My research was made possible through a scholarship grant from the Ministry of Education, Japan (Monbusho).

Finally, my inadequate gratitude goes to my wife, Fanping Li. Her love, patience, understanding and support have made the completion of this research possible.

.... to my wife, my parents and my motherland

献給我的妻子，我的父母和我的祖国

Contents

List of Figures

List of Tables

List of Photographs

NOTATION

A	Cross sectional area; Total interparticle attraction stress
A'	Effective area
a, b	Parameters in hyperbolic equation
A_a, A_s, A_w	Area of air, solid and water, respectively
a_a, a_s, a_w	Area ratio of air, solid and water, respectively
C	Coefficient of Collapsibility
c	Cohesive strength
$\overline{c}$	Effective contact stress
c'	Effective cohesive strength
C_c	Compression index
C_d, C_s, C_w	Collapse, saturation and wetting factors, respectively
CP	Collapse Potential
d	Cohesive intercept
D_{50}	Mean grain size
D_h	Horizontal displacement in direct shear test
D_r	Relative density
E	Young's modulus
e	Void ratio
e_0, e_{max}, e_{min}	Initial, maximum, minimum void ratio, respectively
E_C	Compaction energy
e_c	Void ratio at end of consolidation
e_L	Void ratio at liquid limit
e_p	Void ratio in oedometer under pressure p
E_r	Rebounding modulus
e_w	Void ratio at end of wetting
G	Secant shear modulus
G_0	Initial secant shear modulus
G_s	Specific gravity of solids
H	Height of sample; Dropping height of rammer
H_0	Initial height of sample
$\overline{h}_a$, $\overline{h}_w$	Average height of air and water, respectively
H_c	Height of specimen at end of consolidation or before soaking
H_s	Height of sample before shearing
I_p	Plasticity index
K	Coefficient of Subsidence or coefficient of lateral stress
K_0	Coefficient of earth pressure at rest

K_d	Susceptibility to collapse
K_L	Criterion of collapse
m_v	Volumetric compressibility
N	Number of cycles
N_B	Compaction times of each soil layer
N_L	Layers of compacted soil
P	Normal force at contact point of grains or axial load
p	Overburden pressure
P_0	Vertical pressure due to overburden stress
p_0	Initial total overburden pressure
p_1, p_2	Pressures
p_c	Precompression pressure
P_{C_n}	Collapse pressure for soil at natural moisture content
P_{C_s}	Collapse pressure for saturated soil
Q	Shear force
R	Collapse ratio; Total interparticle electrical repulsion stress
R_c	Relative compaction
R_p	Pressure p induced deformation
R_t	Subsidence caused by pressure p and saturation
S_0	Natural degree of saturation
S_f	Shear strength
S_r	Degree of saturation
S_{r0}	Initial or molding degree of saturation
$(S_r)_{crit}$	Critical value of degree of saturation for collapse to occur
$S.F.$	Safety factor
T	Shear force at contact point of grains
u, u_w	Pore water pressure
u_a	Pore air pressure
$\overline{u}_a$, $\overline{u}_w$	Effective pore air, pore water pressure, respectively
U_c	Uniformity coefficient
u_c	Capillary-induced pore water pressure
V	Volume
V_a, V_s, V_w	Volume of air, solid and water, respectively
V_c	Volume at the end of consolidation
w	Moisture content
w_0	Natural or molding moisture content
w_L	Liquid limit
w_{opt}	Optimum water content
w_p	Plastic limit
W_R	Weight of rammer
w_s	moisture content at 100% saturation, $w_s = \dfrac{\gamma_w}{\gamma_d} - \dfrac{1}{G_s}$
β	Angle of shearing resistance

γ	Shear strain
γ_a	Amplitude of shear strain
γ_d	Dry unit weight of soil
γ_{d0}	As-compacted dry unit weight of soil
γ_{DA}	Double amplitude shear strain
γ_{dc}	Dry unit weight before wetting
γ_{LL}	Dry density of soil at full saturation with the moisture content equal to the liquid limit
γ_{max}	Maximum dry unit weight
γ_{proc}	Maximum dry density from Proctor Compaction
γ_r	Reference strain
γ_t	Natural in-situ density
γ_w	Unit weight of water
ΔD	Displacement at top of sample in shearing direction
Δe_s, Δe_c	Deformation caused by consolidation and by collapse, respectively
$\Delta\sigma_h$, $\Delta\sigma_v$	Increments of horizontal and vertical stresses, respectively
$\Delta\sigma'_h$, $\Delta\sigma'_v$	Increments of horizontal and vertical effective stresses, respectively
Δh	Consolidation deformation
Δh_c	Collapse deformation
Δh_r	Rebounding deformation
Δh_s	Swelling deformation
ΔH_w	Wetting-induced the change of specimen height
Δp	Increment of overburden pressure
ΔS	Axial settlement
ΔV_w	Volume change caused by wetting
Δu	Excess pore pressure
ε_a	Axial strain
ε_c	Axial strain at end of consolidation or before soaking; and
ε_v	Volumetric strain
$(\varepsilon_v)_c$	Volumetric strain at end of consolidation
$(\varepsilon_v)_w$	Volumetric strain at end of soaking
ε_w	Axial strain at end of wetting.
ζ	Coefficient of lateral pressure
η	Collapsibility Coefficient
κ	Rebounding index
μ	Coefficient of friction of grain material
ν	Poisson's ratio
σ	Total normal stress
σ'	Effective normal stress
σ_1, σ_3	Total principal stresses
σ'_1, σ'_3	Effective principal stresses
σ_a	Effective vertical stress
σ'_E, σ'_I	Exogenous, endogenetic effective stresses, respectively

$\sigma_h,\ \sigma_v$	Horizontal, vertical stresses, respectively
$\sigma'_h,\ \sigma'_v$	Effective horizontal, vertical stresses, respectively
τ	Shear stress
τ_d	Dynamic shear stress
τ_f	Shear strength
ϕ	Internal friction angle
ϕ'	Effective internal friction angle
χ	Empirical parameter in Bishop's effective stress equation

Chapter 1

INTRODUCTION

1.1 BACKGROUND

With the development of technology and economy, the activities of human race have gone deep into everywhere on the earth. In the past, few people lived in the regions of considerable desiccation. Water was rare and was moved into these areas with great efforts. During that time, water was even not enough for people to drink to say poured out on the ground around building and for irrigation. However, the recent development of the means of economically moving large volumes of water into these territories has changed the economics of the situation. The availability of water in large quantities makes irrigation possible in regions where farming had not been attempted before and opens up arid areas to industrial and urban development. At same time, it provides the opportunities for spillage of water in large quantities and rises a neglected problem of additional subsidence of the foundation of structures (Bull, 1964; Leonards and Narain, 1963) or even slope failures (Kézdi, 1969; Ishihara, *et al.*, 1990) because of the change in water content in soils.

The phenomenon of additional subsidence of foundations due to change in water content in soils is usually referred to as *collapse* (Jennings and Knight, 1957, 1975; Dudley, 1970), although some writers insisted on using the terms *hydroconsolidation, hydrocompaction, hydrocompression*, or *near surface subsidence* (Lobdell, 1981; Brandon, *et al.*, 1990). The collapse phenomenon was first recognized by Terzhagi. However, little has been mentioned about it until after Word War II. Since the 1950's and especially in the 1970's, a lot of studies have been done on the phenomena and on the soils which have been suspected of being collapsible. Now, more and more geotechnical engineers recognize the destructiveness of collapsible soils and the importance of the study on them.

It seems that collapsible soils cover a wide variety of unsaturated soils from natural to compacted (Chen *et al.*, 1987) and they are found in many parts of the world (Dudley,

1970; Clemence and Finbarr, 1981). From experience, it is generally recognized that the volume decrease due to collapse by water permeation can potentially take place in sandy or silty soils containing some percentage of clay fraction, if they are deposited or placed in a loose and partially saturated state. In natural environments, they are usually present in regions of considerable desiccation. Loess and loessic soils are well known as some of the most typical and significant collapsible soils and many studies have been made so far to identify the resulting subsidence (Dudley, 1970; Chen *et al.*, 1987). Soils compacted dry of optimum and with low dry density have been known as another type of soils exhibiting high vulnerability to hydraulic collapse. Many studies have been made as well to investigate the mechanism and the factors influencing the collapse of compacted soils (Booth, 1975; Cox, 1978; Lawton *et al.*, 1989; Alwail *et al.*, 1991).

At present, the majoring of the research have been devoted to the determination of the mechanism (Barden, *et al.*, 1973). Other studies have been devoted to predictive methods (Jennings and Knight, 1975; Houston, 1988), treatment methods (Sokolovich, 1971; Qian, 1987), and case histories(Knight, 1963). In most of the studies, researchers only dealt with the collapse in a relatively small area, *e.g.*, the foundations of buildings or certain parts of pipe lines, *etc.* In these cases, the collapsible soil layers were considered as being horizontal layers, though it was not point out by the researchers, and soil layers as a whole only loaded by vertical loads in spite of the shearing in micro-structures. Therefore, attentions have been drawn primarily to the prediction of the amount of settlement or volume change and in devising preventive methods against settlement. Few attentions were paid to the strength and deformation behavior of collapsible soils when they were soaked (Yi *et al.*, 1990; Yi *et al.*, 1991). However, in more situations, the collapsible soils, for example, the soils present in earth dams, hillsides or river banks, will bear not only vertical compression load but also shearing load before, during and after collapse has occurred, and sometimes, even earthquake load. Collapse may occur due to initial store of reservoir, irrigation, long term leakage in open channel, heavy rain or sudden increase in water level in the river. In fact, there were many large scale failures reported which were caused by collapse of soils. Leonards and Narain (1963) reported the upstream failure of Portland Dam in southern Colorado, U.S.A., because of the collapse of foundation material when it was first wetted. Kézdi (1969) reported a tremendous landslide in loess along the bank of the Danube river because of the rise of the ground water table. Ishihara *et al.*, (1990) reported a series of catastrophic landslides in the loess deposit in Soviet Tajik due to an earthquake. The loess deposit was wetted over the years by permeation of irrigation water. All these case histories of failures show that consideration of only the additional subsidence is not enough. There is urgent need

for investigating the collapsibility of soils in relation to its shear strength both under static and dynamic loading conditions. The shortage of the basic test data in this aspect requires that researchers pay more attention to it.

1.2 COLLAPSE PHENOMENON IN SOIL STRUCTURE DUE TO WATER INFILTRATION

There are some soils which are often relatively stiff and will suffer small compressions under normal foundation loads if they are in a partly saturated state. However, when wetted under load, many such soils undergo a marked increase in subsidence. This additional subsidence sometimes happened in a very short time. Its rate mainly depends on the rate at which water is available to soil. In the case where water has an easy access, the additional subsidences are rapid. In the unsaturated state, these soils usually possess very loose and unstable structure but with relatively high strength due to the existence of capillary force and/or cementing agents between grain particles. However, as the water content increases, capillary force becomes zero and the cementing agent loses its effectiveness, thereby the temporary strength disappeared. The original structure is destroyed by local shear. This is the typical phenomenon of the collapse of soils.

There are many definitions related to the collapse of soils as proposed by various researchers. Jennings and Knight (1975) define the collapse settlement as an additional settlement of a foundation due to the wetting of a partly saturated subsoils, normally without any increase in applied pressure. Booth (1977) defines the collapse as the settlement that occurred in partially saturated soils solely because of the increase in the degree of saturation. Lawton (1986) defines it as a reduction in total volume of soils caused by an increase in water content at constant total pressure. Although there is no large difference among these definitions, the author prefers to define collapse as the additional volume change because of the change in water content without any change in external pressure.

The quantification and criteria of collapse are expressed in several ways (this will be discussed in Chapter 2). In this thesis, the quantification of collapse is expressed in term of *Collapsibility Coefficient*, η, which is defined as the wetting-induced additional volume change of unit volume of soil without change in external pressure, *i.e.*:

$$\eta = \frac{\textit{the decreased bulk volume due to wetting at constant external load}}{\textit{bulk volume before wetting}} \tag{1.1}$$

In terms of void ratio, it can be rewritten as (see Fig: 1.1):

$$\eta = \frac{e_c - e_w}{1 + e_c} \times 100(\%) \tag{1.2}$$

where e_c is the void ratio corresponding to the equilibrium state of soil at external load, p, and e_w is the void ratio corresponding to the equilibrium state of soil after wetting without any change in p.

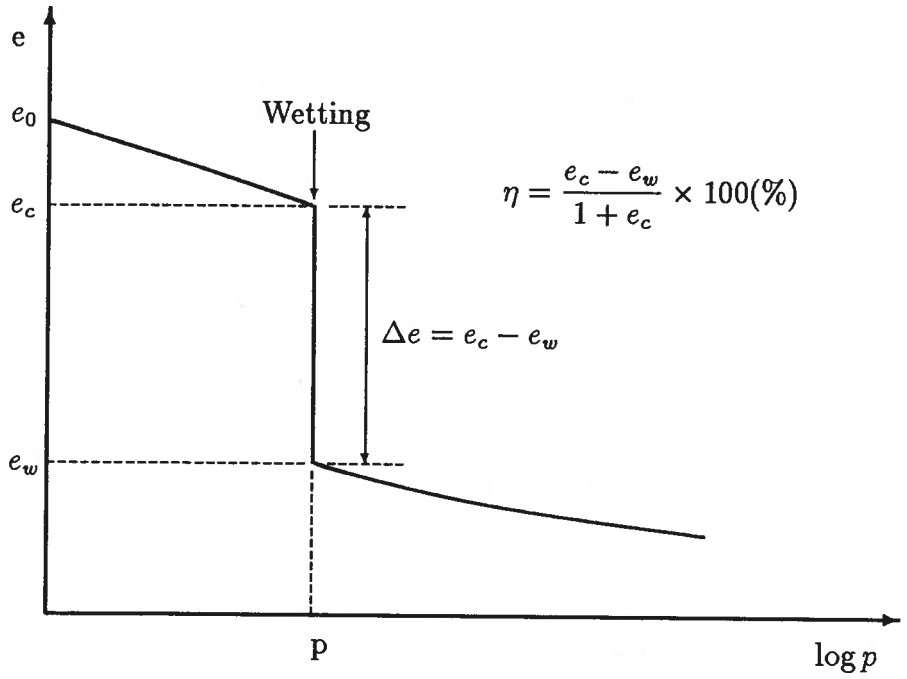

Figure 1.1: Definition of collapsibility coefficient

1.3 COLLAPSIBLE SOILS

Collapsible soils are defined as unsaturated soils with unstable structures that go through a radical rearrangement of particles and great loss of volume upon wetting with or without additional loading (Bara, 1976). These soils usually exist in loose structures of honeycomb-type or bulky-shaped grains often in the form of silt to fine sand (see Fig. 1.2) at relatively low densities. The most extensive deposits of collapsible soils are aeolian or wind-deposited sands and silts (loess). Other collapsible soil deposits are subaerial deposits, alluvial flood plains, fans, mud flow, colluvial deposits, residual soils, volcanic tuffs and decomposed granites or other acid igneous rocks (Dudley, 1970; Clemence and Finbarr, 1981; Chen *et al.*, 1987). Soils derived from volcanic tuff (Morland and Hastings,

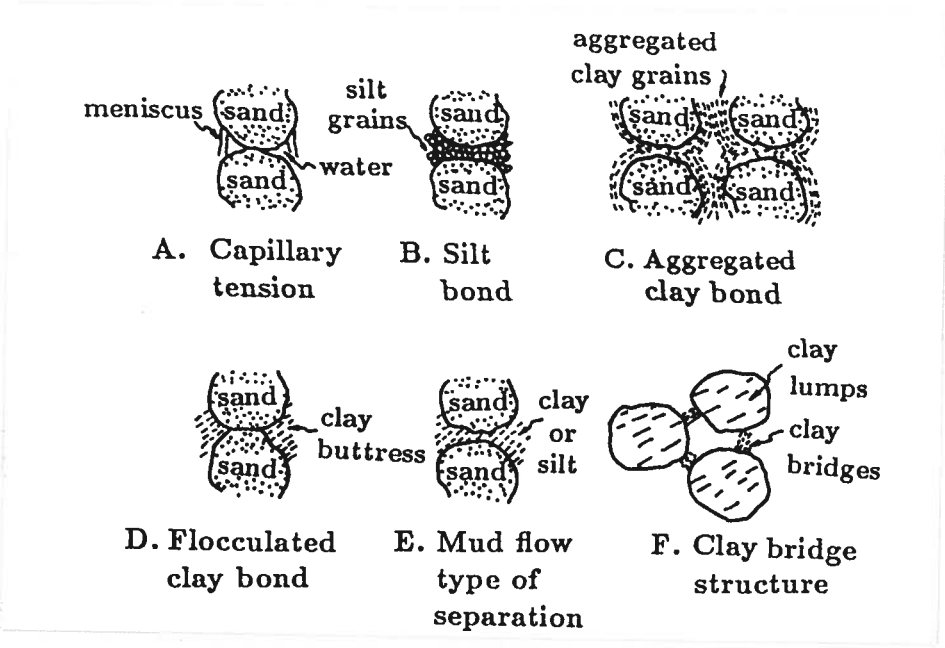

Figure 1.2: Typical collapsible soil structures (from Clemence and Finbarr, 1981)

1973), gypsum (Toulemont, 1970; Al Mohammadi and Nashaat, 1987), loose sands cemented by soluble salts, dispersive clays and sodium-rich montmorillonite clays (Sowers, 1962; Aitchison, 1973) are also collapsible. Another types of soils which are collapsible are loose fills and compacted soils. Lawton (1986) stated that almost all compacted soils can collapse under certain conditions. Some of the main collapsible soils will be discussed below.

1.3.1 Aeolian Deposits

These deposits consist of materials transported by wind which form dunes, loess, loessial-type deposits, and large volcanic dust deposits. They consist of cohesionless or slightly cohesive soils and may have low relative densities. The natural structure of these soils may contain clay cement binders such as loessial soils. These deposits are usually present in arid regions where the underground water table is at great depth below the ground surface. As the water content increases, the clay cement binder loses its strength and soil structure collapses. In some cases, the fine aeolian sediments are found protected from weathering in nature by crusts of impermeable clay. These crusts protect the entrance of large quantities of water, thus preserving the natural structure. Therefore, even in climates of medium rainfall, fine aeolian deposits are either partially modified or not at

all.

Loess, a yellow to reddish-brown soil which usually undergoes large decrease in bulk volume when saturated, covers a large area of the earth's surface – 17% of United States, 15% of Russia and Siberia, $600,000 km^2$ in China (about 60% of which are collapsible), and parts of France, Germany and Eastern Europe. It is also found in New Zealand and the plain regions of Argentina and Uruguay. It is formed by wind-borne deposits traveling over glacial outwash causing precipitation of the soil particles.

1.3.2 Water-Laid Deposits

Water-laid deposits consist primarily of loose water-deposited sediments which form alluvial fans, flows, and flowslides. These materials are originally deposited by flash floods or mud flows derive from small watersheds subjected to cloudbursts at infrequent intervals. The deposits dry out and are never again saturated until the arrival of another flow. The flows consist of poorly consolidated materials that contain considerable amount of clay. The amount of clay in a flow has an important bearing on the soil's behavior. Bull (1964) has shown that maximum collapse occurs when the clay content is about 12% of the solid. Below 5%, there is little collapse, and above 30%, the soil swells.

1.3.3 Residual Soils

Residual soils are the products of weathering, *i.e.*, the disintegration and mechanical alteration of the components of the parent rocks. Their grain sizes vary tremendously from large fragments to gravel, sand, silt, and colloids. The collapsible grain structure has developed as a result of leaching of soluble and colloidal materials. This leaching of the soluble and fine materials results in a high void ratio and unstable structure.

1.3.4 Compacted Soils

Compacted soil is present in all manufactured fills. Its collapse depends on the type of soil used and compaction conditions. The most collapsible compaction conditions are those compacted at low water content (drier of optimum) and with low compacted density. This soil usually has certain fine content, especially clay content. Clay compacted dry of optimum also shows significant collapse (Barden *et al.*, 1969; Barden and Sides, 1970).

1.4 PURPOSE AND SCOPE OF THE PRESENT STUDY

The engineering significance of collapsible soils has been recognized in connection with the failures of structures, natural slopes and manufactured fills. However, the studies on the shear strength behavior in relation to the collapsibility of soils are limited and the behavior is unknown. The present study aims to have a broad understanding of the behavior of this type of soils. Specially, the purposes of this study are:

1. To study the collapse behavior of collapsible soils when soaked under pressure. The factors influencing the collapsibility coefficient will be investigated in detail. By performing this study, the validity of certain concepts can be verified. In case some of these concepts create misconceptions or pose problems in the application, the study aims to make some clarification.

2. To investigate the shear strength and deformation behavior of collapsible soils under cyclic and monotonic loading conditions. The study addresses itself to the investigation of the behavior of different conditions: different collapsibility coefficient, with or without wetting. It tries to get a clear understanding of the strength and deformation behavior of collapsible soil at different collapse conditions.

3. To study the effects of the types of materials on collapse properties and strength and deformation behavior.

4. To examine the mechanism of hydraulic collapse and the mechanism of different strength behaviors under different collapsibility. This study will try to discover the reason why collapsibility affects strength behavior.

In order to perform more collapse conditions, compacted samples of several soils will be used. The conclusions will be applicable mainly to compacted soils. However, some of them can be applied to natural collapsible soils.

1.5 ORGANIZATION OF THE PRESENT STUDY

A brief description of the underlying motivation for this research work, the definition of collapse and the soils which are suspected to be collapsible have been given in this chapter. In order to have a better understanding of the study, a comprehensive discussion of the current state of research work on collapsing soils is presented in Chapter 2. The studies

both on natural and compacted soils are reviewed. The contents include the mechanism of collapse, the predictive method, the treatment method, the factors influencing collapse of compacted soils, and the studies on strength and deformation behaviors of partly saturated soils.

Chapter 3 reviews the case histories of collapse induced failures which intend to emphasize the importance of investigating the shear strength and deformation properties of collapsible soils in relation to collapsibility of soils. The test materials, apparatuses and experimental procedures are given in Chapter 4. The mineral component analysis of the materials as well as the conventional physical properties are illustrated. A detailed discussion is given in the unsuitability of the conventional method in measuring the minimum void ratios of the soils. The procedures of sample preparation and the conduct of tests are also discussed in detail.

The bulk of the experimental study is given in Chapters 5, 6 and 7. Chapter 5 covers the factors influencing the collapsibility coefficient, η, of soils. The results are from 250 wetting tests under overburden pressure of 98 kPa on 5 materials and 80 double oedometer tests on 4 materials. The effects of initial water content, degree of saturation, dry density and the overburden pressure on η of collapsible soils are discussed in detail. The seismic behavior of collapsible soils of different η is investigated in Chapter 6. It also discusses the influence of η on the dynamic strength of the soils. Chapter 7 deals with the behavior of collapsible soils under monotonic loading condition. The strength properties of collapsible soils with different η, and with or without wetting are investigated. The effects of η and wetting on shear strength are discussed. The effects clay content and the mineral properties of clay components are discussed in each chapter.

The applicability of the classical *principle of effective stress* is discussed in Chapter 8. The strength and deformation characteristics of soils with different initial degrees of saturation are studied to show that these properties are affected by saturation ratio of the soil. A modified version of the principle of effective stress is proposed. A new model of the mechanism of the collapse of soil structure is given based on the modified principle of effective stress. The mechanism of the effect of η on shear strength is investigated in Chapter 9 by means of *Scanning Electron Microscope (SEM)* method.

The main conclusions obtained from the present study are briefly summarized in Chapter 10. It also gives some recommendations regarding the constructions on collapsible soil deposits or by use of collapsible soil materials.

Chapter 2

LITERATURE REVIEW

2.1 INTRODUCTION

The collapse of soil structures under the permeation of water is recognized to have important engineering significance in relation to the additional settlements of structures constructed on collapsible soil deposits as well as to the sliding failures of slopes of the soil deposits, fills and embankments. The phenomenon is found to have occurred in many types of soils from natural to compacted ones and in almost all over the world. Since the 1950's, many researches have been carried out on the problem. Most of the studies focused on the mechanism of collapse, factors influencing the magnitude of collapse, prediction of collapse settlement and the improvement of collapsible soil foundations. Several state-of-the-art papers can be found on the field (Northey, 1969; Sultan, 1969; Dudley, 1970; Aitchison, 1973 and Clemence and Finbarr, 1981). The recent state-of-the-art paper was presented by Chen *et al.* (1987). Lawton (1986), Alwail (1990) and Pientong (1989) have also given literature reviews in their theses. The first two authors concentrated their reviews on the studies on compacted soils. In this dissertation, a literature review of the studies on the problems pertaining to both natural and compacted soils will be given in following sections.

2.2 RECOGNITION OF COLLAPSIBLE SOILS

There are two ways, field and laboratory, which are employed to identify whether the soils are collapsible or not. With an understanding of the basic principles of the phenomenon and with a little experience, it is not difficult to recognize the likelihood of collapse settlement from a fresh soil profile in the field. For example, collapse settlement will not occur in soils which lie below the water table. Soil deposits most likely to undergo collapse are: (1) loose fills; (2) altered wind-blown sands; (3) hill wash of loose consistency; (4) decomposed granite or other acid igneous rocks and (5) those compacted dry of

optimum. Jennings and Knight (1975) believed that there exists a critical value for degree of saturation, S_r, below which collapse can occur and above which it will not occur. The critical values are given as follows:

Table 2.1: Critical values of degree of saturation for collapse to occur (after Jennings and Knight, 1975)

Soil	Grain size	$(S_r)_{crit}$ (%)
Fine gravels	1 - 6 mm	6 - 10
Fine silty sands	150 - 2 μ	50 - 60
Clayey silts	150 - 0.2 μ	90 - 95

Most of the methods used to detect collapsible soils in the field are based on experience and some simple tests which can be run in-situ. Mackechnie (1967) stated that collapsible soils can be recognized in the field by the presence of small lumps of soil which break down readily between the fingers. Jennings and Knight (1975) proposed a very simple test, called *sausage test*, to identify potentially collapsible soils in the field. A hand-size sample of the soil to be tested is broken down into two pieces, and each is trimmed until they are approximately equal in volume. One of them is then wetted and molded in the hands to form a damp ball. The two volume are then compared again. If the wetted ball is obviously smaller, then collapse may be suspected. Jennings also proposed another method which was reportedly used with success (Knight and Dehlen, 1963). The principle of the test is the same as the above mentioned one. The difference is that the wetted sample is reformed into a 2-inch diameter cylinder and compared with another undisturbed sample in identical cylinder. If the heights of the two samples are appreciably different, collapsing soil may be suspected. Brink *et al.* (1982) also suggested almost the same method.

The susceptibility to collapse can also be determined by some simple criteria in the field. B. A. Kantey (Mackechnie, 1967) suggested the following criteria to recognize collapsible soils: (1) small lumps which break down easily by hand; and (2) excavate a hole in the soil and break down the removed material and replace into the hole. The susceptibility to collapse can be indicated from the degree of filling of the hole. Potentially collapsible soils will not fill the hole completely. Nowatzki (1980) also suggested that potentially collapsible soils have the following characteristics: low in-situ dry density (less than $14.13 kN/m^3$), desiccated, fines in a coarse-grained matrix, presence of carbonate or oxide cementation, and the presence of voids due to decay or vegetation. On the other

hand, Mackechnie (1989) pointed out that soils with dry unit weights below $16kN/m^3$ which are partially saturated either on a continuous basis or seasonally are susceptible to collapse. "*Not all soils with low unit weights are necessarily collapsible, but partial saturation is generally a prerequisite to collapse.*"

In the laboratory, various criteria are formulated for determining the susceptibility to collapse. The criteria are based on different parameters. Some of them have been listed out by Sultan (1969) and Northey (1969). A summary is given here.

(I). Expressions based on void ratios

1. Denisov (1951) defined the *Coefficient of Subsidence* as:

$$K = \frac{e_L}{e_0} \tag{2.1}$$

where e_L is void ratio at liquid limit, and e_0 is the natural void ratio. The criteria are given as:

K = 0.5 - 0.75 : Highly collapsible soil.

K = 1.0 : Non-collapsible loams.

K = 1.5 - 2.0 : Non-collapsible soils.

2. In USSR Building Code, a parameter is expressed as:

$$\frac{e_0 - e_L}{1 + e_0} \tag{2.2}$$

e_L and e_0 have the same meaning as in Eq. 2.1. For soils with degree of saturation less than 60%, the parameter gives a value of -0.1 or less for a collapsing soil.

3. Denisov (1951) presented another factor as:

$$\frac{e_p - e_w}{1 + e_p} \tag{2.3}$$

where e_p is the void ratio in oedometer under pressure p, and e_w is the void ratio after wetting under the same pressure p. This relationship may be used to evaluate the collapse magnitude due to load application, and due to the combined effect of loading and saturation. For the part due to loading only,

$$R_p = \frac{e_0 - e_p}{1 + e_0} \tag{2.4}$$

For total subsidence,

$$R_t = \frac{e_0 - e_w}{1 + e_0} \tag{2.5}$$

Similar relationships were also presented by Milovic (1969) and Marin (1969). Abelev (1968) suggested the same relation as Eq. 2.5 using different signs and indicated that if the relation gives a value greater than 0.02, the soil is collapsible. Austerlitz *et al.* (1983) modified Abelev's relation by regression method and stated that the criteria of collapse are $R_t \geq 0.05$ and $S_0 \leq 50\%$, where S_0 is the natural degree of saturation.

4. *Collapse Potential (CP)* was defined by Jennings and Knight (1975) as:

$$CP = \frac{\Delta e_c}{1 + e_0} \times 100(\%) \tag{2.6}$$

where Δe_c is the change of void ratio upon wetting under a pressure level equal to $200kPa$. The criteria which have been suggested by Jennings and Knight (1975) are shown in Table 2.2.

Table 2.2: Criteria of collapse potential (after Jennings and Knight, 1975)

CP (%)	Severity of Problem
0 - 1	No problem
1 - 5	Moderate trouble
5 - 10	Trouble
10 - 20	Severe trouble
> 20	Very severe trouble

(II) Expressions based on moisture content and Atterberg Limits

1. Priklonskij (1952) suggested a relationship for determining the susceptibility to collapse as:

$$K_d = \frac{w_L - w_0}{I_p} \tag{2.7}$$

in which, w_L is the liquid limit, w_0 is the natural moisture content, and I_p is the plasticity index. The following relations distinguish between collapsible and non-collapsible soils:

$K_d < 0$: Highly collapsible soil.

$K_d \geq 0.5$: Non-collapsible soils.

$K_d > 1.0$: Swelling soils.

2. Feda (1964) gave a expression as:

$$K_L = \frac{\frac{w_0}{S_0} - w_p}{I_p} \tag{2.8}$$

where w_p is the plastic limit. Partially saturated soils ($S_0 < 1$) with K_L values greater than 0.85 are termed *Subsident Soils.* For these soils, collapse should be expected upon saturation when S_0 =0.6 or less.

(III). Expressions based on density and Atterberg Limits

1. Gibbs (1961) defined the *Collapse Ratio, R* as:

$$R = \frac{w_s}{w_L} \tag{2.9}$$

where
w_s: moisture content at 100% saturation. $w_s = \frac{\gamma_w}{\gamma_d} - \frac{1}{G_s}$.
γ_w: unit weight of water.
γ_d: dry unit weight of soil.
G_s: specific gravity of solids.
It is reported (Northey, 1969) that Gibbs has been developed a relationship between dry density and dry unit weight on the basis of this criteria to predict soil collapse by plotting the values on a chart.

2. Several researchers have made studies to develop criterion based on the liquid limit value and the in-place dry density (Denisov, 1946; Gibbs and Holland, 1960). If the field density is so low that the water content at saturation is greater than the liquid limit, near-zero shear strength will exist upon saturation and the soil structure is subjected to collapse even without appreciable loading. Holtz and Hilf (1961) have made a chart based on the observed data in loessial soils in U.S.A. (Fig. 2.1). Gibbs and Bara (1962) have also proposed similar method based on the premise that a soil which has sufficient void spaces to hold liquid limit moisture at saturation is susceptible to collapse upon wetting.

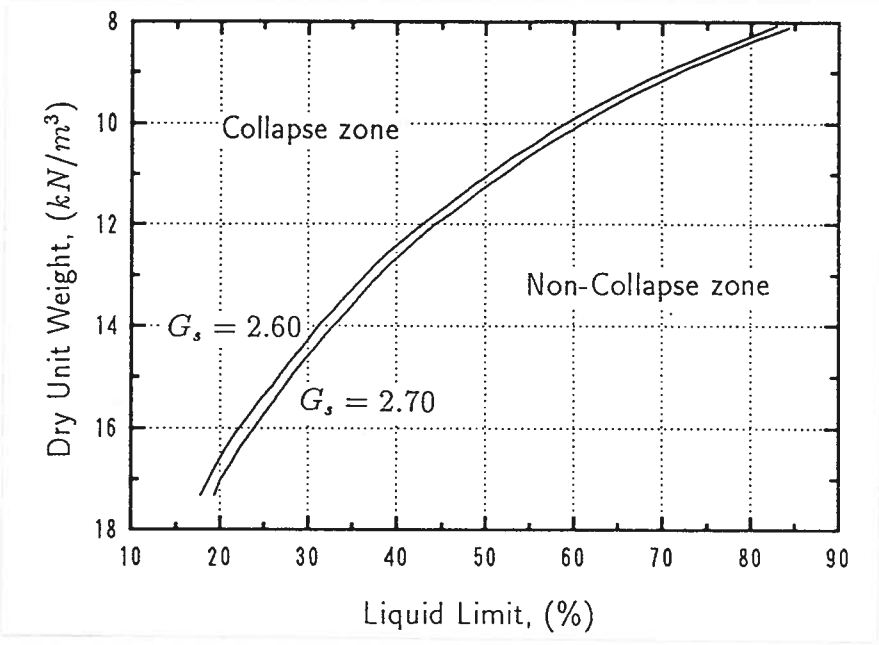

Figure 2.1: Collapsible and non-collapsible loess (after Holtz and Hilf, 1961)

(IV). Expressions based on other parameters

1. Kassif (1956) suggested a relationship which only requires the determination of the natural in-situ density, γ_t, and moisture content, w:

$$\gamma_t \cdot w \leq 1.5 \tag{2.10}$$

2. Zur and Wiseman (1973) related the collapse potential for a density ratio as follows:

$$\frac{\gamma_d}{\gamma_{LL}} < 1.0 \sim 1.1 \tag{2.11}$$

where γ_d denotes the in-situ dry density and γ_{LL} refers to the dry density of the soil at full saturation with the moisture content equal to the liquid limit.

3. Reginatto and Ferrero (1973) proposed a criterion for identifying the susceptibility to collapse of soils in exactly different way. They defined *Coefficient of Collapsibility* as:

$$C = \frac{P_{C_s} - P_0}{P_{C_n} - P_0} \tag{2.12}$$

where

P_0: Vertical pressure due to overburden stress.

P_{C_n}: Collapse pressure for soil at natural moisture content.

P_{C_s}: Collapse pressure for saturated soil.
The definition of each pressures are given in Fig. 2.2. The criteria are given as:

$C < 0$: Truly collapsible soil.

$0 < C < 1$: Conditionally collapsible soils.

$C = -\infty$: Non-cemented, normally consolidated soils.

When $C = 1$ the soil behavior will be the same for any degree of saturation. Very few soils will behavior like this. C is usually smaller than 1 for most of soils, including non-collapsible ones.

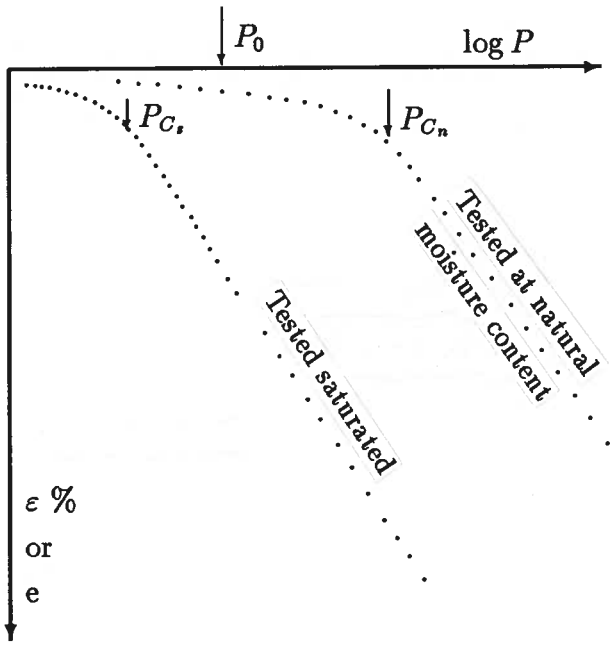

Figure 2.2: Definition of pressures

(V). Experimental methods

1. Benites (1967) suggested a simple laboratory dispersion test to indicate the susceptibility of the soil to collapse upon saturation. It consists of dropping a 2 gram soil sample block at natural moisture content into a cup containing 125 *cc* of distilled water, and recording the time it takes for the sample to disperse completely. For collapsing soils found in the Benson, Arizona area, the dispersion time is approximately 20 to 30 seconds.

2. Jennings and Knight (1975) have developed a *Double Oedometer Method.* Two identical samples are consolidated in oedometers under natural water content and soaking conditions, respectively. The amount of additional subsidence can be estimated from the difference between the two $e \sim \log p$ curves of the two tests.

2.3 MECHANISM OF COLLAPSE

Numerous studies have been done on the mechanism of the collapse of soils when subjected to water permeation (wetting or soaking). It seems that Casagrande (1932) was the first to hypothesize a model regarding the arrangement of soil particles (Fig. 2.3). At

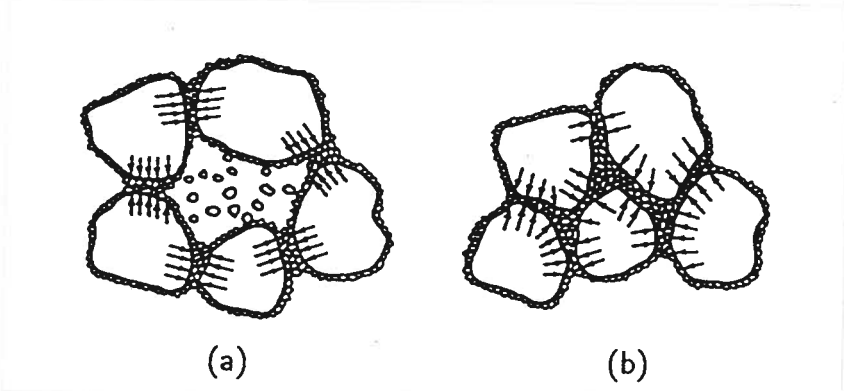

Figure 2.3: Silt/Clay structure suggested by Casagrande (1932). (a). Loaded soil structure before inundation; (b). Loaded soil structure after inundation. (after Houston *et al.*, 1988)

the state of low moisture content, the bonding material at the particle contacts provides shear strength required to resist densification. When water is allowed to get into the highly voided structure, the salt, clay, or silt bonder will soften, weaken, and/or dissolve to some extent. If more water is provided, the bonding materials will not be able to resist the shear stress existing between the interface of the large particles and the structure collapses. Knight (1961) presented similar hypothesis suggesting the mechanism of collapse involving clay bridges between unweathered grains in an open structure. Barden *et al.* (1969) have studied the collapse process in terms of two components of effective stress proposed by Bishop and Donald (1961) and Bishop and Blight (1963). Barden *et al.* (1973) summarized it as the three prerequisites for collapse.

1. An open potentially unstable partly saturated structure.

2. A high enough value of applied stress component to develop a metastable condition.

3. A high enough value of soil suction (or other *bonding* or *cementing* agent) to stabilize intergranular contacts, and whose reduction on wetting will lead to collapse.

These three prerequisites are based on the studies on clay. By means of *Scanning Electron Microscope (SEM)* method, Barden *et al.* (1973) confirmed the three typical collapsible soil structures (B, C, and D in Fig. 1.2, Chapter 1) proposed by Dudley (1970). They have been perfected by Knodel (1981) and Clemence and Finbarr (1981).

The mechanisms mentioned above suggest that collapse is controlled by the appearance of *bonding action* between soil particles. The increase in water content in soil makes this bonding action disappear and collapse takes place.

The *SEM* has been proven to be a good tool in investigating the fabric structure of collapsible soils. There has a growing tendency in the use of *SEM* in recent years (Gao, 1988; Huret *et al.*, 1988; Derbyshire and Mellors, 1988; Grabowska-Olszewska, 1988; and Alwail, 1990). Gao (1988) confirmed that loess in arid areas is still developing. The results of studies of Huret *et al.* (1988) show the effect of temperature on the void ratio of loess. The micrographics of the loess in Poland (Grabowska-Olszewska, 1988) shows that the calcium carbonate occurs in a form of irregular growths, not as coatings surrounding the quartz grains. The latter is the conventional consideration of one of the structures of loesses. Alwail (1990) used the *SEM* method to investigate the structure of compacted soils before and after wetting. He found that the dominant mechanism in the collapse of soils is the disintegration of the clay macropeds into a continuous or discontinuous clay blanket. This kind of micro-structure change is found in samples with clay content up to 50%. The shape of the silt grains and the amount of clay in the silt fines are also found to be significant in influencing the amount of collapse.

The mechanism of collapse of soil is also explained in other ways. The collapse of soils both in the laboratory and in-situ can be explained by recognizing that the process of confined compression is accompanied by shear in the soil mass. It is possible to express the stress state at a point in the soil by a Mohr-Coulomb circle in $\tau \sim \sigma'$ plane as in Fig. 2.4 (Holtz and Hilf, 1961). When the soil is in a relatively dry state, the stress state can be represented by Circle 1 in the figure. Its safety factor against collapse can be taken as the ratio of shear resistance to shear stress. Neglecting intermolecular attraction, that is, assuming cohesion is zero, the safety factor can be expressed as:

$$S.F. = \frac{\sigma' \tan \Phi'}{\tau} = \frac{(\sigma - u) \tan \Phi'}{\frac{\sigma_1 - \sigma_3}{2} \sin(\frac{\pi}{2} + \Phi')} \tag{2.13}$$

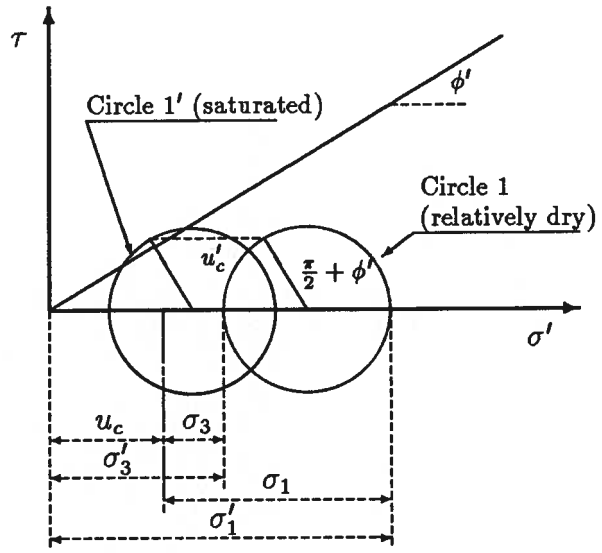

Figure 2.4: Settlement due to saturation in the confined compression test (after Holtz and Hilf, 1961)

For unsaturated soil, the pore water pressure, u, has been shown to be the algebraic sum of pore air pressure, u_a, and the capillary pressure, u_c, resulting from the curvature of the meniscus at air-water interface (Hilf, 1956). In the drained condition, the air pressure in the unsaturated soil is equal to atmospheric pressure, that is, $u_a = 0$. The pressure in the water films of the soil is negative. Therefore, $u = -u_c$ (u_c is a positive value). Hence, Eq. 2.13 becomes:

$$S.F. = \frac{(\sigma + u_c)\tan\Phi'}{\frac{\sigma_1 - \sigma_3}{2}\sin(\frac{\pi}{2} + \Phi')} \tag{2.14}$$

As water is introduced into soil under constant external load, the capillary pressure decreases with the increase in water content and it will finally vanish when the soil is fully saturated. This decreases the safety factor indicated in Eq. 2.14. This is illustrated by Circle 1 being translated toward the origin by an amount equal to the value of u_c to give Circle 1′. Since Circle 1′ intersects the Mohr envelope, failure occurs in this point.

Similar approaches have been made by other individuals. Aitchison and Donald (1956) have calculated the effective intergranular stress induced by negative pore pressure. Donald (1956) validated the calculated values by laboratory tests. Jennings and Burland (1962) described the role of menisci as the *bounding* between grain contact points. Dudley (1970) pointed out that the stresses due to capillary and gravity must become proportionally less of the total when the grains reach the size of the clays. At this size, the forces of osmosis, Van der Waals, and molecular attraction must become relatively

more prominent. Therefore, he demonstrated the use of different mechanisms for different type of soils.

A meaningful work has been done by Newland (1965) who hypothesized the existence of two kinds of effective stresses. The two effective stresses are:

1. The endogenetic effective stresses are due to forces arising at the contact points of particles which act entirely normal to the tangent at the point of contact, *i.e.*, there are no shear components present. Forces included in this category are the various attractive and repulsive forces (electrical, osmotic, Van der Waals and molecular, *etc.*) that give rise to true cohesion in saturated clays, plus the meniscus forces that give rise to the additional strength in unsaturated soils.

2. The exogenous effective stresses are due to external forces acting at contact points of particles accompanied by a component of shear. Forces included are the applied load and gravity force.

The collapse of soils is due to the reduction in the endogenetic effective stress upon wetting.

At the same time that Newland proposed the two effective stress theory, a new model which is some what similar to this concept has been postulated by Burland (1965). This model is based on the concept of grain contact stability. At any contact point of the grains, there exists a normal force, P, and a shear force, T, which are transmitted to the soil grains. It is assumed that the displacement, in the form of translation and rotation of a grain, can only take place as a result of slip at the grain contact points. The stability against slip is controlled by the ratio of the two force components. For a grain to be in equilibrium under its contact forces, it must satisfy the following relationship at every contact point,

$$T/P \leq \mu \tag{2.15}$$

where μ is the coefficient of friction of the material composing the grains.

Burland separated the grain contact forces induced by the transmission of boundary stresses and those induced by grain contact menisci in the same way that Newland did. The two different grain contact forces play different roles in stabilizing the grains. The increase in the contact forces resulting from increments in boundary stress tends to induce grain slippage and distortion and, hence, the irrecoverable volume decreases. However, the increase in the contact forces caused by the increase in the negative pore water pressure within grain contact menisci will tend to stabilize the contacts and will in fact inhibit

grain slippage. This is because only the normal components of the contact forces will increase so that the ratio T/P at any contact point will decrease. When water is added to the soil, the contact menisci diminish with the increase in the degree of saturation in the soil and vanish when the degree of saturation reaches to 100%. Therefore, the normal components of contact forces decrease and collapse occurs in the soil structures.

This model is derived for granular soils. However, because of the phenomenon of *micro-shattering* encountered in most desiccated clays, Burland believed that the effect of increasing the negative pore water pressure in a partly saturated clay soil will be in general the same as for a granular soil, *i.e.*, to increase the rigidity and stability of the soil structure by increasing the contact forces at grain and *packet* contact points. Therefore, the model can also be applied to clay soils.

In order to qualitatively predict the volume change in partly saturated soils, Burland suggested the use of the average value, $\overline{T/P}$, for all the contact points.

A model similar to that of Burland's was proposed by Moore and Millar (1971).

2.4 FACTORS INFLUENCING COLLAPSE

Many individuals have studied the factors which control the magnitude and rate of collapse both on undisturbed and compacted collapsible soils. Barden *et al.* (1973) indicated that the basic prerequisite for a soil to be collapsible is the open metastable structure, whether the soil is made up of sand, silt or clay. Even though the amount of collapse is a function of variations in the material (*i.e.*, kinds of materials and relative proportions of each component including water), initial void ratio, stress history of the materials, thickness of the soil layer involved, and amount of the added load, Dudley (1970) stated that there are two prime requirements for soil to be collapsible, namely a loose soil structure and a moisture content less than saturation. Booth (1975) also showed that the above two factors are the most important. On the other hand, Reginatto and Ferrero (1973) pointed out that dry density is not a governing factor regarding the collapse of soils they used and some of the most stable soils have the lowest densities. Lobdell (1981) has studied the collapse properties of the loess in Southeastern Washington State, USA, and concluded that a key factor in evaluating the collapse potential of a loessial soil appears to lie in the mineralogy of the soil, especially that of the clay minerals which comprise the majority of the cement.

It is clear that the magnitude of collapse depends on many factors. In some soils,

some of the factors are more important than others, while in other types of soils, these factors may not be important. The difference in the conclusions is mainly because of the variation of soils studied. In this section, some of the main factors will be discussed.

2.4.1 Influence of Initial Moisture Content

As many researchers indicated, the initial moisture content is one of the most important factors in the phenomenon of collapse. There is no doubt that fully saturated soil will not collapse (Jennings and Knight, 1975). A number of reports state that the amount of collapse increases continually as the initial moisture content decreases. Others found that there is an optimum degree of saturation for maximum collapse (Dudley, 1970). For compacted soil, there are two states of moisture content before wetting. One corresponds to state at the time of filling, *i.e.*, the placement moisture content, and the other corresponds to the state at the time before adding water, *i.e.*, the after consolidation moisture content. According to Lawton (1986), the placement moisture content contributes to the initial fabric of compacted soil, while the after consolidation moisture content determines the volume change characteristics of the fill. Booth (1975) conducted tests wherein specimens were compacted at the same moisture content (slightly above standard Proctor optimum) and then either moisturized or dried to other moisture contents to simulate the post-construction moisture change in the field. He found that the moisture content prior to collapse is one of the most important factors influencing the amount of collapse in soil. However, changes in the compaction moisture content make little difference to subsequent collapse.

When dealing with the collapse behavior of compacted soils, the state of moisture of soil is usually divided into *dry* and *wet* of optimum. It has been reported by several researchers that clays compacted dry and wet of optimum possess different structures (Lambe, 1958; Barden *et al.* 1969; Yoshinaka and Kazama, 1973). The general transition from a flocculent structure on the dry side of optimum to a dispersed structure on the wet side results in a very different compression behavior for clay. It is also contended that soils compacted *wet of optimum* do not collapse (Barden *et al.* 1969; Barden *et al.* 1973; Barden and Slide, 1970; and Booth, 1975; Lin and Lovell, 1983; DiBerbardo and Lovell, 1979, 1984). Booth (1975; 1977) pointed out that collapse can occur in some soils with moisture contents a little above the Proctor optimum when the densities are low. Lawton (1986) found that with same dry density and overburden pressure, the magnitude of collapse decreases with increasing molding water content. He also indicated that the *optimum* should be replaced by the *line of optimum* because the optimum moisture

content for a given soil varies depending on the compaction energy and the compaction method. This concept was also proposed by Lin and Lovell (1983).

It is also found (Booth, 1975) that there exists a critical moisture content below which collapse may occur and above which no collapse would occur. This critical moisture content varies slightly with the initial dry density and the applied pressure, and is usually higher than the Proctor optimum moisture content.

2.4.2 Influence of Initial Dry Density

Booth (1975) investigated the effect of the initial dry density on the collapse of compacted soils. He found that the amount of collapse at any particular moisture content has a maximum value which occurs at a lower initial dry density for lower moisture content. For any degree of saturation, there is a dry density above which collapse is negligible. For the soils used in the study, this critical value is $15.70kN/m^3$. When initial dry density is lower than this value and at a low moisture condition, collapse can be as much as twenty percent. At a low value of initial dry density, the magnitude of collapse and critical moisture content increase.

Lawton (1986) indicated that the placement dry density is the most important factor in determining the magnitude of collapse when the soil is compacted very dry of the line of optimum. However, near the line of optimum, the collapse potential is controlled by the degree of saturation rather than by the initial dry density. He confirmed the existence of an upper limit of initial dry density for the occurrence of collapse. It is reported that this upper limit increases with the increase in the overburden pressure.

A valuable work was done by El-Sohby and Elleboudy (1987) on naturally cemented sand. The natural moisture content was quite low and close to 2% in all samples. The natural dry densities vary noticeably, ranging from 1.65 to 1.95 t/m^3. The results confirmed the conclusions from compacted soils. It is also found that at high natural density, the soil swells upon wetting if the applied pressure is not high enough.

2.4.3 Influence of Overburden Pressure

According to Booth (1975), for any set of initial conditions there is an applied pressure at which collapse will be maximum. Both this pressure and the amount of collapse increase with the reduction in moisture content. For a given degree of saturation, the amount of collapse increases with the increase in applied pressure. The same conclusions are

obtained by Cox (1978) and Lawton (1986). Huang (1989) found that the magnitude of collapse increases linearly with the increase in applied pressure. El-Sohby's and Elleboudy's (1987) results on natural soils show that at given initial dry density, the amount of collapse increases as the applied pressure increases. At high initial dry density, on the other hand, soil swells in low pressure range and collapses in high pressure range.

2.4.4 Influence of Other Parameters

There are many factors affecting the collapse of soils. Except for the factors mentioned above, the amount of collapse and its rate are affected by the mineralogy of the materials present, the percent of each type of clay mineral, the shape of the bulky grains and their grain size distribution, the pore size and shapes, the cementing agents, the absorbed ions and the type of ions and their concentration in the pore water (Dudley, 1970).

El-Sohby *et al.* (1987) investigated the effect of clay mineralogy. Soils containing more active clays collapse more than those which contain less active clays if the clay content is less than a certain value (about 40% under a pressure of 100 kN/m^2). This value increases with the increase in the applied pressure. Lobdell (1981) reported that loess containing montmorillonite collapses more than those containing illite. The reason is that montmorillonite has high ability to absorb hydrogen cations, thus, it has a higher ability to absorb water than illite.

Effects of clay content and grain size distribution have been studied by El-Sohby and Rabbaa (1984) and El-Sohby *et al.* (1987). Collapse occurs when the clay content ranges from 15% to 40%. For the same clay content, soils containing higher proportions of sand undergo greater amount of collapse than those containing higher proportions of silt. For those free of clay, soils containing silt and sand collapse more than clean silt or clean sand. For natural soils, Dudley (1970) stated that collapse occurs in a range of clay content between 5% to 30%. Maximum collapse occurs when the clay amounts to about 12% of the solids. Alwail (1990) found that the amount of the clay and the shape of silt grain, rather than the capillary force, are the controlling factors in determining the magnitude of collapse of silty sand.

Often times, soil-water chemistry is shown to be an important factor to the collapse of soils (Reginatto and Ferrero, 1973; Reginatto, 1989). Some soil shows no collapse when wetted with normal water, while the same soil undergoes large amount of collapse when wetted with septic tank effluent. The literature is limited in this aspect.

Day (1990) stated that collapsible soil can be sensitive to the sampling process. Different sampling methods may give different amount of collapse. Ismael (1989) compared the results of undisturbed and remolded samples of the same material under the same densities. The remolded sample gives higher collapse potential. El-Sohby *et al.* (1989) have investigated the influence of sample disturbance and side conditions on the amount of collapse. They found that by improving the side conditions of specimen by wax injection, the collapse potential is reduced by 27%. Using equal unit weight method, this reduction is 41%. When the specimen diameter is enlarged and the specimen fitting is improved, the collapse potential decreases by 56%. Milovic (1988) pointed out that the laboratory test results are very often on the unsafe side for the mechanical disturbance. Other researchers (Barden and Sides, 1971; Houston *et al.*, 1988; and Robinson, 1989; Houston and El-Ehwany, 1991) also paid attention to these effects.

Several compaction methods (static, impact, kneading and vibratory) were used in the tests conducted by several individuals (Holtz, 1948; Booth, 1975; Cox, 1978, and Lin and Lovell, 1983). Although Booth mentioned that the changes in the method of compaction may influence collapse, little research has been done to compare the effects of different compaction methods on collapse. Lawton (1986) was the first to investigate the effects. He found that the magnitude of maximum collapse is the greatest for static compaction and the lowest for kneading method. However, the difference is insignificant.

The effect of stress ratio on collapse behavior of soil has been investigated by Lawton (1986) and Lawton *et al.* (1991) by using double-triaxial test method. They found that the magnitude of volumetric strain resulting from a change in stress ratio or from wetting depends on mean normal total stress and is independent of the principal stress ratio. However, the individual components of volumetric strain—axial and radial strain—depend significantly on principal stress ratio.

2.5 PREDICTION AND THEORETICAL ANALYSIS OF COLLAPSE

2.5.1 Prediction of Collapse Deformation

The amount of collapse, or the additional subsidence, is a problem most researchers interested in because it directly relates to the bearing ability of structures to additional deformation. Jennings and Knight (1975) have proposed a method to predict the collapse settlement for design purposes by using the results of *double oedometer* consolidation tests.

Two samples are prepared as identical as possible from the same *undisturbed* sample. Great care is taken to preserve the natural water content. Both samples are carefully trimmed into consolidmeter rings, and are placed in a consolidmeter under a light 1 kPa seating load for 24 hours. At the end of 24 hours, one sample is inundated by flooding with water, while the other sample is kept at its natural water content. Both samples are then left for another 24 hours. The test is then carried out as in an ordinary consolidation test and the results are plotted in $e \sim \log p$ plane. The total overburden pressure, p_0, at the depth of the sample is calculated and plotted on the $e \sim \log p$ curves obtained from the two tests. The precompression pressure, p_c, is found from the soaked curve and compared with p_0. If $p_c/p_0 = 0.8 \sim 1.5$, it is normally consolidated case. If $p_c/p_0 \geq 1.5$, it is overconsolidated case. The test results are adjusted according to different cases, as shown in Fig. 2.5.

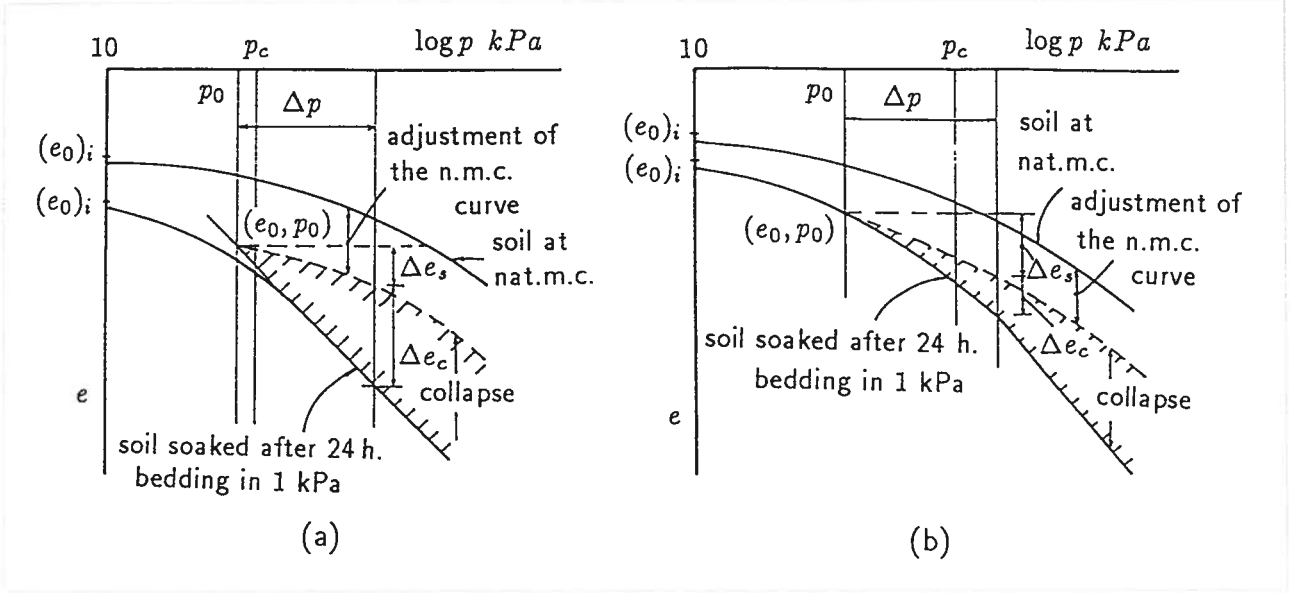

Figure 2.5: Double oedometer curves. (a). Adjusted for normally consolidated soil; (b). Adjusted for overconsolidated soil.(after Jennings and Knight, 1975)

With an additional loading, Δp, the unit settlement (mm/mm) for the soil without change in natural moisture content is $\Delta e_s/(1+e_0)$. If the applied loading remains constant and the soil increases in water content, the unit *additional* settlement is $\Delta e_c/(1+e_0)$. If these values are used with the various selected layers in the profile, the total settlements under both conditions may be calculated.

In Jennings' and Knight's method, the un-soaked $e \sim \log p$ curve is adjusted to pass the (e_0, p_0) point on soaked curve to try to eliminate the effect of the difference in initial

void ratio. This gives a results that no collapse occurs if the total overburden pressure, p_0, at the depth of sample does not change, even though the sample is soaked. It seems that it is not true. Many failure cases show that the collapse often occurs without any change in total overburden pressure.

A modified version of the Jennings and Knight oedometer test was proposed by Houston *et al.* (1988). This modified method consists of three steps: (1) The soil profile beneath the foundation is first divided into a number of different zones, each corresponding to a representative sample. The initial vertical normal stress, the change in stress due to the footing load, and the final vertical normal stress are then calculated at the midpoint of each zone; (2) Soaking test is run on each sample corresponding to each vertical normal stress . The collapse strain for each zone is determined from the $e \sim \log p$ curves. The additional settlement of the zone is equal to the collapse strain multiplied by the thickness of the zone; and (3) The total collapse settlement is obtained as the sum of those in each zone. It is said that this method can predict the collapse settlement better because only one sample is needed and this will reduce the error caused by the difference in two samples.

The procedures for predicting the amount of collapse in this method is of significance. However, the assumption that no deformation caused by soaking will occur at overburden pressure of 5 kPa is doubtful. For some soil, this assumption may be tenable but not for all the soils. For example, for lightly swelling soils, collapse deformation will be resulted if they are wetted under high pressure, while if they are soaked under low pressure, swelling deformation will occur. Therefore, it would be better to investigate the collapse behavior of soil at low pressure before any adoption of the procedures.

2.5.2 Mathematical Approach

Based on the stability of large voids, or macro-pores, a mathematical model has been suggested by Amirsoleymani (1989). The derivation of the mathematical approach is based on the properties of: (1) An open, potentially unstable partly saturated soil with macro-pore structure; (2) a two dimensional stress systems to measure stability conditions; and (3) a strong soil bonding or cementation agent to stabilize intergranular contacts. It assumes that macro-pores are made up of various sizes and shapes of ellipsoids having random orientations with respect to the main principal stress and are located within the *densely packed zones.* Collapse occurs when the tensile strength around the boundary of macro-pores is less than the tensile stress produced by the imposed external stresses.

Because the tensile strength is caused by capillary suction and by the bonds between the particles, it decreases upon wetting accompanied by collapse. After a series of mathematical derivation and other assumptions, an equation of the change of void ratio is derived. The procedures of collapse can thus be approached by numerical calculation.

A model of yield function was developed based on Cam Clay type energy equation and experimental results in unsaturated soils (Karube, 1987; Karube and Kato, 1989). Solutions on compacted kaolin clay reveal the relevancy of the model for both potential collapse and potential heave as applied to real soil.

Finite element method approach for collapsing soils was first proposed by Miranda and Van Zyl (1989). The unsaturated constitutive relationships that take into account the change in the set of independent variables $(\sigma - u_a)$ and $(u_a - u_w)$ are incorporated into the finite element method. The method is used in the analysis of two small dams which are poorly and well-compacted, respectively, and the results show that this method can reasonably simulate the observed behavior of the dams.

Several others models were suggested by individuals in connection with unsaturated soils. Toll (1990) proposed a model based on the critical state (steady state) model for saturated soil, incorporating other variables which are needed for formulating unsaturated soil behavior. The effects of total stress and suction are considered separately. A model based on hardening plasticity was derived by Alonso *et al.* (1990). As in the work of Toll, two independent sets of stress variables: the excess of total stress over air pressure and the suction, were used, in the model. It is stated that upon reaching saturation, the model becomes a conventional critical state model.

2.6 STRENGTH AND DEFORMATION PROPERTIES

2.6.1 Behavior Under Static Loading Condition

A number of reports can be found dealing with the strength and deformation properties of collapsible soils (Williams, 1957; Uchida *et al.*, 1968; Berezantzev *et al.*, 1969; Uriel and Serrno, 1973; Ohta and Hata, 1977; Fukuda, 1978; Allam and Sridharan, 1981; Gulhati and Satija, 1981; Wu *et al.*, 1985; Liu *et al.*, 1985; Akinmusuru, 1987; Pientong, 1989; Stark and Duncan, 1991, and Day and Axten, 1991). Fukuda (1978) performed direct shear test on weathered granite soil in a special way to investigate the effect of hydraulic collapse on the strength and deformation properties of the soil. First, an overburden pressure and an initial shear force are applied on a compacted sample in direct shear

box. The specimen is allowed to reach equilibrium under the applied loads. Then, water is introduced into the specimen from the bottom and a new equilibrium under soaking condition is allowed. When the sample does not fail, the shear force is increased until failure occurred in sample. For different states of applied initial shear force, three different behaviors of failure during further wetting and shearing are observed (see Fig. 2.6). In

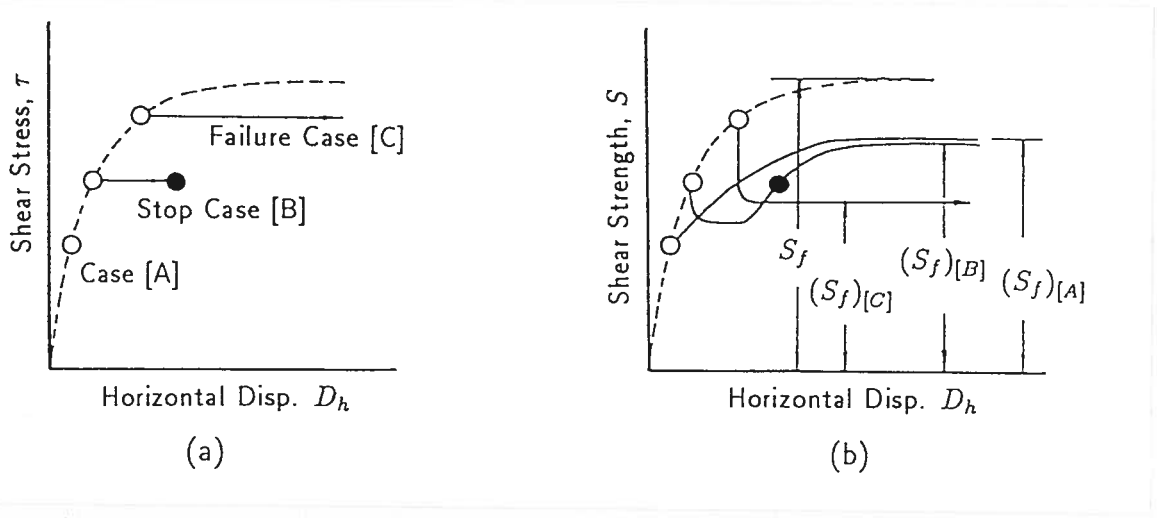

Figure 2.6: Behavior of shear strength upon wetting. (a). Horizontal displacement during wetting, (b). Change of shear strength. (after Fukuda, 1978)

case A, the sample is wetted when the initial shear force is relatively small. No additional horizontal deformation takes place during wetting. Further shearing is needed to cause sample failure. In case B, water is introduced when the sample has borne moderate shear force. Horizontal displacement is recorded during wetting but it stops at a certain deformation. Indicating that additional shear is still needed. In case C, sample has born relatively large shear force before wetting and unlimited deformation is recorded and failure occurs during wetting.

Liu *et al.* (1985) have studied the deformation behavior of intact structural loess of Shaanxi, China and concluded three type of failures and four kinds of *stress* $\sim$ *strain* curves, as shown in Fig. 2.7. The softening deformation behaviors corresponding to a brittle failure where the strain at failure is usually small. This is the typical behavior of loess having high density and low moisture content. If water is introduced into the soil, its behavior changes from strong softening to weak softening. For the soil possessing loose texture with low moisture content, the behavior is either a strain hardening, strong hardening or weak hardening, depending on the stress level, sometimes even weak softening if shear shrinkage occurs during shearing. Mathematical models have been developed

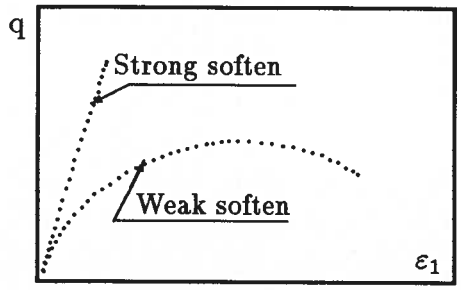

(a). Brittle failure type

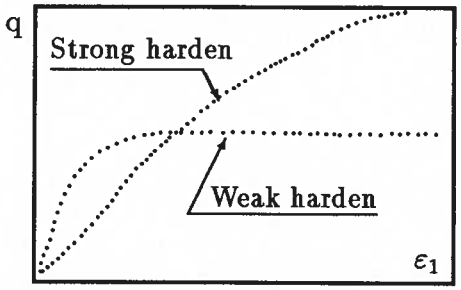

(b). Plastic failure type

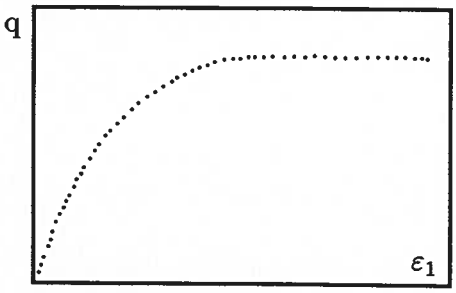

(c). Ideal plastic type

Figure 2.7: Stress – strain relations of loess soils (after Liu *et al.*, 1985)

for each type of stress strain curves.

2.6.2 Seismic Behavior

The seismic behavior of collapsible soil is one area of research in geotechnical engineering which has just been dealt with. The existing research in the area is extremely limited. The available literatures are the work done by Prakash and Puri (1982) and Bhatia and Quast (1984). Prakash and Puri (1982) tested undisturbed samples of loess from Memphis (USA) under cyclic traxial conditions and found that, unlike clean sands, large axial deformation develops before the initial liquefaction. They also reported that there is no large difference in behavior between undisturbed and reconstituted samples under saturated conditions. Bhatia and Quast (1984) performed tests on undisturbed and fabricated (keeping the same grain size distributions and the same states of density and water content) samples under partly saturated and saturated conditions, and reported that under partly saturated condition, cyclic resistance is significantly affected by soil structure, while under saturated condition, this effect is negligible.

According to Bhatia and Quast (1984), the behavior of collapsible soils under seismic loading conditions have also been investigated by several individuals (Rovinovich, 1960;

Gibbs and Bara, 1967; Musaelyan, 1972; and Xie *et al.*, 1980). Rovinovich (1960) carried out a study in which the slump like deformation of loess soil under simulated earthquake conditions was investigated. The study points out that there are two causes of collapse under cyclic loading: 1) due to the weight of the soil and 2) due to cyclic load. Rovinovich observed that the dynamic settlements in a loessial soil increases with the acceleration and duration of the vibration. Gibbs and Bara (1967) studied a collapsible soil being subjected to cyclic loading and their results show that a 10% reduction in shear strength parameters (c and ϕ) is observed due to cyclic loading equivalent to 0.39 earthquake. Musaelyan (1972) reported that seismic loads of varying intensity causes further collapse in collapsible soils. Xie *et al.* (1980) performed an extensive series of experiments and found that the modulus of elasticity depends on the void ratio, the water content, the confining stress and the number of cycles.

2.7 THE CHANGE OF STRENGTH AND DEFORMATION PROPERTIES WITH DEGREE OF SATURATION

The shear strength of partly saturated soils have been investigated by many individuals (Cooling and Smith, 1936; Williams, 1957; Blight, 1967; Berezantzev, *et al.*, 1969; Uchida, *et al.*, 1968; Huang, 1983; Stark and Duncan, 1989). The change of shear strength parameters has been reported in all of these studies.

The effect of degree of saturation (or water content) on shearing resistance of partly saturated soils has been noted almost at the same time as the estimation of modern soil mechanics. As early as in 1930's, Cooling and Smith (1936) have investigated the shearing resistance of typical English clays under different water contents. The test program included three kinds of samples, namely samples remolded from natural state, samples prepared from the air-dried condition by thorough manipulation with different proportions of water, and undisturbed samples, and two test methods: pure shear test on torsional shear test apparatus and unconfined compression. Their results (Fig. 2.8) indicated that the shearing resistance of soil is affected significantly by initial water content of the soil. It is obvious that the lower the initial water content, the higher the shearing resistance. The gradient of the strength reduction decreases as the initial water content increases.

Blight (1967) pointed out that the procedure used by Bishop and Blight (1963) and Blight (1965) to evaluate the value of χ was not completely satisfactory because

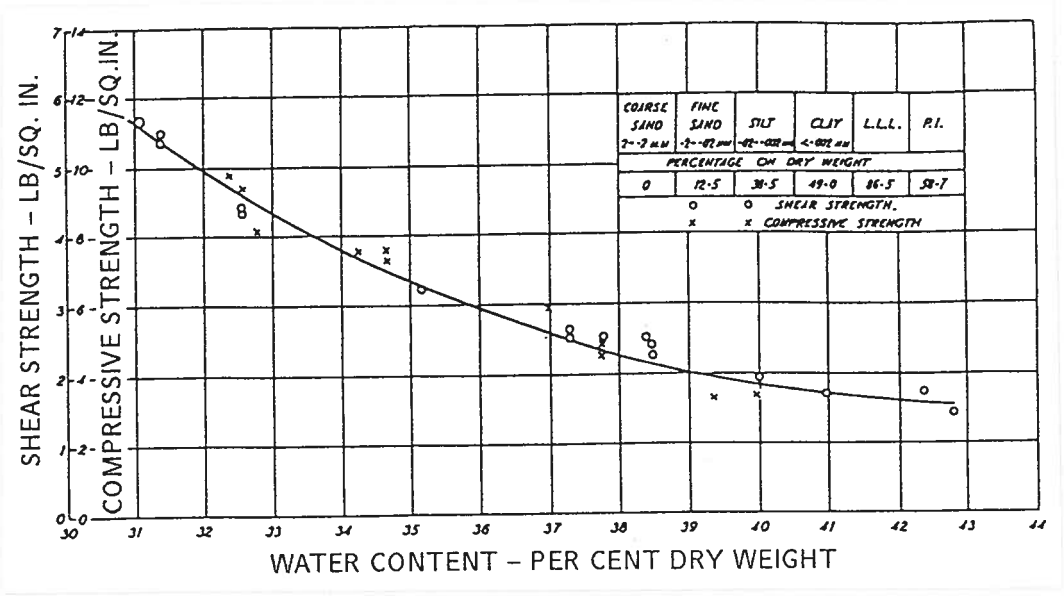

(a). London clay (Sample No. 129)

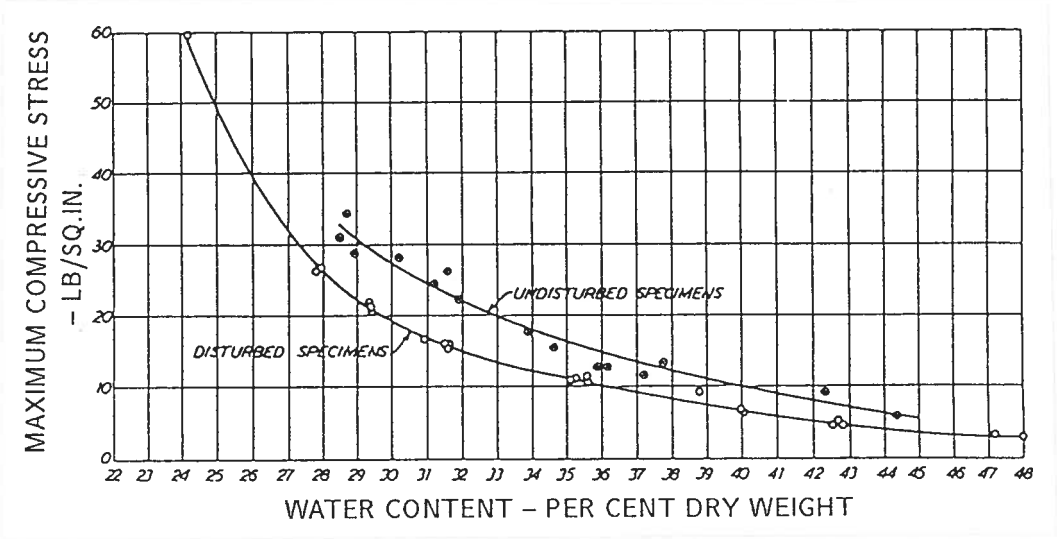

(b). London clay

Figure 2.8: Effect of initial water content on shearing resistance (after Cooling and Smith, 1936)

it assumed that the strength parameters are independent of water content and are the same whether the soil is fully saturated or unsaturated. His results show the change of these parameters with water content. Uchida *et al.* performed three series of triaxial compression tests on compacted samples of various void ratios and degrees of saturation. They found that the shearing resistance decreases and pore pressure increases with the increase in the degree of saturation and void ratio.

A meaningful work was done by Berezantzev *et al.* (1969). They studied the strength and bearing capacity properties of several soils, especially loessial soils, and obtained relationships between cohesive force, internal friction angle and moisture content. They stated that "*wetting will affect, above all, the values of cohesive force (c) and of an angle of internal friction (ϕ), as these soil characteristics are* single-*valued function of humidity*". Laboratory tests were performed on loessial soils to investigate the variation of cohesive force, internal friction angle and lateral pressure coefficient. The results (Fig. 2.9) show that in loessial soils both cohesive force and internal friction angle decrease significantly with the increase of humidity. The internal friction angle decreases by an amount as large as 24 degrees (60%) when moisture content is increased from 2% to 30%. Moreover, the cohesive force is reduced to 67% when moisture content is changed from 2% to 10%. They claimed that the test data are in rather good agreement with the results of field experiments on the same soils. Similar results were obtained by Stark and Duncan (1991) on desiccated clay. Their results show that cyclic soaking further reduces the strength to residual values. This implies that the main reason of collapse is the dramatic reduction of shear strength of soils upon wetting.

The literature on the effect of degree of saturation on deformation properties of partly saturated soils is extremely limited. The only two works which could be found are those by Wu *et al.* (1984, 1985). The results (Fig. 2.10) are of important significance. It is obvious, in Fig. 2.10, that both initial shear modulus and the shear modulus at different strain level change with degree of saturation. It is to be interestingly noted that the initial shear modulus is the same at degree of saturation of 0 and 100%. This is because the phase relationship of soil is the same at the two extreme conditions of saturation ratio: soil is two-phase medium. The only difference is the replacement of water phase by air phase. If no chemical reaction occurs between the solid particles and water or air, the characteristics of the soil will be the same. This is consistent with the case of collapse which shows the existence of optimum degree of saturation at which the magnitude of collapse is maximum.

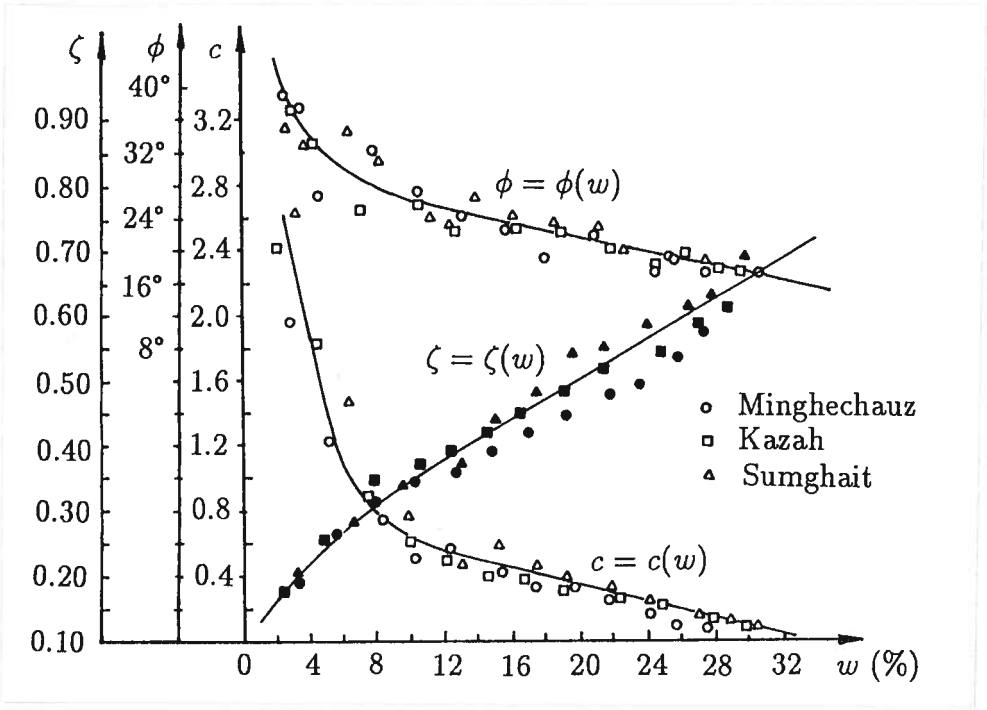

Figure 2.9: Variation of cohesive force c, angle of internal friction ϕ and coefficient of lateral pressure ζ of loessial soils with humidity (after Berezantzev *et al.*, 1969)

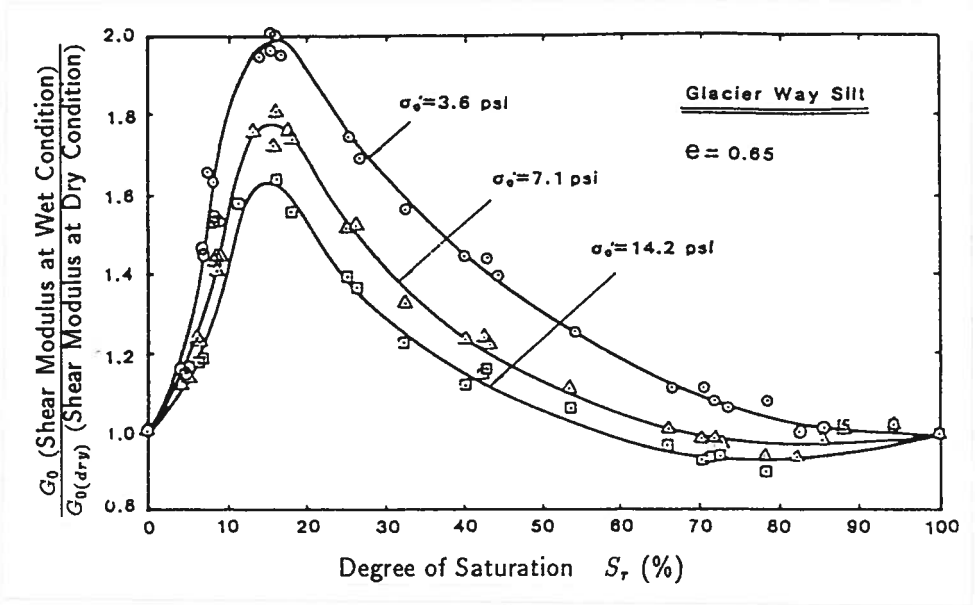

(a). $G_0/G_{0(dry)}$ vs. degree of saturation (after Wu *et al.*, 1984)

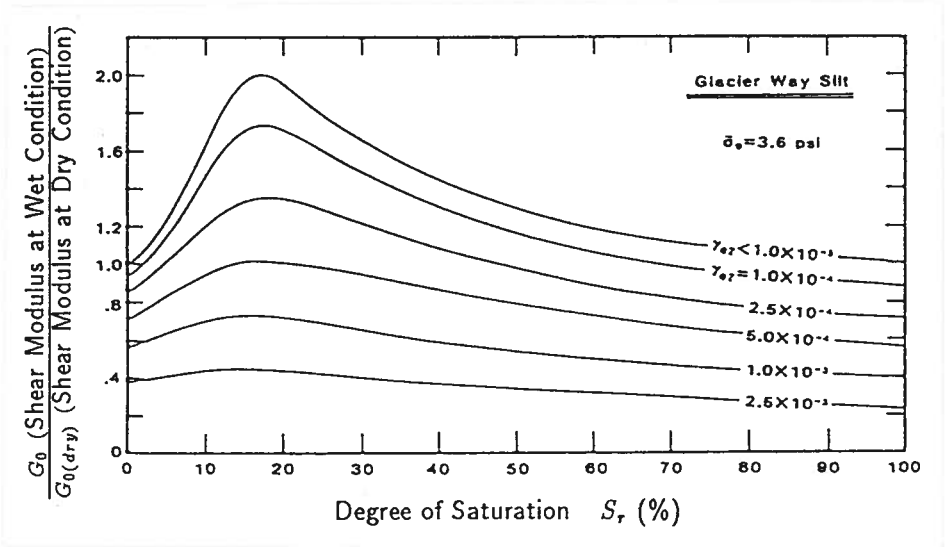

(b). $G/G_{0(dry)}$ vs. degree of saturation for different strain levels(after Wu *et al.*, 1985)

Figure 2.10: Change of shear modulus with degree of saturation

2.8 SUMMARY

Up to this date, the studies on collapsible soils have gone far from recognizing the problem. Not only experimental but also theoretical works have been done by individuals. However, scanning the state-of-the-art in the field, there are a lot of problems left. For example, a general criterion for identifying the susceptibility to collapse of soils has not been widely accepted though so many have been proposed. Some of the methods have limitations in application, *e.g.*, the method proposed by Jennings is unsuitable for soil which will swell at low pressure and will collapse at high pressure. The study on the mechanism of collapse of soil structure is still in a stage of explaining the observing data. Holtz and Hilf explained the phenomenon using Mohr-Coulomb theory and assumed that cohesion, the most important component of strength of unsaturated collapsible soil, is zero and the failure envelop is unity. However, this assumption is not in keeping with the experimental results that the shear strength decreases with increasing in water content. The two-effective stress theory and the grain contact equilibrium model can explain the collapse phenomenon quite well.

The studies on the strength properties lag behind the development in other aspects. A lot of the work are concentrated on the strength properties of soils having different moisture contents. Few works have been done to compare the properties before and after collapse. It is found that no work has been done to investigate the strength properties at different amount of collapse, *e.g.*, in the case of compacted soils, soil compacted dry of line of optimum collapses a lot, while it collapses little if it is compacted wet of line of optimum. The different behaviors under different collapse needs more detailed investigation. Moreover, little literature can be found which deals with the behavior of collapsible soils under seismic loading condition when subjected water permeation. It is noted that the liquefaction of saturated loessial soil is found to have occurred in reality. These works will be done in this study.

Chapter 3

REVIEW OF FAILURE CASES IN COLLAPSIBLE SOIL DEPOSITS OR EMBANKMENTS

3.1 INTRODUCTION

Many failures have been reported to occur in both natural collapsible soil deposits and compacted embankments because of the collapse of soil structures. The lists in Table 3.1 are those available from literature. In fact, almost every year, landslides occur during the rain season in the loess area, located in northwest China and there are also many failures which have occurred because of collapse of soils in USSR. Because of the availability of the literatures that deal with the failures occurred in these area, they are not listed in the lists. These failures usually were triggered by the increase in water content in soils followed by the collapse of soil structure. Some of them did not show large damages at the time of collapse. However, as the external loads was applied, especially earthquake load, catastrophic failure took place. In this chapter, three of the cases listed in Table 3.1 will be discussed in detail. Two of them (Sec. 3.3 and 3.4) are related with this study. The test materials employed in the experiments were sampled from these sites.

3.2 LANDSLIDES IN SOVIET TAJIK

Gissar village is located on a gently sloping hilly terrain about $30km$ southwest of Dushanbe, the capital city of the Tajikistan Republic of USSR. The terrain is covered by a mantle of loess which is deposited windblown from Karakumy desert west of Tajikistan and Kirgistan Republic during the Pleistoncine era. On January 23, 1989, a series of catastrophic landslides accompanied by a large scale mud flow took place in this area during an earthquake of magnitude 5.5. At least 270 villagers were estimated to have died or were missing in the debris and more than 100 houses were buried in 5 meters

Table 3.1 Case Histories of Failures Related to Collapse of Soils

Date	Location	Soil type	Type of failure	Damage	Reason	References
1907		Loess	Landslide		Karatag earthquake	Gubin, 1960
1907		Loess	Landslide		Chuyanchinsk earthquake	Gubin, 1960
1920	Kansu Province, China	Loess	Landslide	The loss of nearly two hundred thousand lives and the destruction of hundreds of towns and cities	Kansu earthquake	Close and McCormick, 1922
1941		Loess	Landslide		Garm earthquake	Gubin, 1960
1943		Loess	Landslide		Faizabad earthquake	Gubin, 1960
1949	Surchob and Yasman River valleys	Loess	Landslide		Chait earthquake	Gubin, 1960
1949	Rector Creek Dam, California, U.S.A.	Clayey-gravelly-sand	Settlement	Cracks in dam	Collapse of embankment materials	Leonard and Narain, 1963
1955	Transvaal, South Africa	Red silty sand	Settlement	Settlement of building	Unusually heavy rain induced collapse of soil	Jennings and Knight, 1957
1955	South Africa	Red silty sand	Settlement	Settlement of ore storage	Collapse of soil	Jennings and Knight, 1957
1956	Transvaal, South Africa	Silty sands and residual granites	Settlement	Settlement of road	Periods of rain triggered collapse	Knight, 1963
1956	Portland Dam, Colorado, U.S.A.	Silt and clay deposits	Settlement	Longitudinal crack and horizontal movement of crest in upstream direction	Collapse of upstream foundation material when it was first wetted	Leonards and Narain, 1963
1961	Luanda, Angola	Ferruginous clay Sand	Settlement	Settlement of airport runway and breakage in the drainge system	Heavy rain triggered collapse	Novais-Ferreira and Meireles, 1967

	Nebraska, U.S.A.	Loess	Settlement	Cracking and settlement of canal embankment	Collapse when was water introduced into the canal	Holtz and Hilf, 1961
	Washington, U.S.A.	Loose silty soil	Settlement	Failure of wasteway chute structures	Collapse when water was introduced into the system	Holtz and Hilf, 1961
	San Joaquin Valley, California, U.S.A.	silty alluvial soil	Settlement		Collapse in test pond which was induced by the leakage in irrigation canal	Holtz and Hilf, 1961; Bull, 1964
1964	the bank of the Danube, Hungary	Loess	Landslide	Damage of pump station, pipe lines etc.	Rise in ground water level triggered collapse	Kezdi, 1969
1968	Aomori Prefecture, Japan	Silty sand with clay fraction	Slide	Several slide failures of railway embankment	Collapse and earthquake	Yamada et al., 1968
1983	Shimane Prefecture, Japan	Weathered residual soil	Landslide	More than hundred lives lost	Heavy rain. total amount rainfall of 500 mm and the maximum intensity exceeded 145 mm/hr.	Nishida and Aoyama, 1987
	Southern California, U.S.A.	Compacted fill	Settlement	Cracks in the concrete slab-on-grade floors	Collapse	Lawton, 1986
	Arizona and New Mexico, U.S.A.	Compacted fill	Settlement	Waviness and roughness of the roadway surface	Nonuniform collapse	Houston, 1988
1987	Chonan Middle School, Japan	Silty sand with clay fraction	Slide	Failure of a portion of the road	Earthquake	Ishihara, et al., 1989
1989	Girrar, Soviet	Loess	Landslide	Landslides followed by mud flow; 270 villagers died, more than 100 houses buried	Collapse and earthquake	Ishihara, et al., 1990

of mud. The earthquake itself was nowhere astonishing. However, the new phenomenon that liquefaction can occur in collapsible soil will make it at an important position in the history of geotechnical engineering.

In total, there were four landslides which have occurred in that event. A plan view of the failures is shown in Fig. 3.1. The landslide at Sharara (Fig. 3.2) was about $800m$ in

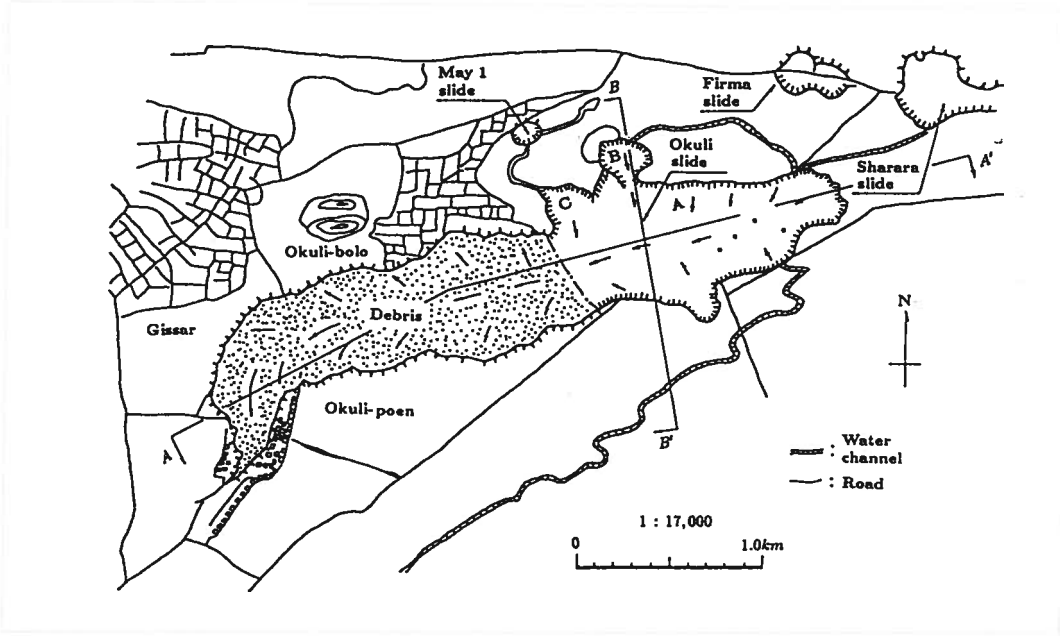

Figure 3.1: Plan view of the landslides in Gissar area (after Ishihara et al., 1990)

frontage and the debris spread out as far downward as $300m$ from the original toe of the fill. Many houses in the village immediately downhill were buried in the mud resulting in the largest number of casualties. On the top part of slide mass (used to be the hilltop), two water tanks used to be installed to supply water for domestic use and agricultural irrigation (Fig. 3.2). A pump station stands on the east side of slide just beyond the scarp. It was used to pump up water to the water tanks or directly to the water channel for irrigation. The bluff line produced by the slide was almost coincident with the line of the water channel. About $500m$ west of Sharara slide, Firma slide was located (Fig. 3.3). This slide was quite similar to the Sharara slide in conditions and features. It also had a small ditch which existed along the scarp line. It was noticed that a crack was found over the hill slopes extending about $50m$ rearward from the slide scarp. This indicated that a movement of a larger soil mass behind the slide occurred and this provides a possibility of another failure due to further wetting in the following years.

May 1 slide (Fig. 3.4) was the smallest among the slides. Because of the buttress

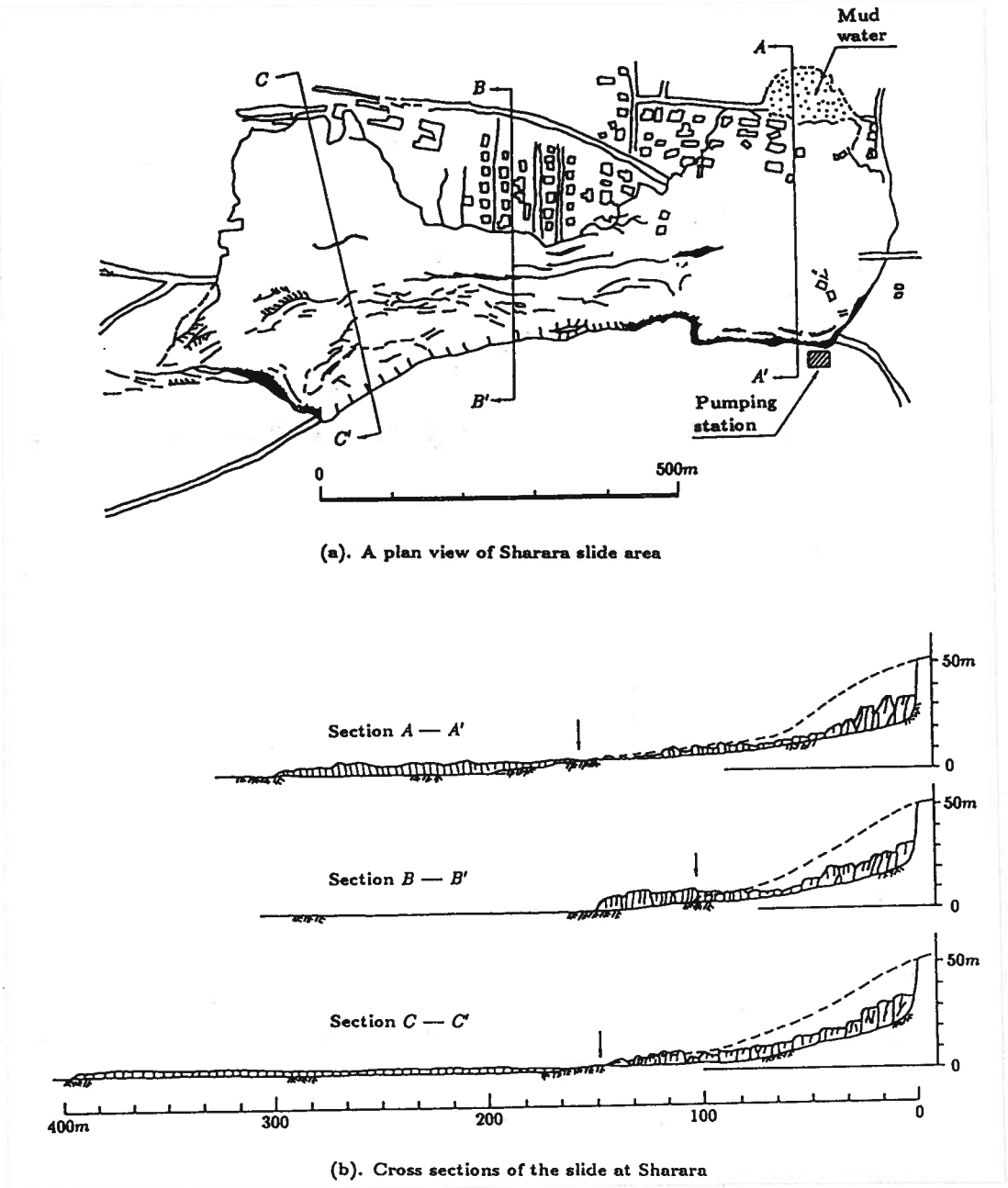

Figure 3.2: Sharara slide (after Ishihara et al., 1990)

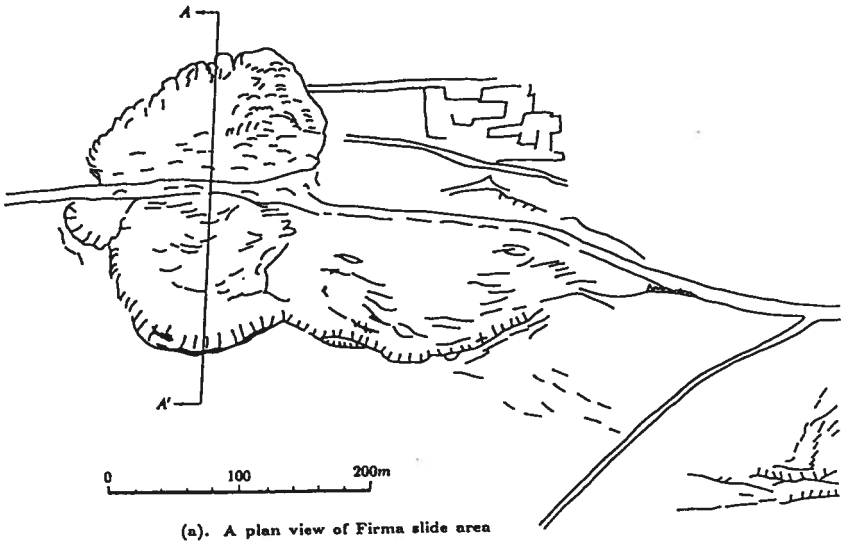

(a). A plan view of Firma slide area

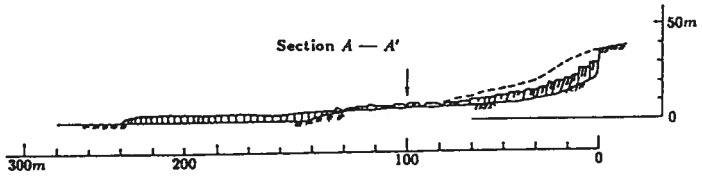

(b). Cross section of the slide at Firma

Figure 3.3: Firma slide (after Ishihara et al., 1990)

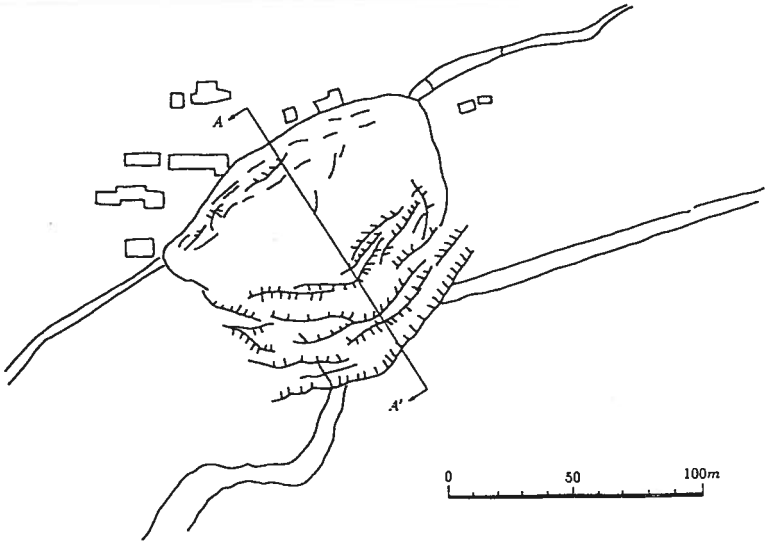

(a). A plan view of May 1 slide area

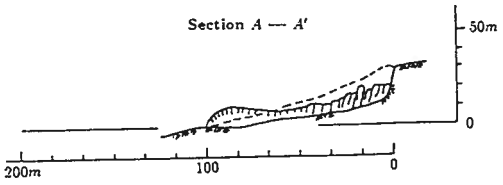

(b). Cross section of the slide at May 1

Figure 3.4: May 1 slide (after Ishihara et al., 1990)

action of the firm ground in front of the slide, the soil did not spread as in the Sharara and Firma slides but formed a pressure ridge about $7m$ high.

The largest and the most cataclysmic failure was the multiple slides at Okuli (Fig. 3.1) which was generated in a slightly depressed area over hilly farmlands. The sliding mass of the loess soil turned into a huge-scale debris flow and traveled through a distance of about $2km$ on nearly flat surface of the ground (Fig. 3.5). This phenomenon

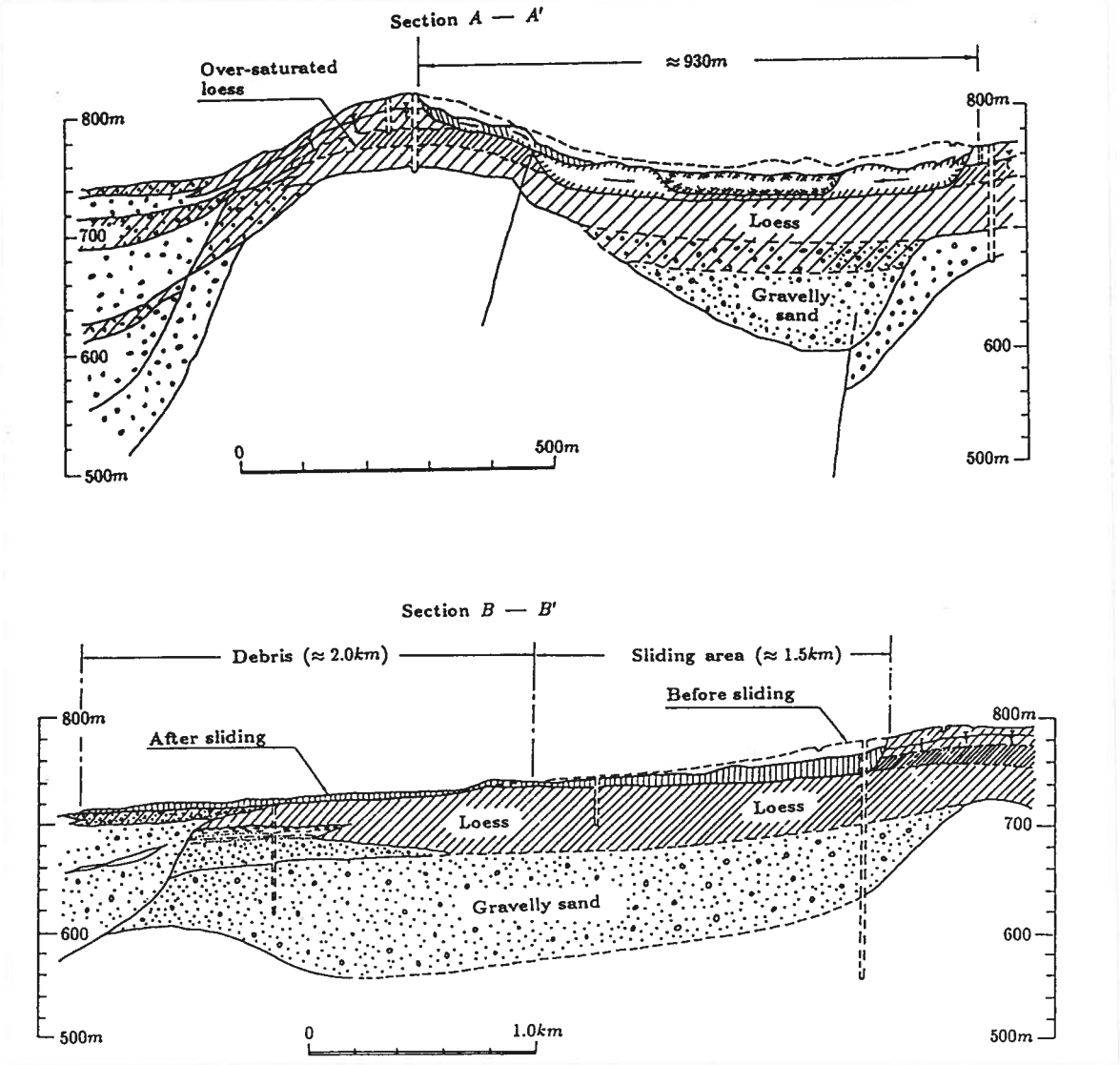

Figure 3.5: Cross sections of Okuli slide (after Ishihara et al., 1990)

suggested that the liquefaction in saturated loess soil took place during the earthquake. It was found that the ground water table was located about $5m$ beneath the ground surface, but the water content diminished around the depth of $20m$ followed by dry loess layers. It was also found that the water content in the layer below the ground water table

of about $3m$ in thickness was around 20%. However, the loess layer beneath this level possessed a high water content with maximum of which was 40% and this was larger than the liquid limit of the soil of 30%. In the other slides, muddy water was also observed spurting and oozing from broken pieces of the loessial soils indicating large quantity of water accumulating in the soils.

The landslides in Gissar were considered to be caused by liquefaction due to the earthquake after the loess deposit was wetted by water for years (Ishihara, et al. 1990). The initially uncultivated land in Gissar area was developed and used for agriculture with the recent development of the area and the increasing population in the urban area of Dushanbe. A network of water channels and ditches was constructed in the hilly area in Gissar for agricultural irrigation. Most of the sections of the channels were not lined with concrete. Water in the canals had been leaking and permeating into the ground through the vertical fissures in the loess deposit over the years and the large quantity of absorbed water had been filling up the pores in the loess. A noticeable amount of ground settlement was reportedly observed over the surface of the farmland. Because of the small slopes in the area, no further failures occurred. However, great loss in strength occurred in loess soils. With the earthquake load acting on the soil layers, excess pore water pressure built up in the over saturated loess layer and the soil layer liquefied followed by catastrophic landslides and mud flow.

3.3 FAILURES IN RAILWAY EMBANKMENTS IN AOMORI

About $120km$ south of Erimo strait ($40.7°N, 143.7°E$), Hokkaido, Japan, an earthquake of magnitude 7.8 took place on May 16, 1968. In this earthquake, there were 48 lives lost, 4 people missing and 329 wounded. The total losses were about 13,400 million yen.

One of the striking characteristics of this earthquake was the damage to railway embankments. Most of the damage were concentrated on two kinds of sites, one was soft and weak natural ground with organic soils on which the embankments were constructed, and the other was the border area between alluvial lowland and diluvial tableland where the earthfills were usually high. In this area, there were five main rivers and other small rivers pass though a diluvial tableland of 40 to $50m$ above sea level. In the glacial epoch, deep valleys were formed by the erosion of water to the diluvial tableland because of the sea level was about 60 to $100m$ lower at that time. Due to the rising of sea level, lakes and mashes were created. Soft ground was formed by the deposition of peat. The earthfill on

this kind of natural ground bore more damage. The typical damage are shown in Fig 3.6 and 3.7. In this type of damage, failure appeared as cracks which were as deep as $3m$ or more. They almost reached the bottom of the fill. Another distinguishing feature was that the cracks were almost parallel to the longitudinal line of the railway (Photo. 3.1). The thickness of the peat ground in this area was about 5 meters. It was considered that the cracks were caused by the failure of soft peat ground under earthquake shaking.

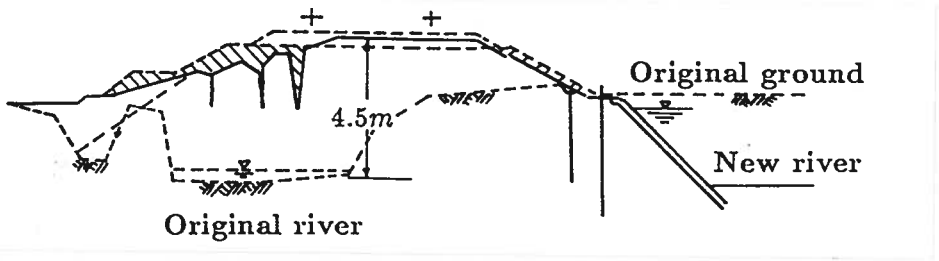

Figure 3.6: Cracking failure at station 683+680 between Ottomo and Ishibumi

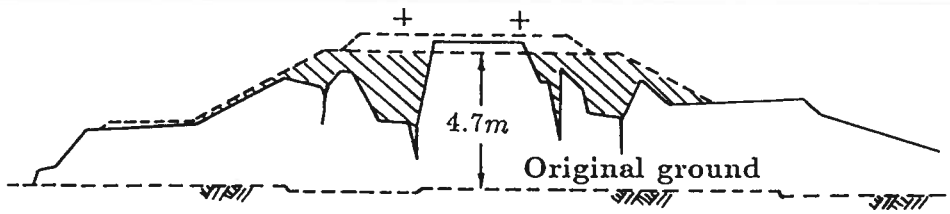

Figure 3.7: Cracking failure at station 684+160 between Ottomo and Ishibumi

In the border area between alluvial lowland and diluvial tableland, the earthfills were usually high. Mostly the damage were found to have occurred in these areas. Fig. 3.8 shows the failure which occurred in Mutsuichikawa between stations $648+250$ and $648+350$ in old earthfill. This was one of the typical types of failure due to this earthquake. A thin soil layer on a slope surface as a whole gushed from the surface like a liquid to the toe of the embankment (Photo. 3.2). The slide was about $80m$ in frontage and the debris spread out as far as $80m$ from the original toe of the fill. One farm house was half buried in debris. This failure looked similar to the one that occurred in a rock-fill dam under strong earthquake action, which was characterized by the triangular shaped shallow block sliding down to the toe area of dam. However, they were different. The filled material in this embankment was well graded silty sand with silt content of about 15% and 9% clay fraction. The material was almost saturated because of the unusually heavy rain before earthquake.

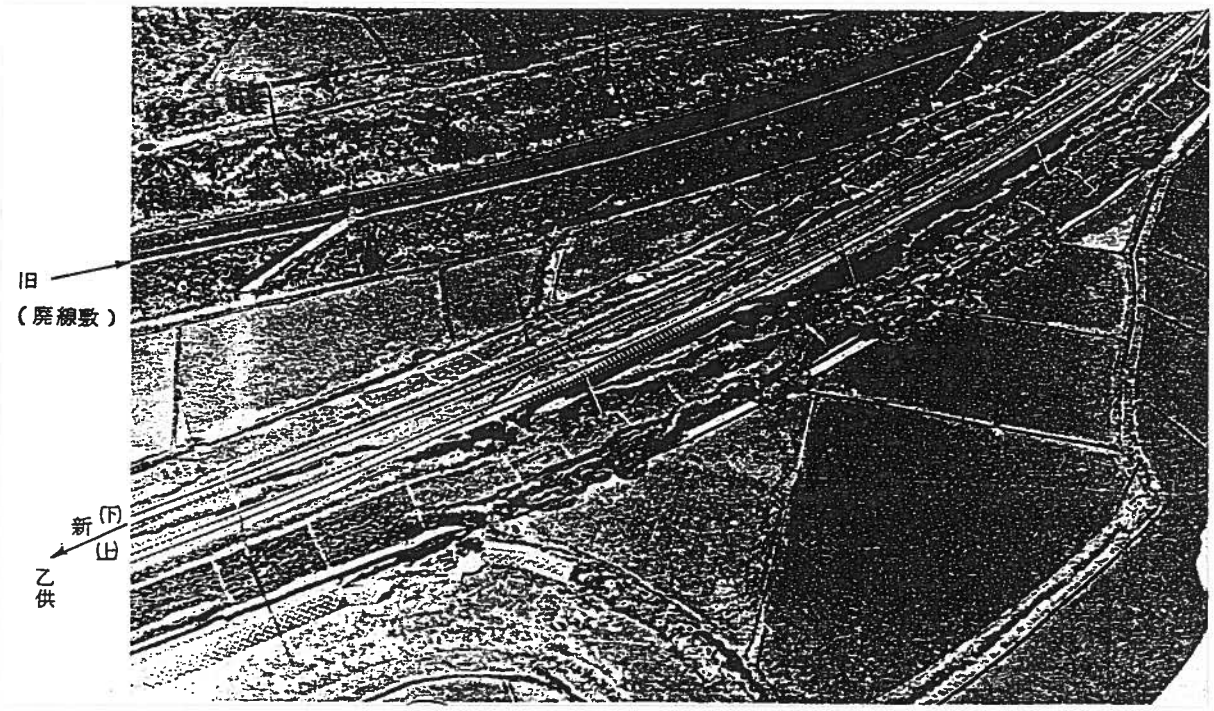

Photo. 3.1: Cracks in railway embankment at station 683 + 900 between Ottomo and Ishibumi

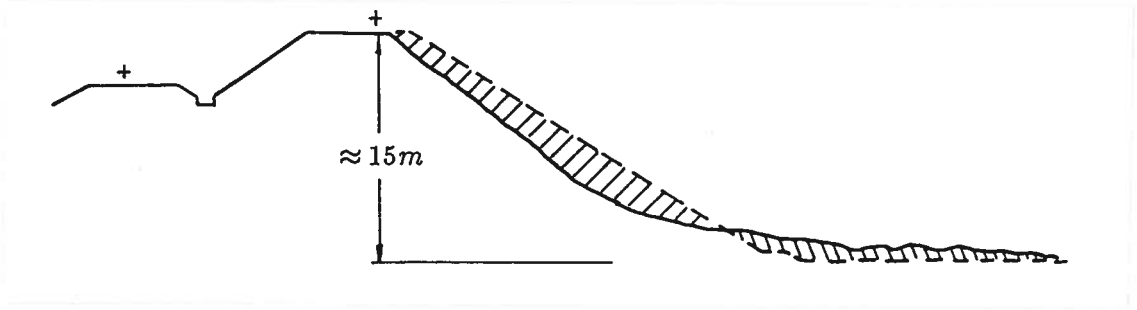

Figure 3.8: Slide flow between stations 648 + 250 and 648 + 350 between Shiriuchi and Mutsuichikawa

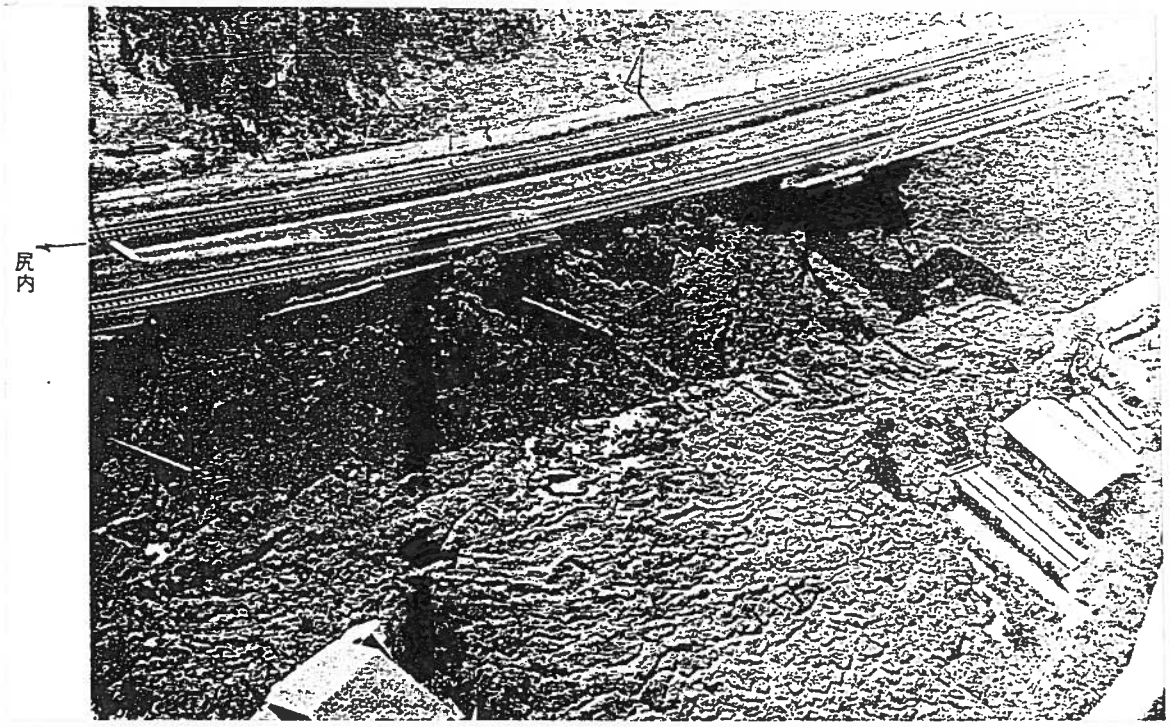

Photo. 3.2: Slide flow between stations 648 + 250 and 648 + 350 between Shiriuchi and Mutsuichikawa

Another type of failure was the conventional type of slide combined with the settlement in earthfill. These failures occurred in new embankment fills, as shown in Figs. 3.9 and 3.10. In Fig. 3.9, failure took place in the two sides of the railway and about $100m$

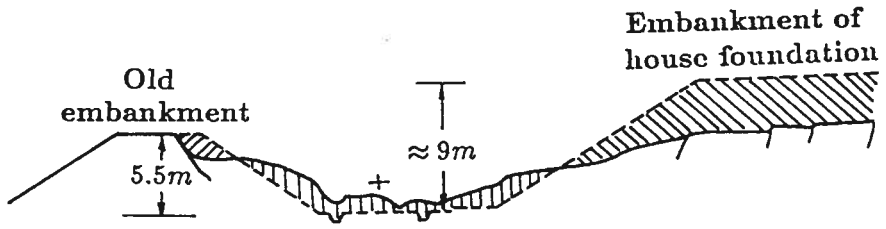

Figure 3.9: Slides and settlement at station 649 + 380 between Shiriuchi and Mutsuichikawa

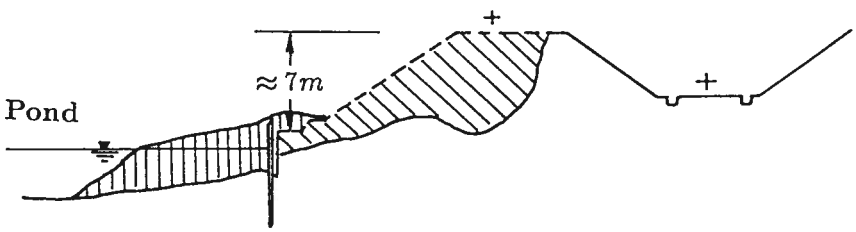

Figure 3.10: Slides and settlement at station 649 + 540 between Shiriuchi and Mutsuichikawa

portion of the railway line was buried. The fill on the left side was old and the one on right side was new. It can be seen that the scale of failure in the new fill was larger than that in old fill (Photo. 3.3). This case was not rare. It was found that the higher embankments were damaged more than the lower embankments and that new embankments were damaged more than the old embankments. One of the reasons cited was that the consolidation settlement in new embankments and the grounds had not finished yet.

Although the first type of damage was caused by the failure in soft peat ground, it seems that the second and third types of failure were related to the collapse and collapse-induced strength lose of compacted soils. In fact, there was an unusually heavy rain before the earthquake took place. The three day rainfall was as large as $165mm$. Especially from 6 to 10 o'clock in the morning of May 14, the amount of rainfall per hour was $25mm$ (see Fig. 3.11). Therefore, the soils were almost saturated at the time the earthquake took place on May 16. Another reason was that the soils were poorly compacted. Even at the time the author conducted sampling, the measured natural dry densities were $1.032g/cm^3$ at Mutsuichikawa at station 649 + 500 and $0.964g/cm^3$ in Ottomo at station 684 + 300. These natural dry densities were almost the same as the minimum dry densities of

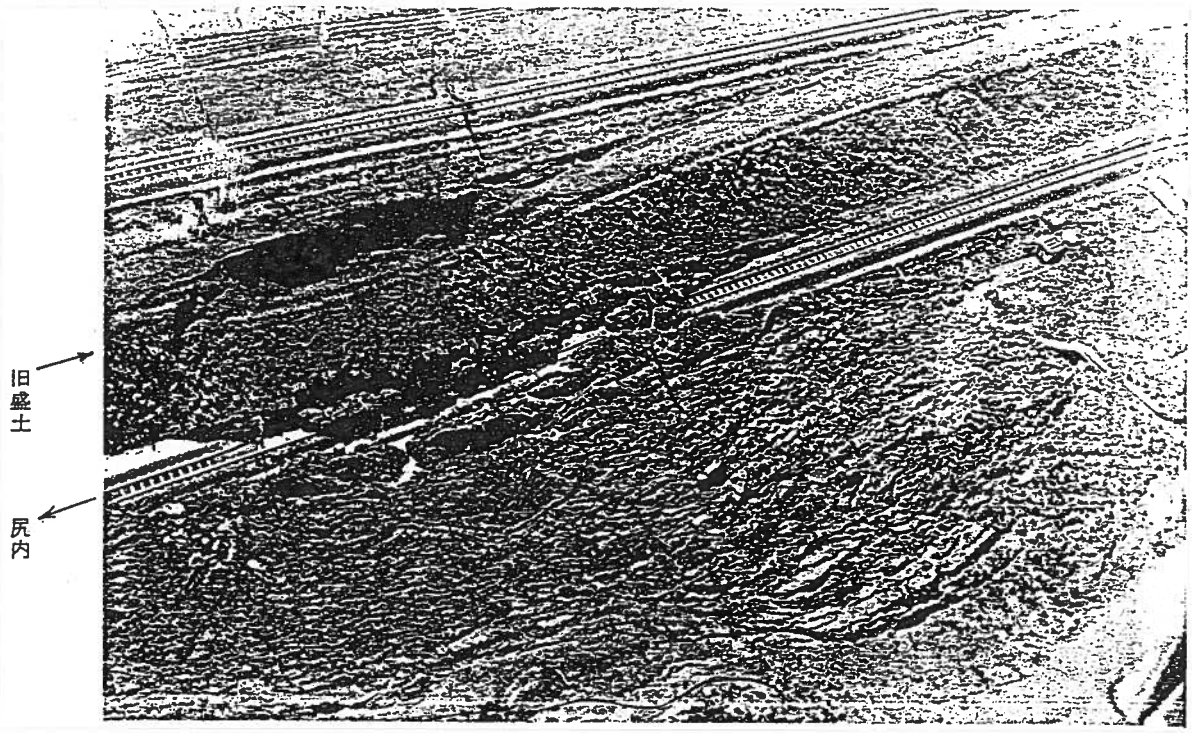

Photo. 3.3: Slides and settlement at station 649 + 380 between Shiriuchi and Mutsuichikawa

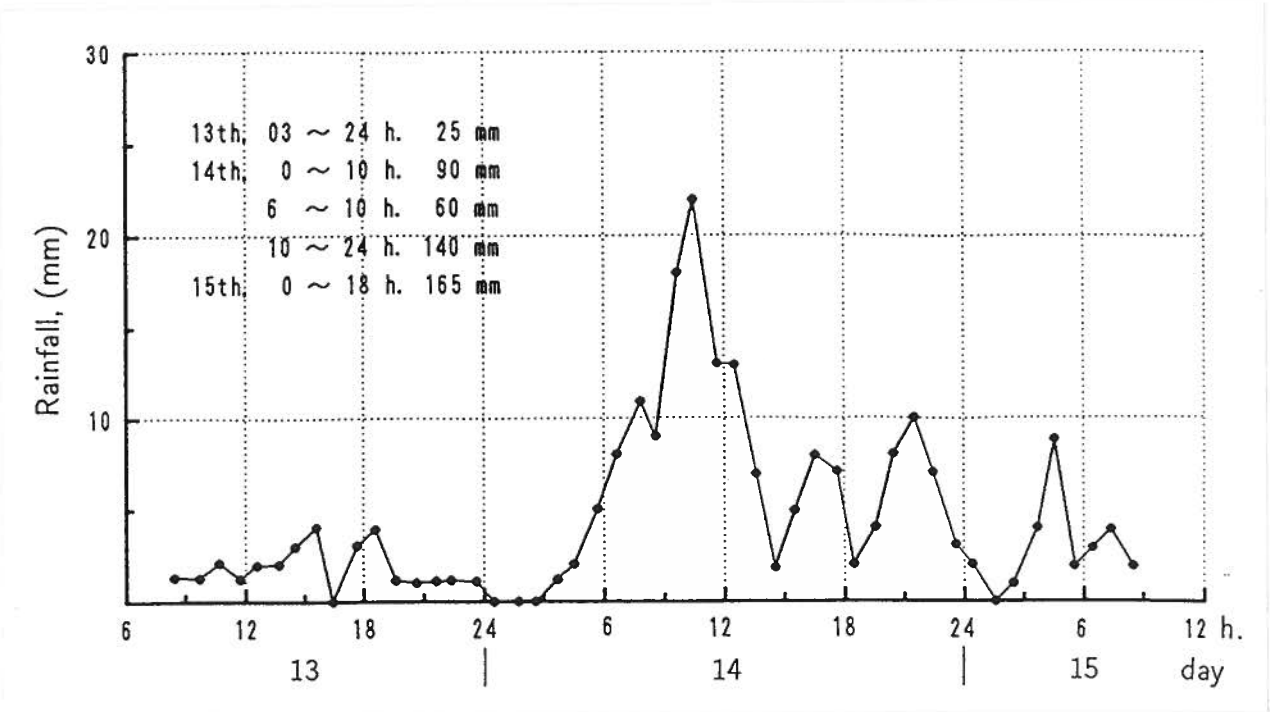

Figure 3.11: Rainfall before earthquake (Aomori)

$0.860 g/cm^3$ and $0.917 g/cm^3$ of the materials, respectively. Considering that the samples were obtained at about 50 cm beneath the slope surface, it can be concluded that the embankment fills were poorly compacted. The poorly compacted embankments had been in a barely stable state on the verge of hydraulic collapse before earthquake, and this led easily to a complete collapse in a form of liquefaction upon being further subjected to seismic shaking.

3.4 FAILURE IN CHIBA PREFECTURE

On October 17, 1987, an earthquake of magnitude 6.7 occurred in Toho-oki, Chiba Prefecture, Japan (Kiso-Jiban Consultants Co., Ltd., 1987). In this earthquake, a small scale slide took place in the sand fills near the edge of the playground of the Chonan middle school, as shown in Fig. 3.12. Fig. 3.12(a) is the plan view of the slide and the cross section of it is shown in Fig. 3.12(b). Swedish cone penetration tests were performed after the failure helped to identify the approximate location of the sliding surface across the fill, as shown in Fig. 3.12(b), which coincided with a loose silty layer a few meters below the ground surface. It was possible that before the earthquake, the fill had pre-collapsed with the rise of the ground water level induced by and the rainfall during the rainy seasons. Shear strength was lost as the collapse took place. As the earthquake shock the fill, it liquefied in saturated area resulting in the failure in both liquefied and non-liquefied soils.

3.5 SUMMARY

Several case histories of collapse-induced failures are reviewed in this chapter. Up to this date, more attentions have been paid to the failures of ground or structure foundations. However, the case histories reviewed here show that the collapse-induced sliding failures are more dangerous and may result in more loss of people's lives and properties. Although, sometimes these kinds of failure are not triggered only by collapse, collapse took important role in causing the failures. Some case histories show that collapse is the only factor which triggered the failure, for instance, the landslides which occurred in the bank of Danube, Hungary and in Shimane, Japan (Table 3.1). This means that more attentions should be paid to the properties of the collapse-induced strength loss not only under static loading condition but also under seismic loading condition.

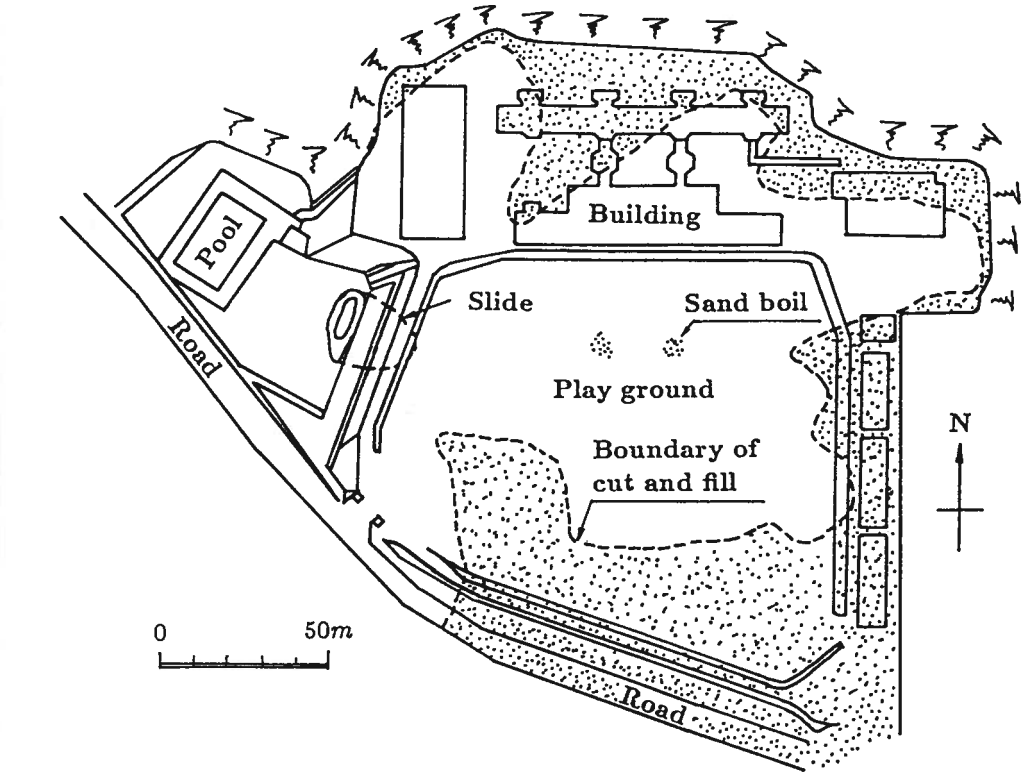

(a). Plane view of the slide at Chyounan site

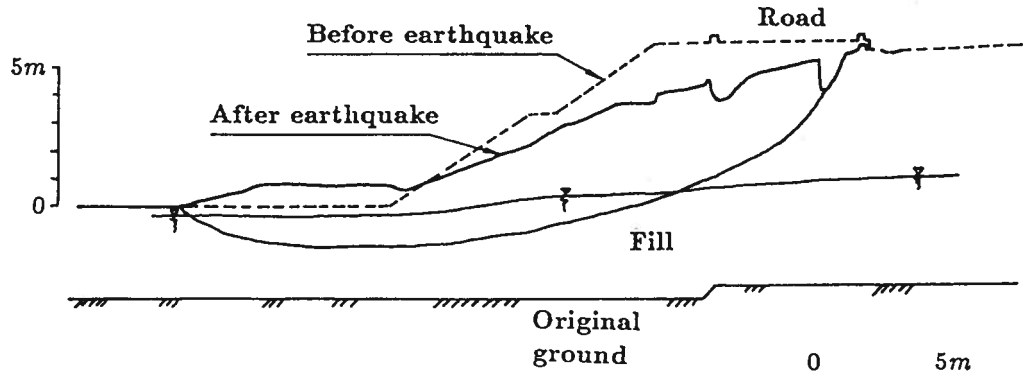

(b). Cross section

Figure 3.12: Slide at Chonan middle school (after Ishihara, Yasuda and Yoshida, 1990)

Chapter 4

TEST MATERIALS, APPARATUS, SCHEDULE AND EXPERIMENTAL PROCEDURES

4.1 INTRODUCTION

There are five materials used in the present study and they can be divided into two types: artificial and natural materials. The artificial material is a mixture of Toyoura standard sand and kaolinite. On the other hands, the four natural materials are sampled from four different sites where sliding failures have occurred during past earthquakes.

The tests presented in this study mainly consist of four kinds of experiments as well as mineral components analysis. The first series of tests are compaction tests having different compaction energies. Based on the results of the compaction tests, the second series of tests, wetting tests, are performed using conventional oedometer to investigate the parameters affecting collapse. Then, simple shear tests are done on the same materials to study the influence of collapse on shear strength and deformation properties of the materials. The simple shear tests are conducted on multi-directional simple shear test apparatus used by Ishihara and Yamazaki (1980) and Ishihara and Nagase (1988). Although the simple shear test apparatus is capable of applying cyclic loads independently in two directions, only one direction is used in the present study. Therefore, it is used as a conventional simple shear test. Following the simple shear tests, scanning electron microscope (*SEM*) tests are conducted to detect the difference in the micro-structure of the samples undergoing large and small wetting-induced collapse.

This chapter presents a discussion of the test materials, apparatus, schedule and the experimental procedures.

4.2 TEST MATERIALS

Two types of materials, artificial clayey sand and natural silty or clayey sands, are used in the present investigation.

4.2.1 Artificial Mixture of Sand and Clay

The artificial mixture of sand and clay (*TKSC*) is obtained by blending commercially available Toyoura sand, the Japanese standard sand, and kaolinite. The Japanese standard Toyoura sand is classified as a uniform fine sand consisting of mostly subrounded to subangular particles with mostly quartz composition. A series of compaction tests are performed to compare the possible collapse properties of the mixtures having different kaolinite contents. The compaction curves of the mixtures are given in Figure 4.1. Based

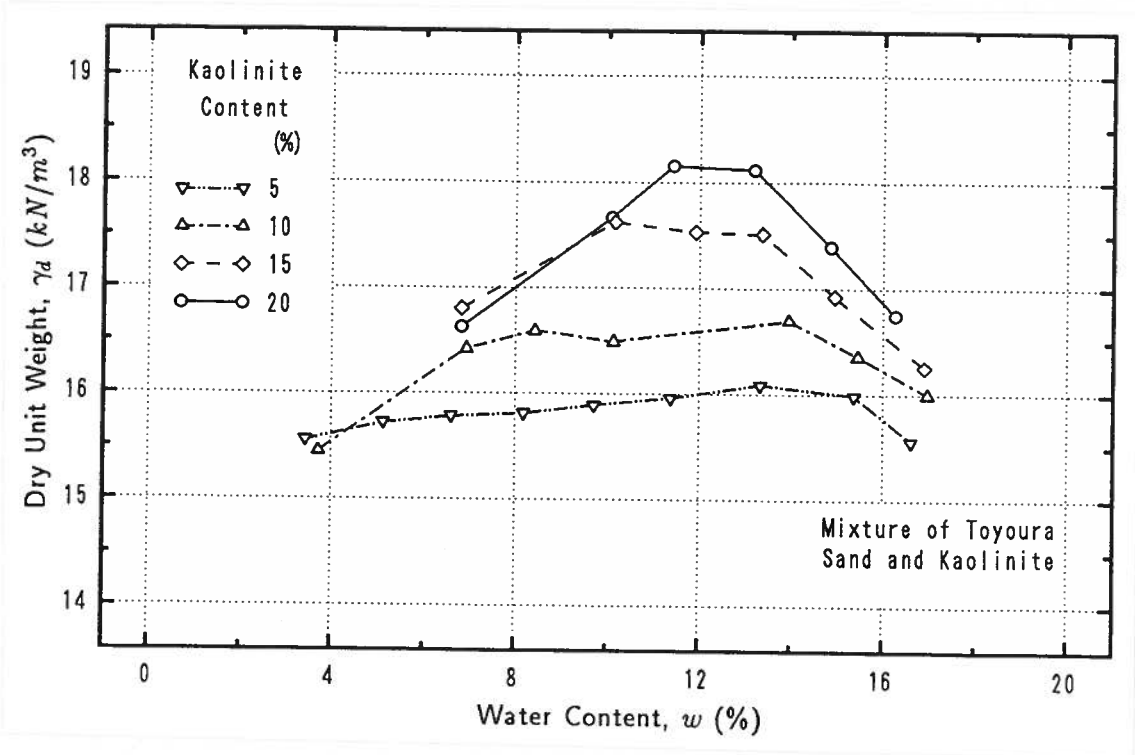

Figure 4.1: Compaction curves of mixtures

on the curves, it is decided that the mixture having a proportion of sand to kaolinite of 1 to 0.15 by weight is to be used in the investigation. The physical properties of the new material are given in Table 4.1 and its grain size distribution curve is illustrated in Fig. 4.2. It is classified as *SC* based on Unified Soil Classification System (USC)(Kézdi,

1974).

Table 4.1: Physical properties of artificial clayey sand

Specific Gravity, G_s	2.655
Mean Grain Size, D_{50} (mm)	0.181
Uniformity Coefficient, U_c	57.5
Silt Content, (%)	0.3
Clay Content, (%)	13.04
Liquid Limit, w_L (%)	18.40
Plastic Limit, w_P (%)	12.75
Classification	SC

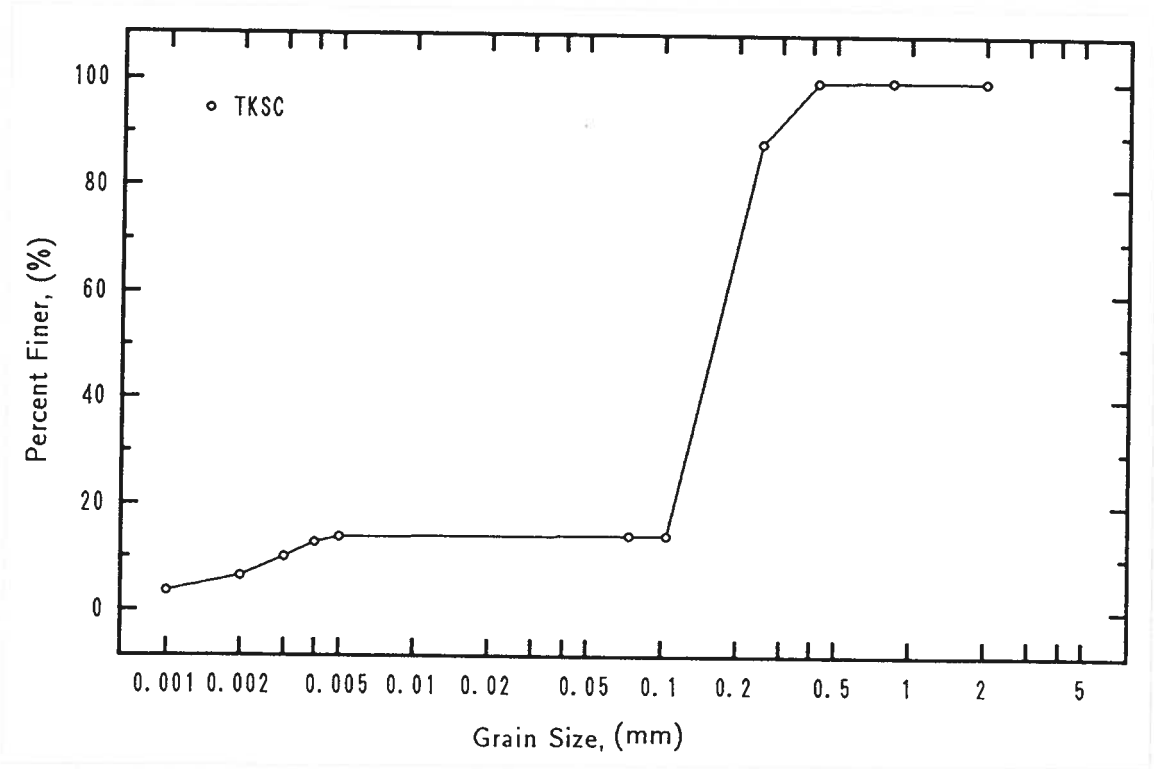

Figure 4.2: Grain size distribution curve of artificial clayey sand

Photo 4.1 shows the mixture of Toyoura sand and kaolinite in a ratio of sand to kaolinite of 1 to 0.15. Photo 4.1(a) is the mixture which is obtained by simply mixing sand and kaolinite together in dry condition. It can be seen clearly that under this condition, sand and kaolinite are separated from each other. However, in natural environment, the

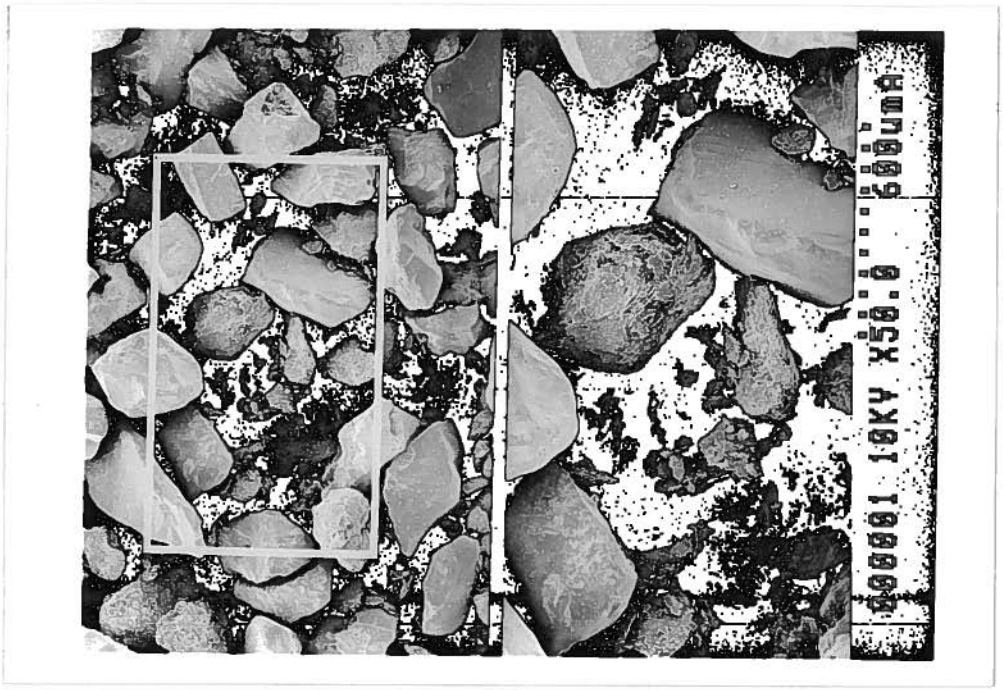

(a)

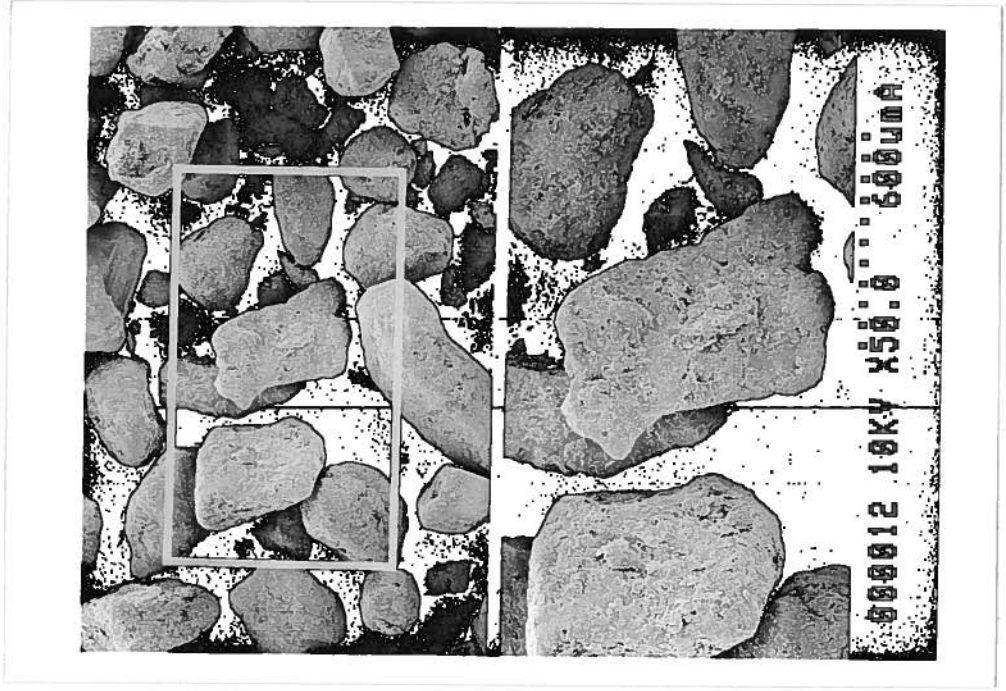

(b)

Photo. 4.1: SEM Micrograph of artificial clayey sand: (a) Blended in dry state; (b) Blended at 5% water content and dried

usual situation is that sand and/or silt particles are coated or bridged by clay. In order to make the blended clayey sand more similar to natural material, the sand and kaolinite are mixed at 5% water content and dried for 24 hours in thermostat at 120 °C. The mixture obtained by using this new method, as shown in Photo 4.1(b), is quite different from the mixture shown in (a). It is visible that all the sand particles are coated by kaolinite.

4.2.2 Silty and Clayey Sands Sampled from Manufactured Fills

In order to make sure that the results of artificial clayey sand can represent the general properties of collapsible soils, four natural silty and clayey sands are used in the present study. Two of them, which are referred to as Chonan A (*CASM*) and Chonan B (*CBSM*), are sampled from Chonan Middle School, Chiba prefecture, where a sliding failure has taken place due to an earthquake in 1987 (Ishihara, 1990). The other two materials, Ottomo sand (*OTSC*) and Mutsuichikawa sand (*MUSC*), are borrowed from railway embankments in Ottomo and Hachinohe-Mutsuichikawa, respectively, in Aomori prefecture, where a series of sliding failures of the railway embankments occurred in Tokachioki earthquake in 1968 (Yamata, et al., 1968).

The physical properties of these materials are given in Table 4.2 and their grain size distribution curves are illustrated in Fig. 4.3.

Table 4.2: Physical properties of natural silty and clayey sands

	CASM	CBSM	OTSC	MUSC
Specific Gravity, G_s	2.668	2.645	2.641	2.681
Mean Grain Size, D_{50} (mm)	0.111	0.110	0.105	0.182
Uniformity Coefficient, U_c	9.83	17.36	19.39	104.00
Silt Content, (%)	20.6	31.9	20.8	23.7
Clay Content, (%)	7.0	8.5	7.5	16.0
Liquid Limit, w_L (%)	30.75	25.55	33.00	40.8
Plastic Limit, w_P (%)	25.10	22.32	22.78	29.2
Classification	SM	SM	SC	SC

4.2.3 Mineralogy of Materials

It is well known that the mineralogy of materials, especially the clay component, affects the collapse properties to a certain extent (Dudley, 1970; Lobdell, 1981; and El-Sohby *et*

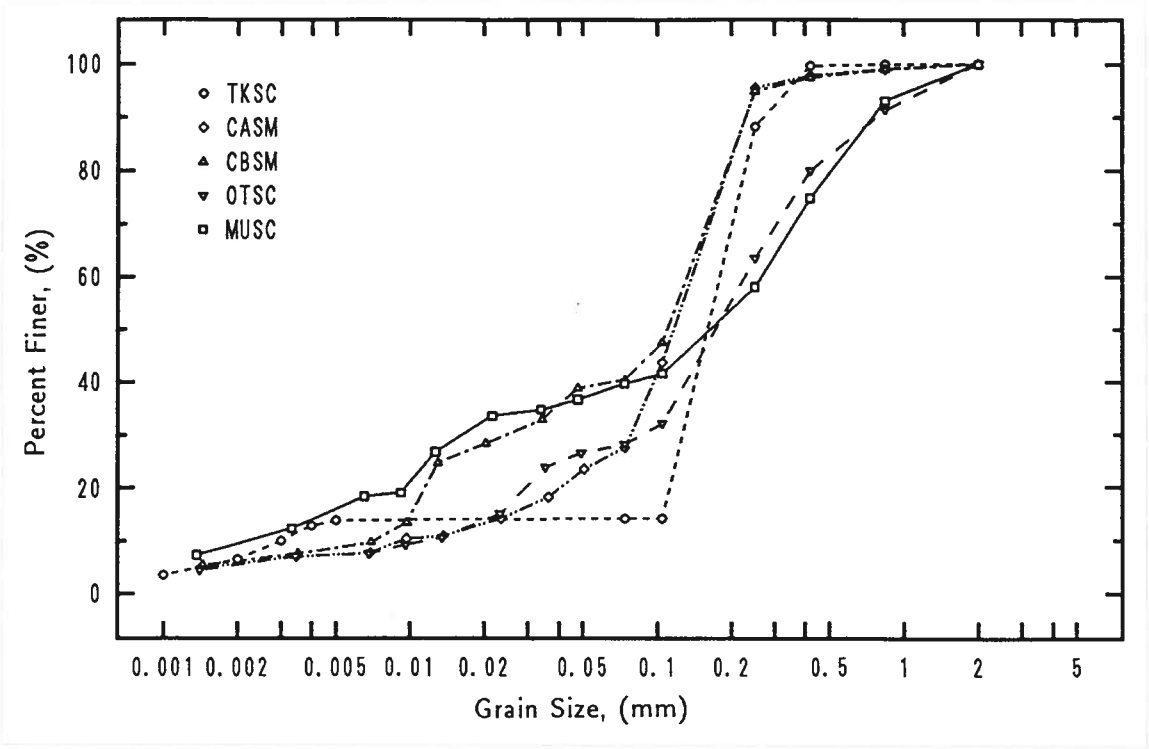

Figure 4.3: Grain size distribution curve of natural silty sands

al., 1987). In order to investigate this influence, mineral component analysis is performed using two methods: X-ray diffraction analysis and polarizing microscope analysis for the grain size smaller or larger than 74 μm, respectively. The polarizing microscope used is *OLYMPUS-POM* and the photograph is taken using *OLYMPUS PM-6* camera. Samples with grain size smaller than 74 μm are obtained got by washing the materials through No. 200 sieve. The results of the analysis are given in Table 4.3 and Appendix A. In the table, the order of minerals is arranged according the quantity of the mineral which is present in the soil. The results show that for those grain size larger than 74 μm, the main minerals are almost the same. The polarizing microscope demonstrates that *CASM* material is fresher than *CBSM* and the particle are also larger (this can be seen in Fig. 4.3). On the other hand, *CBSM* is more weathered. The particle size of *OTSC* are also relatively large (Fig. 4.3). The X-ray diffractograms of the four materials (the test is not applied on *TKSC* material because its clay component is kaolinite) are given in Fig. 4.4. *CASM* and *CBSM* have three clay minerals present, kaolinite, halloysite and montmorillonite, while *OTSC* and *MUSC* contain only kaolinite mineral. It seems that there is no big difference on the clay minerals in all the materials.

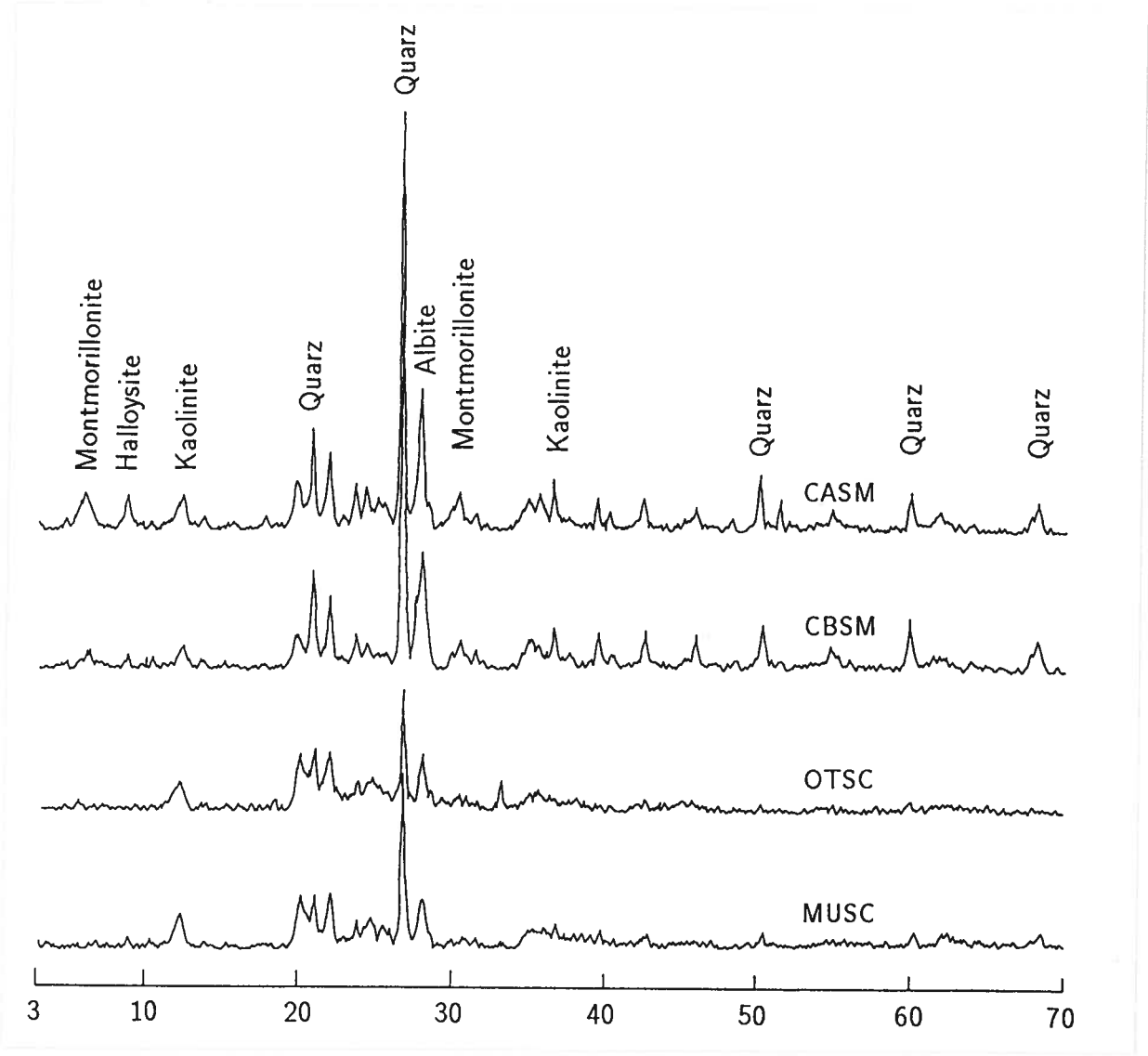

Figure 4.4: X-ray diffractograms of $< 74\mu m$ fraction of the materials

Table 4.3: Mineralogy of materials

Grain Size (μm)	Mineral Components				
	TKSC	CASM	CBSM	OTSC	MUSC
> 74	quartz, feldspar	quartz, feldspar, amphibole, magnetite, clay aggregate	quartz, feldspar, magnetite, hematite, chlorite, clay aggregate	quartz, feldspar, magnetite, hematite, pyroxene, clay aggregate	quartz, feldspar, magnetite, hematite, hydrated iron, zircon, pyroxene
< 74	kaolinite	quartz, montmorillonite, halloysite, kaolinite, albite	quartz, albite, kaolinite, halloysite, montmorillonite	quartz, kaolinite, albite	quartz, kaolinite, albite

4.2.4 Maximum and Minimum Void ratios and Relative Density

The in-situ denseness of non-cohesive soil usually is described in terms of by relative density, D_r, which is defined by the following equation:

$$D_r = \frac{e_{max} - e}{e_{max} - e_{min}} \tag{4.1}$$

where e, e_{max} and e_{min} are the in-situ void ratio, maximum void ratio and minimum void ratio, respectively. However, there is no clear definition of D_r for soils with silt and clay content. The standard relative density test is limited to soils with fine content less than 5% (JASM, 1979). In order to give a quantitative description of the denseness of the soils having fine content, different methods are used to measure the maximum and minimum void ratios in addition to standard methods.

The new method for e_{min} measurement is as follows: The test mold and procedures are the same as those used in the standard method. The difference is that the mold is full of water. Soils are poured into water in ten layers and after the material of each layer is poured into the water, the mold is tapped 100 times. Before the sand of the following layer is tipped into the mold, several minutes are allowed to pass to let the fines settle. Following the placement of the last layer, the sample is covered by filter paper and the extra water is taken off from the top of filter paper using tissue paper. Then the extension of the mold is taken off and the extra sand is removed. The sand is dried in thermostat

and the weight is measured after being dried for 24 hours.

e_{max} is measured by collapse method[1]. The materials are prepared to have a certain initial water content and sprinkled homogeneously in a lucite top open tank. During the process of sprinkling, the material in the tank is made as loose as possible. After all the materials are sprinkled in the tank, the surface is smoothened gently. Water is then introduced into tank from bottom to infiltrate the material and collapse is allowed to occur under the own weight of soil (without overburden pressure). The height of the sample is measured at the end of collapse and the dry weight of the sample is weighed after the test.

Test results of Toyoura Standard Sand showed that the measured e_{max} is larger than that obtained from the standard method and the value increases as the initial water content is increased from 0% to a certain value, beyond which the measured e_{max} is independent of the initial water content of the material. However, the results using other materials demonstrate the existence of an optimum water content in which the measured e_{max} is maximum. All the results, therefore, correspond to these optimum water contents.

The e_{max} and e_{min} measured using the different methods are given in Table 4.4[2]. It also contains the minimum void ratios obtained from standard Proctor compaction tests. Void ratios in Table 4.4 can be plotted as a function of the clay content in Fig. 4.5. It can

Table 4.4: Void Ratio Measured Using Different Methods

	Standard Method		New Method		Standard
	e_{max}	e_{min}	e_{max}	e_{min}	Proctor
TKSC	1.420	0.734	1.061	0.722	0.475
CASM	1.714	0.827	1.543	0.831	0.711
CBSM	1.648	0.996	1.456	0.846	0.570
OTSC	1.880	0.752	1.418	0.752	0.656
MUSC	2.117	1.288	2.029	1.145	0.830
Toyoura sand	0.99		1.17		
Sand B	0.96		1.20		

be seen that the maximum and minimum void ratios measured by the standard method is larger than that measured using the new method except in the case of Toyoura sand and Sand B wherein the clay contents are 0%. This means that the loosest state can be

[1]This method is proposed by Mr. R. Verdugo.

[2]The results of Toyoura sand and Sand B (a clean sand) are from Mr. R. Verdugo.

obtained by the standard method while the new method can result in the densest state.

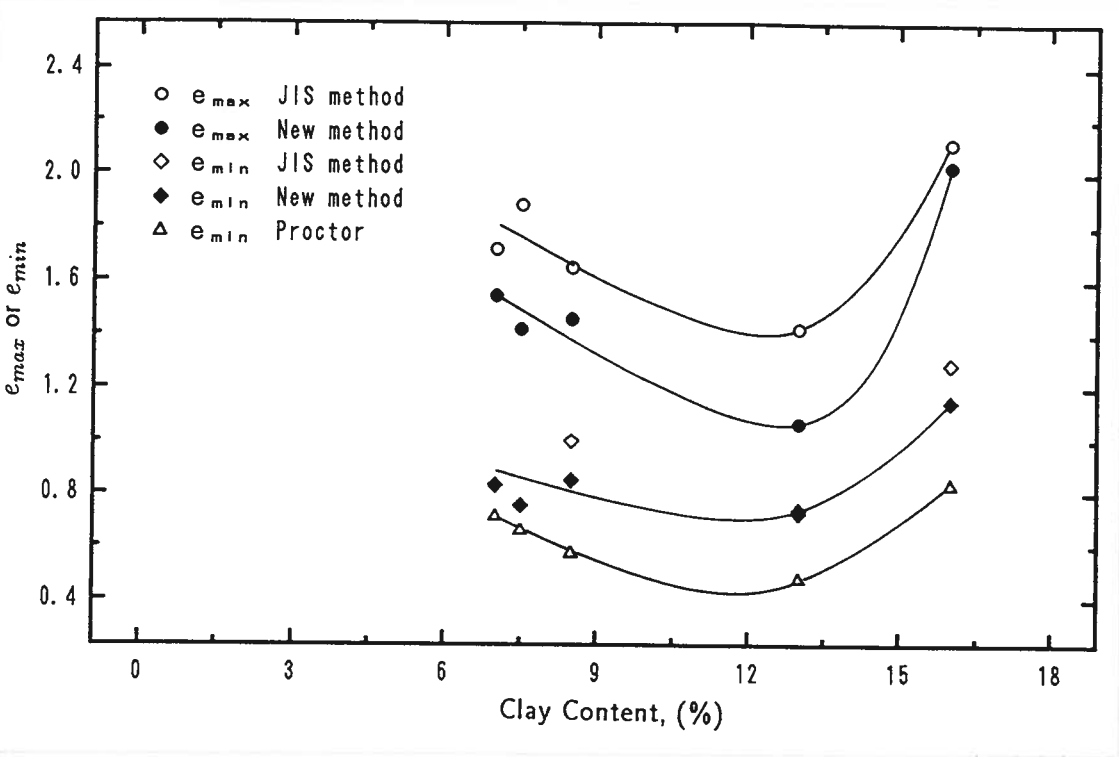

Figure 4.5: Void ratios for different method against clay content

It is noted that although the new method produces the smaller e_{min}, the values are still much higher than those obtained from *Standard Proctor compaction.* Similar results are also obtained by other researchers, as shown in Fig. 4.6. These results show that as the fine content increases, the maximum dry density for the standard method changes from larger to smaller than that obtained from *Standard Proctor Compaction* test for a material with fine content. For another material with clay content, this tendency starts from the very beginning. In fact, in the range of clay contents from 4.98% to 76.4%, the maximum dry densities from standard method are smaller than that from *Standard Proctor Compaction.* It is found that the relative densities of some samples are over 100% when the values of e_{min} measured using standard or new method are used in the calculation. This indicated that the densest state could not be obtained by either standard or new method. Therefore, the minimum void ratios from proctor compaction are used in the calculation.

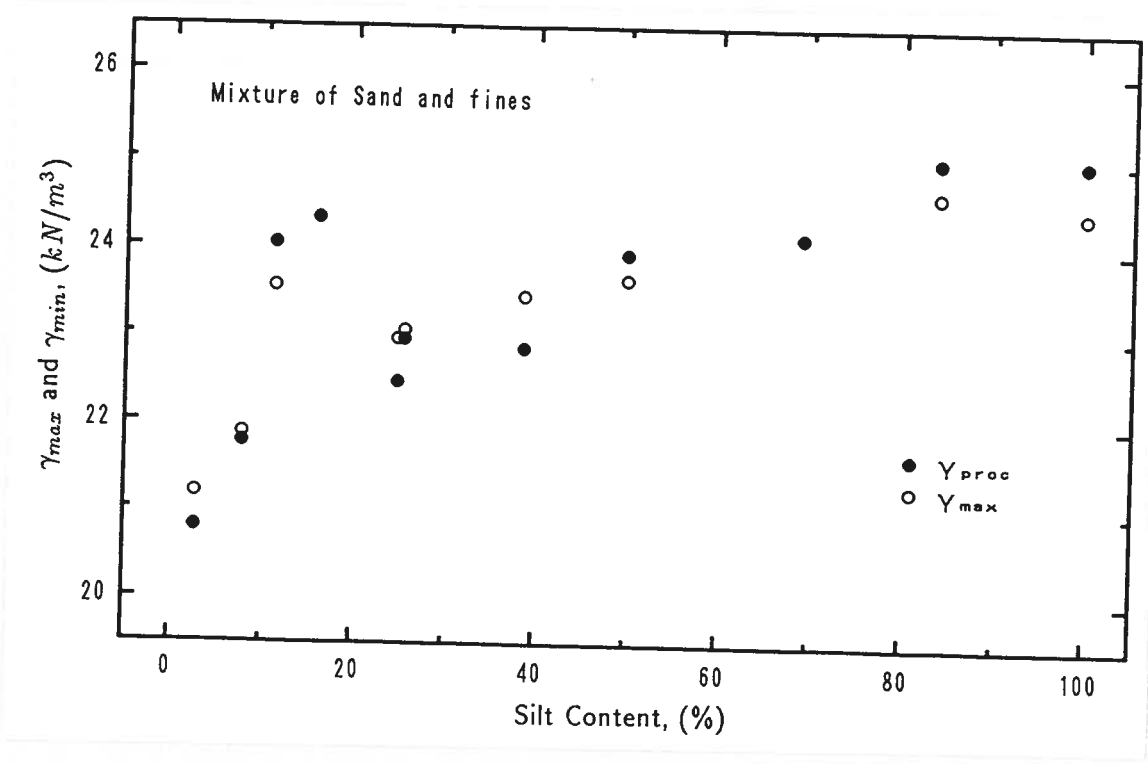

(a). Effect of silt content on maximum dry density

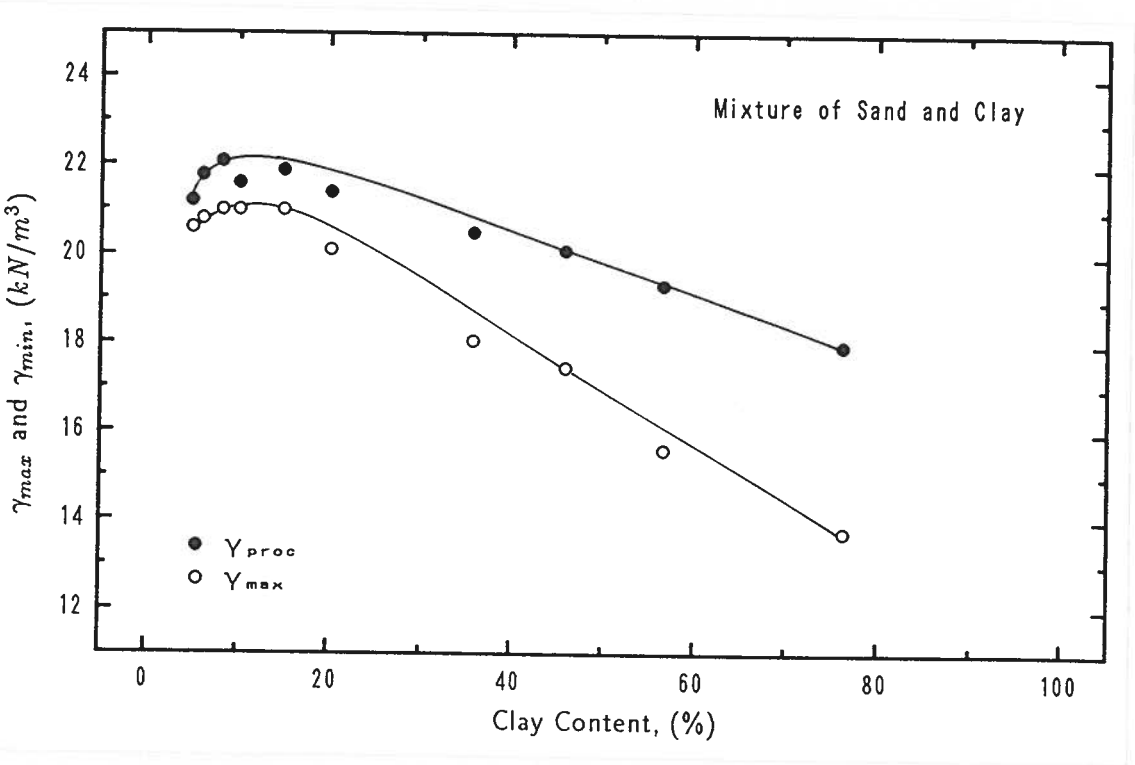

(b). Effect of clay content on maximum dry density

Figure 4.6: Effect of silt and clay content on maximum dry density(data from R. Verdugo)

4.3 TEST APPARATUS

In this section, three main test apparatuses: compaction test device, oedometer and simple shear test machine, are discussed. The mineral components analysis is performed by using X-ray diffraction for $< 74\mu m$ samples and polarizing microscope for $> 74\mu m$ samples. The scanning electron microscope used in this study is *HITACHI S-450 DX* at 10 kv. They will not be discussed in detail in this section.

4.3.1 Compaction Test Device

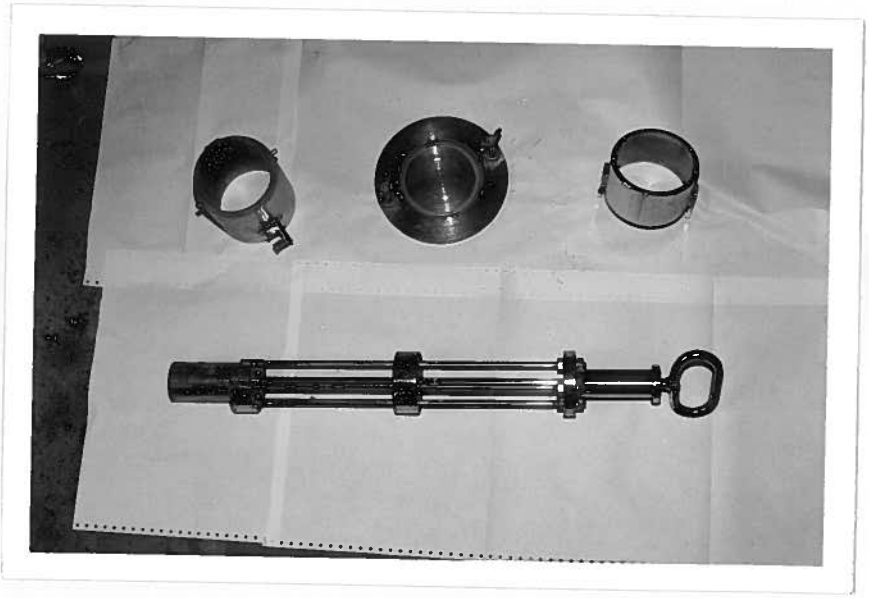

Photo. 4.2: Compaction device

The Compaction test device used in the present study is shown in Photo. 4.2, which has model capacity of 1000 cm^3 and rammer weight 2.5 kilogram. The standard Proctor compaction is obtained by dividing the soil into three layers, with each layer compacted 25 times with rammer dropping height 30 cm (Ishihara, 1989). Different compaction energies are obtained by changing the compaction times and the height of drop of the rammer.

4.3.2 Wetting Test Device

One dimensional loading-wetting tests are performed on conventional oedometer. The device is shown in Photo. 4.3 and Fig. 4.7. Photo. 4.4 is the loading system of the collapse test device. The specimens used in this series of tests are disk-shaped of 2 cm thickness and 6 cm in diameter.

Photo. 4.3: Oedometer

4.3.3 Simple Shear Test Apparatus

The same multi-directional simple shear apparatus as that employed in the previous studies (Ishihara and Yamazaki, 1980; Nagase and Ishihara, 1987) is used in the present study. This equipment is similar to NGI type simple shear apparatus but the reinforced rubber membrane which is used to prevent the lateral deformation of the specimen is replaced by a stack of teflon coated annular plate made of stainless steel. The axial stress is applied from the bottom of the specimen while the top is fixed in vertical direction but freely movable in the horizontal. Shear force is applied by load carriage which is capped to the specimen from the top of it. Although this apparatus is capable of applying shear loads in the two perpendicular directions independently, only one direction is used in the present study. Therefore, the tests in this research work are conventional simple shear tests. A schematic illustration of the apparatus is shown in Fig. 4.8.

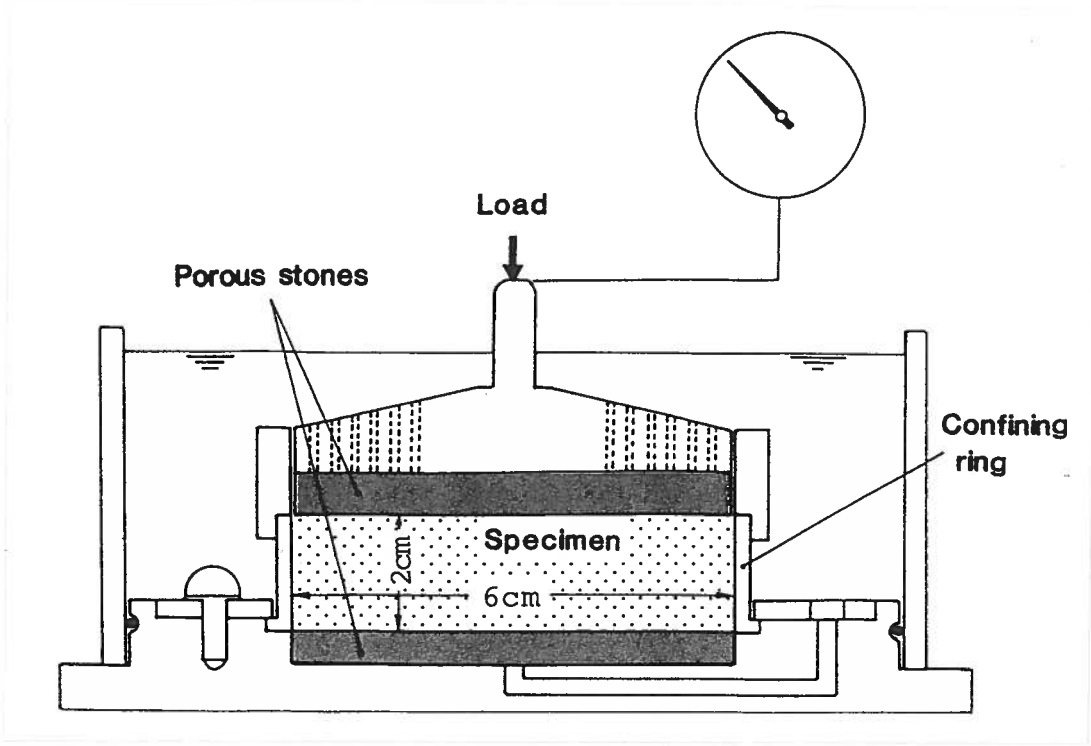

Figure 4.7: Oedometer

Photo. 4.4: Loading system of wetting test

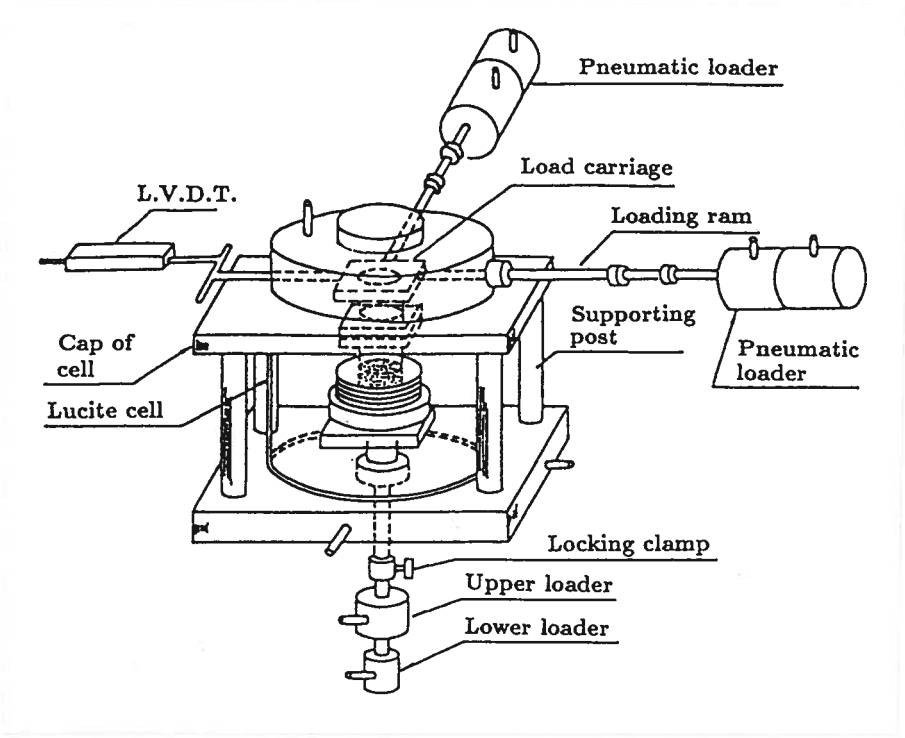

Figure 4.8: Schematic illustration of the two-directional simple shear apparatus

The simple description of the apparatus is given below. Yamazaki (1978) and Nagase (1981, 1984) gave a detailed description in their respective theses about the equipment.

(I). The main part of the apparatus

The general layout of the main part of the apparatus is demonstrated in Photo. 4.5 and Fig. 4.8. It consisted of three main components: two mutually perpendicular horizontal loading device, an assemblage for specimen placement, and an equipment for applying vertical load.

(1). Assemblage for specimen placement

The assemblage for specimen placement is shown in Fig. 4.9. The soil specimen is enclosed in a rubber membrane which is secured to the top cap and base by means of O-rings. The flank of the membrane-enclosed specimen is surrounded by a stack of annular plates to prevent lateral displacement during monotonic or cyclic simple shear test. These annular plates are made of stainless steel and coated with teflon. The outer diameter is 100 mm and the inner diameter is 71 mm with thickness of 1 mm. A total of

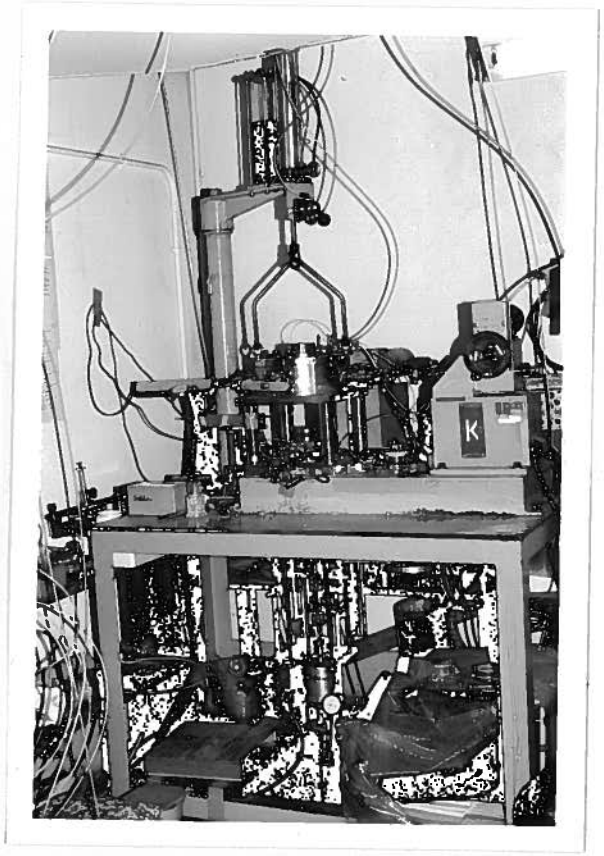

Photo. 4.5: General layout of the apparatus

37 plates are used. Photo. 4.6 shows the shape of the plates.

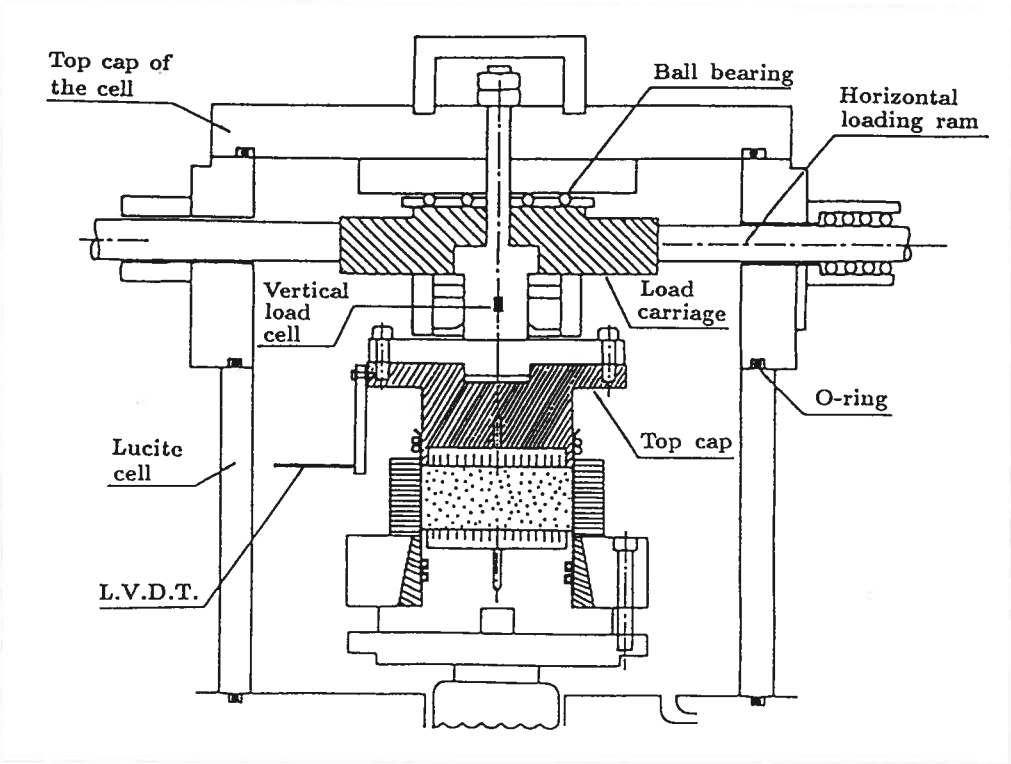

Figure 4.9: Setup of the simple shear test apparatus

The top cap and base of the specimen is shown in Photo. 4.7. They have a diameter of 70 mm. Porous stone disks of 66 mm in diameter are embedded in both of them. In order to prevent the sliding between the porous stone disk and the specimen surfaces and to make sure that friction is large enough to transfer the shear loads to the specimen, blades made of stainless steel are laid crosswise in the porous stone (see Photo. 4.7 and Fig. 4.10). Drainage lines are provided both through top cap and base plate of the specimen. One of the drainage line is connected to the pore water pressure transducer (Kyowa, PGM, $500kN/m^2$) installed at the pedestal of the test cell. An auxiliary device is provided to apply back pressure through the drainage line. The top cap is rigidly secured to the unit of the load carriage so that the horizontal load could be transferred with minimum rocking to the top surface of the specimen.

(2). Horizontal loading unit

Two identical loading rams are arranged to apply cyclic force on the specimen along the two mutually perpendicular horizontal directions. Each ram is capable of applying a maximum static load of $3500kN$ and a maximum cyclic load of $2200kN$. The load is

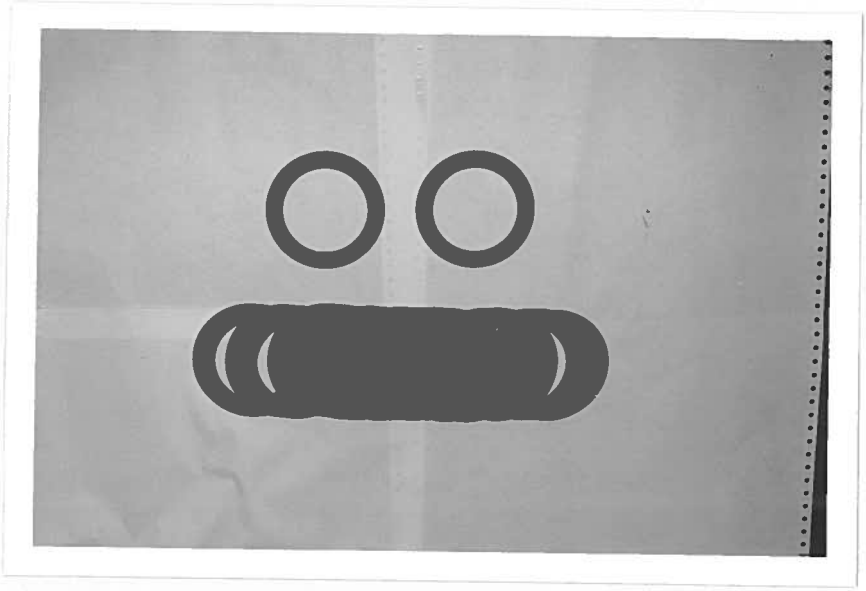

Photo. 4.6: Plates for preventing lateral deformation

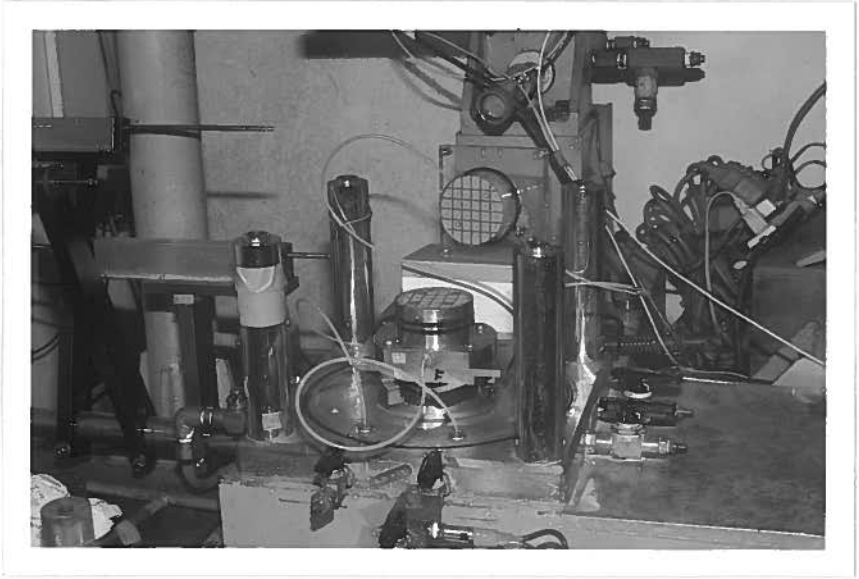

Photo. 4.7: The top cap and base of the specimen

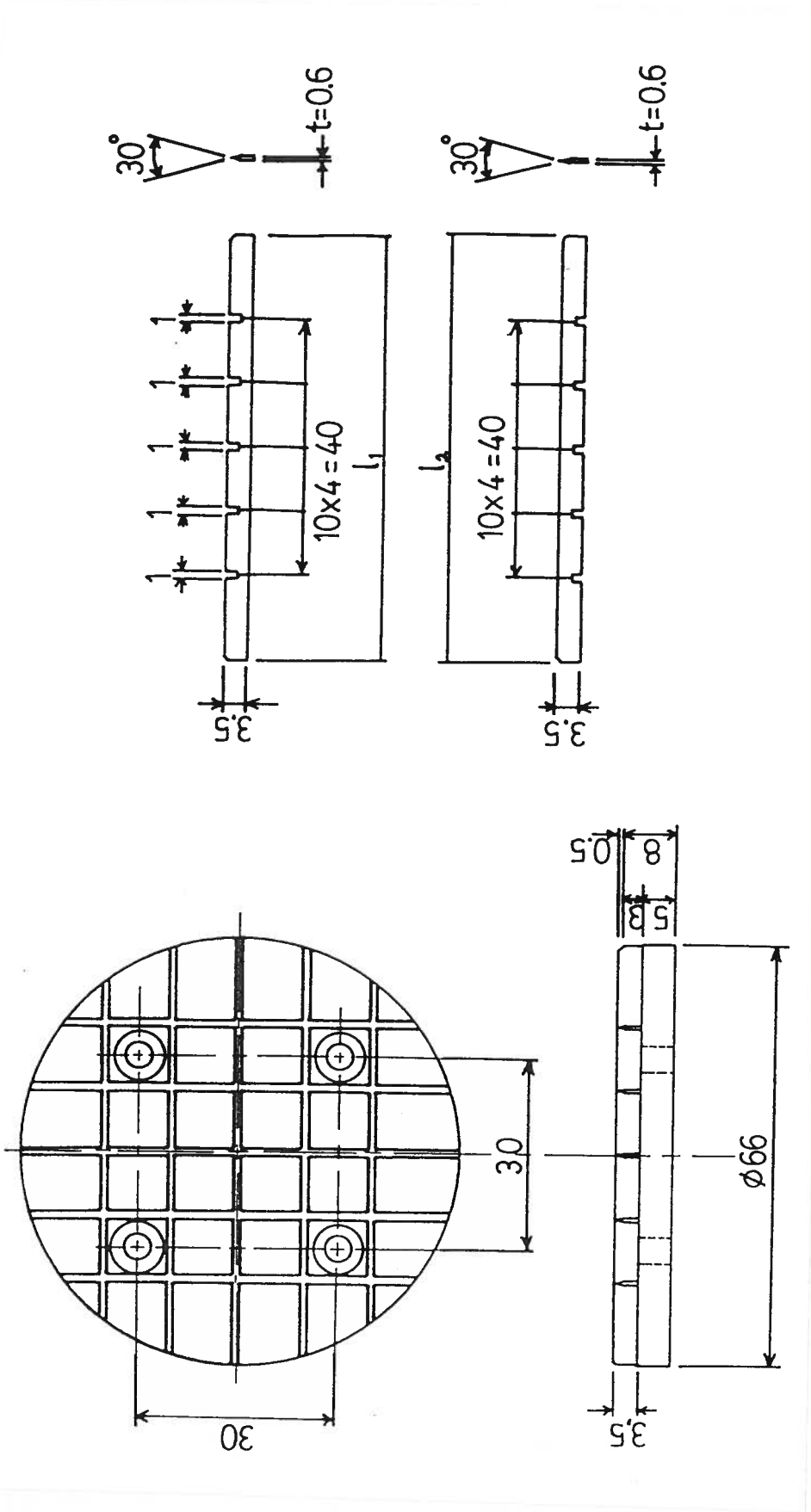

Figure 4.10: Steel blades inlaid in pore stone

transmitted to the specimen through a specially designed carriage fitted to the top of the cell. The schematic plan of the load carriage is shown in Fig. 4.11. The carriage is

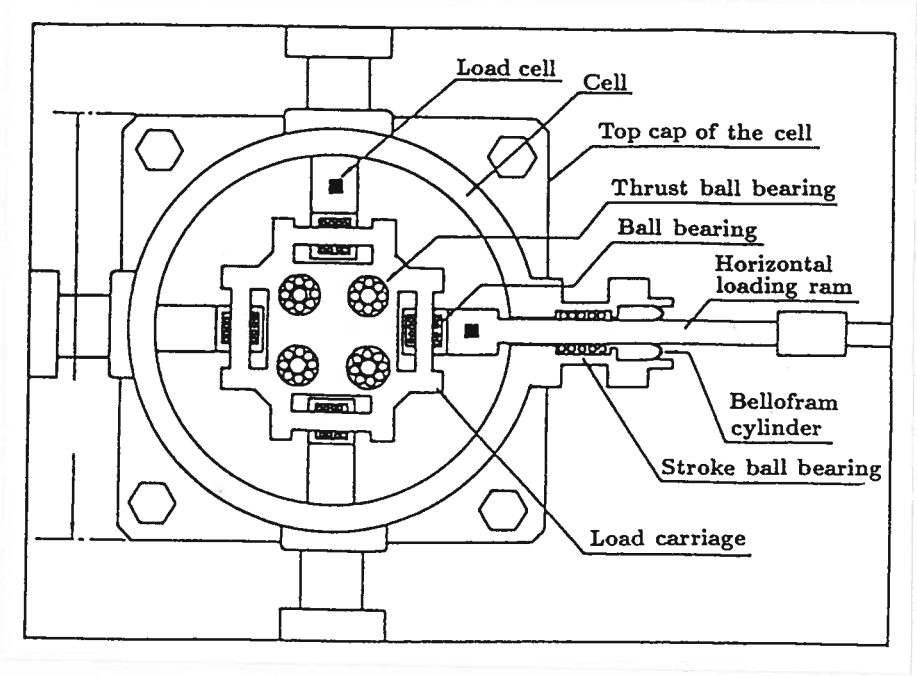

Figure 4.11: Load carriage

designed to apply load to the specimen only along the thrust axis of its activating jack while, at the same time, permitting free horizontal movement perpendicular to this axis. This is achieved by the arrangement of a ball bearing system as shown in Fig. 4.11. The motion of the load carriage is restricted to a movement in the horizontal plane by guide ball bearings. Thus, it is possible to obtain independent operation of loading in the two mutually perpendicular directions without generating undesirable interactions between the two horizontal loading devices during cyclic loading tests. Each of the loading ram is connected to a pneumatic loader through a load cell which monitor the intensity of load transmitted to the specimen. The load cells (U.S. Trans, INC, SG-type), which are placed inside the cell, have a maximum capacity of $2270kN$. Linear variable differential transformers (Shinko, SG-type) having a maximum stroke of $\pm 20mm$ are connected the horizontal rods on the opposite side of the loading ram as shown in Fig. 4.8 to monitor the horizontal displacement at the top of the specimen.

(3). Vertical loading unit

Two independently operating pneumatic rams are installed below the test cell to apply vertically upwards loads. The upper cylindrical ram, having a maximum capacity of $4910kN$, is installed to apply static vertical stress to the specimen during consolidation. It is also used to support the weight of the platform and any auxiliary device which might be placed on it. The lower ram (maximum capacity $2220kN$) shown in Fig. 4.8 is designed to provide a force to counterbalance the vertical pressure produced in the cell due to the application of the cell pressure. A mechanism to clamp the vertical loading rod in any position is provided just beneath the test cell. In order to monitor the vertical stress during test, a load cell (Seiken No. 123) with a maximum capacity of $3000kN$ is attached to the vertical shaft above the specimen cap inside the test cell.

(4). Appendages for sample preparation

(a). Tapered sleeve and annular plate supporter (Photo. 4.8)

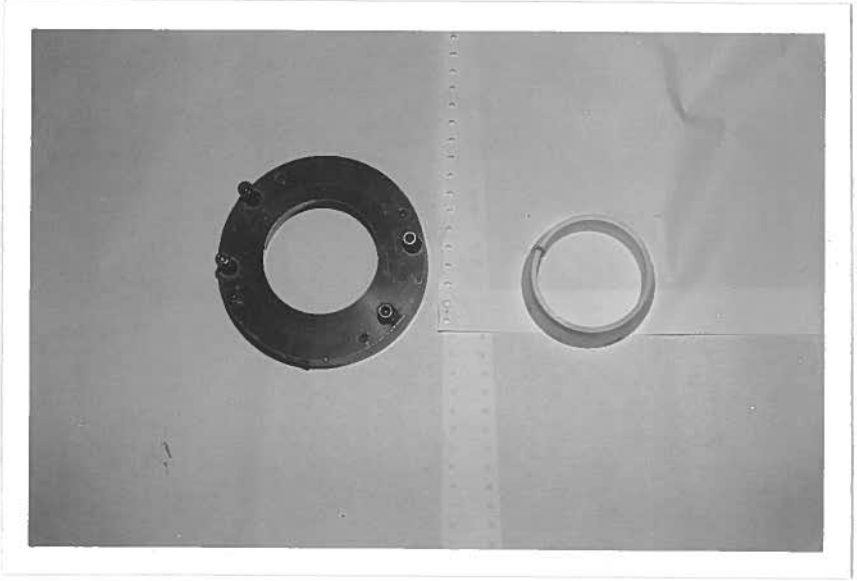

Photo. 4.8: Tapered sleeve and plates supporter

Tapered sleeve and annular plate supporter are used to secure the rubber membrane to the base plate and support the annuals plates. Although the sleeve is used to secure the membrane and at same time to prevent the leakage between the O-ring and the membrane, there are still some leakage. Moreover, because the O-ring is inlaid in the periphery of the base plate, there exists a chink between the base and the membrane after the mold is set up and the vacuum is applied. The material quite easily fills up this chink. Therefore, a narrow membrane tape is tied on the membrane at the part above

the O-ring.

(b). Mold for exerting suction (Photo. 4.9)

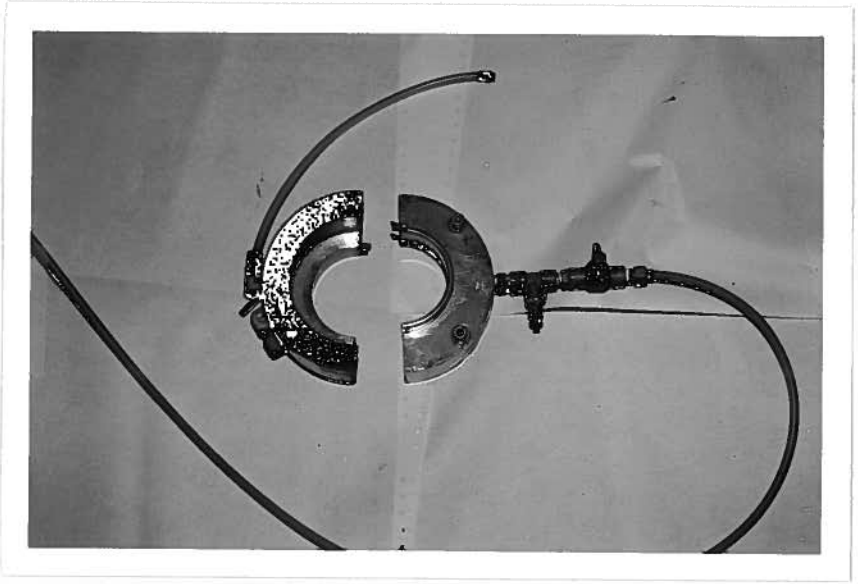

Photo. 4.9: Suction mold

A specially designed mold is used to hold the annular plates and apply suction to make the rubber membrane tight to the stack of annular plates.

(c). Specimen surface smoother and top cap holder (Photo. 4.10)

The smoother is designed to smooth on the surface of the specimen during sample preparation. The holder is used to support the sample top cap, allowing it to be lowered gently on the surface of the specimen. It also serves the function of guiding the top cap and making it in the right position for connecting with load carriage.

(II). Shear force loader

(1). Pneumatic cyclic loader

The pneumatic cyclic loader consisted of two main parts: pneumatic actuator (Photo. 4.11) and sine load generator (Photo. 4.12).

(a). Pneumatic actuator of horizontal load

As shown in Fig. 4.12, there are two pneumatic rams in the actuator which formed two air pressure cells, one is for static pressure, p_2, and the other is for dynamic air

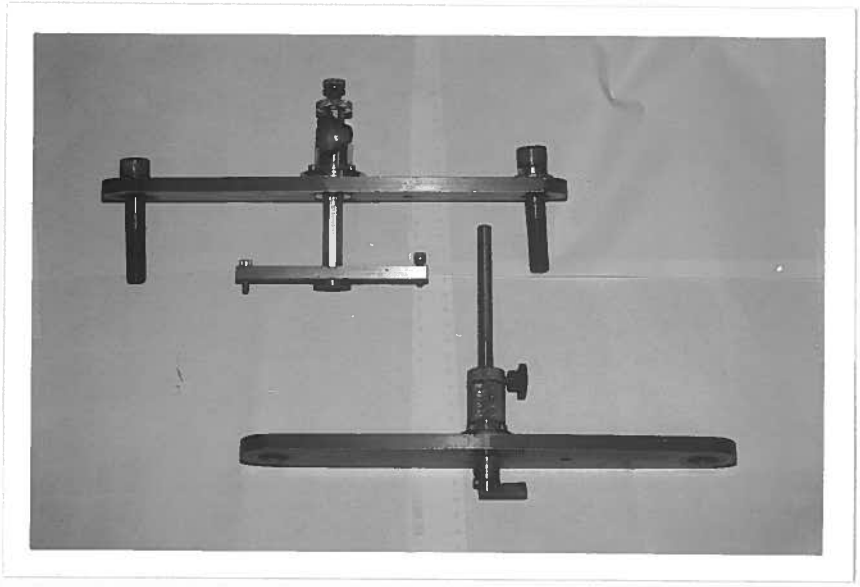

Photo. 4.10: Surface smoother and cap holder

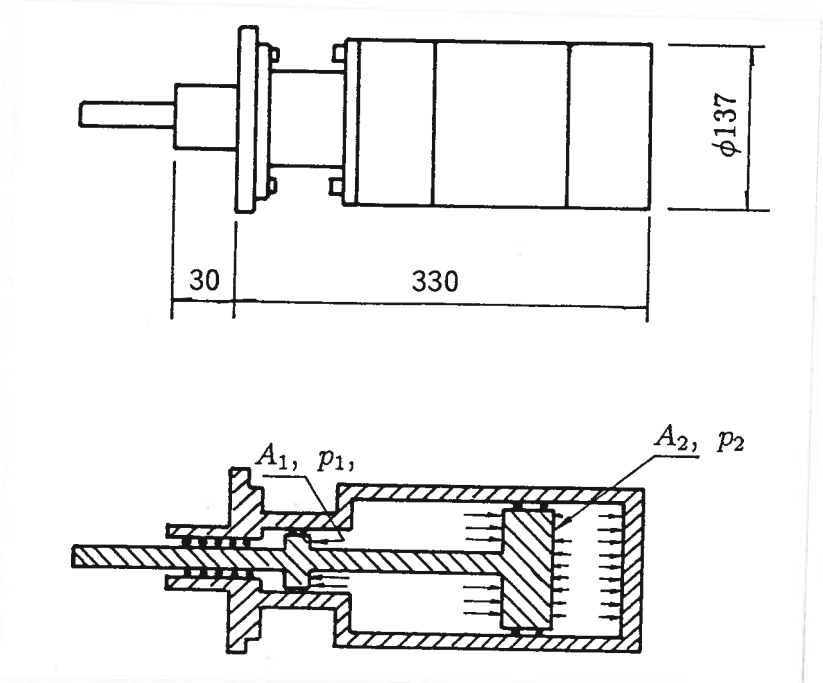

Figure 4.12: Pneumatic actuator

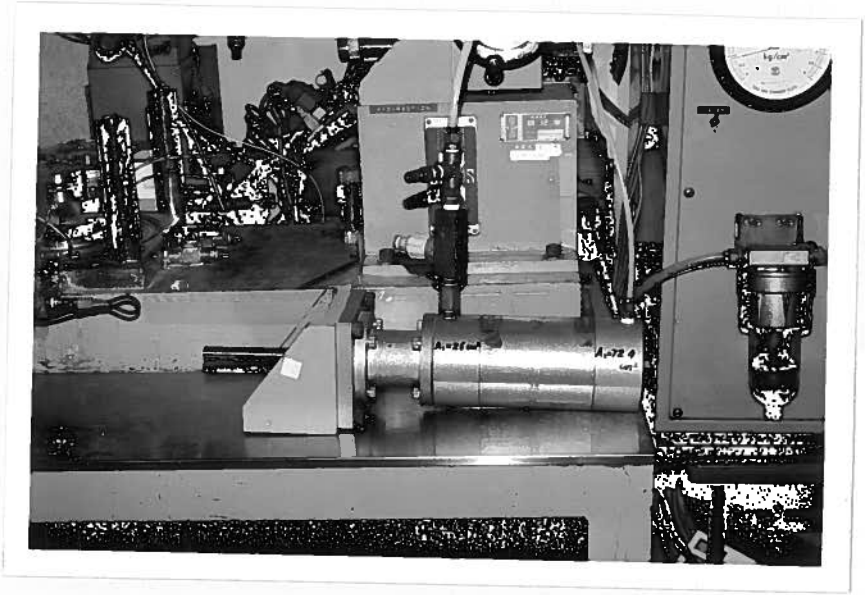

Photo. 4.11: Pneumatic actuator

Photo. 4.12: Sine load generator

pressure, $p_1 \pm \Delta p$. The cross section area of pistons are A_1 and A_2 for dynamic and static pressure cells, respectively. The effective piston area was $A' = A_2 - A_1$. Therefore, the load transmitted to rod, Q, was

$$\begin{aligned} Q &= (p_1 \pm \Delta p) \times A' - p_2 \times A_2 \\ &= \pm \Delta p \times A' + (p_1 \times A' - p_2 \times A_2) \end{aligned} \tag{4.2}$$

The air pressure in static cell is adjusted to $p_1 \times A' = p_2 \times A_2$ before applying dynamic load. Therefore, the load during cyclic loading is

$$Q = \pm \Delta p \times A' \tag{4.3}$$

(b). Pneumatic sine load generator

Photo. 4.12 shows the layout of the generator while the schematic diagram of the pipe lines is illustrated in Fig. 4.13. The static pressure is adjusted through a pressure adjuster. The static part of the dynamic pressure is set by Dc Offset. The magnitude of dynamic pressure, Δp, is adjusted by Amplitude.

(2). Strain controlled monotonic loader

The simple shear test apparatus is original designed to perform cyclic tests. In order to be able to run monotonic tests on the apparatus, the pneumatic loader is replaced by a specially designed strain controlled monotonic loader. Shear load is applied either manually or automatically. Ten speeds ranging from $0.06mm/min$ to $1.22mm/min$ can be freely selected in automatic loading. The investigation of the strength properties of soils shows that the strength of a sand is virtually uninfluenced by the rate of strain, especially when the rate of strain is between 0.1 to 10 *percent/min* (Mogami, 1969). On the other hand, the strength of a clay depends to an appreciable extent on this factor (Skempton and Bishop, 1950). By considering the fact that the soils used in this study are non-clay soils, and other factors, a speed of $0.70mm/min$ is used in the present study. The rate of strain was about 2.3~2.6 *percent/min.* The strain controlled monotonic loader is demonstrated in Photo. 4.13.

(III) Control plate

Photo. 4.14 shows the control plate. All the applied pressures except the shear load are controlled by it. Fig. 4.14 is the layout of the pipe lines and controlling system.

(IV) Measuring equipment

The test data are measured by a *transducer–amplifier–recorder* system. Data are

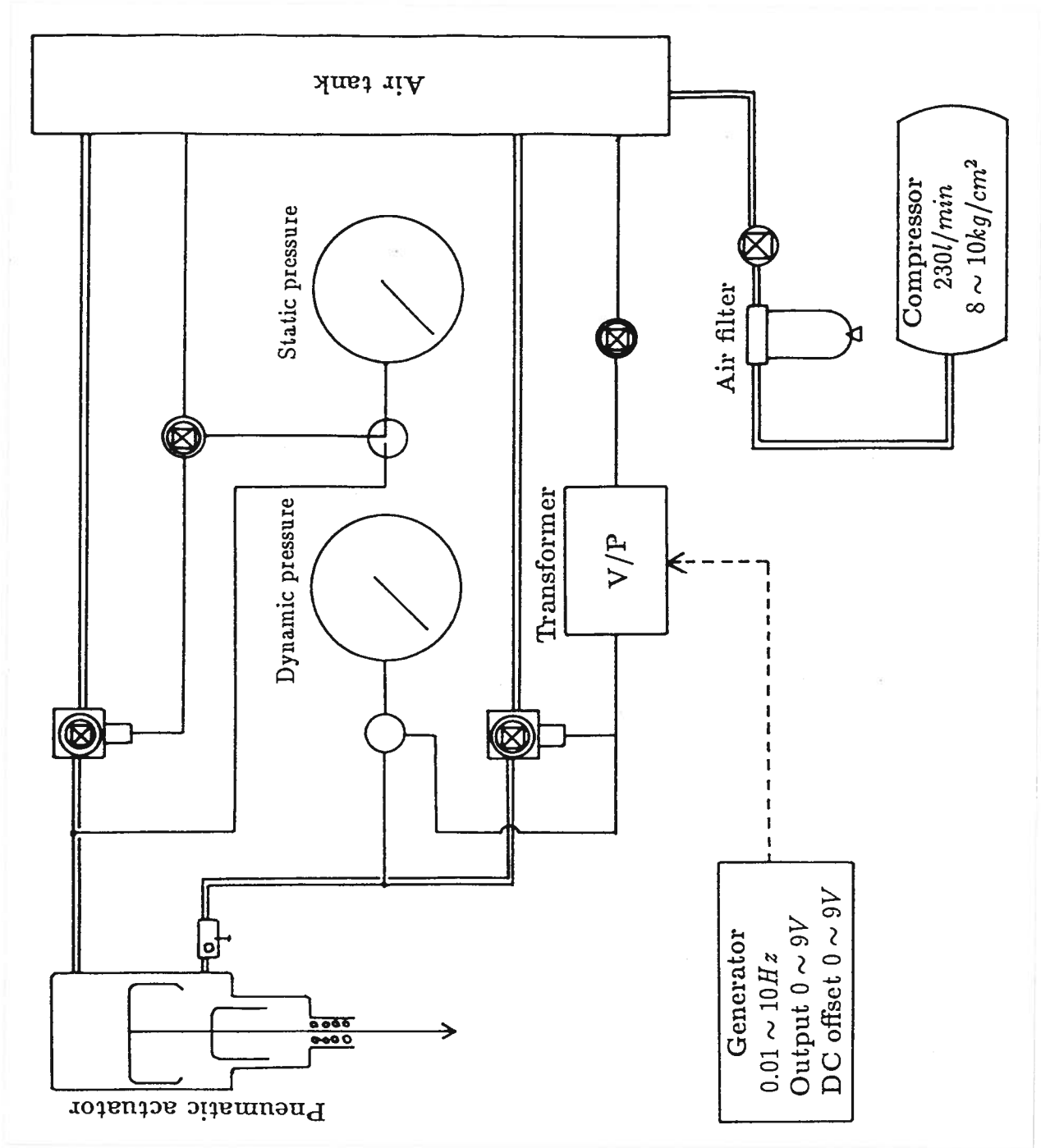

Figure 4.13: Layout of pipe lines of sine load generator

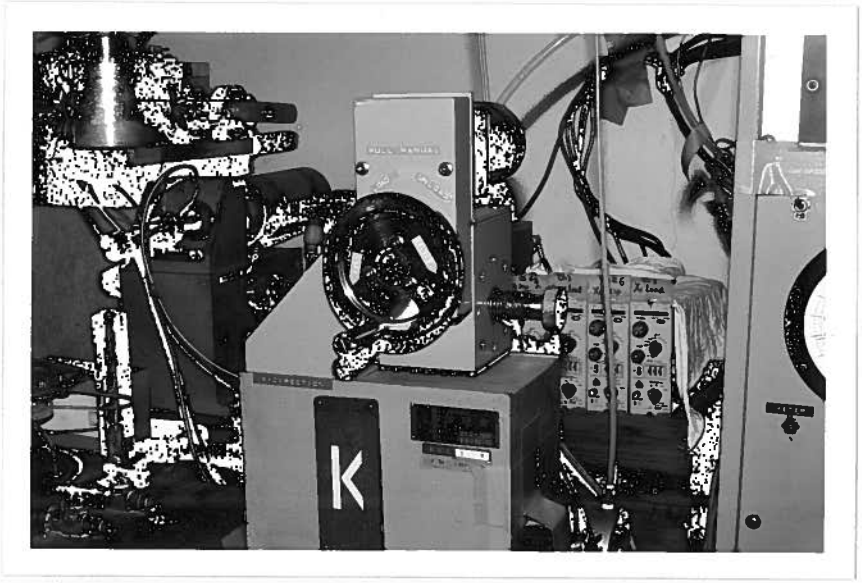

Photo. 4.13: Strained controlled monotonic loader

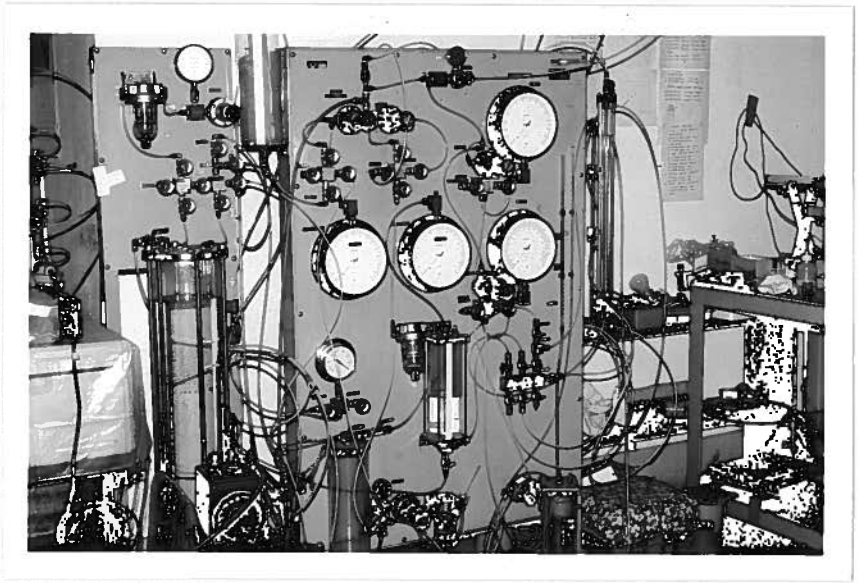

Photo. 4.14: Control plate

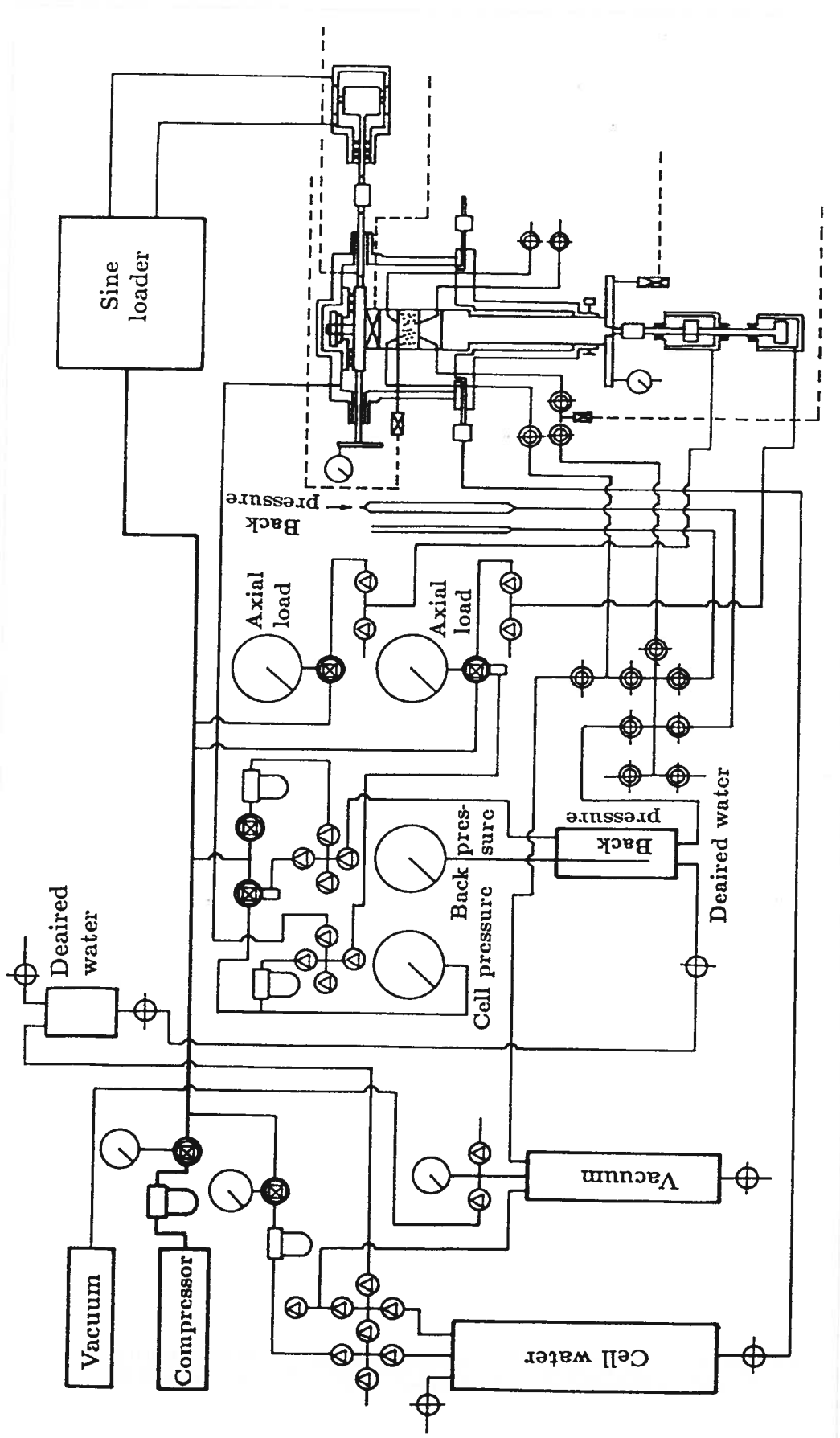

Figure 4.14: Pipe lines and controlling system on control plate

recorded by DRF1 data recorder and are saved in floppy disk. The data are read and calculated directly from the disk.

4.4 TEST SCHEDULE

The test schedule is discussed in this section. There are five materials used in the present study. The main tests performed are compaction test (*CT*), wetting test (*WT*), monotonic shearing test (*MST*) and cyclic shearing test (*CST*) as well as mineral component analysis (*MCA*) and scanning electron microscope (*SEM*). The test schedule is illustrated by the following flowchart:

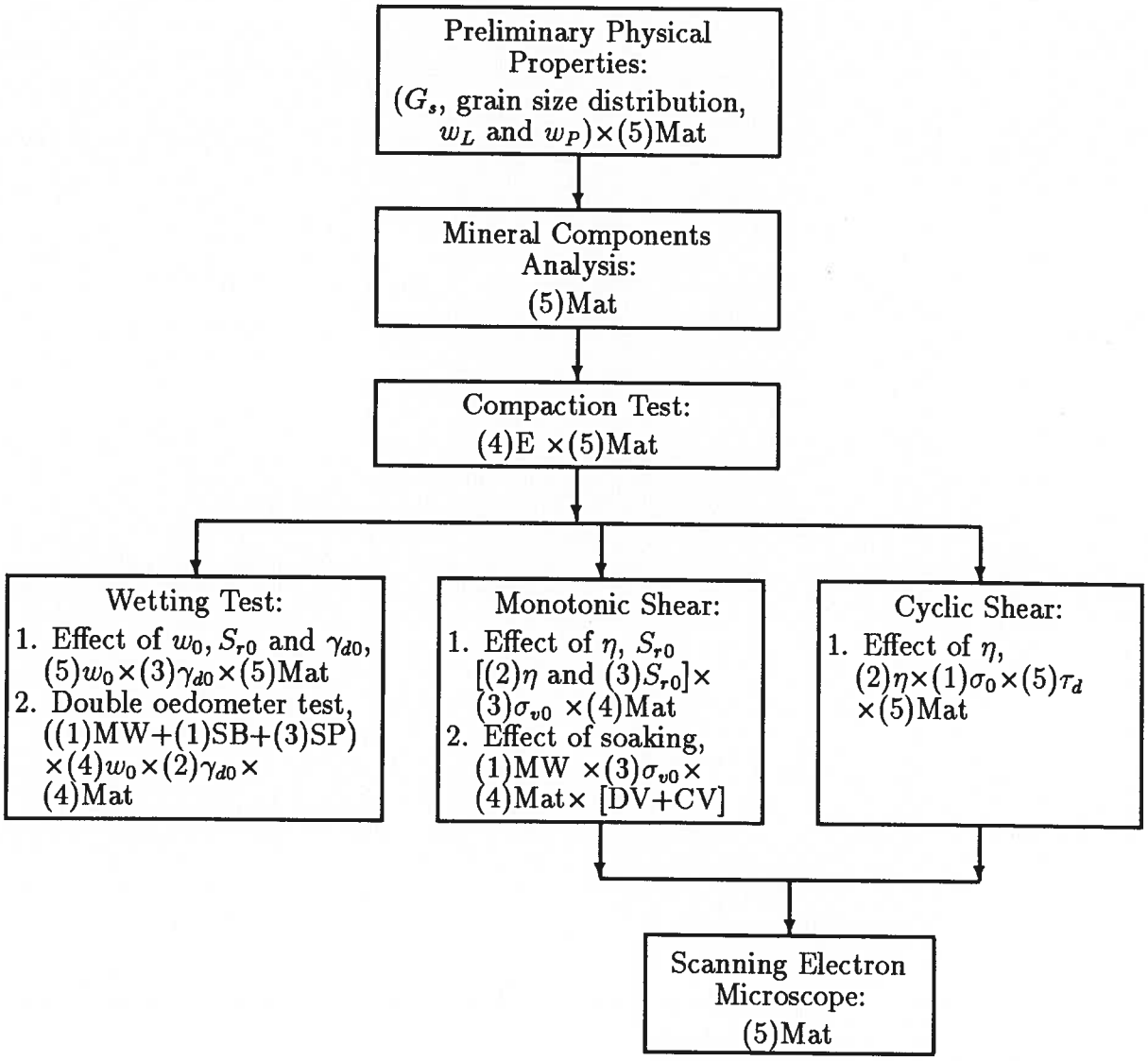

Figure 4.15: Flowchart of research schedule

In the flowchart,

G_s : the specific gravity;

w_L : the liquid limit;

w_P : the plastic limit;

Mat : materials, and (5)Mat means 5 different materials (the same meaning for other variables);

w_0 : the initial water content;

S_{r0} : the initial degree of saturation;

γ_{d0} : the initial dry density;

σ_{v0} : the initial overburden pressure;

τ_d : the amplitude of cyclic shear stress;

E : energy;

MW : tested at molding (initial) water content;

SB : soaked from beginning;

SP : soaked at certain overburden pressure;

DV : drained volume changeable tests; and

CV : constant volume tests.

4.5 EXPERIMENTAL PROCEDURES

Although as much as five kinds of tests are performed in the present study, only the experimental procedures of oedometer test and simple shear test will be discussed in detail in this section. Compaction test is conducted by following the standard steps.

4.5.1 Oedometer wetting test

(I). Sample preparation

A standard procedure is followed in the sample preparation to ensure a desired initial conditions in the test. The general steps for sample preparation are given in the following:

1. Fit the sample ring on the base of oedometer and secure it with a ring shaped plate by three screws.

2. Measure the height of ring, from pore stone surface to the top of ring, at six points. Use the mean value, H_0, to calculate the volume of the sample.

3. Compute the weight of the material needed based on the volume calculated above with the predetermined dry density. Prepare the materials to have the required initial water content. Weigh half of the computed weight.

4. Fill the weighed out material in sample ring carefully with spoon, smoothen the surface and use a brass-made flat-bottom rammer to tamp the material to the desired height $\frac{1}{2}H_0$.

5. Put on the extension ring on the sample ring and repeat step 4. When the sample in the ring is tamped to a height a little higher than H_0 by trial and error, take off the extension ring and use a flat plate cutter to trim the sample to the right height H_0.

6. Put on the extension ring again and place the cap gently on the surface of sample. Place the whole oedometer in loading frame. Fix the dial gauge on oedometer and zero it.

(II). Test procedures

After completion of sample preparation, the following procedures are followed to test the sample:

1. Apply a seating load of $5kPa$ for a period of about 10 minutes. Note the dial gauge reading at the end of the seating period.

2. Load the sample at as-compacted conditions to the desired load level. Take the dial gauge readings at time 0.1, 0.15, 0.25, 0.5, 1, 2, 3, 5, 10, 20, 30, 60, 120 minutes, *etc.* A velocity of deformation of $\frac{1}{100}mm/h.$ is considered as the standard at the end of sub-consolidation. If the velocity of deformation at the end of 120 minutes is larger than this standard value, the consolidation should be continued until the standard value is reached.

3. Pour de-aired, distilled water into the cell to a level slightly above the cap, providing the sample with access to the water from both the top and the bottom under a small positive head. The water level above the cap is maintained throughout the test. Take the dial gauge readings at the same time intervals as described in step 2. The same standard of deformation is used as the end of collapse.

4. Drain the cell and remove it from loading frame. Remove the wet sample together with the ring from the cell. Take out the wet sample from the ring and weigh

and then dry it in the thermostat at a temperature of 120 °C for 24 hours. Clean the ring, cap and base porous stone and hold the waste in another vessel and dry it. Weigh the dried sample and the residual from the ring and porous stone. The as-compacted and oven-dried weights of material are used to determine the initial dry density and molding water content of sample. The weight of the wet sample is used to estimate the degree of saturation. The equilibrium dial gauge readings are used to determine the volume change which occurred during consolidation and soaking.

The above test procedures are used in wetting tests. In double oedometer tests, the test procedures are almost same as above. The only difference is that two nearly identical samples are prepared, with one sample being consolidated under as-compacted conditions in all load increments until the required load level, while the other sample is soaked at 10 kPa equilibrium load and then loaded with the other load increments. The collapse of the sample is computed based on the volume changes of the two identical samples.

4.5.2 Simple shear test

(I). Sample preparation

Fig. 4.16 illustrates the preparation of the sample in simple shear test. The following steps are observed during sample preparation.

1. Increase the air pressure in the upper pneumatic ram located under test cell. Insert two steel made ties under the support plate which is linked up with the top of loading rod, decrease the pressure to zero and lock the rod. Screw the base of specimen and the support plate together. Measure the thickness of rubber membrane and stretch it over the periphery of the base. Tie up a narrow membrane tape over the membrane at the part above the O-ring.

2. Sheathe the teflon tapered sleeve and annular plate supporter. Screw the supporter with four screws to the base plate to ensure that the rubber membrane is fastened on the base and that there is no leakage between the membrane and the periphery of the base.

3. Place a stack of teflon coated annular plates outside membrane together with the mold and fix them by four screws on the supporter. Use a fixture in clamping the two pieces of the mold together.

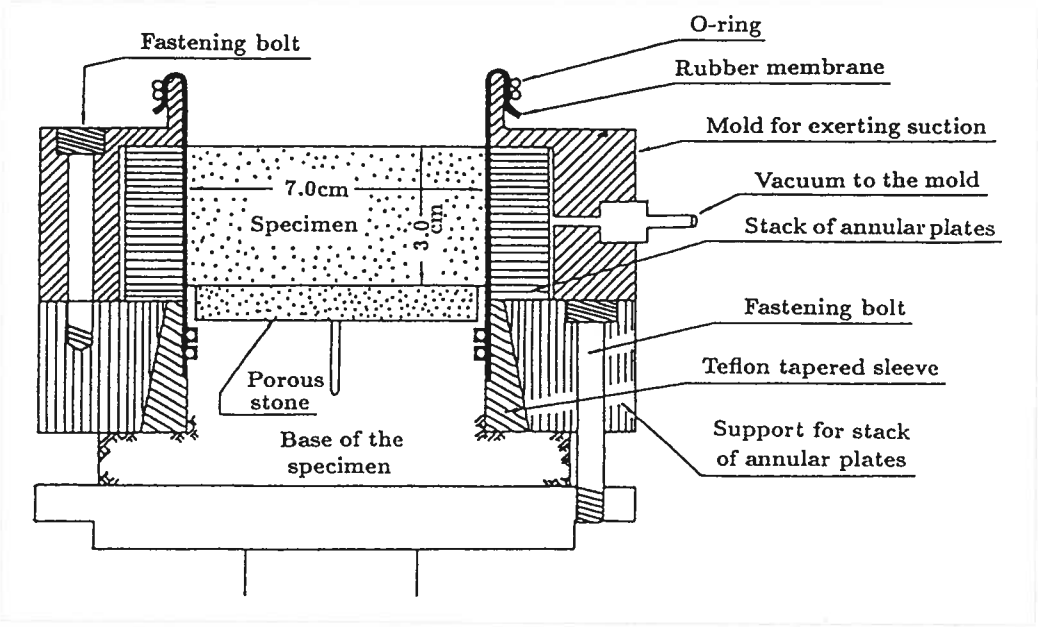

Figure 4.16: Illustration for sample preparation

4. Pull the rubber membrane through the mold, stretch it over the top of the mold such that there are no wrinkles in the membrane and roll it back over the top edge of the mold. Apply vacuum to the space among the membrane, annular plates and the mold through a vacuum line attached to a nipple on the outside of the mold, thereby stretching the membrane tightly against the inside of the annular plates.

5. Compact the sample in three layers, each having a height of 1 cm. Each layer is compacted by loosely placing a predetermined amount of moist soil in the membrane room and tamping the soil to the required height. The surface of compacted soil is roughened before the next layer is compacted. The same procedures are repeated two times to obtain the whole sample.

6. Screw the top cap and the top cap holder together by two bolts, placed diagonally on the two supporting posts and screw them. Gently lower the top cap onto the surface of specimen. A small force is needed to push the cap, thereby getting a better touch between the pore stone disk and the specimen surface, because of the existence of steel blades in pore stone. A mark for the required specimen height is placed on the cap holder based on the calibration.

7. Fix the top cap temporarily to the holder, thereby preventing any vertical move-

ment. Remove the vacuum line. Roll over the rubber membrane and secure it by one O-ring to top cap. Apply a vacuum of 5 kPa inside the specimen. Remove the fixture and mold. Secure the rubber membrane to the top cap with another rubber membrane tape. Screw a small plate, which is used to measure the shear displacement, on the top cap. Separate the holder from the top cap and remove it.

8. Unlock the rod. Increase the air pressure in the pneumatic ram, take out the ties and decrease the pressure to zero again.

9. Lower gently the cell cap to the four supporting posts by means of a small crane. Fix it to the posts by four bolts.

10. Zero the amplifiers of the shear and vertical load cells. Gently lift the base platform, on which the specimen with the cap now rests, by increasing the air pressure in the upper pneumatic ram. When the specimen top cap touch the plate beneath the vertical load cell, connect them rigidly by means of four screws.

11. Connect the load carriage to the horizontal loading rod. Set the linear variable differential transformer to the right position. Note the vertical dial gauge reading.

The apparatus has a lucite cell which is formerly used to apply cell pressure on specimen. In the present study, the samples are consolidated and sheared under plane strain condition, thus, no additional cell pressure is applied. Therefore, the lucite cell is not used.

(II). Test procedures

The test procedures in the specimen consolidation and wetting in simple shear tests are almost the same as in oedometer wetting tests. A seating load of 5 kPa is applied at end of the sample preparation. The initial vertical dial gauge reading is noted. Then, an overburden pressure of 98 kPa (an increment of 93 kPa) is applied. All the samples in present study are consolidated and wetted at this overburden pressure. The dial gauge readings are taken at the same time intervals as in the oedometer wetting test. The main consolidation is usually finished in two minutes and the sub-consolidation in two hours. At the end of sub-consolidation, water having a head of about 40 cm from one water tank is supplied though bottom by two drainage lines to specimen. The drainage lines in top cap are connected to another tank, allowing the extra water to be drained. Dial readings are recorded at the same time intervals.

In case of monotonic test, samples are tested under three different overburden pressures, 98, 196 and 294 kPa. However, all the samples are consolidated and wetted at an initial overburden pressure 98 kPa. Then, at the end of wetting induced deformation, the specimen is loaded to the required load level and consolidated until a new equilibrium is obtained. The collapsibility coefficients are calculated corresponding to an overburden pressure 98 kPa.

When the soaked specimen has stopped shrinking thereby indicating a new equilibrium state of vertical displacement, the drainage lines for the water supply are closed and some minutes are allowed to pass to let the pore water pressure in the specimen to dissipate. When the pore water pressure has dissipated to zero, the vertical loading rod is clamped to inhibit any vertical displacement during shear loading. The top drainage lines are closed. Then, shear loading (monotonic or cyclic) is applied on the specimen. The test is performed at plane strain, constant volume and undrained conditions. Data are recorded by DRF1 data recorder.

At the end of the test, the wet sample is removed, weighed and dried and weighed again after drying. The waste from the cleaning membrane and the top and base porous stone is dried and weighed. These data are used to calculate the initial dry density, the dry density and the degree of saturation before shearing. The collapsibility coefficient is computed based on the equilibrium dial gauge readings before and after wetting and the initial height of the sample.

(III). Calibration, calculation and correction of variables

There are five variables, vertical stress and strain, shear stress and strain and pore water pressure, which are measured in the tests using *transducer-amplifier-data recorder* system. The calibration, calculation and correction of the variables will be discussed here.

(1). Calibration of transducer

There are five transducers which are used in the test to monitor the shear stress, shear displacement, axial load, axial displacement and pore water pressure, respectively.

(a) Load cells

The shear load cell is taken out from the equipment and calibrated using a standard load cell calibrator. The axial load cell is placed in the samples cell. It is very difficult to take it out and to calibrate it in standard load cell calibrator. Therefore, in order to calibrate it accurately, a calibrated standard load cell is placed in the place where specimen is placed. Load is applied on load cell by increasing the pressure in vertical pneumatic

ram. The applied load is read out by the output from standard load cell. Another kind of output in the form of voltage is derived from real load cell. The relationship between the two outputs is set up and used in calculation. If the amplifier is zeroed for load zero, the output is the net load acting on the load cell.

(b) Displacement transducer

A linear variable transformer is used to monitor the horizontal displacement. It is calibrated by using a series of standard plates with thickness of 1, 1.25, 1.5, 2, 3, 5, 10 mm *etc.* The accuracy of the plates is validated by a standard thickness calibrator. The vertical displacement transducer is a dial gauge capable of outputting voltage signal. It can be used as a linear variable transformer as well as a conventional dial gauge. It is calibrated using the standard thickness calibrator. The dial gauge readings are also calibrated. The results show that the error is negligible.

(c) Pore water pressure transducer

Pore water pressure transducer is calibrated by using a standard pressure gauge which is directly connected to the back pressure line. Air pressure is applied from the back pressure valve. A relationship is established between the pressure gauge readings and the output voltage signal from the transducer.

(2) Calculation of variables

It is well known that there are uneven distribution of stress and strain (Vucetic, 1982; Finn, 1985) in simple shear test. However, it is very difficult to measure the distribution of stress and strain along specimen surface. An average value is used in the present study. Following are the formulas used in calculation:

Shear stress:

$$\tau = \frac{Q}{A} \tag{4.4}$$

Axial stress:

$$\sigma_v = \frac{P}{A} \tag{4.5}$$

Shear strain:

$$\gamma = \frac{\Delta D}{H_s} \tag{4.6}$$

Axial strain:

$$\varepsilon_a = \frac{\Delta S}{H} \tag{4.7}$$

where A is the cross fictional area of the specimen, Q is the shear force, P is the axial load, ΔD is the displacement at top surface of specimen in shearing direction, ΔS is

the vertical settlement, H_s is the height of specimen before shearing and H is the height corresponding to each state of testing.

Note that the pore water pressure is modified data directly from recorder.

(3). Correction of variables

For the intrinsic problems in apparatus design, some correction must be made in the measurement and in the calculation of the variables. There are two main problems: one is the friction between the loading rod and stoke ball bearing, and the other is the rocking motion around horizontal axis of the top cap.

For the problem of friction, there exists difference between the vertical and horizontal directions. In the case of vertical direction, the load cell is installed above the top cap (see Fig. 4.9). The load acting on the load cell is equal to the overburden force acting on the specimen plus the friction between the periphery of the specimen and the rubber membrane and that between rubber membrane and the inner surface of the annular plates. In the part of top cap insetting in annular plates, the rubber membrane is secured on the periphery of the top cap and the radius of the top cap (35.00 mm) plus the thickness of the rubber membrane (usually $0.275 \sim 0.325$ mm) is less than the inner radius of annular plates ($35.50mm$). The rubber membrane and annular plates do not touch each other. Therefore, no friction exists in this part. Because the lower loading rod is fixed thereby maintaining the specimen in a constant condition during shearing, it is considered that the above mentioned friction is negligible. Therefore, the output of load cell represented the load actually acting on the specimen if it is zeroed for zero load.

As shown in Fig. 4.9, the shear load cell is connected with loading rod. Shear load is transmitted to the specimen by load carriage. The outputs of this load cell include shear force acting on the specimen, extension force in the rubber membrane, friction in the annular plates and friction between the load rod and the ball bearing. In order to measure these forces, simple shear tests under monotonic and cyclic loading conditions are performed on dummy water samples. Because water has no shear resistance, the measured force in load cell is the sum of these forces. A relationship between these forces and shear displacement is established. In real tests, these forces corresponding to a certain shear displacement is deducted from the output of the load cell.

Because of the rocking motion around the horizontal axis of top cap (this will be discussed later in Chapter 6), the horizontal displacement measured at the level of the horizontal load ram is greater than the displacement occurring at the top of the specimen. This means that the shear strain calculated using the measured displacement of the load

ram is larger than the real shear strain induced in the specimen. It is found that this error increased with the increase in the overburden pressure and dry density of specimen. In order to measure the real displacement in the specimen, a small plate is fixed rigidly on the top cap at the opposite side of load ram, as shown in Fig. 4.9. The linear variable differential transformer is installed at the level of the bottom surface of top cap as shown in Photo. 4.5 and acted on the small plate. The measured displacements at this level are used in calculation. The difference between the measured displacements at the two levels of a dummy rubber specimen is illustrated in Fig. 4.17.

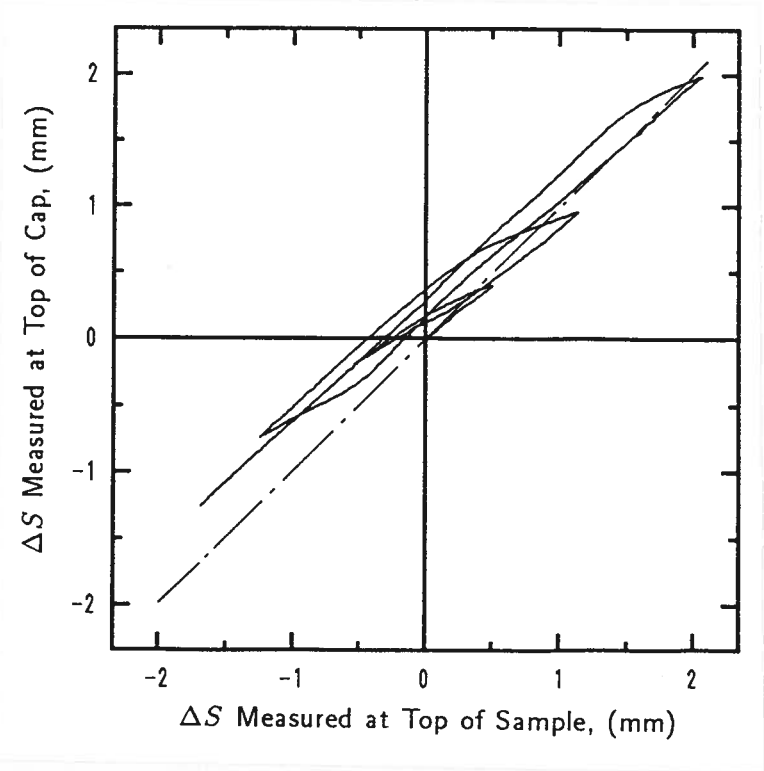

Figure 4.17: Displacements measured at two levels which illustrate the rocking motion of top cap around the horizontal axis

4.6 SUMMARY

The test materials, apparatus, schedule and experimental procedures have been discussed in this chapter. The mineral component analysis shows that there is no big difference in the mineralogy of the materials used in the present study. The test results of e_{min} suggest that the value corresponding to the maximum dry density from *Standard Proctor Compaction* should be used in estimating the relative density of soils with fine or clay content.

The discussion of test apparatus is concentrated on the simple shear test device. The sample preparation and test procedures which have been strictly followed in all the tests in the present investigation have been presented in detail.

Chapter 5

HYDRAULIC COLLAPSE AND THE INFLUENCING FACTORS

5.1 INTRODUCTION

It is well known that partly saturated soil usually possesses an unstable structure because of the presence of suction and bonding or cementing agents. This metastable structure will collapse when subjected to water permeation. The amount of collapse depends on many factors. A review of previous studies on this aspect has been given in Section 2.4. The review indicates that, despite these studies, several questions and divergences remain as to the effect of each influencing factors.

In this chapter, the collapse and the effects of different factors on the magnitude of collapse of compacted clayey and silty sands are investigated both by *Wetting* and *Double-Oedometer* tests. The so called *Wetting test* is performed in the following way: the prepared specimen in the oedometer ring is consolidated under a given load until secondary consolidation is finished; once the stress equilibrium is obtained, the specimen is soaked in water under the same overburden pressure. The test follows the real stress history in in-situ condition. A detailed discussion of the sample preparation and test procedures has been given in Section 4.5.1. The *Double-Oedometer test* was first proposed by Jennings and Knight (1957). In this method, two approximately identical specimens are prepared in oedometer rings, and placed in a consolidometer under a light 10 kPa seating load (in the original method, the seating load was 1 kPa) until stress equilibrium is achieved. Once the stress equilibrium is obtained, one sample is inundated by flooding with water, while the other sample is kept at its molding water content. Both samples are then left for a certain time interval until new a stress equilibrium is achieved. The test is then carried out in ordinary manner, adding load increment each time interval, and the results are plotted. In this method, the stress history is different from the real one.

The tests are conducted in the manner discussed in chapter 4. In the following

discussion, the process of deformation under constant overburden pressure and molding moisture content is called *consolidation* and the process of deformation during which additional water is added is referred to as *wetting* or *soaking.*

The quantification of collapse is expressed in terms of *Collapsibility Coefficient*, η (See section 1.2.). In a general stress condition, it can be expressed as:

$$\eta = \frac{\Delta V_w}{V_c} \tag{5.1}$$

or

$$\eta = \frac{(\varepsilon_v)_w - (\varepsilon_v)_c}{1 - (\varepsilon_v)_c} \tag{5.2}$$

The meanings of the signs in the equations are:

ΔV_w : the volume change because of wetting;

V_c : the volume at end of consolidation or before soaking;

$(\varepsilon_v)_c$: the volumetric strain at end of consolidation or before soaking; and

$(\varepsilon_v)_w$: the volumetric strain at end of wetting.

In plane strain condition, it can be written as:

$$\eta = \frac{\Delta H_w}{H_c} \tag{5.3}$$

or

$$\eta = \frac{\varepsilon_w - \varepsilon_c}{1 - \varepsilon_c} \tag{5.4}$$

where

ΔH_w : the change of specimen height because of wetting;

H_c : the height of specimen at end of consolidation or before soaking;

ε_c : the axial strain at end of consolidation or before soaking; and

ε_w : the axial strain at end of wetting.

Eq. 5.3 is used in the calculation of collapsibility coefficient, η, in all the tests because they are performed in plane strain condition.

5.2 DETERMINATION OF MOLDING CONDITIONS

It is considered that almost all the compacted soils can collapse under certain conditions when they are subjected to water infiltration (Lawton, 1986). The main conditions under which collapse would most possibly occur are when the soil is compacted dry of optimum and with small dry unit weight (Booth, 1975). In order to identify the range of moisture content and dry unit weight in which collapse would most possibly take place, a series of compaction tests are performed first for all the five materials. The tests are conducted

following the manner of standard compaction test. The energy absorbed per unit volume of soil can be calculated by the following equation (Ishihara, 1988):

$$E_C = \frac{W_R \cdot H \cdot N_L \cdot N_B}{V} \tag{5.5}$$

where

W_R : the weight of rammer;

H : the dropping height of rammer;

N_L : the layers of compacted soil;

N_B : the compacting times of each soil layer; and

V : the volume of soil.

In order to obtain different compacting energy, different combinations of parameters were used as shown in Table 5.1. The family of compaction curves employing different

Table 5.1: Combination of parameters for different compacting energy

E_C $(cm \cdot kgf/cm^3)$	W_R (kgf)	H (cm)	N_L	N_B	V (cm^3)
5.625	2.5	30	3	25	1000
3.375	2.5	30	3	15	1000
1.125	2.5	30	3	5	1000
0.075	2.5	2	3	5	1000

compacting energies are presented in Figs. 5.1 to 5.5 for five materials, respectively, along with the lines corresponding to degree of saturation , S_r, of 10, 20, 30, 40, 50, 60, 70, 80, 90, and 100% and the *line of optimum* which is obtained by connecting the coordinates of optimum water content and maximum dry unit weight in each compaction curves.

The curves yielding the highest densities are obtained by the so called *Standard Proctor Compaction Test* (Proctor, 1933) in which the compacting energy employed is $E_C = 5.625 cm \cdot kgf/cm^3$. The others are determined to be imparting lesser compacting energy. It is noted that the line connecting the coordinates of optimum water content and maximum dry unit weight coincides, *line of optimum*, approximately with a certain contour line of degree of saturation. For the five materials tested, the values are approximately 70%, 74%, 80%, 70%, and 80%, respectively. It is noticeable that the *line of optimum* falls in a range of 70 to 80% of contour lines of degree of saturation for all the materials.

The optimum water content and the corresponding maximum dry unit weight are illustrated in Figs. 5.6 as a function of compacting energy. It can be seen from Fig. 5.6

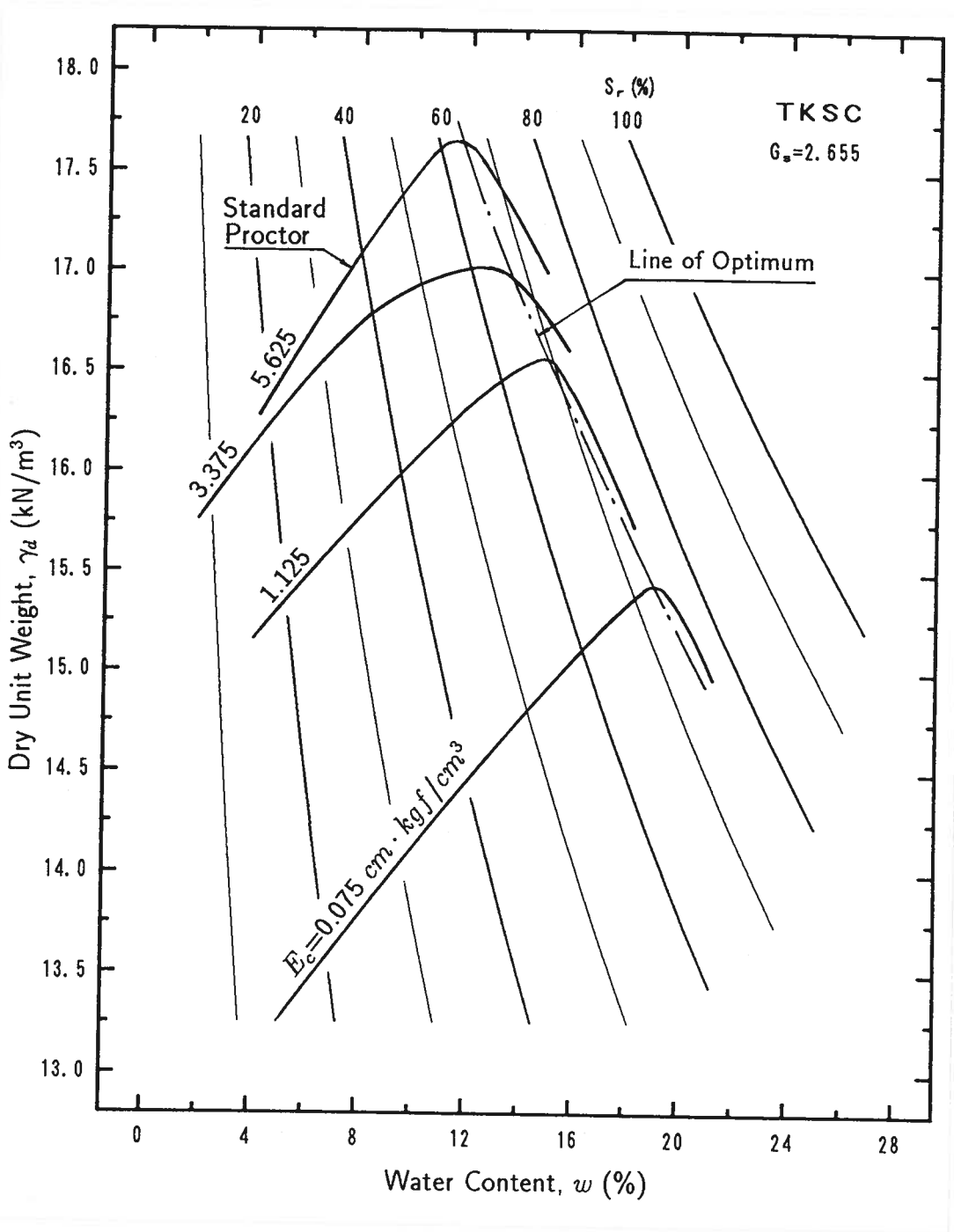

Figure 5.1: Compaction curves of an artificial mixture

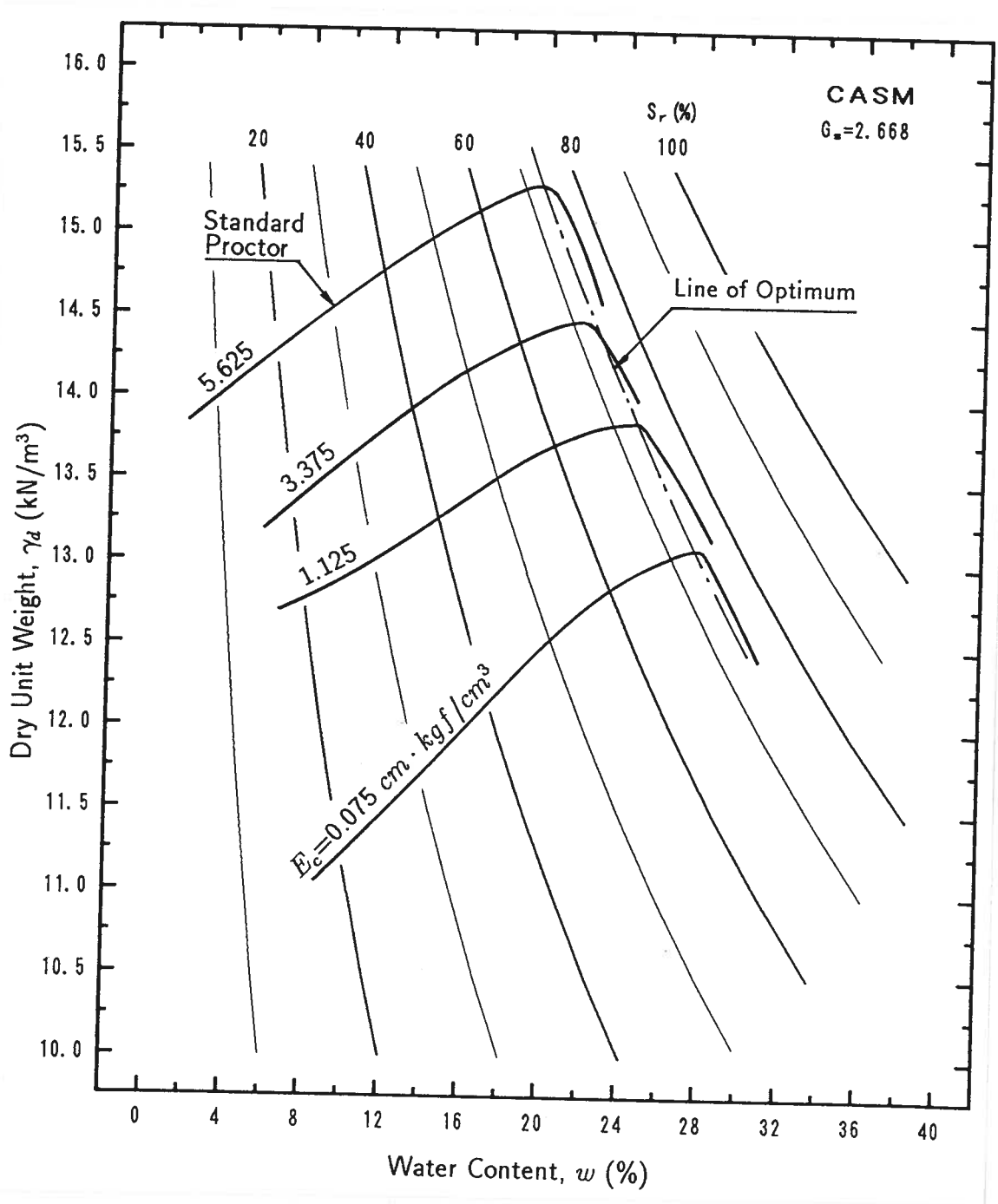

Figure 5.2: Compaction curves of Chonan A silty sand

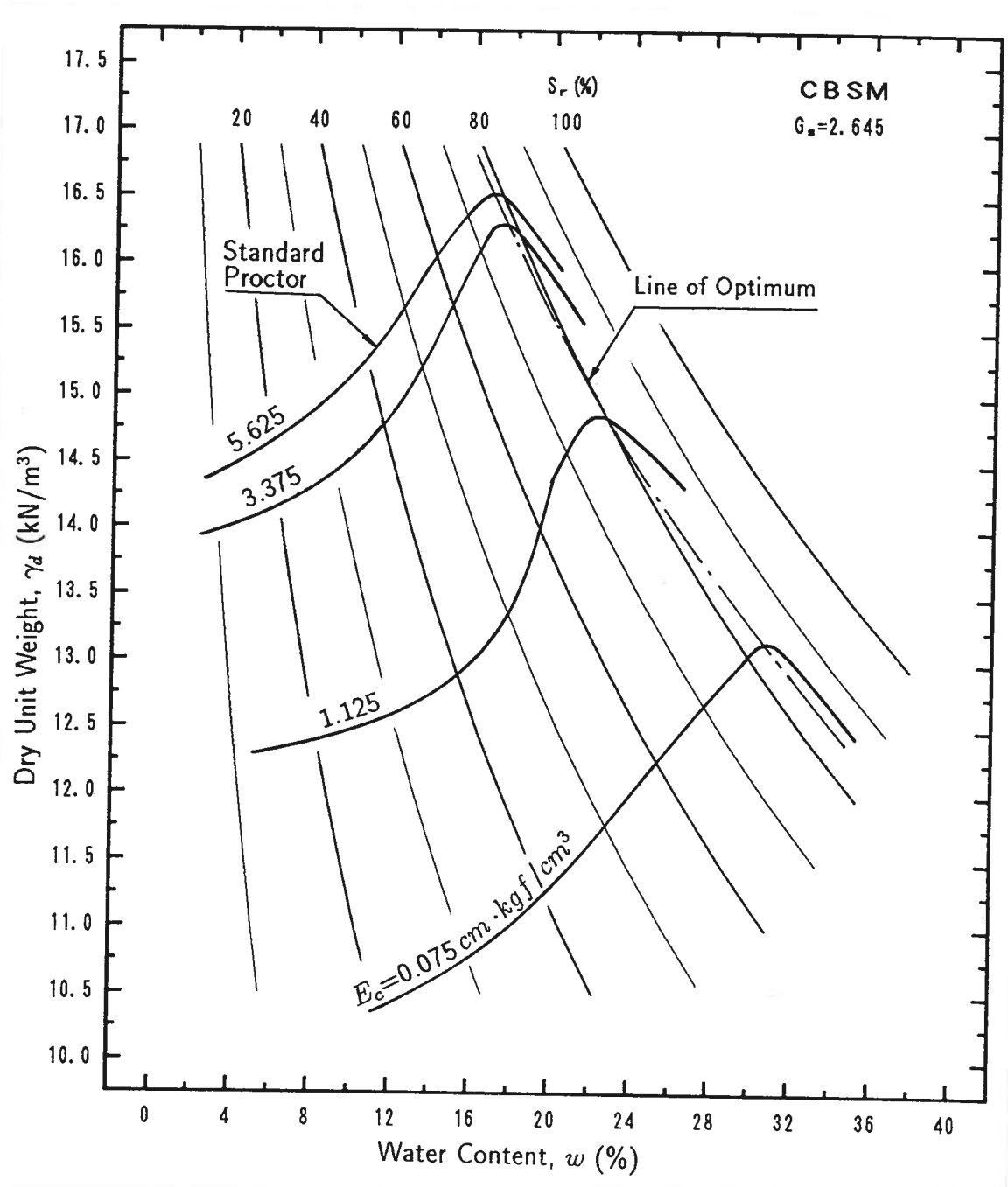

Figure 5.3: Compaction curves of Chonan B silty sand

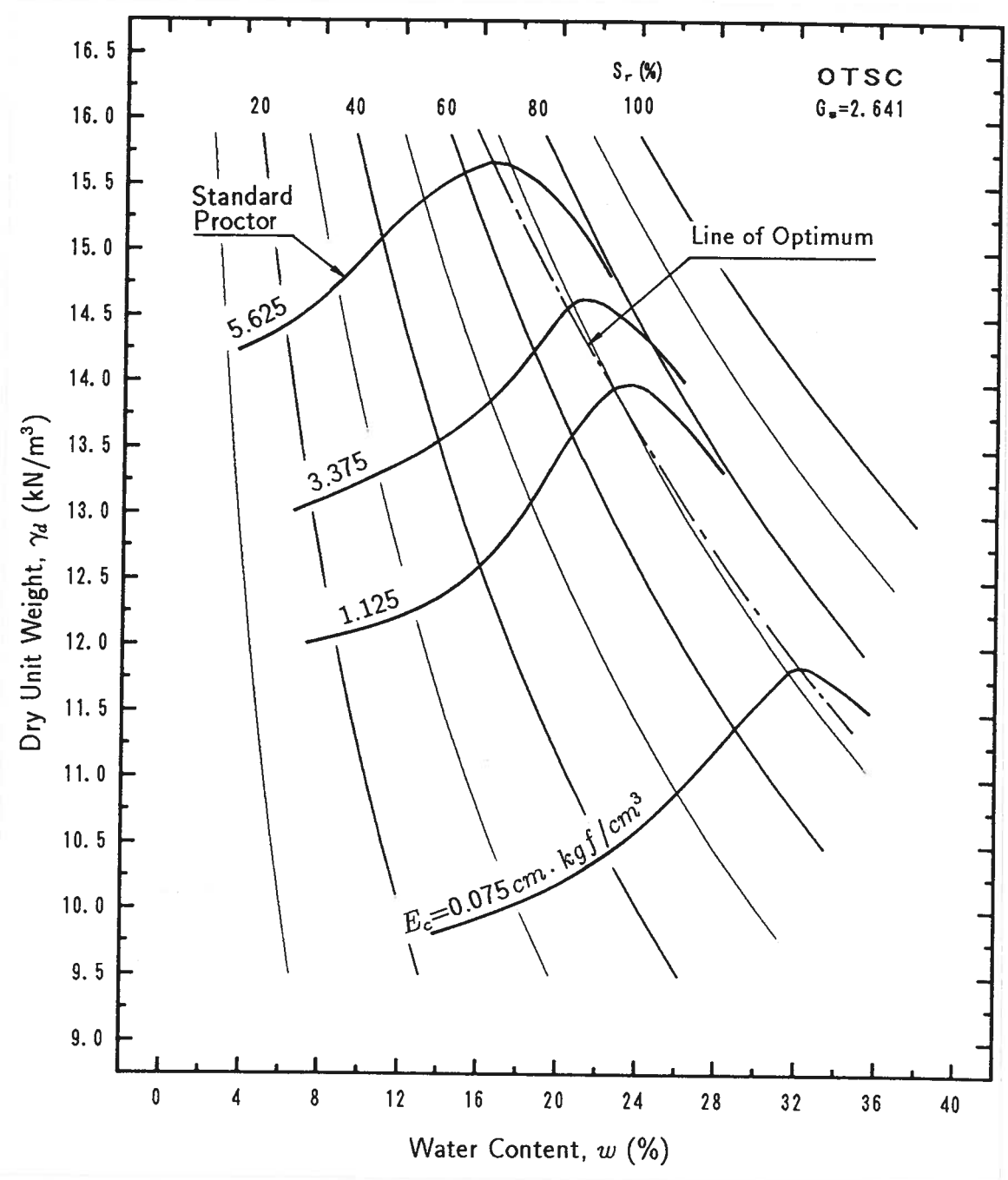

Figure 5.4: Compaction curves of Ottomo clayey sand

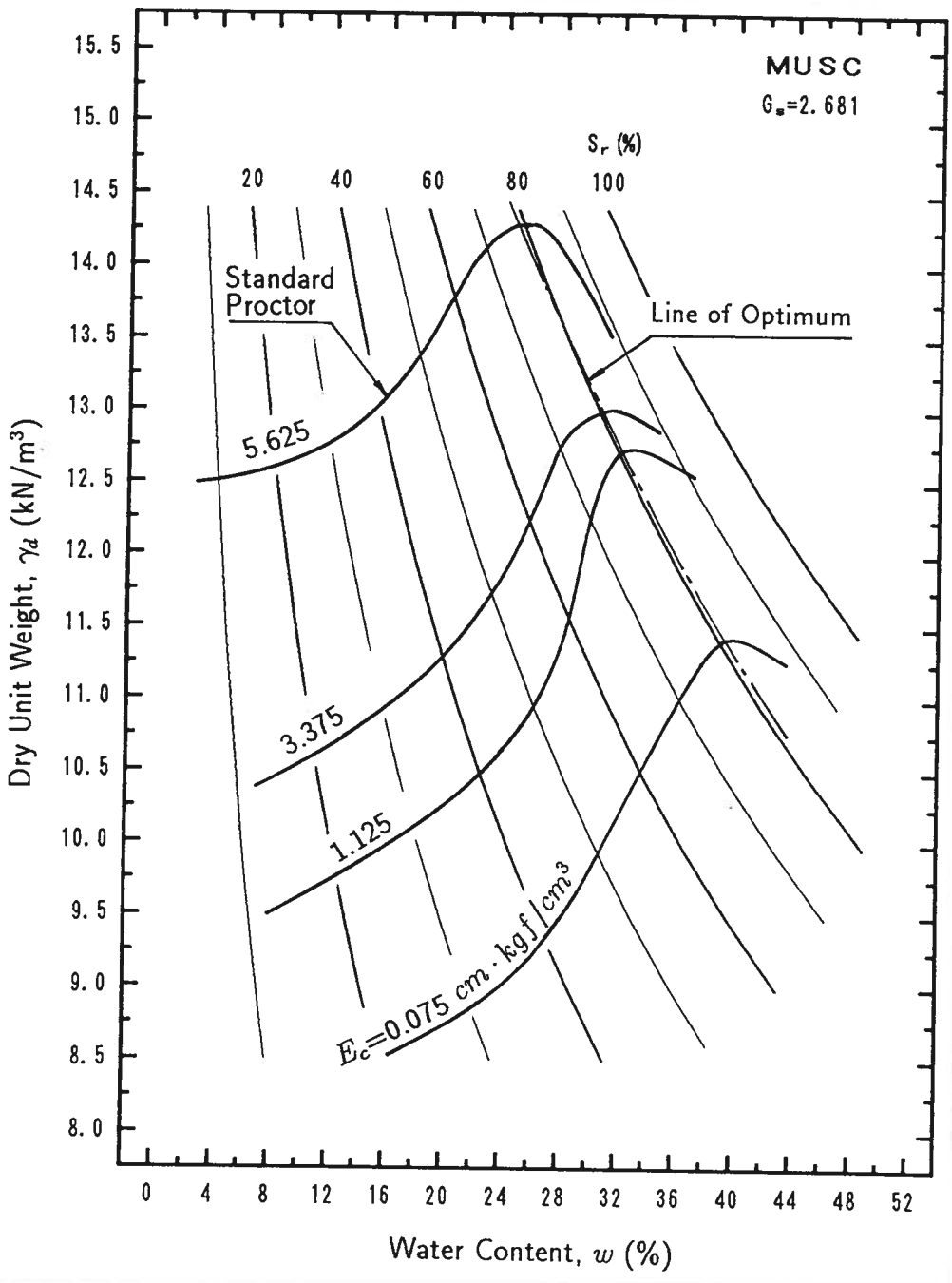

Figure 5.5: Compaction curves of Mutsuichikawa clayey sand

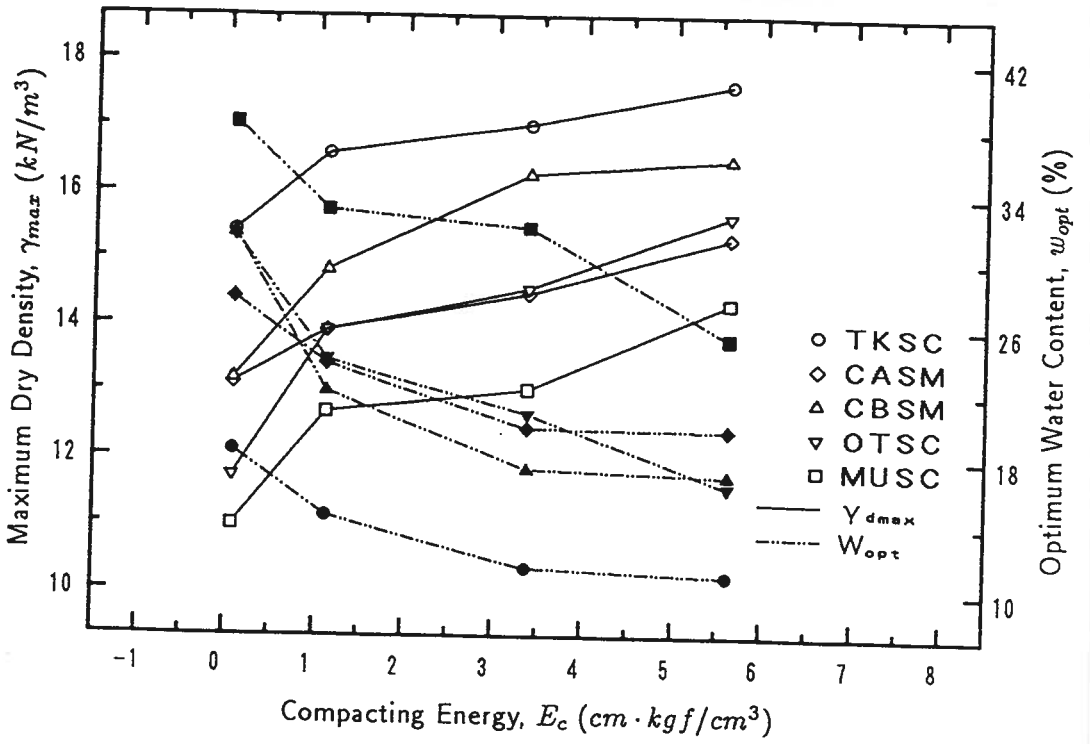

Figure 5.6: Relationship between maximum dry unit weight and compacting energy

that the dry unit weight corresponding to an optimum water content for each compacting energy increases, but the gradient decreases as the applied compacting energy increases, especially when the compacting energy is larger than 1.125 $cm \cdot kgf/cm^3$. It also shows clearly that the optimum water content and its gradient decreases as the compacting energy increases. This figure also demonstrates that the maximum dry density of *TKSC* (mixture of Toyoura sand and 15% kaolinite), which are yielded during compaction corresponding to each energy level, are the largest among all the five materials used, while that of *MUSC* (Mutsuichikawa clayey sand) are the smallest. The effect of clay content on maximum dry unit weight is illustrated in Fig. 5.7. The maximum dry unit weight increases as the clay content increases up to about 12%, and then it decreases as the clay content increases. The maximum value is obtained at clay content about 12%. This means that the clay content has an important effect on the compacting properties of soils. It is known that the densification of a soil during compaction is caused by the local shear deformation between soil particles. With low clay content, the local shear is occurred between sand particles. Because sand particles possess higher shearing resistance, the compacting deformation will be small and as a result, the density is small. As the increase in clay content, some sand particles will be coated by clay. Clay lubricates the

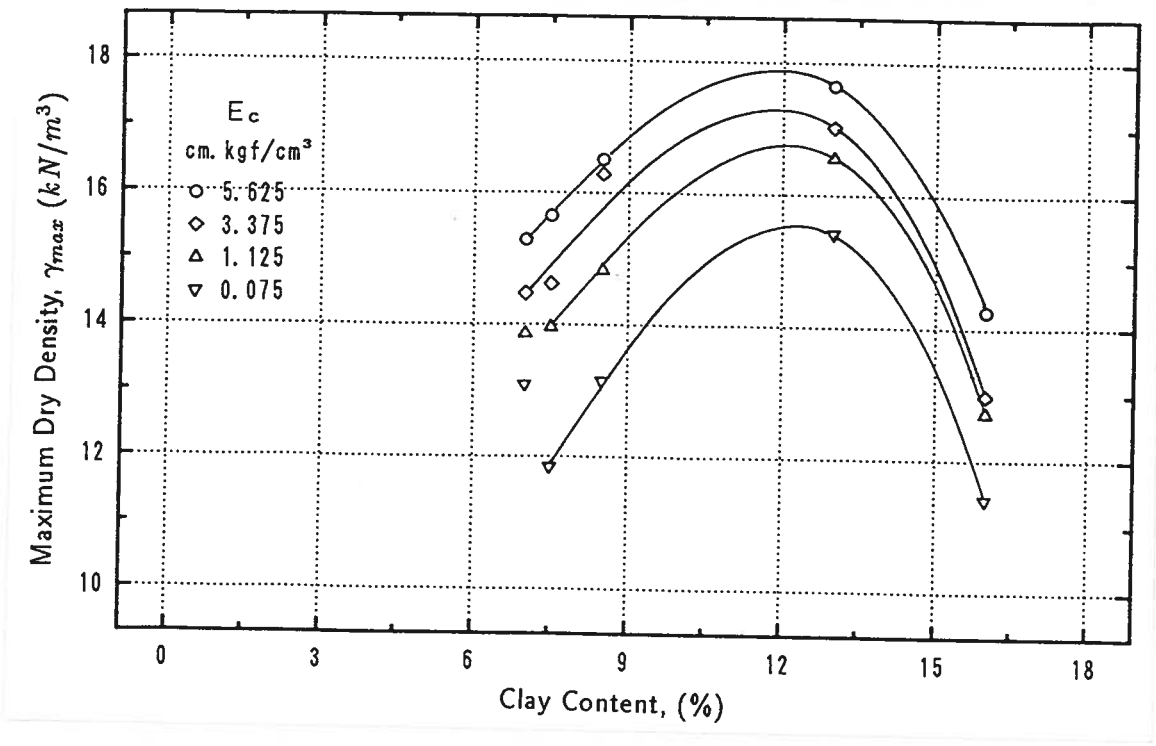

Figure 5.7: The effect of clay content on maximum dry unit weight

sand particles and reduces the shearing resistance. As the clay content increases to a certain value, The lubricating action is the maximum and the soil undergoes maximum deformation under the same compaction energy. This corresponds to such a soil structure that all the sand particles are coated by a thin clay film. The further increase in clay content will increase the thickness of clay film and some shearing action occurs between clay particles. The interparticle electrical repulsion and attraction of clay will increase the shearing resistance. Therefore, soil will show smaller compaction deformation and further smaller dry density, under the same compaction energy.

5.3 INFLUENCE OF MOLDING CONDITIONS

Based on the results of compaction tests, collapse tests using oedometer test device are run within an estimated possible range of moisture content and dry unit weight. The first set of tests is the *wetting test* which is intended to investigate the effects of molding condition on the collapse properties of soils. All the tests are conducted under an overburden pressure of 98 *kPa*.

A special test is designed to illustrate the phenomenon and the process of collapse.

This test is conducted in a top open lucite tank of 30 cm in height and 10 cm in inner diameter. The thickness of the wall of lucite tank is 1 cm. A porous stone 10 cm in diameter is embedded in the bottom of the tank and then a filter paper is overlain on the porous stone. In order to reduce the friction between the sample and the wall of the tank, a grease coat is applied to the wall of the tank, then a extreme thin polyethylene made lap film is used to stick on the grease coat before preparing the sample. The test results show that grease and polyethylene made lap film work well in reducing the friction.

Specimen of 20 cm in height is prepared following the same procedures as in oedometer test. At the end of the specimen preparation, filter paper, porous stone and loading pad are put in that order on the top of the specimen. Then, the whole tank is placed in the loading frame. The loading frame is borrowed from a conventional triaxial apparatus. In this test the material used is *TKSC* (Toyoura sand mixed with 15% kaolinite). The specimen has an initial dry unit weight of 13 kN/m^3. The phenomenon and the process of collapse are shown in Photo. 5.1. Photo. 5.1(a) shows the sample at end of preparation. Photo. 5.1(b) demonstrates the sample after consolidation. It is to be noted that there is some deformation due to the application of an overburden pressure of 98 kPa. However, although the relative compaction of the specimen is relatively small (73.6%), the consolidation deformation at overburden pressure 98 kPa is not large enough. Photo. 5.1(c) indicates the state of sample at time that water infiltrated to 1/4 of the height of sample. It demonstrates clearly how the collapse develops as water infiltrates into soil. The collapse deformation can be seen from the displacement of black mark lines. It can be seen that there is a sudden reduction in bulk volume upon water infiltrating into the specimen. This deformation, at the top of sample, is almost the same order as that of consolidation. Photo. 5.1(d) and (e) are the states of sample when water infiltrates into 1/2 and 3/4 of the height of specimen, respectively. Photo. 5.1(f) shows at the end of hydraulic of collapse. A total collapse deformation as great as the collapsibility coefficient, η, of 13% is observed in this test.

One of the results of the *wetting test* using the oedometer ring is presented in Fig. 5.8 in which specimens prepared having identical molding dry unit weight of γ_{d0}=13.71 kN/m^3 but with varying water content are consolidated and subsequently inundated with water. It can be seen in Fig. 5.8 that, at relatively low molding water content, while there is some change in the specimen height under an overburden pressure of σ_{v0}=98 kPa, a sudden decrease in the height of the specimen takes place as a consequence of hydraulic collapse due to water inundation. At relatively high molding water content, the specimen undergoes large deformation during consolidation, but the reduction of specimen height due to wetting is small. The amount of wetting-induced volume change tends to signifi-

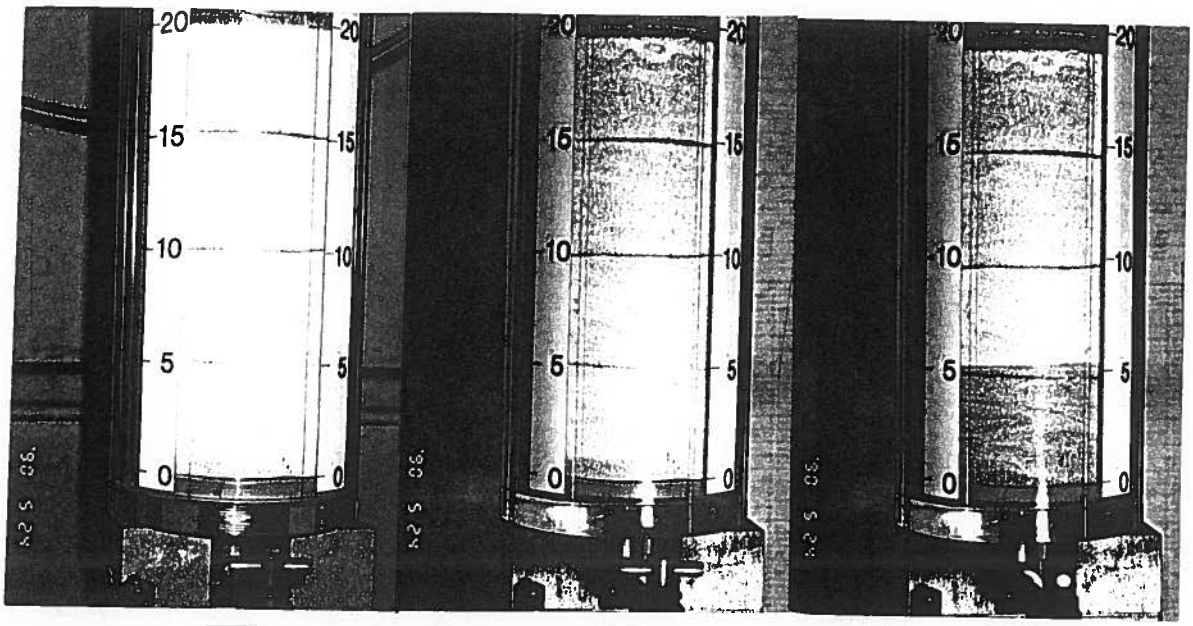

(a) (b) (c)

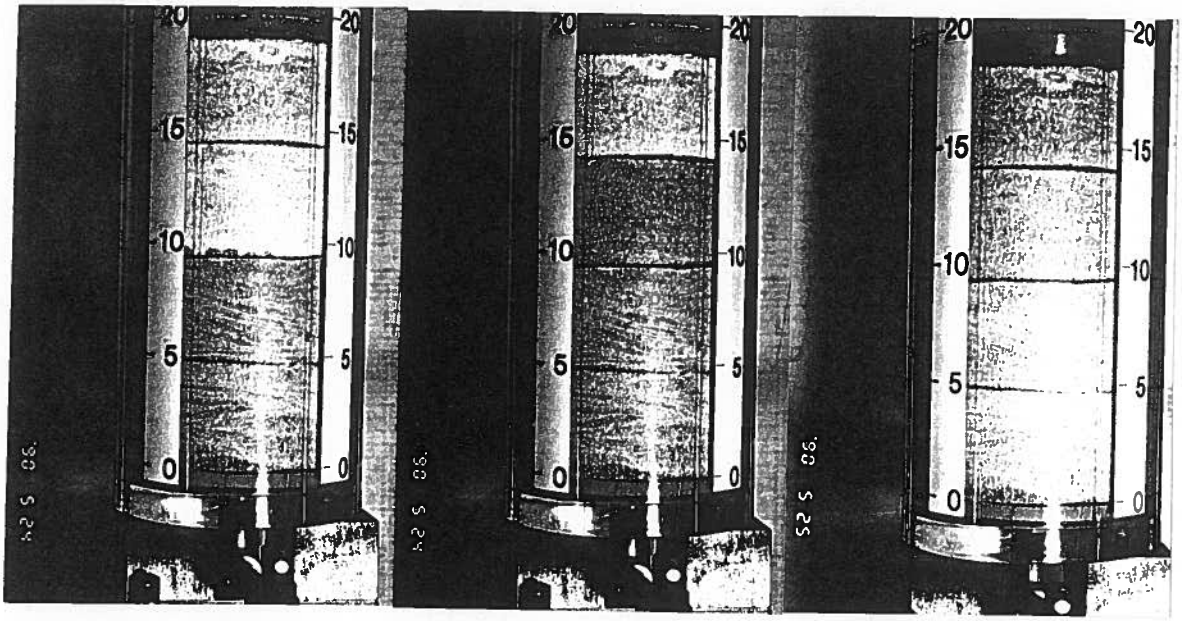

(d) (e) (f)

Photo. 5.1: Process of collapse. (a). Before consolidation; (b). After consolidation; (c). 1/4 of the soil layer being infiltrated; (d). 1/2 of the soil layer being infiltrated; (e). 3/4 of the soil layer being infiltrated; (f). End of collapse.

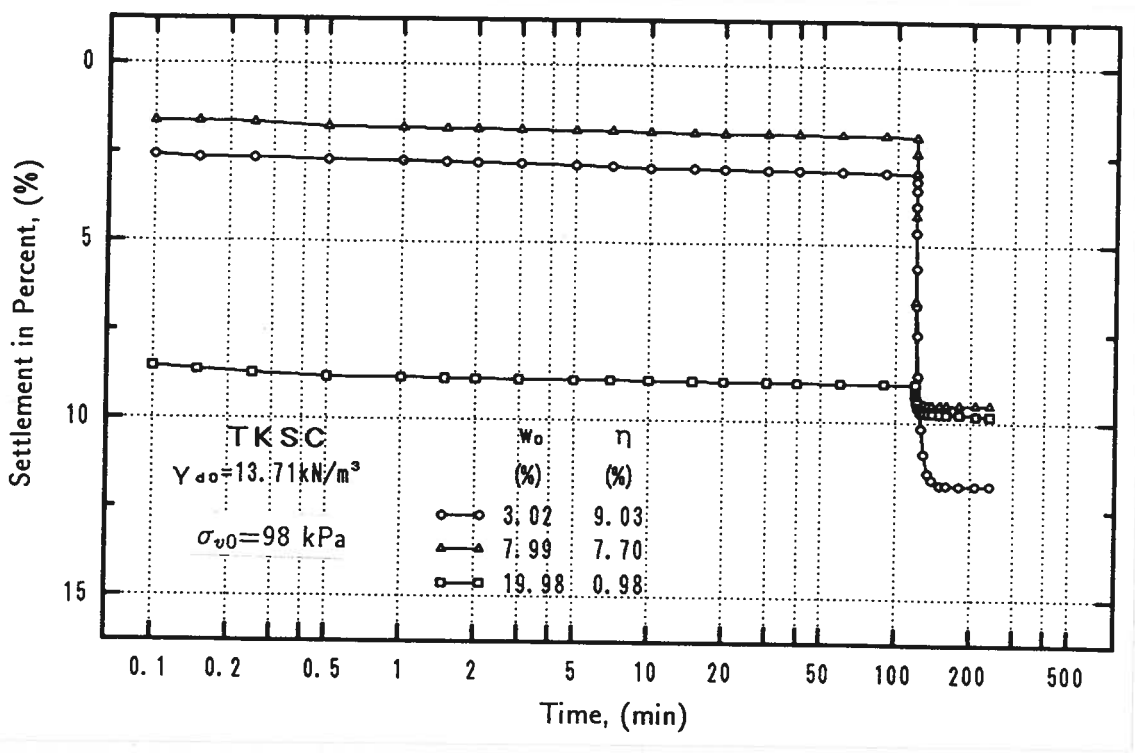

Figure 5.8: Time history of consolidation and collapse

cantly increase with decreasing water content at which sample has been compacted. The amount of consolidation is also affected by this molding water content. The higher the molding water content, the greater is the magnitude of consolidation deformation.

In order to illustrate the influence of molding water content on the amount of volume change before wetting, graphs are plotted as in Fig. 5.9 to 5.13, in which the dry unit weights of the specimens at molding and after consolidation (before inundation) are demonstrated as a function of the molding water content. The graphs show that the dry unit weight after consolidation changes with the variation of the molding water content, even though the specimens are almost of identical molding dry unit weights. With the increase in the molding water content, a minimum value of dry unit weight after consolidation appears; in other words, dry unit weight initially decreases and then increases as the molding water content increases. This is evident in specimens of low molding dry unit weights. The tendency of dry unit weight to first increase and then decrease with the increase in water content decreases as the molding dry unit weight increases. In the decreasing region, the change of the gradient of the dry unit weight is relatively smaller than that in the increasing region. In the increasing region, the increase in the dry unit weight with the increase in the molding water content is significant.

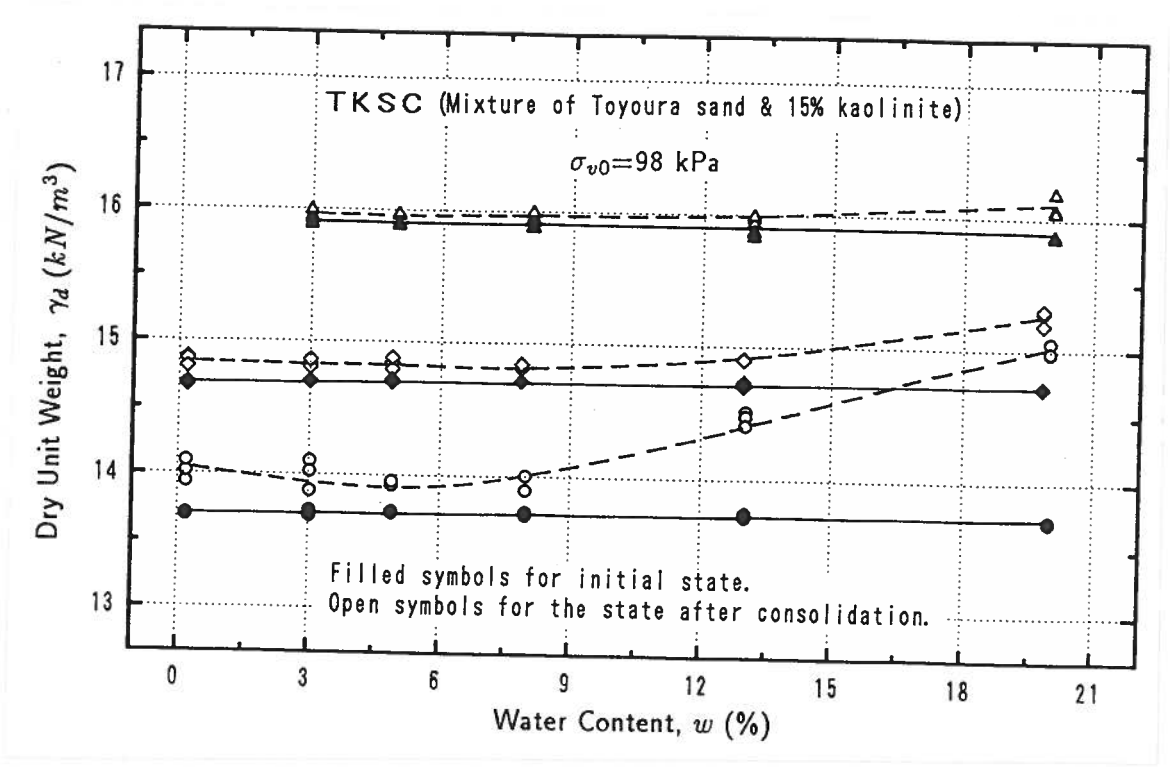

Figure 5.9: Change of dry unit weight during consolidation

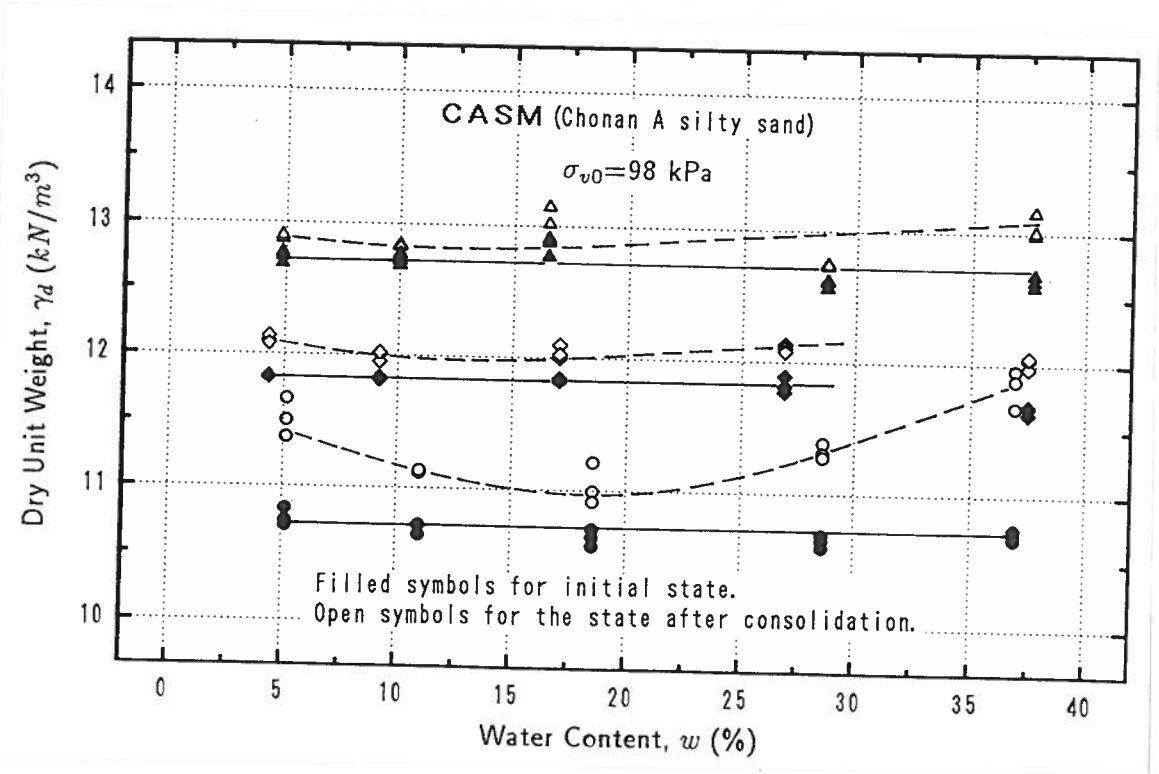

Figure 5.10: Change of dry unit weight during consolidation

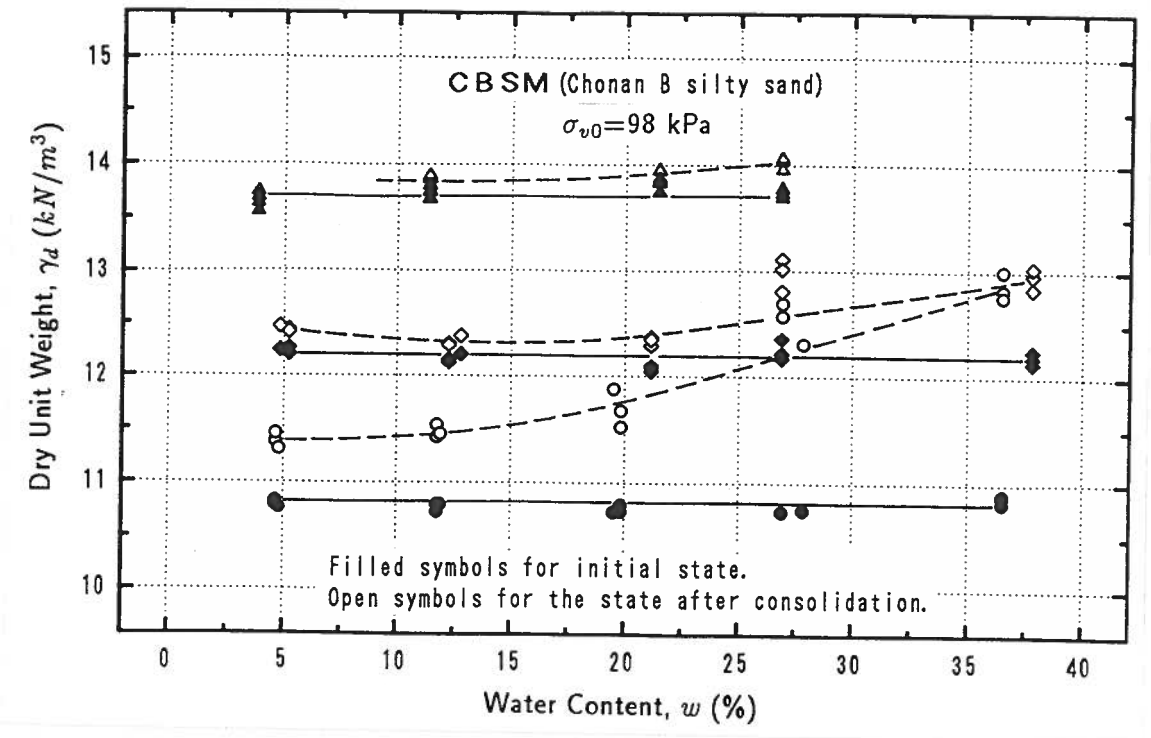

Figure 5.11: Change of dry unit weight during consolidation

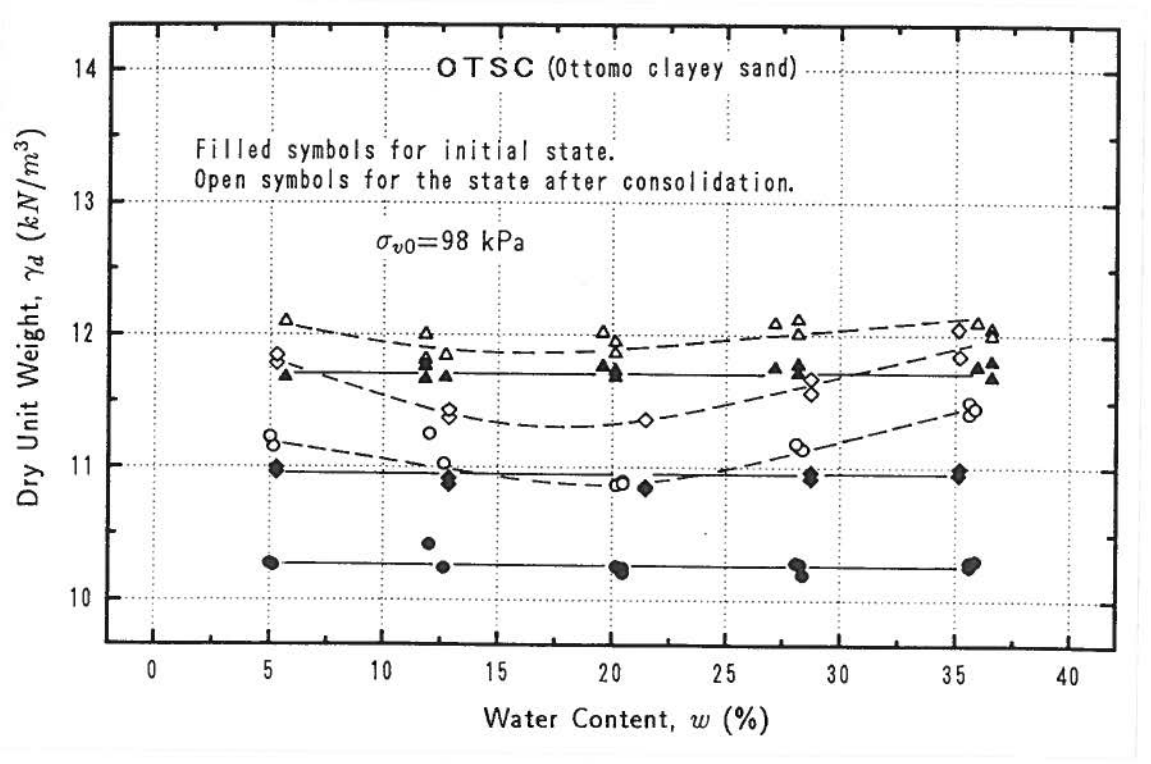

Figure 5.12: Change of dry unit weight during consolidation

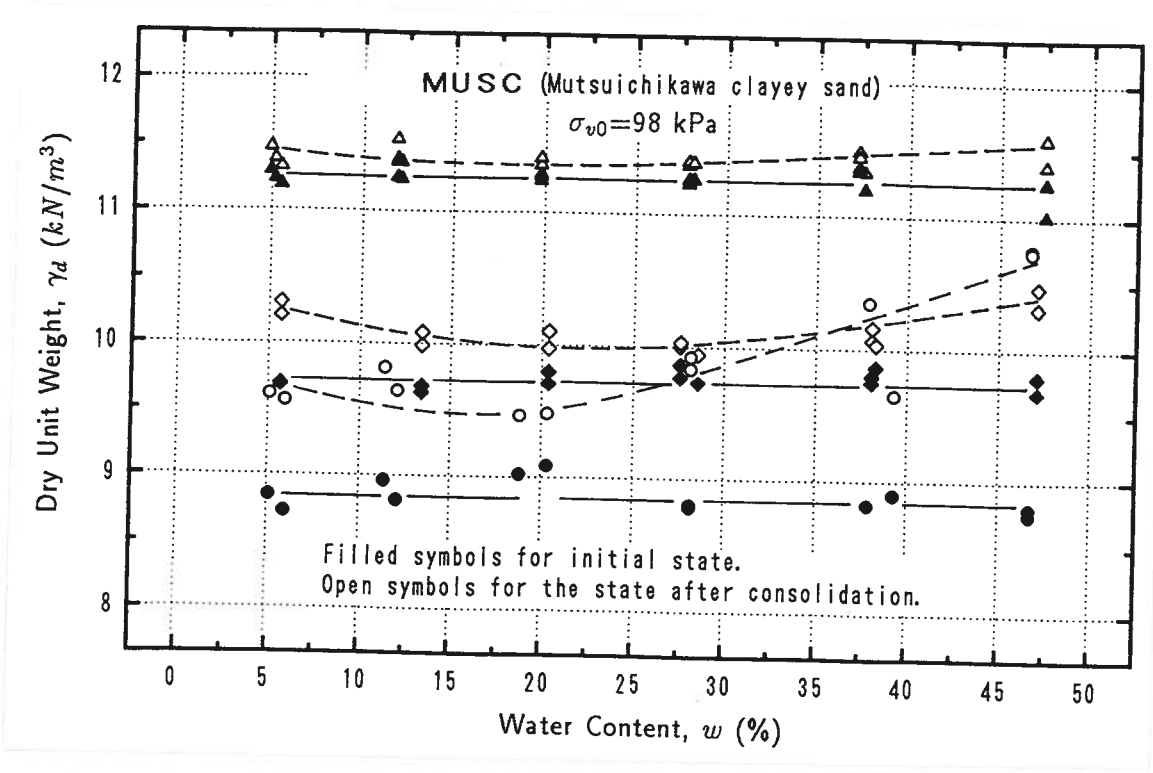

Figure 5.13: Change of dry unit weight during consolidation

This can be reasonably explained as a result of suction action (effective stress caused by suction). As moisture content in the soil increases from zero to a relatively large value (corresponding to degree of saturation of about 100%), three limits of suction action exist: the minimum limits of zero suction action occur at zero moisture content and at the moisture content in which the degree of saturation is 100%, and the maximum limit occurs at a certain moisture content–a critical value. When moisture content is less than this critical value, suction action, as well as the stiffness of the soil, increases as the moisture content increases and reaches the maximum value at this critical moisture content. When the moisture increases and exceeds the critical value , further increase in the moisture content reduces suction action. During the variation in suction action, the behavior of the soil changes from more compressible to less compressible and then to more compressible state. While in the case wherein the molding dry unit weight is relative high, soil behavior is more incompressible. Even if the moisture content is far from the critical value, the compression deformation is small and therefore, the difference in dry densities after consolidation is also small.

The existence of a critical moisture content at which the effect of suction action (the component of effective stress caused by capillary force) is maximum has been confirmed

by Aitchison and Donald (1956). They pointed out that for uniform spherical grains in an open or cubical packing (six contact points per grain) the maximum added pressure due to capillary effect occurs at a moisture content of about 32%. For the densest packing of these uniform spherical grains, the maximum added pressure occurs at about 10% moisture content. The effect drops off as the moisture content varies from the peak pressure condition.

The results of the *wetting test* series to examine the effects of water content at compaction under a given density are demonstrated for the five tested materials in Figs. 5.14 to 5.18, respectively, in terms of *Collapsibility Coefficient*, η, versus molding water content curves. It is to be noted that different compaction energies are employed in preparing

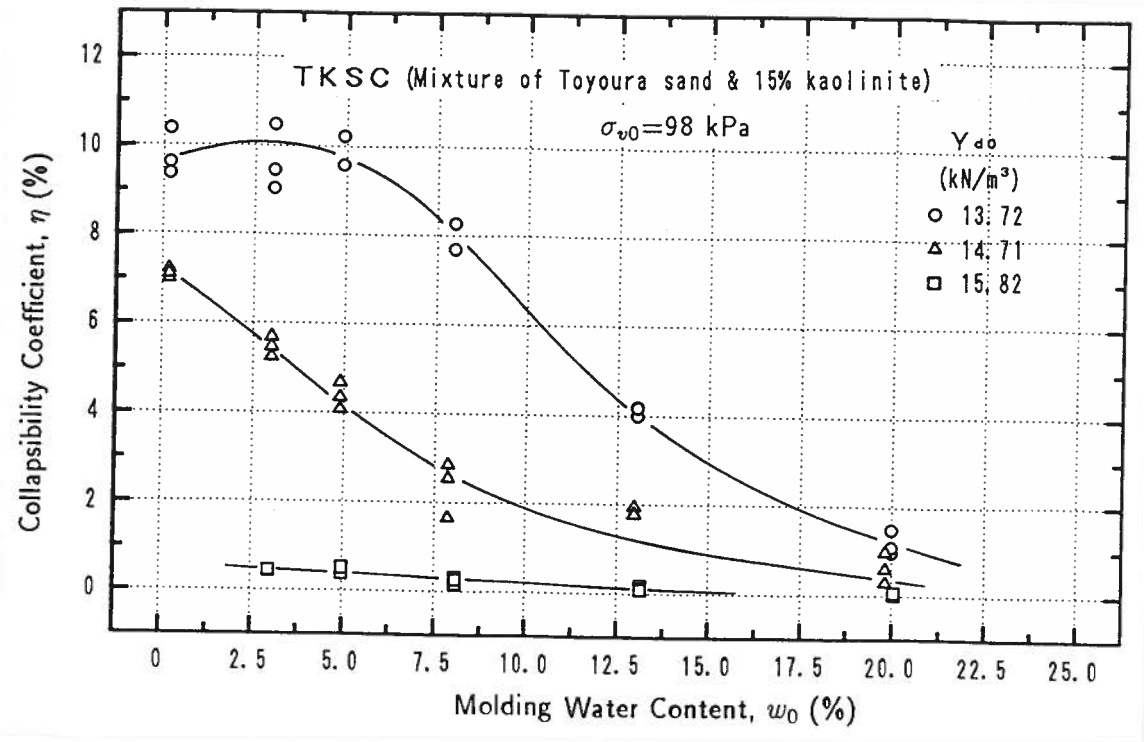

Figure 5.14: Effect of molding water content on collapsibility coefficient, η

specimens with different water contents while maintaining a constant density at compaction. In these figures, the effect of molding dry unit weight on the η versus molding water content curves for a constant overburden pressure is also illustrated. The graphs show that the amount of wetting-induced collapse under a given overburden pressure depends mainly on the water content and dry unit weight at which the soil has been compacted. It can generally be stated that the drier the soil at compaction, the larger is the amount of collapse due to soaking. This conclusion is identical with those obtained

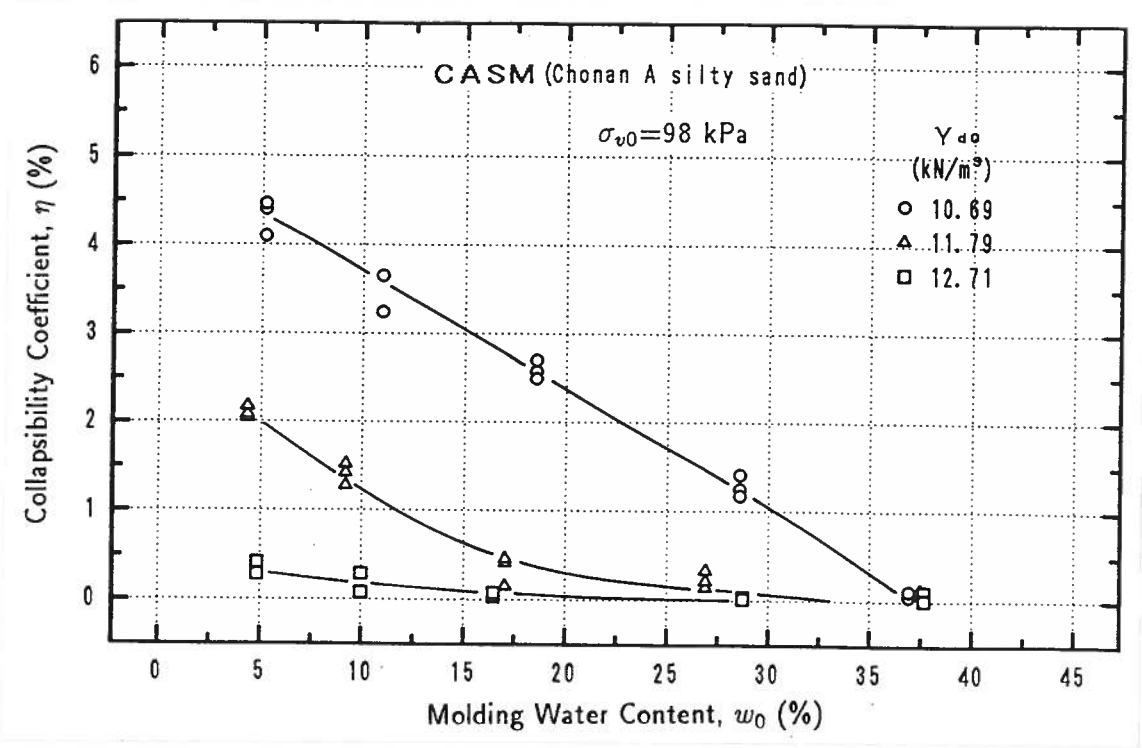

Figure 5.15: Effect of molding water content on collapsibility coefficient, η

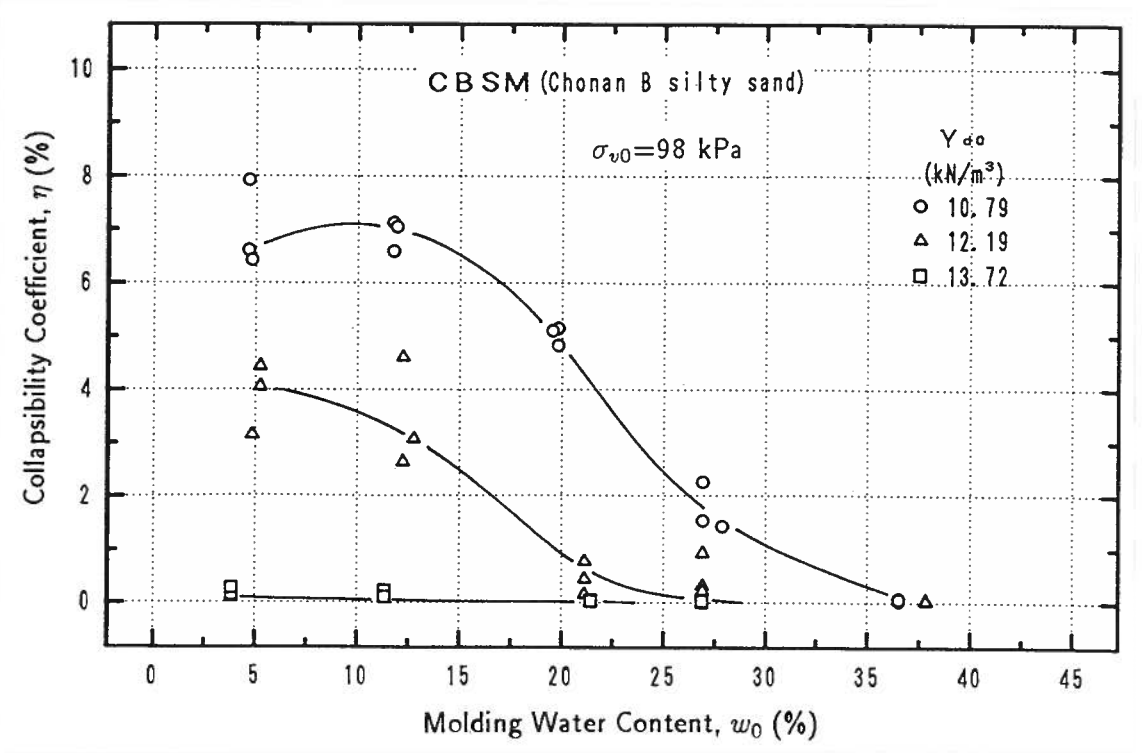

Figure 5.16: Effect of molding water content on collapsibility coefficient, η

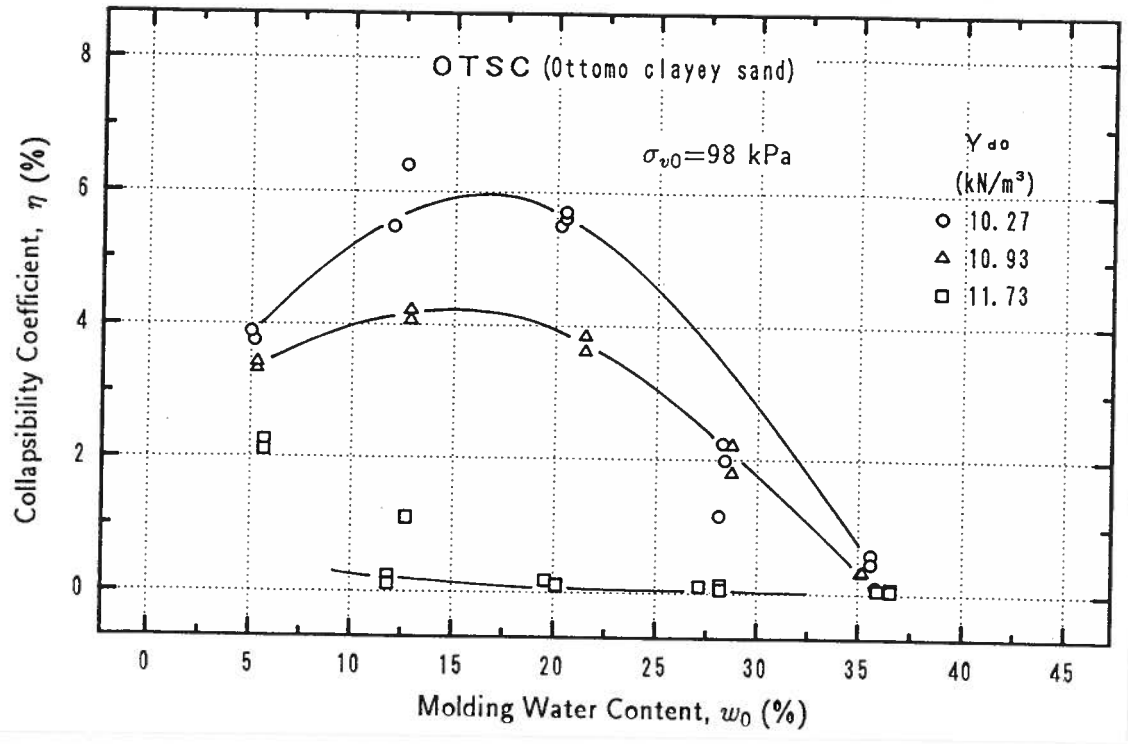

Figure 5.17: Effect of molding water content on collapsibility coefficient, η

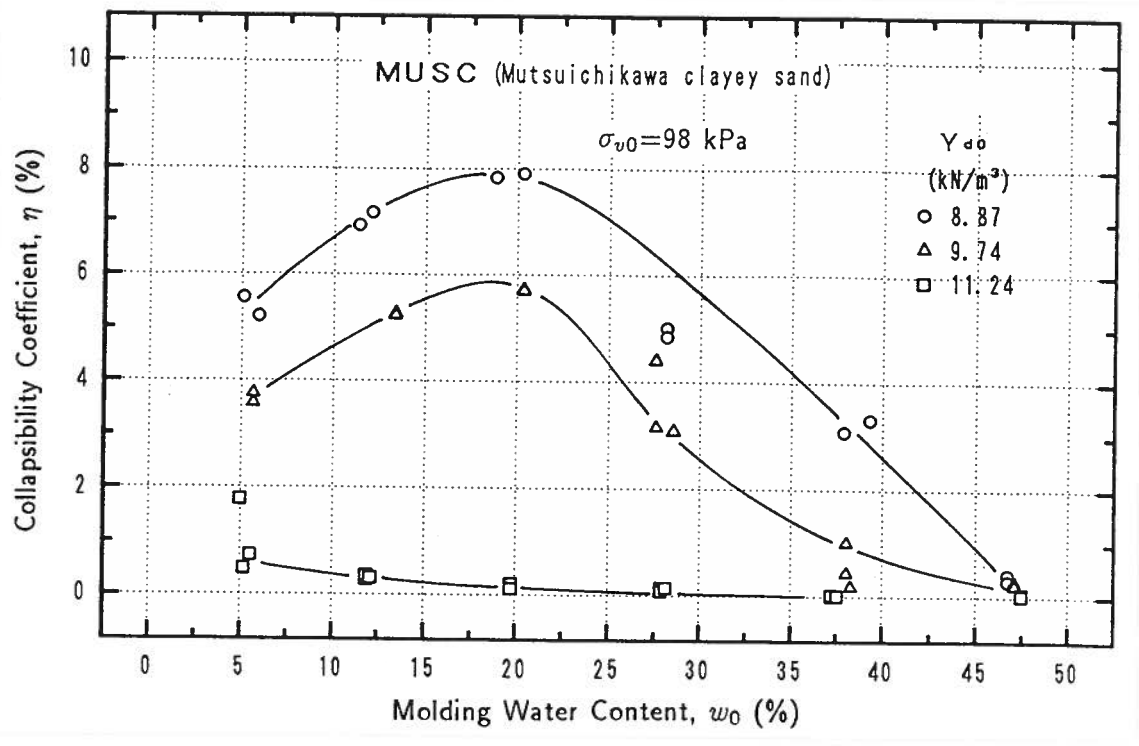

Figure 5.18: Effect of molding water content on collapsibility coefficient, η

by Booth (1975) and Lawton (1986). However, this is not true for the whole collapsible range of dry unit weight and for all the soils. Most of the soils, including the artificial mixture of Toyoura sand and 15% kaolinite, show that under low molding dry unit weight, there exists a critical value of molding water content, for a given dry unit weight, at which the wetting-induced collapse is maximum. When the water content at compaction is less than this critical water content, collapse increases as the water content increases; on the other hand, when the molding water content is larger than this critical value, collapse decreases with the increase in water content. The existence of an optimum water content at which maximum collapse occurs can be reasonably explained as the capillary effect. As discussed in the previous paragraphs, for specimens with the same molding dry unit weights but of varying moisture contents, the density after consolidation varies with the change in the moisture content and reaches a minimum value at a critical value of moisture content because of capillary effect. At the end of consolidation (before soaking), the soil in the region near the critical moisture content is looser and possesses more nominal strength than those outside this region. Upon inundation in water, this nominal strength is lost because of the disappearance of capillary effect. Therefore, sample collapses more than those outside the critical region. It can be seen that the critical value of moisture content is identical for both minimum after-consolidation dry unit weight and maximum collapse to occur.

It is noted that few literature can be found having given similar results. Although Dudley (1970) stated that the existence of an optimum moisture content for maximum collapse to occur, no test results can be found to support the statement. A probable reason that the existence of a critical value of moisture content has not been found by previous researchers is that their tests are performed on samples which are relatively dense and of relatively high water content and also the variation of soils employed. For example, the results of material *CASM* (Chonan A silty sand) used in this study do not show any critical value of moisture content. For this material, the relative compaction, which is defined as the ratio of any dry unit weight to the maximum dry unit weight obtained by standard proctor compaction test, $\gamma_d/(\gamma_d)_{pmax}$, at molding condition is greater than 70%, which is larger than other materials (except material *TKSC*).

It can be seen from Figs. 5.14 to 5.18 that beyond the critical value of moisture content, the amount of collapse decreases rapidly as the molding water content increases. For a given molding dry unit weight, there is a molding water content beyond which collapse will not occur. For materials *TKSC* (Mixture of Toyoura sand and 15% kaolinite), *CASM* (Chonan A silty sand) and *CBSM* (Chonan B silty sand), it is difficult to say that there is a critical molding water content beyond which no collapse will occur under all

the molding dry unit weight, while for materials *OTSC* (Ottomo clayey sand) and *MUSC* (Mutsuichikawa clayey sand), it seems that there exists a critical value of water content beyond which collapse will not occur under all the molding dry unit weight. These values are 37% and 47.5%, respectively.

In order to see the effect of molding dry unit weight on collapse, test results are plotted in terms of collapsibility coefficient, η, versus molding dry unit weight, as shown in Figs. 5.19 to 5.23. It is apparent that the looser the density at compaction, the larger the decrease in soaking-induced volume, and hence, the larger the value of η. It is noted in the figures that the change of η is different for different molding moisture contents. When the molding water content is relatively small, η initially decreases slowly and then rapidly as the dry unit weight increases; on the other hand, when the molding moisture content is high, the tendency changes to rapid and then followed by slow decrease with the increase in dry unit weight. However, no matter how η changes with dry unit weight, the $\eta \sim \gamma_{d0}$ curves tend to be concentrated to one point, which gives zero value of η. This has been found in all the materials tested, *i.e.*, for a given overburden pressure, there is a critical value of dry unit weight beyond which no volume change whatsoever will be caused in a soil upon inundation regardless of the molding water content. The critical values of dry unit weight, $(\gamma_d)_{crit}$, and the corresponding relative compaction, R_c, and relative density, D_r, are given in Table 5.2.

Table 5.2: Critical value of dry unit weight

	TKSC	CASM	CBSM	OTSC	MUSC
$(\gamma_d)_{crit}(kN/m^3)$	16.0	13.0	13.8	12.0	11.5
R_c (%)	90.6	85.0	83.6	76.6	80.6
D_r (%)	83.9	65.7	71.4	58.9	65.2

The same test results as those given in Figs. 5.14 to 5.18 can be re-expressed as a function of degree of saturation, S_r, as in Figs. 5.24 to 5.28 by using the following relationship:

$$S_r = \frac{w}{\frac{\gamma_w}{\gamma_d} - \frac{1}{G_s}} \tag{5.6}$$

The physical meaning of the signs in above equation is the same as those discussed in chapter 2. For a given a value of dry unit weight, γ_d, the degree of saturation can be computed by Eq. 5.6 for a known water content, w. The degree of saturation in the abscissa of Figs. 5.24 to 5.28 is obtained in this way from the water content values shown

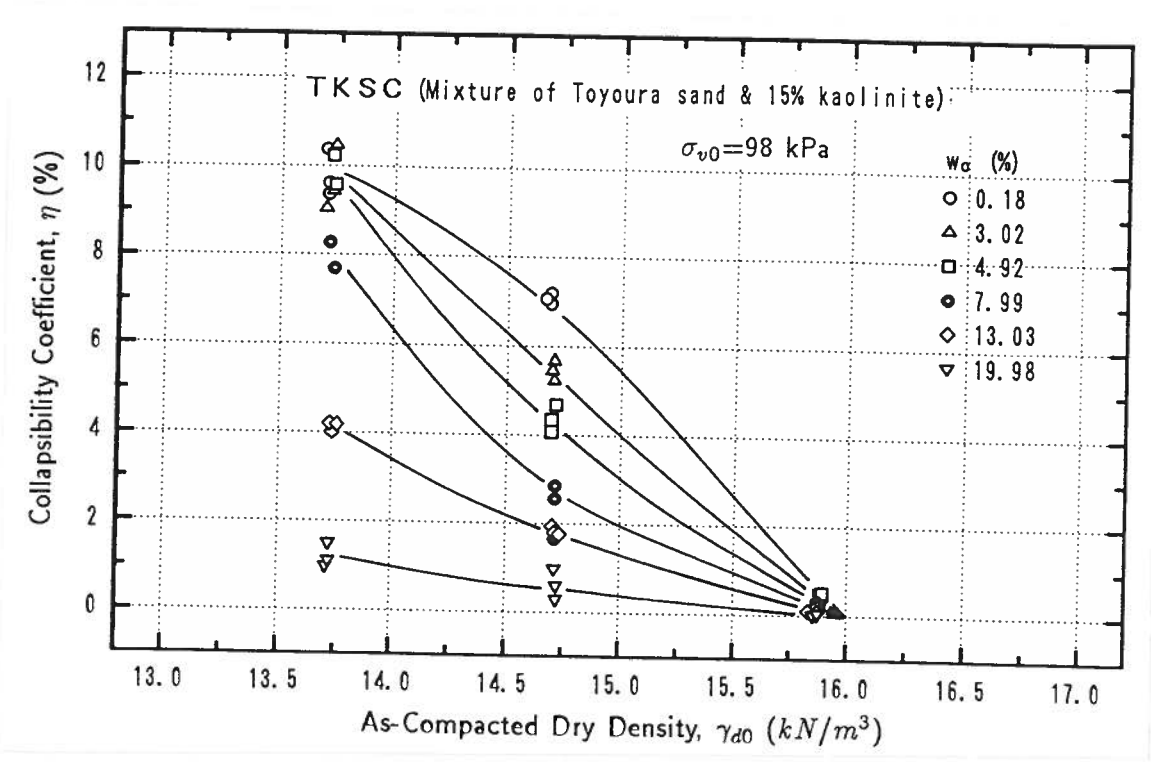

Figure 5.19: Effect of molding dry unit weight on collapsibility coefficient, η

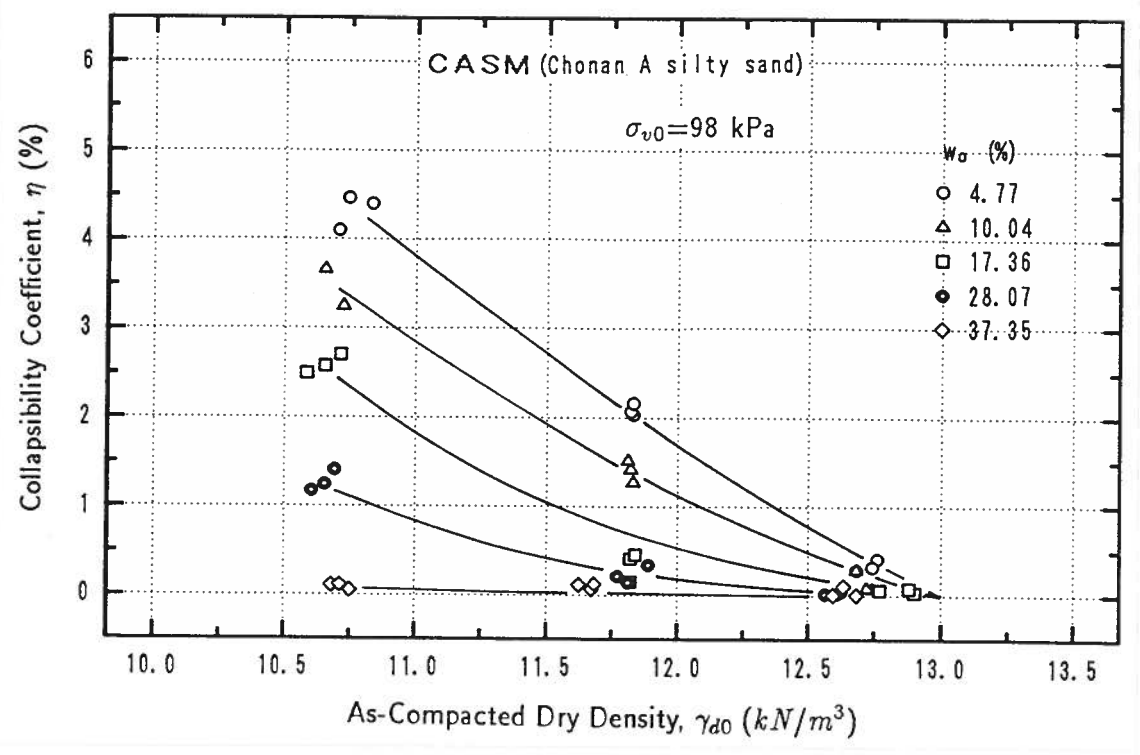

Figure 5.20: Effect of molding dry unit weight on collapsibility coefficient, η

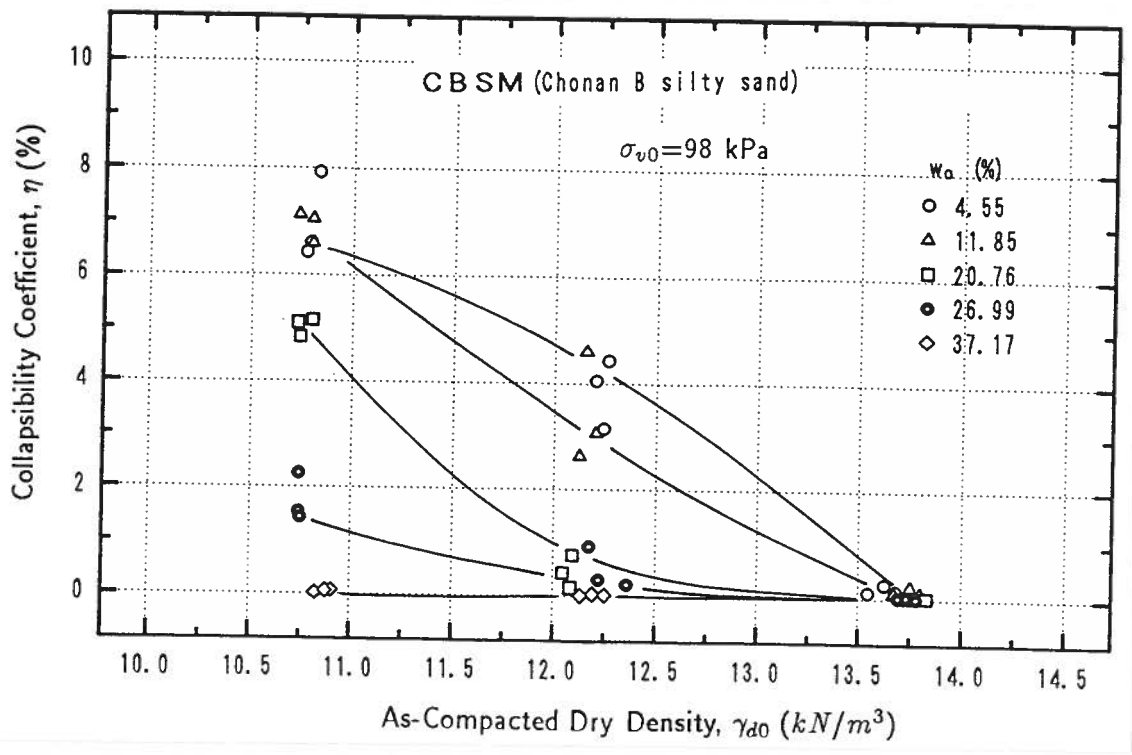

Figure 5.21: Effect of molding dry unit weight on collapsibility coefficient, η

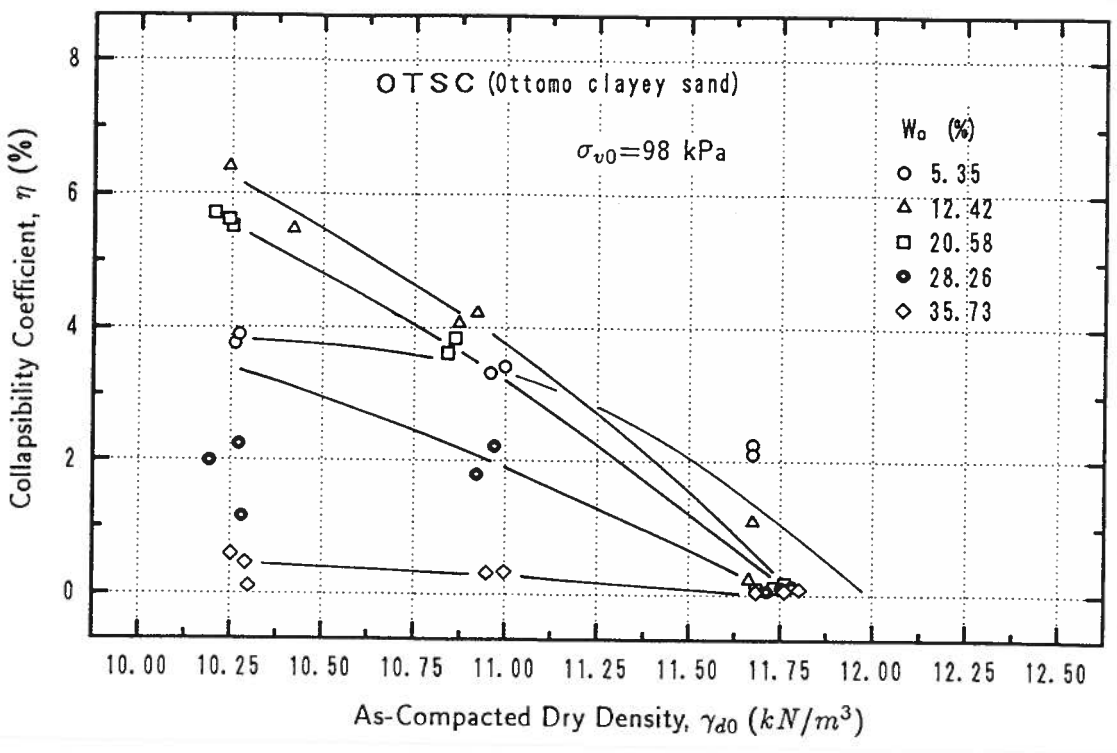

Figure 5.22: Effect of molding dry unit weight on collapsibility coefficient, η

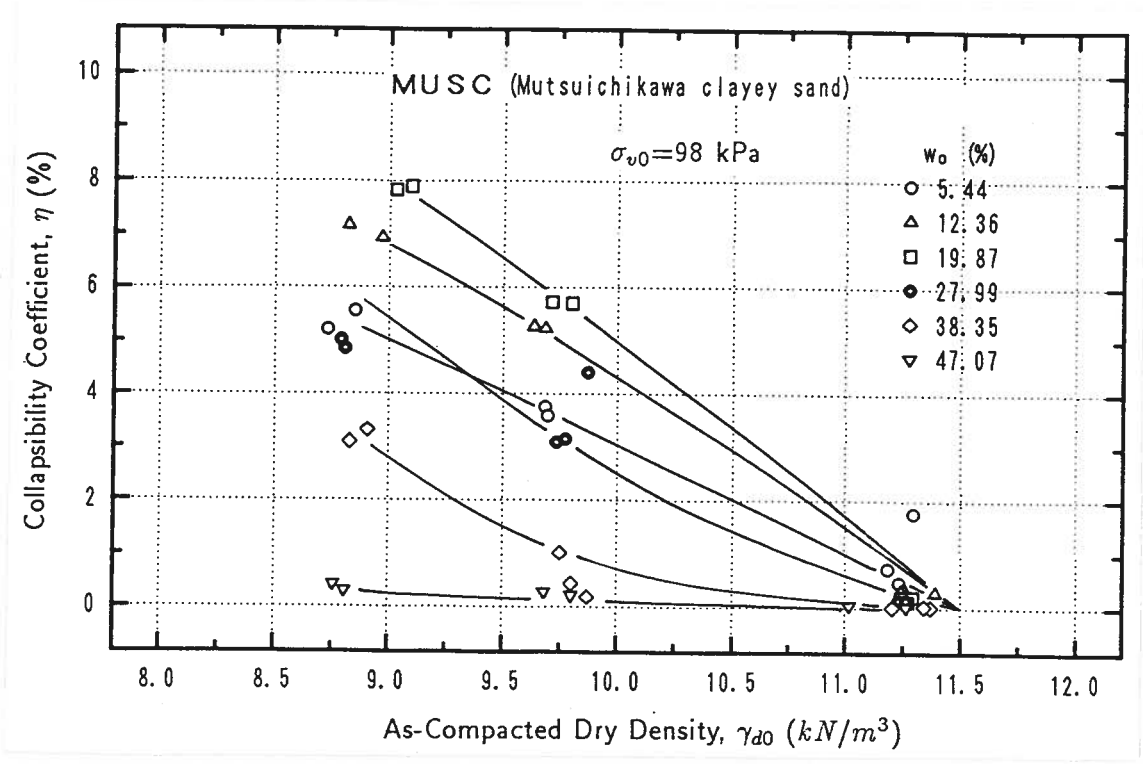

Figure 5.23: Effect of molding dry unit weight on collapsibility coefficient, η

in Figs. 5.14 to 5.18, respectively. Figs. 5.24 to 5.28 indicate the characteristic relationship among the collapsibility coefficient, the degree of saturation and the as-compacted density of the materials tested under the external overburden pressure of $\sigma_{v0} = 98kPa$. It is apparent that the conclusions from the effect of as-compacted moisture content are also suitable, *i.e.*, there is a value of degree of saturation at which the amount of collapse is maximum. Collapse decreases as degree of saturation varies from this value. The decrease in the amount of collapse is more rapid if the degree of saturation is larger than this value. The difference is that there exists a critical value of degree of saturation for each tested material at which no collapse will take place if the molding degree of saturation is larger than this critical value, no matter what the value of the as-compacted density is. These critical values for the tested materials are given in Table 5.3.

Table 5.3: Critical value of degree of saturation

	TKSC	CASM	CBSM	OTSC	MUSC
$S_r(\%)$	80	70	70	72	75

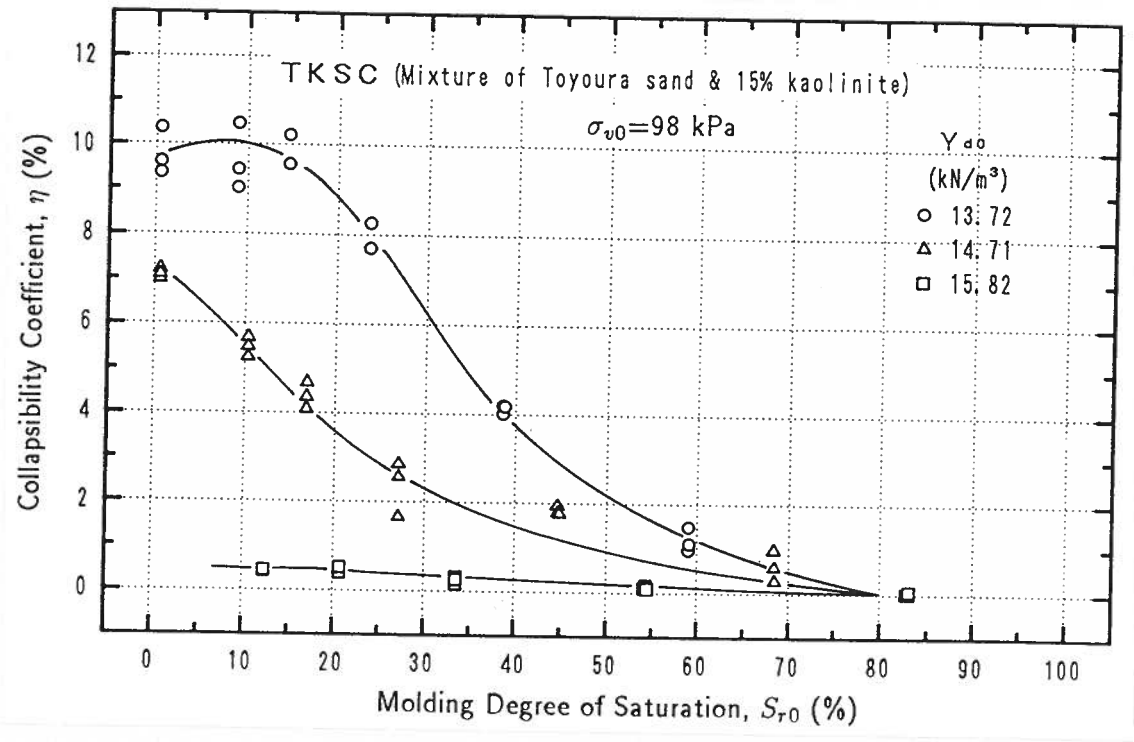

Figure 5.24: Effect of degree of saturation on collapsibility coefficient, η

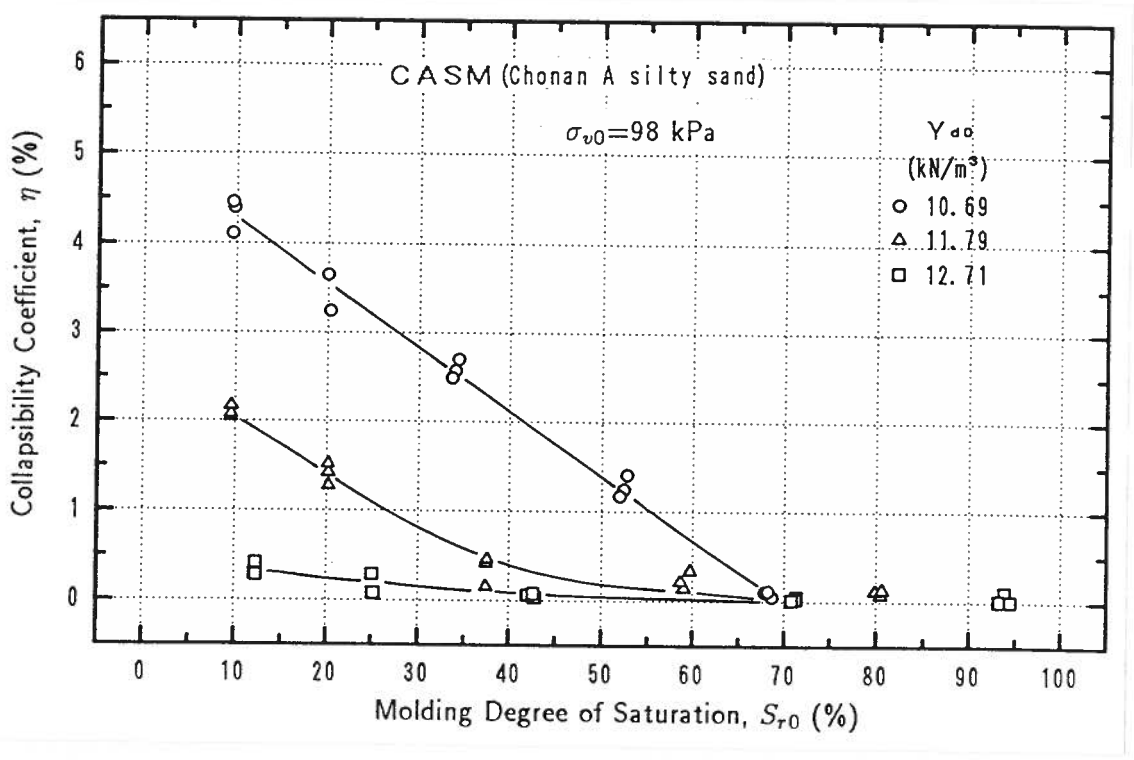

Figure 5.25: Effect of degree of saturation on collapsibility coefficient, η

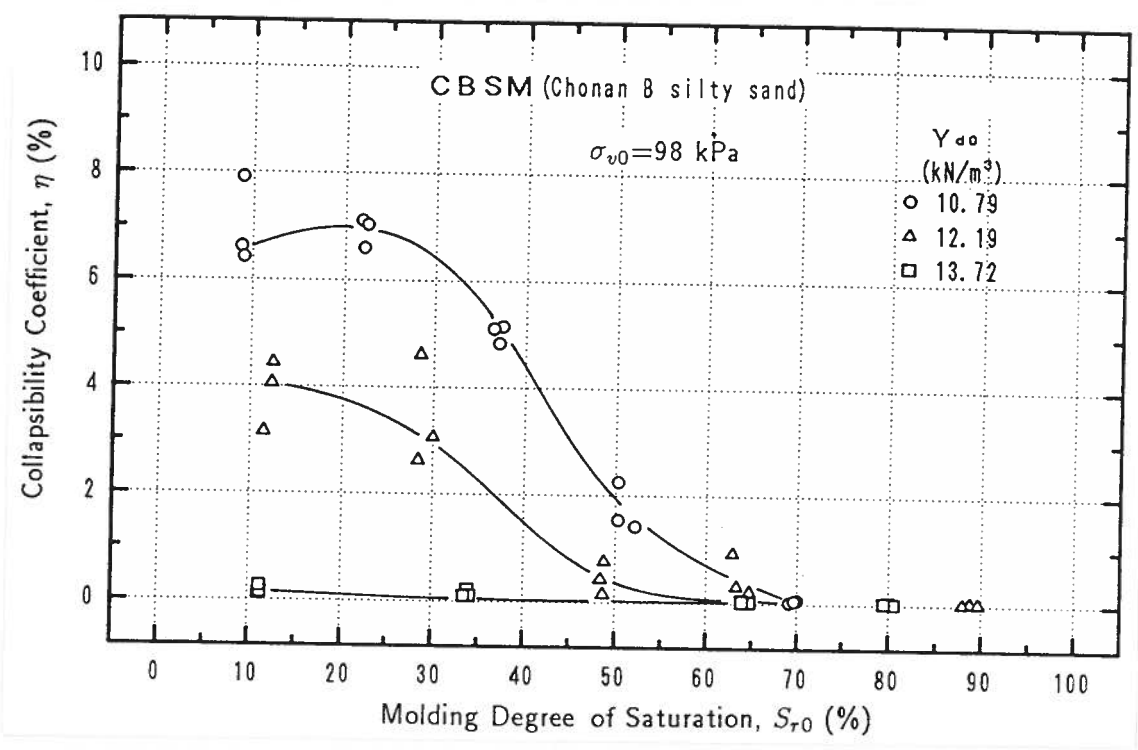

Figure 5.26: Effect of degree of saturation on collapsibility coefficient, η

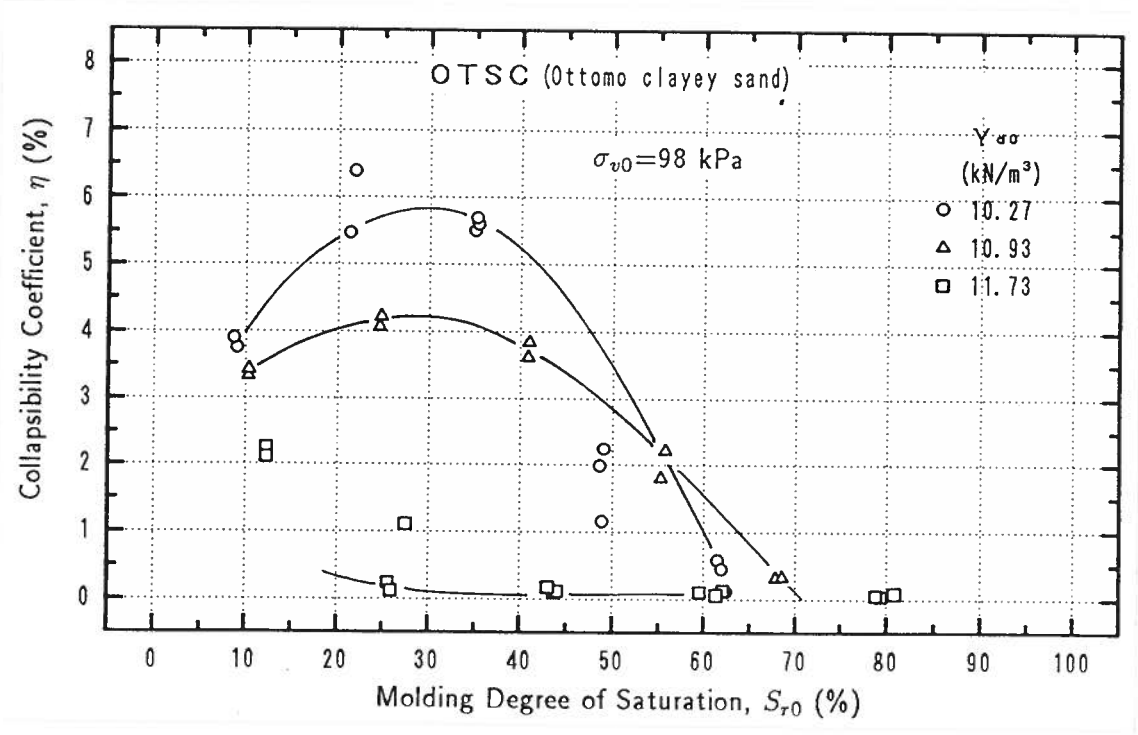

Figure 5.27: Effect of degree of saturation on collapsibility coefficient, η

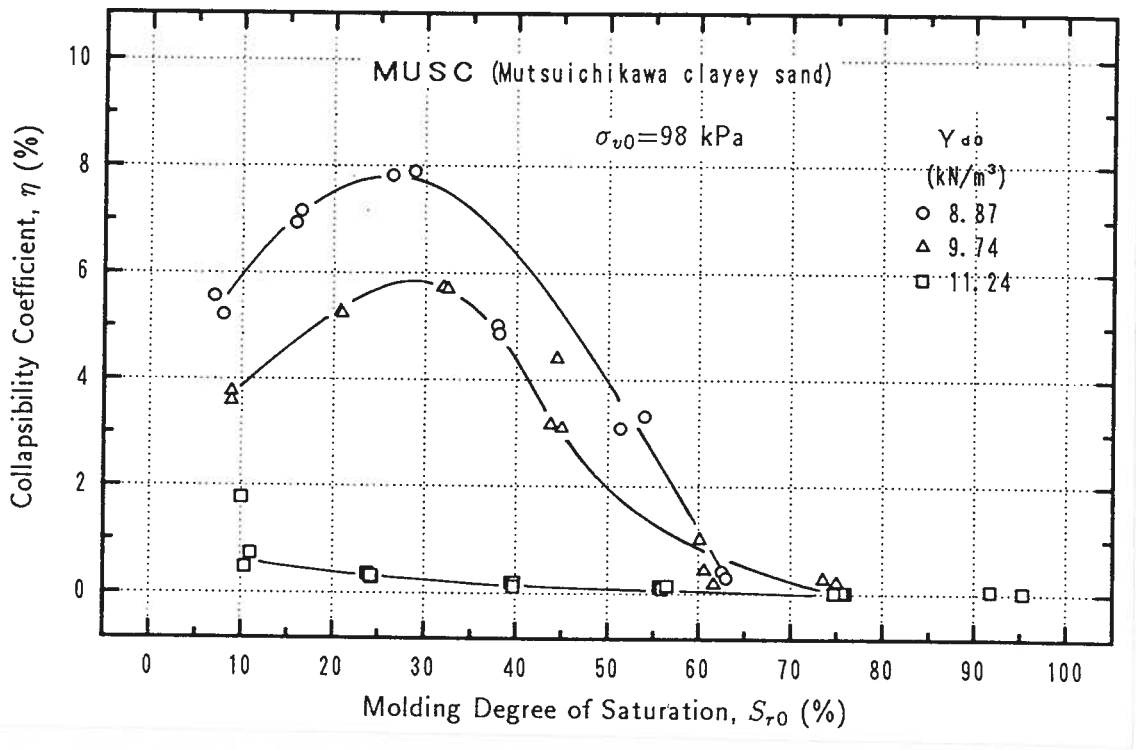

Figure 5.28: Effect of degree of saturation on collapsibility coefficient, η

As discussed above, the consolidation deformation is different because of the difference of suction effect at different molding water contents. This means that the dry unit weight before soaking is different even if it is identical in molding condition. In order to clarify whether the dry unit weight before soaking is a better parameter in investigating the effect on collapse, it is chosen as an independent variable of collapse. The results are shown in Figs. 5.29 to 5.33. The figures indicate that all the conclusions obtained from $\eta \sim \gamma_{d0}$ curves are suitable. The curves of different molding content appear to be closer to each other than those in $\eta \sim \gamma_{d0}$ plane. This is because the difference among the degrees of saturation is smaller after consolidation than before consolidation. If the test is run in such a way that the samples are prepared with different initial conditions but go to identical condition of density or saturation after consolidation, the results will be the same as in $\eta \sim \gamma_{dc}$ plane. However, the test is much difficult to control than those which require controlling only the initial conditions. Therefore, the molding dry unit weight is good enough as a parameter in studying the influence on collapse in compacted soils.

The results of the hydraulic collapsibility tests shown in Figs. 5.14 to 5.23 can be displayed alternatively in a form of contours of equal η as a function of as-compacted dry unit weight and water content. In fact, it is easy to read off the combination of

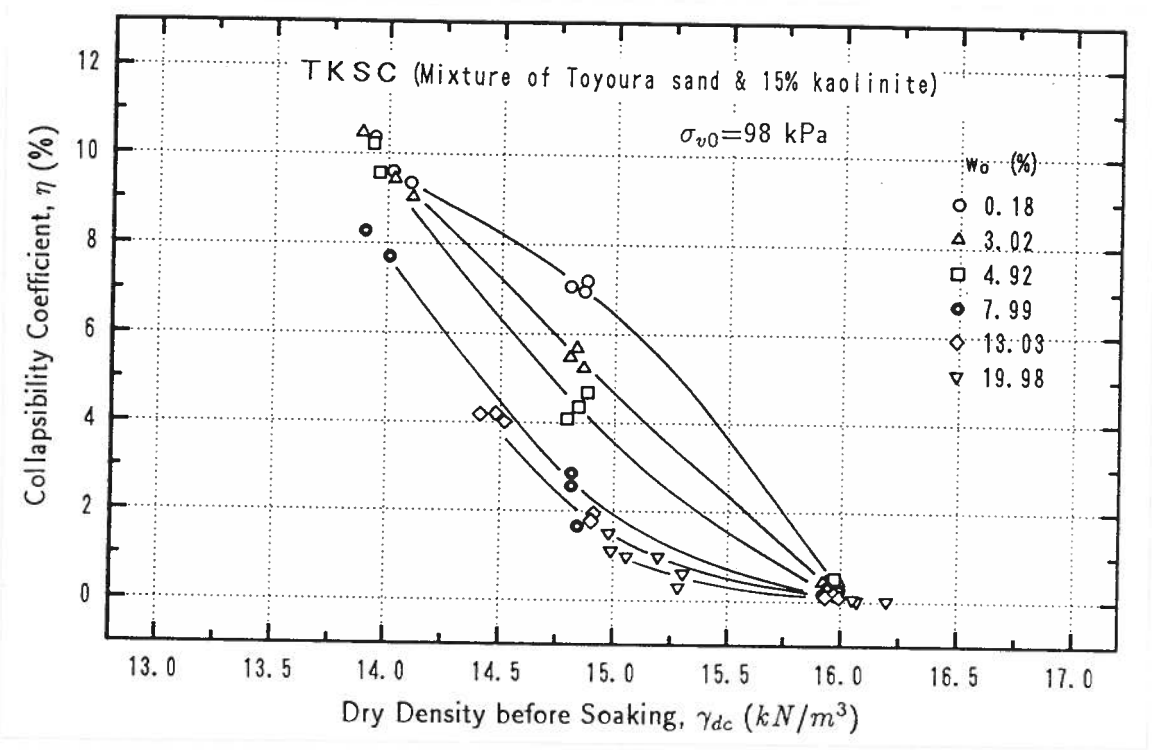

Figure 5.29: Effect of dry unit weight before wetting on collapsibility coefficient, η

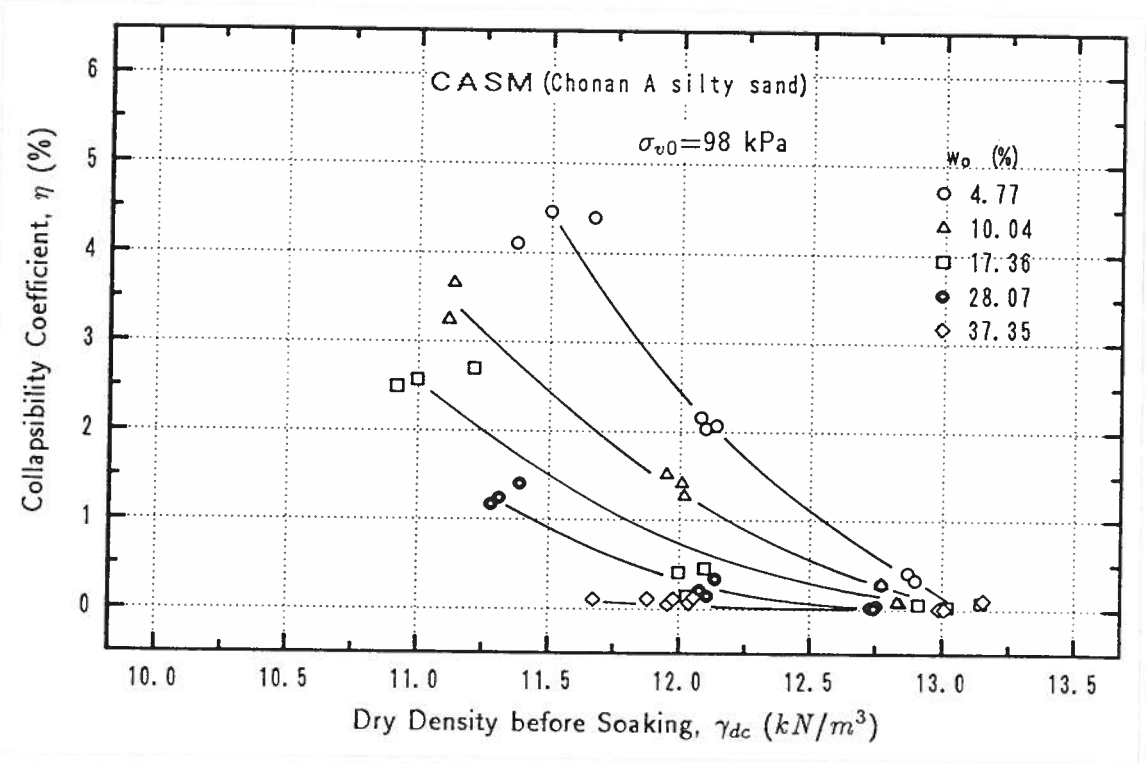

Figure 5.30: Effect of dry unit weight before wetting on collapsibility coefficient, η

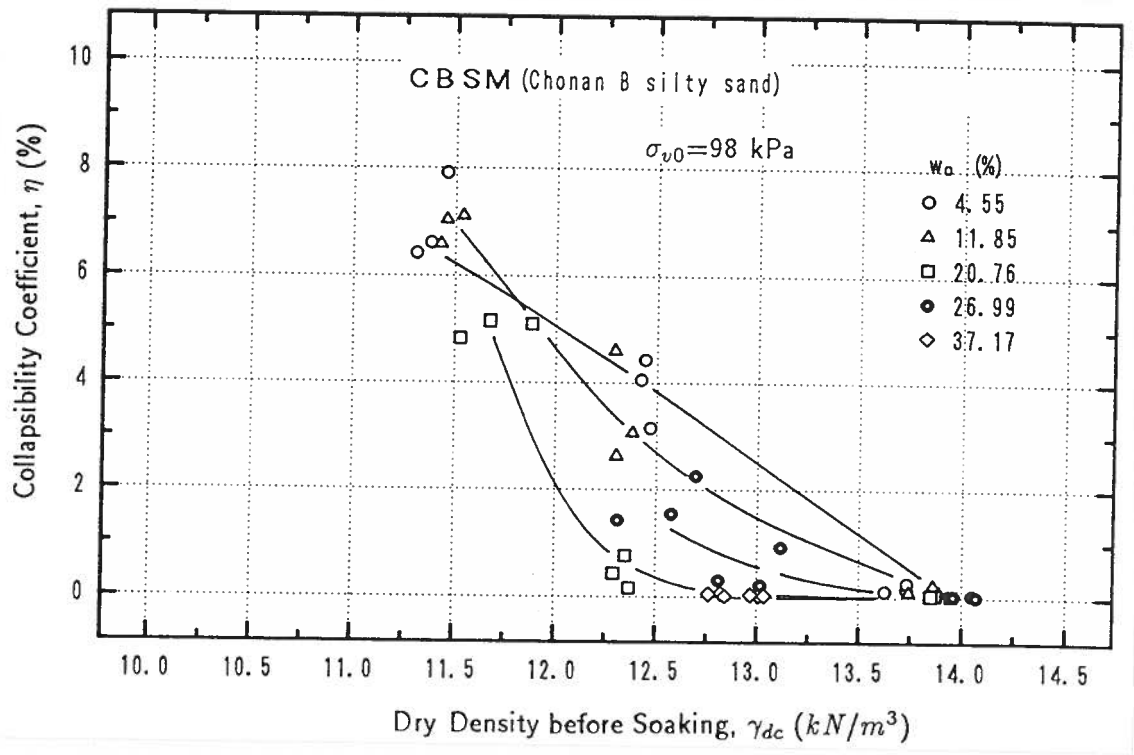

Figure 5.31: Effect of dry unit weight before wetting on collapsibility coefficient, η

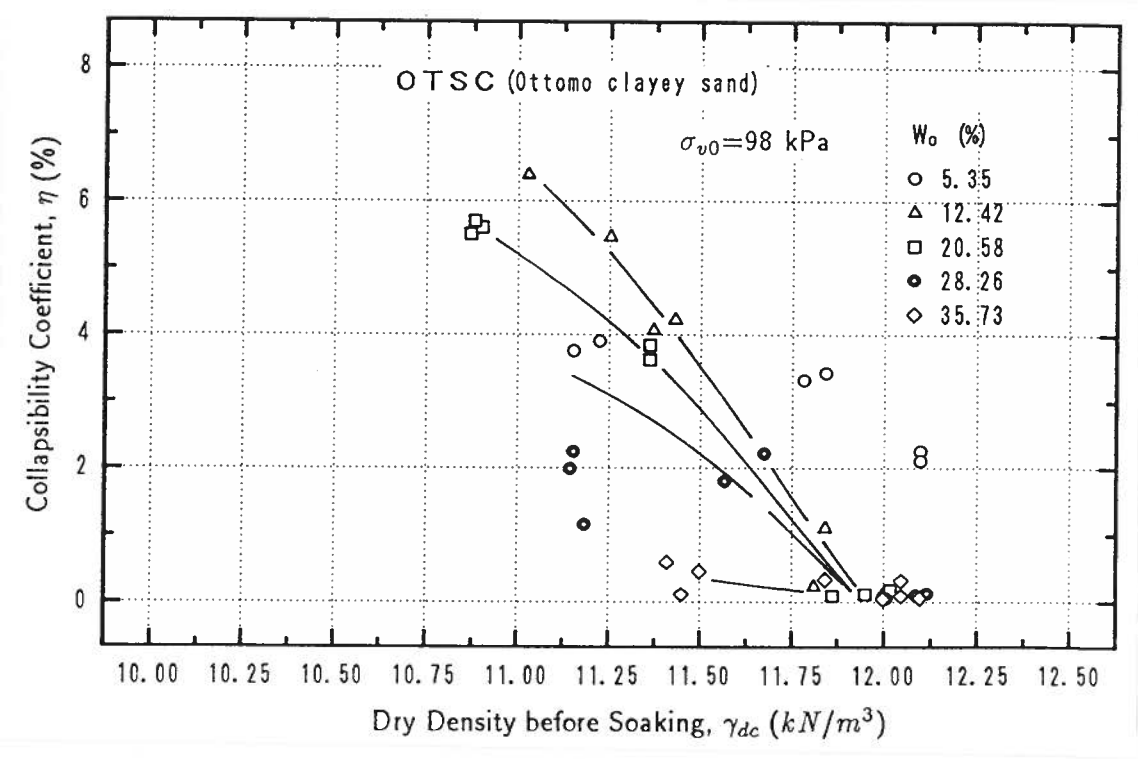

Figure 5.32: Effect of dry unit weight before wetting on collapsibility coefficient, η

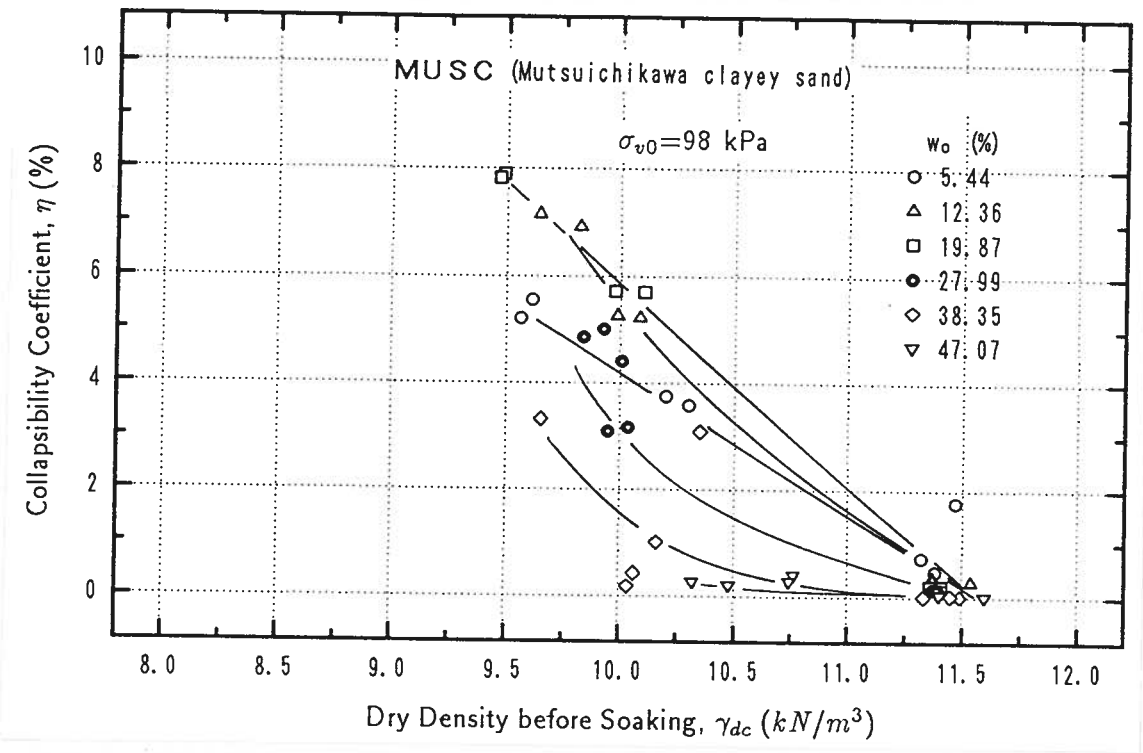

Figure 5.33: Effect of dry unit weight before wetting on collapsibility coefficient, η

η and water content, w, on equal density lines and the combination of η and density, γ_d, on equal water content lines. Pairs of such data are laid down in $\gamma_d \sim w$ plane to draw up a family of contour lines giving equal value of collapsibility coefficient. The results are shown in Figs. 5.34 to 5.38. The characteristic shape of the curves in these figures is similar to those of Booth's and Lawton's contours of equal volume change for non-expansive and expansive soils, respectively. However, a difference exists among the results. In Booth's results, the existence of an upper limit of dry unit weight for the occurrence of collapse is not presented. On the other hand, Lawton's results show that the upper limit of degree of saturation which collapse can occur does not exceed the line of optimum. The results from this study show that there exists an upper limit of both as-compacted dry unit weight and degree of saturation at which collapse can occur. The upper limit of the degree of saturation may exceed the line of optimum, depending on the type of soil. The difference may be due to the difference of soil types used in the corresponding studies. In fact, the shape of contours in this study is more like Booth's in the region of relatively low density, while in the region of relative high density, it is more like Lawton's. It is also to be noted that the shape of contours is different for different soils. For materials *TKSC* (Mixture of Toyoura sand and 15% kaolinite), *CASM* (Chonan

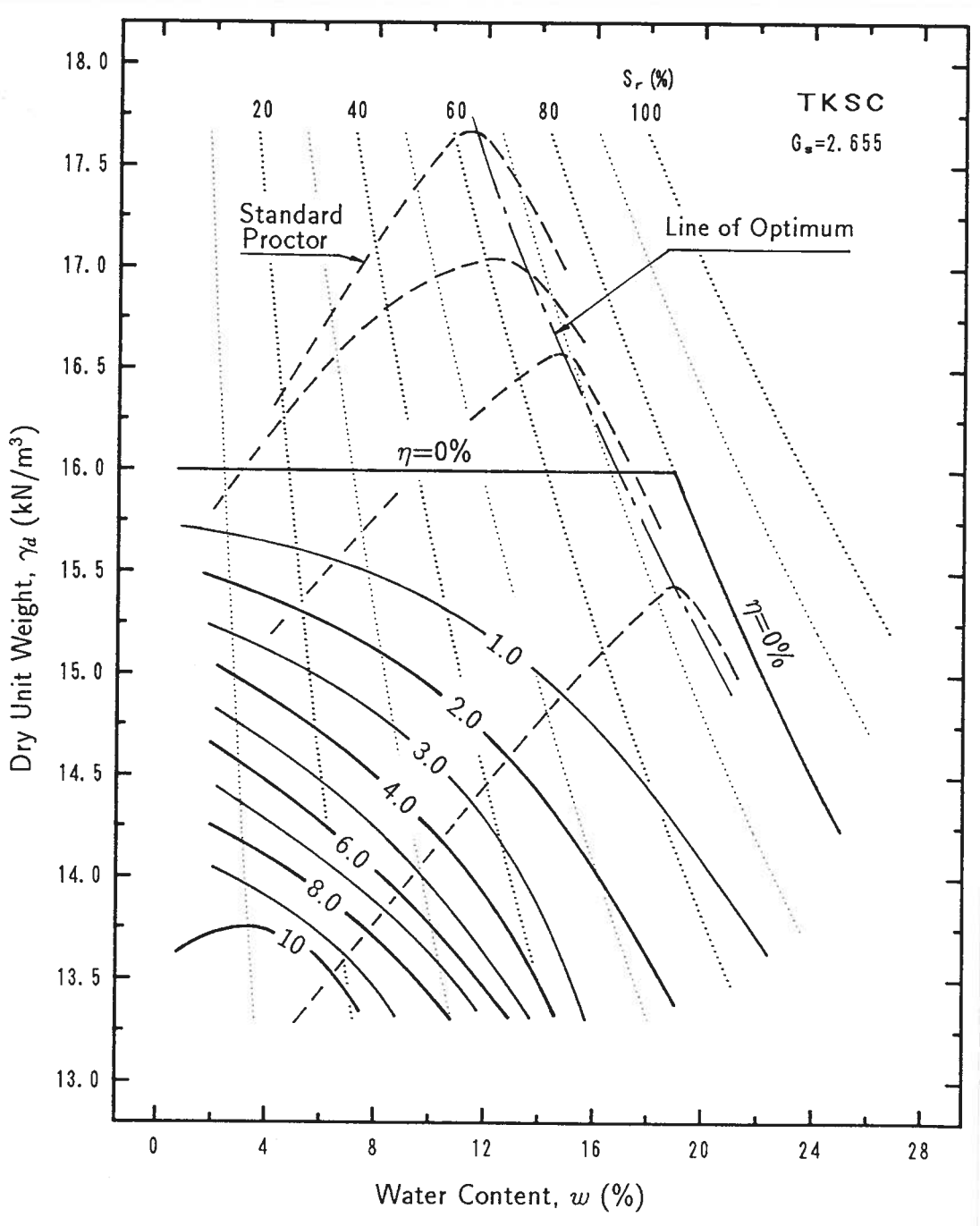

Figure 5.34: Isogram of equal collapsibility coefficient as a function of molding dry unit weight and water content

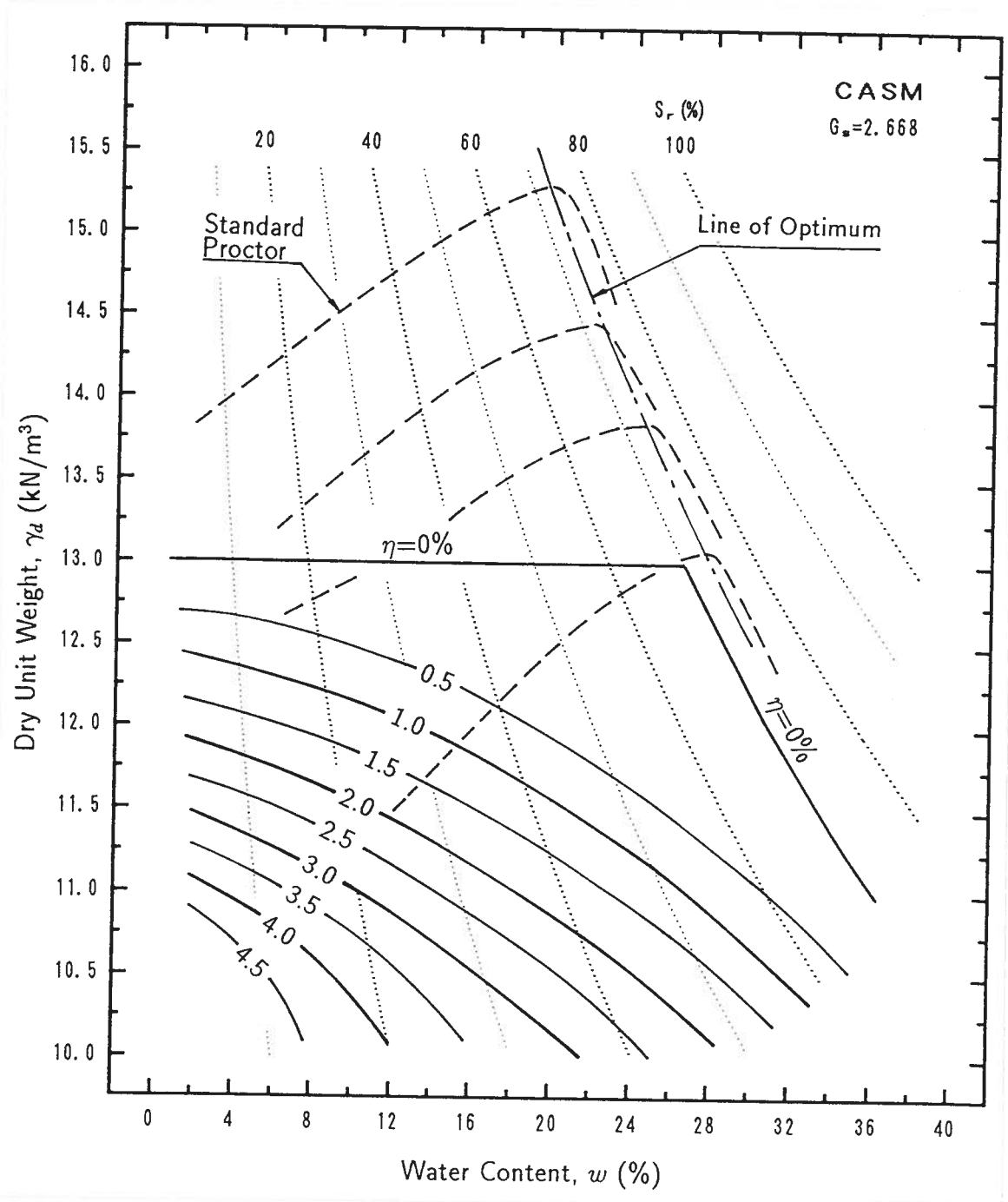

Figure 5.35: Isogram of equal collapsibility coefficient as a function of molding dry unit weight and water content

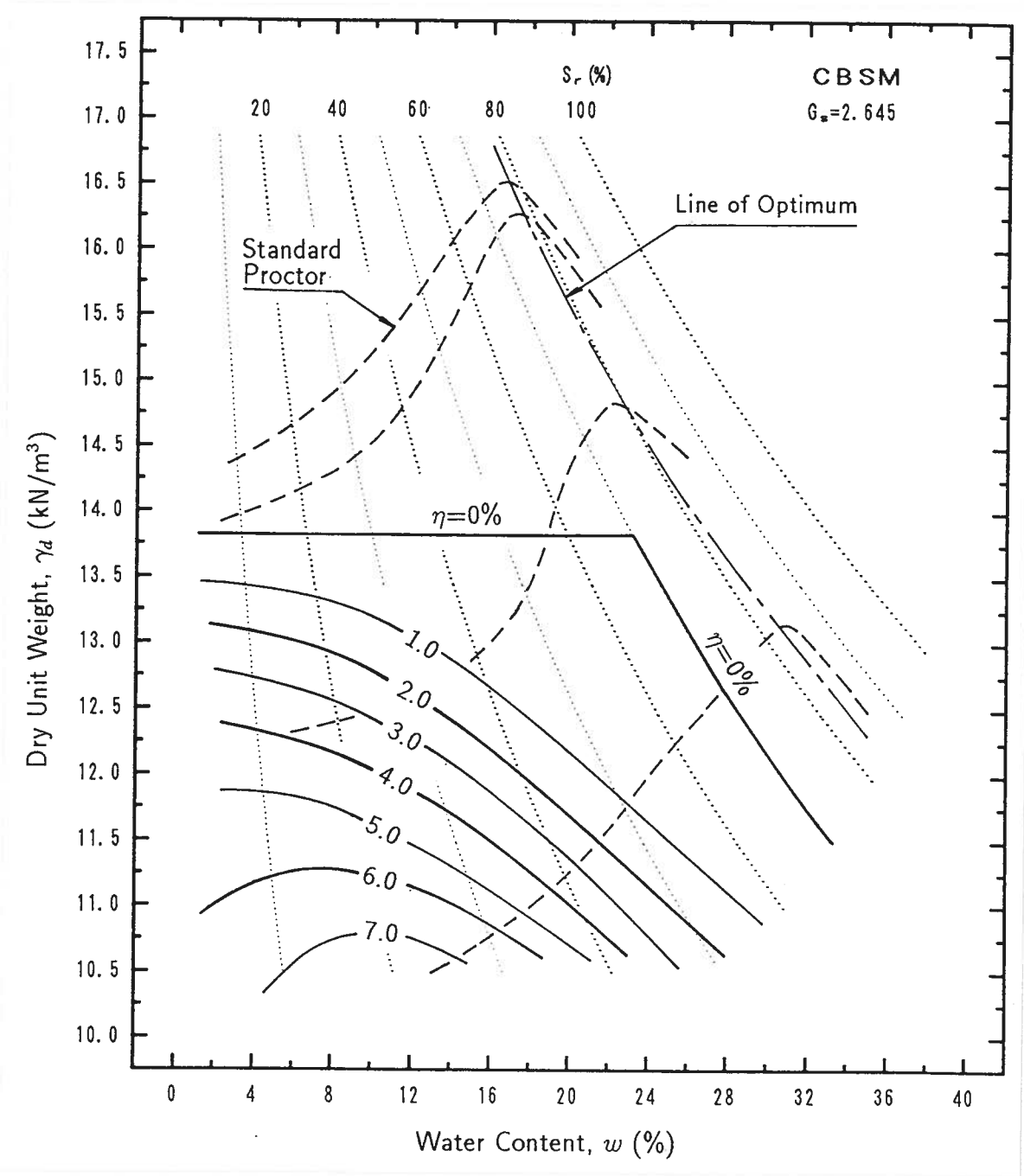

Figure 5.36: Isogram of equal collapsibility coefficient as a function of molding dry unit weight and water content

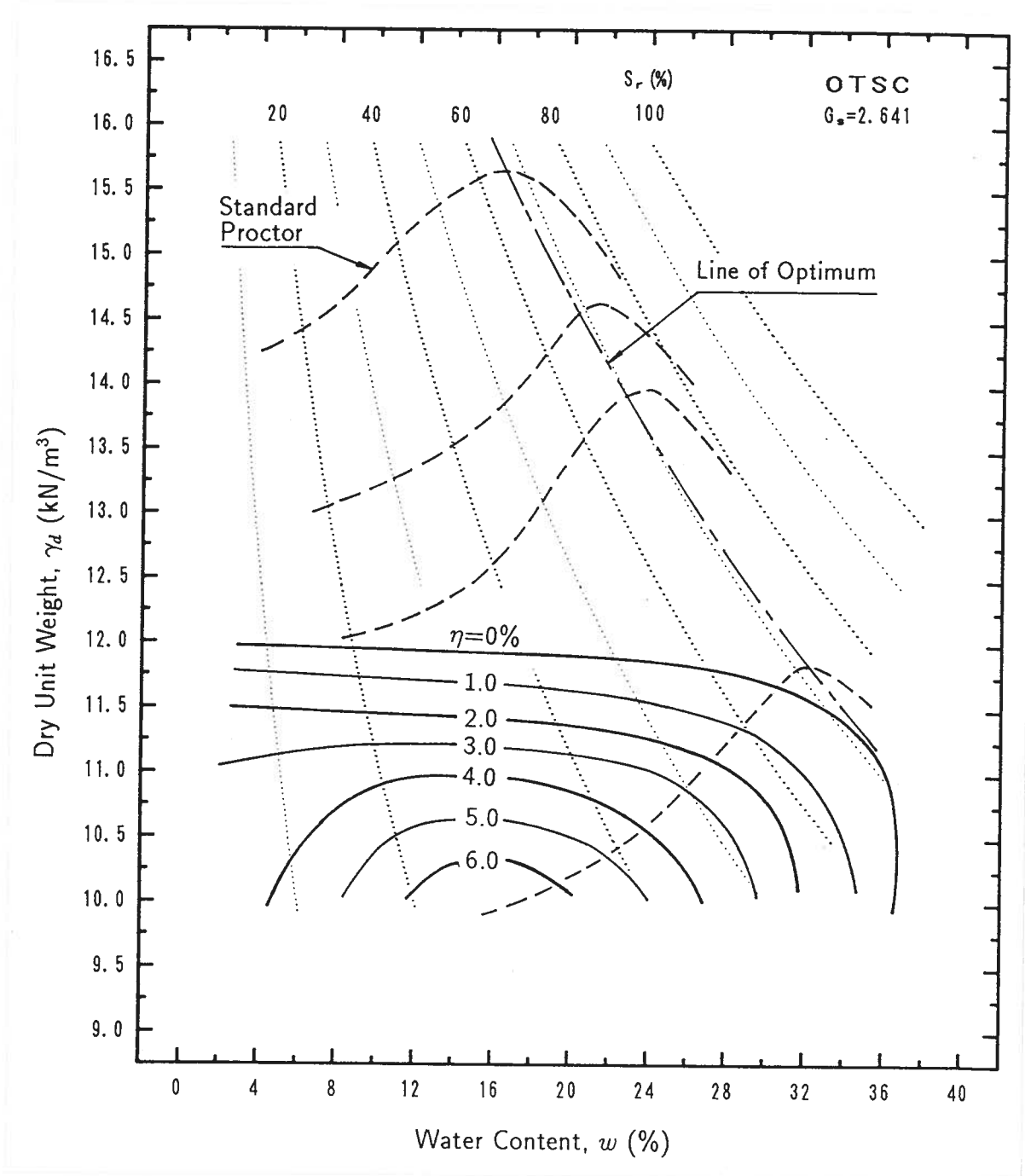

Figure 5.37: Isogram of equal collapsibility coefficient as a function of molding dry unit weight and water content

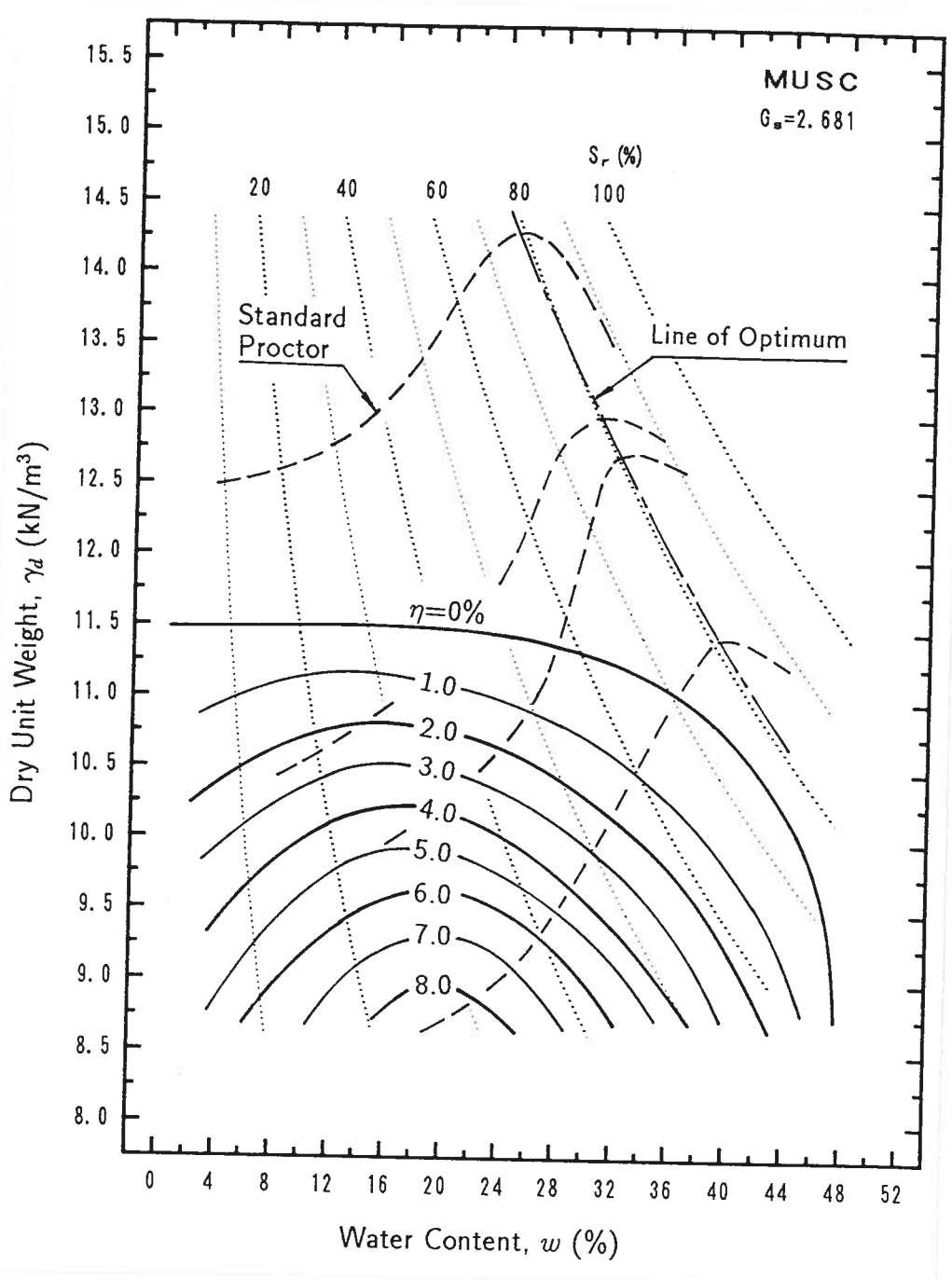

Figure 5.38: Isogram of equal collapsibility coefficient as a function of molding dry unit weight and water content

A silty sand) and *CBSM* (Chonan B silty sand), the change of collapsibility coefficient with water content is rapid even at relatively high dry unit weight. On the other hand, for materials *OTSC* (Ottomo clayey sand) and *MUSC* (Mutsuichikawa clayey sand), the change of collapsibility coefficient with water content is relatively slow at relatively high dry unit weight and rapid at low dry unit weight.

It seems from the test results shown in Figs. 5.34 to 5.38 that for a soil under certain overburden pressure, there exists a critical state of molding water content and dry unit weight at which the magnitude of collapse is maximum. The amount of collapse at all the other state of water content and density will never exceed this value. This is because under a given overburden pressure, there is a minimum value of dry unit weight which comes from the loosest state of soil; in other words, if a sample is prepared to be of the loosest state of density, the density will come to a certain value after being consolidated at the given overburden pressure and obtaining stress equilibrium. This value of density is the minimum value of soil which can exist at the given overburden pressure. It will yield the maximum value of collapse.

5.4 INFLUENCE OF OVERBURDEN PRESSURE

A second series of test are performed on the same materials (except material *CASM*) as in the *wetting test* using the so-called *double-oedometer* test method. This test is not conducted on material *CASM* (Chonan A silty sand) because the material has been used up. The results from a *double-oedometer* test are plotted as in Fig. 5.39, in which the void ratio is shown as a function of the overburden pressure for the samples tested at both molding and saturated conditions. The collapsibility coefficient is the ratio of the difference of void ratios between the two curves to the unit volume before soaking, $(1+e_c)$. The predicted collapsibility coefficient of all the tests are presented in Figs. 5.40 to 5.47 as function of the overburden pressure. To illustrate the correlation of the two methods, several wetting tests have been conducted under overburden pressures 30, 98 and 294 kPa. The results are illustrated in Figs. 5.40, 5.41, 5.42, 5.43, 5.44, and 5.45 by filled symbols. The results show that although there are some difference among the results, the two methods are comparable.

The effect of overburden on collapse are clearly demonstrated in these figures. For a given molding dry unit weight and water content, there is a critical overburden pressure at which the magnitude of collapse is maximum. The more the overburden pressure deviates from this critical value, the smaller the collapse. This is reasonable because compacted soil behaves as over-consolidated soil. For over-consolidated soil, there exists

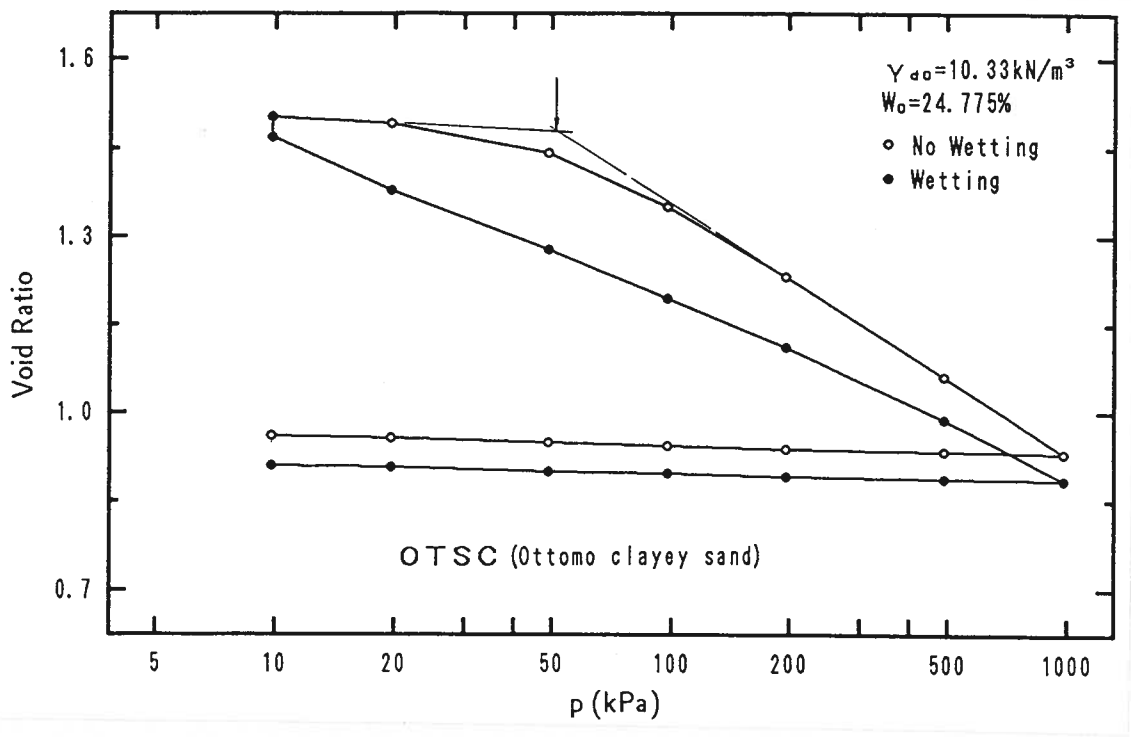

Figure 5.39: Typical compression curves of samples in molding and saturated states

a pre-stress, p_0, beyond which the compressibility of soil becomes much higher than at stress levels less than this value. On the other hand, soaked sample is more likely to behave as a normally consolidated soil. Although its compressibility is higher at low pressure than that of unwetted sample, its compressibility increases slowly as the consolidation pressure increases. This can be seen in Fig. 5.39. Therefore, a critical pressure at which the maximum collapse can take place is evident. It is noticeable that this critical pressure decreases significantly as the molding water content increases. This is because the pre-stress decreases as the moisture increases, and this is shown in Fig. 5.48 for materials *OTSC* (Ottomo clayey sand) and *MUSC* (Mutsuichikawa clayey sand).

The results given in Figs. 5.49 to 5.54 illustrate the effect of molding water content on collapse under different overburden pressures. It is noted that the critical value of molding moisture content at which maximum collapse occurs at specified overburden pressure is also evident in the results. This critical value decreases as the overburden pressure increases. This is because for specimens having the same moisture content and dry unit weight, and one is loaded under a larger overburden pressure, this specimen will show more compression during the process of consolidation and possesses higher degree of saturation after consolidation. The effect of capillary will decrease because of high

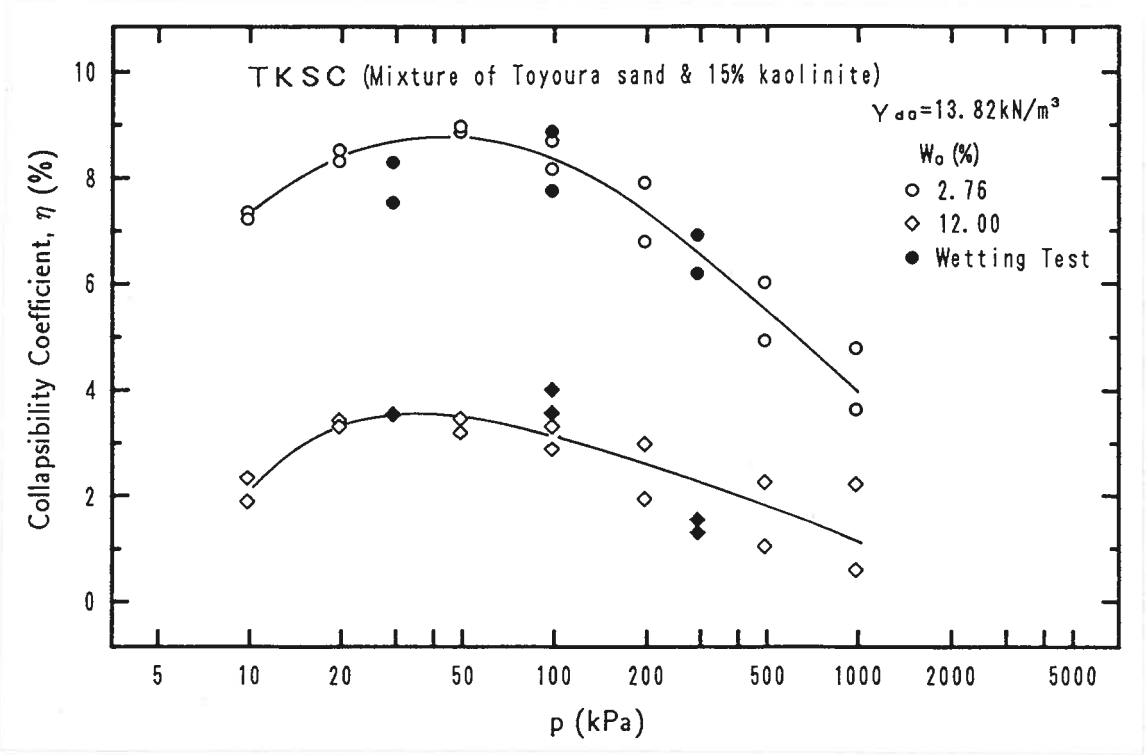

Figure 5.40: Collapsibility versus overburden pressure

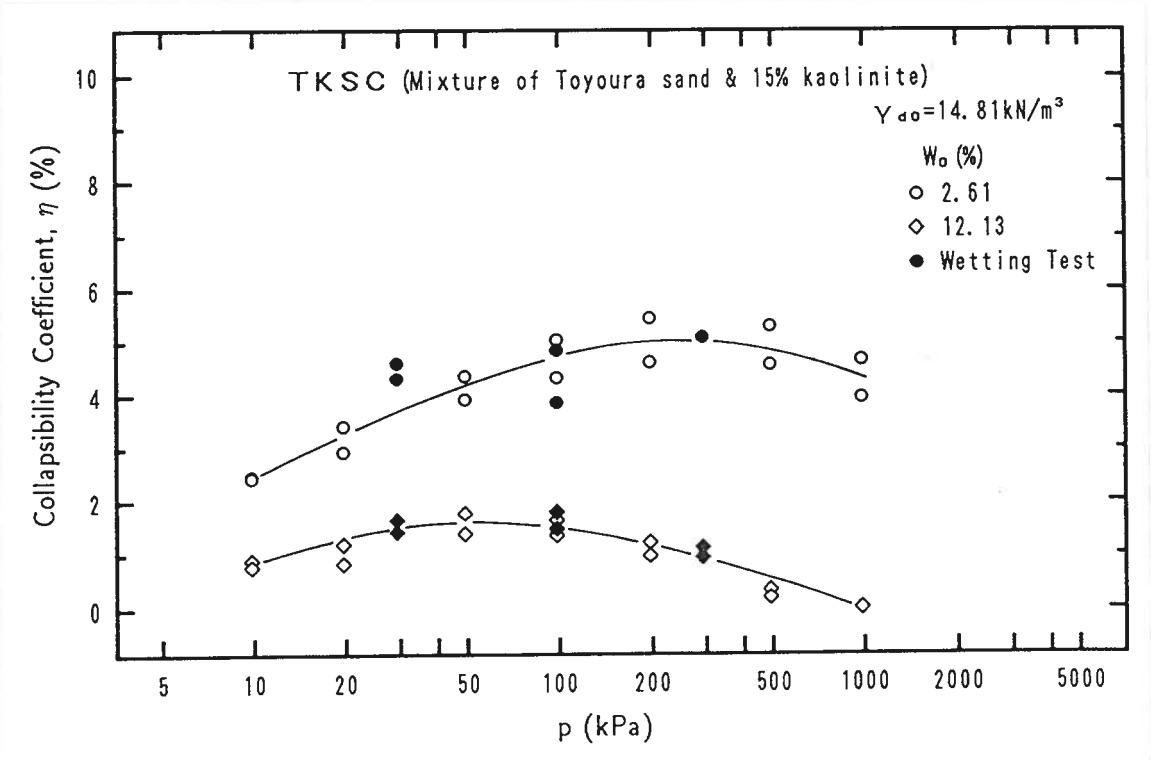

Figure 5.41: Collapsibility versus overburden pressure

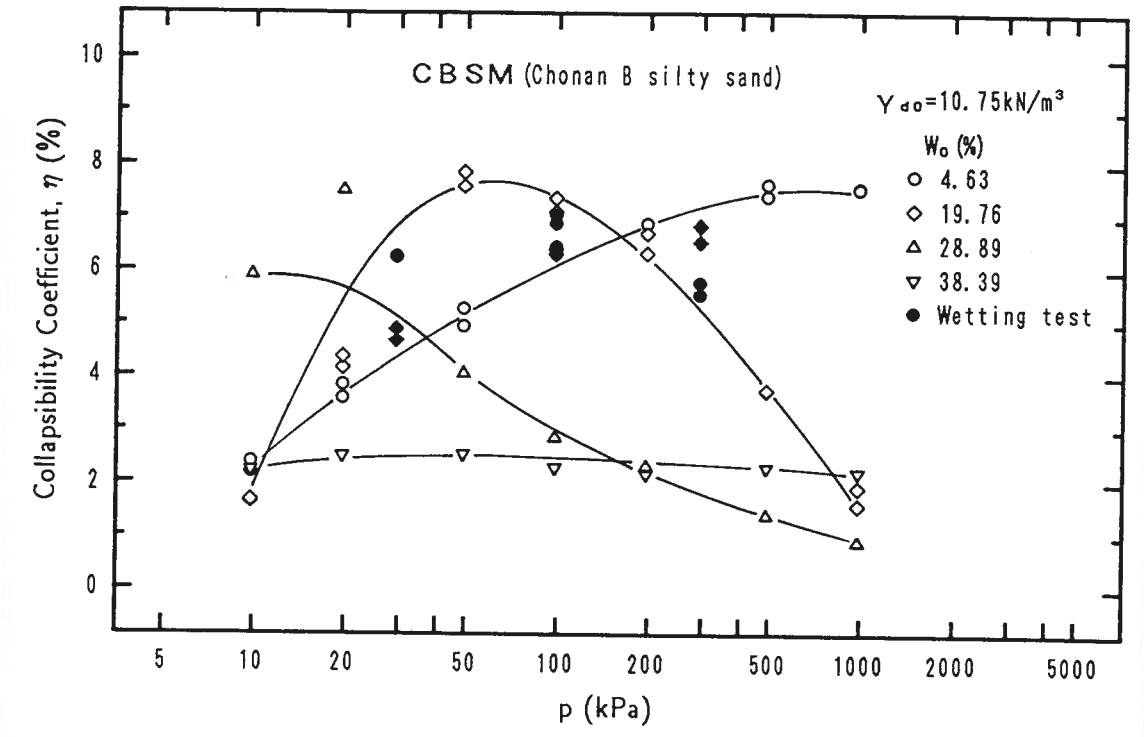

Figure 5.42: Collapsibility versus overburden pressure

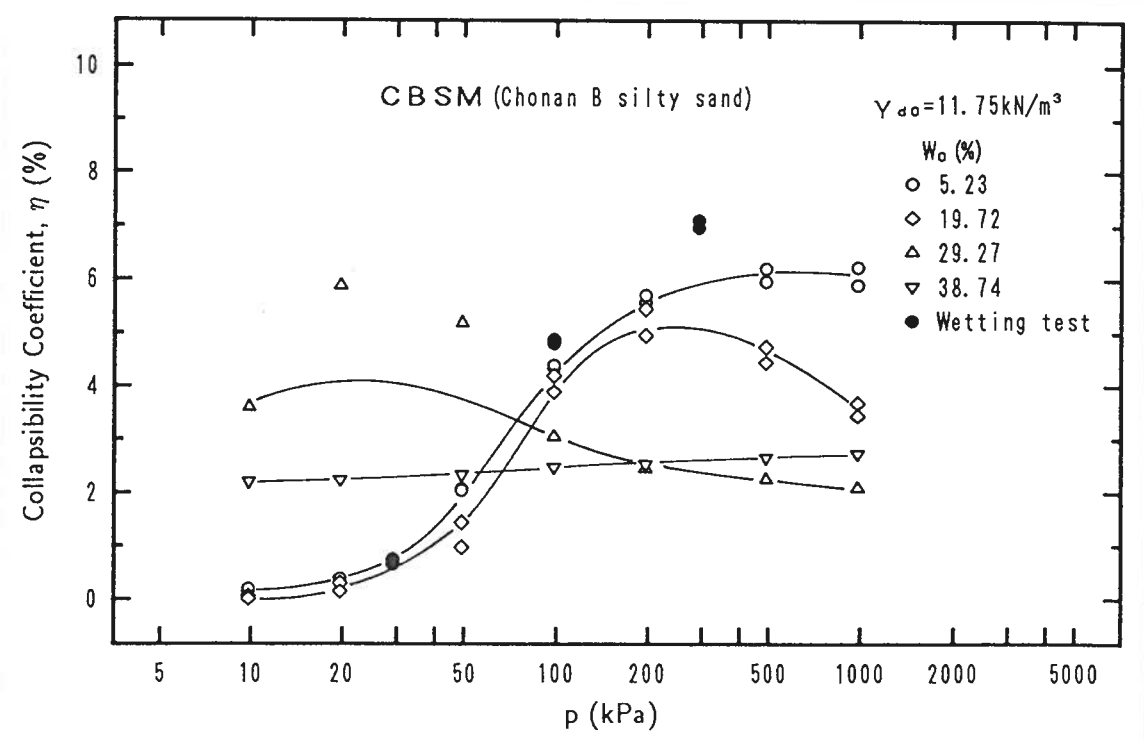

Figure 5.43: Collapsibility versus overburden pressure

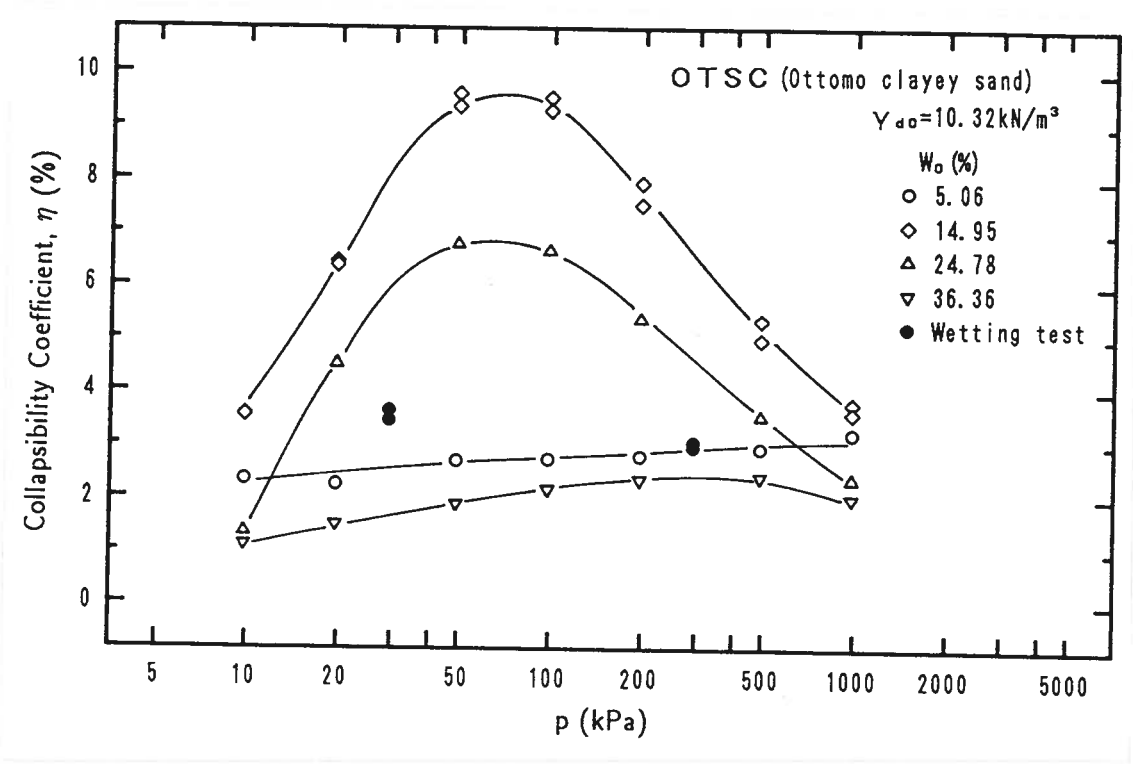

Figure 5.44: Collapsibility versus overburden pressure

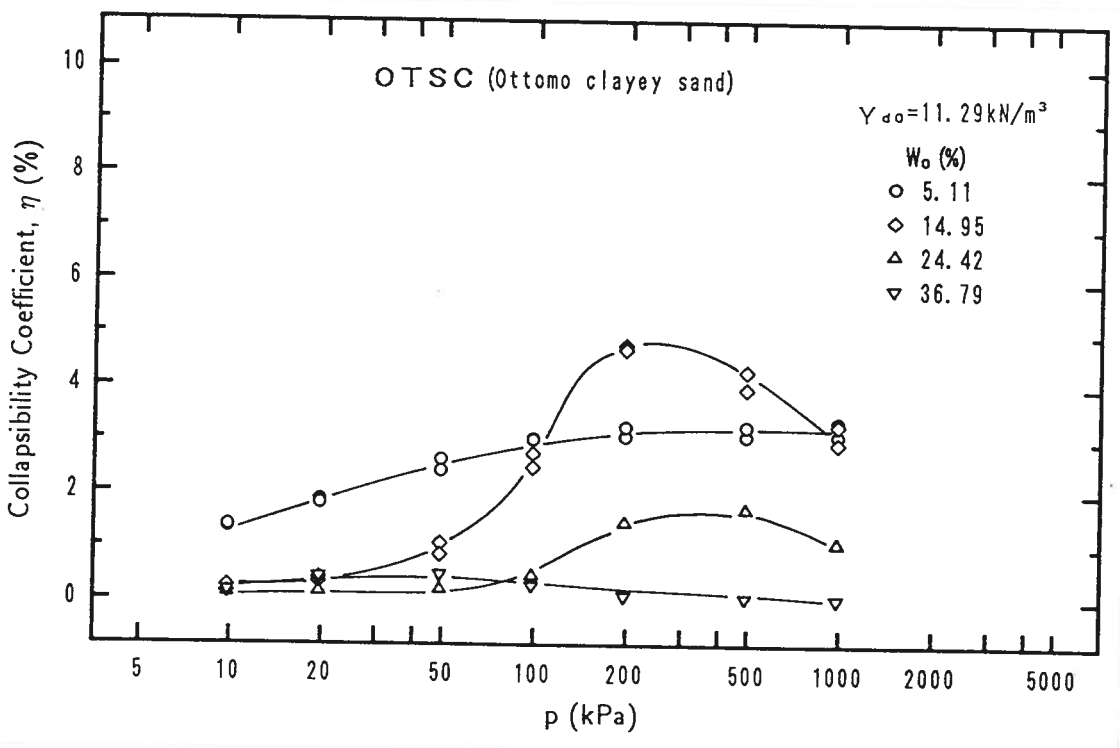

Figure 5.45: Collapsibility versus overburden pressure

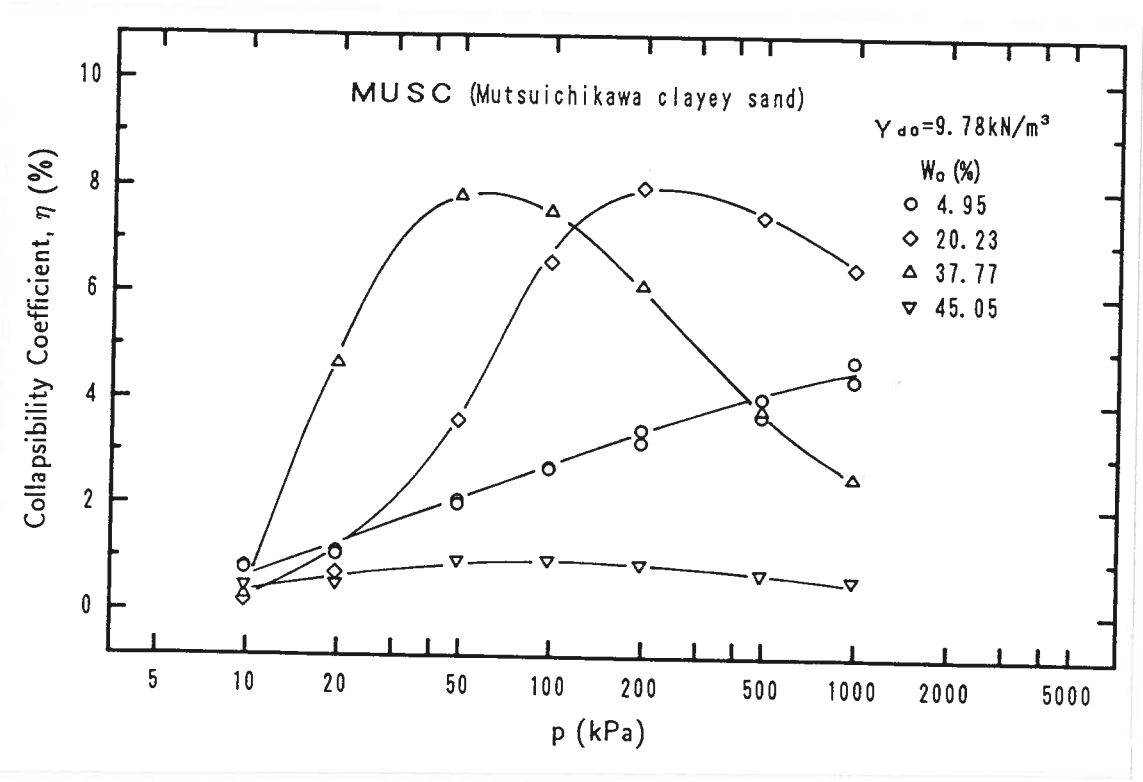

Figure 5.46: Collapsibility versus overburden pressure

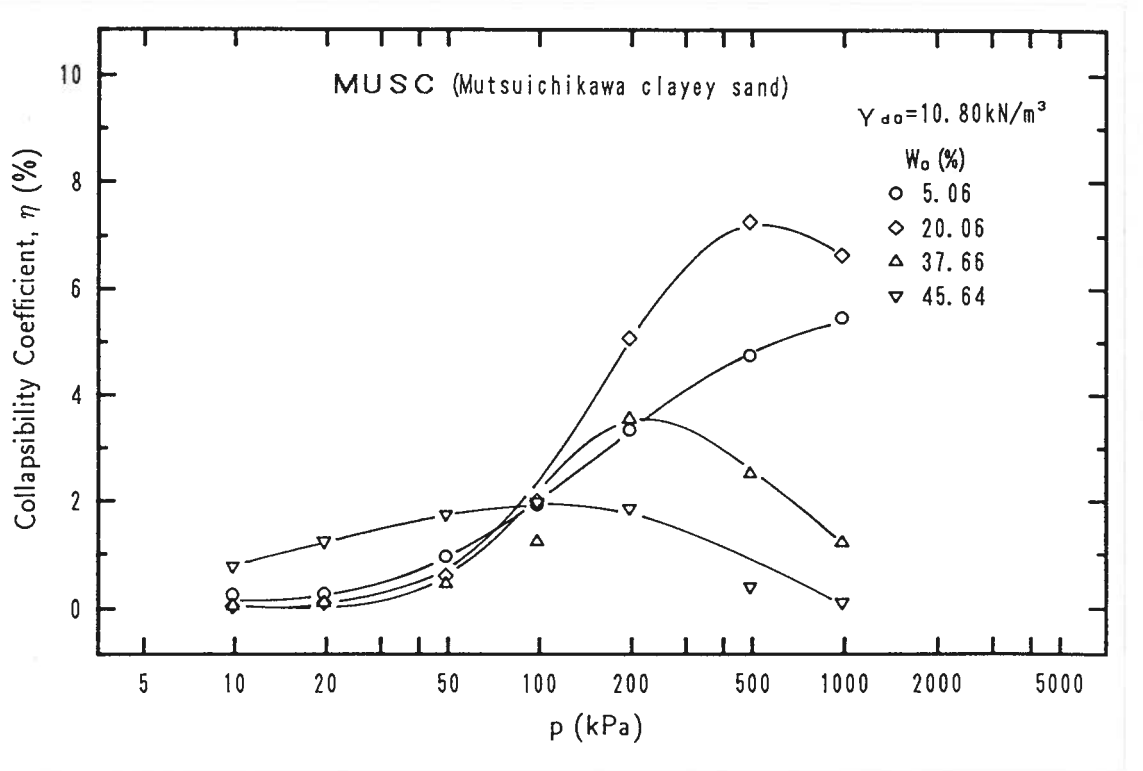

Figure 5.47: Collapsibility versus overburden pressure

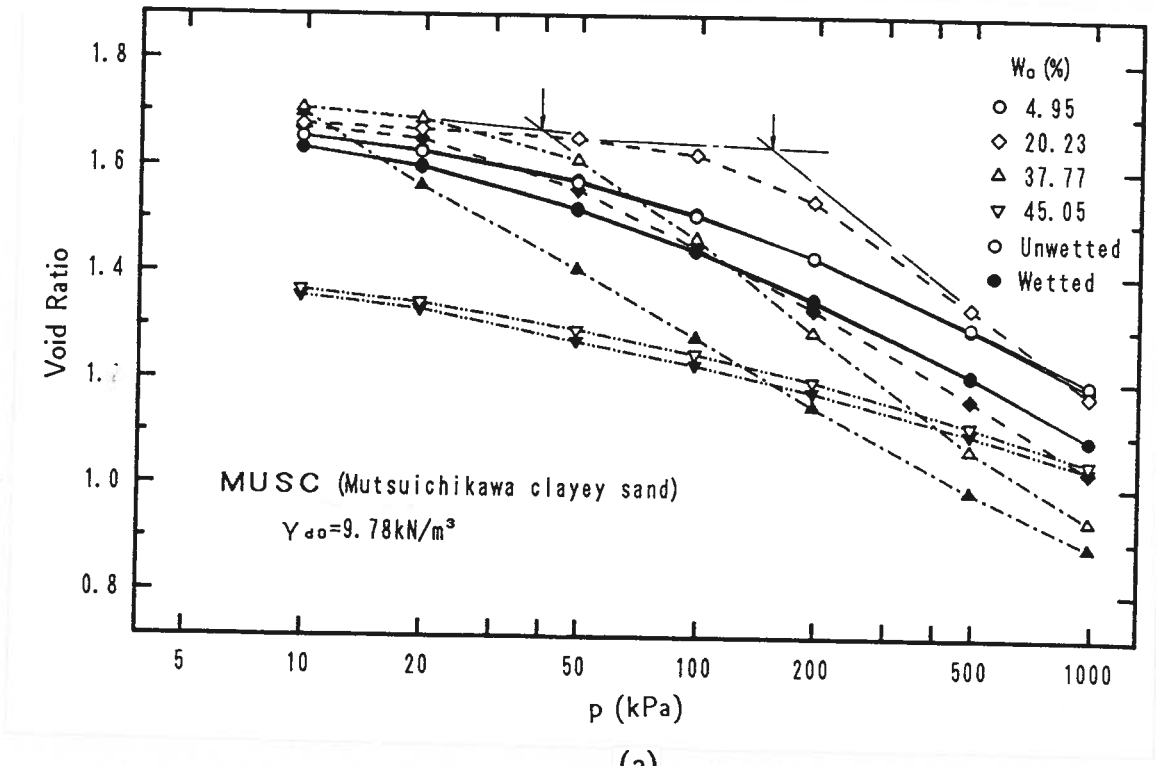

(a)

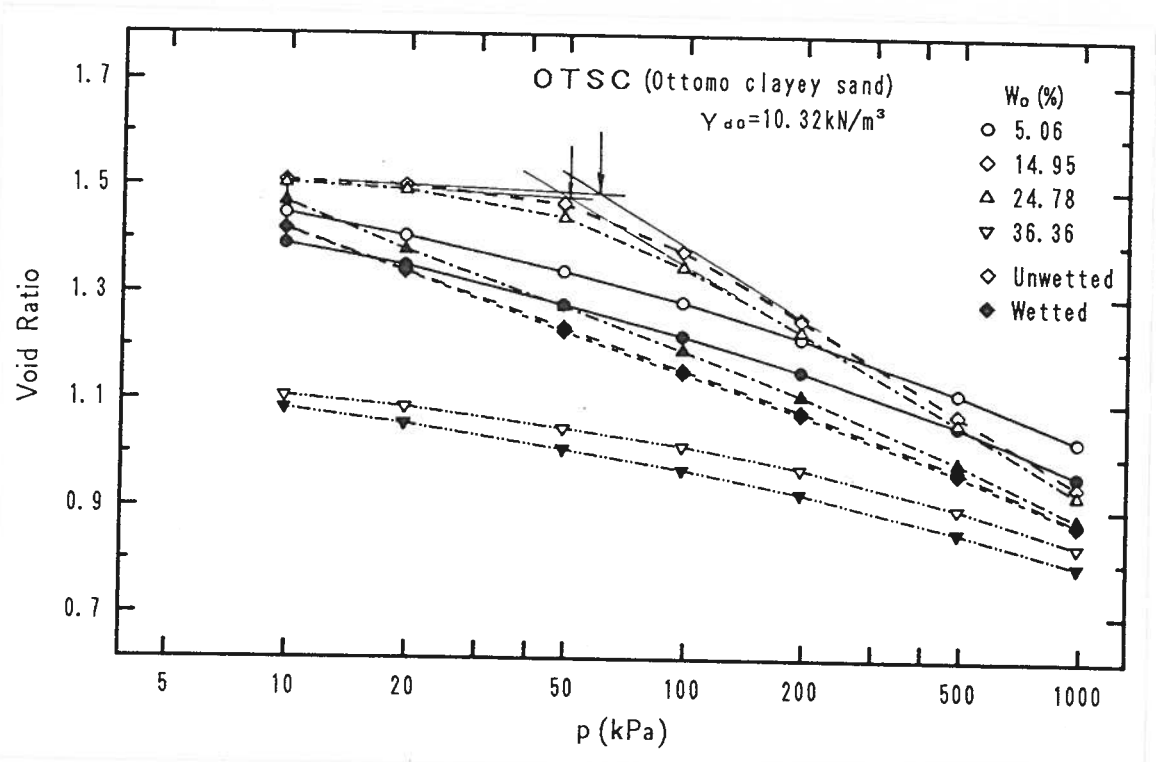

(b)

Figure 5.48: Relationship between void ratio and overburden pressure together with the effect of molding content on pre-stress

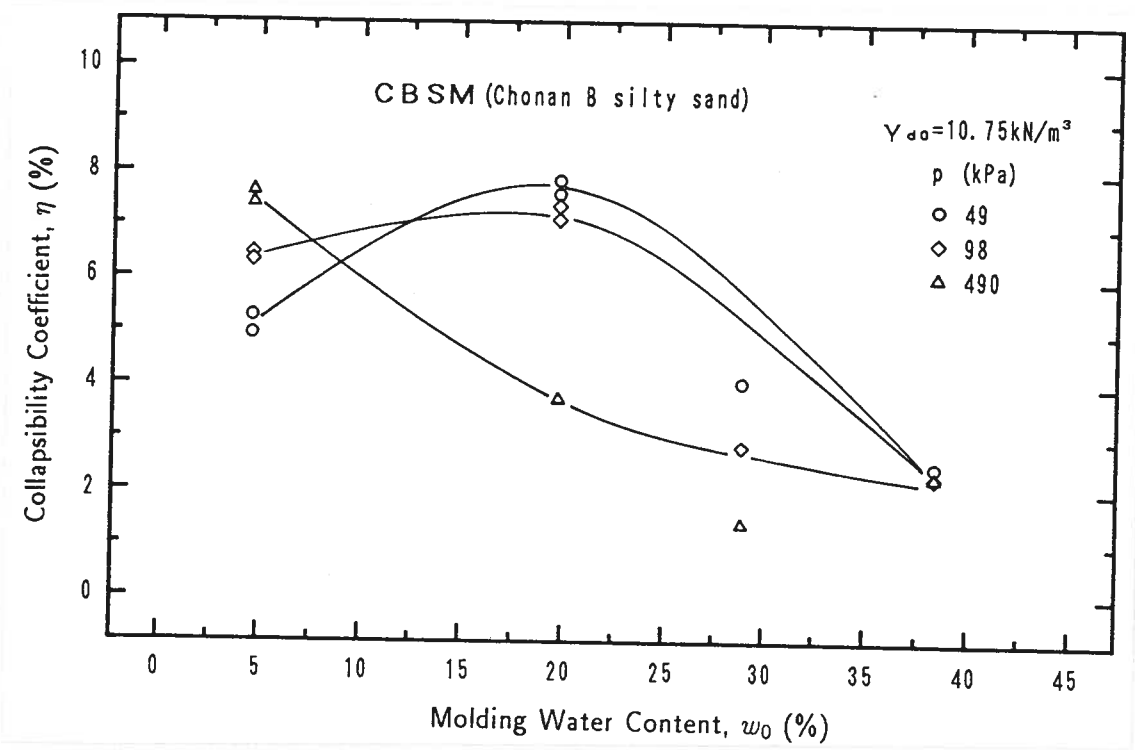

Figure 5.49: Collapsibility versus molding water content

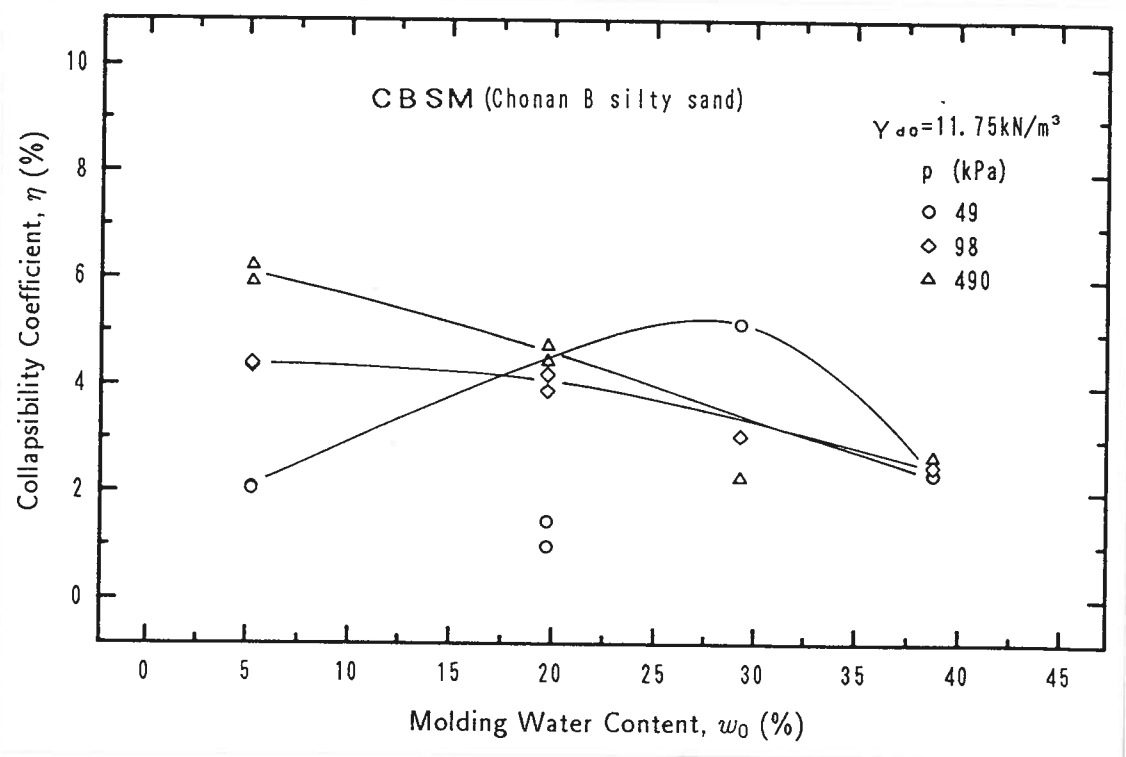

Figure 5.50: Collapsibility versus molding water content

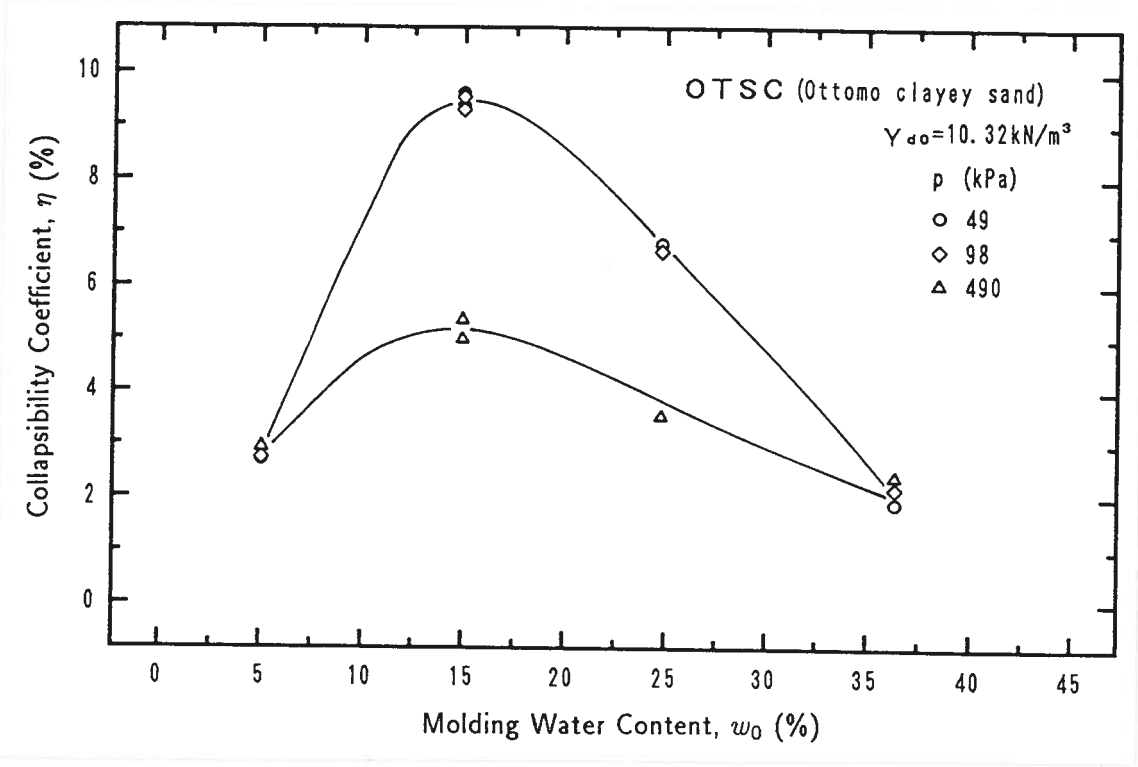

Figure 5.51: Collapsibility versus molding water content

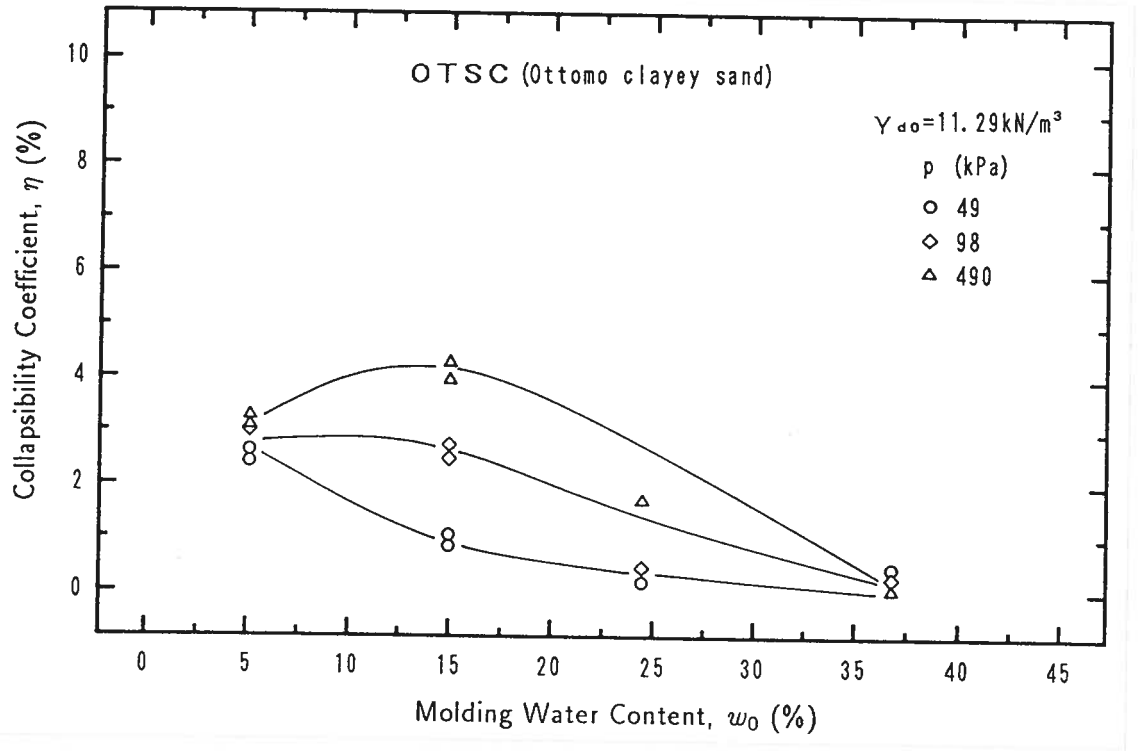

Figure 5.52: Collapsibility versus molding water content

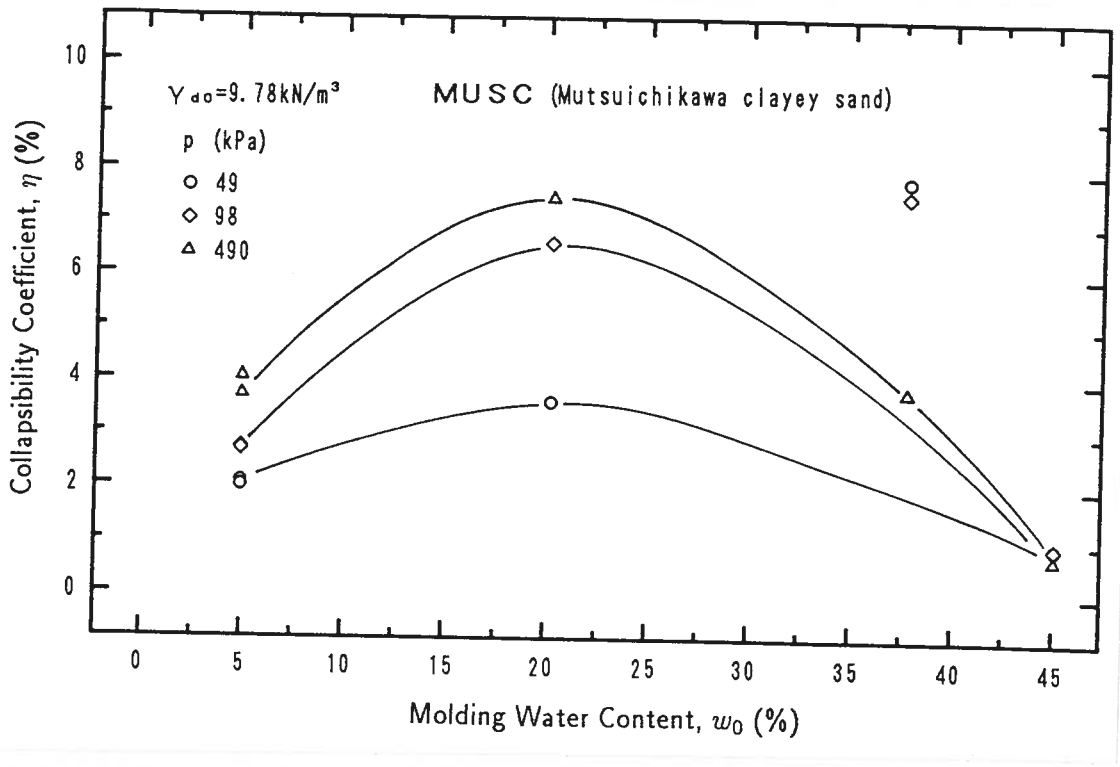

Figure 5.53: Collapsibility versus molding water content

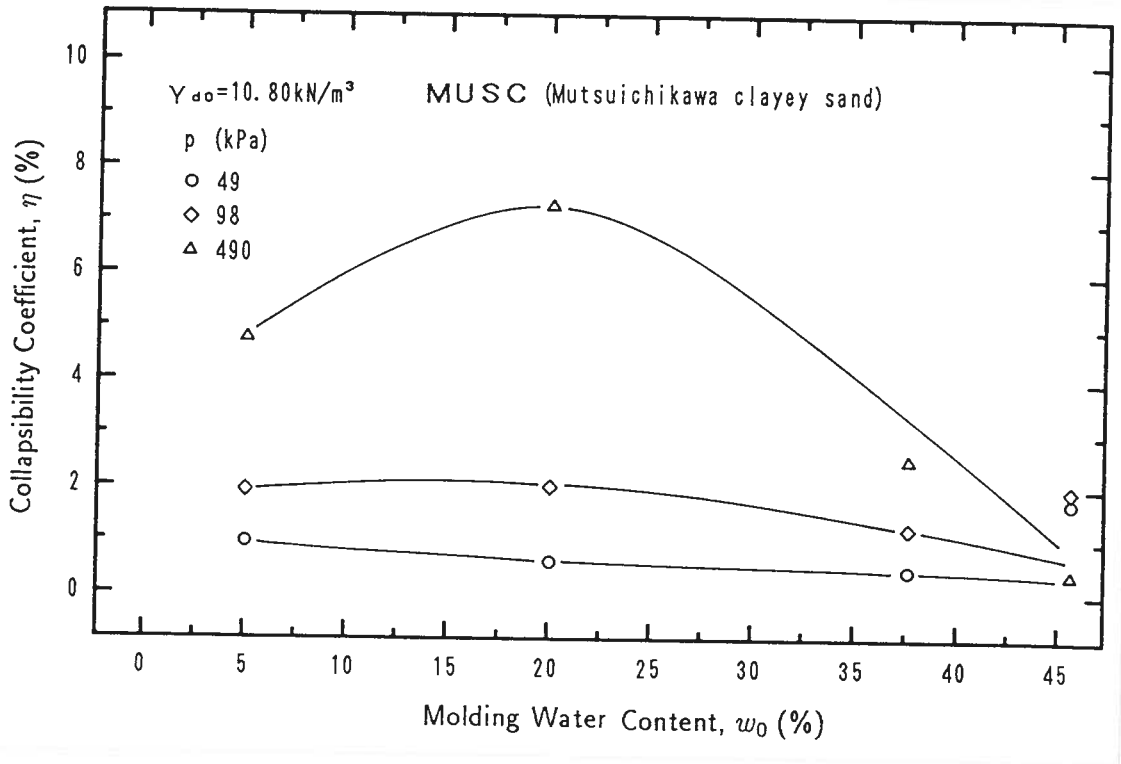

Figure 5.54: Collapsibility versus molding water content

degree of saturation. On the other hand, if the molding water content is smaller and the pressure is maintained as before, the degree of saturation after consolidation is also small even if the sample undergoes the same amount of compression. Consequently, the capillary effect will be larger. Therefore, more collapse will take place upon inundation. This means that the value of moisture content at which the effect of suction is maximum will move to the direction of lower degree of saturation, *i.e.*, lower water content, as the overburden pressure increases.

5.5 INFLUENCE OF MATERIAL TYPES

From the results shown in Figs. 5.14 to 5.18 and 5.40 to 5.47, it can be seen that for different materials, the response to water infiltration is quite different. In order to analyze the influence of different materials on the amount of collapse, the magnitude of collapse corresponding to a relative compaction of 75% is given in Fig. 5.55 for five materials. These results are derived from Figs. 5.14 to 5.18. Tests are performed under an overburden

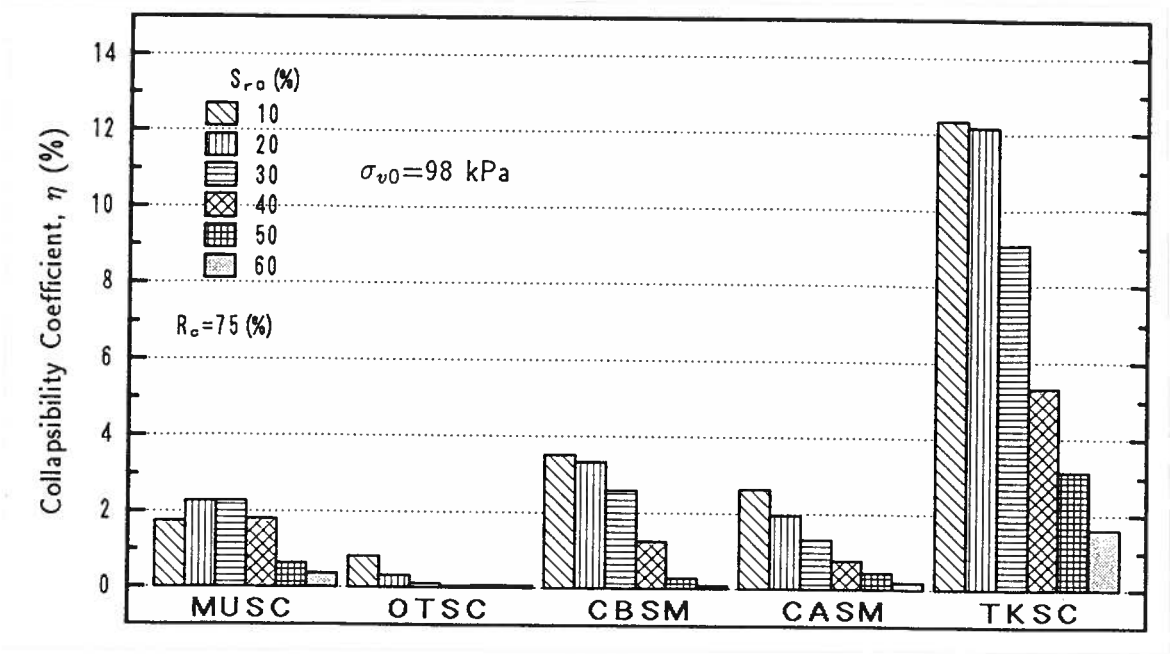

Figure 5.55: Collapse response of different materials

pressure of 98 kPa. This figure clearly shows the difference of collapse response of different materials. It is noted that material *TKSC* (Mixture of Toyoura sand and 15% kaolinite)

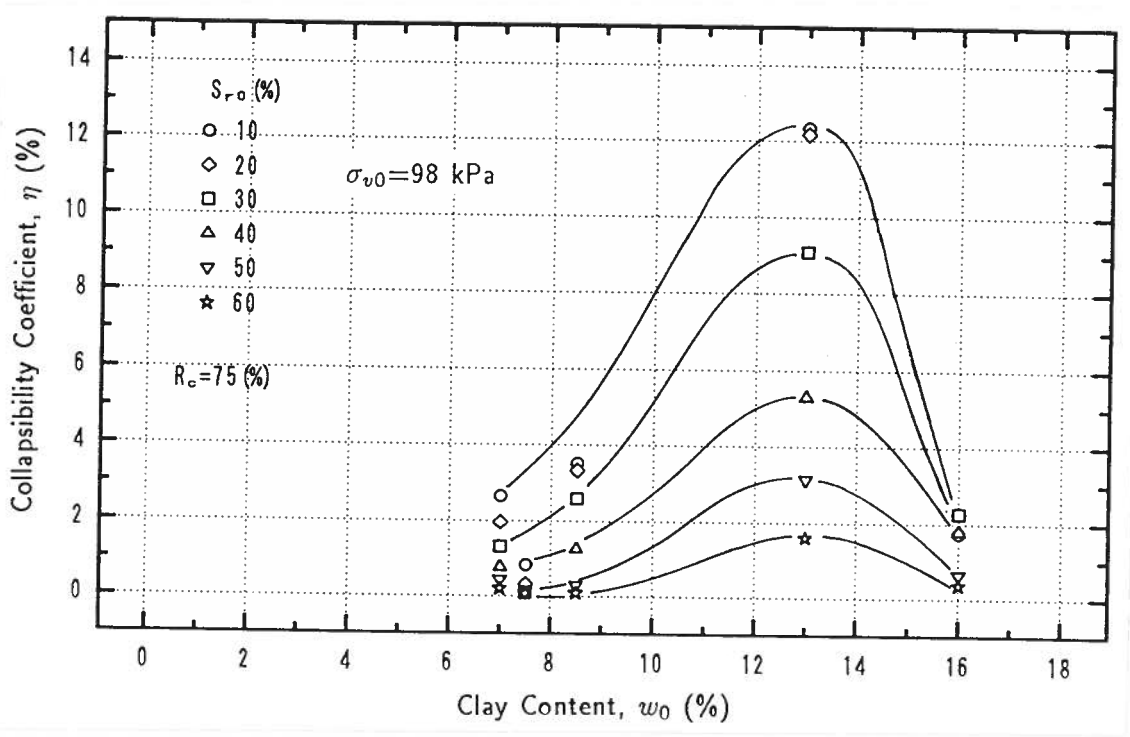

Figure 5.56: Collapsibility coefficient versus clay content

gives maximum collapse, while the magnitude of collapse of material *OTSC* (Ottomo clayey sand) is the smallest under the same condition of relative density and overburden pressure. In order to be able to quantitatively investigate the effect of material difference, clay content is chosen after a series of comparisons, as a parameter to represent the material difference. The amount of collapse as a function of clay content is shown in Fig. 5.56. This figure demonstrates that there exists a critical clay content which gives the maximum value of the magnitude of collapse. Collapse decreases when the clay content of the material deviates from this critical value. The existence of an critical clay content for maximum collapse has been verified by Bull (1964), El-Sohby and Rabbaa (1984) and El-Sohby *et al.* (1987). Bull indicated that the amount of clay for maximum collapse is about 12% of the total solids. This value is quite close to that obtained in this study (13%). However, it seems that the critical clay content is not the only reason for the appearance of extremely high value of collapse at low degree of saturation. It is also noted that there is a relatively small value of η at clay content of 7.5% (Ottomo clayey sand). This means that only the parameter clay content can not represent the whole properties of materials. The difference of grain size distribution and the minerals contained must also be important factors which influence the amount of collapse. The mineral component

analysis (see section 4.2.3) shows that in the portion of grain size smaller than $74\mu m$, material *TKSC* (Toyoura sand mixed with 15% kaolinite), *OTSC* (Ottomo clayey sand) and *MUSC* (Mutsuichikawa clayey sand) contain single clay mineral – kaolinite, while in material *CASM* (Chonan A silty sand) and *CBSM* (Chonan B silty sand), there are three clay minerals, kaolinite, montmorillonite and halloysite. The proportion of the three clay minerals are different in the two materials. In material *CASM*, the proportions are about 32.1%, 35.4% and 32.5%, respectively, while in material *CBSM* (Chonan B silty sand), they are 42.1%, 33.1% and 24.8%, respectively. In view of grain size, it can be seen from Fig. 4.2 and 4.3 that the grain size distribution of material *TKSC* (Mixture of Toyoura sand and 15% kaolinite) is quite different from the other four materials. It is a mixture of uniform fine sand and kaolinite without silt portion, and therefore, it is gap-graded. On the other hand, material *OTSC* (Ottomo clayey sand) is well graded. Comparing the response to collapse of these two materials (the clay mineral in the two material is the same), one can find that not only clay content but also grain size distribution affect the amount of collapse. Well graded material collapses less than the material containing only clay and sand portion. It is also noted that the clay content of material *MUSC* (Mutsuichikawa clayey sand) is larger than *TKSC*. However it collapses much less than *TKSC*. This means that besides the existence of the above mentioned critical clay content for maximum collapse, the grain size distribution takes important function in influencing the amount of collapse.

For materials *OTSC* (Ottomo clayey sand) and *MUSC* (Mutsuichikawa clayey sand), the mineral components and silt content are almost the same and the grain size distributions at grain size larger than 0.2 *mm* are similar. The only difference is the clay content. It is clear that the magnitude of collapse increases as the clay content increases. Materials *CASM* (Chonan A silty sand) and *CBSM* (Chonan B silty sand) also give the same conclusion. It is noted that the material *OTSC* (Ottomo clayey sand) has almost the same clay and silt content as material *CASM* (Chonan A silty sand). However, they respond differently when subjected to water permeation. One reason is that material *OTSC* is well graded and, therefore, shows less collapse. Another possible reason might be the presence of montmorillonite in material *CASM*, which has a high ability to absorb hydrogen cation and consequently, a high ability to absorb water (Lobdell, 1981).

The upper limit of relative compaction at which collapse ceases to occur, together with relative density for the five materials are given in Fig. 5.57 . It is noted that for material *TKSC* (Mixture of Toyoura sand and 15% kaolinite), the upper limit of relative compaction is 90.6%, while for material *OTSC* (Ottomo clayey sand), this upper limit is only 76.6%. These upper limits as a function of clay content is illustrated in Fig. 5.58.

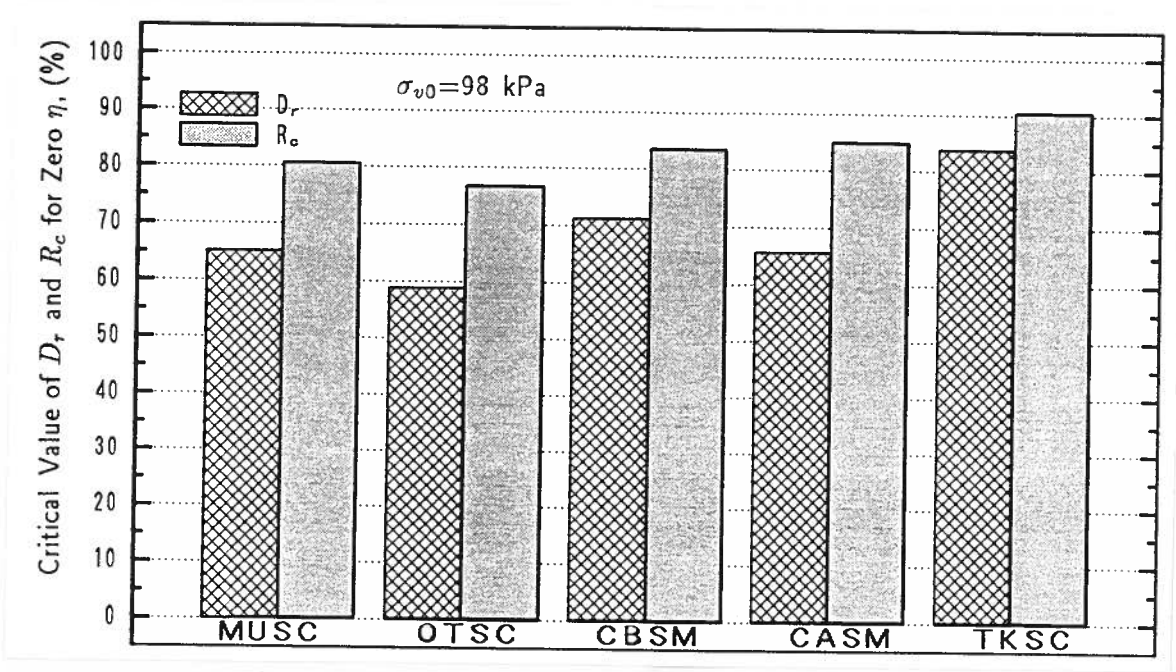

Figure 5.57: Critical value of D_r and R_c of different materials for zero η

It is found that there is still a critical value of clay content at which the upper limit of relative compaction or relative density for zero collapse is maximum.

The relative compaction and corresponding maximum collapse in the test are demonstrated in Fig.5.59. This figure clearly shows that the maximum collapse of *TKSC* (Mixture of Toyoura sand and 15% kaolinite) for a given relative compaction is the largest among the five materials. The collapse of the other four materials is relatively close to each other. However, they still demonstrate dome difference. The collapse of *OTSC* (Ottomo clayey sand) for a given relative compaction is the smallest.

5.6 SUMMARY

The wetting-induced collapse and the influencing factors, such as as-compacted dry density, molding water content, and overburden pressure, of compacted soils have been studied in this chapter by use of conventional consolidmeter. For compacted soil, there is a certain range of molding moisture content and dry unit weight within which collapse can most possibly occur. In order to determine this range, a series of compaction tests are performed first on the tested materials by employing different compaction energies.

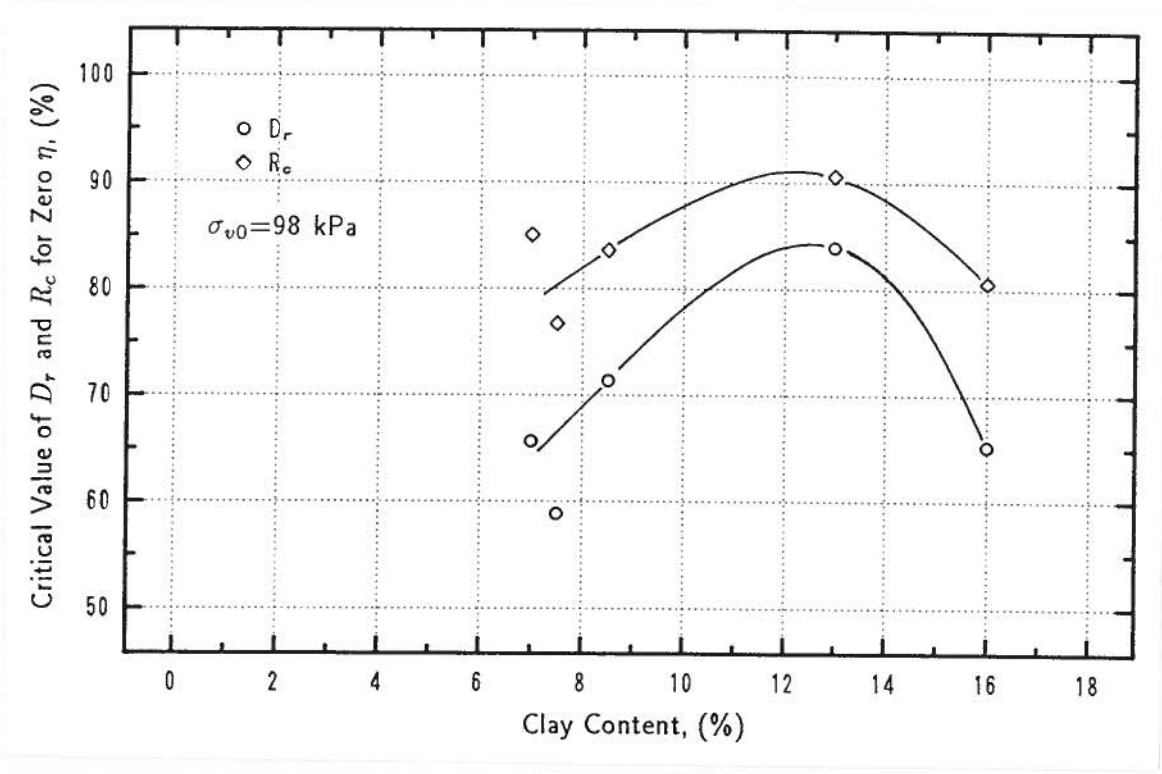

Figure 5.58: Critical value of D_r and R_c for zero η as a function of clay content

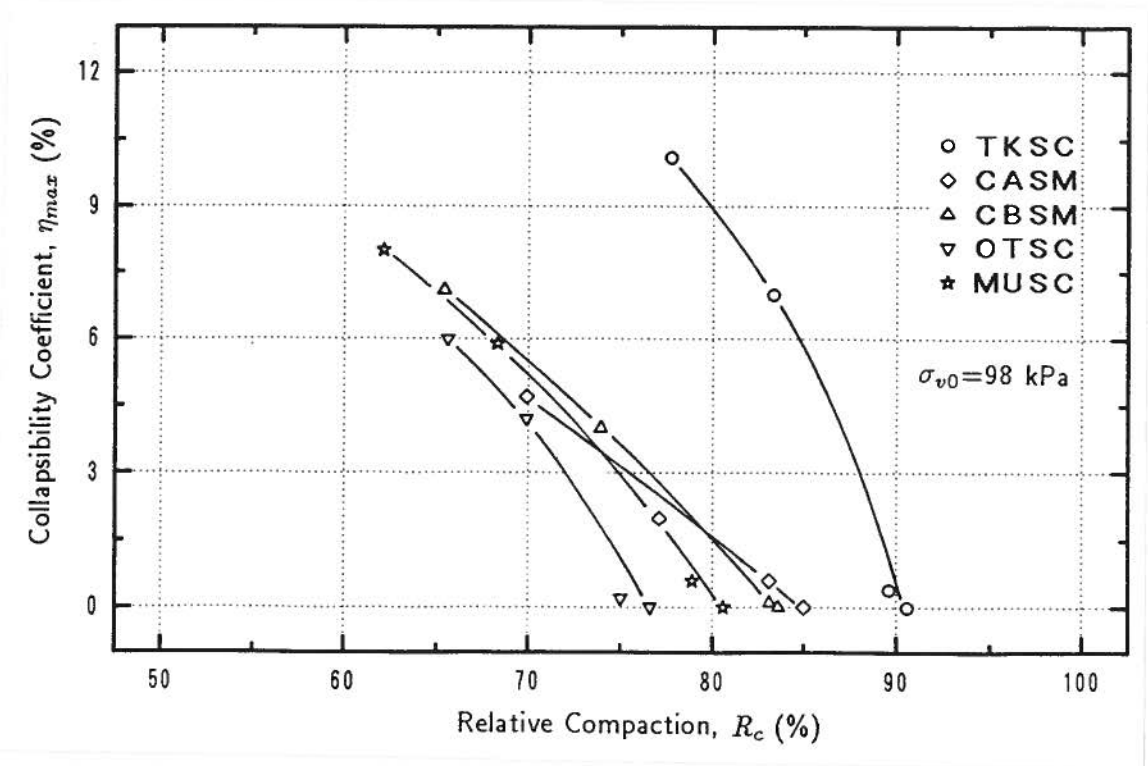

Figure 5.59: Maximum collapse as a function of relative compaction

The molding conditions of the samples in the collapse tests are based on the results of compaction tests.

Two kinds of test methods, wetting tests and double-oedometer tests, have been used to investigate the influence of different factors on the collapse of soils. Comparison of the tests shows that the results from the two test methods are comparable.

Analysis of the results from this category of tests yields following conclusions:

- With constant overburden pressure and identical as-compacted dry density, the amount of collapse decreases with the increase in molding degree of saturation if the relative compaction is high. On the other hand, if the relative compaction is low, there exists a critical molding degree of saturation which gives the maximum value of collapse. The collapse decreases as the degree of saturation diverges from this critical value. The decline of $\eta \sim S_{r0}$ curve is larger on the side in which the degree of saturation is larger than the critical value than on the side in which the degree of saturation is less than the critical value.

- No matter how much is the as-compacted dry density, there exists an upper limit of degree of saturation beyond which no collapse could occur. This upper limit of saturation ratio depends on the material but the value usually falls in the range of about 70~80%.

- With constant overburden pressure and molding water content, the amount of collapse decreases significantly with the increase in as-compacted dry density.

- An upper limit of as-compacted dry density also exists in the soil. Collapse will never occur, no matter how dry the soil is, if the state of soil falls in the range wherein the as-compacted dry density is larger than the upper limit. This upper limit is a function of the material type and changes greatly.

- With the same state of molding water content and as-compacted dry density, the magnitude of hydraulic collapse increases and reaches a maximum value with the increase in the overburden pressure. Further increase in the overburden pressure results in the reduction in the magnitude of collapse.

- The magnitude of collapse is also affected by material properties, *e.g.*, grain size distribution, clay content, clay mineralogy, *etc.* Well graded soil collapses less than poorly graded soil. It seems that there exists an critical clay content which yields the maximum amount of collapse. If the clay content of the soil is less than this critical value, soil behaves more cohesionless, and if, on the contrary, its clay content

is larger than the critical value, it is more cohesive. In both cases, the soil will show less collapse when subjected to water infiltration.

Chapter 6

BEHAVIOR UNDER CYCLIC LOADING CONDITIONS

6.1 INTRODUCTION

The behavior of collapsible soil under cyclic loading is one area in geotechnical engineering in which little has been known by soil engineers. Most of the research on collapsible soils are concentrated on the additional settlements caused by water infiltration, mechanism of collapse phenomenon, and predicting methods. Some of the investigations have draw attention to the shear strength characteristics of this type of soils under static loading. In the area of behavior of collapsible soils under cyclic loading, the research that has been down is extremely limited (Some of them which the author has found with great effort have been reviewed in Chapter 2). However, there are several catastrophic landslides which occurred in the loessial areas during earthquakes (Seed, 1968; Ishihara *et al.*, 1990). The biggest landslides may be those that occurred in Kansu, China (Close and McCormick, 1922), and in Tajik, Soviet Union (Ishihara, *et al.*, 1990). The first event occurred in 1920 in China during the Kansu earthquake. Large landslides developed in deposits of loess. The area of greatest destruction, 100 miles by 300 miles in extent, contained ten large cities aside from numerous villages. Nearly two hundred thousand lives were lost and hundreds of towns and cities were totally destroyed in the event. "*Landslides that eddied like waterfalls, crevasses that swallowed houses and camel trains, and villages that were swept away under a rising sea of loose earth, were a few of the subsidiary occurrences that made the earthquake in Kansu one of the most appalling catastrophes in history*" (Close and McCormick, 1922). "*The condition of the loess deposits at the time of this earthquake is not known but it is clear that liquefaction occurred, if not from the development of pore water pressures, then presumably from the development of pore air pressures*" (Seed, 1968). In the later event, extensive liquefaction developed in the loess deposit of aeolian origin in the gently sloping hilly terrain which lead to a series of landslides accompanied by a large-scale mud flow (see Chapter 3). These examples in-

dicate that liquefaction, which have usually occurred in water-sedimented sand deposits, occurred in the deposits of loessial soils, the most typical collapsible soils. Therefore, it is necessary to investigate the behavior of collapsible soils under dynamic loading action and, especially, the factors influencing those behavior. In this study, it is intended to fill the inadequate knowledge in this field.

Under cyclic loading condition, the soil in natural partly saturated collapsible soil deposits or manufactured embankments can be considered as in an undrained and volume changeable state because of the high compressibility of pore air in the soil. Unless the pore air pressure developed in the soil is so high that it offsets the total stress and suction action, liquefaction will never occur. On the contrary, when the soil is soaked and collapse occurs, the degree of saturation usually increases to a relative high value (usually more than 80%, see Chapter 5) and the soil even is fully saturated. Therefore, an undrained and constant volume condition is possible when subjected to seismic load. Because the stability of these soils under partly saturated condition is usually out of the problem at seismic loading condition, the response to cyclic load is insignificant. Therefore, only the seismic behavior under soaked and collapsed conditions is investigated in this chapter. All the tests are performed under plane strain and constant volume conditions. The discussions on stress states and stress changes in constant volume test are given in the first part of this chapter. Then, both strength and deformation behaviors of collapsible soils are discussed.

The test apparatus used is simple shear test device and the experimental procedures discussed in Chapter 4 are followed. The axial stress is constant before shearing for all the tests in this chapter and is equal to 98 kPa.

6.2 CONSTANT VOLUME SIMPLE SHEAR TEST

There are many test apparatuses which can be used to investigate the stress-strain and strength properties. Nowadays, the main devices used are the triaxial test apparatus, simple shear apparatus and torsional shear apparatus. Of the three tests, the triaxial test is the easiest to perform and the necessary apparatus is the cheapest, simplest, and more widely available. On the other hand, the torsional test is the most complicated to perform and the apparatus is the most expensive. However, the simple shear test appears to permit a considerably better approximation of the field stress patterns (Seed and Peacock, 1971), although it is more complicated than triaxial test and its boundary conditions are not as clear as in torsional shear test (Finn, 1985). In this study, a more important factor to have chosen the simple shear apparatus is the measurement of

the wetting-induced volume change (collapse). To measure the volume variation during collapse, special facilities are needed in triaxial or torsional shear devices, while in simple shear apparatus, this can be done very simply because of the plane strain condition of specimens. Another advantage of the simple shear device is the shorter time needed to execute water permeation uniformly within the samples.

Pickering (1973) pointed out that the chief disadvantages of simple shear testing are the complexity of the machine and the difficulty of test procedure. Undrained liquefaction testing also suffers from inaccuracy due to volume change in the apparatus as the pore pressure rises. Pickering (1973) had analyzed the effect of the compliance of machine and obtained a conclusion that even with a machine compliance as low as the compressibility of water, the vertical strain which must be induced is twice that in nature. The number of cycles to liquefaction in the test are therefore greater than that in nature, and the testing error is on the unsafe side. Another problem is the sensitivity of the bulk modulus of water to degree of saturation. For values of $S_r \simeq 99\%$, the effective bulk modulus of water, K_w, becomes the same order as $\overline{E}_r$ (tangent modulus of the one-dimensional unloading curve at a point corresponding to the initial vertical effective stress) and, thus, the increase in pore-water pressure per cycle would be reduced considerably (Martin *et al.*, 1973). In considering the experimental difficulties of cyclic simple shear tests on saturated sands (including that of compliance), a new method, *drained constant volume simple shear test*, has been used widely by several individuals (Pickering, 1973; Moussa, 1975; Martin *et al.*, 1978; and Finn, 1985).

The method of constant volume test is initially used in the direct shear test owing to the difficulties in the prevention of drainage (Taylor, 1953; Bjerrum, 1954). Bjerrum and Landva (1966) have investigated the shear strength by drained constant volume simple shear test on a Norwegian quick clay. Later studies (Pickering, 1973; Moussa, 1975; Martin *et al.*, 1978; and Finn, 1985) are concentrated on liquefaction problems on cohesionless soils. Because the shear strength of cohesionless soil is not appreciably affected whether the soil is fully saturated or dry (Terzaghi and Peck, 1967), constant volume test on dry sand samples can be used to represent the undrained properties of totally saturated ones. It is found that the results obtained from the two kinds of tests are in good agreement (Feda, 1971; Moussa, 1975). This is of great advantages because the preparation of dry samples is easier and less time consuming than that of totally saturated ones.

In the drained constant volume test, the change in the applied vertical stress on the specimen is equivalent to the change in the pore water pressure which would have

occurred in the specimen if the specimen had been prevented from draining under a constant applied vertical stress (Bjerrum and Landva, 1966). The various stress states and changes in stress in the two kinds of tests are discussed in the following paragraphs.

For simplicity, the complications of seating loads and overconsolidated samples are ignored. Assume that the loading head moves freely under the applied load, is supported by the sample and the test system is perfectly rigid, therefore, the horizontal stress coefficient of the machine is equal to the coefficient of earth pressure at rest, K_0. Let the stress acting on the sample be σ_v in a vertical direction, σ_h in a horizontal direction, with a pore water pressure u. Let the subscripts 1 and 2 denote the conditions before and after liquefaction (or failure). Let the effective vertical stress acting before shearing be σ_a.

First, consider the stress changes in saturated undrained test. As the sample liquefies, the effective vertical stress tends to become zero. Therefore, for clean sand, the effective horizontal stress presumably tends to approach zero. The various stress states and the changes in stress are as follows:

$$\left.\begin{array}{lll} \sigma'_{v1} = \sigma_a; & \sigma'_{v2} \to 0; & \Delta\sigma'_v \to -\sigma_a \\ \sigma'_{h1} = K_0\sigma_a; & \sigma'_{h2} \to 0; & \Delta\sigma'_h \to -K_0\sigma_a \\ \sigma_{v1} = \sigma_a; & \sigma_{v2} = \sigma_a; & \Delta\sigma_v = 0 \\ \sigma_{h1} = K_0\sigma_a; & \sigma_{h2} \to \sigma_a; & \Delta\sigma_h \to (1-K_0)\sigma_a \\ u_1 = 0; & u_2 \to \sigma_a; & \Delta u \to \sigma_a \end{array}\right\} \tag{6.1}$$

In the drained constant volume test, $u = 0$ is constant. The measured vertical stress decreases. Stresses before and after testing and the stress increments are:

$$\left.\begin{array}{lll} \sigma'_{v1} = \sigma_{v1} = \sigma_a; & \sigma'_{v2} = \sigma_{v2} \to 0; & \Delta\sigma'_v = \Delta\sigma_v \to -\sigma_a \\ \sigma'_{h1} = \sigma_{h1} = K_0\sigma_a; & \sigma'_{h2} = \sigma_{h2} \to 0; & \Delta\sigma'_h = \Delta\sigma_h \to -K_0\sigma_a \\ u_1 = 0; & u_2 = 0; & \Delta u = 0 \end{array}\right\} \tag{6.2}$$

Therefore, the reduction of vertical stress in drained constant volume test is equivalent to the increase of pore water pressure in saturated undrained test.

For unsaturated soil, the stresses are a little different from those in totally saturated or dry soils because of the existence of suction. According to Bishop's theory (1959), the effective stress in unsaturated soils can be expressed as:

$$\sigma' = (\sigma - u_a) + \chi(u_a - u_w) \tag{6.3}$$

where, u_a is pore air pressure, u_w is pore water pressure, and χ is an empirical parameter representing the proportion of the soil suction $(u_a - u_w)$ that contributes to the effective stress. Let

$$\Delta u = (u_a - u_{a0}) - \chi[(u_a - u_w) - (u_{a0} - u_{w0})] \tag{6.4}$$

be the *excess pore pressure*, where the subscript 0 refers to the state before application of shear load. The stress changes before and after testing are:

$$\sigma_1' = (\sigma_1 - u_{a0}) + \chi(u_{a0} - u_{w0}) \tag{6.5}$$

$$\sigma_2' = (\sigma_2 - u_{a0}) + \chi(u_{a0} - u_{w0}) - \Delta u \tag{6.6}$$

In the constant volume test, the *excess pore pressure* is constant and is equal to 0 and pore air pressure u_{a0} is equal to atmosphere. During shearing, vertical stress decreases and tends to become zero, *i.e.*, $\sigma_2 \rightarrow 0$. Therefore, Eq. 6.6 becomes

$$\sigma_2' \rightarrow \chi(u_{a0} - u_{w0}) \tag{6.7}$$

This means that unsaturated sample will never reach initial liquefaction.

The stress in the intermediate state is expressed by Bishop's effective equation as in Eq. 6.3. Because in drained constant volume test the pore air pressure equals atmospheric pressure, Eq. 6.3 becomes:

$$\sigma_v' = \sigma_v + \chi(u_a - u_w) \tag{6.8}$$

Rearranging the order of Eq. 6.8 leads to:

$$\sigma_v = \sigma_v' - \chi(u_a - u_w) \tag{6.9}$$

This equation means that the measured vertical stress during the test represents the algebraic difference of effective vertical stress and suction action. The change in vertical stress is equivalent to the increase in *excess pore pressure.*

Besides the aforementioned reasons, another important reason to compel the adoption of constant volume test is the rocking motion of the top cap of the specimen. The simple shear apparatus used in this study has a defect as it produces rocking motions around horizontal axis and this induces vertical stress near the edge of the specimen. It is found that this rocking motion becomes more violent as the overburden pressure or the density of specimen increases. Because of the rocking motions, the horizontal displacement measured at the level of the horizontal load ram is larger than the displacement occurring at the top of specimen (see Figure 4.17 in Section 4.5.2). In an undrained, volume changeable test, this rocking motion becomes more violent because the specimen tends to be denser (especially unsaturated sample), and, therefore, additional stress acts on the specimen. In constant volume test, the rocking motions diminish as the vertical stress decreases during shearing and will vanish if the vertical stress becomes to zero. It may not be justified to assume that the behavior of the specimen is exactly equivalent to one in which there is no any rocking motion. However, at least in considering the portion

of large deformation (failure or liquefaction), the constant volume test seems likely to give a better approximation of the natural stress condition than the undrained and volume changeable test. Therefore, all the tests in this catalogue are tested under plane strain and constant volume conditions. Because samples are unsaturated, the measured vertical stress during shearing is the algebraic difference of the effective vertical stress and suction action.

6.3 STATE HISTORY BEFORE SHEARING

In laboratory test, it is the simplest way to prepare samples having identical initial states of as-compacted dry density. However, because of the consolidation and collapse deformation, the dry densities before cyclic shearing change remarkably. It is well known that the strength and deformation properties of soil depend in a certain extent on its density. If the densities of the samples are different before shearing, the effect of amount of collapse on the strength and deformation properties will mix with that of density. In order to demonstrate this mixing action of the two effects, a set of tests is performed on material *TKSC* (Mixture of Toyoura sand and 15% kaolinite). Samples are prepared such that they have the same as-compacted dry densities and different molding moisture contents. The results are given in Fig. 6.1 in terms of cyclic shear stress ratio versus number of cycles. In this set of tests, the as-compacted dry densities of specimens are relatively high (94% relative compaction). Therefore, the resulting collapsibility coefficients, η, are very small (as given in the legend in Fig. 6.1). Although the results are relatively scattered, they still show that the cyclic shear strength decreases as η increases, especially those with η of 1.455%. However, the trend of strength decrease is not as clear as desired because of the small value of η. In order to obtain larger value of η, a second set of tests is performed similarly but of lower as-compacted dry density (82% relative compaction). The results are presented in Fig. 6.2. The results seem to give a contrary conclusion to that obtained from Fig. 6.1. It is to be noted that the dry density before cyclic shearing is relatively different upon being subjected to consolidation and water permeation. It is evident that the effect of collapsibility mingles with that of dry density. This indicates that the as-compacted dry density may not be a good parameter in investigating the effect of collapse on strength behavior, although it is quite important to collapse itself.

In order to separate the two effects, tests are performed such that the specimens in the mold of the simple shear test are prepared at different molding moisture contents and dry densities, but upon being consolidated at an overburden pressure of $\sigma_{v0} = 98kPa$ and subjected to water infiltration, the specimens reduce their volume, accompanied by an

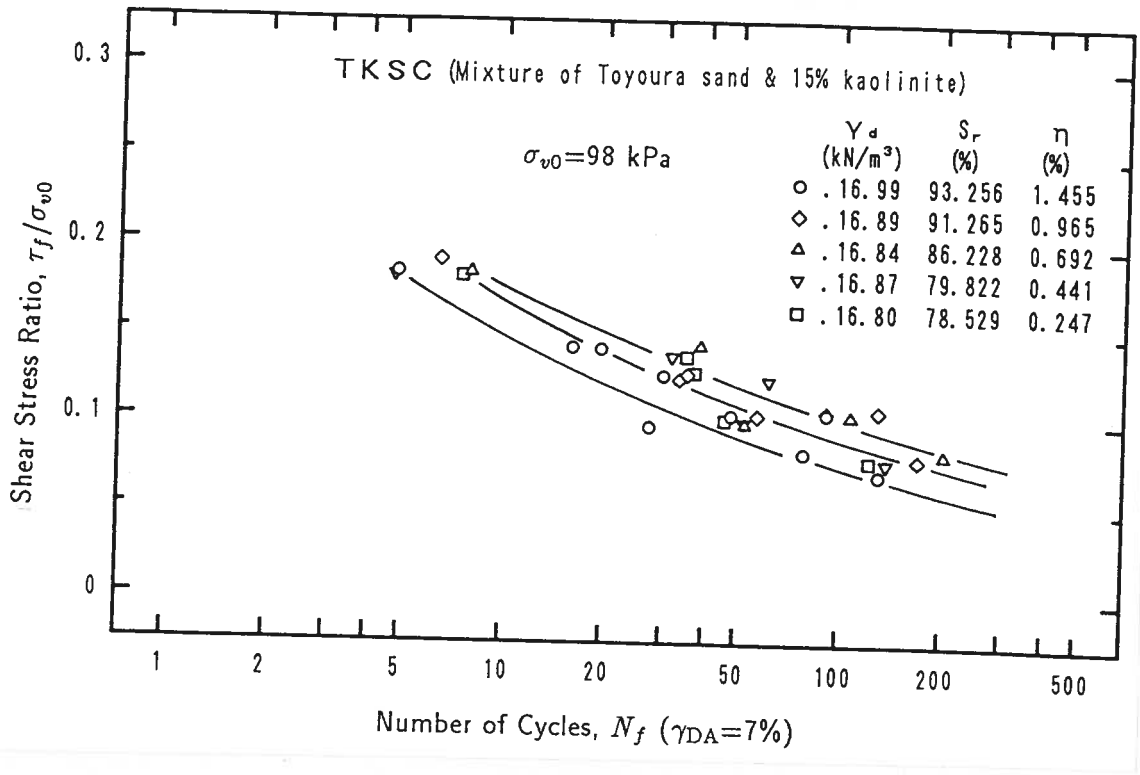

Figure 6.1: Cyclic shear stress ratio versus number of cycles

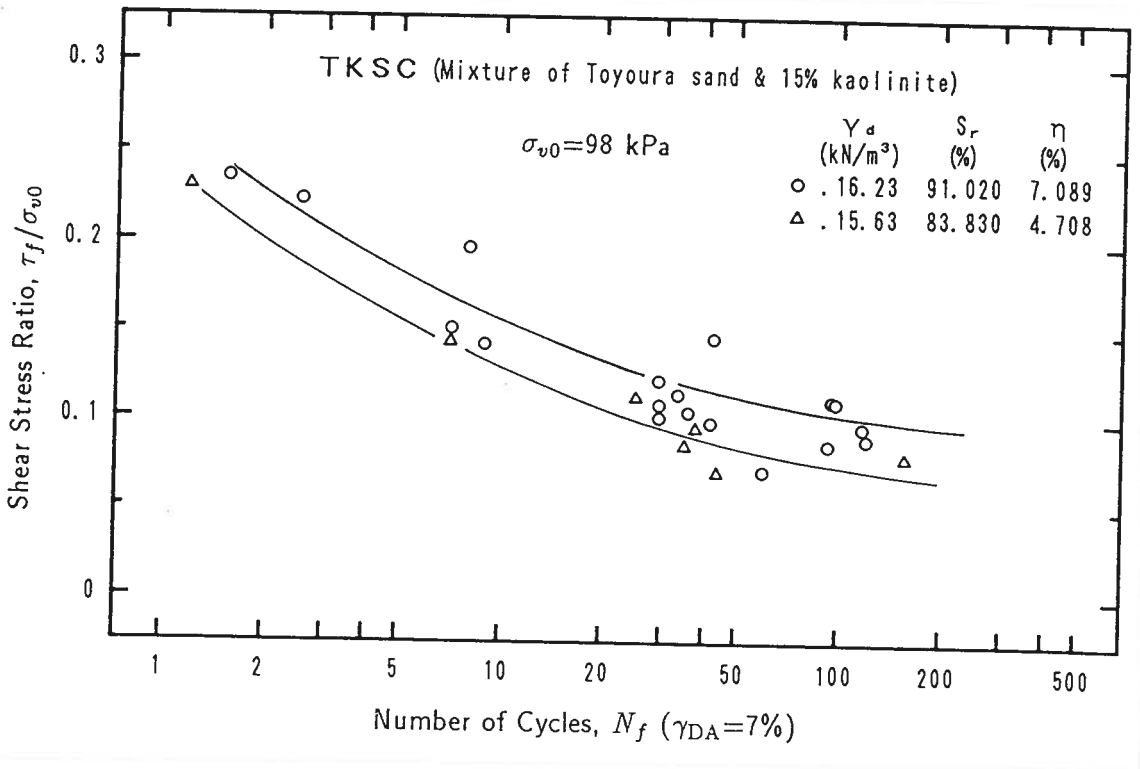

Figure 6.2: Cyclic shear stress ratio versus number of cycles

increase in water content, and reach an almost identical condition at the end. This change in the state of the samples is illustrated by arrows in Fig. 6.3 for material *TKSC* (Mixture of Toyoura sand and 15% kaolinite). For example, point A in Fig. 6.3 indicates an initial state of loose sample compacted to an as-compacted dry unit weight of $\gamma_{d0} = 14.39kN/m^3$ at an initial water content of $w_0 = 3\%$. When the overburden pressure of $\sigma_{v0} = 98kPa$ is applied to the sample, the density increases to a value of $15.10kN/m^3$ as indicated by point A' in Fig. 6.3. When the sample is subsequently infiltrated with water, its water content increases to a value of 21%, accompanied by a further increase in dry density to a value of $16.29kN/m^3$, as indicated by point A'' in the figure. During this water absorbing process, a hydraulic collapse as high as 7.34% is observed. Similar process of state change of other samples which are densely compacted initially is indicated by points $B \rightarrow B' \rightarrow B''$ and $C \rightarrow C' \rightarrow C''$ in Fig. 6.3, wherein the values of collapsibility are as small as 0.82% and 0%, respectively. It can be found that the final state reached after soaking is practically identical with the dry unit weight of 16.22 kN/m^3 and water content about 20%. The corresponding degree of saturation is about 80% which is slightly higher than the value of line of optimum. It is observed, in sample C in Fig. 6.3, that the water content decreases during consolidation and wetting. This is an occlusion phenomenon that air is occluded in pore water and migrated only with pore water. In fact, the change of state of sample C does not follow the locus $C \rightarrow C' \rightarrow C''$ as indicate by solid lines. It might follow the track $C \rightarrow C''$ as indicated by broken line. This is because in the case of sample with high initial water content, the sample is in a state of occlusion. Water and air are drained out during consolidation. Although water passes through the sample during soaking, the sample does not absorb additional water. Similar changes in the state of samples for the other materials used are presented in Figs. 6.4 to 6.7. The occlusion phenomenon also appears in the samples of high molding water content.

6.4 SEISMIC SHEAR STRENGTH BEHAVIOR

In order to investigate the effect of the magnitude of collapse on the seismic behavior of collapsible soils, a series of simple shear tests are performed on five materials. The cyclic loading phase of the tests is executed after the samples have reached the identical state of dry density and water content. The typical time histories of shear strain and developed excess pore pressures are demonstrated in Figs. 6.8 to 6.17. Each figure gives a pair of results of samples which have approximately the same condition of dry density and water content prior to the application of cyclic loading and have born the same amplitude of cyclic shear stress but have undergone different amount of collapse. These figures show

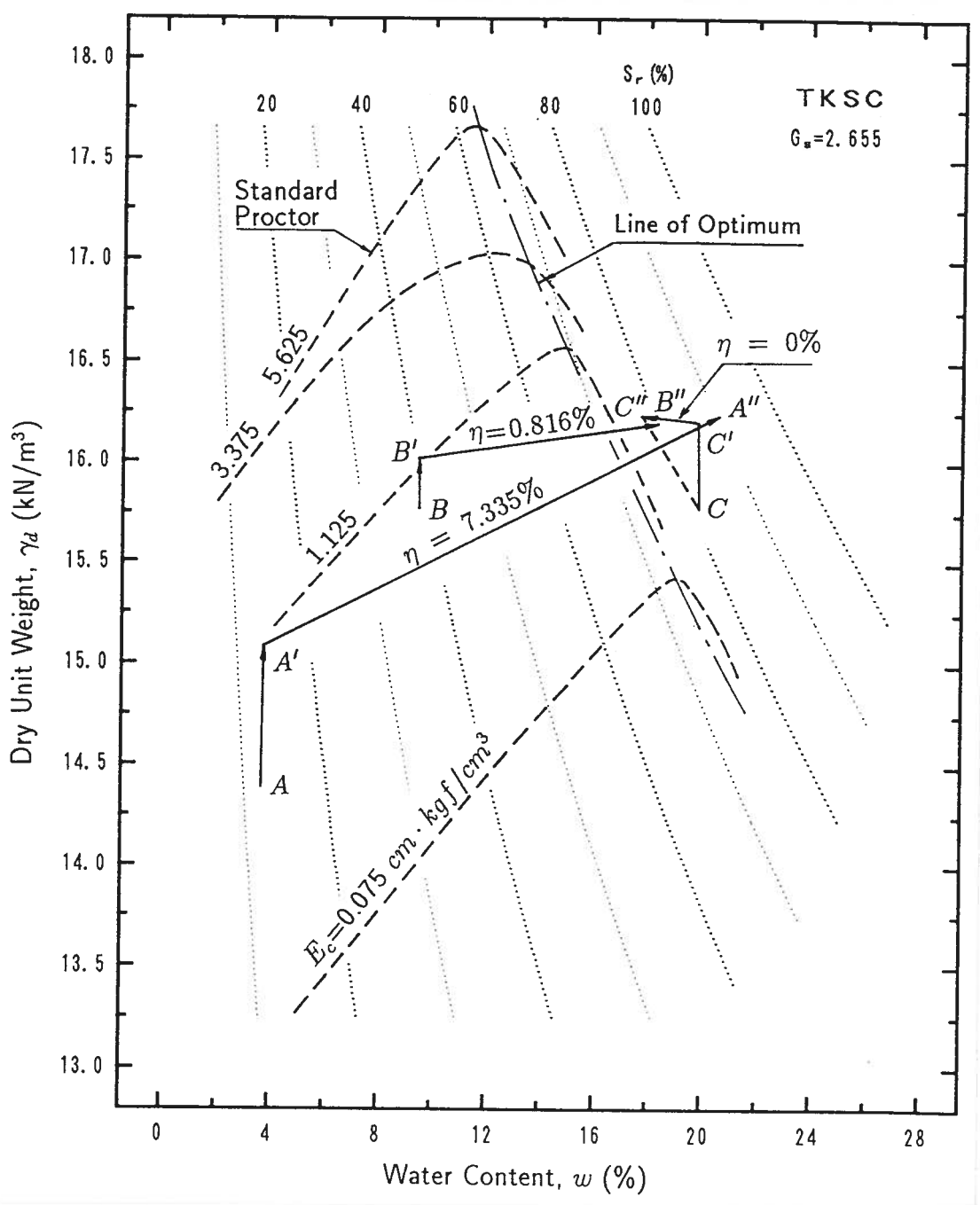

Figure 6.3: Changes in the state of samples during application of overburden pressure and water permeation

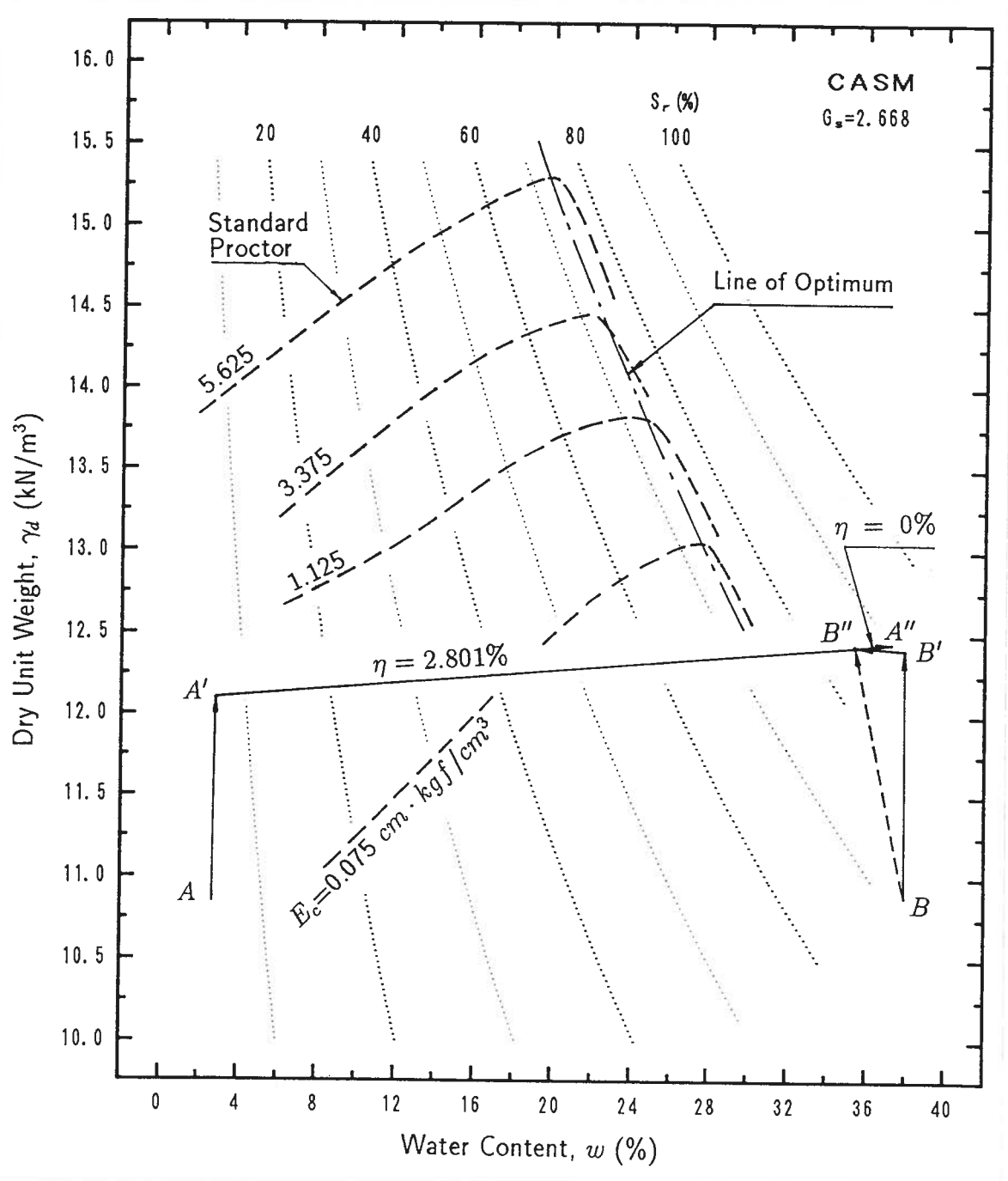

Figure 6.4: Changes in the state of samples during application of overburden pressure and water permeation

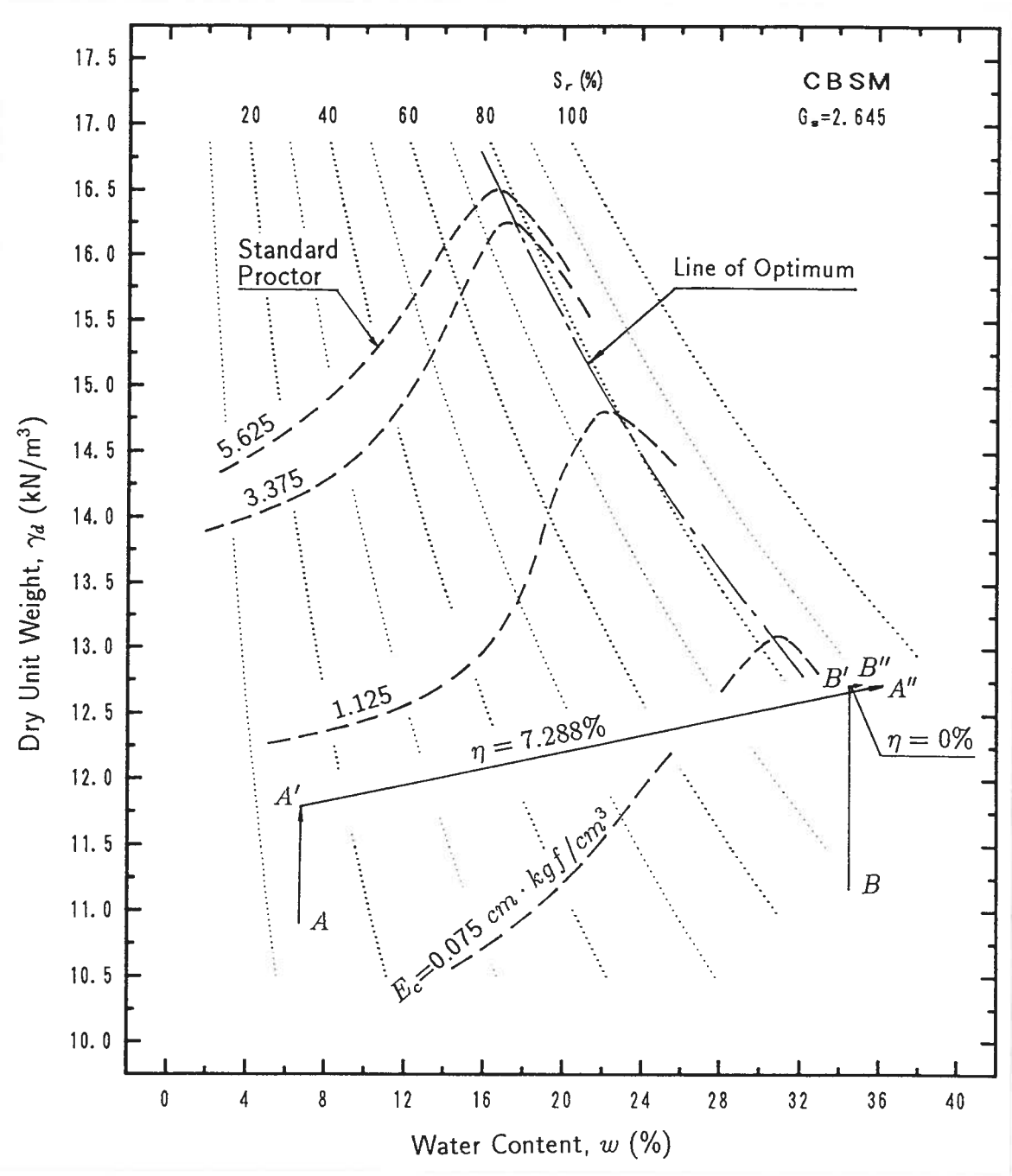

Figure 6.5: Changes in the state of samples during application of overburden pressure and water permeation

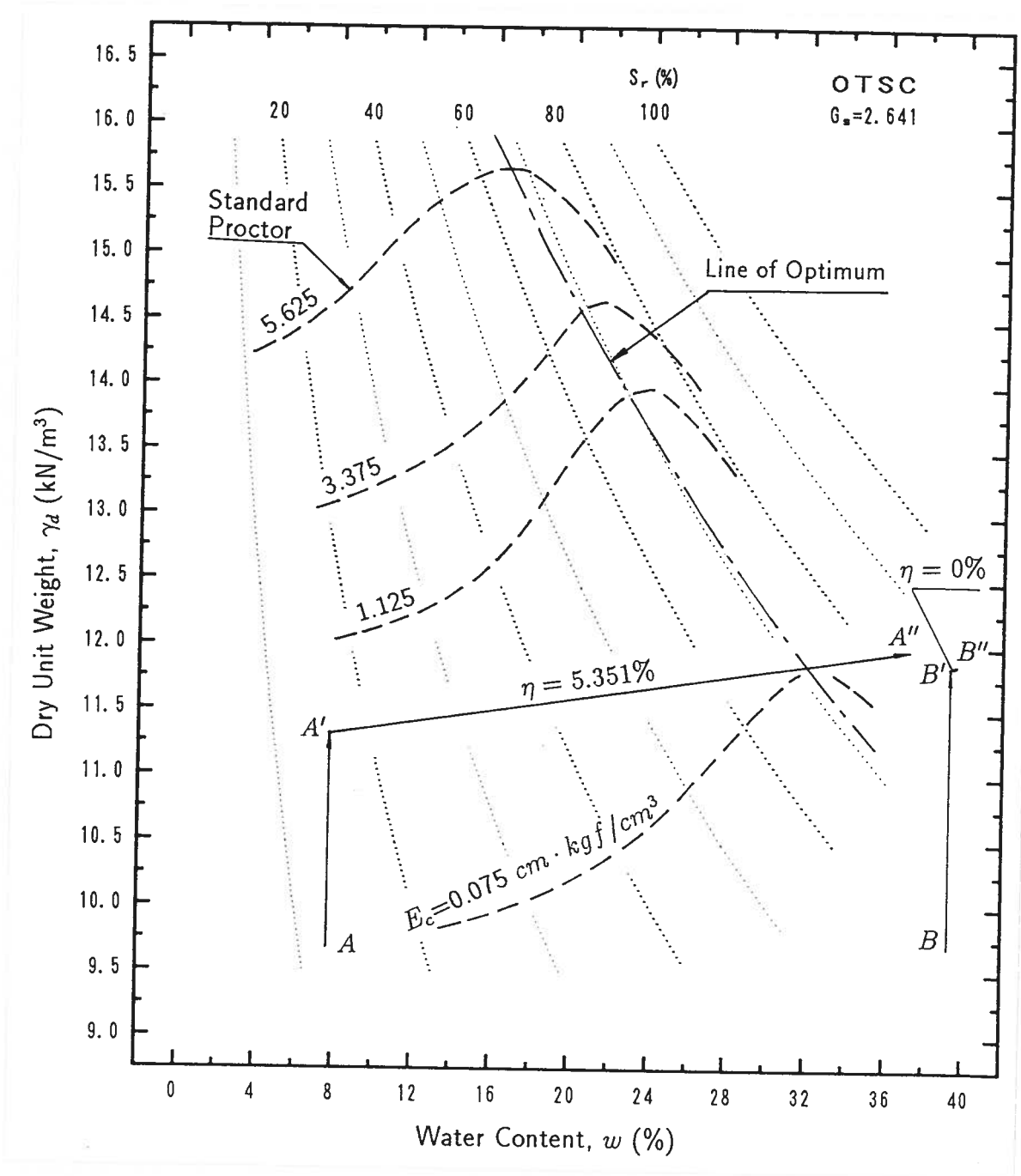

Figure 6.6: Changes in the state of samples during application of overburden pressure and water permeation

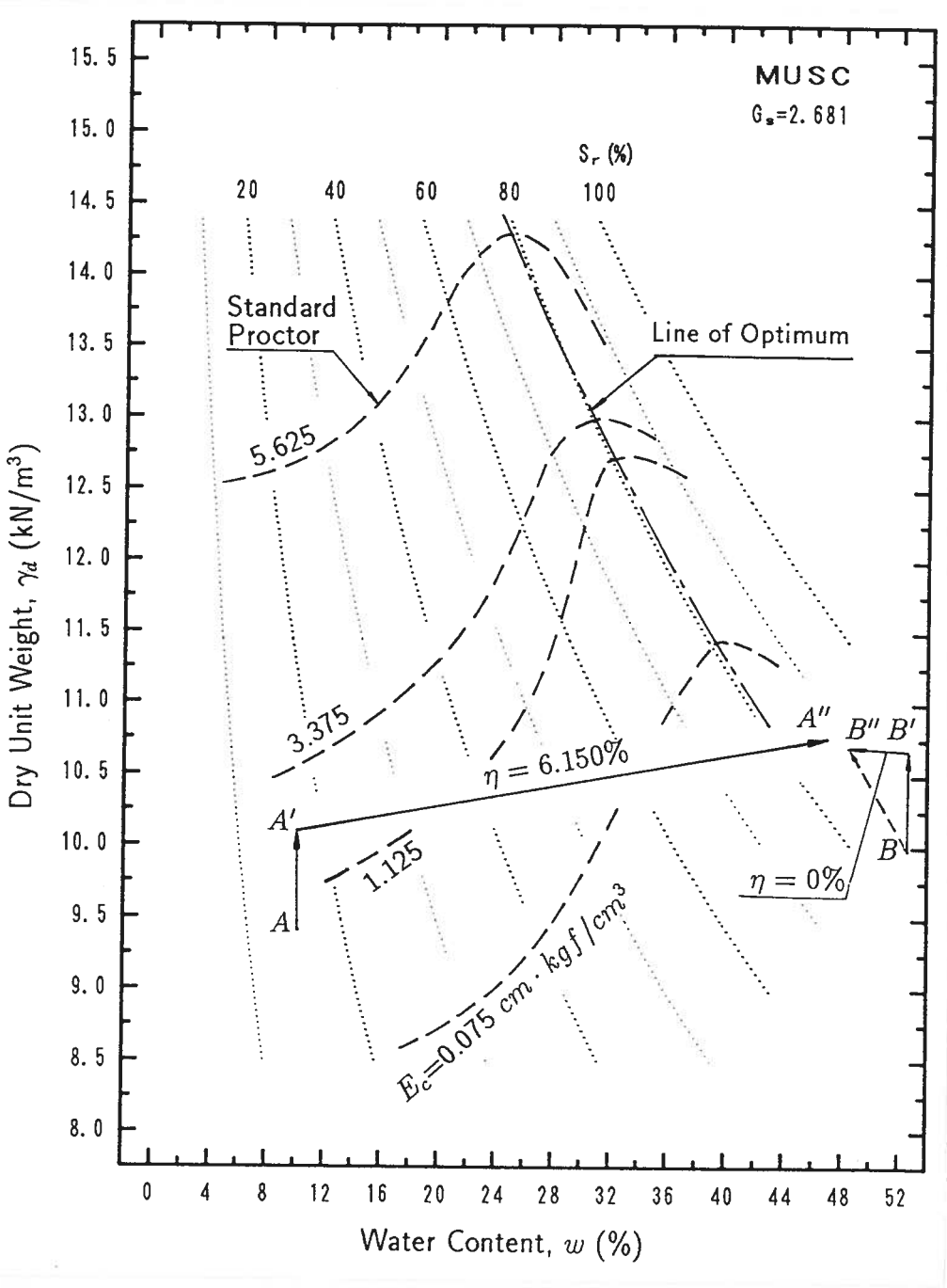

Figure 6.7: Changes in the state of samples during application of overburden pressure and water permeation

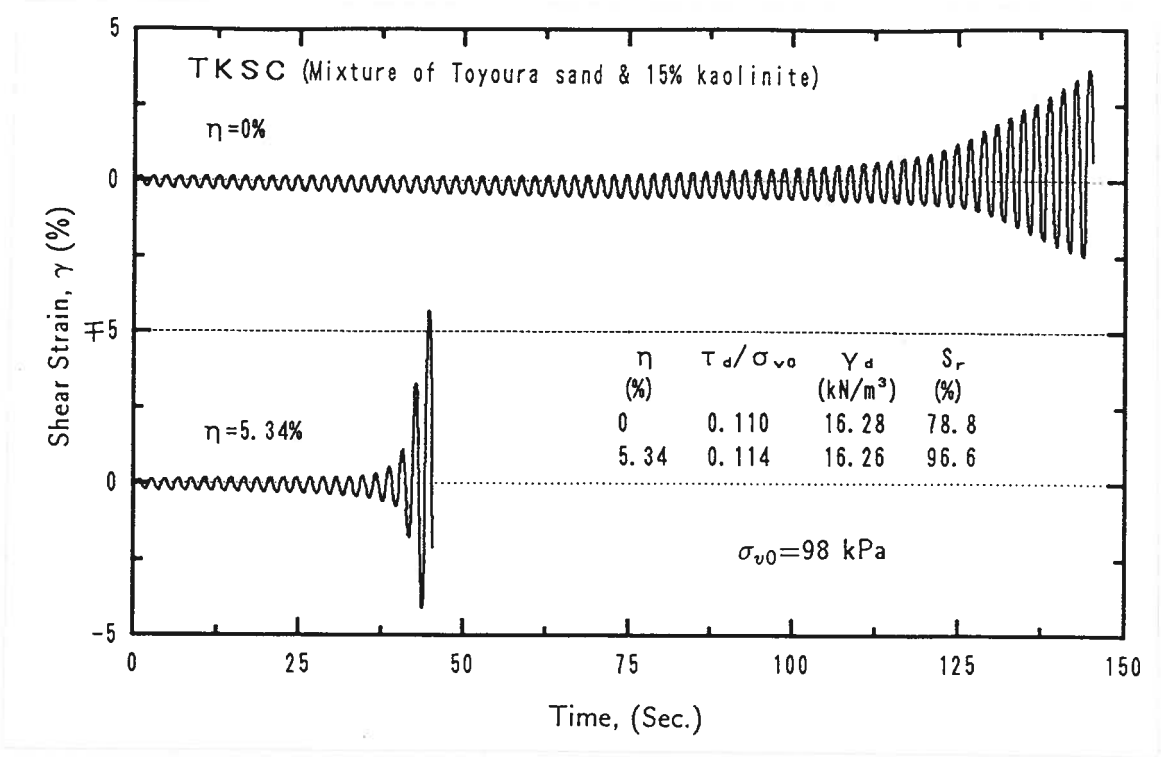

Figure 6.8: Time histories of shear strain of samples with different collapse

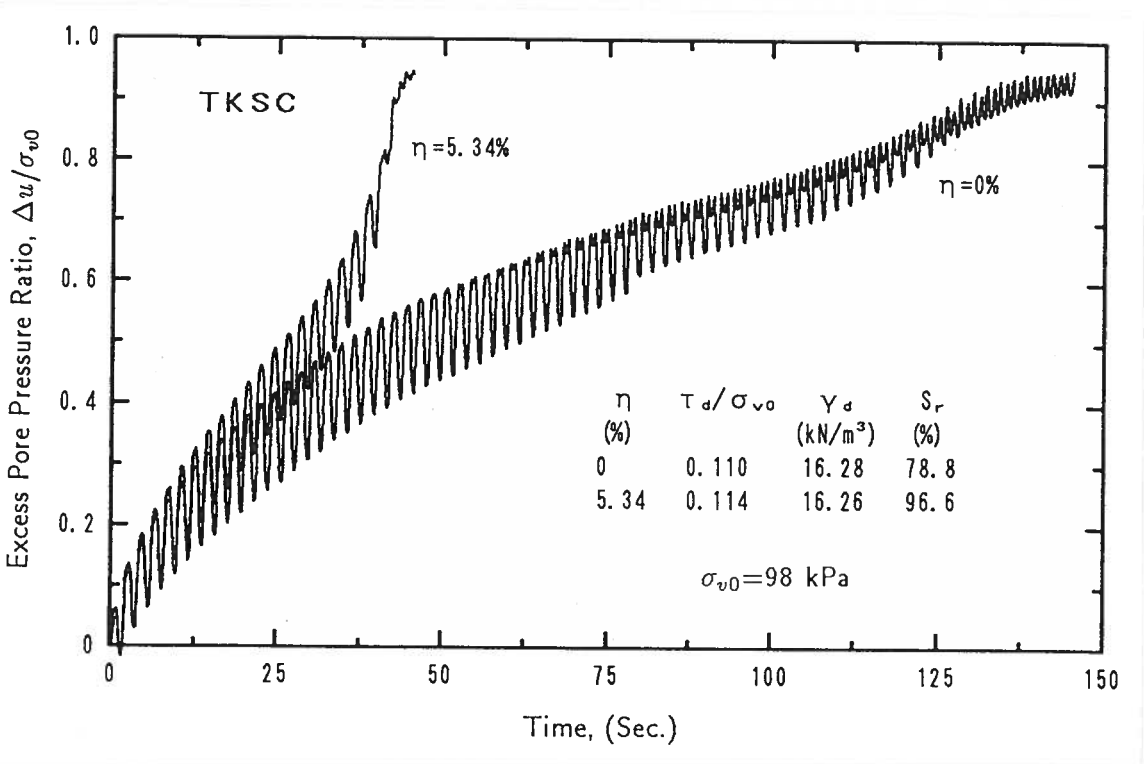

Figure 6.9: Time histories of excess pore pressure ratio of samples with different collapse

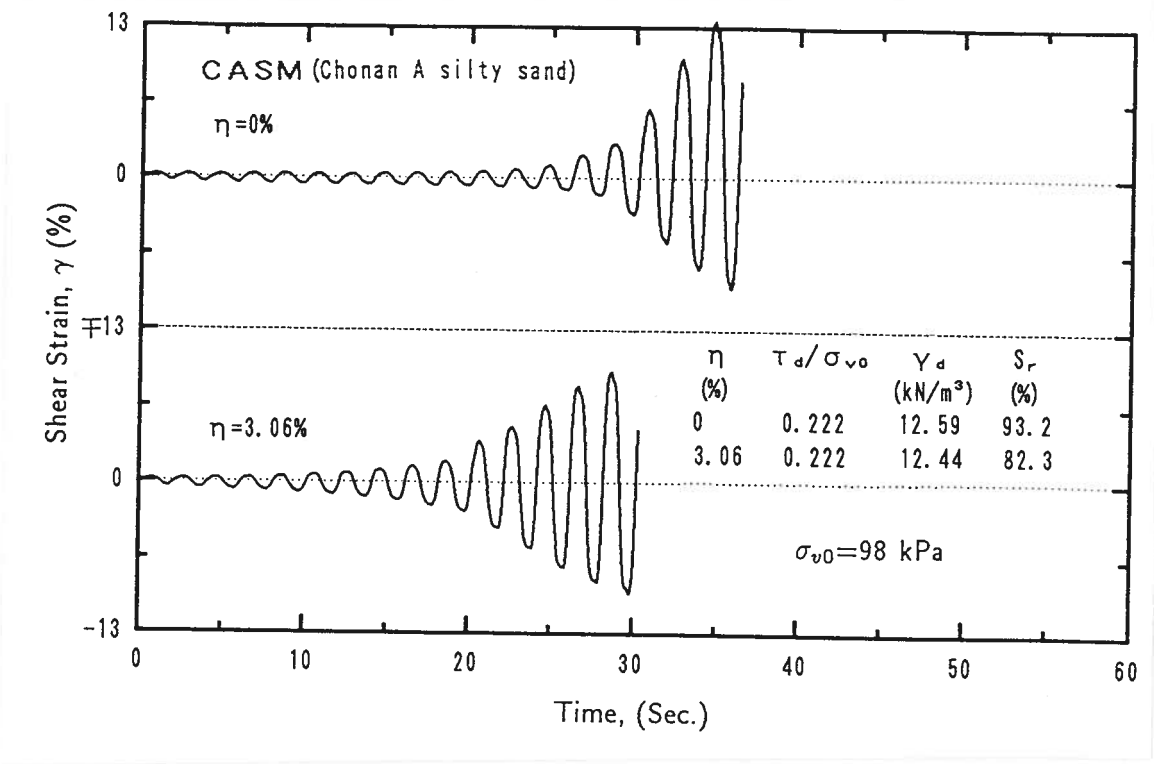

Figure 6.10: Time histories of shear strain of samples with different collapse

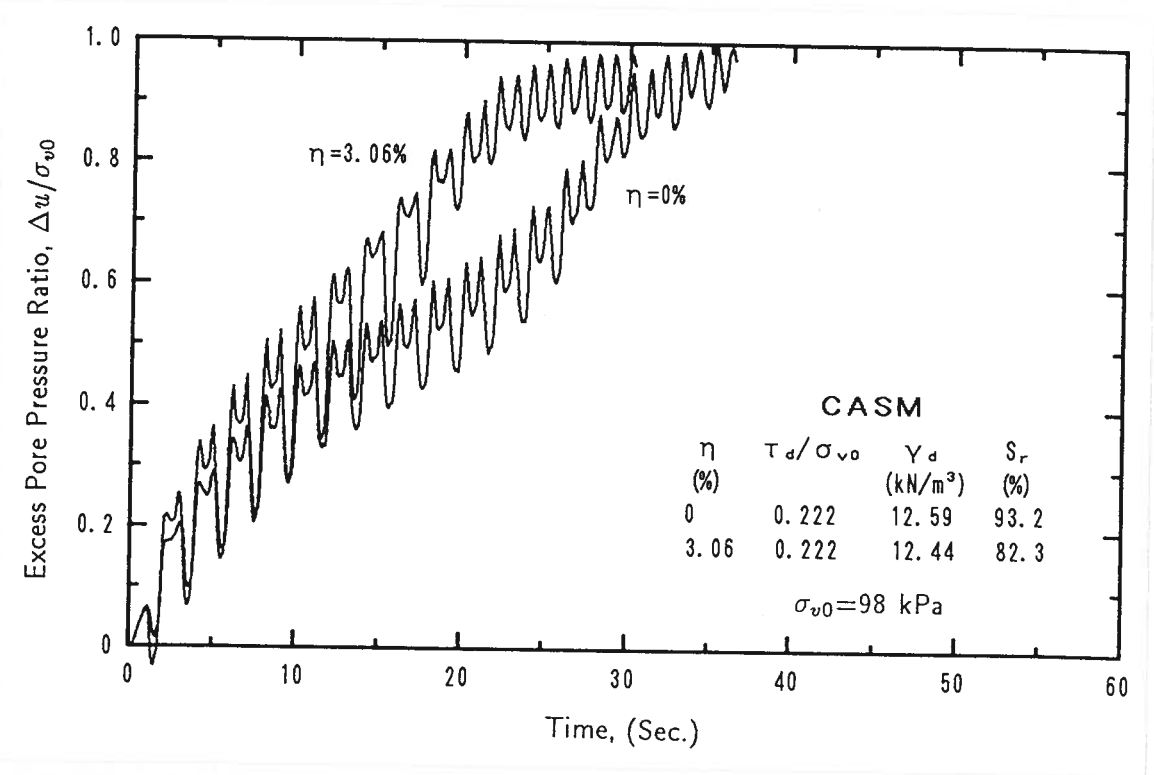

Figure 6.11: Time histories of excess pore pressure ratio of samples with different collapse

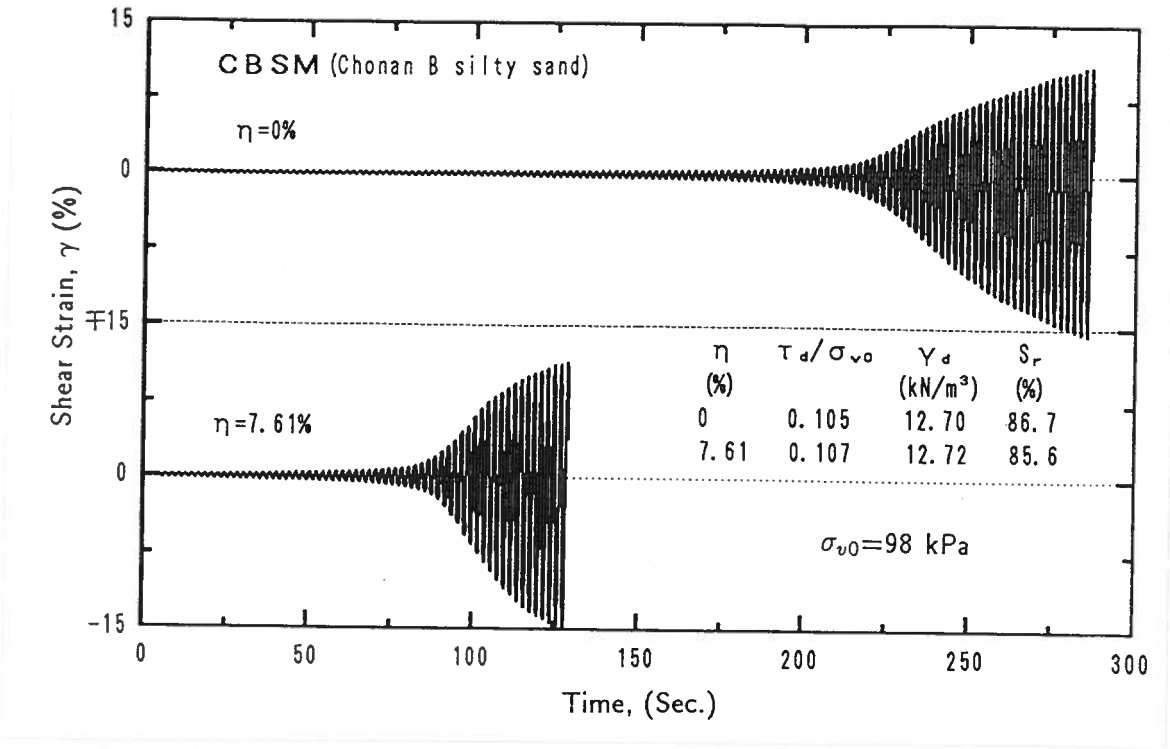

Figure 6.12: Time histories of shear strain of samples with different collapse

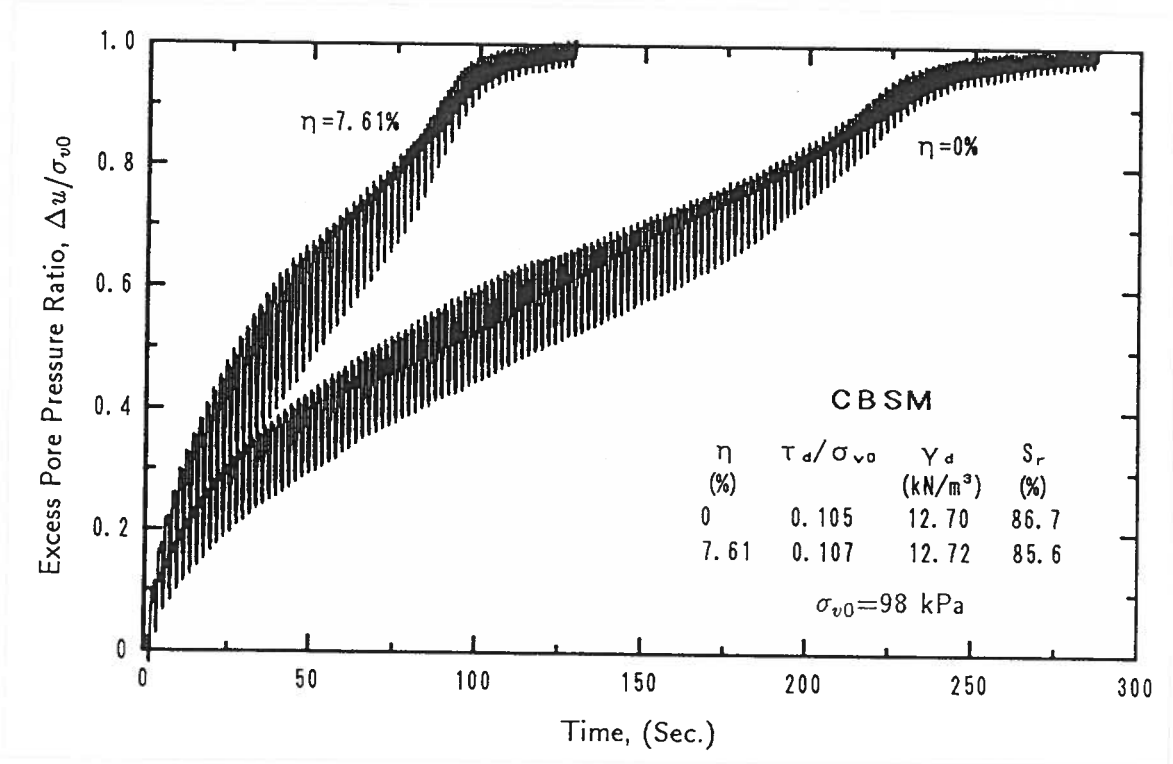

Figure 6.13: Time histories of excess pore pressure ratio of samples with different collapse

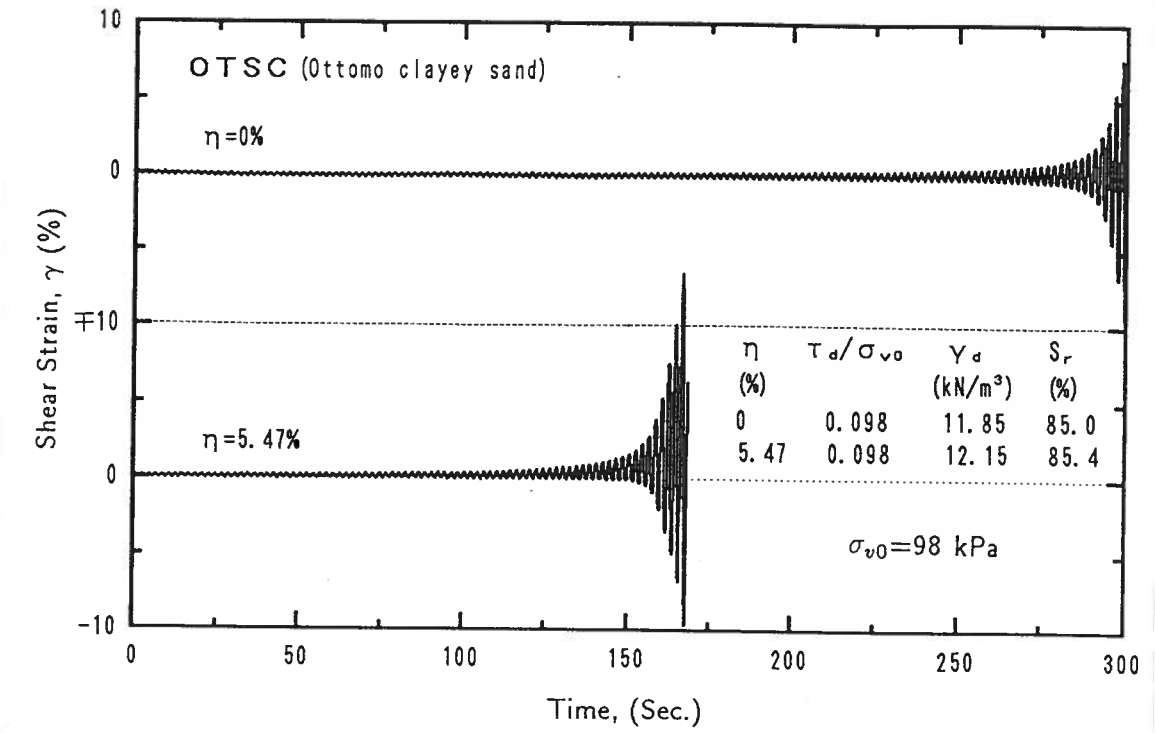

Figure 6.14: Time histories of shear strain of samples with different collapse

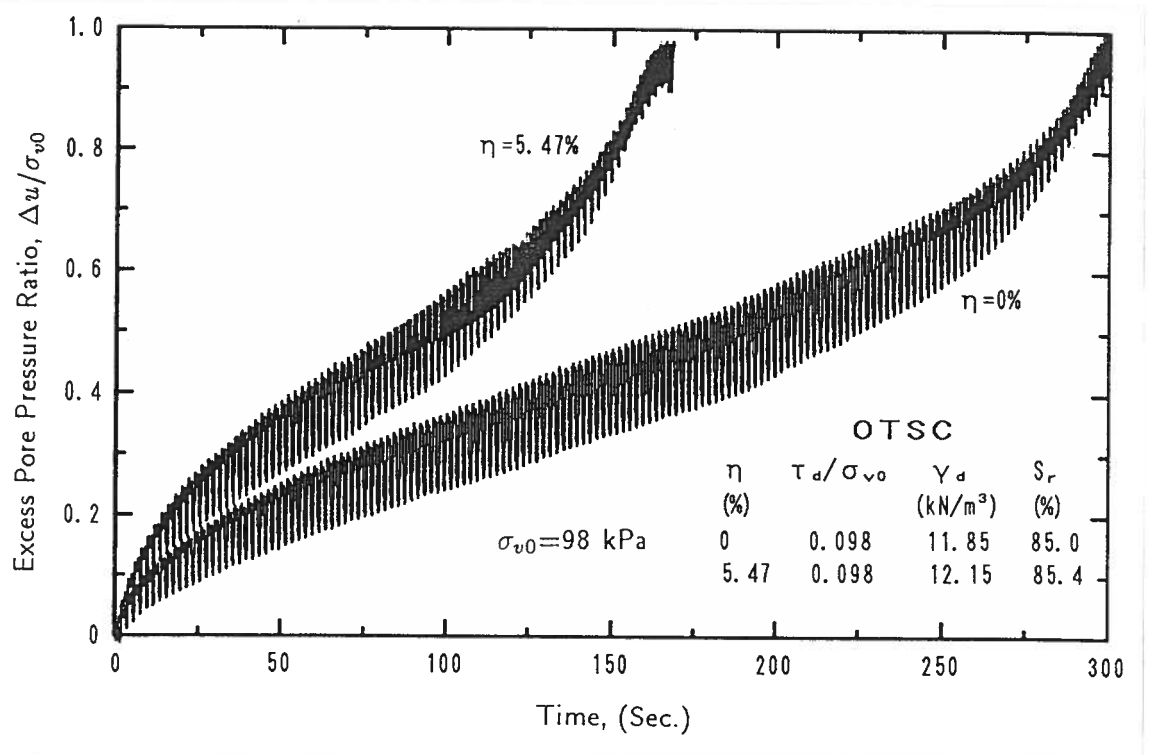

Figure 6.15: Time histories of excess pore pressure ratio of samples with different collapse

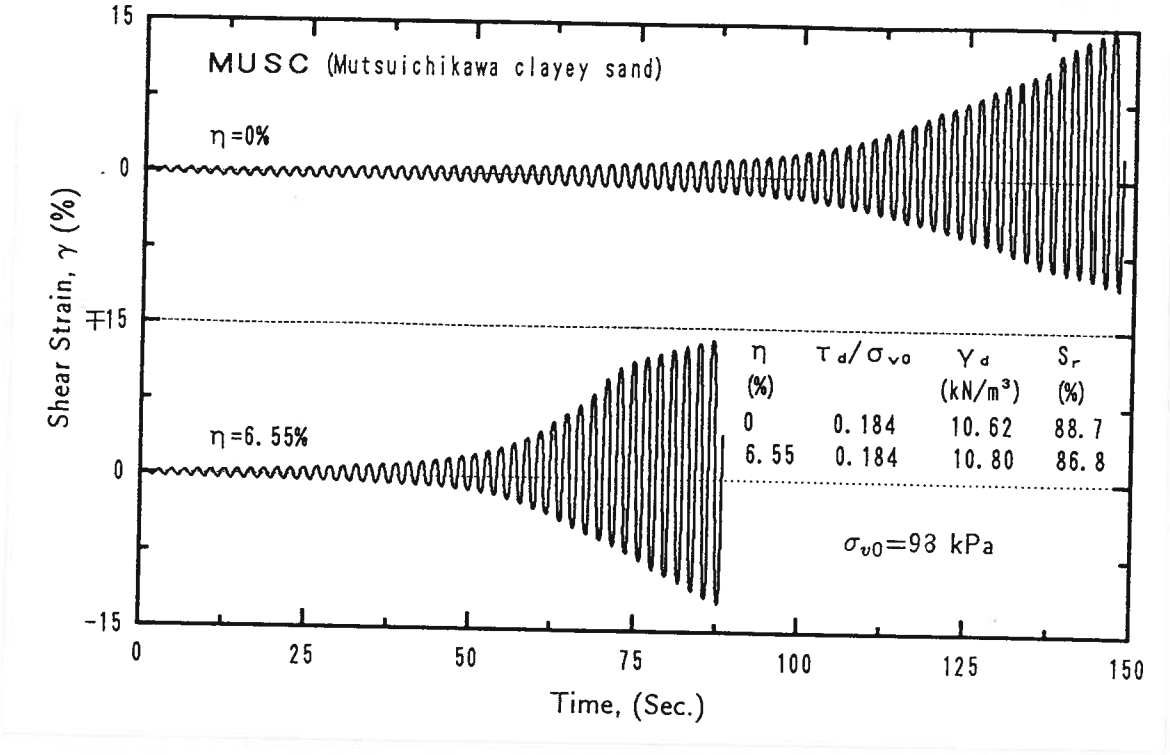

Figure 6.16: Time histories of shear strain of samples with different collapse

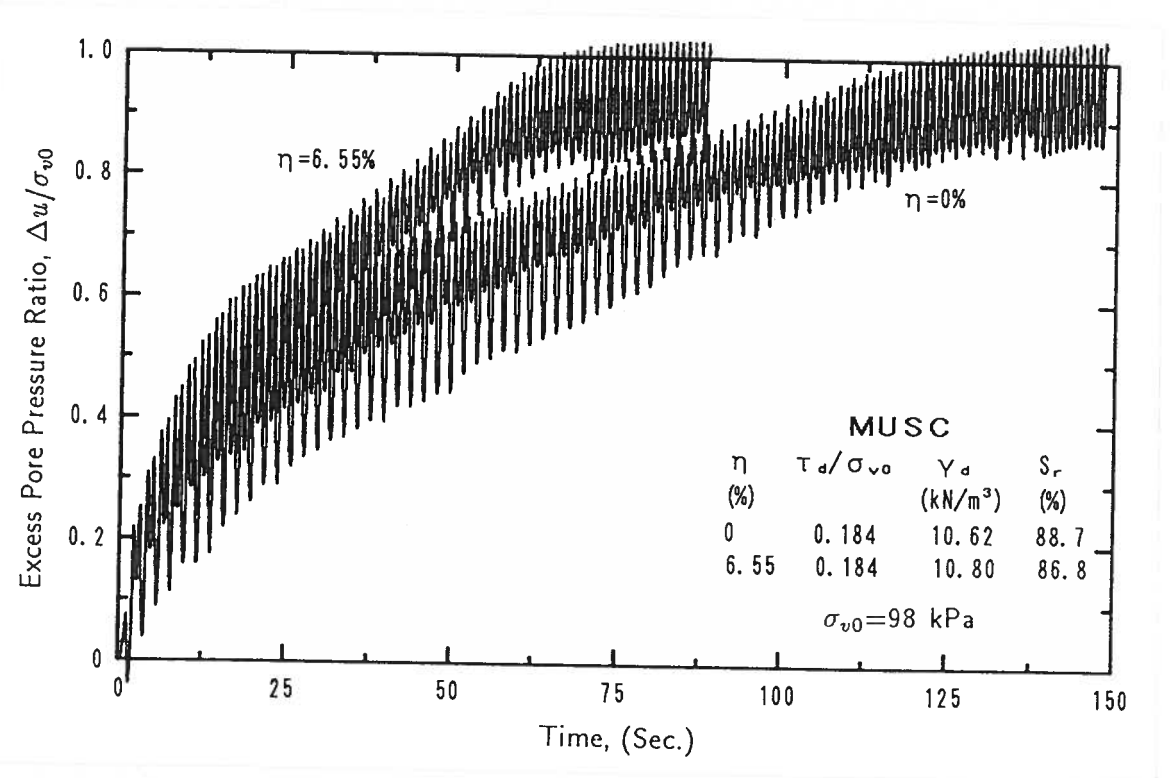

Figure 6.17: Time histories of excess pore pressure ratio of samples with different collapse

that collapse caused by water permeation weakens the capability of collapsible soils to resist seismic loading. In order to illustrate this weakening, the results of cyclic simple shear tests conducted under constant-volume condition are presented in Figs. 6.18 to 6.22 for the five materials, respectively. The cyclic shear stress ratios required to cause ±3.5% shear strain are plotted versus the number of cycles. As indicated in the legend of Figs. 6.18 to 6.22, the samples just prior to cyclic load application have been brought to approximately the same conditions with respect to dry density, water content and degree of saturation. The only difference is the process or history in hydraulic collapse which the samples have experienced until they reached the final state. It is evident that all the results show that for a given number of cycles, the cyclic shear stress ratio required to yield ±3.5% shear strain depends significantly on the magnitude of collapse experienced by the samples prior to cyclic shearing. The greater the degree of collapse, the smaller is the stress ratio needed to develop the same magnitude of shear strain at the same number of cycles or the shorter is the time to sustain at the same stress ratio. The samples in all the tests are wetted and have relatively high and almost identical values of saturation ratios. At these saturation ratios (usually greater than 80%), suction action (the effective stress caused by suction) is considered the same in both samples whether they have undergone high or low collapse. Therefore, the suction is not the factor influencing the strength in this situation. It is considered that it is the microstructure of soil which affect the strength properties. Samples which show different magnitude of collapse have different microstructures (the details will be discussed in Chapter 9).

In order to see the effect of collapse on cyclic strength behavior of collapsible soils, the cyclic stress ratios required to induce ±3.5% shear strain under a certain number of cycles are read off from Figs. 6.18 to 6.22 and are plotted versus collapsibility coefficient in Figs. 6.23 to 6.27. It can be clearly seen in these figures that, for a given number of cycles, the cyclic stress ratio required to induce cyclic softening in all the materials tested tends to decrease as the collapsibility coefficient increases. This decrease can be expressed in terms of the strength reduction factor which is defined as:

$$\frac{(\tau_f)_{\eta 0} - (\tau_f)_{\eta h}}{(\tau_f)_{\eta 0}} \times 100\% \tag{6.10}$$

where, $(\tau_f)_{\eta 0}$ is the shear strength corresponding to zero percent collapse and $(\tau_f)_{\eta h}$ is the shear strength at high collapse. The shear strength is defined as the cyclic shear stress ratio corresponding to ±3.5% shear strain (or 7% double amplitude shear strain). The reduction of shear strength obtained for each materials tested is shown in Fig. 6.28. Except for material *MUSC* (Mutsuichikawa clayey sand), the reduction in cyclic shear strength appears to have a maximum value as the number of cycles increases. However,

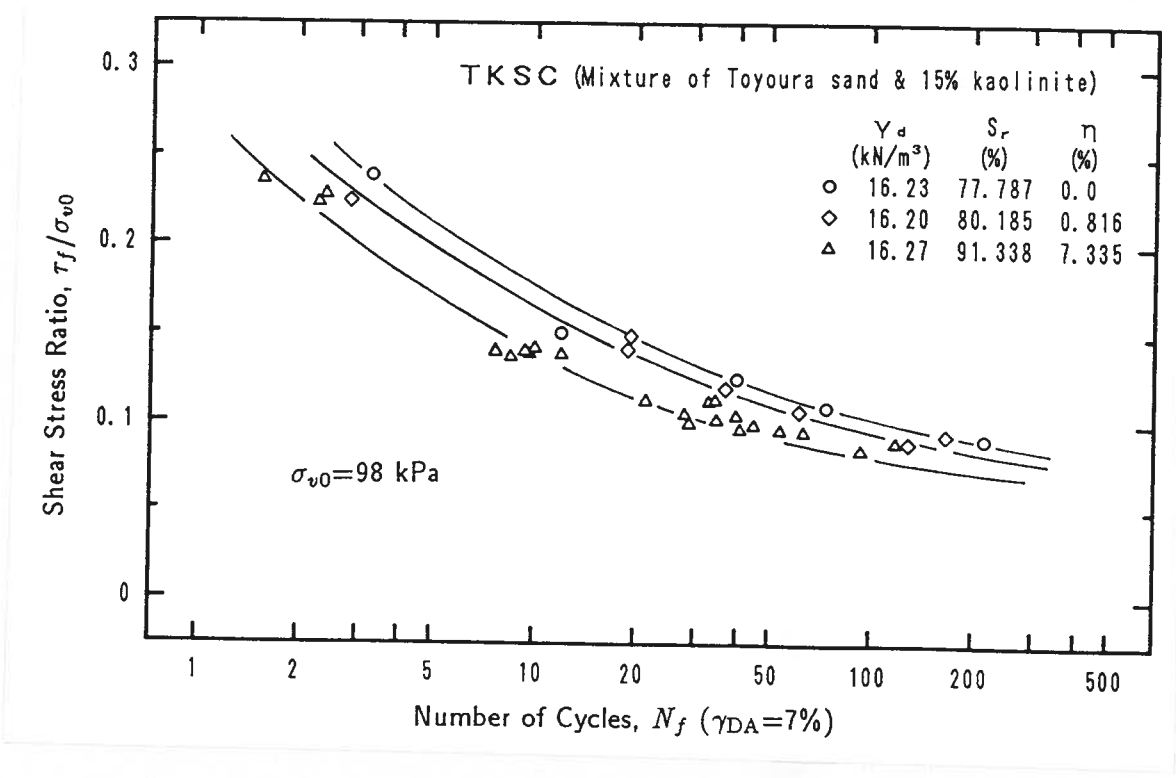

Figure 6.18: Cyclic shear stress ratio versus number of cycles

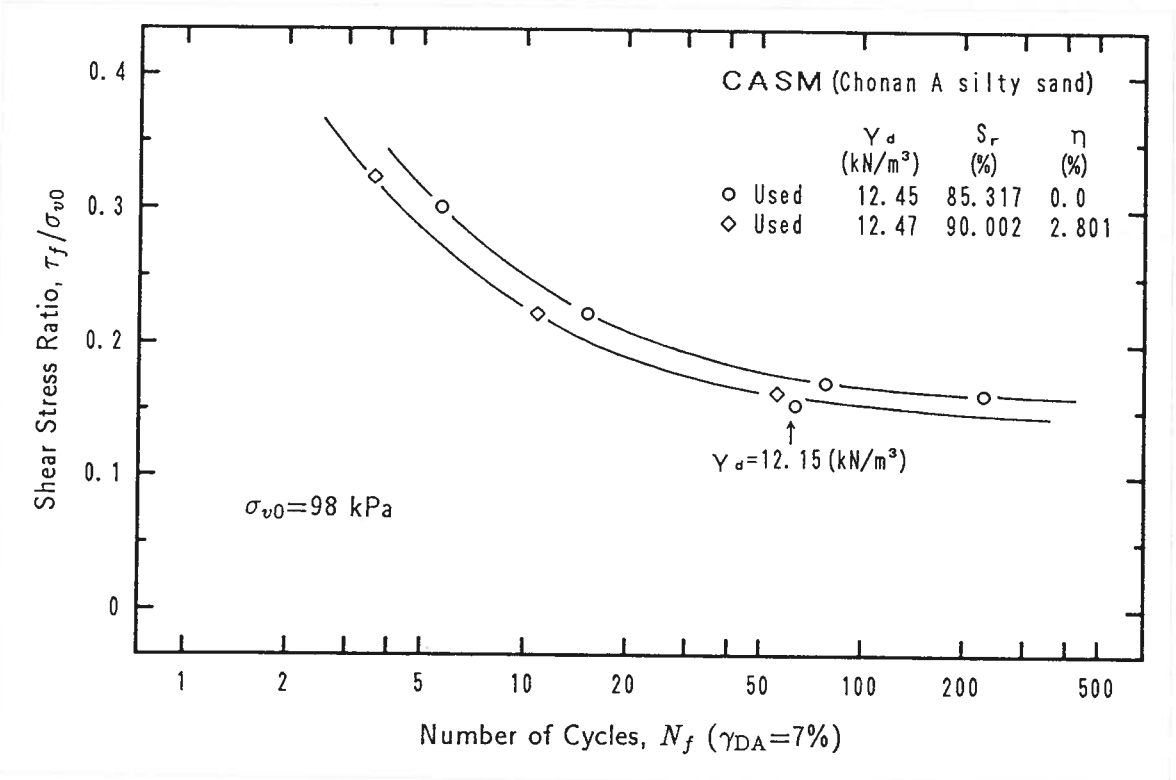

Figure 6.19: Cyclic shear stress ratio versus number of cycles

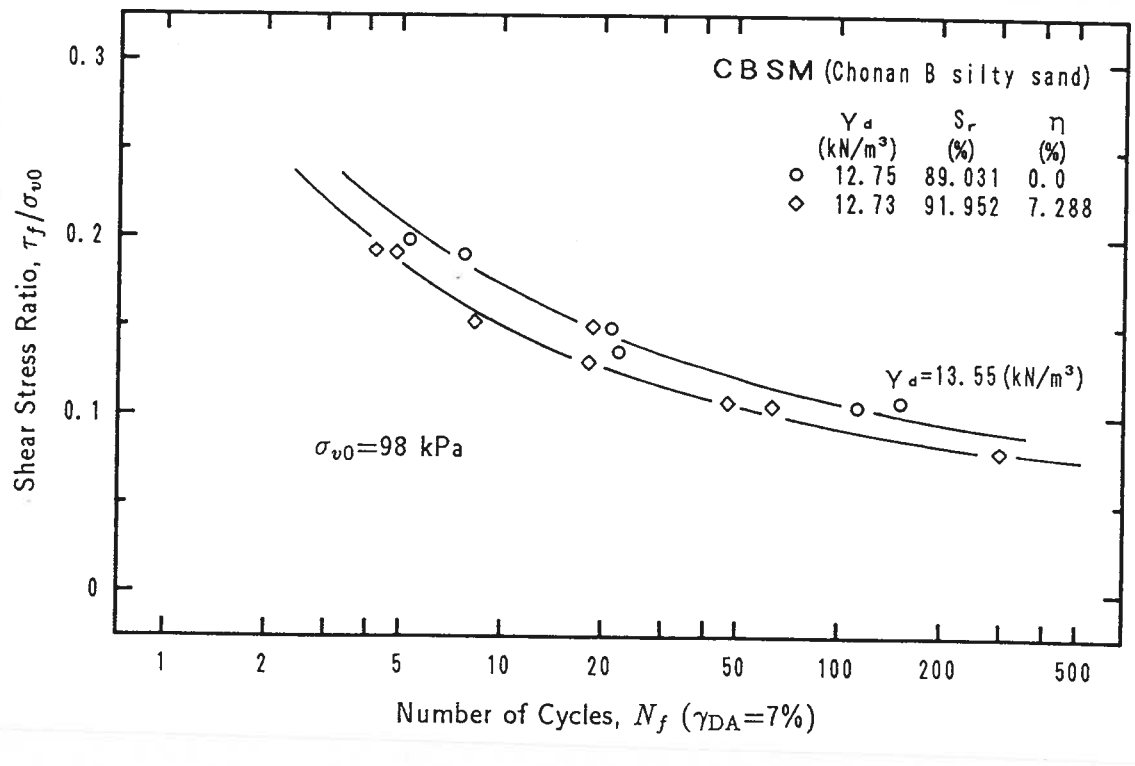

Figure 6.20: Cyclic shear stress ratio versus number of cycles

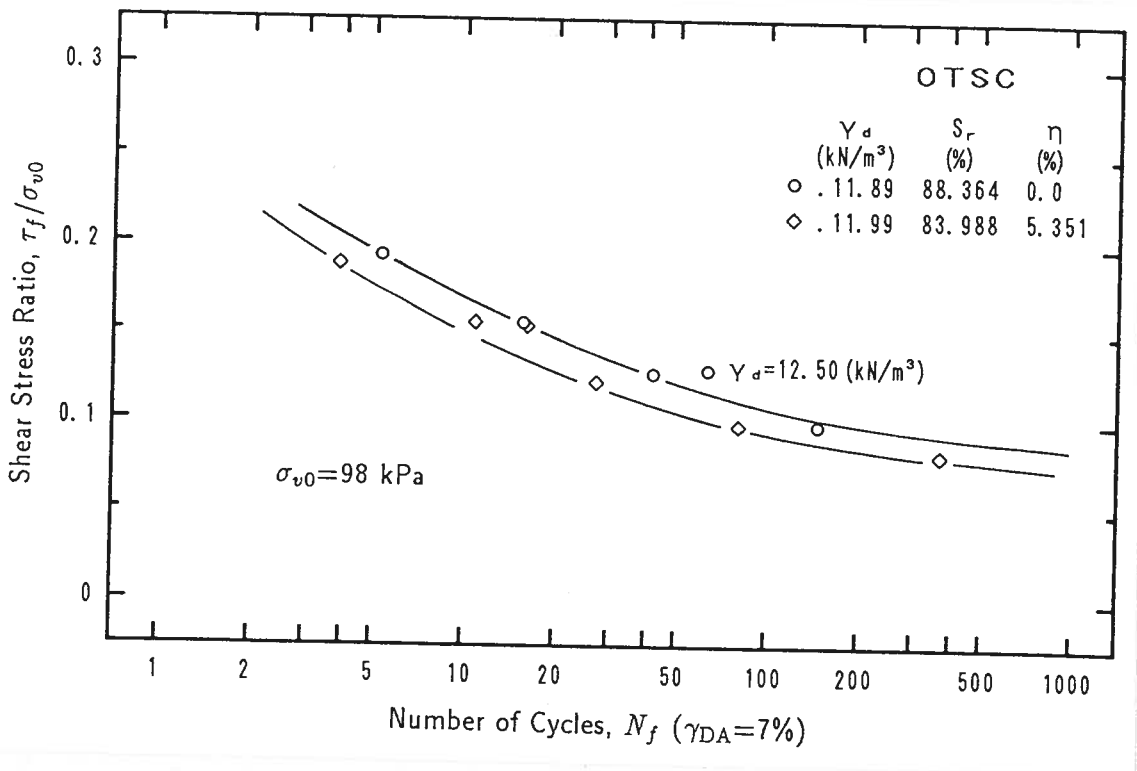

Figure 6.21: Cyclic shear stress ratio versus number of cycles

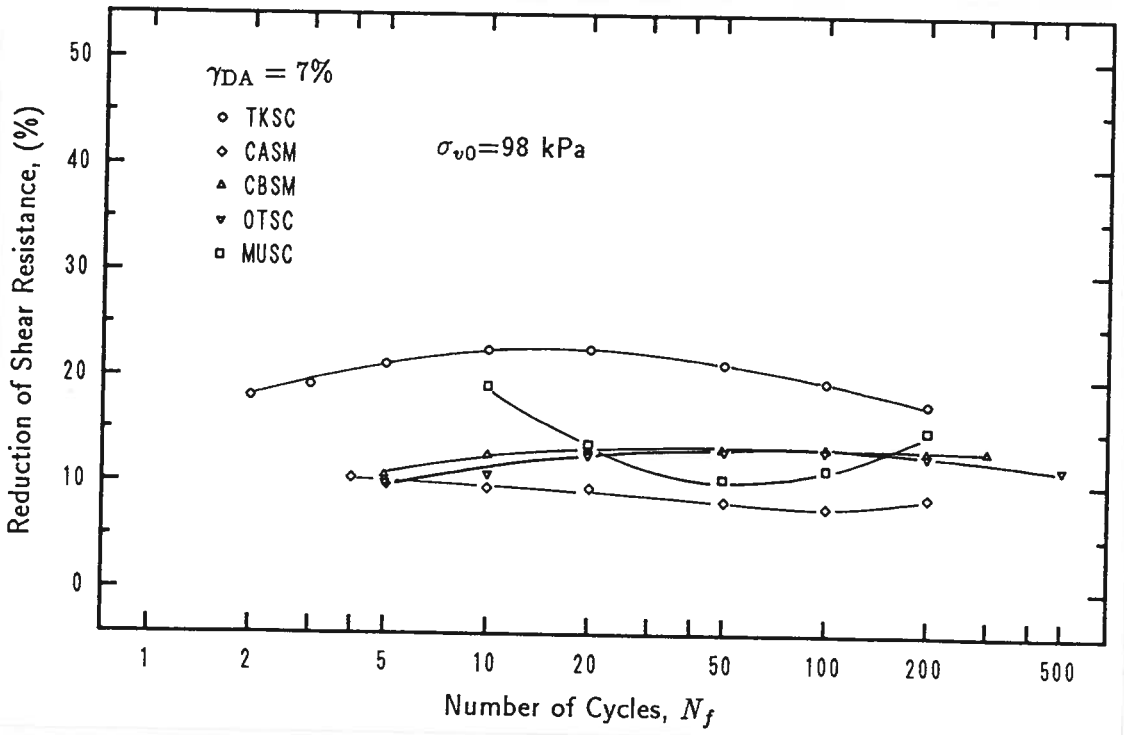

Figure 6.22: Cyclic shear stress ratio versus number of cycles

the variation is so small that it can be treated as a constant with enough accuracy for engineering purpose. Material *MUSC* (Mutsuichikawa clayey sand) gives a contrary trend regarding the change in strength reduction with number of cycles. This material is not special except that the clay content is a little higher. At this stage, it is unknown why this material gives a contrary trend of the change of strength reduction. The strength reduction at number of cycles of 10 and the average values for all the materials are given in Table. 6.1. It is obvious that the amount of collapse, or the history of hydraulic collapse has a significant influence on the cyclic strength properties. The reduction of cyclic shear strength usually is larger than 10%, even higher than 20% for some cases.

6.5 SEISMIC DEFORMATION BEHAVIOR

In the present study, all the cyclic tests are performed under stress controlled condition. Therefore, the stress-strain relationship could not be obtained directly from the test results. In order to get the stress-strain relationships, the relationships between the cyclic shear stress ratio and the number of cycles are plotted for each particular shear strain value. Then, it is possible to read off the combinations of values of cyclic shear

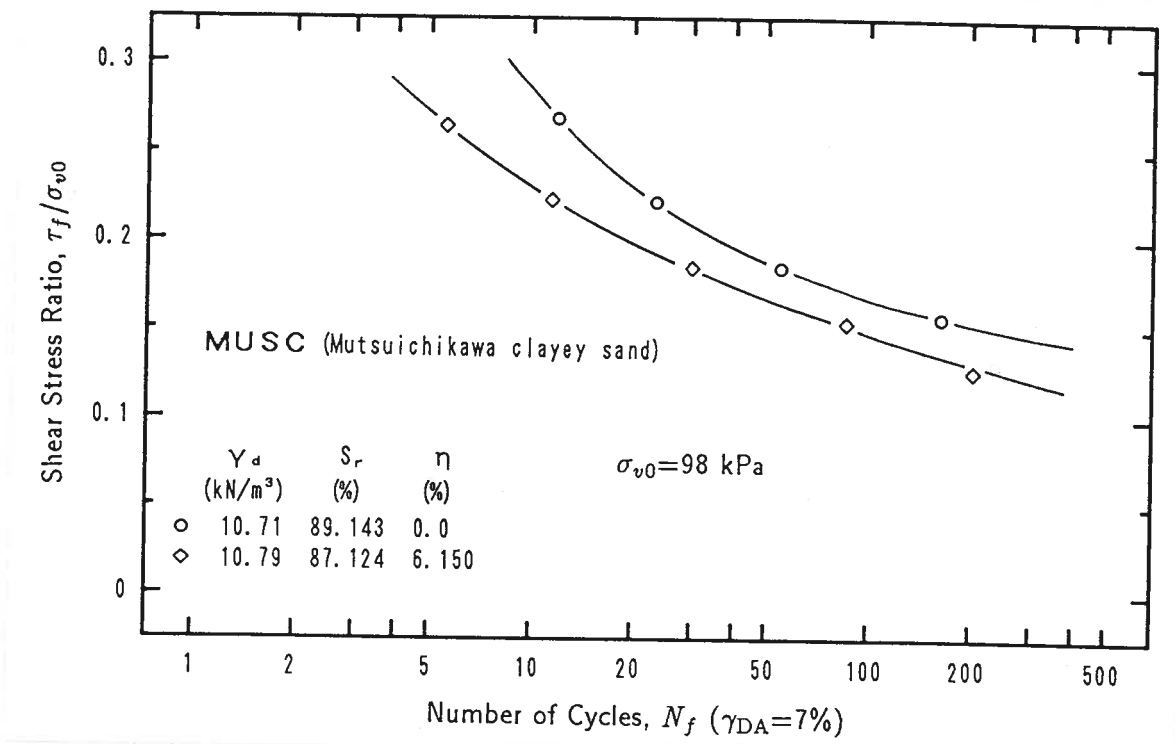

Figure 6.23: Cyclic shear strength versus collapsibility coefficient

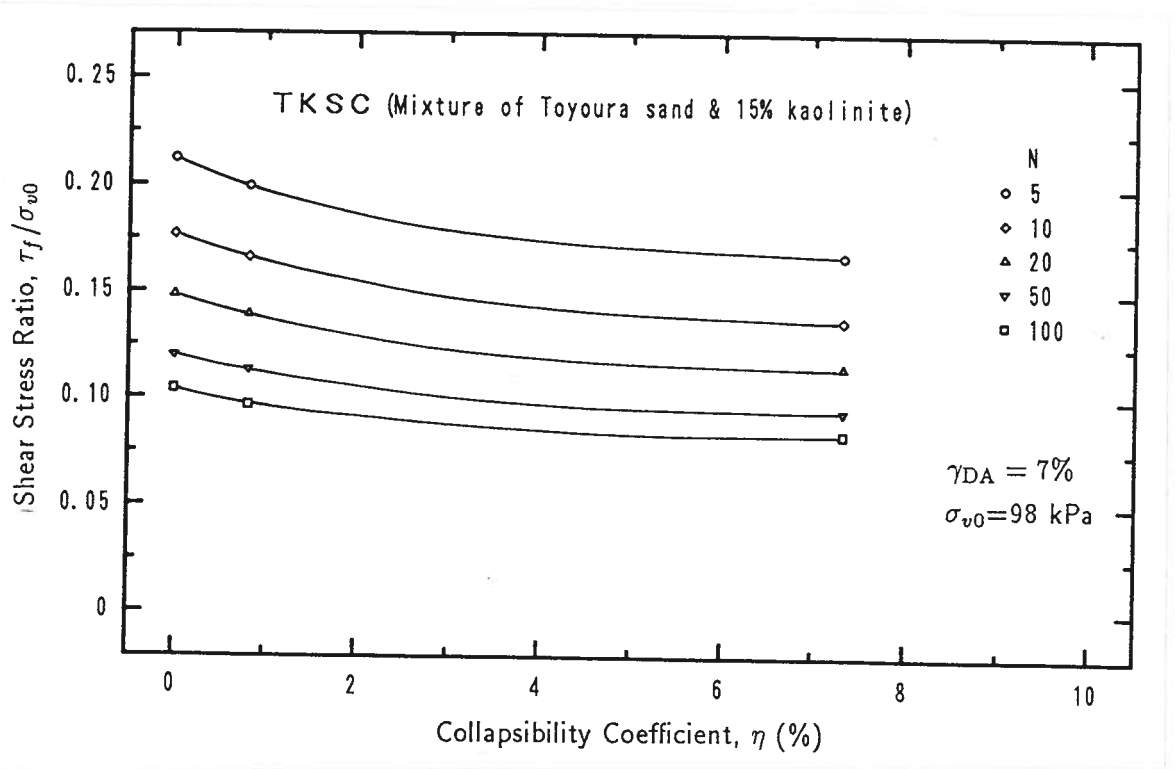

Figure 6.24: Cyclic shear strength versus collapsibility coefficient

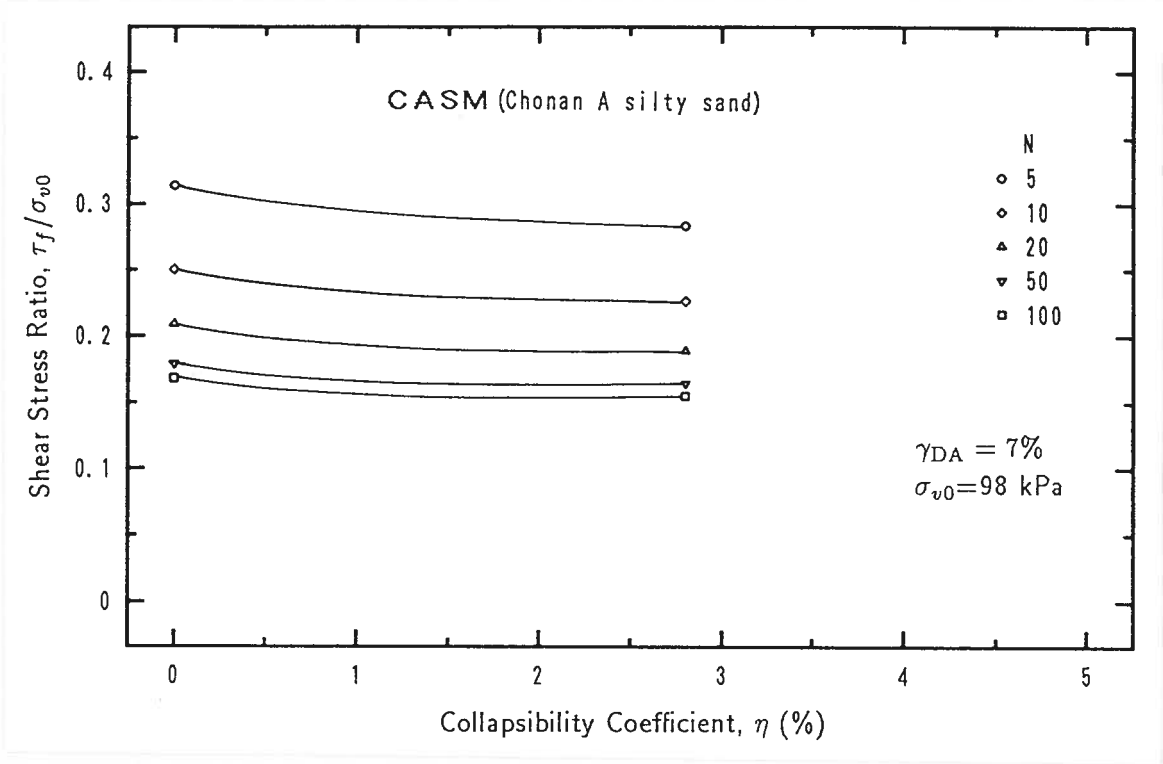

Figure 6.25: Cyclic shear strength versus collapsibility coefficient

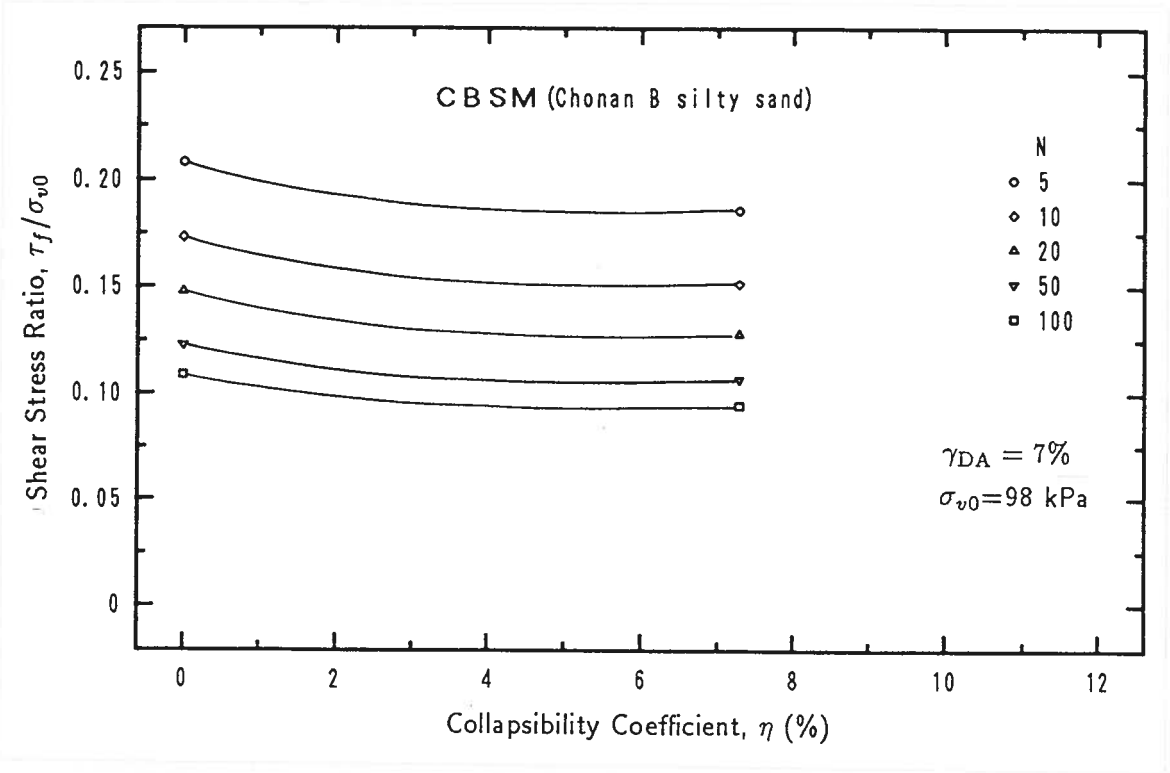

Figure 6.26: Cyclic shear strength versus collapsibility coefficient

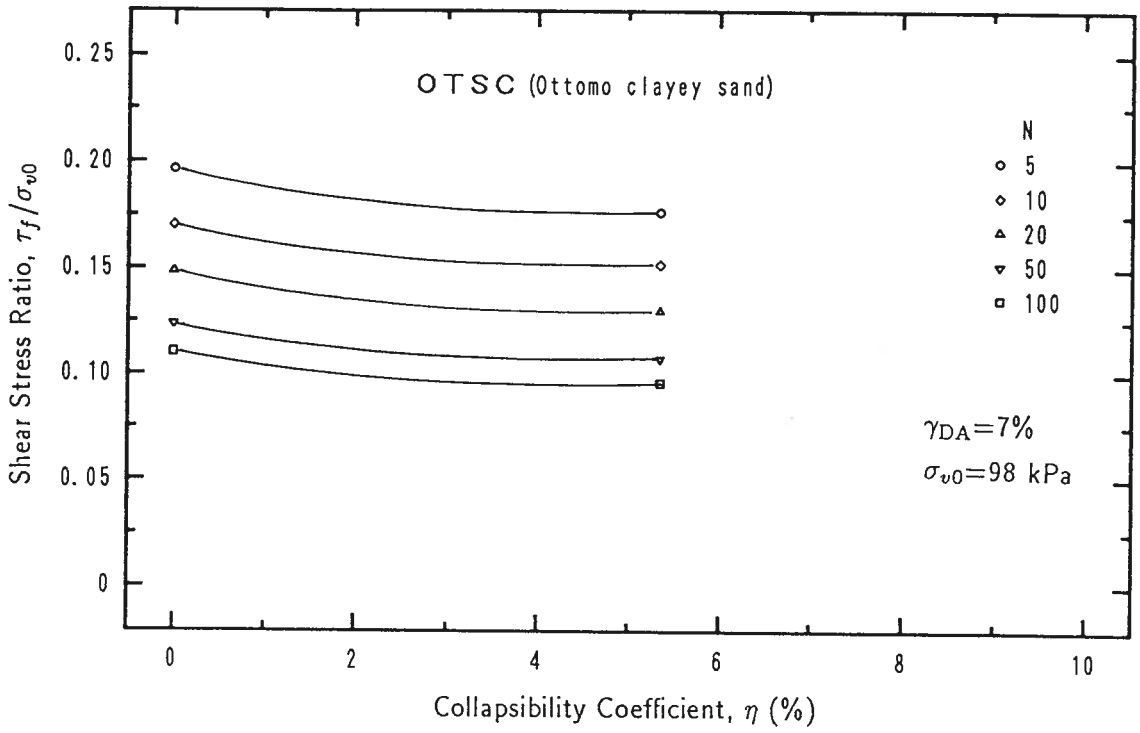

Figure 6.27: Cyclic shear strength versus collapsibility coefficient

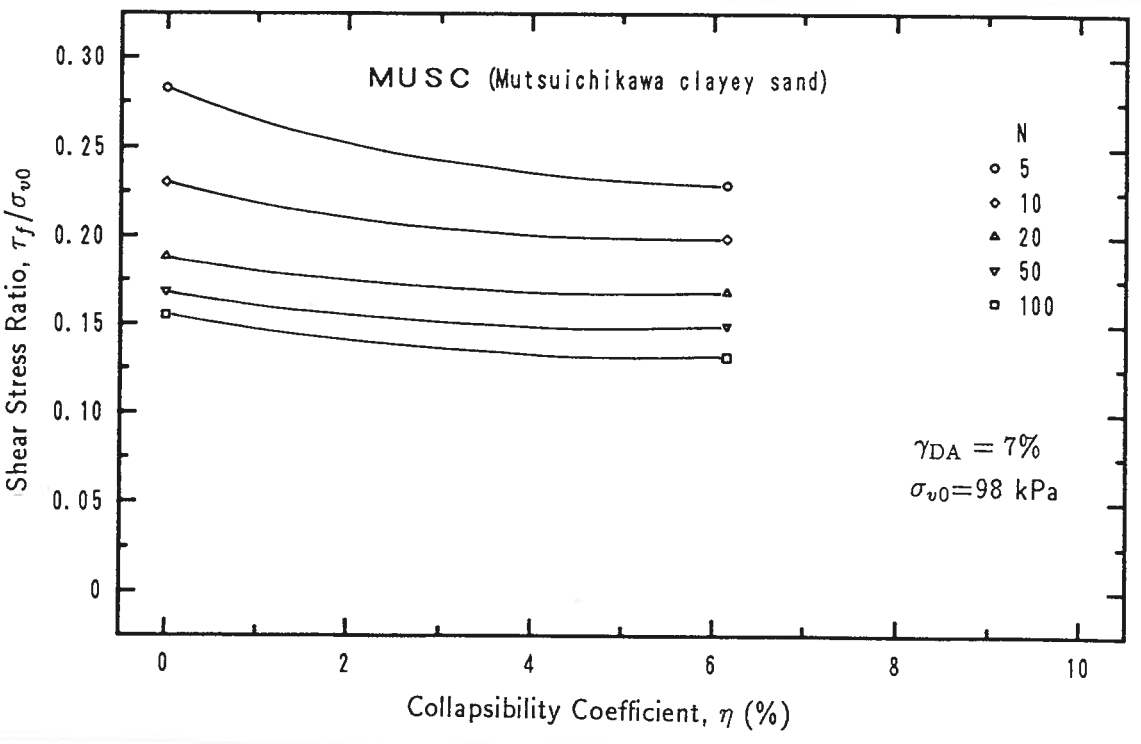

Figure 6.28: The reduction of shearing resistance as a function of number of cycles

Table 6.1: Strength reduction caused by different collapse

Material	Strength reduction (%)	
	N=10	Mean
TKSC	22.5	20.2
CASM	9.5	9.1
CBSM	12.5	12.7
OTSC	10.7	11.9
MUSC	19.1	13.9

stress ratio and shear strain for a given number of cycles. Pairs of such data are plotted down in stress strain plane to draw a curve. All the results which will be presented in the following paragraphs are obtained in such a way.

Typical stress-strain curves of samples having different history of hydraulic collapse are demonstrated in Figs. 6.29 to 6.33. The shear strain in these figures is double amplitude value. Curves of different collapsibility coefficients for the same material are presented in one figure for comparing the deformation behavior of soil which experienced different amount of collapse. State conditions of samples, dry density and degree of saturation, together with the collapsibility coefficient just prior to cyclic shearing are given in the legend for each materials, respectively. The samples have almost the same dry densities and approximately identical saturation ratios before the application of cyclic load. For most of the materials used (except material *TKSC*, a mixture of Toyoura sand and 15% kaolinite, which has a middle value of collapsibility coefficient), the deformation behavior is investigated at two extreme cases of collapse, namely minimum collapse (zero) and maximum collapse. The so-called maximum collapse means that it is the maximum value of collapse among samples of the same as-compacted dry density. These values represent the history of hydraulic collapse undergone by the samples. The stress-strain relationships are those corresponding to number of cycles of 5 and 10 to demonstrate the effect of the cycles on deformation properties. It is evident that the deformation characteristics of samples which experienced different magnitude of collapse are different. Collapse tends to weaken the deformation behavior of collapsible soils. The cyclic shear stress ratio required to yield the same magnitude of shear strain decreases as the collapsibility coefficient increases. This decrease occurs even at a very small shear strain of 0.2%.

It is to be noted that, although the stress-strain characteristics is affected by the collapse history of samples, the shape of the stress-strain curves does not change. The

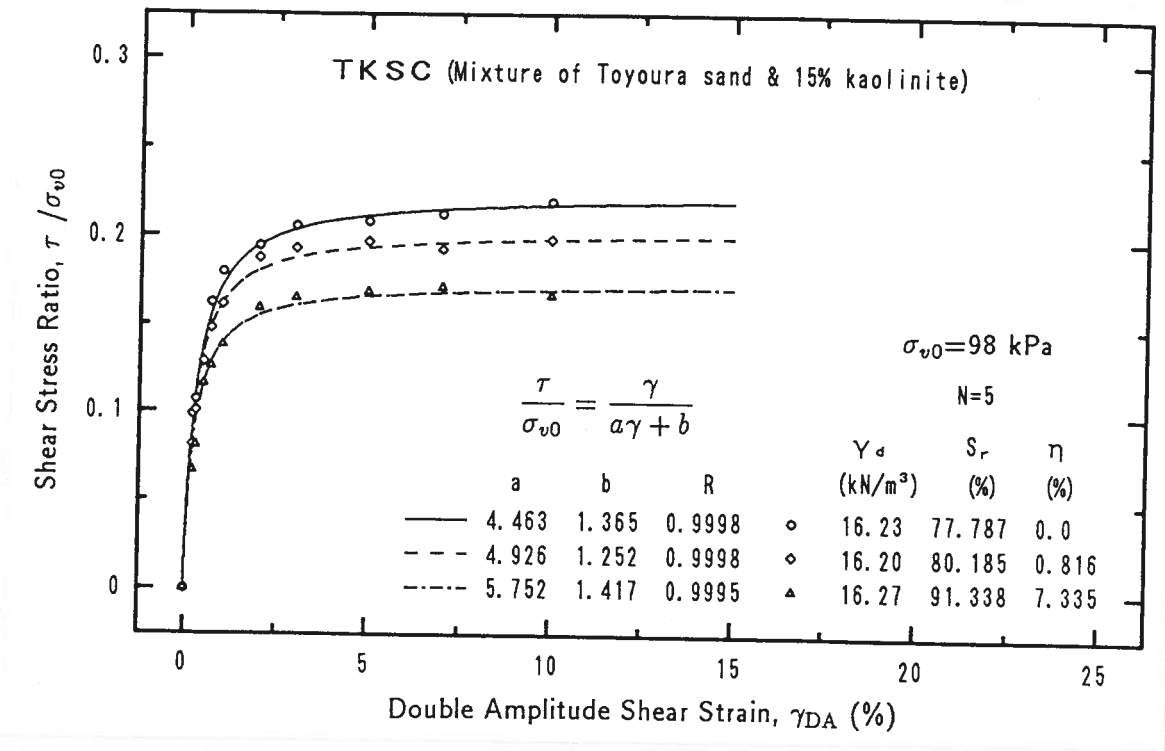

(a). Number of cycles N=5

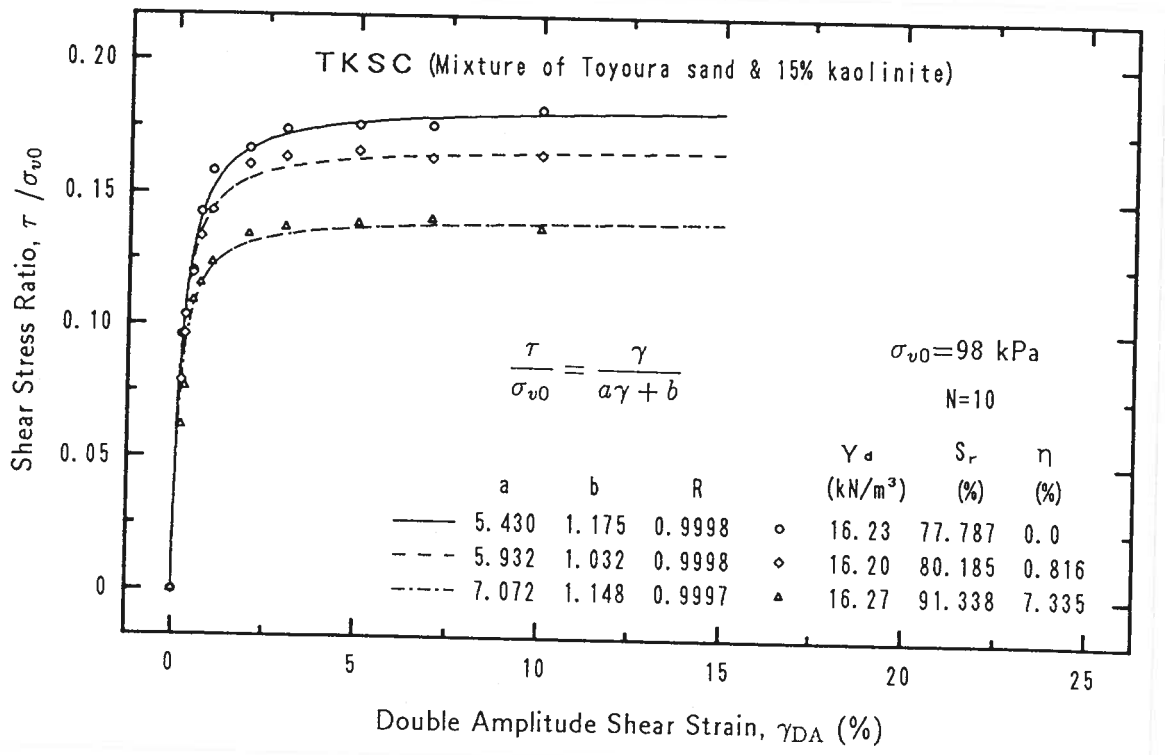

(b). Number of cycles N=10

Figure 6.29: Stress-strain relationships of samples of different collapse history

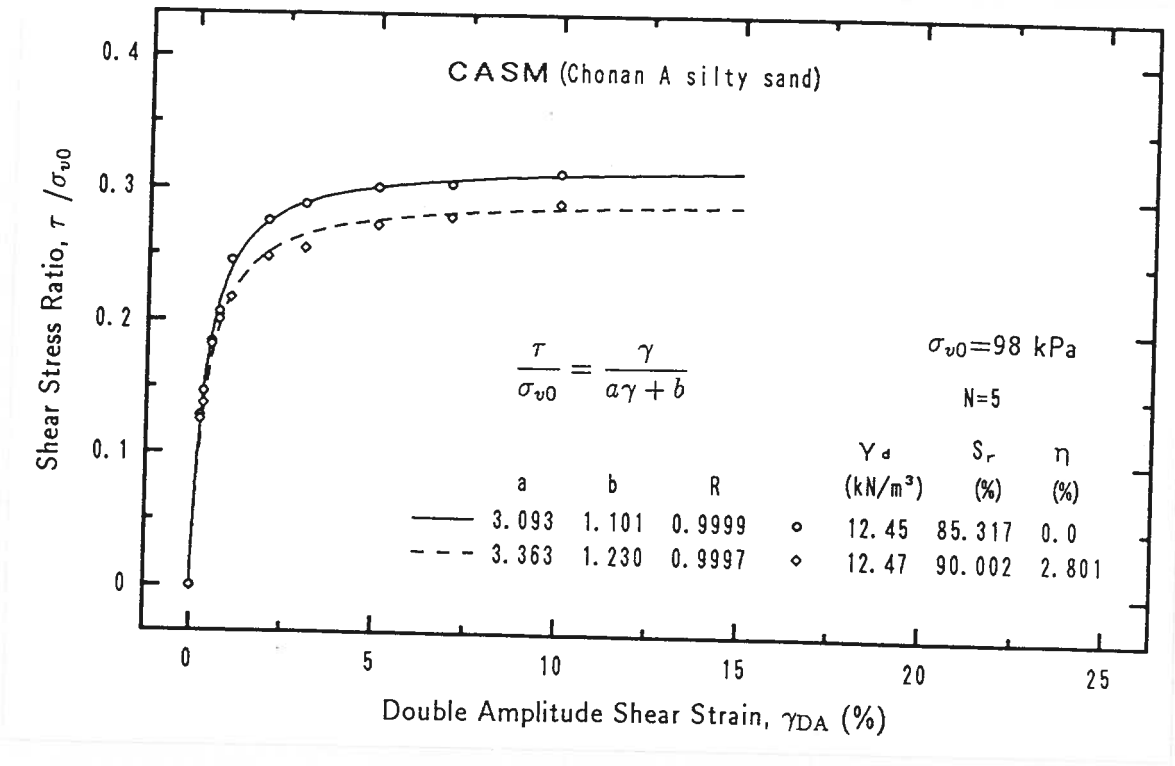

(a). Number of cycles N=5

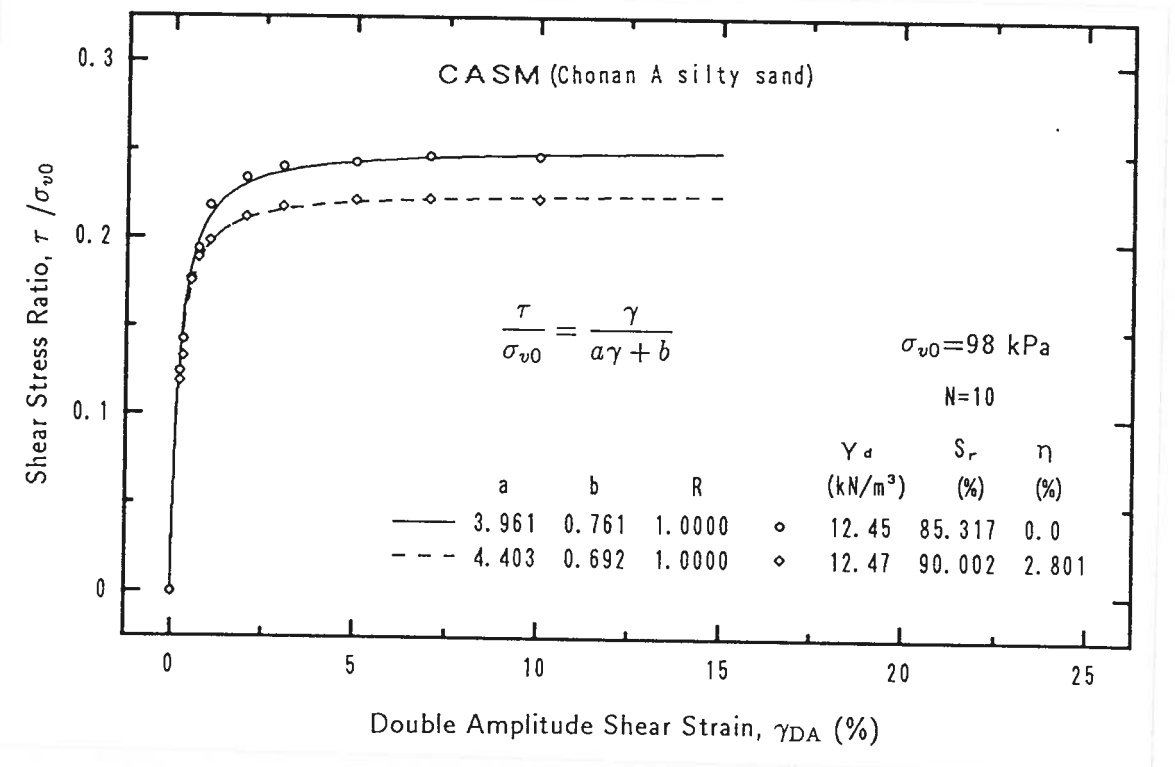

(b). Number of cycles N=10

Figure 6.30: Stress-strain relationships of samples of different collapse history

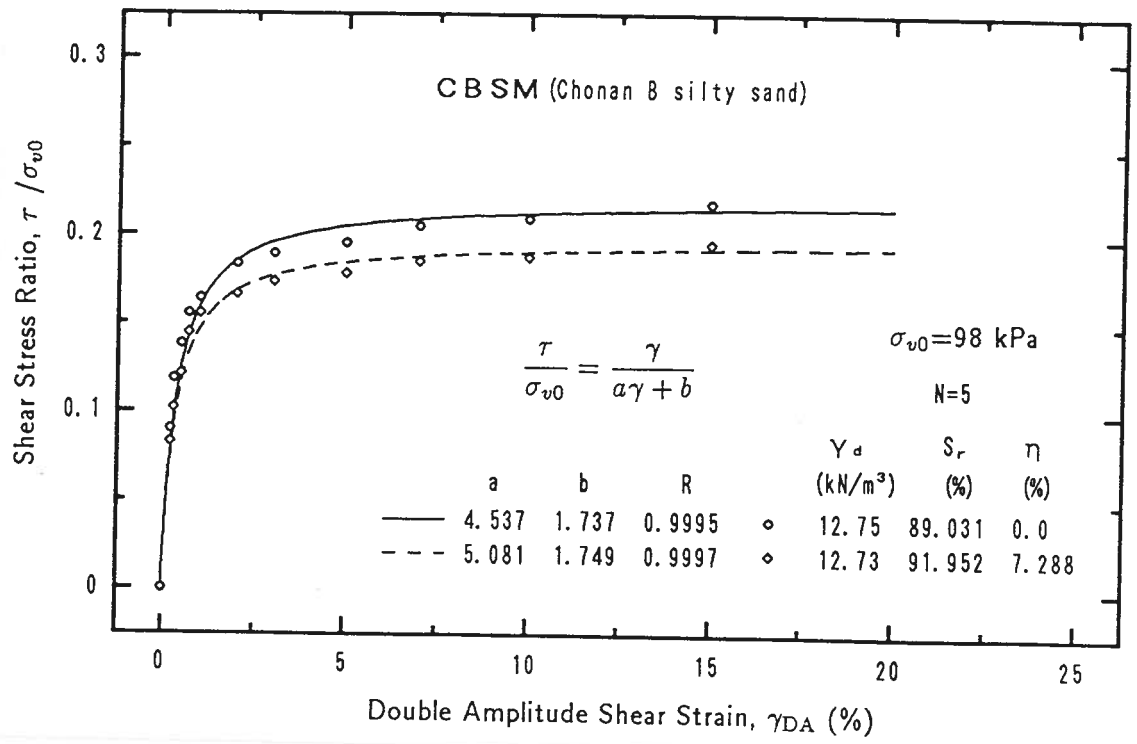

(a). Number of cycles N=5

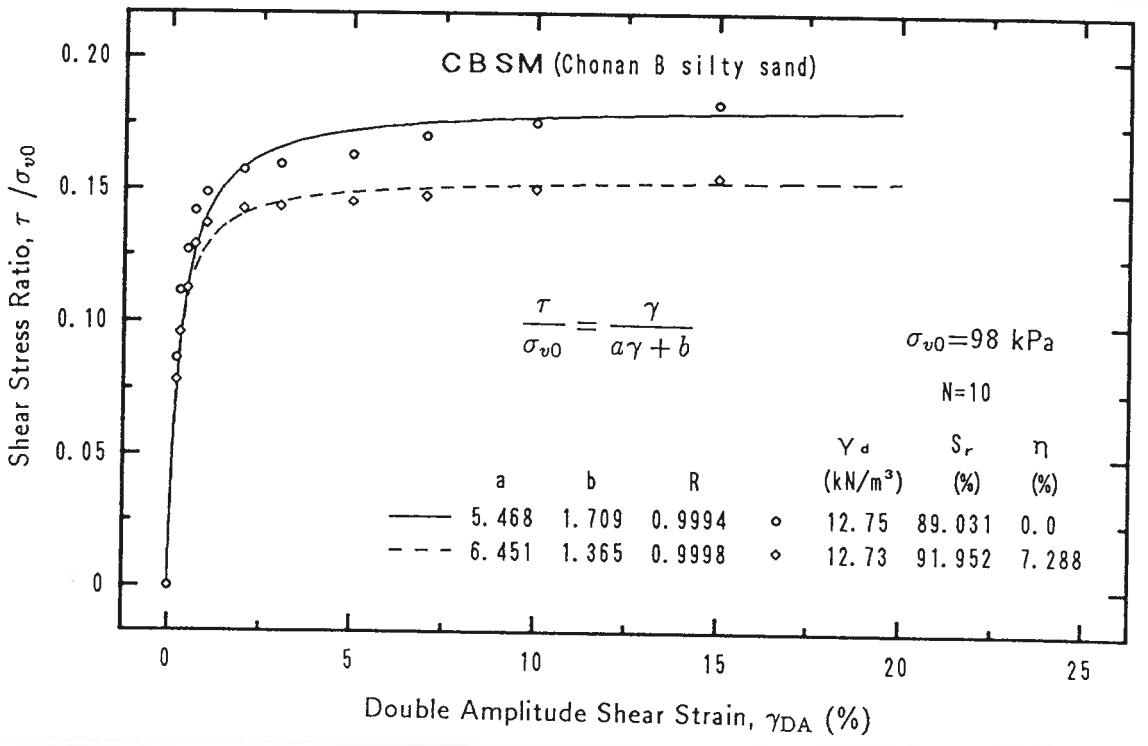

(b). Number of cycles N=10

Figure 6.31: Stress-strain relationships of samples of different collapse history

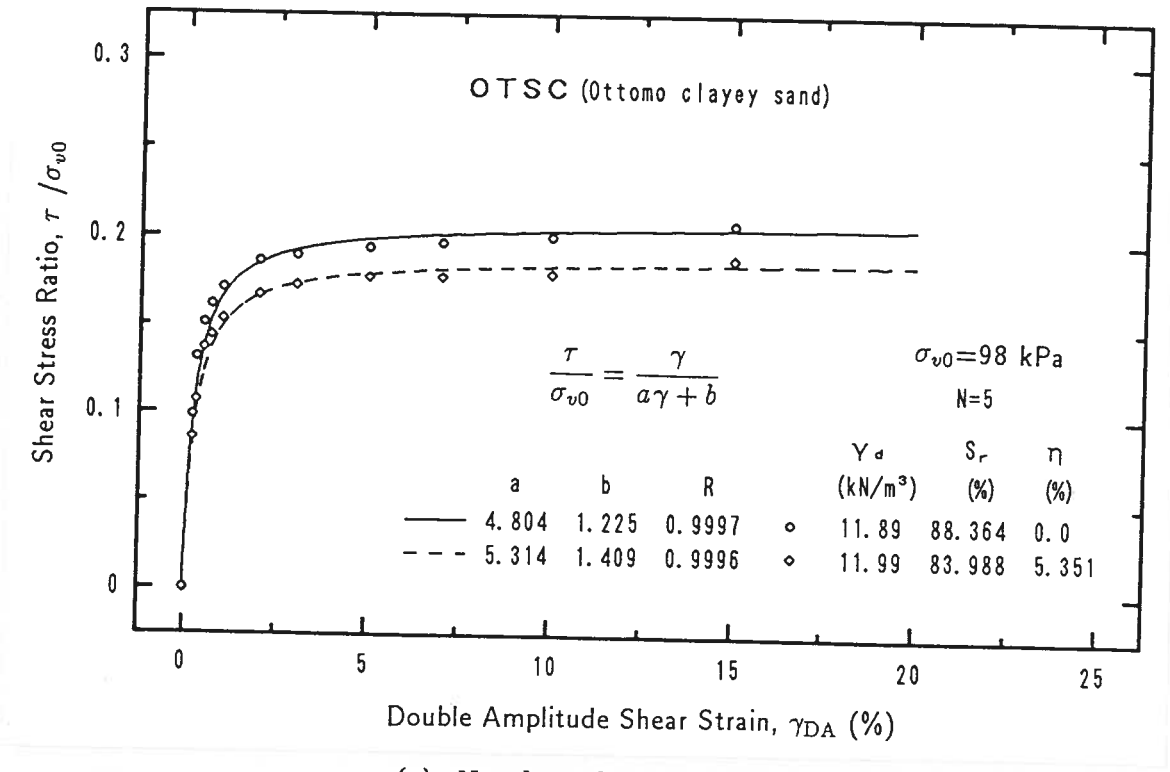

(a). Number of cycles N=5

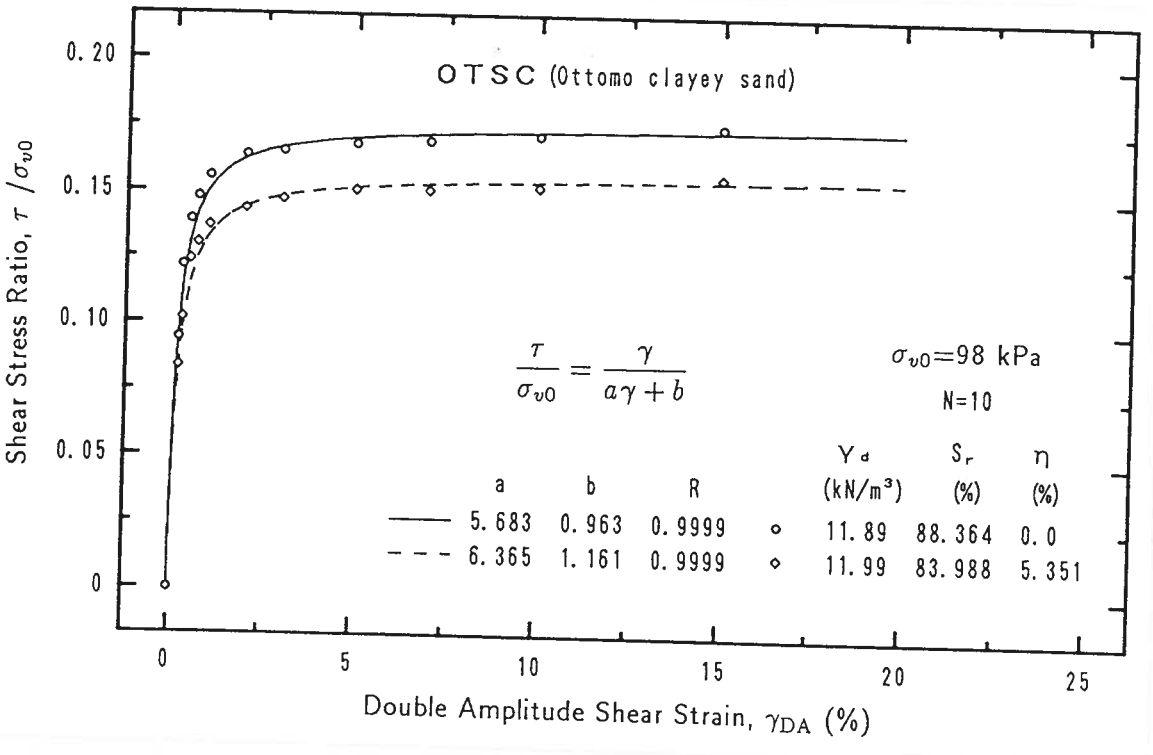

(b). Number of cycles N=10

Figure 6.32: Stress-strain relationships of samples of different collapse history

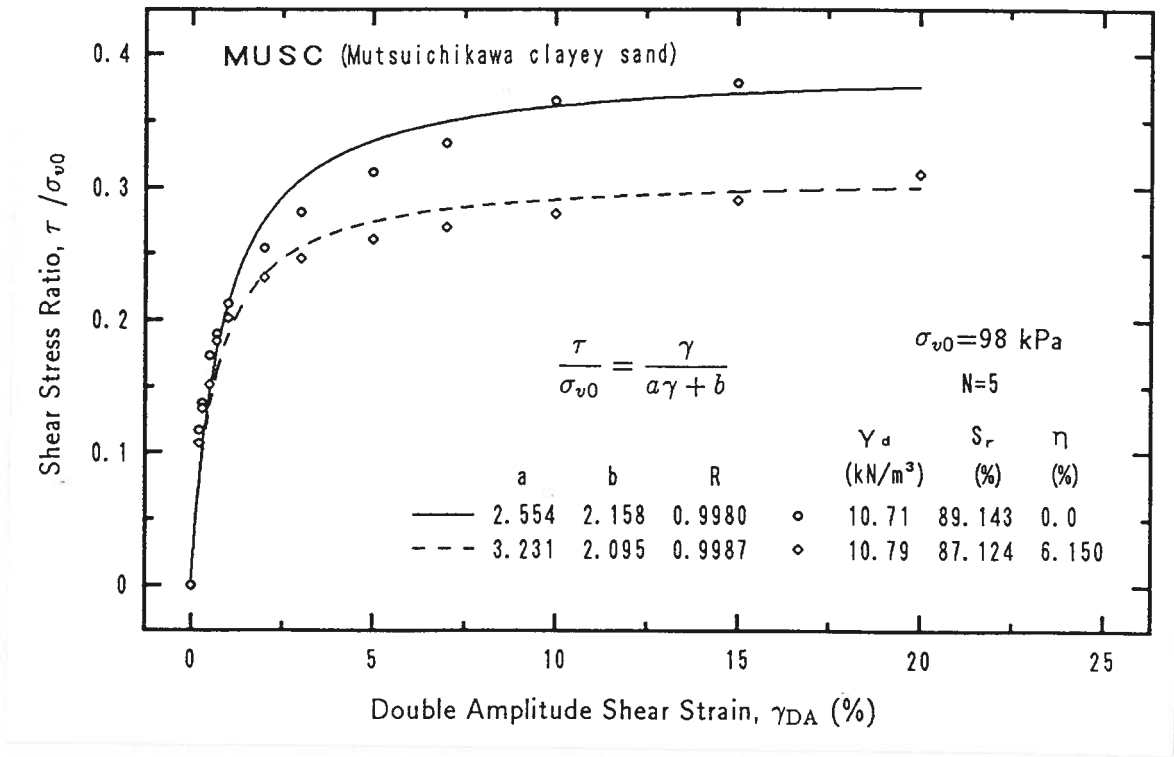

(a). Number of cycles N=5

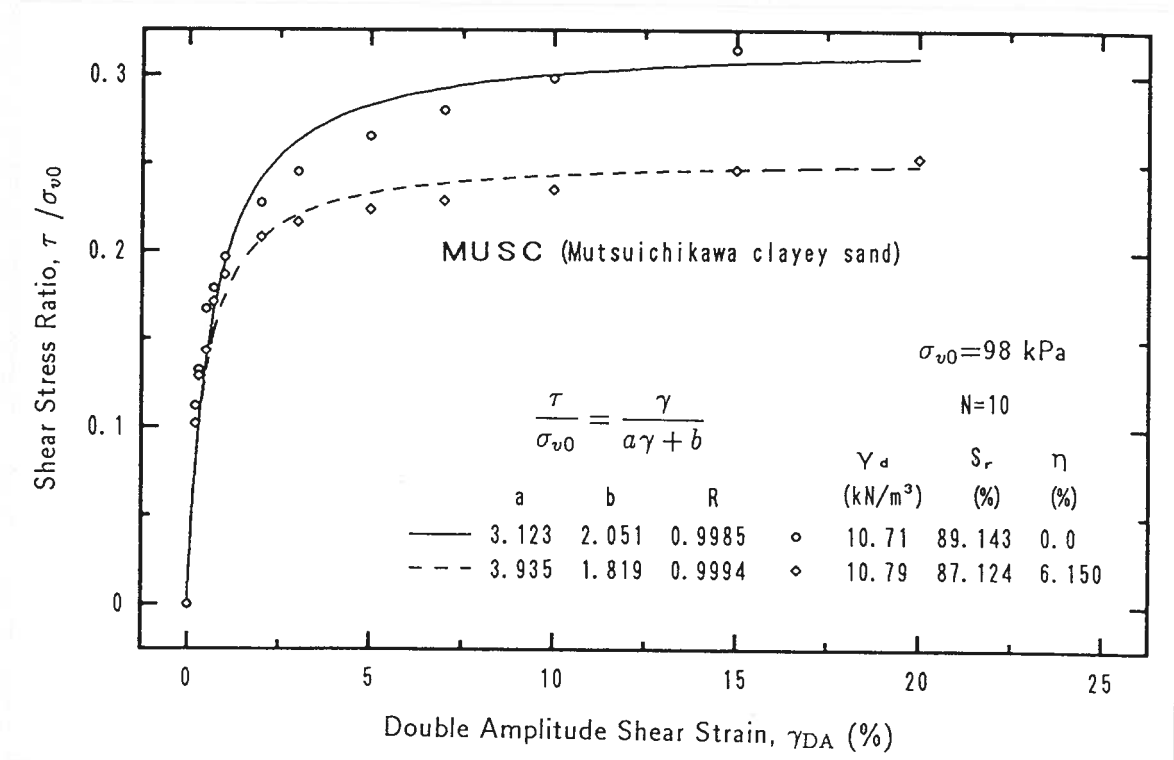

(b). Number of cycles N=10

Figure 6.33: Stress-strain relationships of samples of different collapse history

stress-strain curves can be well fitted by:

$$\frac{\tau}{\sigma_{v0}} = \frac{\gamma}{a\gamma + b} \tag{6.11}$$

where

a and b are test constants; and

γ is the *double amplitude* shear strain in percent.

Coefficient a and b, together with the coefficient of correlation, are indicated in the legend and are summarized in Table 6.2. In Figs. 6.29 to 6.33, lines are predicted by Eq. 6.11 and symbols are test results. These figures and the correlation coefficient in Table 6.2 state clearly that Eq. 6.11 can be used to predict the stress-strain behavior pretty good.

Table 6.2: Coefficient a and b and correlation coefficient

Material	N	η	a	b	Coefficientof correlation
TKSC	5	0.0	4.463	1.365	0.9998
		0.816	4.926	1.252	0.9998
		7.335	5.752	1.417	0.9995
	10	0.0	5.430	1.175	0.9998
		0.816	5.932	1.032	0.9998
		7.335	7.072	1.148	0.9997
CASM	5	0.0	3.093	1.101	0.9999
		2.801	3.363	1.230	0.9997
	10	0.0	3.961	0.761	1.0000
		0.801	4.403	0.692	1.0000
CBSM	5	0.0	4.537	1.737	0.9995
		7.288	5.081	1.749	0.9997
	10	0.0	5.468	1.709	0.9994
		7.288	6.451	1.365	0.9998
OTSC	5	0.0	4.804	1.225	0.9997
		5.351	5.314	1.409	0.9996
	10	0.0	5.683	0.963	0.9999
		5.351	6.365	1.161	0.9999
MUSC	5	0.0	2.554	2.158	0.9980
		6.150	3.231	2.095	0.9987
	10	0.0	3.123	2.051	0.9985
		6.150	3.935	1.819	0.9994

Eq. 6.11 is similar to hyperbolic equation as formulated by Konder and Zelasko

(1963), *i.e.*,

$$\tau = \frac{G_0 \gamma_a}{1 + \frac{G_0}{\tau_f} \times \gamma_a} \tag{6.12}$$

where

G_0 is initial tangent shear modulus at $\gamma = 0$;

τ_f is the shear strength of soil; and

γ_a denotes the amplitude of shear strain in decimal.

The initial shear modulus, G_0, can be taken as being equal to the elastic shear modulus at very small shear strain range. The initial shear modulus, G_0, and the shear strength, τ_f, can be back-calculated from coefficients b and a in Eq. 6.11. The relations between them are:

$$G_0 = \frac{200 \times \sigma_{v0}}{b}, \qquad \tau_f = \frac{\sigma_{v0}}{a} \tag{6.13}$$

If normalized with respect to the initial overburden pressure, σ_{v0}, Eq. 6.13 becomes:

$$\frac{G_0}{\sigma_{v0}} = \frac{200}{b}, \qquad \frac{\tau_f}{\sigma_{v0}} = \frac{1}{a} \tag{6.14}$$

The back-calculated initial shear modulus and shear strength are given in Table 6.3 normalized with respect to the initial overburden pressure, σ_{v0}. The reference strain, γ_r, is also given in this table. It is defined by Hardin and Drnevich (1972b) as:

$$\gamma_r = \frac{\tau_f}{G_0} \tag{6.15}$$

It is evident that the shear strength decreases as the collapsibility coefficient increases. It appears that, for all the materials, there is no consistent rule concerning the change of the initial secant shear modulus with the amount of collapse. This is because there is not enough test data in the range of small shear strain and the test error is relatively large in this range. Therefore, the back-calculated value could not really represent the real value of the initial shear modulus of the soil. However, it is still to be noted that the reference strain and the normalized shear strength decrease with the number of cycles and the normalized initial modulus increases as the number of cycles increases. This is consistent with the results reported by Hardin and Drnevich (1972a, Fig. 8). Hardin's and Drnevich's results indicate that the increase in initial shear modulus with the number of cycles decreases as the number of cycles increases and increases with the increase in the effective mean principal stress. Because the initial shear modulus can be taken as being equal to the elastic shear modulus at very small strain range (Ishihara, 1982), the fact that G_0 increases with the number of cycles means that, under cyclic loading condition, elastic shear modulus of soil is a function of the number of cycles.

Table 6.3: Normalized shear strength, initial modulus and reference strain γ_r

Material	N	η	τ_f/σ_{v0}	G_0/σ_{v0}	γ_r
TKSC	5	0.0	0.224	146.52	0.00153
		0.816	0.203	159.74	0.00127
		7.335	0.174	141.14	0.00123
	10	0.0	0.184	170.21	0.00108
		0.816	0.169	193.80	0.00087
		7.335	0.141	174.22	0.00081
CASM	5	0.0	0.323	181.65	0.00178
		2.801	0.297	162.60	0.00183
	10	0.0	0.252	262.81	0.00096
		0.801	0.227	289.02	0.00079
CBSM	5	0.0	0.220	115.14	0.00191
		7.288	0.197	114.35	0.00172
	10	0.0	0.183	117.03	0.00156
		7.288	0.155	146.52	0.00106
OTSC	5	0.0	0.208	163.27	0.00127
		5.351	0.188	141.94	0.00133
	10	0.0	0.176	207.68	0.00085
		5.351	0.157	172.27	0.00091
MUSC	5	0.0	0.392	92.68	0.00422
		6.150	0.310	95.47	0.00324
	10	0.0	0.320	97.51	0.00328
		6.150	0.254	109.95	0.00231

The above results verify that the behavior of collapsible soils is different for different collapse histories. It gives a qualitative description of the soil properties. As for how much is the effect of collapse history on soil properties, these figures are not able to give a quantitative description. It is necessary to find a rule which can quantitatively describe the effect of amount of collapse on the behavior of collapsible soils. The effect of collapse history on deformation and strength properties of collapsible soils may be evaluated by comparing the secant shear moduli of samples of different collapse history at a given shear strain. As the result of such comparison, the effect of collapse on the stiffness (secant shear modulus) of soils is expressed in terms of *collapse factor*, C_{cl}, which is defined as the ratio of the secant shear moduli between samples having different collapse histories at the same shear strain corresponding to a particular overburden pressure, that is:

$$C_{cl} = \frac{G_{\eta h}}{G_{\eta 0}} \tag{6.16}$$

where, G is the secant shear modulus. The subscript $_{\eta h}$ means high collapse and subscript $_{\eta 0}$ means zero collapse. The secant shear modulus, G, is defined by

$$G = \frac{\tau_a}{\gamma_a} \tag{6.17}$$

where τ_a denotes the amplitude of shear stress. Introducing Eq. 6.15 into Eq. 6.12, the expression of the shear modulus (secant modulus) for the H-D model is obtained from Eq. 6.17 as follows,

$$G = \frac{G_0}{1 + \frac{\gamma_a}{\gamma_r}} \tag{6.18}$$

Substituting Eq. 6.18 into Eq. 6.16, the *collapse factor* becomes,

$$C_{cl} = \frac{(G_0)_{\eta h}}{(G_0)_{\eta 0}} \frac{1 + \frac{\gamma_a}{(\gamma_r)_{\eta 0}}}{1 + \frac{\gamma_a}{(\gamma_r)_{\eta h}}} \tag{6.19}$$

This is a monotonic function on γ_a axis. From Table 6.3, for most of the materials used, it is found

$$(\gamma_r)_{\eta h} - (\gamma_r)_{\eta 0} < 0 \tag{6.20}$$

It can be proven that, under the condition of Eq. 6.20, Eq. 6.19 is a monotonically decreasing function at a range of $\gamma_a \geq 0$. Materials *MUSC* (Mutsuichikawa clayey sand) and *CASM* (Chonan A silty sand, at number of cycles of 5) give $(\gamma_r)_{\eta h} - (\gamma_r)_{\eta 0} > 0$, therefore the *collapse factor* is a monotonically increasing function when $\gamma_a \geq 0$.

The change in *collapse factor* with cyclic shear strain is demonstrated in Fig. 6.34. It can be seen in Fig. 6.34 that for most of the cases, the *collapse factor* decreases as

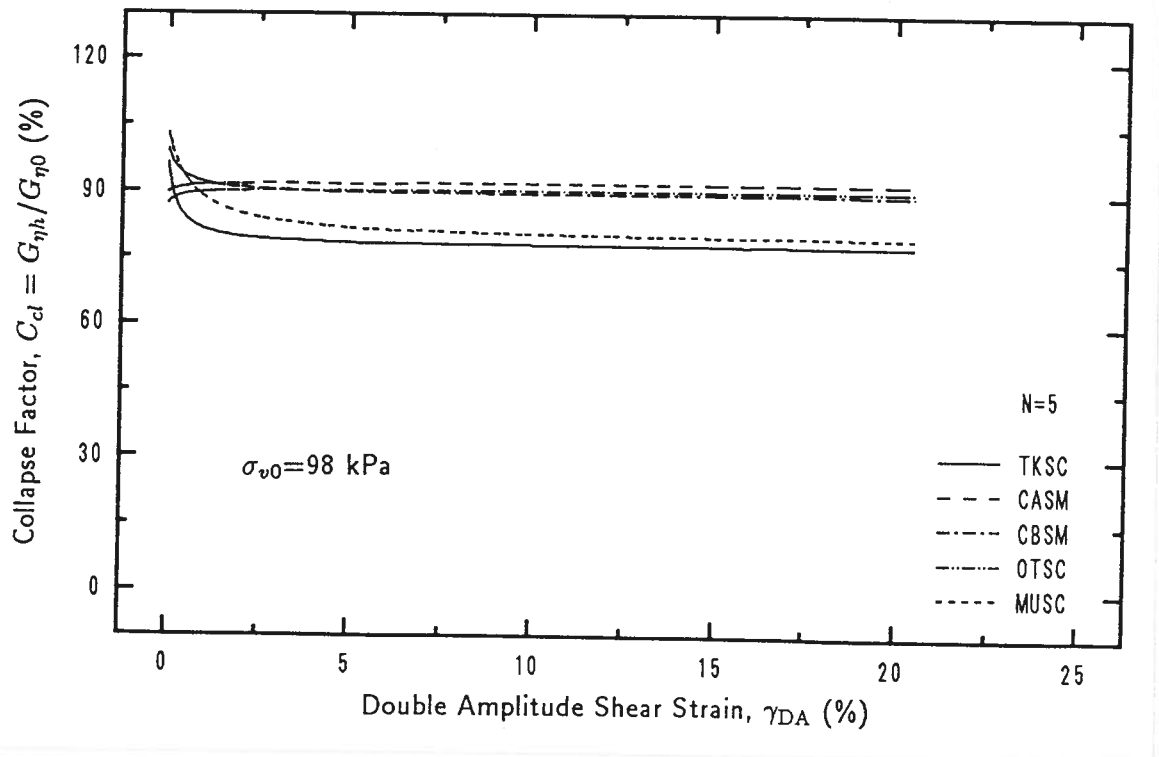

(a). Number of cycles N=5

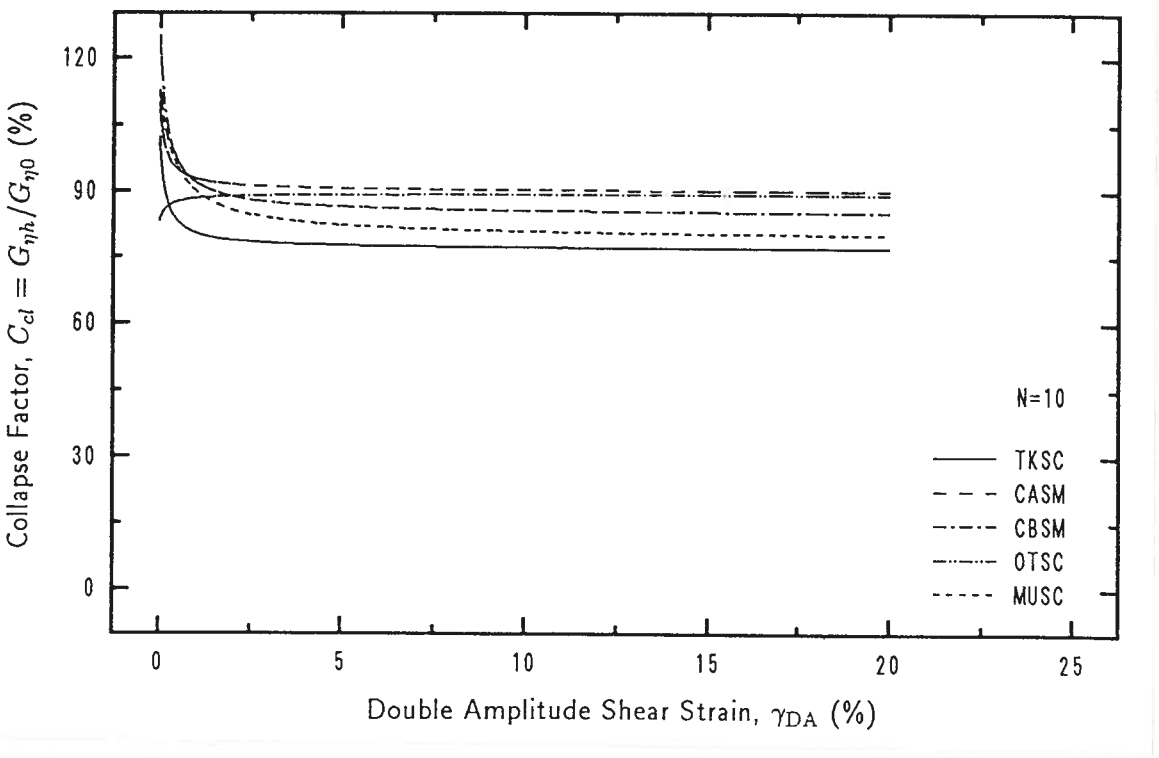

(b). Number of cycles N=10

Figure 6.34: Collapse factor as a function of cyclic shear strain

the cyclic shear strain increases. The opposite trend is shown in the figure. However, the variation of *collapse factor* in the cases having opposite trends is usually small. It is considered that this opposite trend is caused by test error. Although some exceptions exist, it is to be noted that the main change in *collapse factor* including the exceptions, occurred in the range of shear strain less than about 2%. Beyond this critical value of shear strain, the change in *collapse factor* is so small that it practically can be considered as constant with enough accuracy.

The two limits at $\gamma_a \to 0$ and $\gamma_a \to \infty$ can be obtained from Eq. 6.19 as

$$\lim_{\gamma_a \to 0} C_{cl} = \frac{(G_0)_{\eta h}}{(G_0)_{\eta 0}}, \qquad \lim_{\gamma_a \to \infty} C_{cl} = \frac{(G_0)_{\eta h}}{(G_0)_{\eta 0}} \frac{(\gamma_r)_{\eta h}}{(\gamma_r)_{\eta 0}} = \frac{(\tau_f)_{\eta h}}{(\tau_f)_{\eta 0}} \tag{6.21}$$

The second limit gives the lower limit of the reduction of secant shear moduli. The outcomes are illustrated in Table 6.4 for all the materials and all the cases investigated. It

Table 6.4: Limits of the reduction of secant shear modulus

Material	N	$(C_{cl})_{\gamma=0}, (\%)$	$(C_{cl})_{\gamma\to\infty}, (\%)$
TKSC	5	109.0	90.6
		96.3	77.6
	10	113.9	91.5
		102.4	76.8
CASM	5	89.5	92.0
	10	110.0	90.0
CBSM	5	99.3	89.3
	10	125.2	84.8
OTSC	5	86.9	90.4
	10	83.0	89.3
MUSC	5	103.0	79.1
	10	112.8	79.4

is apparent that the history of hydraulic collapse has remarkable effect on the deformation characteristics of collapsible soil. The maximum reduction of secant shear modulus (or stiffness) is as large as 23.4% corresponding to a number of cycles of 10 for material *TKSC* (Mixture of Toyoura sand and 15% kaolinite). For other materials, it is larger than about 10%. This reduction tends to increase with number of cycles.

6.6 INFLUENCE OF MATERIAL KINDS

In the previous sections, it is to be noted that the response to cyclic load is different for different materials. The difference is also presented in terms of the effect of *collapse history* on the cyclic loading response. Of the five materials used in the present study, the mineralogy is similar. The difference mainly is illustrated in the grain size distribution and clay and silt content. In collapsible soils, the clay content is a very important factor influencing the collapse characteristics. In order to investigate the influence of material kinds on the response of collapsible soils to cyclic load, the clay content is chosen here as a parameter to quantitatively describe the material difference. The different collapse-induced reduction in shear strength as a function of clay content derived from the previous test series is illustrated in Fig. 6.35. It is obvious that there is a critical value of clay

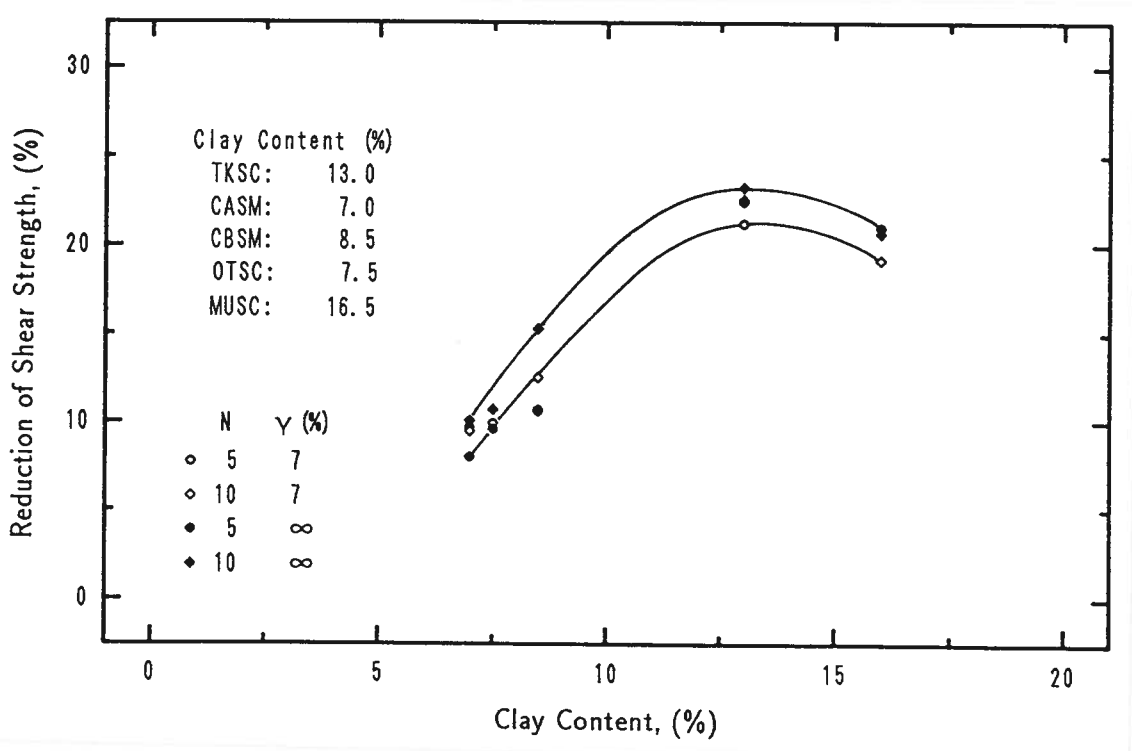

Figure 6.35: Different collapse-induced reduction of shear strength as a function of clay content

content at which the strength reduction caused by different amount of collapse gives a maximum value. The more the clay content deviates from this critical value, the lower is the strength reduction. This result is reasonable because as the clay content decreases, soil possesses less cohesiveness. On the other hand, the larger the clay content, the

higher is the cohesiveness of the soil. Therefore, the soil either becomes cohesionless soil or cohesive soil. In both cases, the influence of different amount of collapse will decease.

6.7 SUMMARY

The strength and deformation behavior of collapsible soils under cyclic loading condition has been discussed in this chapter. A detailed discussion has been devoted to the stress state and stress changes under constant volume condition and during shearing. It has been found that the measured vertical load during shearing is equal to the algebraic difference of effective stress and the proportion of soil suction that contributes to the effective stress; in other words, the measured vertical stress during shearing is the intergranular stress caused by external load. At high saturation ratio, it is approximately equal to effective stress. The state histories of molding moisture content and dry density of the tests have also been described in detail.

Based on the discussion of test results, the following conclusions can be obtained:

- The cyclic shearing resistance of collapsible soil is affected by the collapse history that the soil has experienced before cyclic shearing. The higher the magnitude of hydraulic collapse, the lower is the cyclic shearing resistance. The reduction of cyclic shearing resistance is almost constant with regards to the number of cycles and usually is larger than 10% depending on the materials.

- The cyclic shearing resistance of collapsible soil is affected significantly by the dry density before the application of cyclic loading. The denser the soil before cyclic shearing, the higher is the shearing resistance.

- The stress-strain relationship can be well predicted by the hyperbolic model. It is independent on collapse history.

- The *collapse factor*, C_d, is used to express the effect of collapse history of soil on deformation behavior. At small strain level (double amplitude shear strain less than 2%), this factor decreases rapidly with shear strain and becomes stable as the shear strain increases further. The *collapse factor* is as low as 76.8% at a number of cycles of 10 and high strain level for material *TKSC*. For the other materials, it is usually less than 90%.

Chapter 7

BEHAVIOR UNDER MONOTONIC LOADING CONDITIONS

7.1 INTRODUCTION

The strength and deformation characteristics of collapsible soils under cyclic loading condition when subjected to water permeation and the effect of collapse history of the soil on seismic behavior have been investigated in the previous chapter. The test results indicate that it is possible that the liquefaction occurs in compacted collapsible soil when it is subjected to water infiltration and collapse takes place. The hydraulic collapse history has significant influence on the seismic strength and deformation properties. How does the collapsible soil behave under monotonic loading condition? Does the collapse history affect the monotonic behavior of collapsible soil? How much is the strength loss caused by soaking? Although the properties of collapsible soils under monotonic loading condition whether they are subjected to water permeation or not are of vital concern to the soil engineers in recent years, and a series of studies have been done in the field (see Section 2.6), the answers for these questions are far from satisfactory. Most of the studies were performed on the unsaturated samples without water infiltration. Some have studied the effect of soaking on the strength properties. Few studies are done to investigate the effect of the amount of collapse of soil on the strength and deformation behavior when subjected to water infiltration. When dealing with the collapse problem, the most important aspect is not the strength of soil at natural moisture content but the strength loss caused by the increase in moisture content, especially the sudden infiltration of water. And in the case of compacted soil, different as-compacted conditions will result in different amount of collapse due to the infiltration of water. The effect of the amount of collapse, which the soil has undergone before further loading, on strength is, therefore, also very important.

In this chapter, the effect of different amount of collapse on the strength properties and the loss in strength of soils caused by wetting will be investigated. The deformation

behavior is also studied. The main purposes are to illustrate the tremendous effect of water infiltration on shear strength and deformation properties and the importance of selecting an as-compacted condition such that wetting the compacted soil will result in little collapse.

Under monotonic loading condition, the test conditions are different for different situations. When the soil is subjected to water infiltration, an undrained condition can be assumed reasonably because failure (landslide) usually occurs in a relatively short time duration. Because the degree of saturation after collapse is usually very high and even fully saturated, a constant volume test can be used equivalent to the fully saturated undrained test. On the contrary, if no water infiltration occurs in the soil, soil usually is partly saturated and is in a drained and volume changeable state during monotonic shearing. In this chapter, the plane strain and constant volume tests are performed on soaked samples, while the drained, constant vertical stress, and volume changeable tests are performed on unwetted samples. The stress states and stress changes in constant volume test have been discussed in the previous chapter. The strength and deformation behaviors of collapsible soils will be discussed in following sections. The state histories will be discussed in corresponding sections.

7.2 SHEAR STRENGTH BEHAVIOR

7.2.1 Behavior of Soils Which Have Undergoing Different Collapse

It has been recognized that soils compacted at low water content and of low density will collapse when it is subjected to water permeation (Jennings and Knight, 1975; Booth, 1975; and Lawton, 1986). Jennings and Knight (1975) suggested that the soil be compacted at a moisture content greater than 2% less than the optimum. However, nobody mentioned if there is any difference between the strength properties of the soil if it has undergone different amount of collapse. In order to verify whether the amount of collapse affects the static strength properties of soils, simple shear tests are conducted on samples which have undergone different amount of collapse. As discussed in Section 6.3, if the density of samples is different before shearing, the effect of the amount of collapse on the strength and deformation properties will blend with that of the density. In this set of tests, the main aim is to investigate the effect of different amount of collapse on the strength and deformation behavior of collapsible soil. Therefore, it is necessary to separate the two different effects. Tests in this section are performed, as in the previous chapter, on specimens which are prepared of different as-compacted densities and mold-

ing moisture contents, but after being consolidated at the same overburden pressure and soaked, come to an almost identical state of densities and water contents at the end of collapse (or before shearing). Therefore, if there is any difference in soil behavior, it must be the results of different amount of collapse which have undergone by specimens. The results obtained from so performed tests are presented in Figs. 7.1 to 7.4. Among them, Fig. 7.1 illustrates the peak and residual strengths of material *TKSC* (Mixture of Toyoura sand and 15% kaolinite), represented by the open and filled symbols, respectively. The others represent the strengths corresponding to 15% shear strain. Zero percent collapse is obtained in a way such that the molding water content is so high that no obvious additional settlement occurs at all when additional water is introduced into the specimen and infiltrated into it.

As mentioned before, the dry densities of the samples bearing the same overburden pressure are almost identical at the end of collapse (or before shearing). It can also been seen from the legend in the figures that the degree of saturation before shearing is approximately the same. The only difference is the amount of collapse, which is expressed in terms of *collapsibility coefficient*, η, that the samples have undergone before shearing. These figures indicate that the shear strength of soils is affected by the magnitude of collapse which the soils have experienced. The shear strength of the specimens which have experienced high amount of collapse is smaller than that of those which have undergone little amount collapse. The reductions of shear strength are listed in Table 7.1 in terms of strength parameters, d and β, which represent the cohesive intercept and angle of shearing resistance of $\tau_f \sim \sigma_{v0}$ curves, respectively. For all the materials used in this

Table 7.1: Changes of strength parameters due to different collapse

Material		η_{Low}		η_{High}		Reduction (%)	
TKSC	d, (kPa)	5.5†	10.7‡	3.35†	3.35‡	40.9†	69.6‡
	β, (°)	16.1†	6.8‡	14.7†	4.4‡	8.3†	34.9‡
CBSM	d, (kPa)	0	—	0	—	0	—
	β, (°)	15.6	—	14.3	—	8.3	—
OTSC	d, (kPa)	5.2	—	0	—	100	—
	β, (°)	20.0	—	19.3	—	3.5	—
MUSC	d, (kPa)	32.5	—	3.9	—	88.0	—
	β, (°)	15.7	—	20.3	—	-29.0	—

† Parameters corresponding to peak strength;

‡ Parameters corresponding to residual strength.

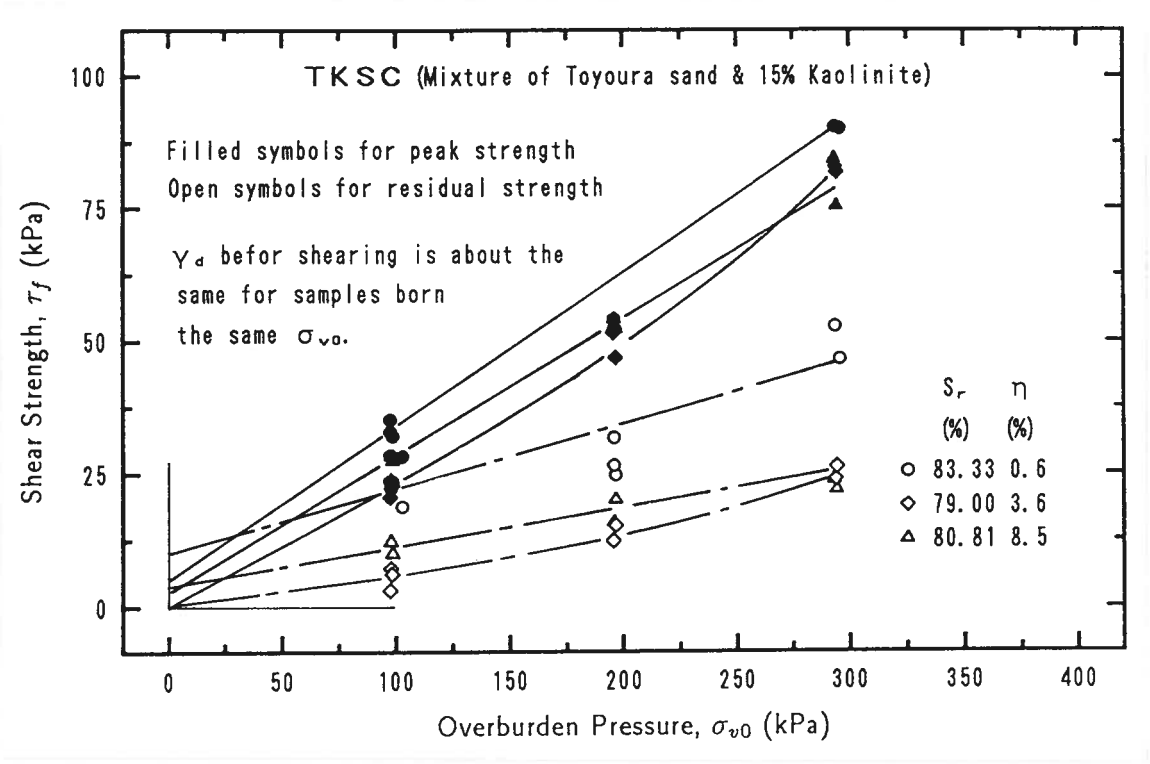

Figure 7.1: Effect of different amount of collapse on shear strength

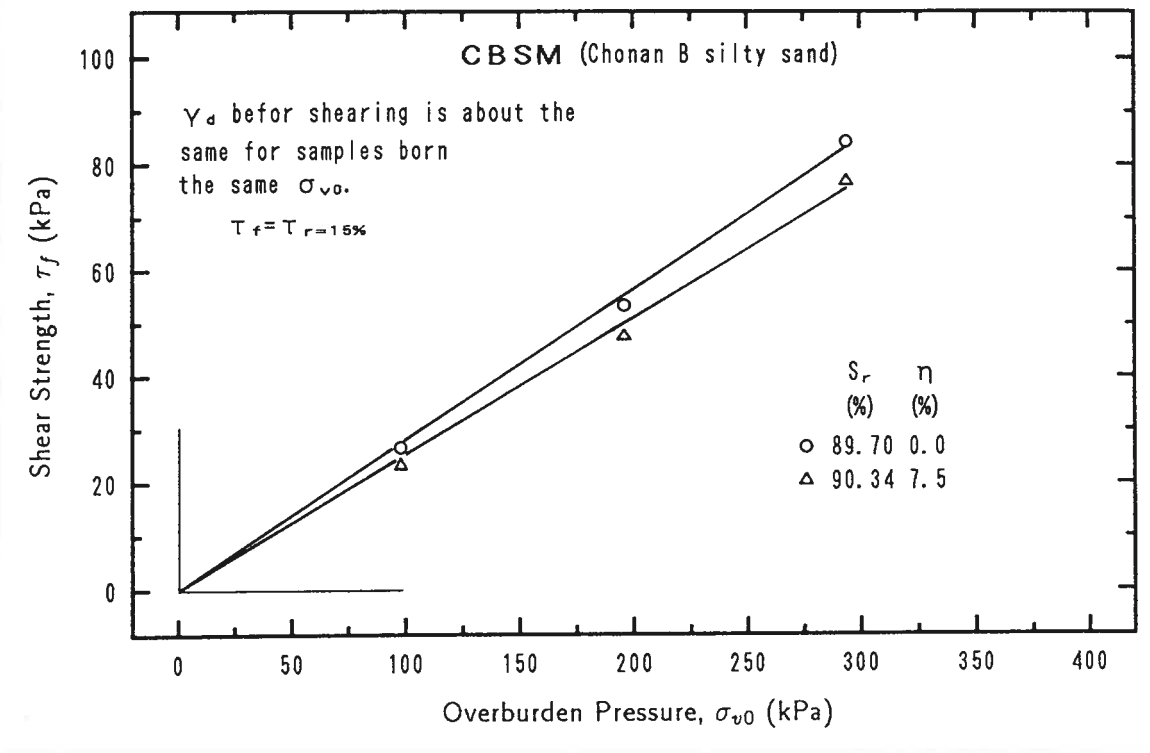

Figure 7.2: Effect of different amount of collapse on shear strength

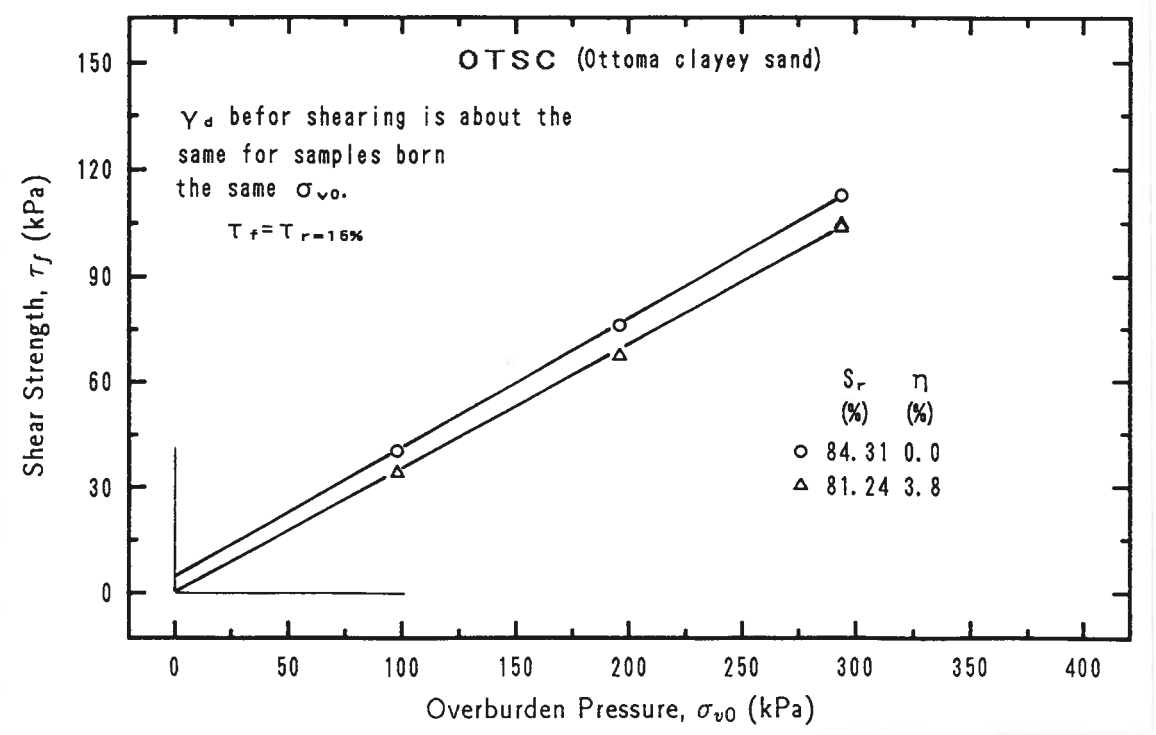

Figure 7.3: Effect of different amount of collapse on shear strength

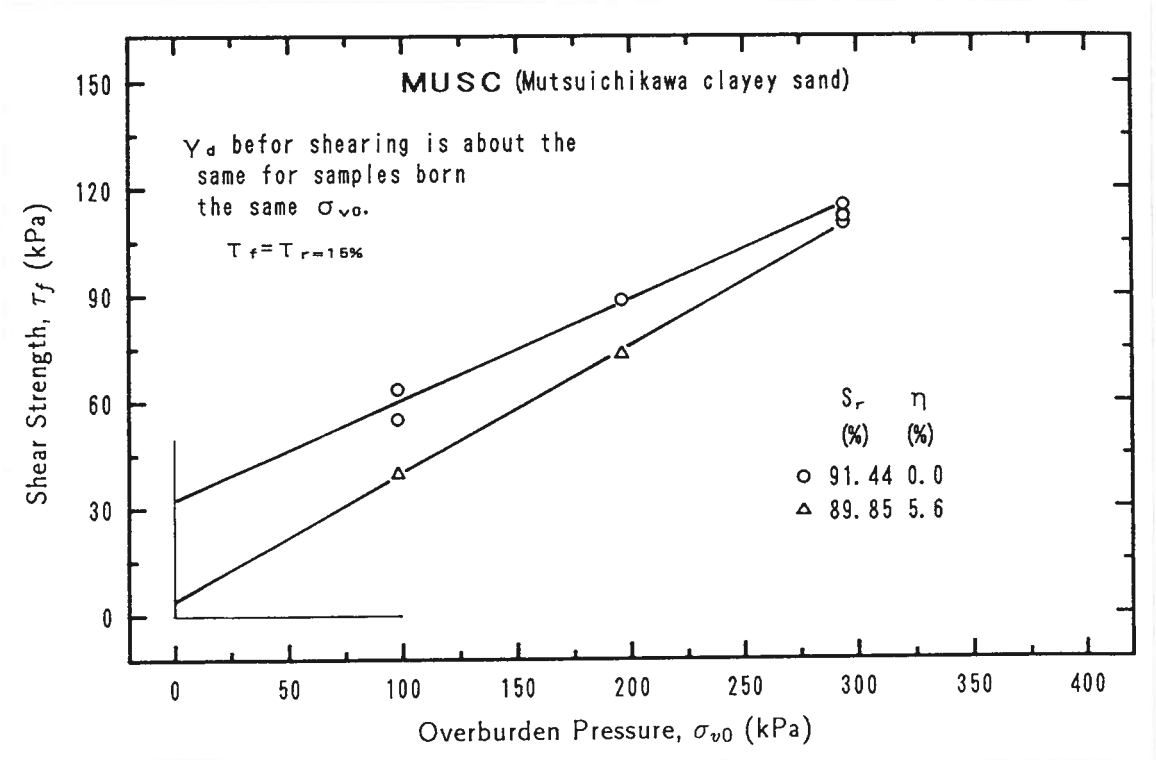

Figure 7.4: Effect of different amount of collapse on shear strength

study, the cohesive intercept, d, decreases if the samples have experienced large amount of collapse. For most of the materials, the angle of shearing resistance, β, also decreases. The only exception is the material *MUSC* (Mutsuichikawa clayey sand) which shows an increase in β. However, it can be seen in Fig. 7.4 that the samples which have undergone little amount of collapse possess relatively high cohesive intercepts. On the other hand, for those which have experienced high amount of collapse, the cohesive intercepts are very small. Although the values of β of the samples with little amount of collapse are smaller than those of samples with high amount of collapse, the strength reduction at a stress range up to 300 kPa is clearly shown in the figure. The different behavior of the materials might be due to the difference of materials. This will be discussed in Section 7.4.

Due to the difficulties in preparing samples which will yield different collapse upon wetting but which will come to an almost identical state of dry density and saturation ratio at the end of collapse, only two extreme conditions, namely maximum and minimum collapse, are adopted for most of the materials tested in this study. *TKSC* (Mixture of Toyoura sand and 15% kaolinite) is the only material on which tests are run on samples with different η. The results are indicated in Fig. 7.5 in shear strength, τ_f, versus collapsibility coefficient, η. In this figure, filled symbols are used to indicate the peak

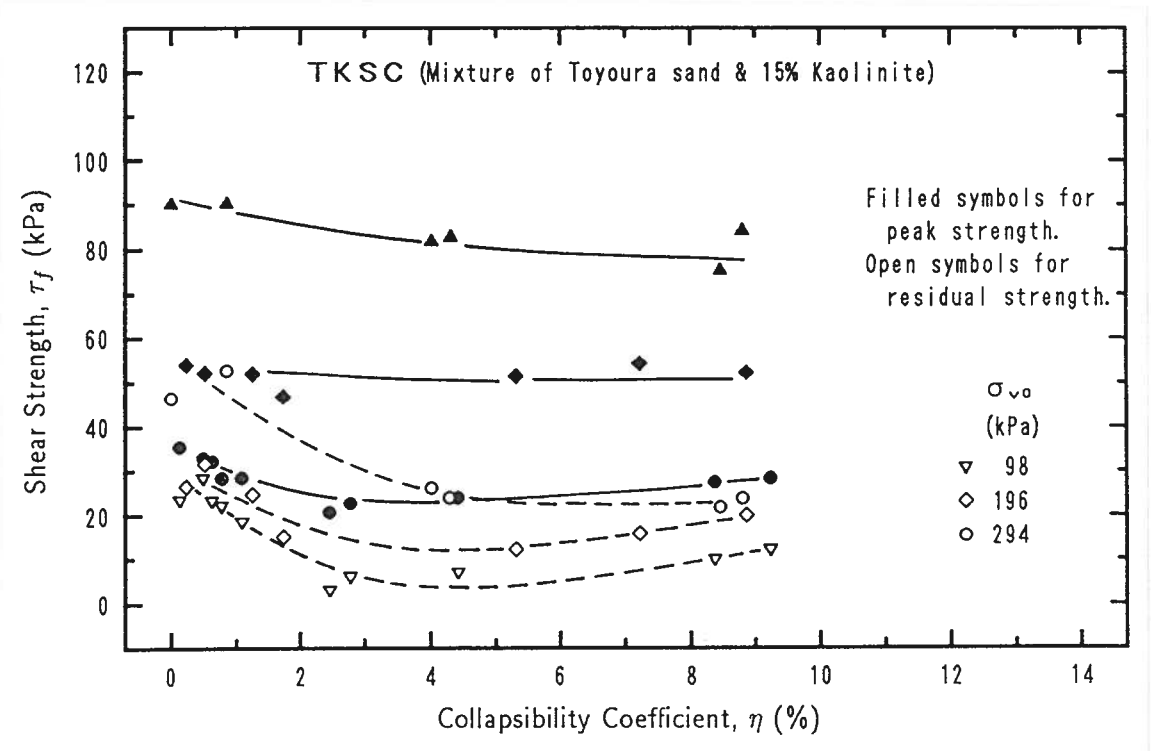

Figure 7.5: Effect of collapsibility coefficient on shear strength

strength and open symbols for residual strength. It is noted that the decrease in peak shear strength as the amount of collapse increases is smaller than that of residual strength. The changes of shear strength with the increase in collapsibility coefficient, η, are different for different load levels. Under a pressure 294 kPa, the shear strength decreases as η increases. For load level less than some value, the shear strength decreases first and then increases as η increases. These are shown in Fig. 7.1 as non-straight lines. Because material *TKSC* (Mixture of Toyoura sand and 15% kaolinite) is relatively different from the other materials, it is not clear if the other materials are of similar properties.

In this set of tests, the saturation ratios of the samples are approximately the same. This means that the effective stress caused by suction is the same, and therefore, under the same external pressure, the effective stresses of specimens are the same. The only difference is the amount of collapse which specimens have undergone. It is believed that the strength difference is caused by the difference in the structure of the samples. Different structures are caused by different molding water contents. The details of this are discussed in Chapter 9.

The strength parameters, d and β, given here are different from the strength parameters, c and ϕ (cohesion strength and angle of internal friction, respectively). The relationships between the two sets of strength parameters can be derived as in follows. In the plane strain condition, it can be assumed that the horizontal stress coefficient under consolidation loading condition is equal to coefficient of earth pressure at rest, K_0 (see Section 6.2). At constant volume condition, the reduction of the overburden pressure during shear is equivalent to the increase in pore pressure. Therefore, the equivalent total stress in vertical direction is constant and is equal to initial overburden pressure σ_{v0}. During the application of shear load, the stresses redistribute in the sample. Assume that at the time of failure the applied shear stress is τ and the horizontal stress coefficient is K. The stress state of the specimen can be expressed as in Fig. 7.6(a). The *Mohr* circle and *Mohr – Coulomb* envelope are given in Fig. 7.6(b). Fig. 7.6(b) also demonstrates the strength parameters d and β. Let

$$\sigma_0 = \frac{\sigma_1 + \sigma_3}{2} = \frac{1+K}{2}\sigma_{v0} \tag{7.1}$$

Considering that the radius of *Mohr* circle is constant yields

$$(\sigma_0 + c\cot\phi)\sin\phi = \frac{(\sigma_0 + d\cot\beta)\sin\beta}{\sin(2\theta - \beta)} \tag{7.2}$$

From Fig. 7.6(b), there has,

$$\tan 2\theta = \frac{\tau}{\frac{1-K}{2}\sigma_{v0}} \tag{7.3}$$

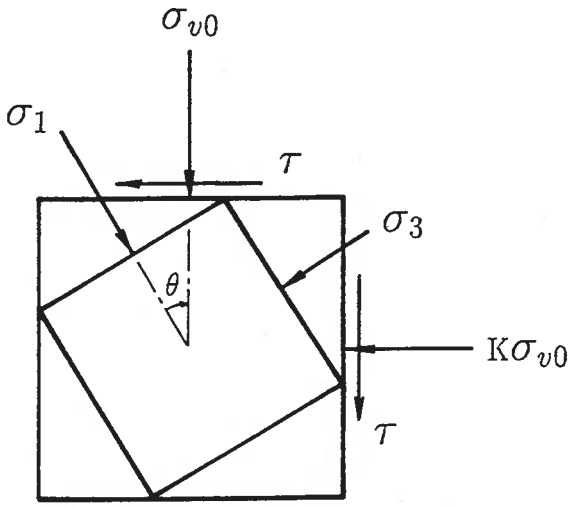

(a)

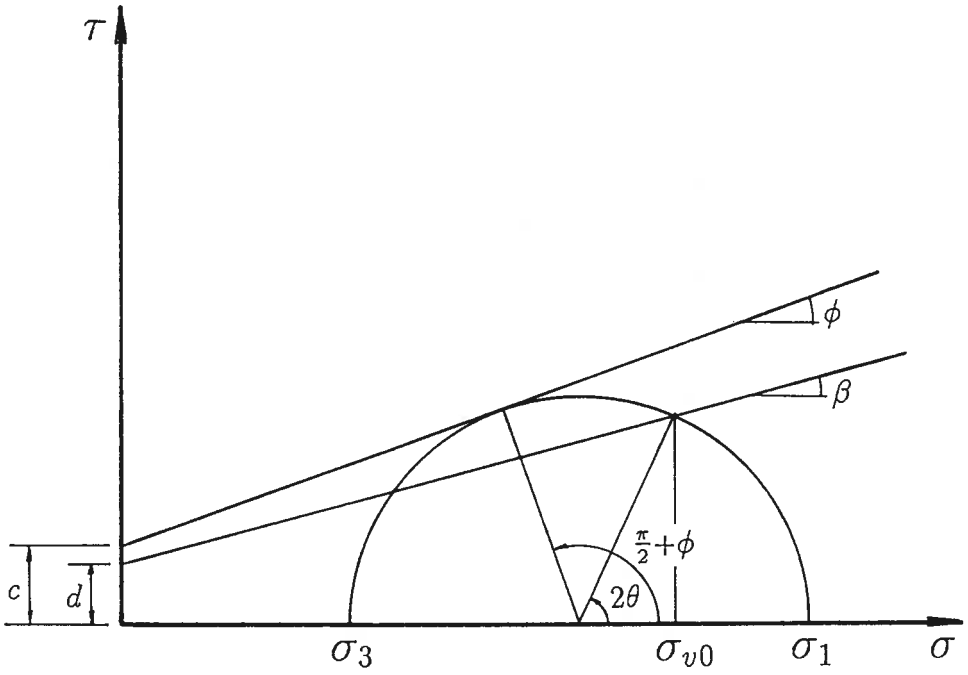

(b)

7.6: Relationships between two sets of strength parameters. (a). Stress state at failure; lohr-Coulomb envelope

Substituting Eq. 7.3 into Eq. 7.2 gives

$$(\sigma_0 + c\cot\phi)\sin\phi = \frac{(\sigma_0 + d\cot\beta)\sqrt{4\tau^2 + (1-K)^2{\sigma_{v0}}^2}\sin\beta}{2\tau\cos\beta - (1-K)\sigma_{v0}\sin\beta} \tag{7.4}$$

This equation gives the relationships among d, β and c, ϕ. If d and c are equal to 0, Eq. 7.4 becomes,

$$\sin\phi = \frac{\sqrt{4\tau^2 + (1-K)^2{\sigma_{v0}}^2}\sin\beta}{2\tau\cos\beta - (1-K)\sigma_{v0}\sin\beta} \tag{7.5}$$

Introducing $\tan\beta = \dfrac{\tau}{\sigma_{v0}}$ into Eq. 7.5 gives,

$$\sin\phi = \sqrt{(\frac{2\tan\beta}{1+K})^2 + (\frac{1-K}{1+K})^2} \tag{7.6}$$

For given β and K, the value of ϕ can be calculated by Eq. 7.6. For example, for material *CBSM* (Chonan B silty sand), assuming $K = 0.5$, Eq. 7.6 gives $\phi = 30.01°$ and $28.46°$ for samples which have experienced low and high magnitude of collapse, respectively. This means that the angle of internal friction also decreases as the sample undergoes high collapse.

7.2.2 Behavior of Wetted and Unwetted Soils

As described in the introduction, the main purpose in this set of tests is to study the strength loss caused by water infiltration. It is the usual case, in practice, that soil deposits arrive stress equilibrium at a certain moisture content. The sudden change in the moisture content, whether it is caused by breakage of pipe lines, heavy rain or rise in underground water level, will destroy the existing stress equilibrium and the collapse of soil structure occurs. To imitate this process of collapse, two samples are prepared having identical state of as-compacted moisture contents and densities and consolidated at a given overburden pressure. After the samples arrive stress and deformation equilibrium at the given overburden pressure, one sample is sheared following the stress and deformation equilibrium under drained, constant vertical stress and volume changeable conditions, and the other sample is flooded by water. Collapse occurs in the wetted sample due to water infiltration. When the collapse completes and the new stress and deformation equilibrium arrive, the sample is sheared. The dry densities of the two samples are about the same after consolidation but different before shearing because of the deformation due to collapse. In other words, the dry density of wetted sample is larger than that of unwetted one before shearing.

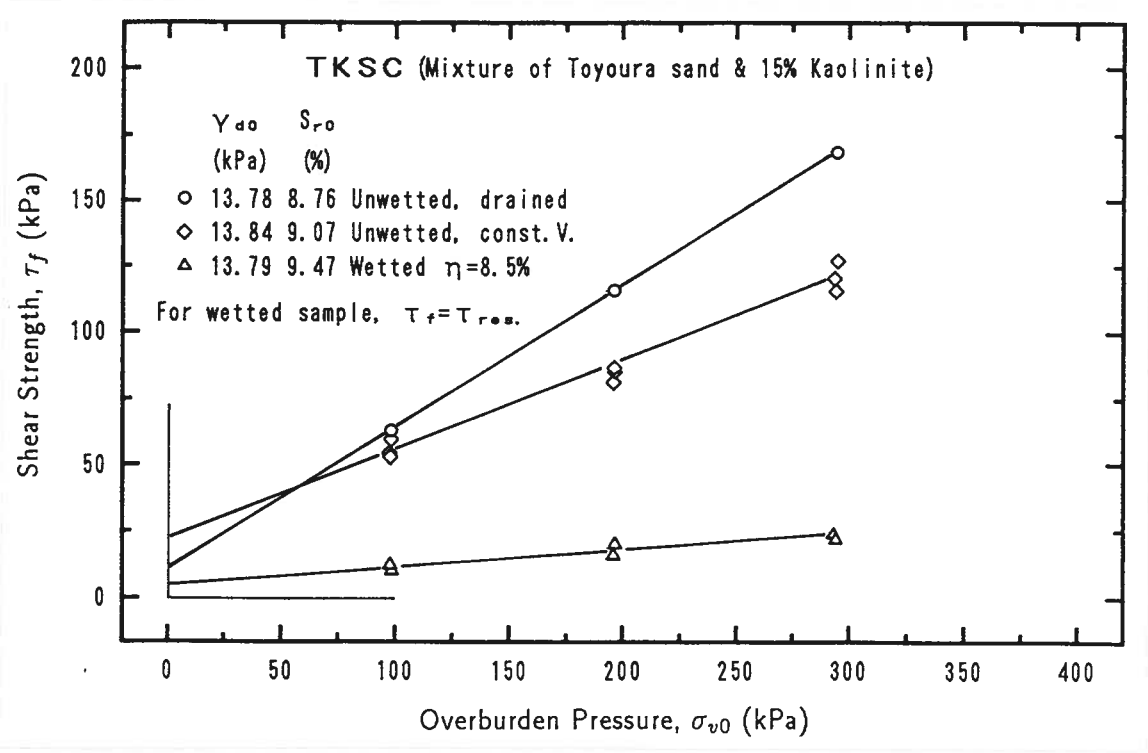

Figure 7.7: Effect of wetting on shear strength

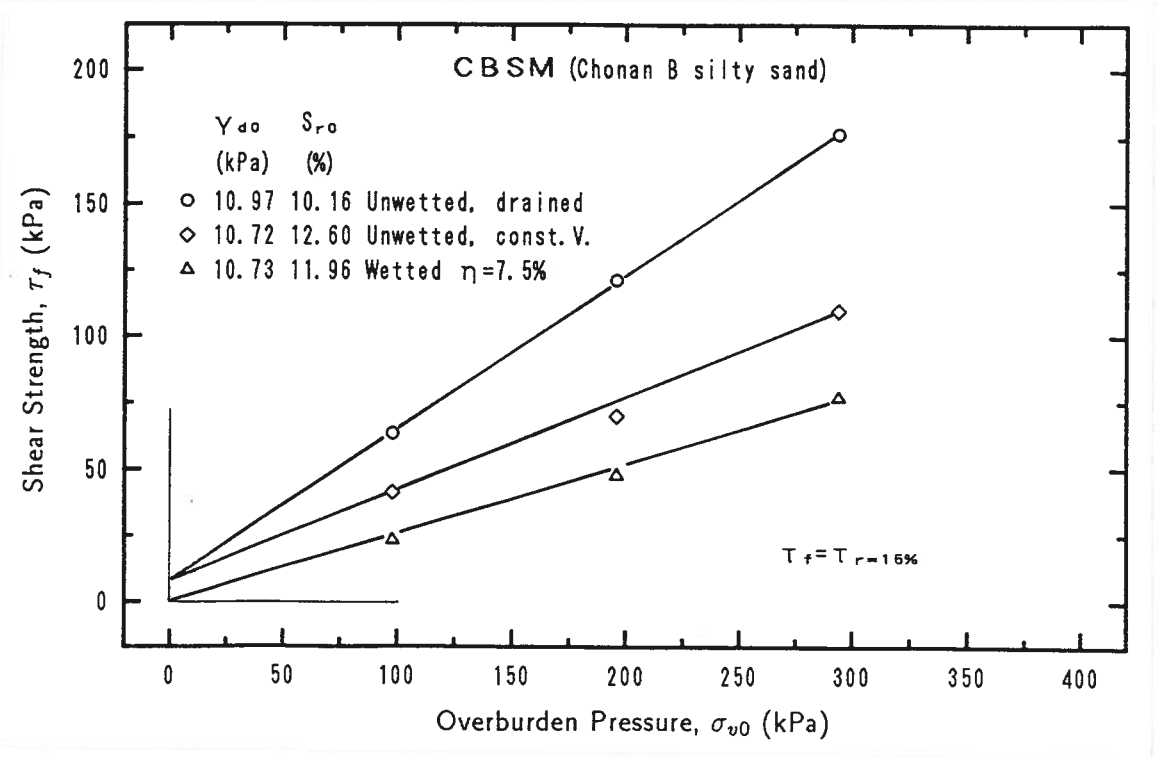

Figure 7.8: Effect of wetting on shear strength

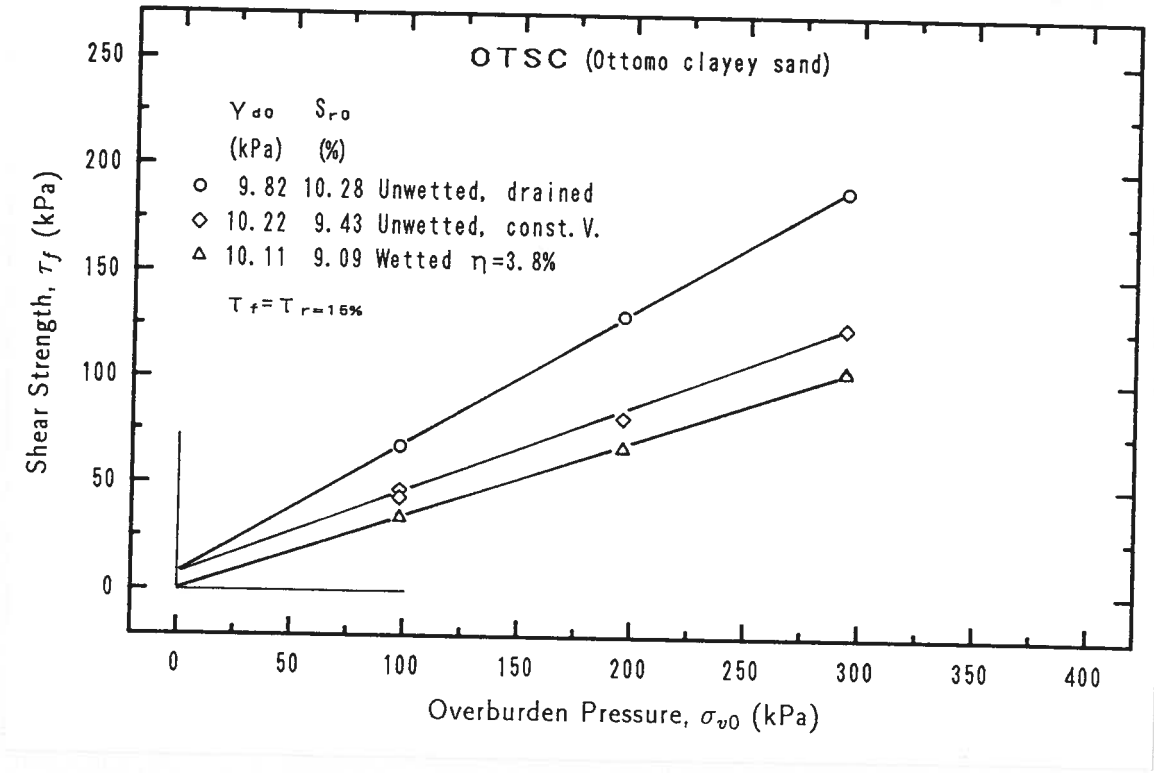

Figure 7.9: Effect of wetting on shear strength

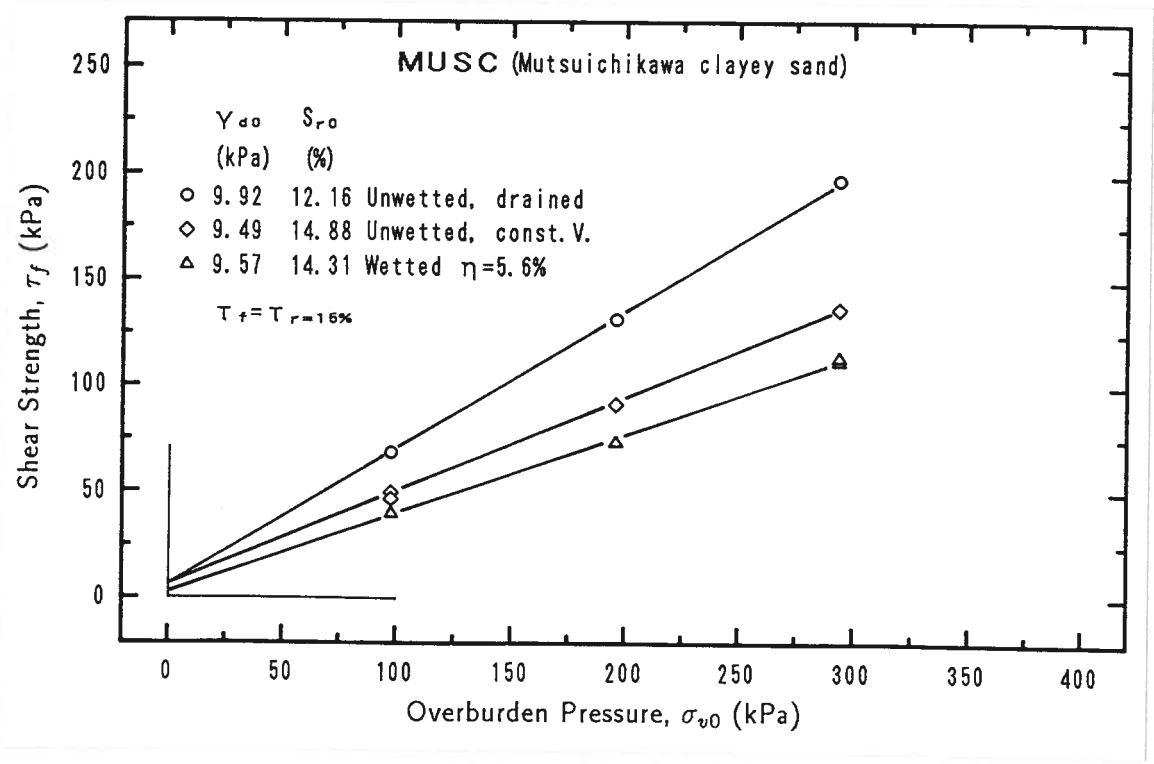

Figure 7.10: Effect of wetting on shear strength

The curves of shear strength versus initial axial stress of the four tested materials are given in Figs. 7.7 to 7.10. For different stress-strain behaviors, the shear strength is defined in different ways. If the soil shows strain softening (peak strength appears in the stress-strain curves), the maximum and residual shear stresses are taken as peak and residual shear strengths, respectively. If the soil has strain hardening behavior (no obvious peak value appears in stress-strain curves), the shear stress required to yield 15% shear strain is taken as the shear strength. In these figures, only the wetted samples in Fig. 7.7 (Mixture of Toyoura sand and 15% kaolinite) show of peak and residual strengths, and only the residual strengths are given in Fig. 7.7. For other test conditions and other materials, the shear strength is the shear stress corresponding to 15% shear strain.

It can be seen in these figures that wetting has significant influence on the strength properties of collapsible soils. The shear strength of soils decreases greatly as the soils are wetted. The strength reduction can be expressed by strength parameters d and β, which represent the cohesive intercept and angle of shearing resistance of $\tau_f \sim \sigma_{v0}$ curves, respectively. Table 7.2 presents the values of d and β for the four materials under wetting and unwetted conditions and the reduction of these values due to wetting. The results

Table 7.2: Changes of strength parameters due to wetting

Material		Unwetted	Wetted	Reduction (%)
TKSC	d, (kPa)	13.3	3.3†	75.6‡
	β, (°)	27.8	4.4†	84.1‡
CBSM	d, (kPa)	8.1	0	100
	β, (°)	29.5	14.3	51.5
OTSC	d, (kPa)	5.8	0	100
	β, (°)	31.3	19.3	38.2
MUSC	d, (kPa)	5.0	3.9	22.5
	β, (°)	32.3	20.3	37.0

† Parameters corresponding to residual strength.

‡ Reduction corresponding to residual strength.

in Table 7.2 show that not only d but also β decreases due to wetting. The reduction of the cohesive intercept depends on the clay content. In the case of low clay content, materials *CBSM* (Chonan B silty sand) and *OTSC* (Ottomo clayey sand), the cohesive intercept completely disappears, while when the clay content is relatively high, materials *TKSC* (Mixture of Toyoura sand and 15% kaolinite) and *MUSC* (Mutsuichikawa clayey sand), there are still some cohesive intercepts after the samples have been subjected to

water permeation. The unstable and relative high strength of collapsible soil in unsaturated state is considered to be the result of suction and the high external load induced effective stress because of the drained condition. In fact, for natural collapsible soils, it also includes the effect of cementation. For laboratory compacted samples, however, cementation agents have not developed yet because of the relatively short time interval between sample preparation and testing. Therefore, in laboratory condition, suction and the drained condition are the only factors which should be considered. The presence of suction increases the effective stress in the normal component and, consequently, the resistance to shear. As the soil is soaked, the increase in the degree of saturation reduces the magnitude of suction followed by the loss of strength. It is noticeable that not only the cohesive intercept but also the angle of shearing resistance changes due to soaking. The decrease in the angle of shearing resistance due to wetting is as large as 26.8 degrees for *TKSC* (Mixture of Toyoura sand and 15% kaolinite) material. The second factor influencing the shear strength is considered to be the test condition. When the sample is unwetted, sample is in a drained condition and no excess pore pressure is developed in the sample, therefore, the effective stress caused by external load is constant during shear. On the other hand, when the sample is wetted and the degree of saturation of it increases to a relatively high value, test condition changes from drained to undrained condition. Excess pore pressure is built up and consequently, the effective stress in the sample decreases. Because of this decrease in effective stress, the shear strength decreases. Therefore, it is evident that the effect of soaking on shear strength is shown in two aspects, the reduction of suction and the change of test condition which results the decrease in external load induced effective stress. In order to separate these two effects, another set of tests are performed on unwetted samples under constant volume and undrained conditions. The test results are presented by diamond symbols in Figs. 7.7 to 7.10 for the four materials tested, respectively. As discussed in the previous chapter, the constant volume test for dry non-clay soils is equivalent to fully saturated undrained test, while for soil which possesses a certain moisture content and is partly saturated, the constant volume test maintains the feature of suction. The measured stress is equal to the algebraic difference of effective stress and the component of effective stress caused by suction; in other words, the measured stress is equal to the effective stress induced by external load, and this effective stress decreases during constant volume shearing. Therefore, the strength difference between unwetted drained test and unwetted constant volume test is resulted by the decrease in external load induced effective stress which is caused by the change of drainage condition. The effective stresses caused by suction are the same in these two type of tests and are constant. This is shown in Figs. 7.8 to 7.10 as a constant

value of cohesive intercept for the two type of tests. It is to be noted that material *TKSC* (Mixture of Toyoura sand and 15% kaolinite) is an exception to the above conclusion. It might be due to test error. On the other hand, the strength difference between wetted tests and unwetted constant volume tests is due to the disappearance of suction. In these two type of tests, the effective stresses which is resulted by external load are the same and decrease during shear loading. In unwetted samples, suction exists, while in wetted samples, suction disappears due to the increase in degree of saturation. The changes in strength parameters in these two type of tests are given in Table 7.3 for the four materials tested. It is to be noted that not only the cohesive intercepts but also the angles

Table 7.3: Changes of strength parameters due to disappearance of suction

Material		Unwetted	Wetted	Reduction (%)
TKSC	d, (kPa)	22.8	3.3†	85.7‡
	β, (°)	18.5	4.4†	76.1‡
CBSM	d, (kPa)	8.1	0	100
	β, (°)	18.8	14.3	23.6
OTSC	d, (kPa)	5.8	0	100
	β, (°)	22.0	19.3	12.3
MUSC	d, (kPa)	5.0	3.9	22.5
	β, (°)	24.3	20.3	16.3

† Parameters corresponding to residual strength;
‡ Reduction corresponding to residual strength.

of shearing resistance change as the suction disappears. This means that the presence of suction affects not only the cohesion strength but also the angle of internal friction of the soil.

It is noted that the dry density of wetted samples are larger than that of unwetted ones prior to the application of shear loading. According to the common knowledge in saturated soils, the denser the soil, the higher is the strength. This is also true in unsaturated soils. However, when talking about the strength change due to wetting, care must be taken. A soil engineer who rarely deals with unsaturated soils is liable to commit the mistake of believing that soils will possess higher strength after they are wetted because of the increase in density due to wetting. This is not true because the magnitude of strength loss caused by the change in drainage condition and the disappearance of suction action is much higher than the strength increase caused by the increase in density due to wetting and collapse. This further indicates that the strength loss caused by the

change in drainage condition and the disappearance of suction action is larger than the measured value.

7.3 DEFORMATION BEHAVIOR

7.3.1 Behavior of Soils Which Have Undergone Different Amount of Collapse

The typical stress-strain curves of samples which experienced different amount of collapse are presented in Figs. 7.11 to 7.14. It can be seen that although both the samples are wetted, there are differences existed between the stress-strain curves due to the different amount of collapse experienced by the samples. At small strain level (about less than 0.2% to 1.5% and different for different soils), there are little differences between the stress-strain curves of the samples which have undergone different amount of collapse. As the shear strain increases beyond this value, soils behave differently. Those which have experienced large amount of collapse have smaller secant shear moduli (at the same shear strain) than those which have undergone little collapse. For material *TKSC* (Mixture of Toyoura sand and 15% kaolinite, Fig. 7.11), the soils behave as strain softening no matter how much collapse it has been experienced. The difference between the stress-strain curves increases with the increase in shear strain. For material *CBSM* (Chonan B silty sand, Fig. 7.12), slightly strain hardening shows in the samples which have experienced low collapse, while for samples which have undergone high collapse, the stress-strain curves demonstrate slightly strain softening. But, both the strain hardening and strain softening are very weak. The stress-strain relationships are almost ideal plastic type. Materials *OTSC* (Ottomo clayey sand, Fig. 7.13) and *MUSC* (Mutsuichikawa clayey sand, Fig. 7.14) have strain hardening behavior in the case of both low and high collapse. The effect of different amount of collapse on the deformation behavior of soil seems to occur mainly at shear strain level between 4% to 24% for material *OTSC* in Fig. 7.13 and this effect decreases when the shear strain is larger than 24%. Fig. 7.14 shows that the effects of different amount of collapse are significant at stress levels of 98 and 196 kPa while it is unnoticeable at axial stress of 294 kPa.

In order to quantitatively describe the effect of the effect of the different amount collapse on the shear characteristics of collapsible soils under monotonic loading condition, *collapse factor* defined in Eq. 6.16 can be used, *i.e.*:

$$C_{cl} = \frac{G_{\eta h}}{G_{\eta 0}} \tag{7.7}$$

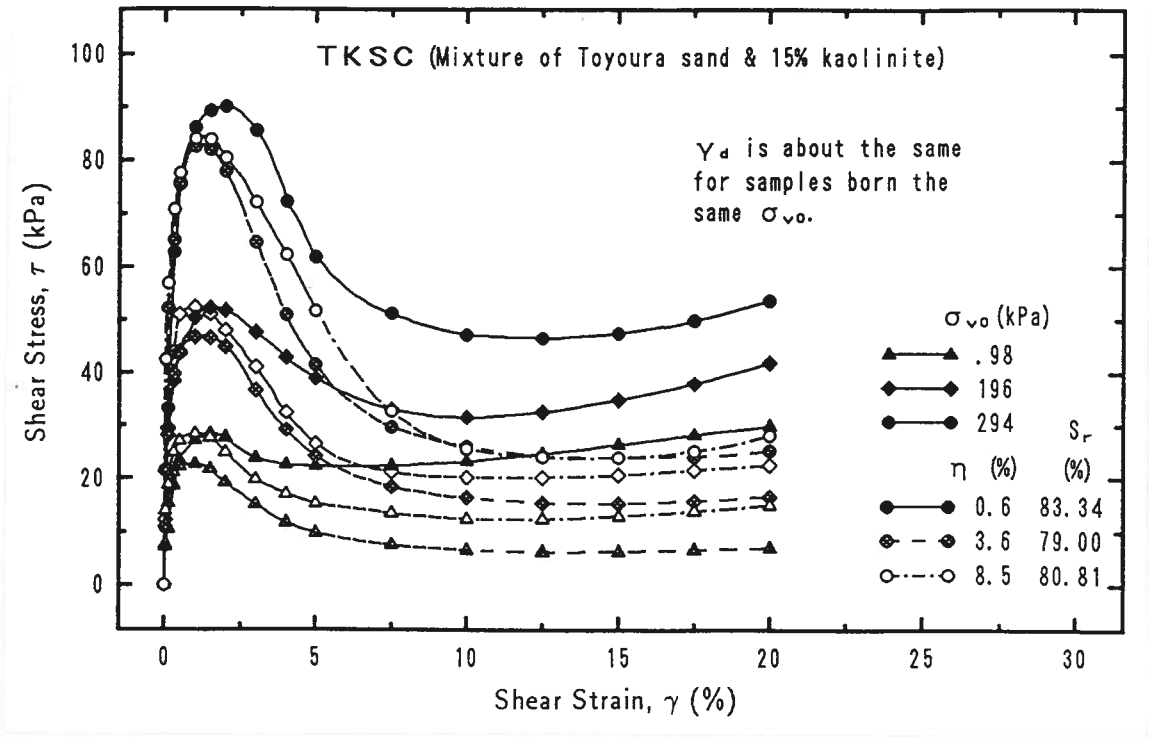

Figure 7.11: Stress-strain curves under different amount of collapse

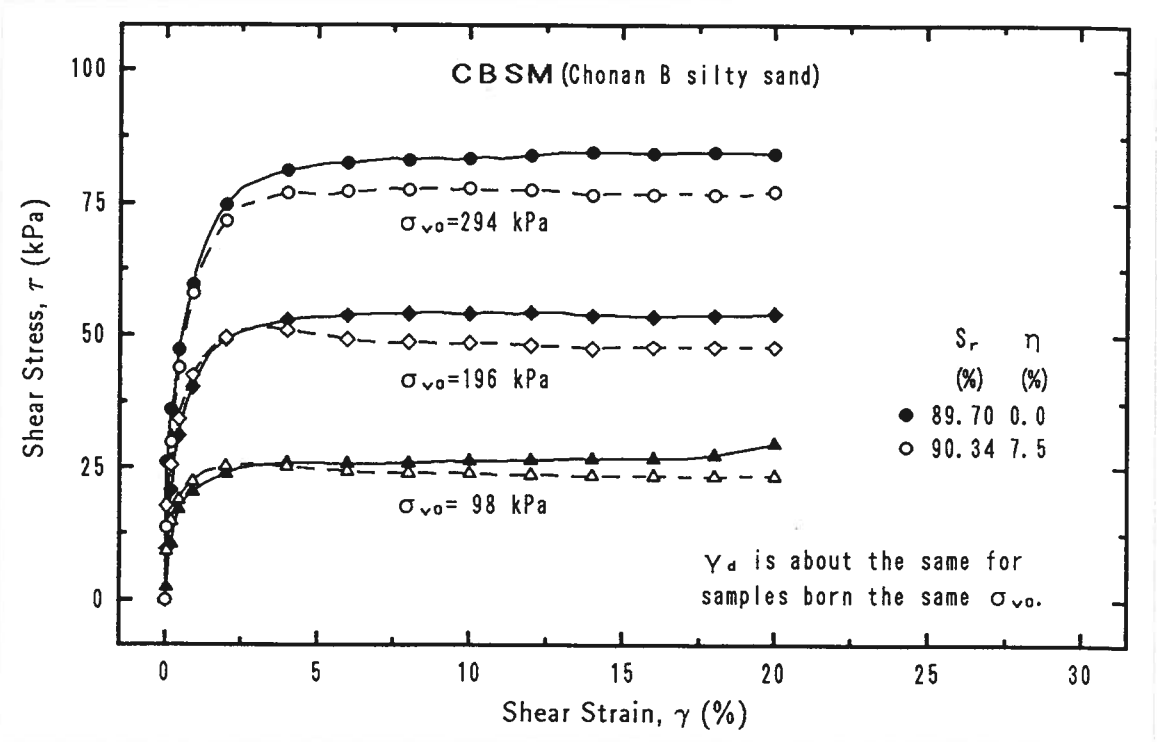

Figure 7.12: Stress-strain curves under different amount of collapse

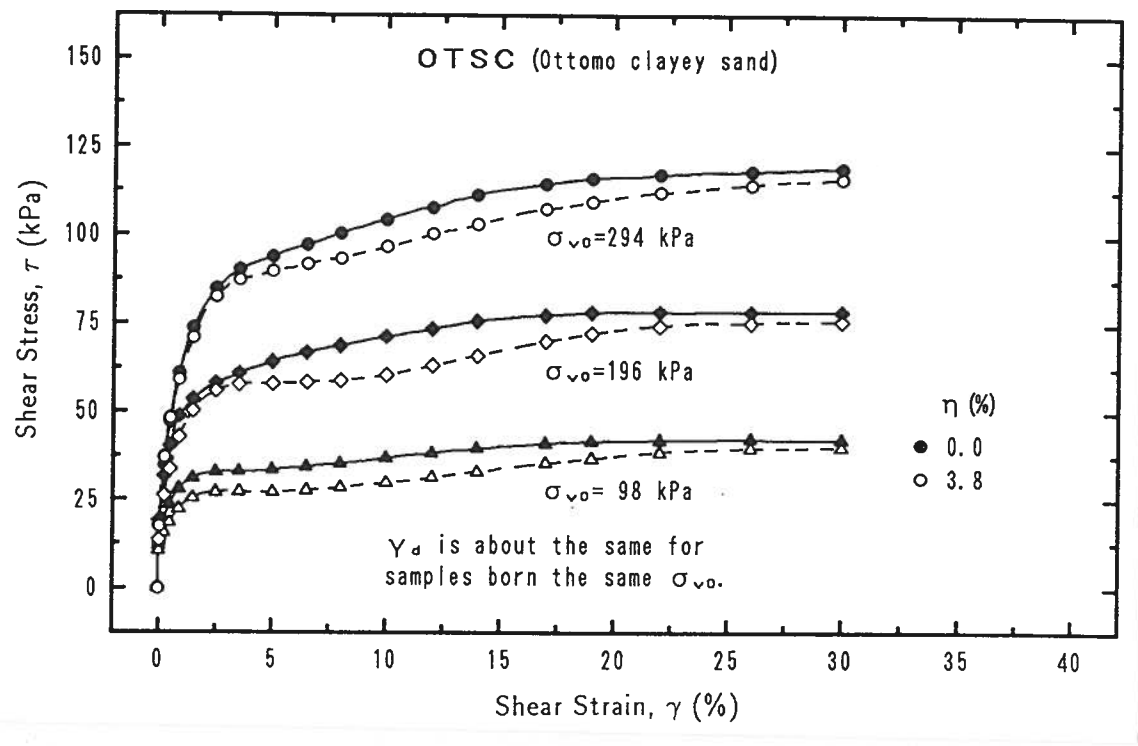

Figure 7.13: Stress-strain curves under different amount of collapse

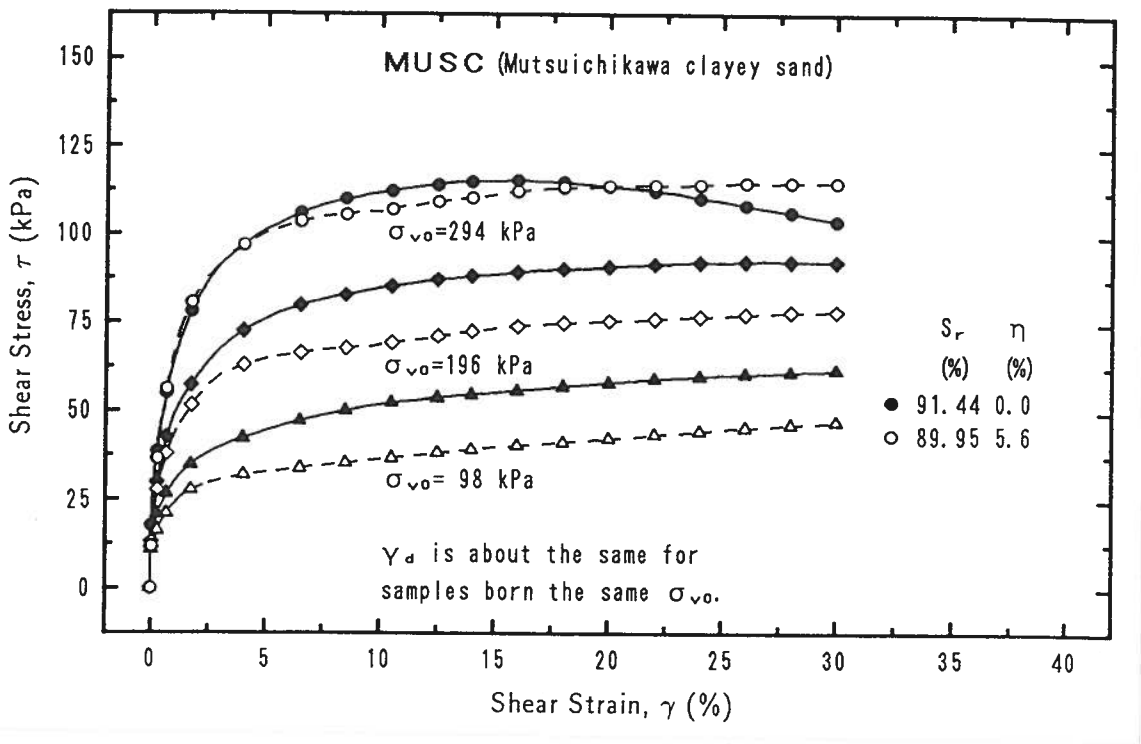

Figure 7.14: Stress-strain curves under different amount of collapse

This definition can also be expressed as:

$$C_{cl} = \frac{G_{\eta h}}{G_{\eta 0}} = \frac{\tau_{\eta h}/\gamma}{\tau_{\eta 0}/\gamma} = \frac{\tau_{\eta h}}{\tau_{\eta 0}} = \frac{(\tau_{\eta h}/\sigma_{v0})}{(\tau_{\eta 0}/\sigma_{v0})} \tag{7.8}$$

where

τ : the shear stress;

σ_{v0} : the initial axial stress; and

The subscript $_{\eta h}$ means high collapse and subscript $_{\eta 0}$ means zero collapse.

Therefore, this ratio can be readily obtained by dividing the shear stress ratio, $\tau_{\eta h}/\sigma_{v0}$, of samples which have experienced high amount of collapse by the stress ratio, $\tau_{\eta 0}/\sigma_{v0}$, of samples which have undergone low amount of collapse or dividing the corresponding shear stresses. For this purpose, the plots such as those shown in Figs. 7.11 to 7.14 can be used most commonly. For each of the tested materials, the *collapse factor*, C_{cl}, is determined and all the results are summarized in Figs. 7.15 to 7.17 for the materials used corresponding to overburden pressure of 98, 196 and 294 *kPa*, respectively. These figures give the trends of variation in *collapse factor* with respect to the shear strain. Although the variations of collapse factors with shear strain are different for different type of materials, the values of collapse factor are less than 1 in a large range of shear strain. This means that the stiffness of the soil decreases in a large range of shear strain if it has experienced large amount of collapse in the history of hydraulic collapse. It is evident that the results are affected by the total stress level. The comparison of the results in Figs. 7.15 to 7.17 show that that the *collapse factor* increases with the increase in total stress level. This tendency is especially demonstrated in the variation with overburden pressure of the collapse factors of the three natural materials which are sampled from manufactured embankments. It means that the effect of collapse history on the strength and stiffness of the soil decreases as the increase in stress level. This is reasonable because the effect of collapse on strength and stiffness properties of soil is considered to be the difference between the microstructure of samples which have experienced different amount of collapse (it will be discussed in detail in Chapter 9). The difference between the microstructures might be reduced as the stress level increases and, therefore, this reduction reduces the effect of collapse on soil behavior.

Figs. 7.18 to 7.21 are the relationships between the excess pore pressure and the shear strain developed during shearing. It is obvious that in samples which have experienced high amount of collapse, the excess pore pressure is easier to build up than in those which have undergone little amount of collapse. Because of the higher excess pore pressure, the effective stress of the samples which have experienced high amount of collapse is smaller, at the same strain level, than those of the samples which have experienced low

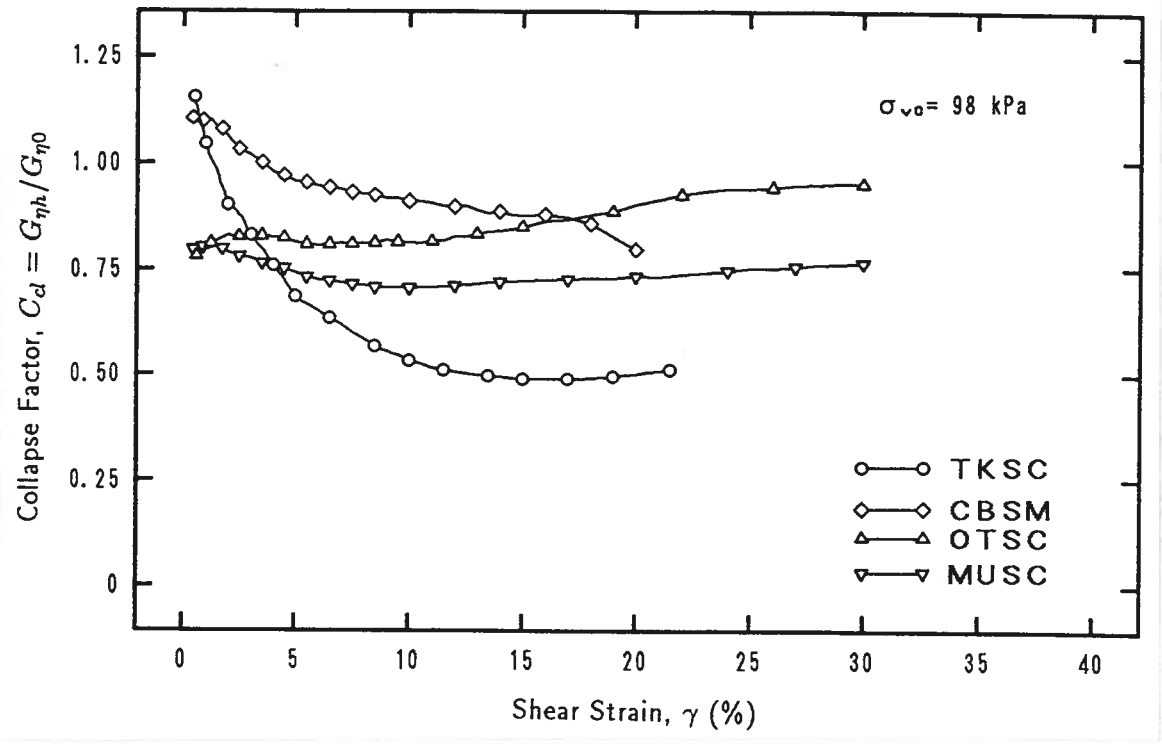

Figure 7.15: Collapse factor as a function of shear strain for an overburden pressure of 98 kPa

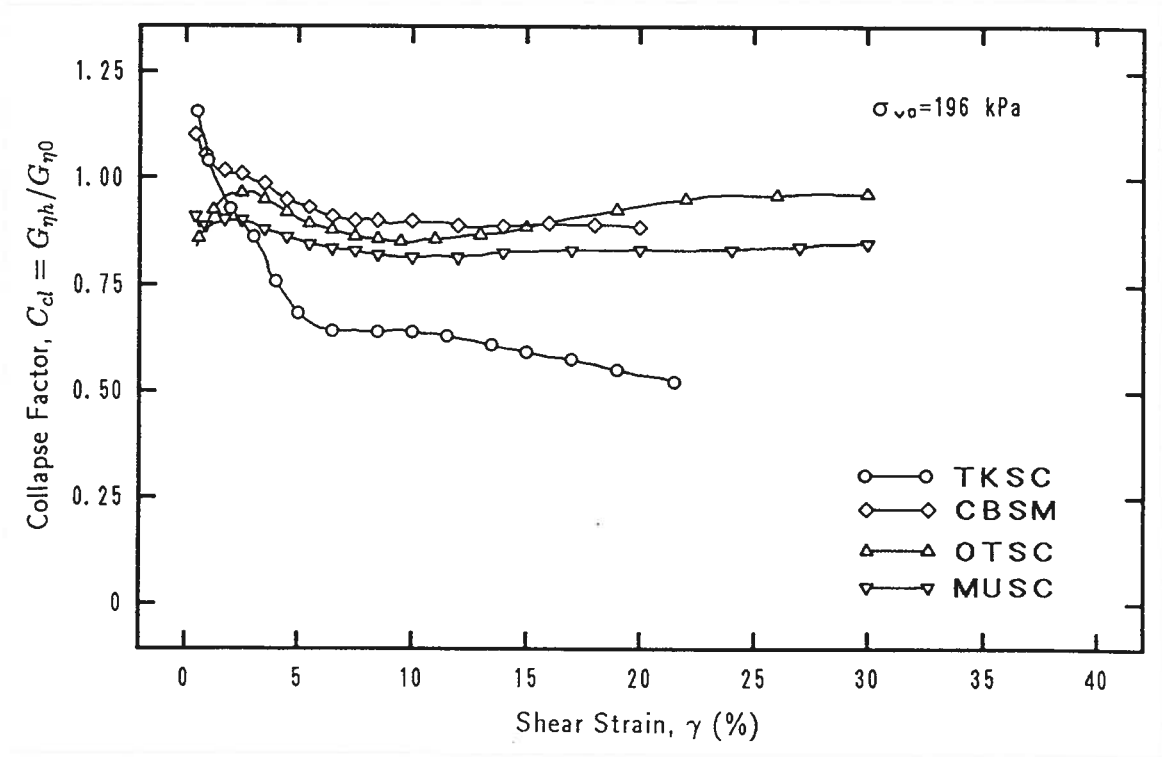

Figure 7.16: Collapse factor as a function of shear strain for an overburden pressure of 196 kPa

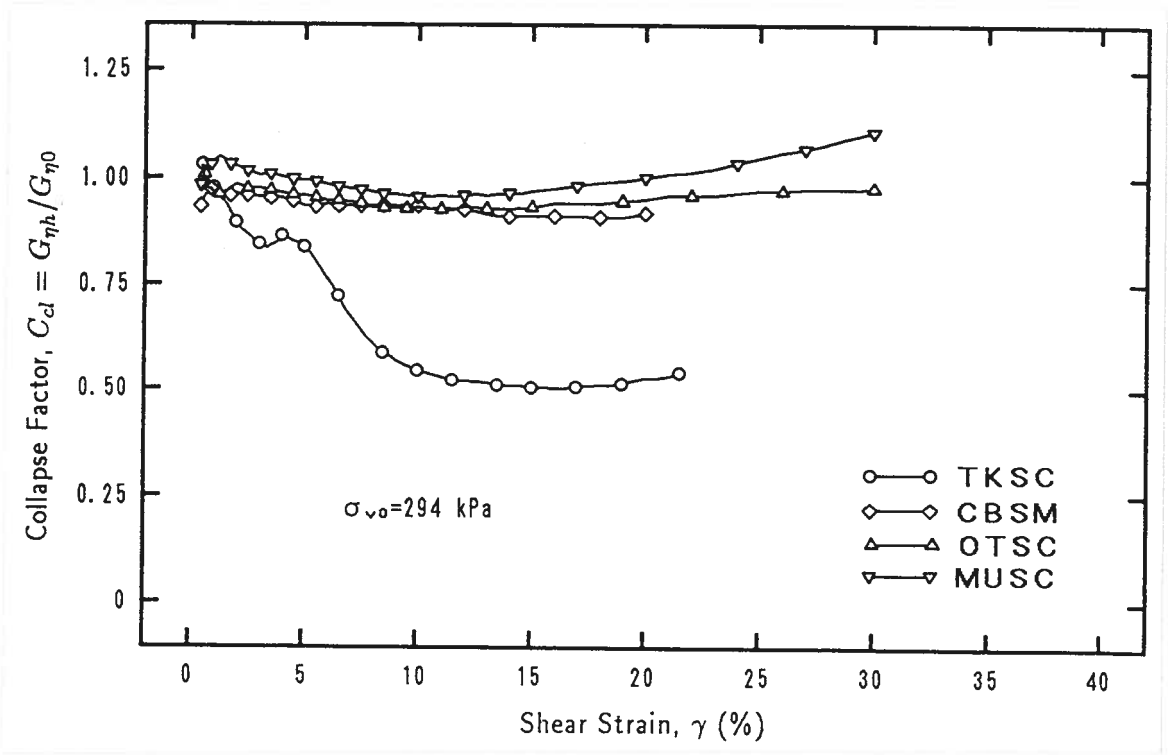

Figure 7.17: Collapse factor as a function of shear strain for an overburden pressure of 294 kPa

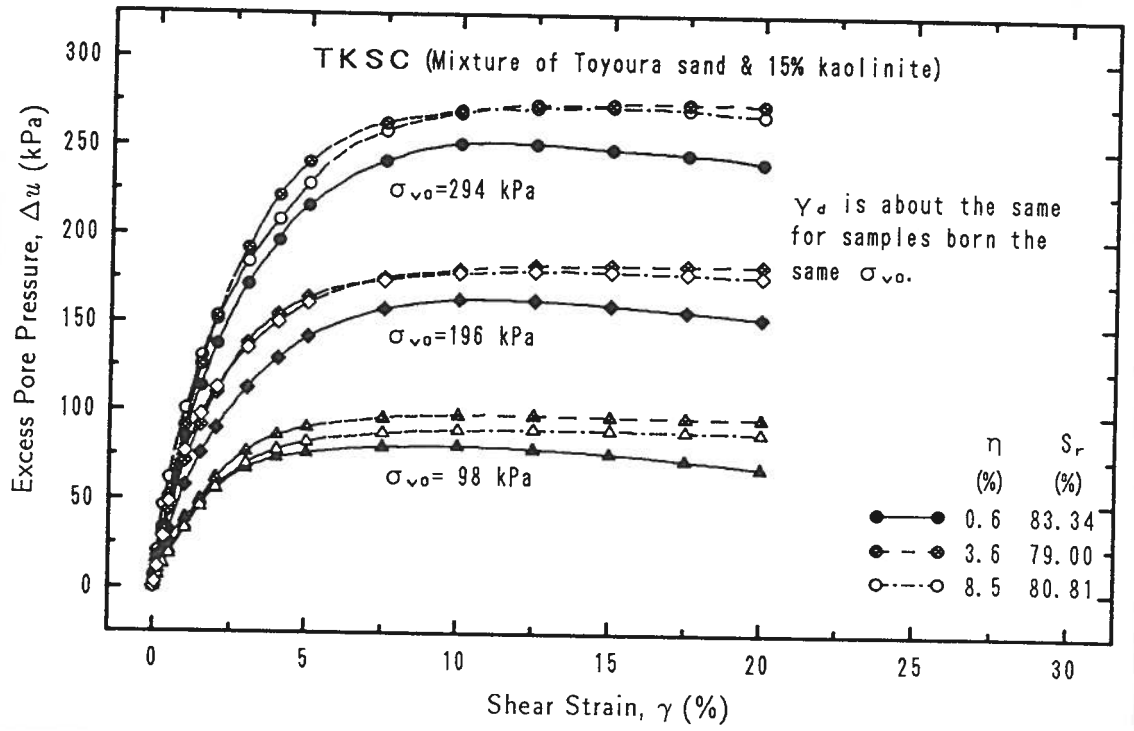

Figure 7.18: Excess pore pressure developed in samples which have undergone different amount of collapse

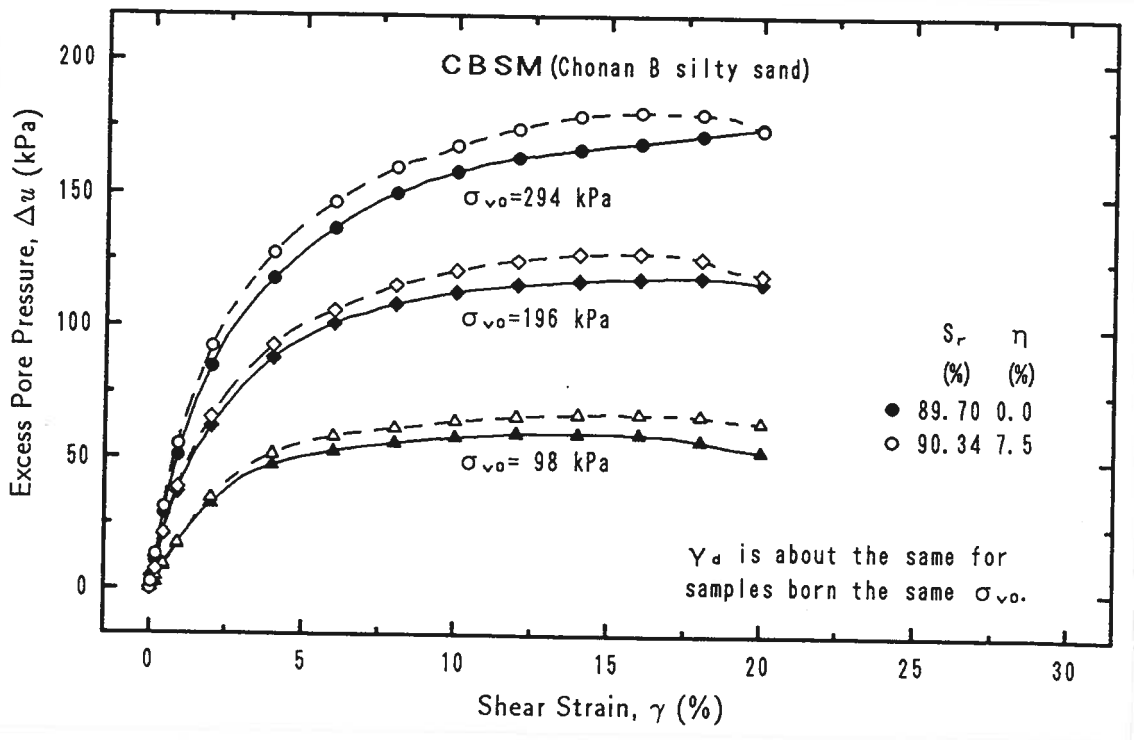

Figure 7.19: Excess pore pressure developed in samples which have undergone different amount of collapse

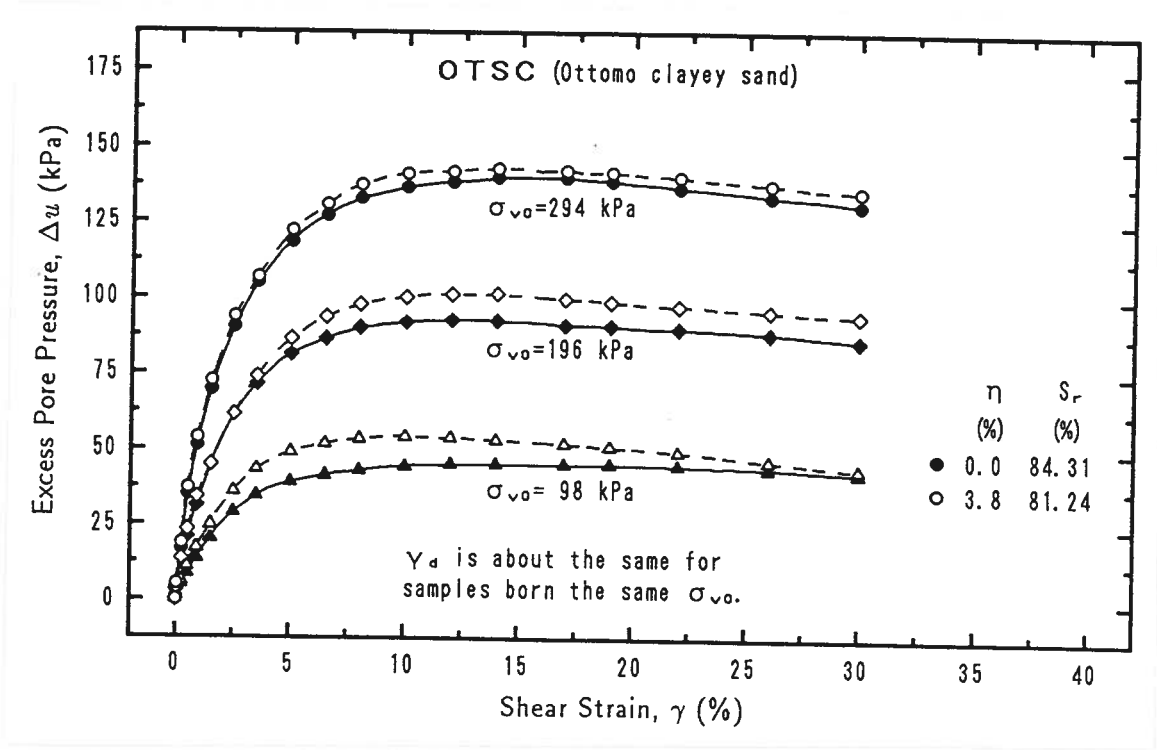

Figure 7.20: Excess pore pressure developed in samples which have undergone different amount of collapse

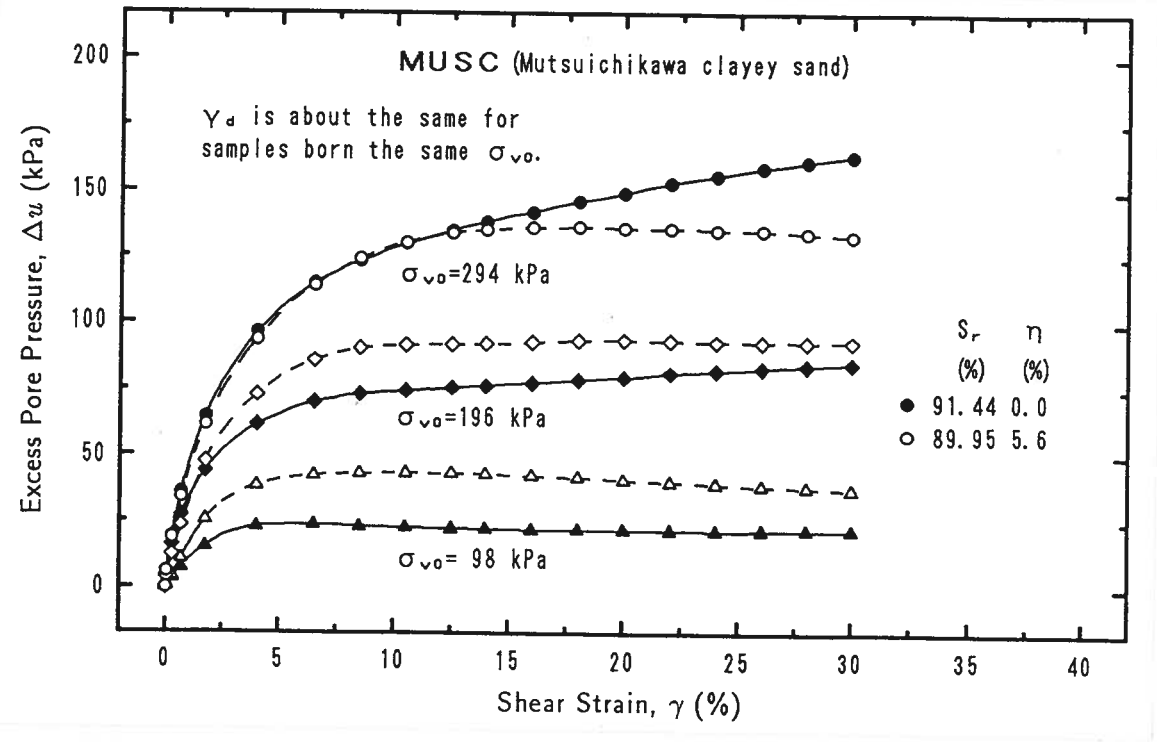

Figure 7.21: Excess pore pressure developed in samples which have undergone different amount of collapse

amount of collapse, and therefore the lower shear strength. The stress paths (Figs. 7.22 to 7.25) show that there is some difference between the failure envelopes although the difference is relatively small. The stress paths of samples which have undergone small amount of collapse are obviously higher than those which have experienced large amount of collapse. Because both of the samples have been wetted and have high and approximately the same saturation ratios, suction induced effective stress is negligible. The stress paths in Figs. 7.22 to 7.25 are equivalent to those in terms of the effective stress. Therefore, the difference between the stress paths really represents the effect of collapse on strength properties of collapsible soils.

7.3.2 Behavior of Wetted and Unwetted Soils

The typical stress-strain relationships of wetted and unwetted samples under different loads are illustrated in Figs. 7.26 to 7.29 for the four materials used. It is observed from the figures that, for materials *TKSC* (Mixture of Toyoura sand and 15% kaolinite) and *CBSM* (Chonan B silty sand), if the samples are unwetted, they have strain hardening behavior, while if the samples are wetted, the behavior is strain weakening. For materials *OTSC* (Ottomo clayey sand) and *MUSC* (Mutsuichikawa clayey sand), soils have strain hardening behavior whether they are wetted or not. But, the hardenability decreases as the samples are subjected to water infiltration. It is also found that the wetting-induced weakening depends on the shear strain level. The stiffness (secant shear modulus) of soils decreases sharply as they are wetted and the reduction in the stiffness increases as the shear strain increases.

As discussed in the previous section, the dry density of wetted specimens are larger than that corresponding to unwetted ones because of the collapse-induced deformation before shearing. Therefore, the stiffness of unwetted samples must be larger than the values presented in the figures if their dry densities are to be equal to those corresponding to wetted ones. This means that the wetting-induced weakening would be larger if the unwetted samples had the same dry densities as the wetted ones.

In Section 7.2.2, it has be discussed that the wetting-induced strength loss is resulted by two factors, namely reduction of external load caused effective stress which is due to the change in drainage condition and the disappearance of suction induced effective stress. The two factors can be separated by unwetted constant volume tests. The stress-strain curves of this set of tests are also illustrated in Figs. 7.26 to 7.29 by shadowed symbols and dash lines. It is evident that suction has significant influence on the deformation behavior of collapsible soils.

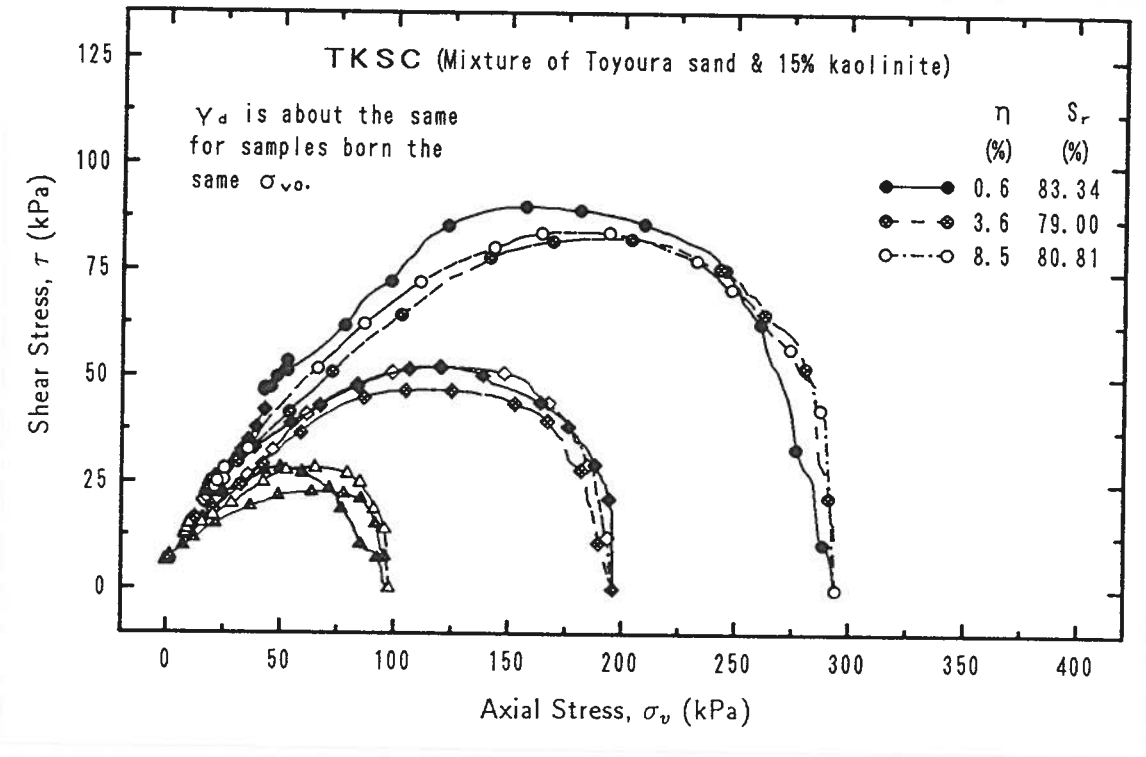

Figure 7.22: Relationships between shear stress and measured axial stress under different amount of collapse

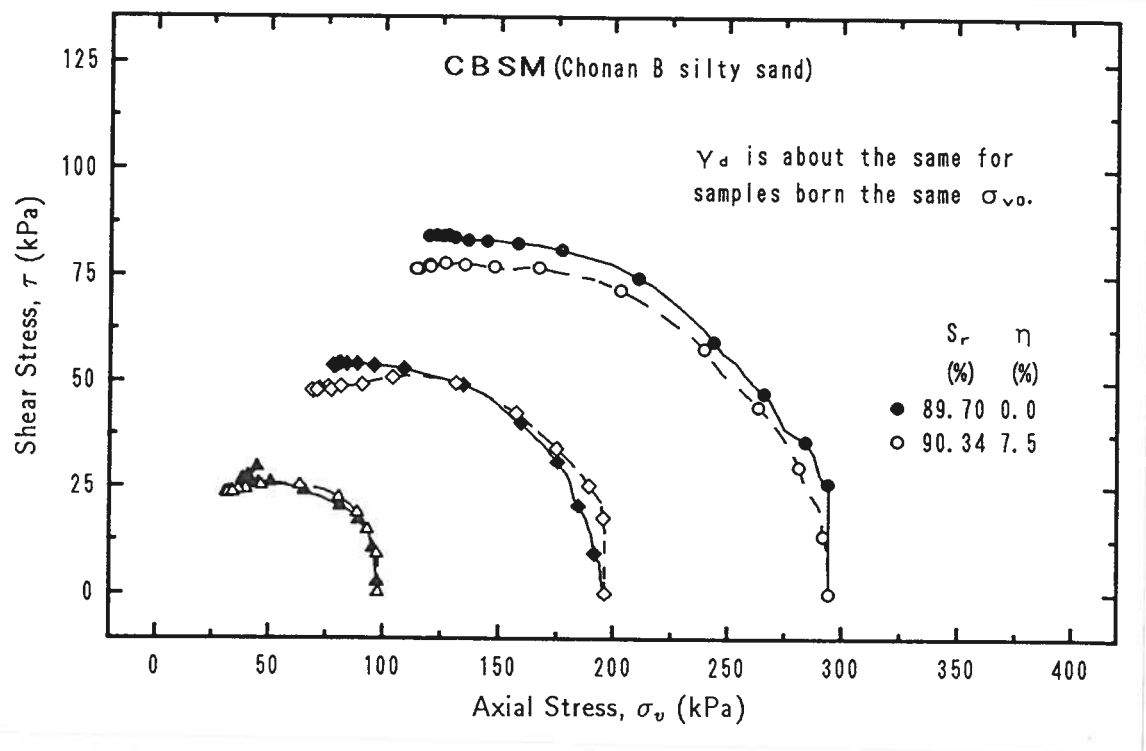

Figure 7.23: Relationships between shear stress and measured axial stress under different amount of collapse

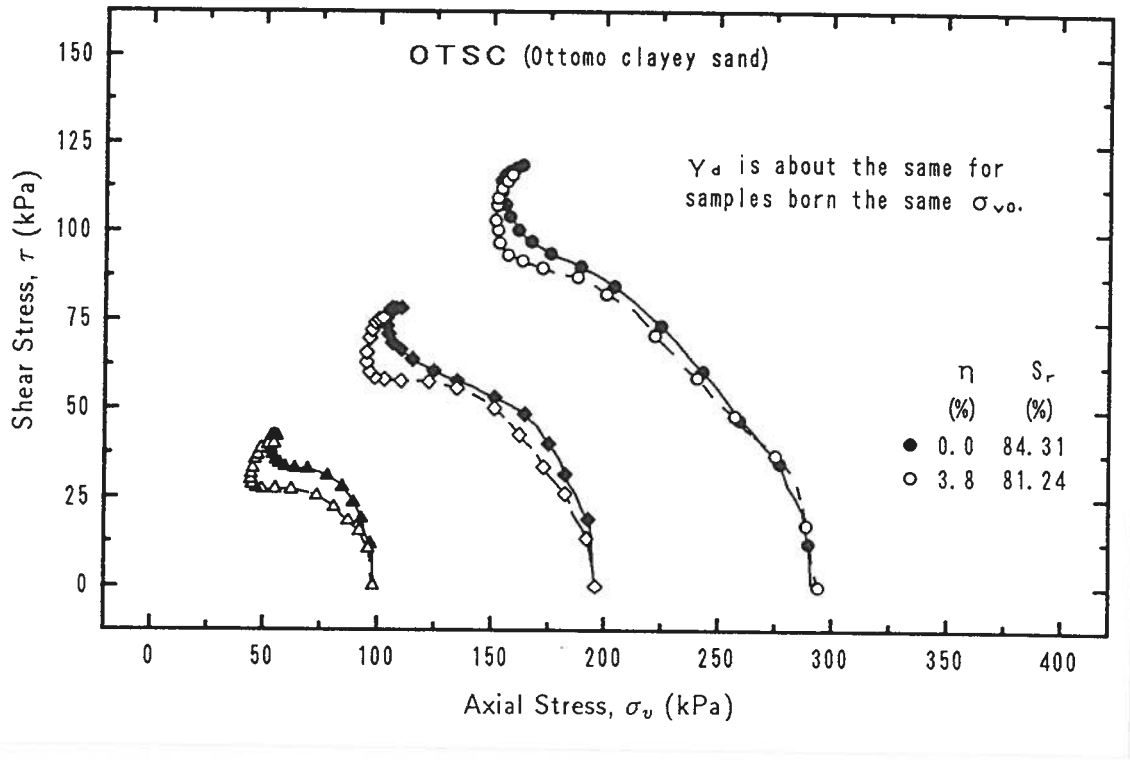

Figure 7.24: Relationships between shear stress and measured axial stress under different amount of collapse

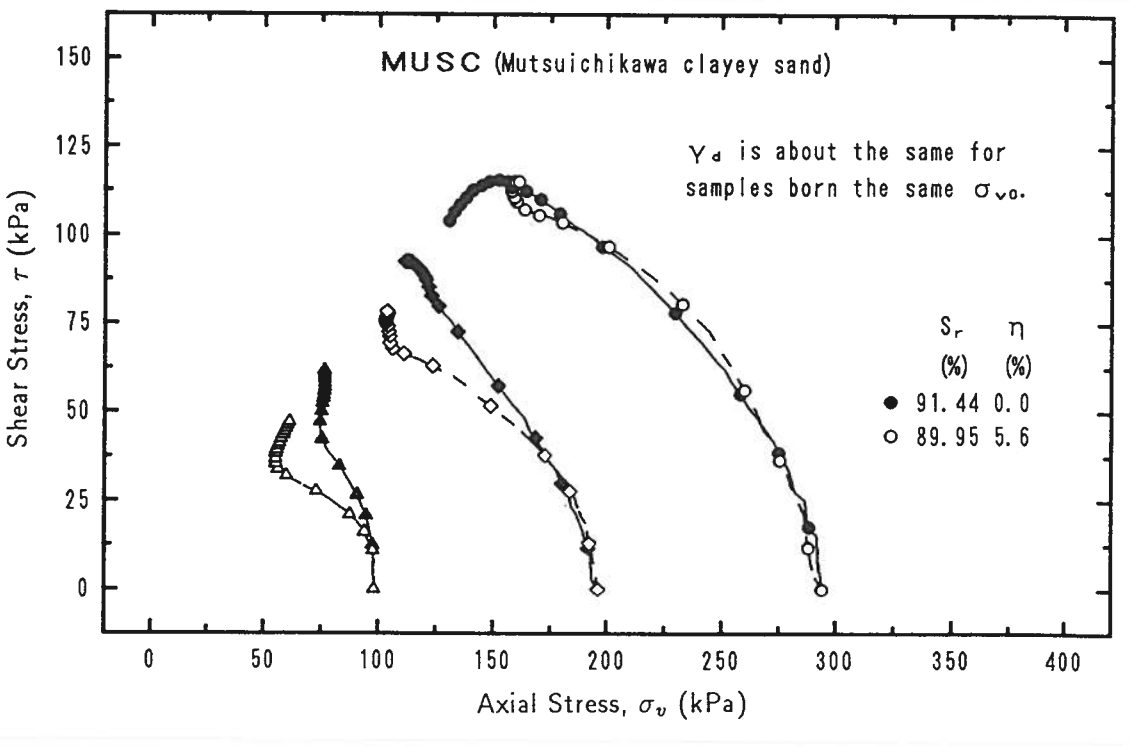

Figure 7.25: Relationships between shear stress and measured axial stress under different amount of collapse

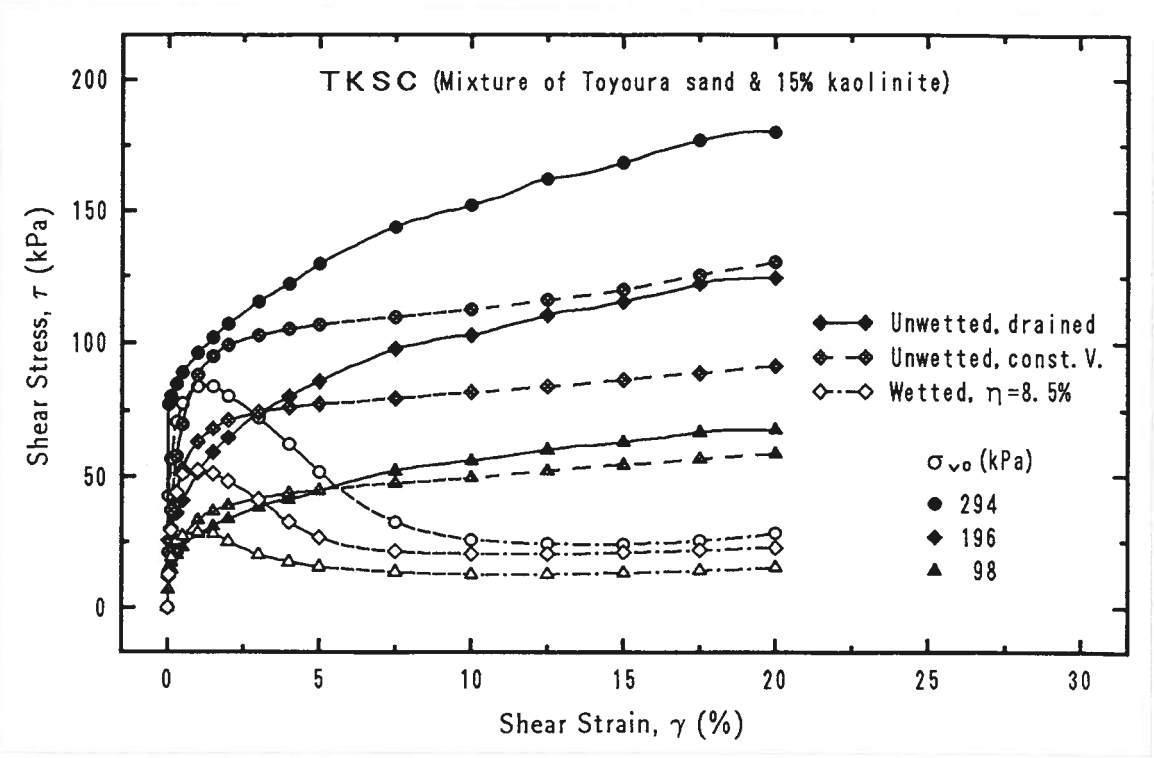

Figure 7.26: Stress-strain curves of wetted and unwetted samples

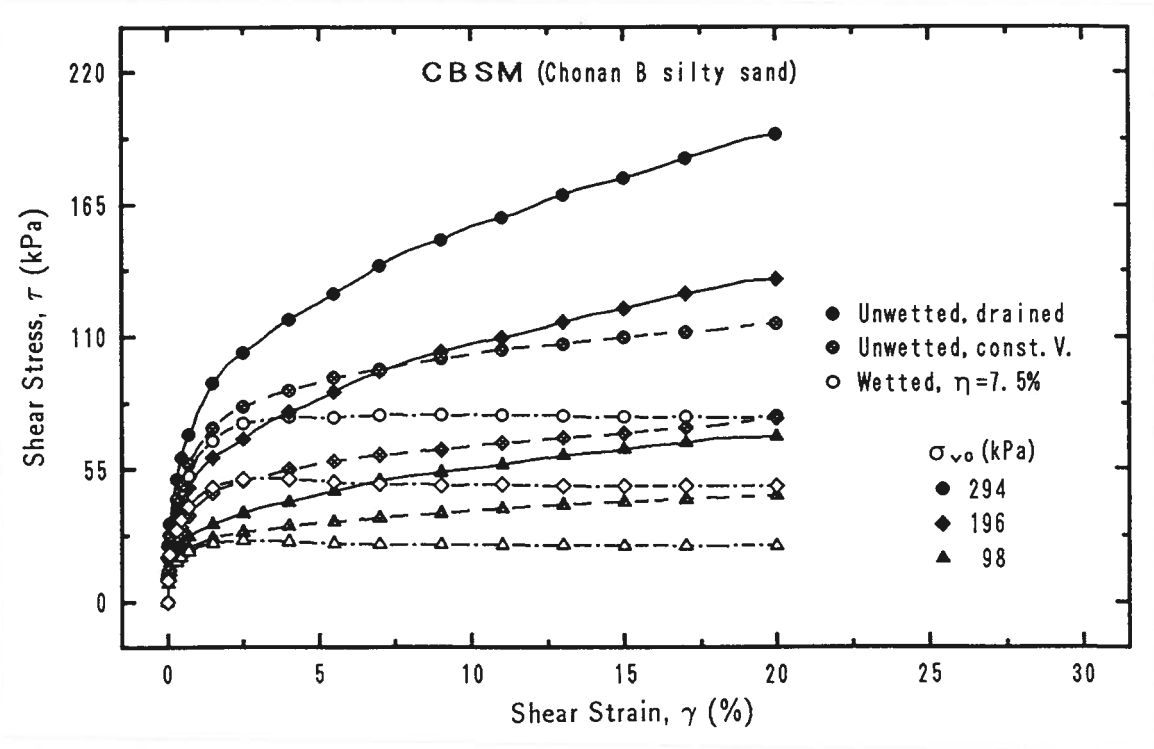

Figure 7.27: Stress-strain curves of wetted and unwetted samples

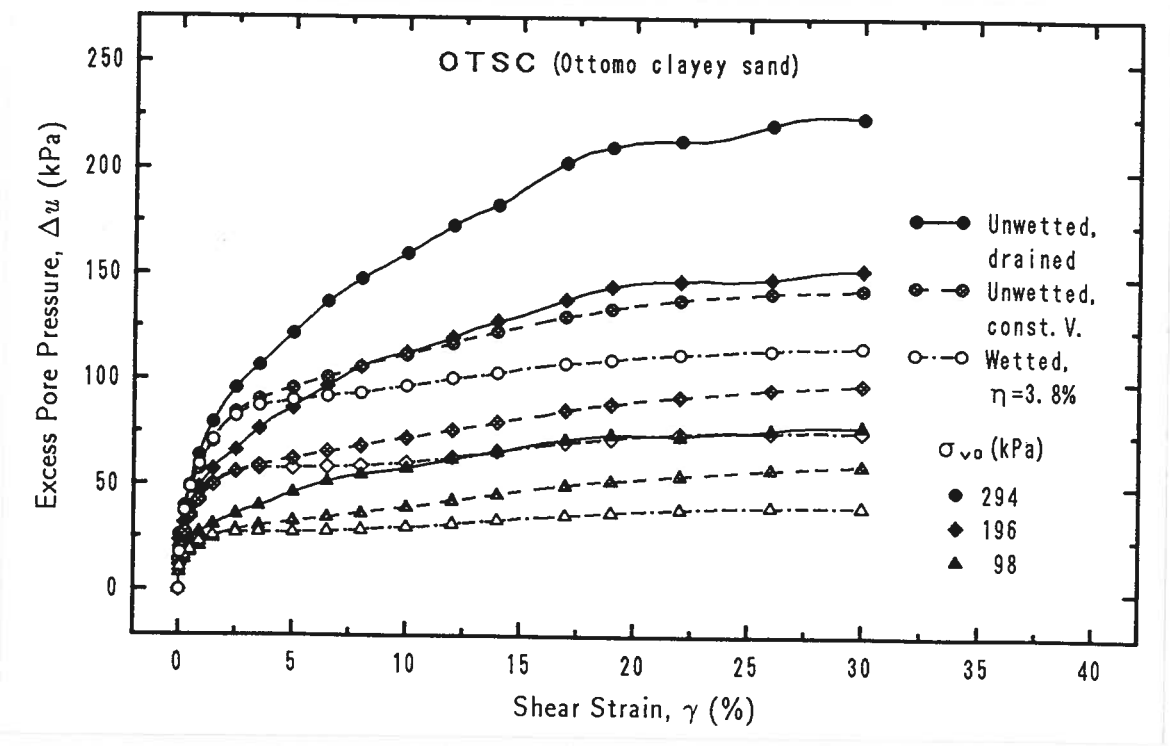

Figure 7.28: Stress-strain curves of wetted and unwetted samples

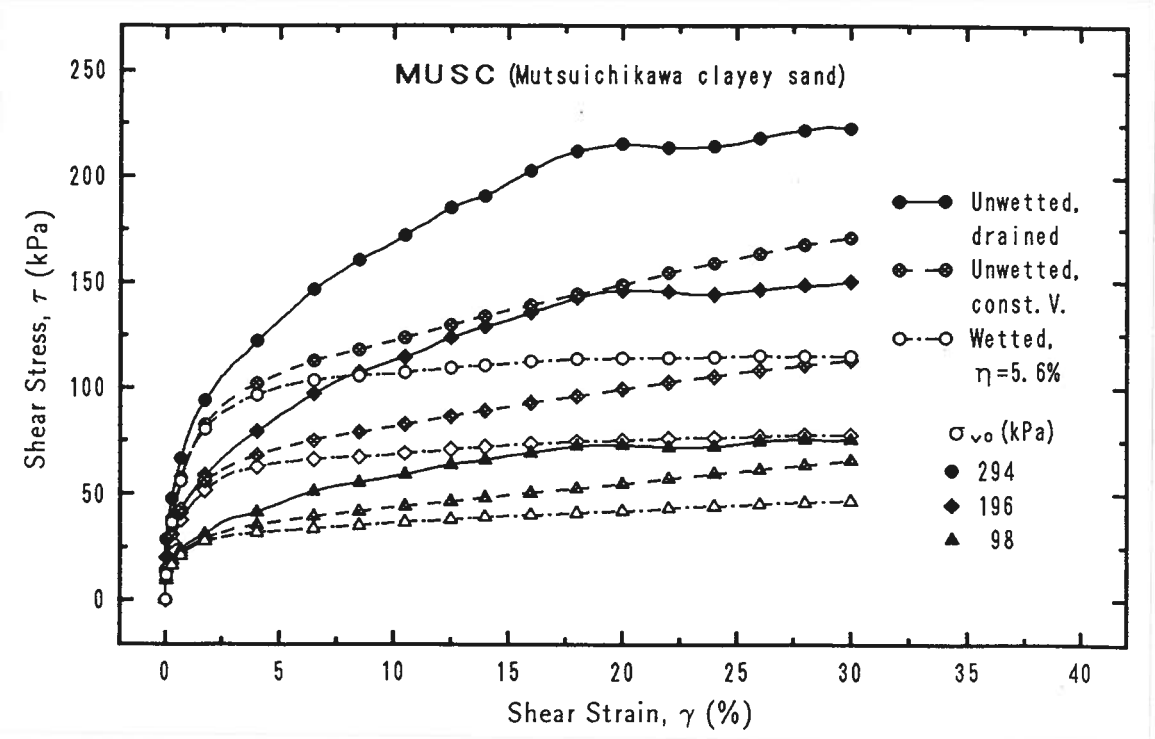

Figure 7.29: Stress-strain curves of wetted and unwetted samples

In the same manner as that used in investigating the effect of collapse history on soil behavior, the ratio of the secant shear moduli of wetted and unwetted samples will be used to describe the effect of wetting on soil properties. This secant modulus ratio is termed as *wetting factor*, C_w:

$$C_w = \frac{G_w}{G_{uw}} \tag{7.9}$$

According to the definition, it can also be expressed as the ratio of shear stress or shear stress ratio:

$$C_w = \frac{G_w}{G_{uw}} = \frac{\tau_w/\gamma}{\tau_{uw}/\gamma} = \frac{\tau_w}{\tau_{uw}} = \frac{(\tau_w/\sigma_{v0})}{(\tau_{uw}/\sigma_{v0})} \tag{7.10}$$

where the subscripts $_w$ and $_{uw}$ mean wetted or unwetted. Similar to the *collapse factor*, the *wetting factor* can be readily obtained by dividing the shear stress ratio, τ_w/σ_{v0}, of wetted samples by the stress ratio, τ_{uw}/σ_{v0}, of unwetted samples or dividing the corresponding shear stresses. The *wetting factor* is obtained based on the test data such as those plotted in Figs. 7.26 to 7.29. The outcomes of such data arrangements versus shear strain are demonstrated in Figs. 7.30 to 7.32 which indicate the trends of variation in wetting factor, which are similar to those for collapse factor, with respect to the shear strain at which the factor is evaluated. The results in the three figures are corresponding to three different overburden pressures. It can be seen from these figures that the wetting factor decreases with the increase in shear strain, in other words, the effect of wetting increases as the shear strain increases. It is also noted that the reduction in the stiffness occurs even at very small shear strain (0.01%) for the three natural materials. For material *TKSC* (Mixture of Toyoura sand and 15% kaolinite), the wetting factor is found to be larger than 1 at a shear strain range between 0.5% to 1% when the overburden pressure is less than 196 kPa. Outside this strain range, the wetting factor is less than 1, and if the overburden pressure is larger than 196 kPa, the factor is less than 1 on whole strain axis. The abnormal value of wetting factor is considered to be caused the strain softening behavior in stress-strain relationships (see Fig. 7.26) and the test error. The results from wetted and constant volume tests are demonstrated in Figs. 7.33 to 7.35 to show the changes of the stiffness of the soil caused exclusively by suction. It is obvious that the same tendency of the variation of wetting factor with shear strain, *i.e.*, wetting factor decreases with the increase in shear strain, is present in the results. It is considered that this variation of wetting factor is related with soil suction. Shear deformation tends to destroy the meniscus bonds between particles. In order to destroy the meniscus bonds, a certain amount of shear stress is needed. The larger the shear deformation, the larger is the shear stress needed to destroy the meniscus bonds. Therefore, soils behave as strong hardening in unwetted condition even when soil is relatively loose. On the other hand,

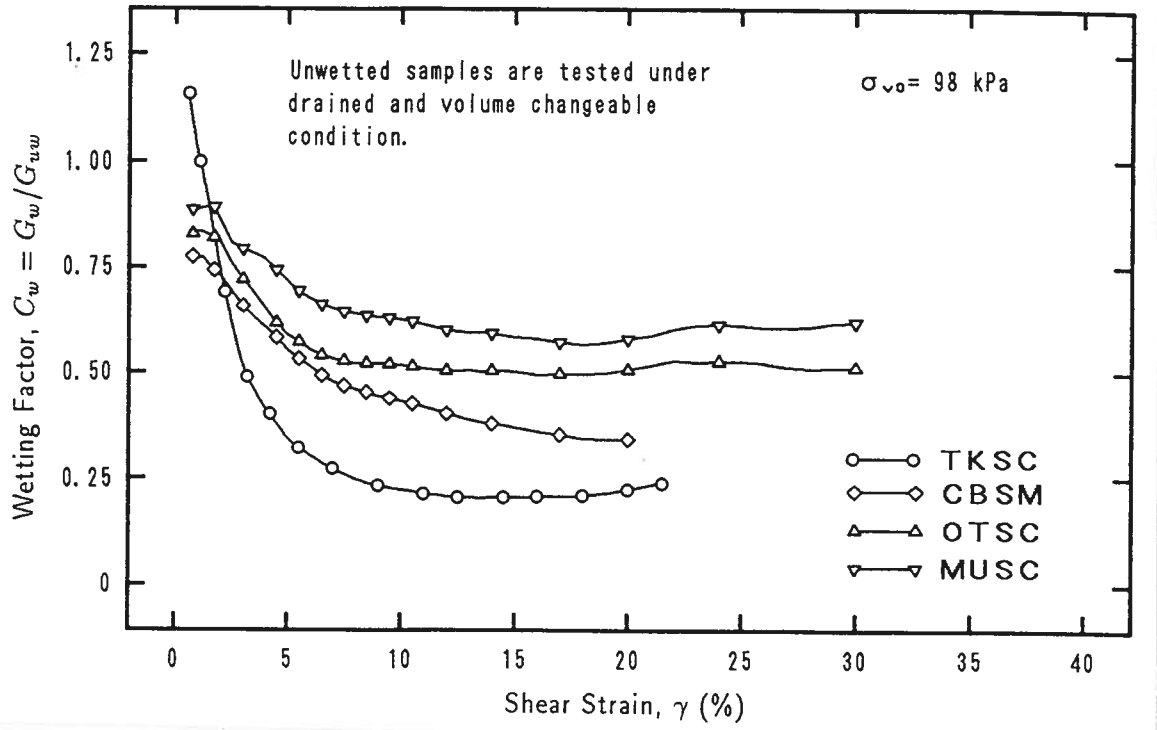

Figure 7.30: Wetting factors as a function of shear strain for an overburden pressure of 98 kPa

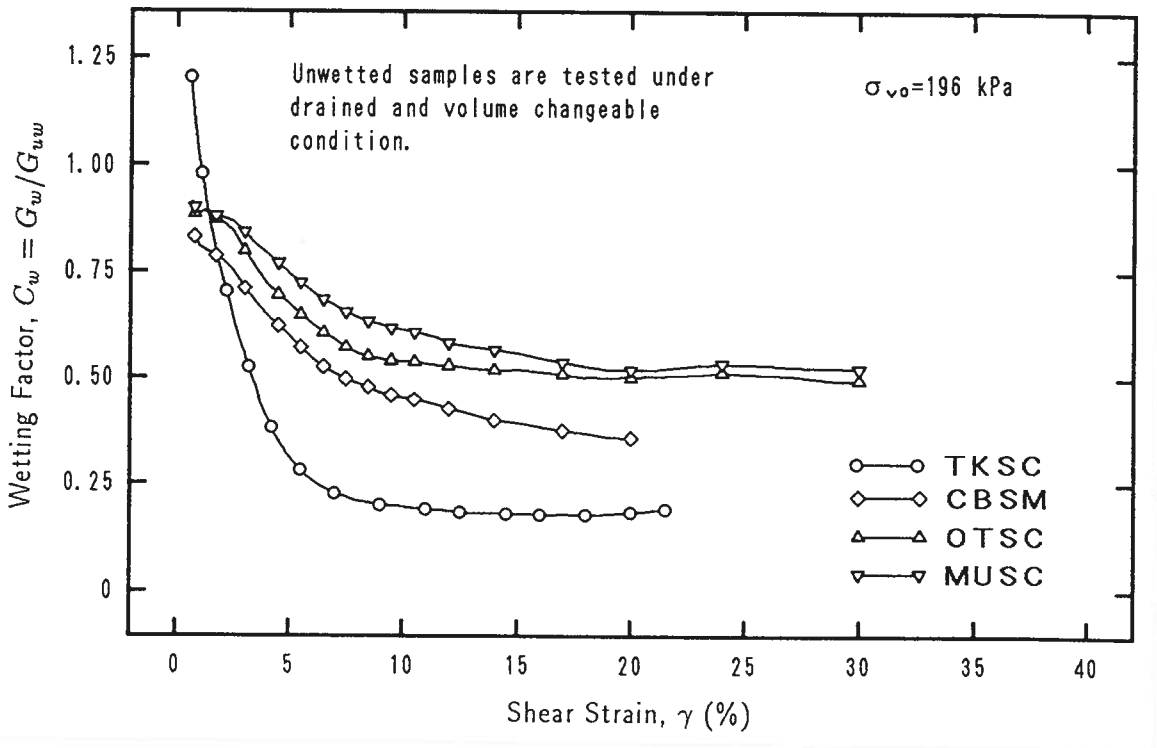

Figure 7.31: Wetting factors as a function of shear strain for an overburden pressure of 196 kPa

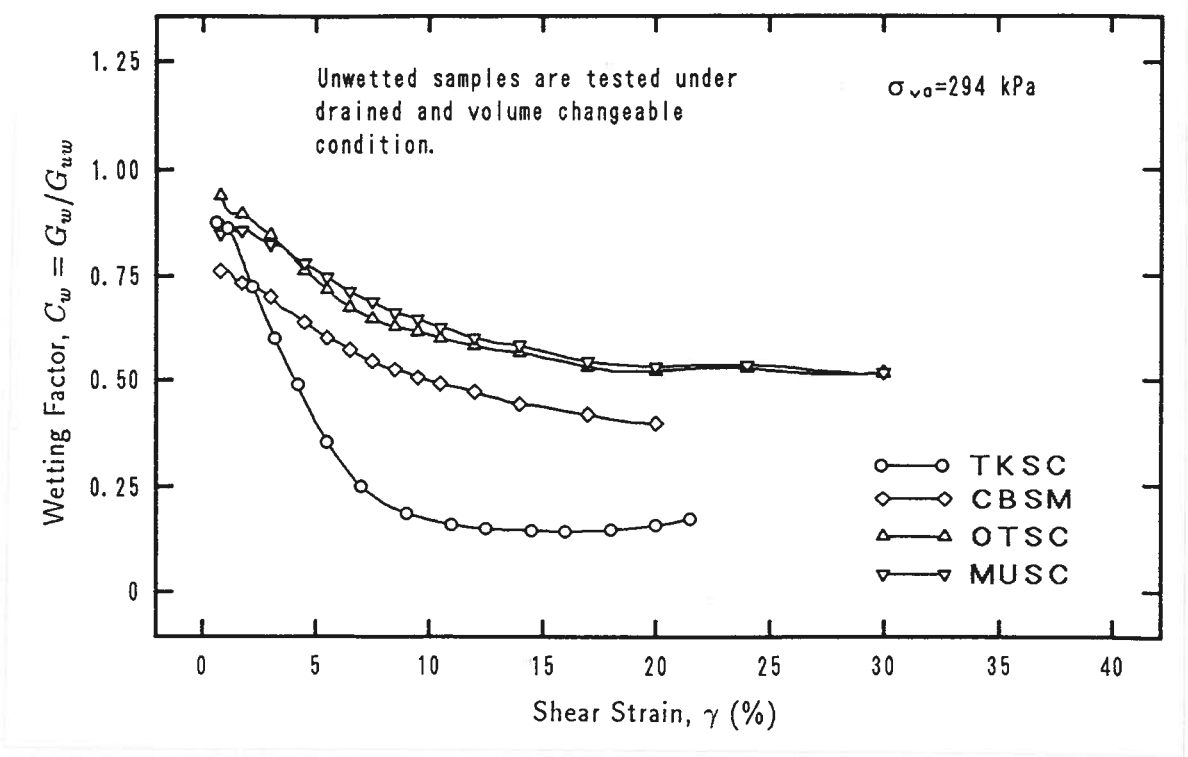

Figure 7.32: Wetting factors as a function of shear strain for an overburden pressure of 294 *kPa*

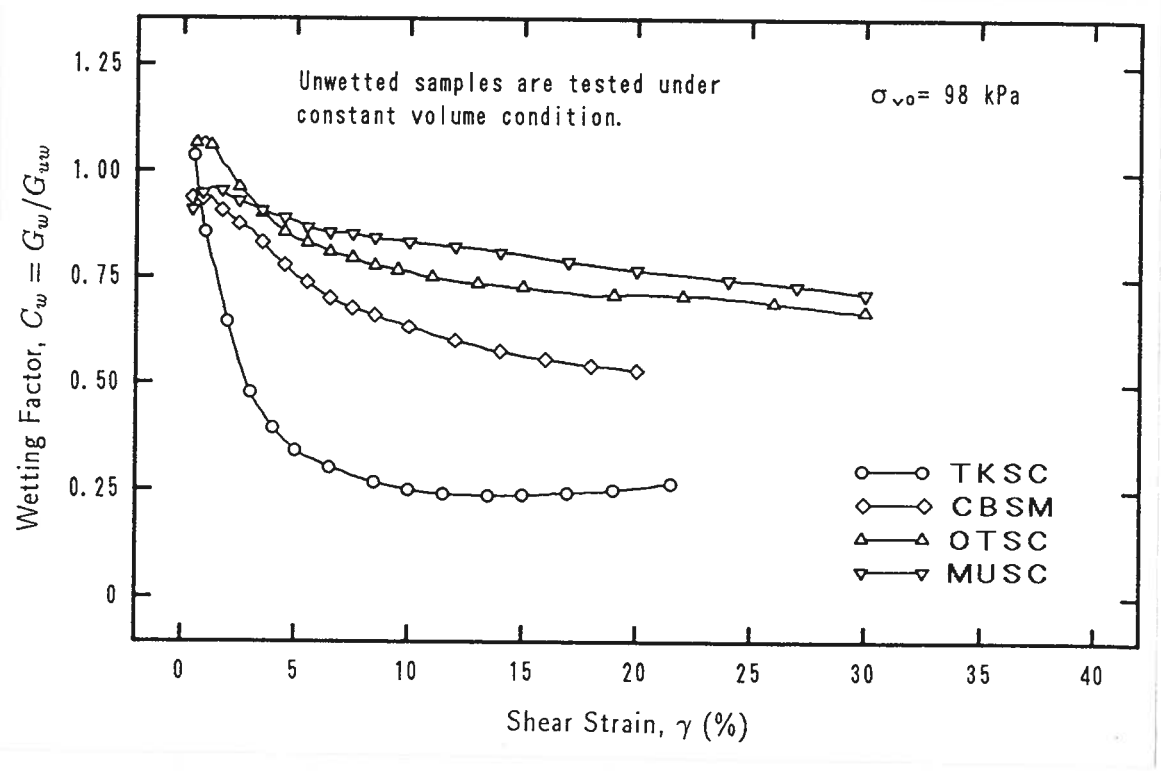

Figure 7.33: Wetting factors as a function of shear strain for an overburden pressure of 98 *kPa*

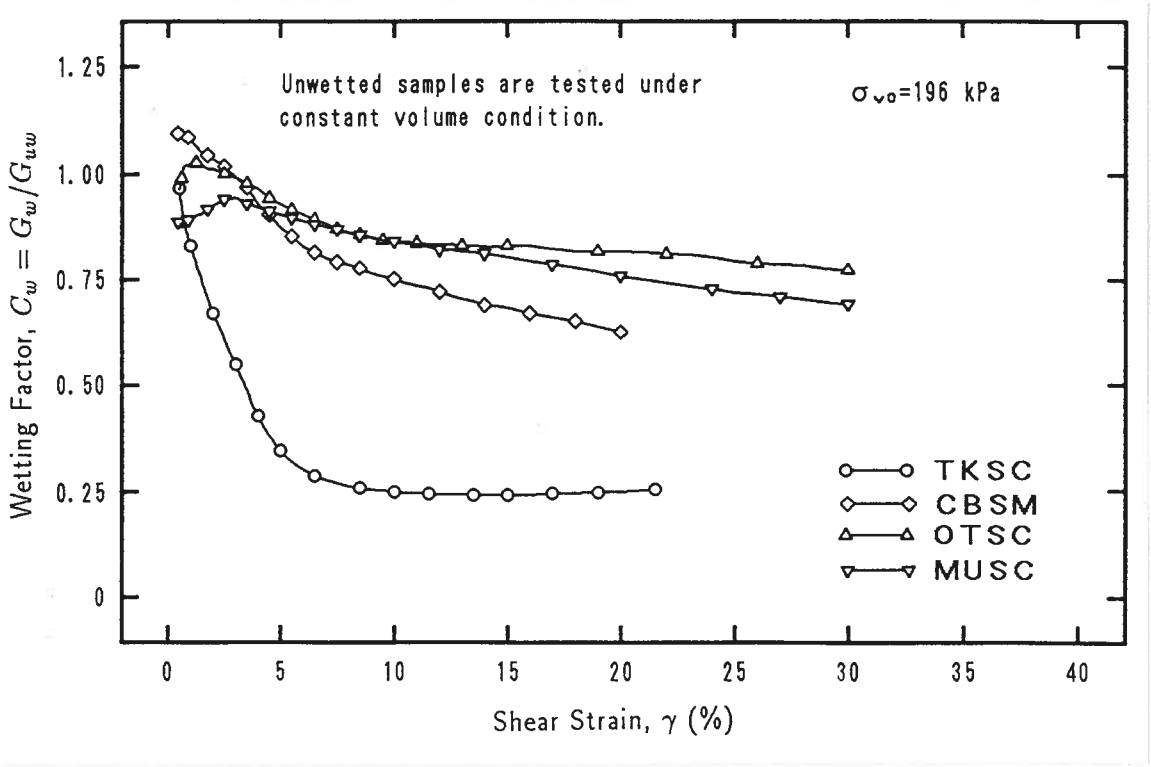

Figure 7.34: Wetting factors as a function of shear strain for an overburden pressure of 196 kPa

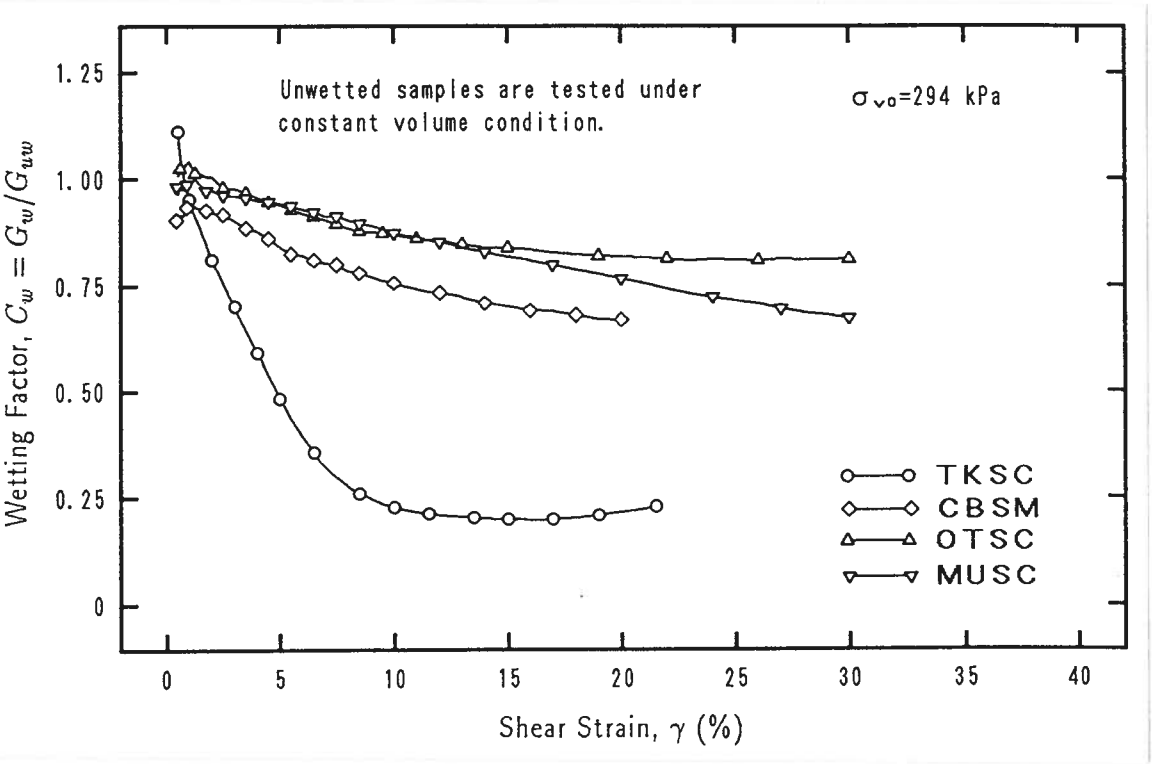

Figure 7.35: Wetting factors as a function of shear strain for an overburden pressure of 294 kPa

in wetted soils, suction disappears due to wetting. Soils behave either as ideal plastic or strain softening material. The larger the shear strain, the larger the difference between the stress-strain curves (see Figs. 7.26 to 7.29). Therefore, the *wetting factor* will increase as the shear strain increases.

The comparison of the results illustrated in Figs. 7.30 to 7.32 and in Figs. 7.33 to 7.35 shows that no significant influence of overburden pressures can be seen from the results. For materials *CBSM* (Chonan B silty sand) and *OTSC* (Ottomo clayey sand), it seems that, at the same strain level, the *wetting factor* increases with increase in confining stress (in other words, the effect of wetting on shear moduli decreases as confining stress increases), while the contrary is found in materials *TKSC* (Mixture of Toyoura sand and 15% kaolinite) and *MUSC* (Mutsuichikawa clayey sand). It is considered that the difference is due to the scatter of results.

It is also observed that the wetting factors of material *TKSC* are quite smaller than those of the other materials. The difference is caused by the difference of materials. Details will be discussed in Section 7.4.

The developed *excess pore pressures* in the constant volume tests as a function of shear strain are presented in Figs. 7.36 to 7.39. For drained unwetted tests, no excess pore pressure is developed. It can be seen from these figures that the excess pore pressure developed in unwetted samples (constant volume test) are relatively low. However, as soon as the samples are wetted, the excess pore pressure developed during shear becomes much higher. This is the reason why the stiffness and strength of soils decrease due to wetting. For unwetted samples, because of the low saturation ratio and the existence of suction action, the effective stresses before shearing are larger than the total stresses and will never become zero during shearing although the excess pore pressure increases. The appearance of suction action increases the apparent strength of soils. On the other hand, for wetted specimens, although they are denser because of the collapse deformation caused by soaking, suction also disappears due to wetting. The higher saturation ratio after soaking accounts for the excess pore pressure to build up more easily, thereby the smaller the effective stress and the larger the strength loss.

Although the measured axial stress during shearing is not equal to the effective stress, it can still be used to approximately show the stress path of the soil. The stress paths in terms of the shear stress versus measured axial stress of samples with or without wetting are given in Figs. 7.40 to 7.43. For drained tests, the vertical stress, σ_v, is constant in stress paths and is equal to initial overburden pressure σ_{v0}. For constant volume tests, the focus of stress path of unwetted samples is going up while those of wetted samples

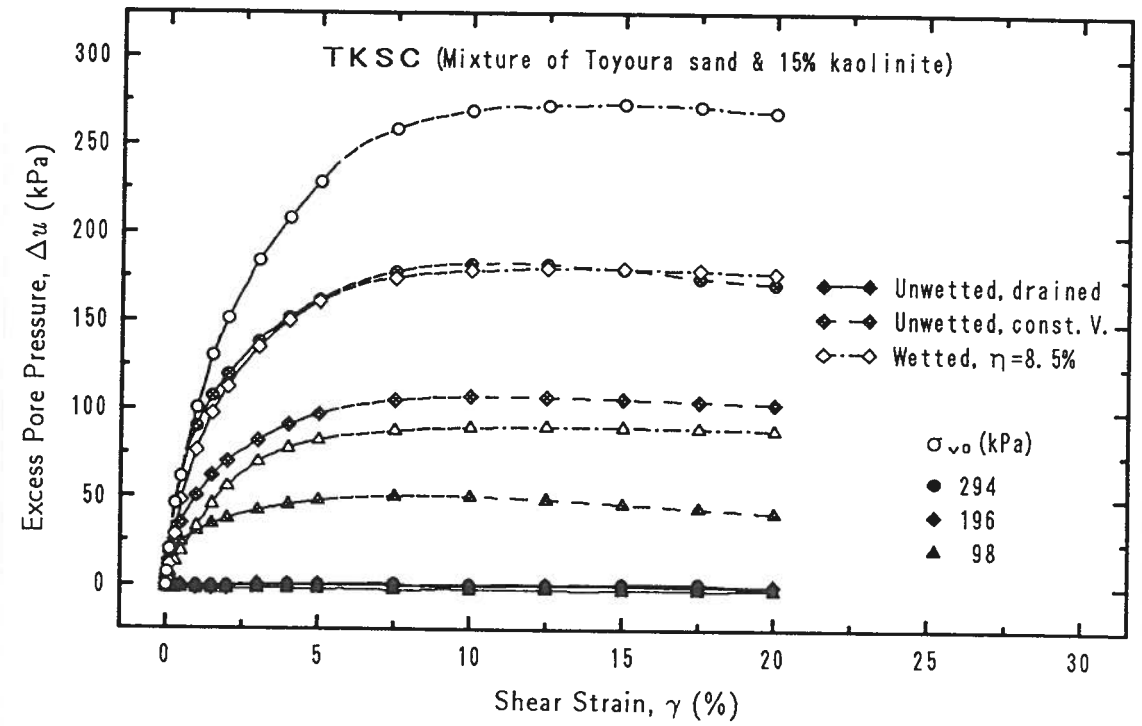

Figure 7.36: Excess pore pressure developed in wetted and unwetted samples

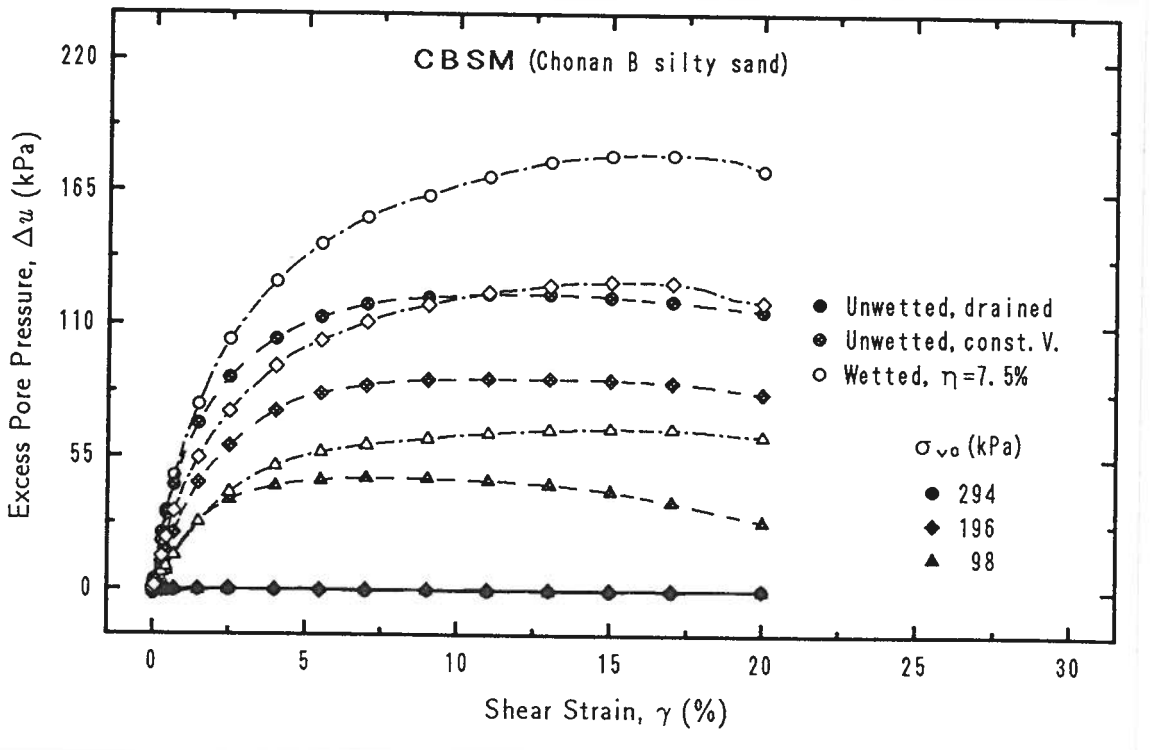

Figure 7.37: Excess pore pressure developed in wetted and unwetted samples

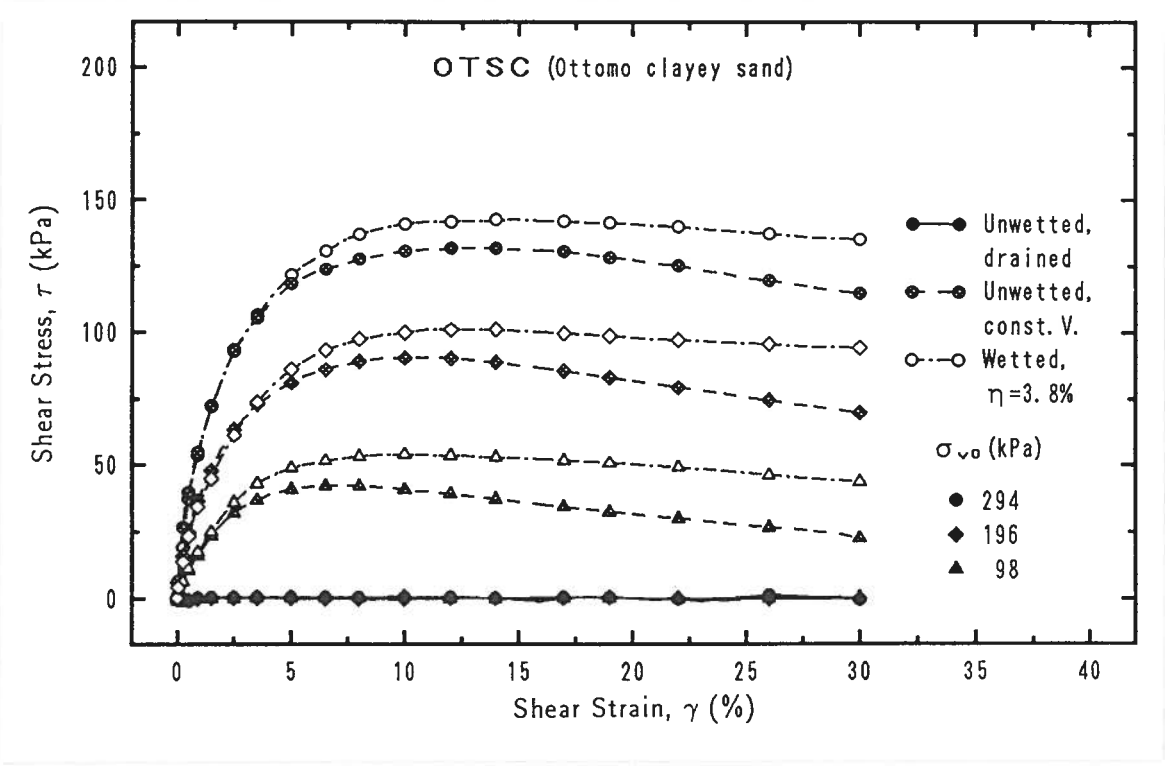

Figure 7.38: Excess pore pressure developed in wetted and unwetted samples

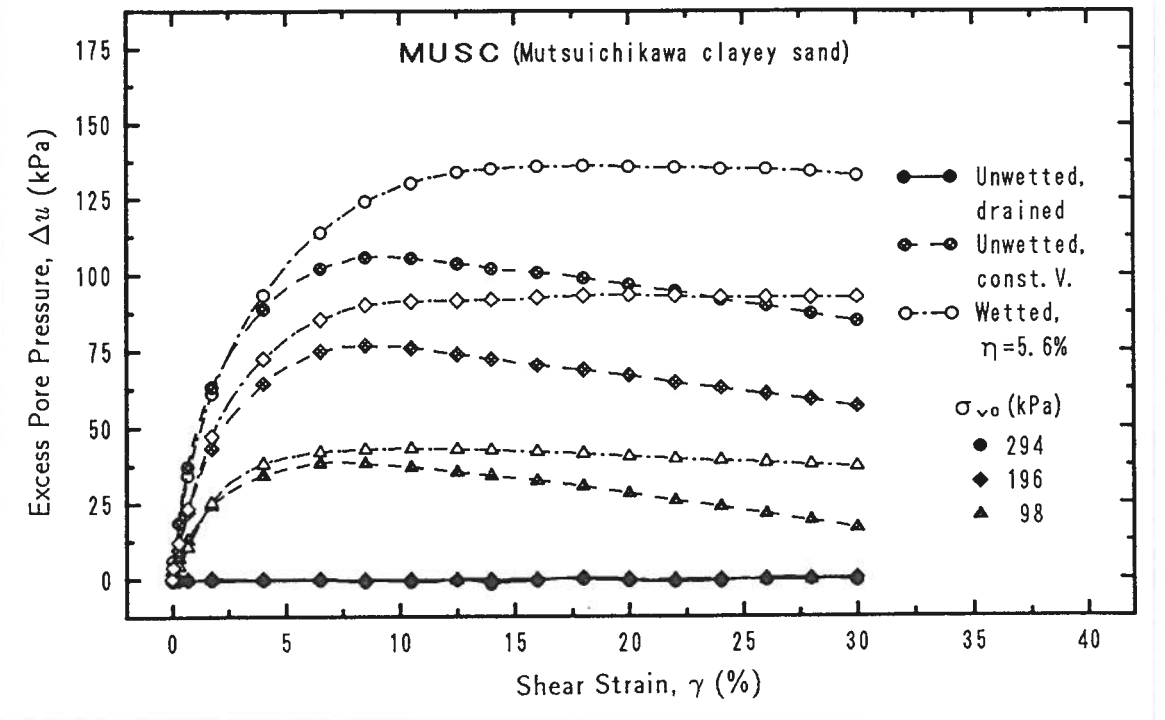

Figure 7.39: Excess pore pressure developed in wetted and unwetted samples

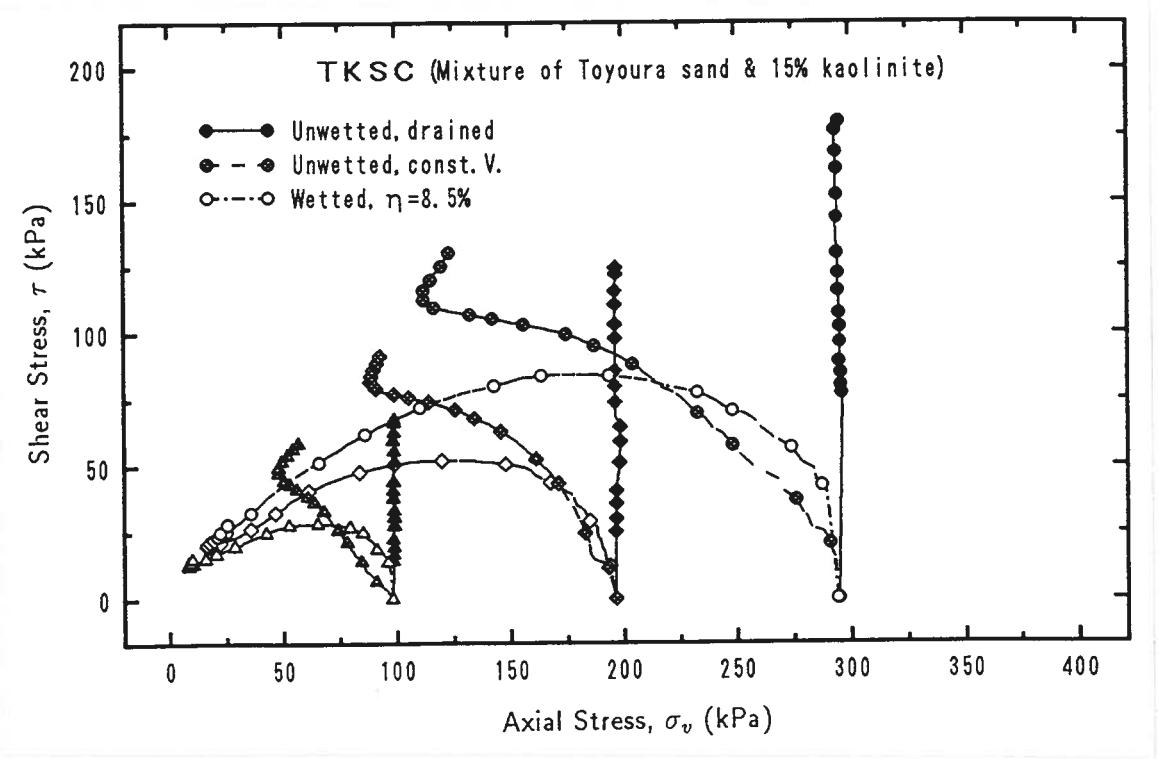

Figure 7.40: Relationships between shear stress and measured axial stress of wetted and unwetted samples

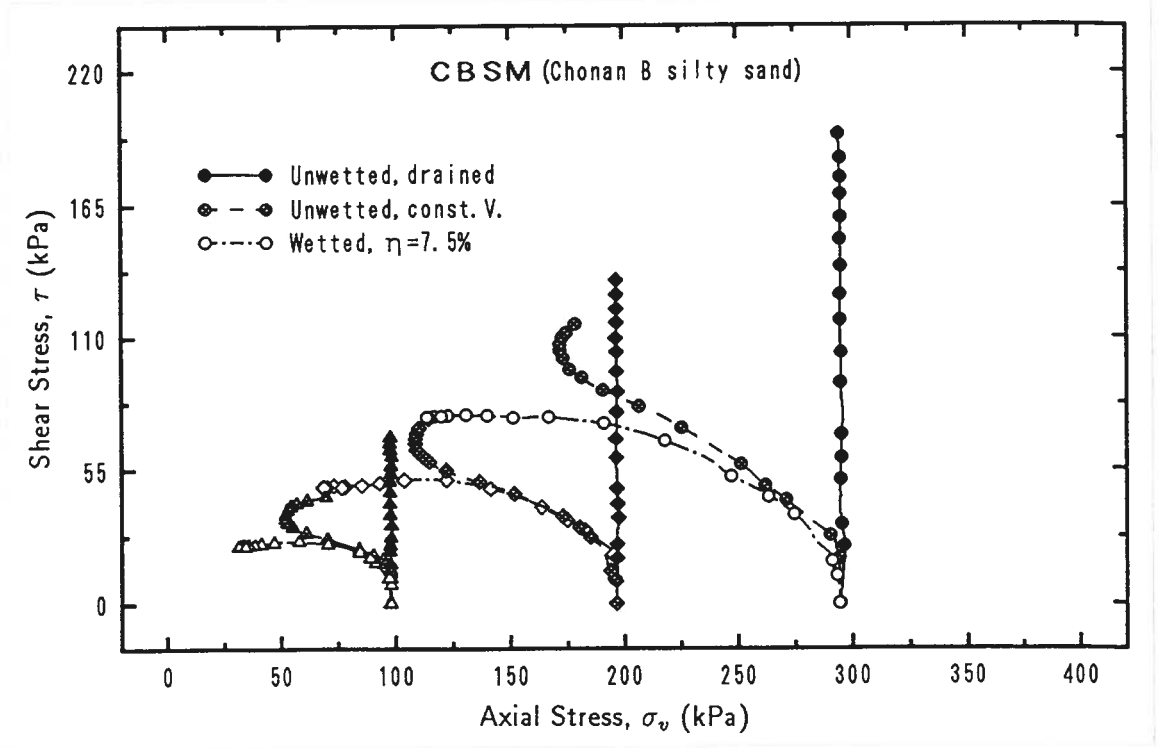

Figure 7.41: Relationships between shear stress and measured axial stress of wetted and unwetted samples

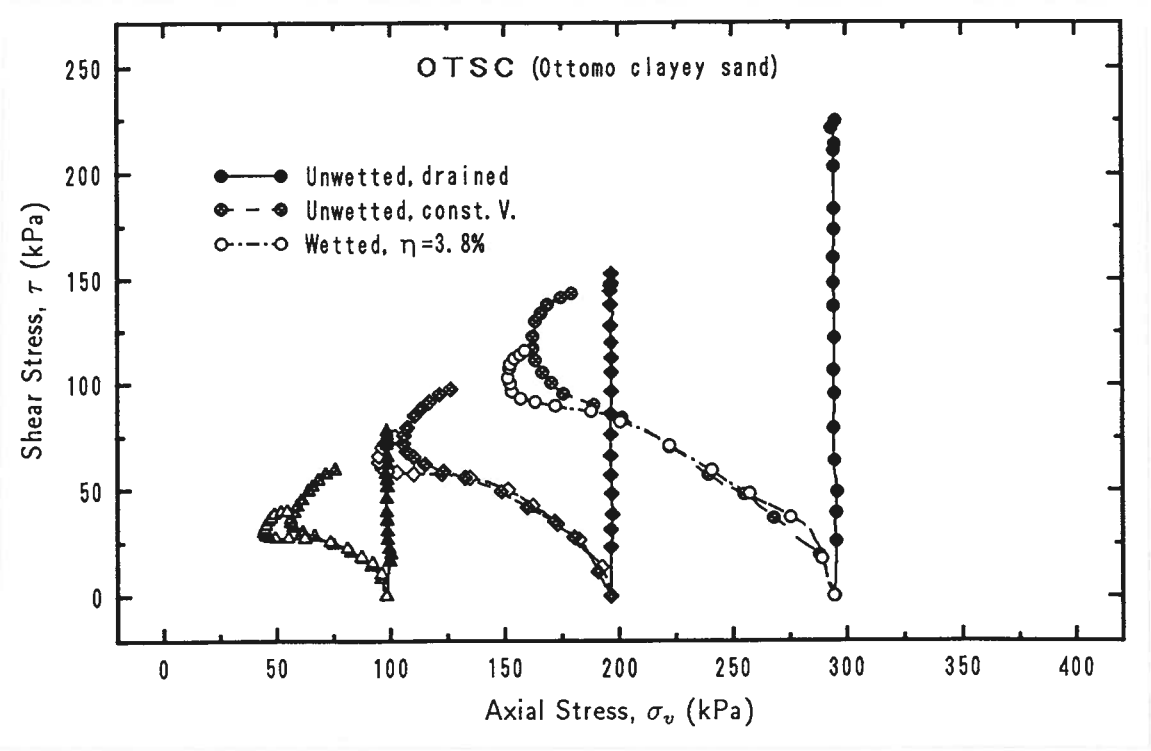

Figure 7.42: Relationships between shear stress and measured axial stress of wetted and unwetted samples

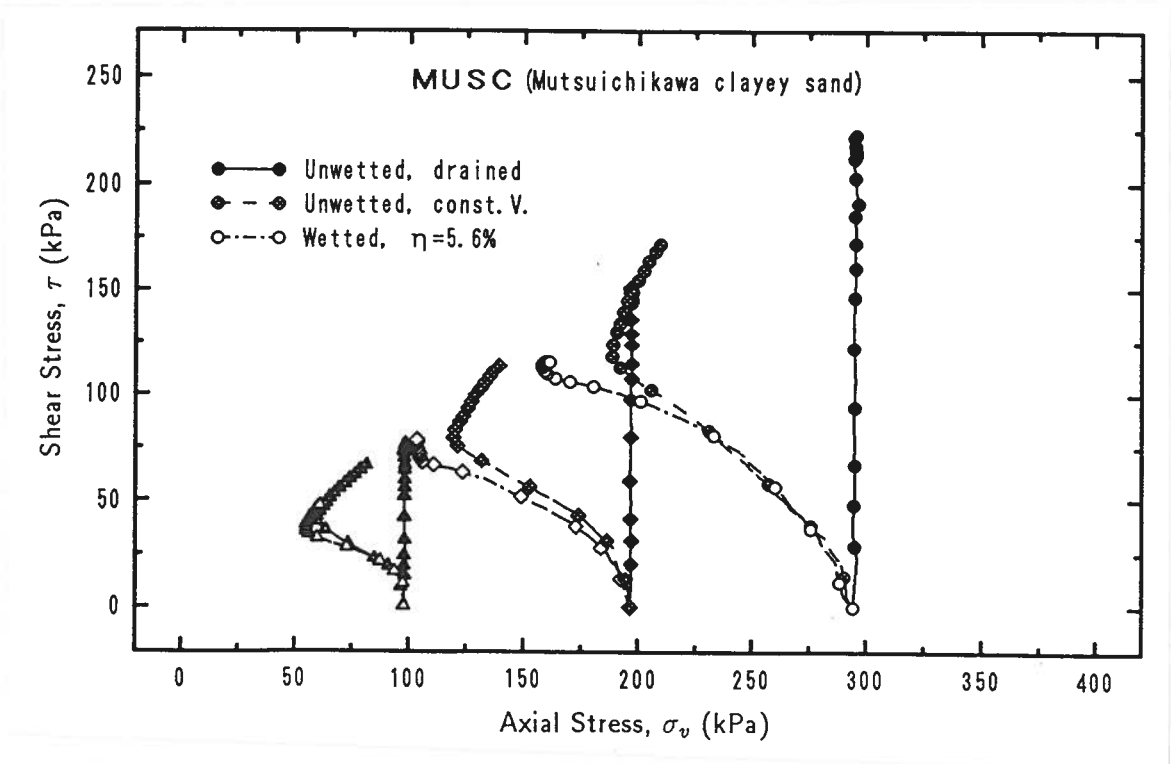

Figure 7.43: Relationships between shear stress and measured axial stress of wetted and unwetted samples

is going down or in some cases, going up but less than those of unwetted ones. In fact, the measured axial stress, σ_v, is the algebraic difference of the effective stress and suction action. For wetted samples, suction action is almost equal to zero because of the relatively high saturation ratios. Therefore, σ_v is approximately equal to effective stress, σ'_v. On the other hand, for unwetted samples, suction is very high especially for low degree of saturation, and σ_v is smaller than σ'_v. Therefore, the difference between the stress paths must be larger in terms of effective stresses than in terms of σ_v.

7.4 INFLUENCE OF MATERIAL KINDS

The results presented in the previous sections show that there exist differences in strength and deformation behaviors of different types of materials. In order to investigate the influence of material types, the reduction in strength parameters, d and β, are plotted as a function of clay content in Fig. 7.44. The data in this figure are from Tables 7.2, 7.3

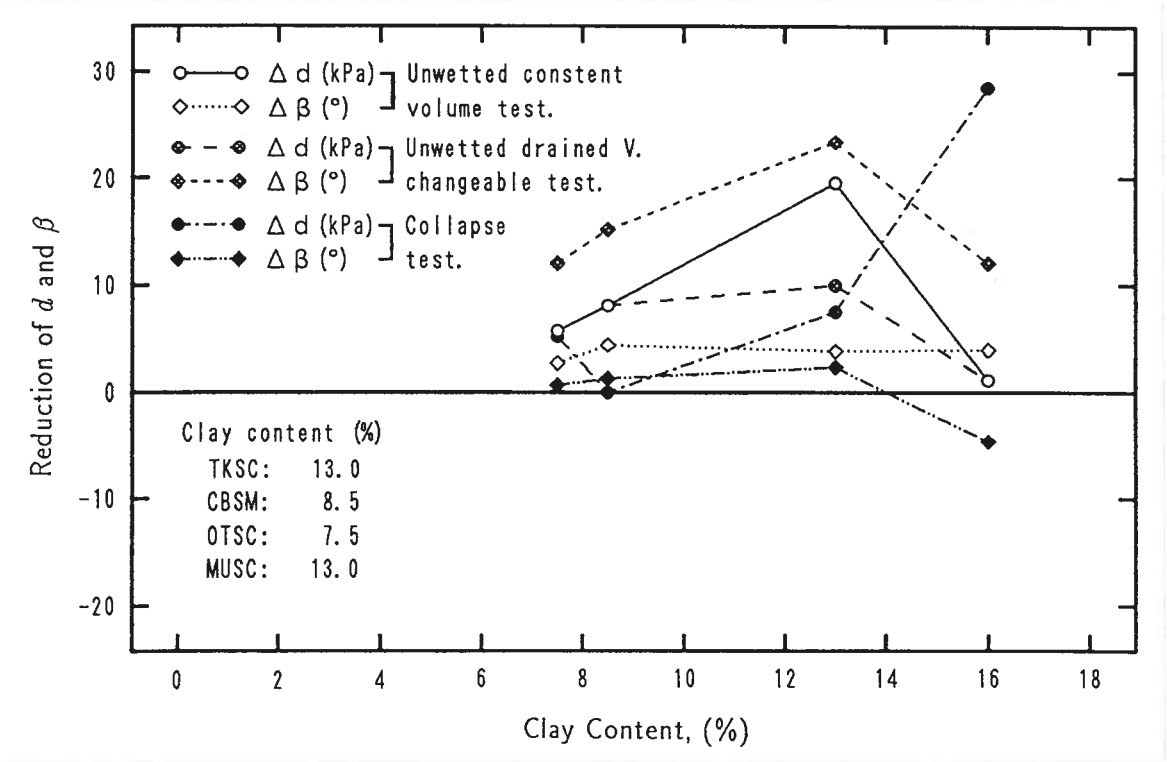

Figure 7.44: Reduction of strength parameters d and β as function of clay content

and 7.1. It is noted that except for the change of cohesive intercept, d, of collapse tests, there is a critical value of clay content at which the reduction of strength parameters is maximum. The existence of exception means that the reduction of strength parameters

of soils depends not only on the clay content of the soils but also on other properties, *e.g.*, the grain size and its distribution, the mineralogy of clay components, *etc.* Clay content is not enough to describe the properties of the reduction of strength parameters caused by wetting or collapse.

The relationships between collapse factor, wetting factor and clay content are plotted in Figs. 7.45, 7.46 and 7.47, respectively. The results of the tests involving three

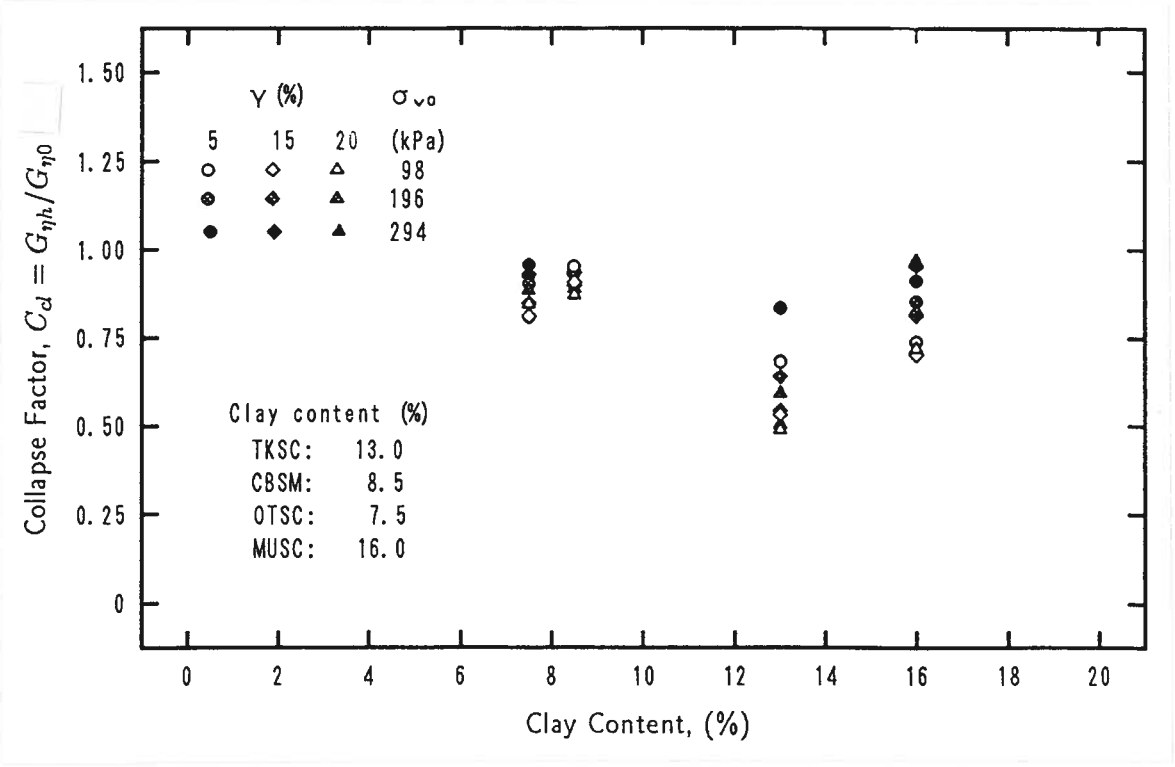

Figure 7.45: Relationships between collapse factor and clay content

different shear strains, namely 5, 10, and 15%, and three overburden pressures are presented in the figures. Although the factors decrease as the shear strain increases, the changes are insignificant when shear strain is larger than 5%. It is observed that a consistent tendency is observed with regards to the changes of the two factors with clay content, that is, there is a critical value of clay content which gives the minimum values of the factors. This is consistent with the results presented in Chapter 5. In the said chapter, the test results verified that there is a critical value of clay content at which the amount of collapse of soils is maximum. This means that at this particular clay content, the soils are more collapsible. It is possible that soil of this clay content possesses a more metastable structure which gives relatively high apparent strength at low degree of saturation. As soon as the saturation ratio increases or as the soil is wetted, the strength

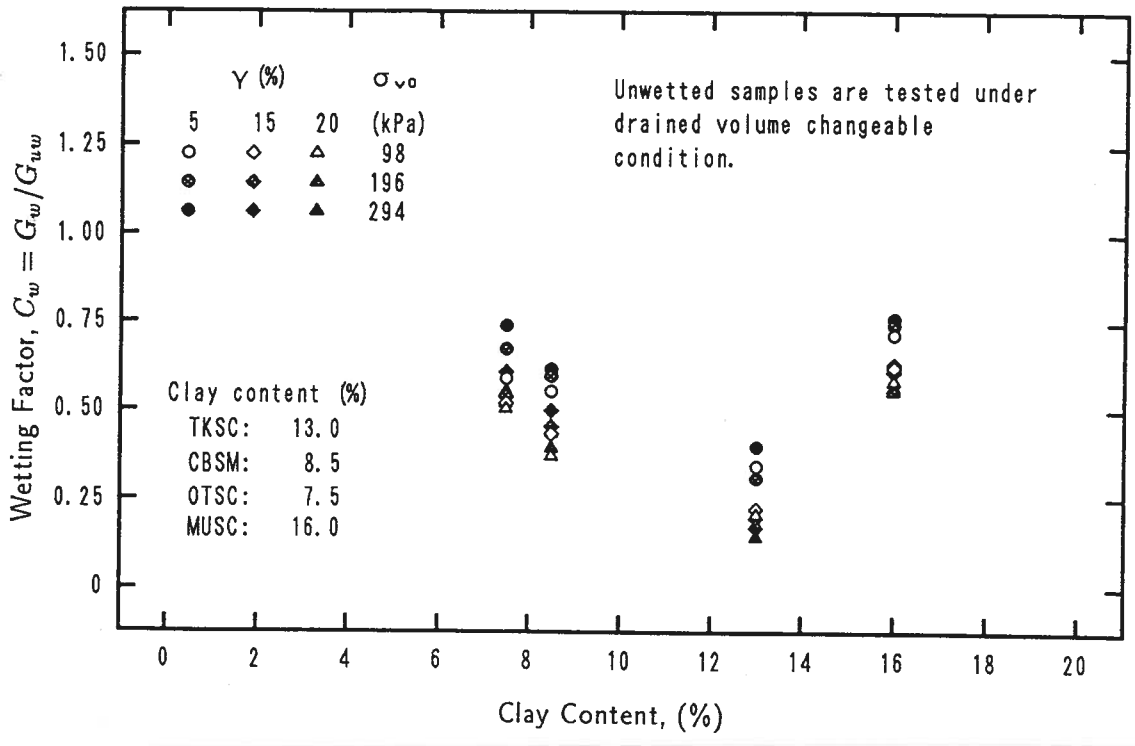

Figure 7.46: Relationships between wetting factor and clay content for drained test

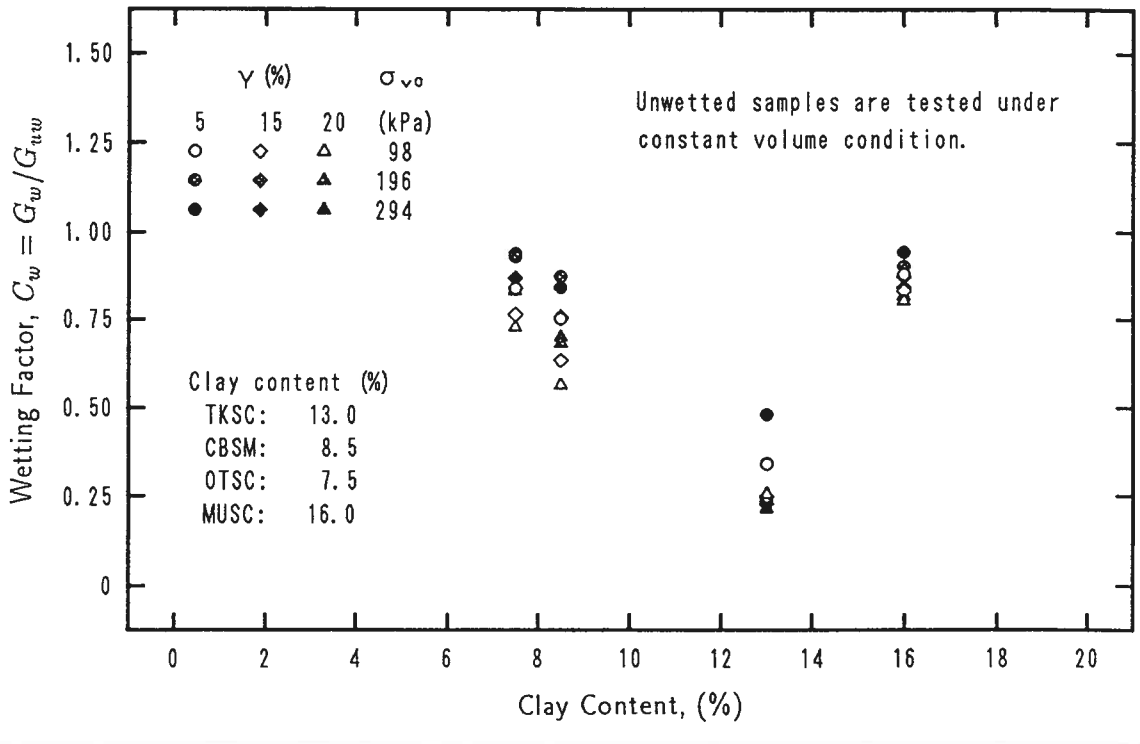

Figure 7.47: Relationships between wetting factor and clay content for constant volume test

decreases significantly. As the clay content deviates from this critical value, the soil has either more cohesionless or more cohesive behavior. In both the cases, the collapsibility of soils will decrease and the reduction in strength caused by collapse and wetting will be less.

7.5 SUMMARY

The tests in this chapter are concerned with the behavior of collapsible soils under monotonic loading condition. Two series of tests are performed: wetted and unwetted, and wetted and of high or low magnitude of collapse. Tests are conducted on simple shear test apparatus under each possibly existed test conditions. For wetted sample, specimen is sheared under plane strain and constant volume condition with the consideration that the degree of saturation of soil after being infiltrated by water is usually very high and even fully saturated, and failures usually occur relatively fast. For unwetted samples, the tests are performed under drained and volume changeable conditions because of the drainage conditions of partly saturated soil deposits in reality.

From the test results, the following conclusions can be made:

- Under identical state of dry density and saturation ratio prior to the application of shearing load, shear resistance decreases as the magnitude of hydraulic collapse increases.

- The loading condition changes as the soil is soaked and is collapsed. Before collapse, soil is in a drained and volume changeable condition. On the other hand, after collapse, soil is in an undrained and almost full saturated condition. With the same initial state of water content and dry density, the wetted samples possess much less shearing resistance than the unwetted ones, although the dry density increases due to wetting-induced collapse deformation. The strength loss is caused by the decrease in external load induced effective stress and the disappearance in suction. The disappearance in suction due to wetting not only reduces the cohesive strength but also changes the internal friction angle of the soil.

- The decrease in shear resistance is shown as the reduction of either the cohesive intercept or the angle of shearing resistance, or both.

- The shear strength reduction caused by unit dry density decreases as the saturation ratio increases.

- The effect of collapse history on the deformation behavior of soil can be expressed in terms of *collapse factor*, C_d, which is defined as the secant shear modulus ratio of the sample which has undergone high collapse to that which has experienced little collapse. The fact that this factor is less than unity means that samples which have experienced high hydraulic collapse have smaller ability to resist deformation. This factor also decreases as the shear strain increases.

- The effect of wetting on deformation characteristics of soil can be expressed in terms of *wetting factor*, C_w, which is defined as the secant shear modulus ratio of wetted sample to unwetted sample. The *wetting factor* is usually smaller than 1 which indicates that the secant shear modulus of wetted sample is smaller than that of unwetted sample. This factor decreases with shear strain.

- Different materials behave differently under monotonic loading condition. There exists a critical clay content at which all the aforementioned factors mentioned attain a minimum value.

Chapter 8

THE MECHANISM OF HYDRAULIC COLLAPSE – THE GENERAL PRINCIPLE OF EFFECTIVE STRESS

8.1 INTRODUCTION

The validity of the Terzaghi's *principle of effective stress* for saturated soils has been adequately verified by the work of Rendulic (1936), Bishop and Eldin (1950), Henkel (1959, 1960), and Skepton (1960). It becomes the basis of modern soil mechanics. For partly saturated soils, several expressions of effective stress have also been proposed by various individuals (Jennings, 1957; Bishop, 1959; Aitchison, 1960). However, the applicability of the effective stress principle in partly saturated soils, especially in explaining the *collapse* phenomenon, has been questioned by many researchers (Jennings and Burland, 1962; Jennings, 1963; Burland, 1965; Newland, 1965; Brackley, 1971; and Sridharan, *et al.*, 1973). Researchers usually assume that Terzaghi's principle of effective stress is valid for partly saturated soils if the pore air pressure is considered in the expression of effective stress. However, a lot of test results obtained by many individuals indicate that this assumption is incorrect. In this chapter, a modified version of the *principle of effective stress*, referred to as the general principle of effective stress, is proposed based on the test observation. The phenomenon of hydraulic collapse, as well as hydraulic swelling, is explained based on the general effective stress principle.

8.2 THE CLASSICAL PRINCIPLE EFFECTIVE STRESS

(I) Saturated Soils

The classical *principle of effective stress*, one of the most outstanding contributions to modern soil mechanics, was summarized by Karl V. Terzaghi (1923, 1932). He stated the principle in the following terms (1936):

"The stresses in any of a section through a mass of soil can be computed from the *total principal stresses* σ_1, σ_2 and σ_3 which act in this point. If the voids of the earth are filled with water under a stress u, the total principal stresses consist of two parts. One part, u, acts in the water *and* in the solid in every direction with equal intensity. It is called the *neutral stress* (or pore water pressure). The balance, $\sigma_1' = \sigma_1 - u$, $\sigma_2' = \sigma_2 - u$, and $\sigma_3' = \sigma_3 - u$, represents an excess over the neutral stress u and it has its seat exclusively in the solid phase of the soil.

"This fraction of the total principal stresses will be called the *effective principal stresses.* ...

"A change in neutral stress u produces practically no volume change and has practically no influence on the stress conditions for failure. Porous material (such as sand, clay and concrete) was found to react on a change of u *as if* it were incompressible and *as if* its internal friction were equal to zero. All the measurable effects of a change of the stress, such as compression, distortion and a change of the shearing resistance are *exclusively* due to change in effective stresses, σ_1', σ_2' and σ_3'. Hence every investigation of the stability of a saturated body of earth requires the knowledge of both the total and the neutral stresses."

The classical *principle of effective stress* described above can be summarized in the form of four propositions:

1. Soil is a two-phase medium: solid and liquid (water). The voids of the solids are filled with water.

2. All measurable effects of a change in the stress, such as compression, distortion, and change in the shearing resistance of a soil, are exclusively due to changes in the effective stress.

3. The effective stress σ' is defined as the excess of the total applied stress σ over the pore pressure u, *i.e.*:

$$\sigma' = \sigma - u \tag{8.1}$$

4. All the parameters concerning the strength and deformation properties of soil, such as cohesive strength (c'), angle of internal friction (ϕ'), volumetric compressibility (m_v), Young's modulus (E), Poisson's ratio (ν), rebounding modulus (E_r), initial shear modulus (G_0), *etc.*, are variables which are independent of the saturation

ratio (because saturation ratio is constant and equal to 1). For a given soil (having the same initial state of void ratio, stress history, and fabric structure), the aforementioned parameters are constant.

Almost in all the papers (Jennings and Burland, 1962; Bishop, 1964) and text books (ECIWC, 1982; Huang, 1983; Craig, 1987) describing the *principle of effective stress*, only the second and third propositions are mentioned. Although people mentioned that they are dealing with saturated soils when they talk about Terzaghi's principle of effective stress, the first proposition has never been emphasized. As the prerequisite of Terzaghi's principle of effective stress, it is necessary for it to be specially emphasized.

The fourth proposition is a tacit assumption of the validity of the principle of effective stress. Terzaghi (1936) pointed out that strength parameters might be affected by water content, therefore, he emphasized that:

> "...All the specimens subjected to the test must have the same initial water content and in *all* the tests of the same series the normal pressure σ' must either be increased from zero to its ultimate value or *all* the tests must have been preceded by consolidating the samples under the same pressure $\sigma_0 > \sigma$. ..."

However, because soil is fully saturated, the difference in the initial water content is caused by different void ratios. Therefore, the so-called effect of initial water content is the results of the difference in initial void ratio. This can be well verified by the example which Terzaghi quoted to illustrate the effect of initial water content on strength parameters. He wrote that for a clay sample with an original water content equal to the liquid limit, the cohesive strength is zero. If the normal pressure σ is reduced subsequently to zero, the cohesive strength is considerably greater and the water content is considerably smaller than that at the beginning of the test. In fact, here he compared the strength of a normally consolidated sample with that of an over-consolidated sample. It is evident that the void ratio of the sample has changed in the second stage due to the virgin loading and unloading, as well as the stress history.

A very good example of the fourth proposition is the analogy of consolidation using the concept of effective stress principle. The mechanics of the one-dimensional consolidation process can be represented by means of a simple analogy as in Fig. 8.1. Fig. 8.1(a) shows a spring inside a cylinder filled with water and a piston, fitted with a valve, on top of the spring. It is assumed that there is no leakage between the piston and the cylinder and there is no friction. The spring represents the compressible soil skeleton, the water in the cylinder the pore water and the bore diameter of the valve the permeability of the

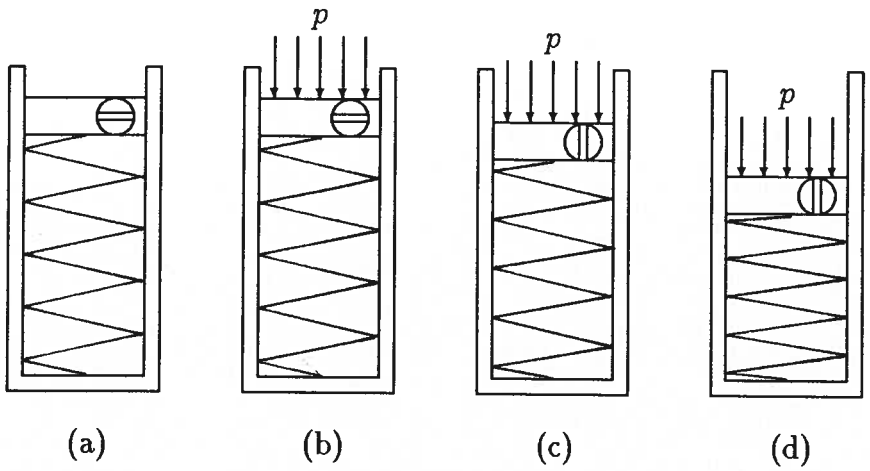

Figure 8.1: Consolidation analogy

soil. The cylinder itself simulates the condition of no lateral strain in the soil.

Suppose a load p is now applied on the piston with the valve closed, as in Fig. 8.1(b). Assuming water to be incompressible, the piston will not move as long as the valve is closed, with the result that no load can be transmitted to the spring; the load will be carried by the water, and the increase in pressure in the water is equal to the load p. This situation with the valve closed corresponds to the undrained condition in the soil.

If the valve is now opened, water will be forced out through the valve at a rate governed by the bore diameter. This will allow the piston to move and the spring to be compressed as the load is gradually transferred to it. This situation is shown in Fig. 8.1(c). At any time, the increase in the load on the spring will correspond to the reduction in pressure in the water. Eventually, as shown in Fig. 8.1(d), all the load will be carried by the spring and the piston will come to rest, and this corresponds to drained condition in the soil. At any time, the load carried by the spring represents the effective normal stress in the soil, the pressure of the water in the cylinder the pore water pressure and the load on the piston the total normal stress. The movement of the piston represents the change in the volume of the soil and is governed by the compressibility of the spring (the equivalent of compressibility of the soil skeleton).

If the load p on the piston is then removed, the spring rebounds, the piston moves upward and water gets back into the cylinder. The magnitude of the movement of the piston depends on the ability of the spring to rebound.

The compressibility and the rebounding-ability of the spring may be changed with applied load p. If p is constant, the compressibility and rebounding-ability are constant.

It is obvious, in the above analogy, that the parameters of deformation are assumed

to be independent of the liquid phase.

(II) Unsaturated Soils

The fundamental role played by Terzaghi's *principle of effective stress* in the prediction of the behavior of fully saturated soils has led researchers to try to extend the theory to cover partly saturated soils. Aitchison and Donald (1956), Jennings (1957), Croney, *et al.*, 1958, Bishop (1959), and Aitchison (1960) all proposed modified forms of the effective stress equation to account for the two-phase nature of the pore fluid in a partly saturated soil. The *Conference on Pore Pressure and Suction in Soils* (1960) brought together all these workers' views. It was generally agreed that the equation proposed by Bishop (1959) is the most general definition of the effective stress. This equation can be written as:

$$\sigma' = \sigma - u_a + \chi(u_a - u_w) \tag{8.2}$$

where

u_a denotes pressure in pore air;

u_w denotes pressure in pore water; and

χ is a coefficient whose value, which must be between 0 and 1, depends primarily on the degree of saturation and the soil type.

The effective stress equation for cohesive soils has been studied by several individuals (Lambe, 1960a, 1960b; Sridharan, 1968; Sridharan *et al.*, 1973). In these studies, researchers considered the intergranular stress between the contacts or near contact points of individual soil particles, with the repulsive and attractive forces especially taken into account. A modified Lambe's equation (1960a) was proposed by Sridharan (1968):

$$\overline{c} = \sigma - \overline{u}_w - \overline{u}_a - R + A \tag{8.3}$$

where

$\overline{c}$ is the effective contact stress;

$\overline{u}_w$ is the effective pore water pressure;

$\overline{u}_a$ is the effective air pressure;

R is equal to the total interparticle electrical repulsion divided by the total interparticle area; and

A is equal to the total interparticle attraction divided by the total interparticle area.

The first three terms in Eq. 8.3 consist the conventional effective stress as in Eq. 8.2.

As pointed out by Burland (1961) and Jennings and Burland (1962), in developing the expression for the effective stress in partly saturated soils, a tacit assumption is made that the effective stress principle is valid over the whole range of saturation. Researchers

assumed that the second and fourth propositions in Terzaghi's *effective stress principle* are valid in partly saturated soils (this has been obviously indicated by Bishop and Donald (1961), Bishop and Blight (1963) and Blight (1965) in the method to calculate the coefficient χ), and if, by some modification, the expression of the effective stress includes the effect of pore air pressure, the principle is valid for whole unsaturated soil.

The validity of the so-defined principle of effective stress (in partly saturated soil) was questioned as soon as it was proposed (Burland, 1961; Jennings and Burland, 1962; Burland, 1965; and Newland 1965). It, by no means, is able to explain the phenomenon of wetting-induced collapse in which the effective stress decreases while the compression deformation increases upon wetting. This is because that the effective stress decreases during soaking. According to effective stress principle, the decrease in effective stress should cause rebounding deformation. While in the problem of hydraulic collapse, compression deformation occurs. In fact, it also can not explain the phenomenon of hydraulic swelling. The deformation caused by hydraulic swelling can be larger than compression deformation. However, the rebounding deformation caused by release of effective stress should be less than the compression deformation because of the plasticity of soil materials. Even for elastic material, the rebounding deformation can only be equal to the compression deformation. The main reason that the modified Terzaghi's principle of effective stress can not explain the phenomena of hydraulic collapse and hydraulic swelling might be the misconception that the fourth proposition of Terzaghi's principle of effective stress is valid in partly saturated soils, *i.e.*, the parameters concerning strength and deformation characteristics for a given soil are unique in partly saturated condition as well as in fully saturated condition. A lot of studies in partly saturated soils show that, for a given soil, these parameters are not unique but a function of degree of saturation.

8.3 THE CHANGE OF STRENGTH PARAMETERS AND STIFFNESS WITH SATURATION RATIO IN PARTLY SATURATED SOILS

In case of partial saturation, soil is a three phase medium: solid, water and air. The pore water pressure (u_w) must always be less than the pore air pressure (u_a) due to surface tension. Unless the degree of saturation is close to unity, the pore air will form continuous channels through the soil and the pore water will be concentrated in the regions around the interparticle contacts. The boundaries between pore water and pore air will be in the form of menisci whose radii will depend on the size of the pore spaces within the soil.

The shear strength of partly saturated soils have been investigated by many in-

dividuals (Cooling and Smith, 1936; Williams, 1957; Blight, 1967; Berezantzev, *et al.*, 1969; Uchida, *et al.*, 1968; Huang, 1983; Stark and Duncan, 1989). The change of shear strength parameters has been reported in all of these studies. A detailed literature review has been given in Chapter 2. In this study, the effect of degree of saturation on volumetric compressibility has been investigated intensively under confining compression condition in Chapter 5. The test results indicate that the volumetric compressibility changes with the change of saturation ratio of the soil. In Chapter 7, the results show that there has tremendous strength loss as the soil is soaked and collapsed, though the initial state (moisture content, dry density and fabric) of the soil is the same. The results also indicate that both the parameters of strength (cohesive intercept d and angle of shearing resistance β) and stiffness (secant shear modulus) change with the variation in saturation ratio of soils. In order to further demonstrate the effect of saturation ratio on strength parameters and stiffness of soil, a series of monotonic tests are performed on samples of different saturation ratio. Samples are prepared such that the dry densities after consolidated at the same overburden pressure are about the same. Because of the difficulty to select such initial dry densities, scatter in dry densities before shearing also shows in the results. The outcomes are presented in the following paragraphs.

8.3.1 Effect of Saturation Ratio on Shear strength

The values of shear strength for different degrees of saturation versus initial axial stress, σ_{v0} are given in Figs. 8.2 to 8.5. In the figures, the values of the shear strength are equal to the shear stresses required to yield 15% shear strain, except for material *TKSC* (Mixture of Toyoura sand and 15% kaolinite) wherein the stress-strain curves show peak and residual values, and therefore, the peak and residual values are taken as peak and residual shear strengths, respectively. Only the residual shear strength is presented in Fig. 8.2.

Figs. 8.2 and 8.3 clearly show that shear strength decreases as the initial saturation ratio increases. The effects of the initial degree of saturation on shear strength are illustrated in Figs. 8.6 and 8.7. For material *TKSC* (Fig. 8.6), the shear strength decreases rapidly as the initial saturation ratio increases up to a value of about 45%. From there on, the reduction in shear strength becomes very slow. For material *CBSM* (Chonan B silty sand, dot broken lines in Fig. 8.7), the shear strength also shows a decrease in value with the increase in initial degree of saturation. The gradient of the strength reduction is not as great as that of material *TKSC* and depends on the stress level. The higher the stress level, the larger is the gradient of strength reduction. For materials *OTSC* (Ottomo clayey

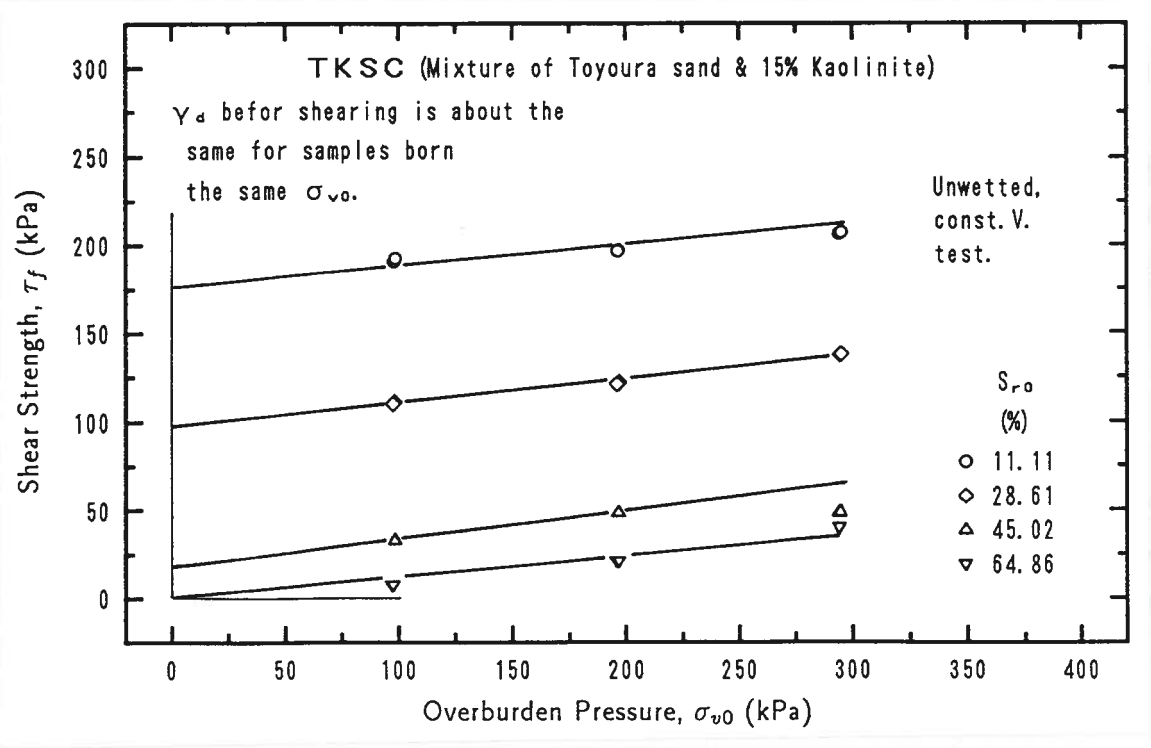

Figure 8.2: Effect of different saturation ratio on shear strength

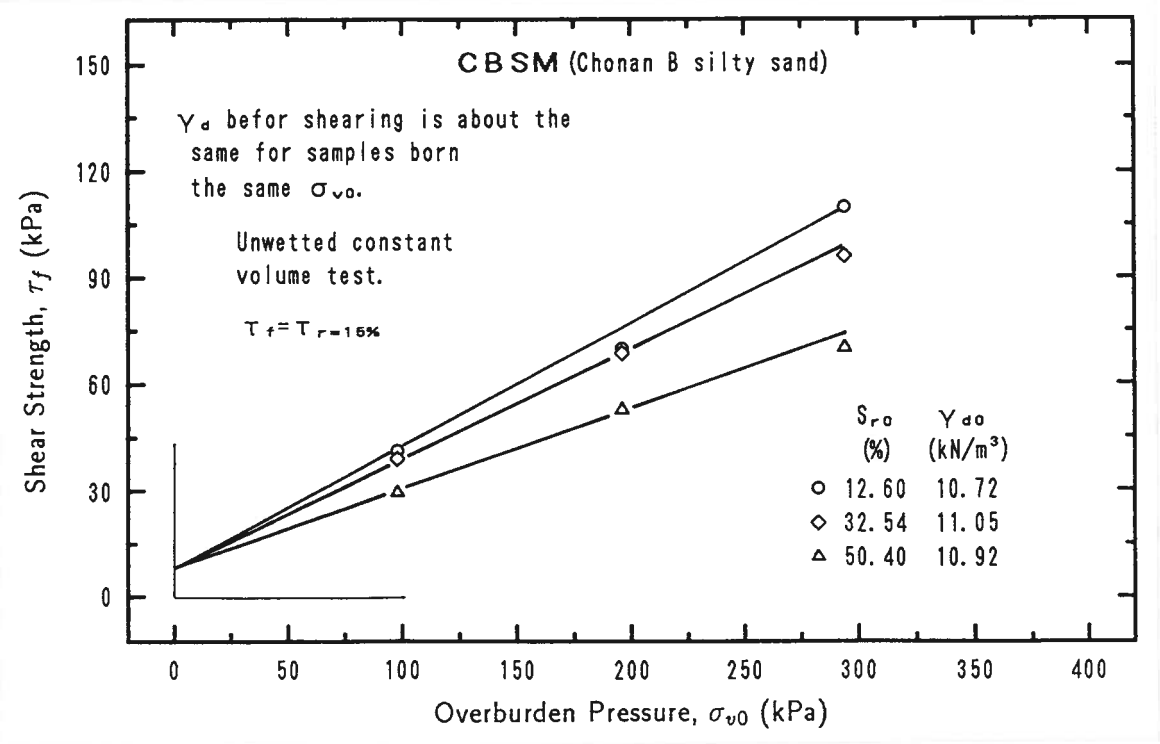

Figure 8.3: Effect of different saturation ratio on shear strength

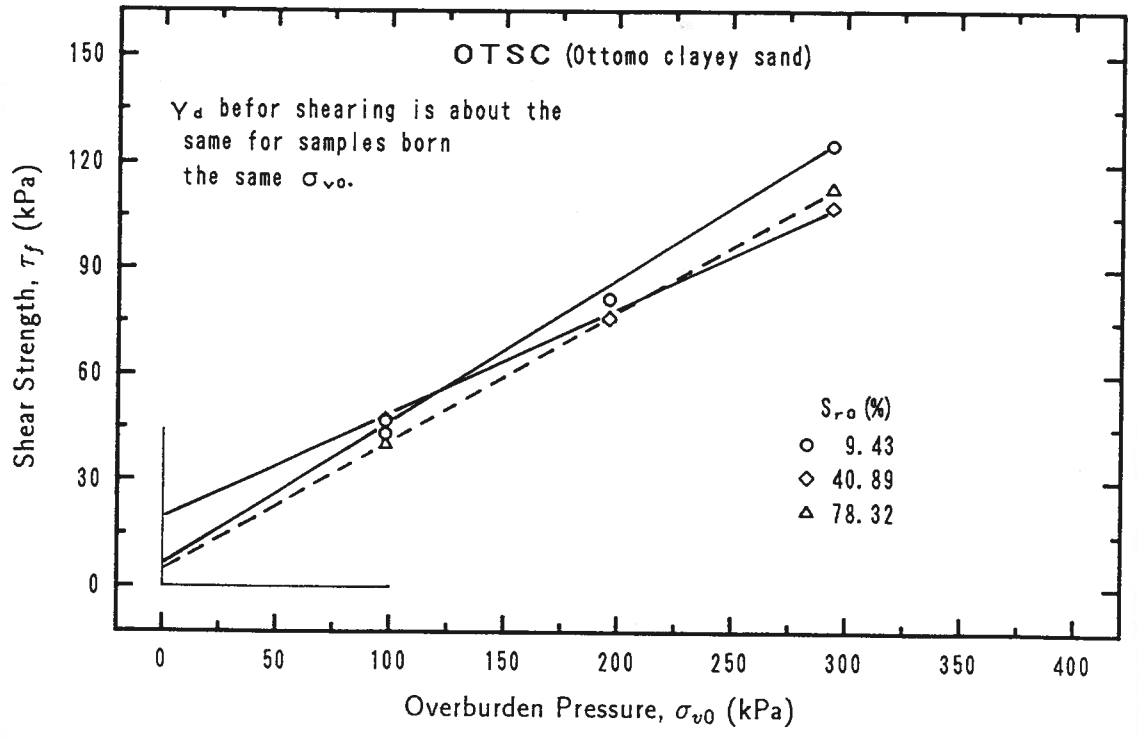

Figure 8.4: Effect of different saturation ratio on shear strength

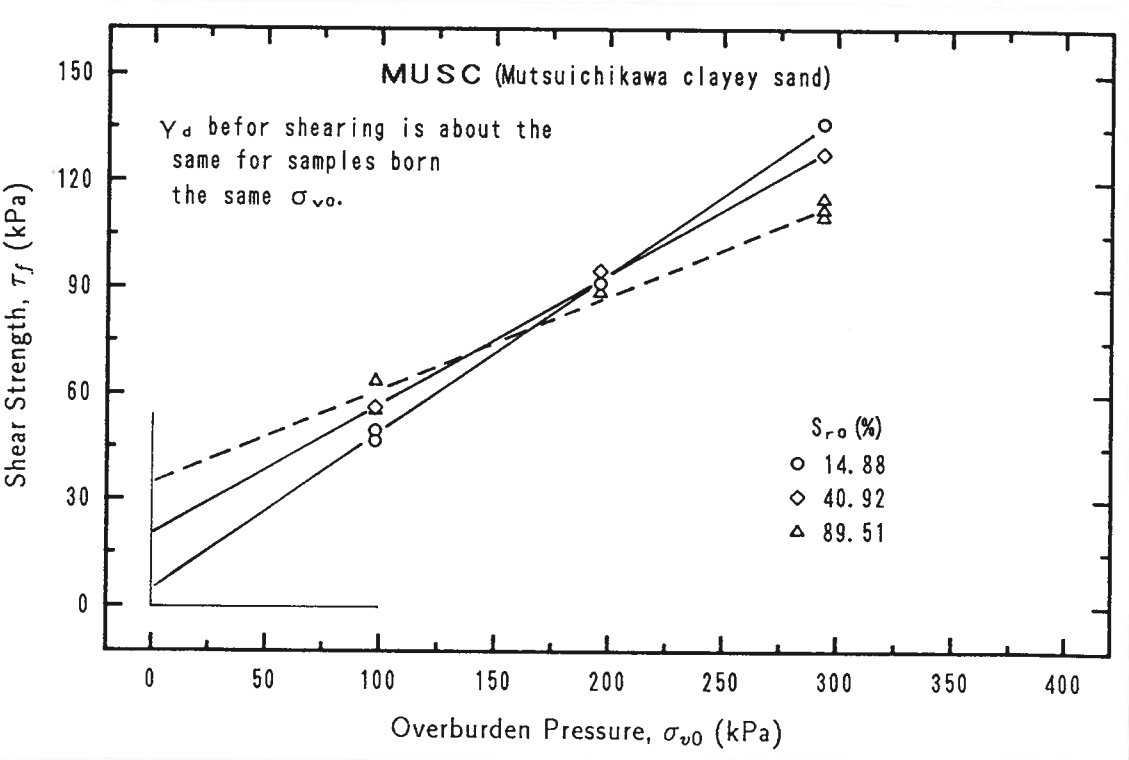

Figure 8.5: Effect of different saturation ratio on shear strength

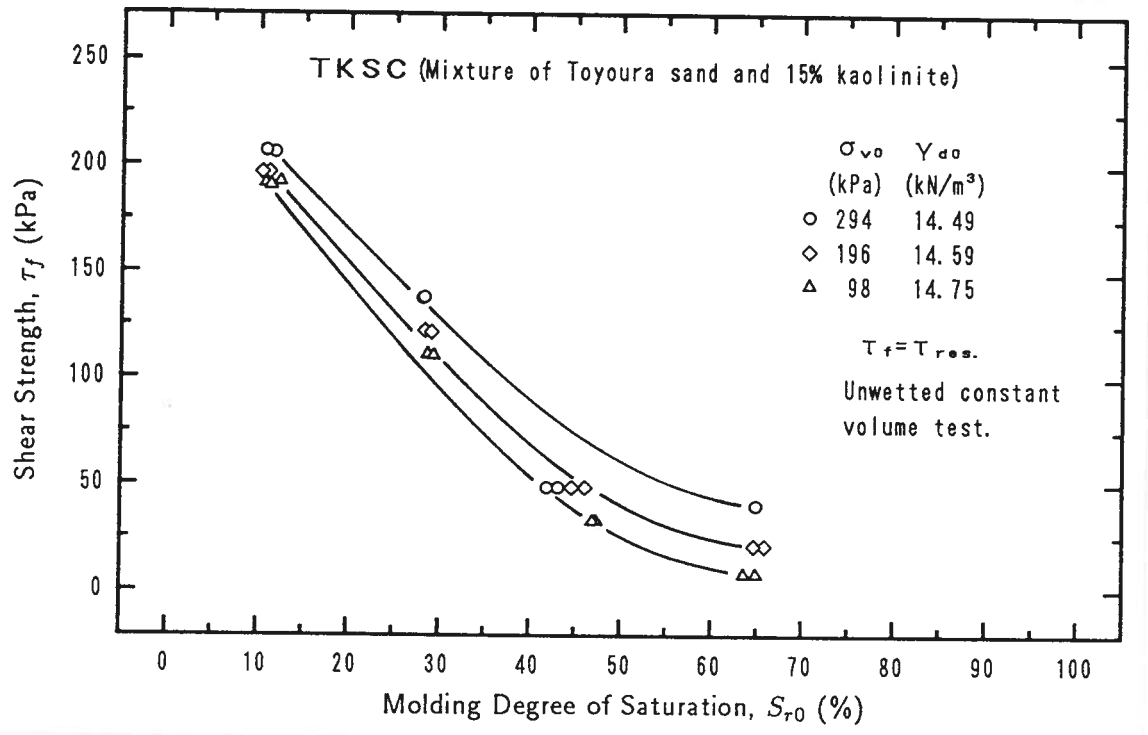

Figure 8.6: Effect of initial saturation ratio on shear strength

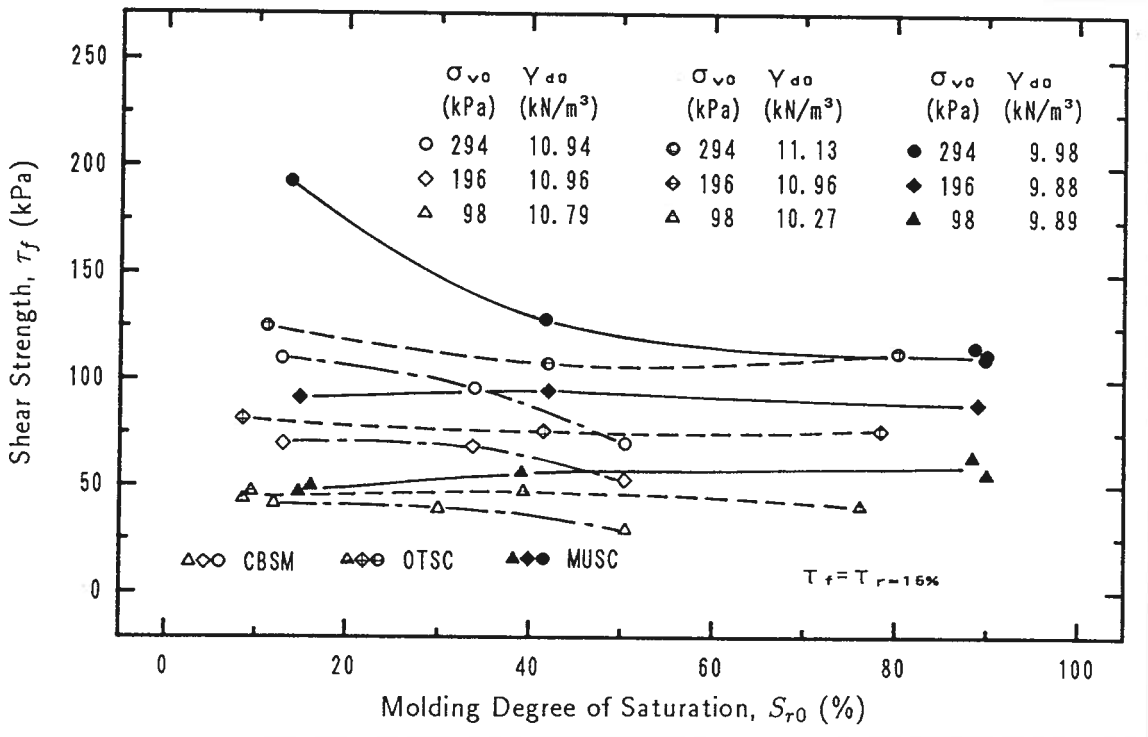

Figure 8.7: Effect of initial saturation ratio on shear strength

sand) and *MUSC* (Mutsuichikawa clayey sand) (broken and solid lines, respectively), the results show that the effect of the initial saturation ratio on shear strength is relatively complicated. However, under higher stress level (294 kPa, in Fig. 8.7), the shear strength still tends to decrease as the initial degree of saturation increases. The inconsistency under lower stress level could be possibly explained by the fact that the shear strength of moister sample at the same initial dry density would decrease more during the application of overburden pressure, while at constant water content, the shear strength of denser samples tend to increase more. The random variations in samples and test procedures, and the difficulties in preparing samples of different molding water contents and dry densities but achieving identical states of density account for the difference in dry density. Because soil is more compressible at higher moisture content during consolidation, samples of higher moisture content are easier to be in a denser condition after consolidation. In this scenario, the denser sample's tendency to increase more in shear strength would control over the moister sample's tendency to decrease more in shear strength. It is beyond reason that moister samples (in the range of relatively high saturation ratios) are of higher shear strength than drier sample if their dry densities are the same. The change in shear strength with dry density of soil *OTSC* (Ottomo clayey sand) is illustrated in Fig. 8.8, which is under the overburden pressure of 98 kPa. The figure clearly indicates that the effect of density variation on shear strength. The scatter of shear strength caused by density variations are also presented in the results of material *TKSC* (Mixture of Toyoura sand and 15% kaolinite). The strength difference caused by unit dry density as a function of initial degree of saturation is given in Fig. 8.9. The effect of overburden pressure on the scatter of strength is also illustrated. It is obvious that the drier the sample and the lower the stress level, the larger is the strength change caused by density although the results are relatively scattered. In fact, the results of material *TKSC* given in the previous figures are corrected for dry densities from a number of tests which have been performed in the same conditions. It is also found that if the dry density is low, the effect of density variation is relatively small (see filled symbols in Fig. 8.9). The strength curves of the two different dry densities are shown in Fig. 8.10. It demonstrates that the effect of dry density on the strength properties of soils is significant.

Generally speaking, there is a tendency for the cohesive intercepts, d, and the angles of shearing resistance, β, to decrease as the initial saturation ratios increase. The reductions of d and β when saturation ratios are changed from 10$\sim$15% to 40$\sim$50% are given in Table 8.1. It can be seen that the exceptions to the trend are indicated in the results. Material *TKSC* (Mixture of Toyoura sand and 15% kaolinite) has an extremely high value of d which almost disappeared as the saturation ratio is increased.

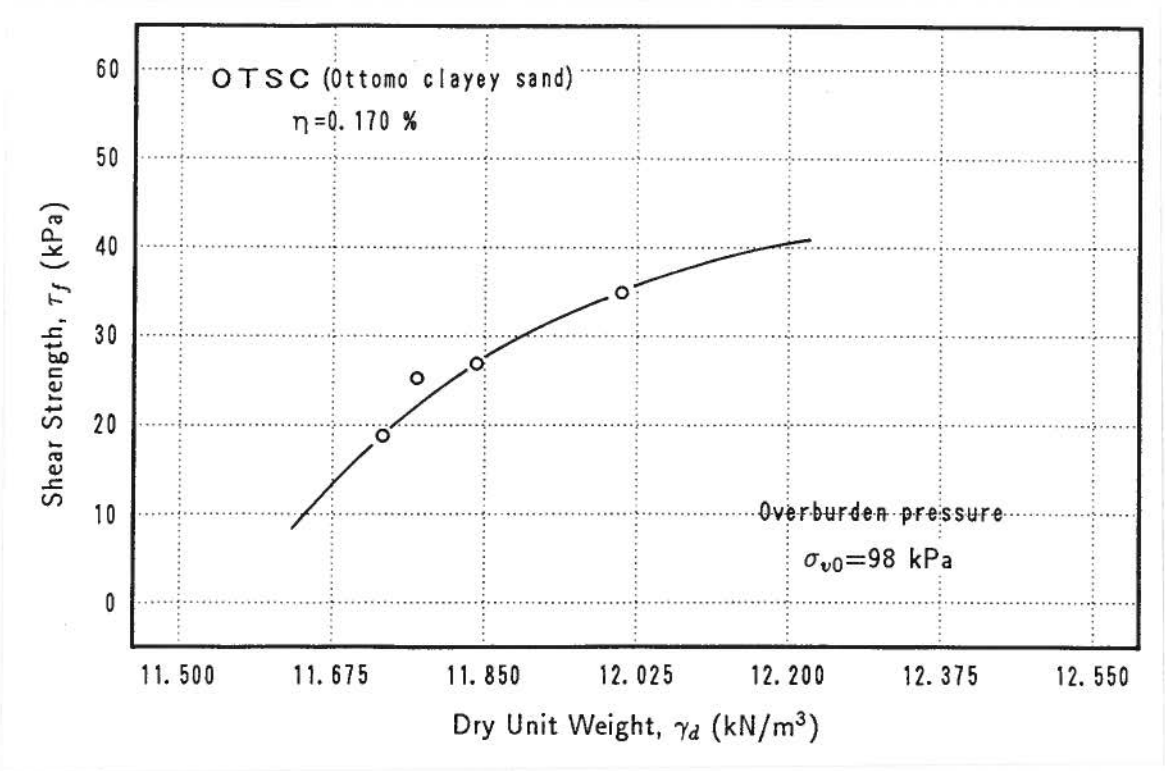

Figure 8.8: Change of shear strength with dry density

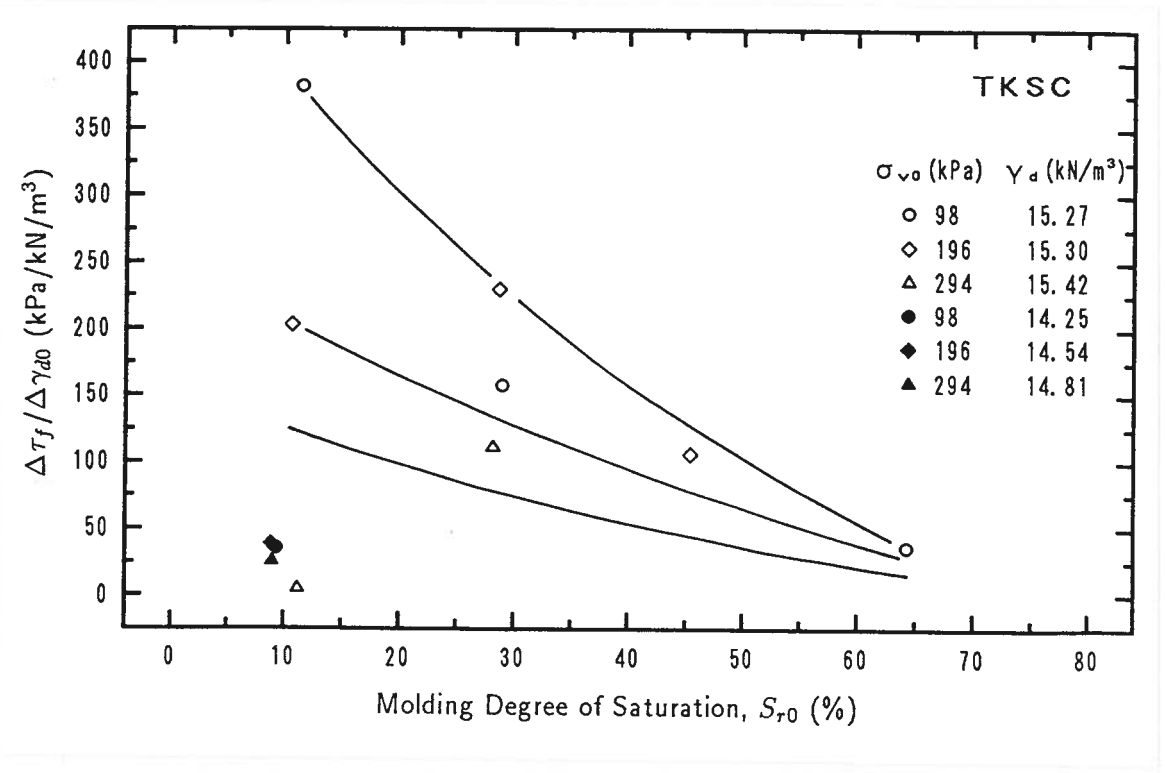

Figure 8.9: Effect of dry density on shear strength

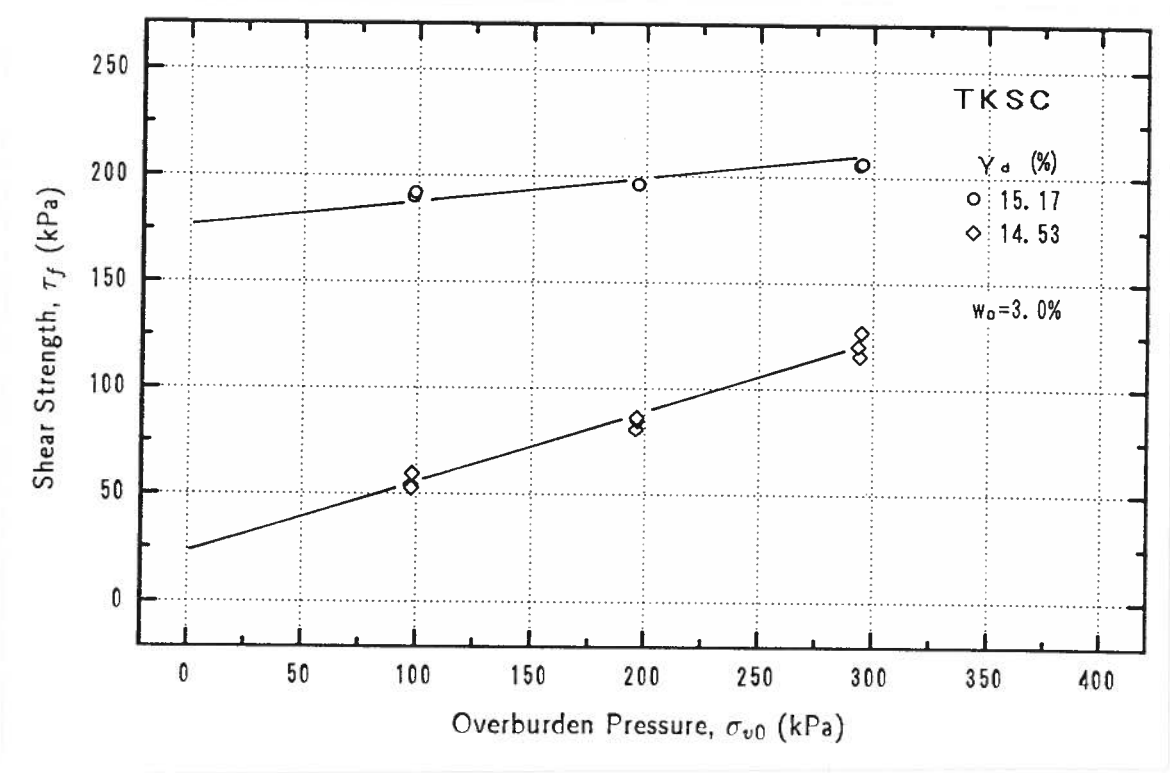

Figure 8.10: Shear strength of soils at different dry density

Table 8.1: Changes of strength parameters due to different saturation ratio

Material		$S_{r0} = 10 \sim 15\%$	$S_{r0} = 40 \sim 50\%$	Reduction (%)
TKSC	d, (kPa)	175.8	16.2‡	90.8‡
	β, (°)	6.9	9.5‡	-38.2‡
CBSM	d, (kPa)	8.1	8.0	1.5
	β, (°)	18.8	12.3	34.2
OTSC	d, (kPa)	5.8	18.9	-227.4
	β, (°)	22.0	16.7	24.3
MUSC	d, (kPa)	5.0	20.7	-311.6
	β, (°)	24.3	20.3	16.3

‡ Parameters corresponding to residual strength.

Materials *OTSC* (Ottomo clayey sand) and *MUSC* (Mutsuichikawa clayey sand) have relatively small values of d which cause very high percentages of the increases in d. These exceptions are considered to be the results of random variations in dry density and test procedures and also the difference of material types.

8.3.2 Effect of Saturation Ratio on Deformation

Figs. 8.11 to 8.16 are the stress-strain relationships of samples with different saturation ratios. All of these tests are tested at molding degree of saturation and without wetting. These figures show that without wetting, soils usually behave as strain hardening materials. The tendency of strain hardening weakens as the degree of saturation increases. Material *TKSC* (Mixture of Toyoura sand and 15% kaolinite) is the most typical material to demonstrate this behavior. At low saturation ratio, it behaves as strong hardening material. As the degree of saturation increases, it changes to weak hardening, ideal plastic and further softening. This feature is affected by applied load. The increasing in stress level tends to weaken the hardenability.

In Fig. 8.15 (material *OTSC*, Ottomo clayey sand), it is noted that in a certain shear strain range, the stress-strain curves of samples having lower saturation ratios are lower than those of samples having higher saturation ratios. The contrary occurs when shear strain increases beyond a critical value. This critical value decreases with the increase in applied load. Other materials, like *CBSM* (Chonan silty sand) and *MUSC* (Mutsuichikawa clayey sand), also show similar characteristics. It is found (Fig. 8.14) that this phenomenon occurred at a saturation ratio less than 50%.

The same data processing used in Chapters 6 and 7 is also employed to investigate the effect of saturation ratio on strength and deformation behavior of soils. The effect of saturation ratio is expressed in terms of *saturation factor*. The saturation factor can be defined, depending on the purpose, as: the ratio of the secant shear moduli of soils at any degree of saturation to those at a given relatively small degree of saturation, which is used to describe the reduction of moduli caused by increasing the saturation ratio, and the ratio of the secant moduli of soils at any degree of saturation to those at fully saturated condition, which describes the increase in shear moduli due to the decrease in saturation ratio. In this study, all the tests are performed in partly saturated conditions. It is intended to investigate the strength loss caused by increasing the degree of saturation. Therefore, the first definition will be used to express the effect of saturation ratio on soil

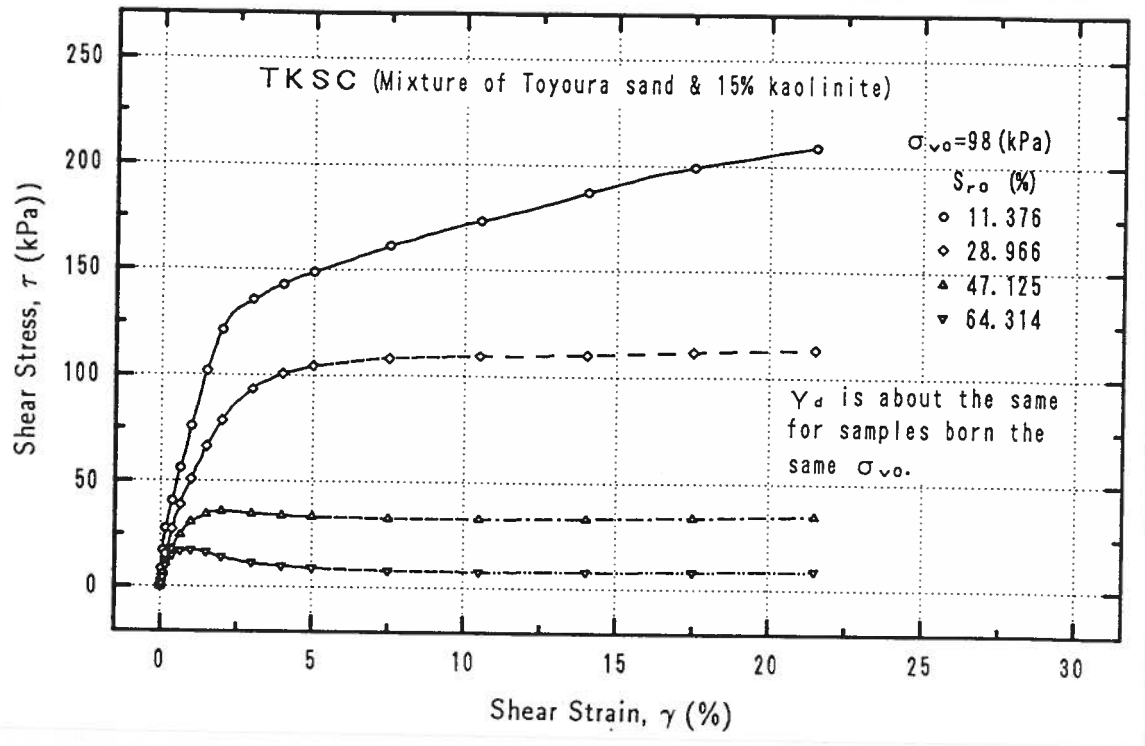

Figure 8.11: Stress-strain curves of samples with different saturation ratios

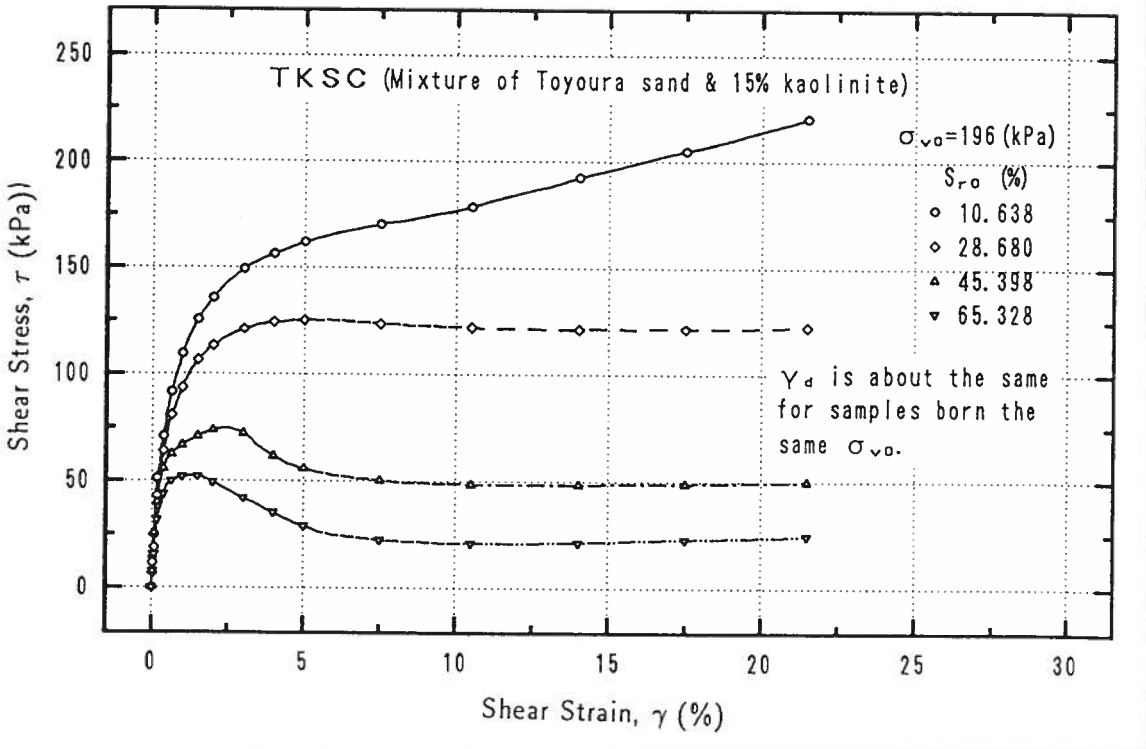

Figure 8.12: Stress-strain curves of samples with different saturation ratios

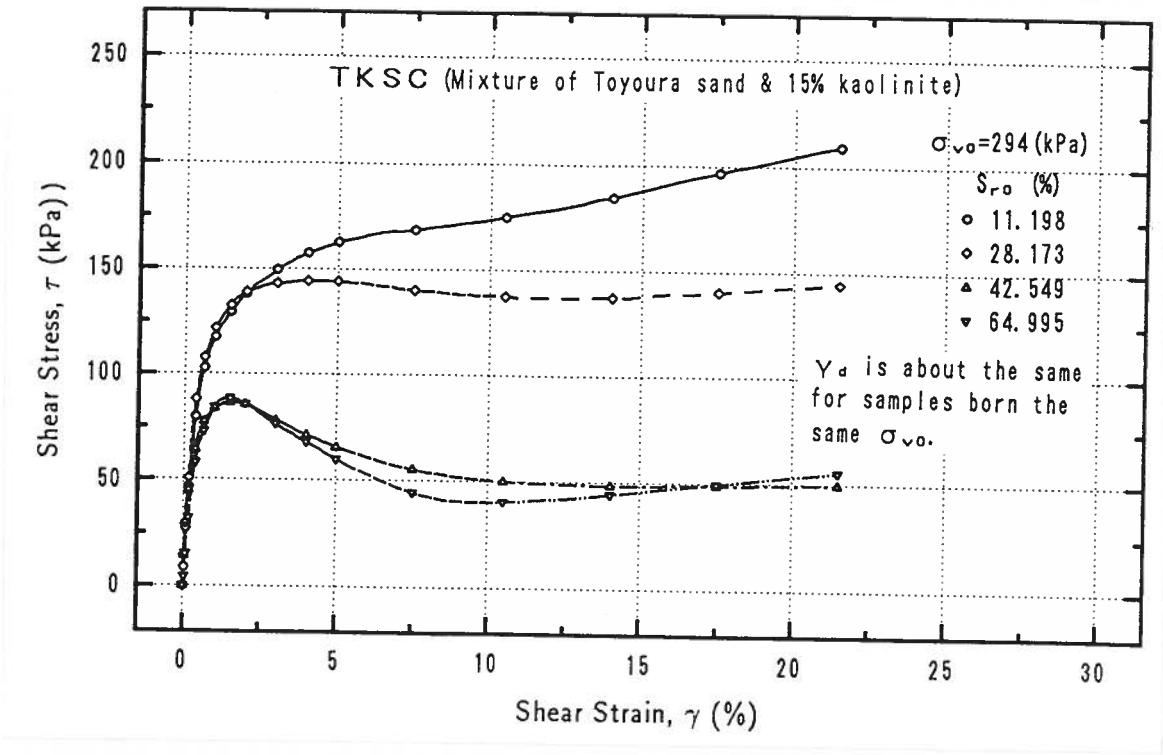

Figure 8.13: Stress-strain curves of samples with different saturation ratios

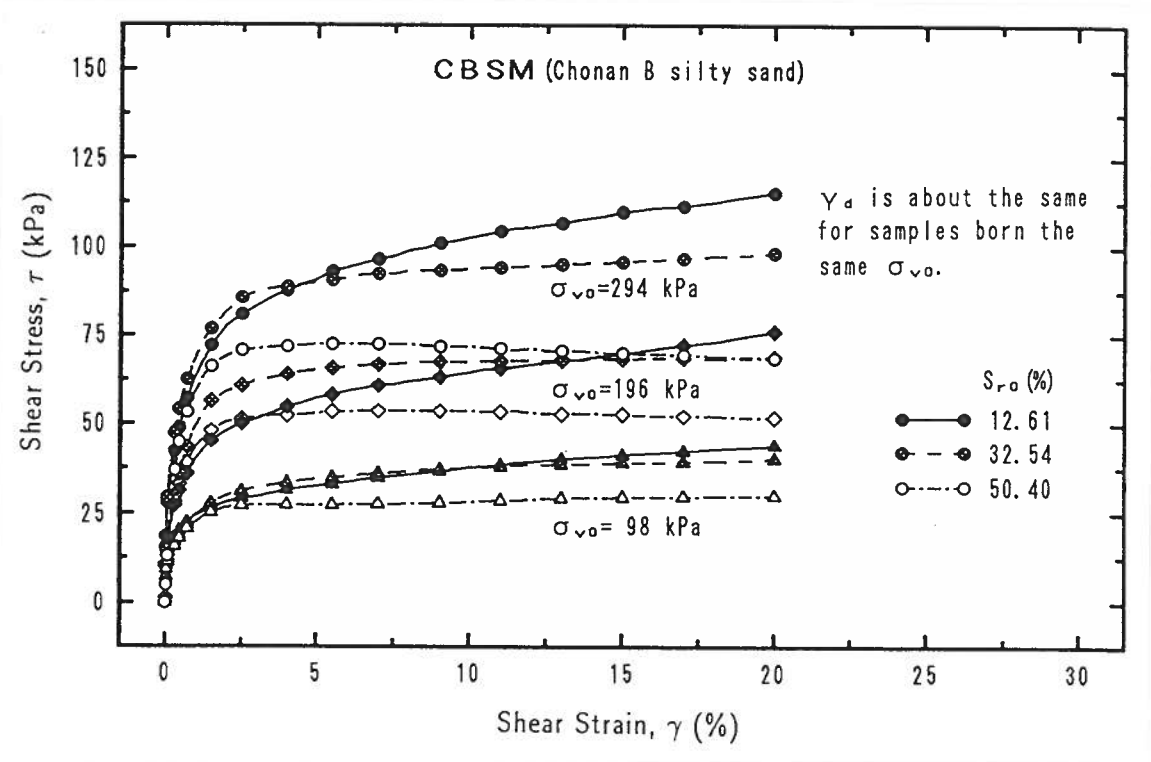

Figure 8.14: Stress-strain curves of samples with different saturation ratios

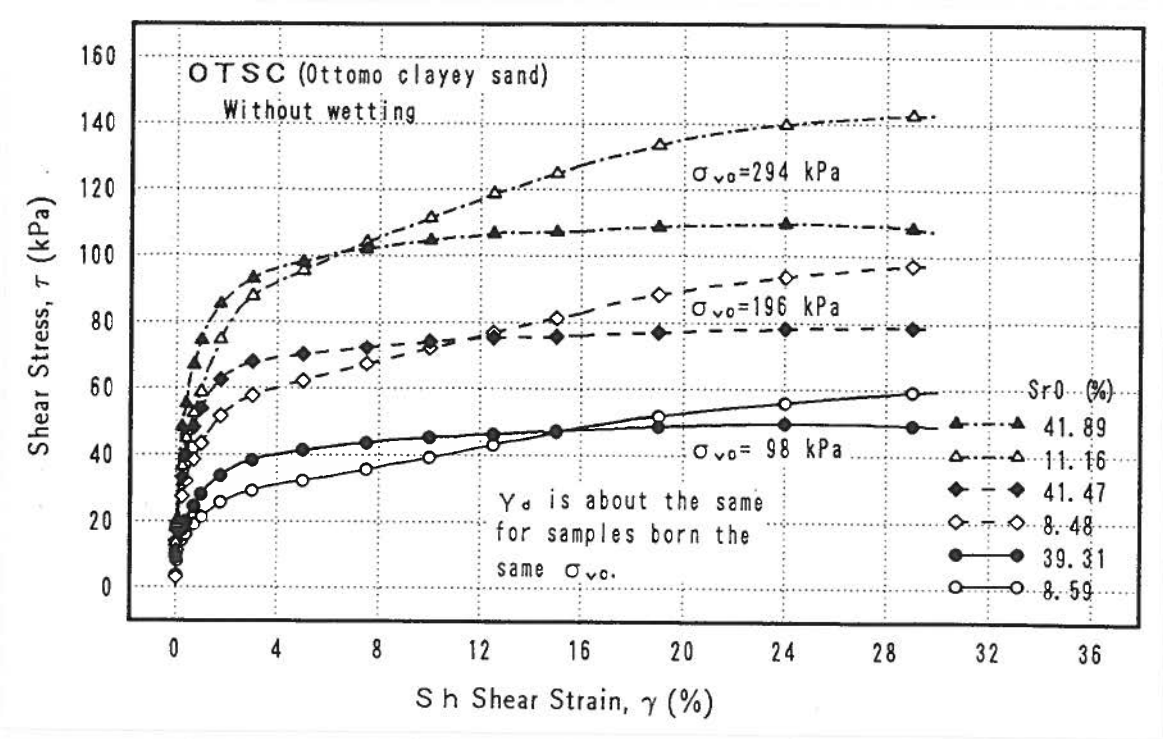

Figure 8.15: Stress-strain curves of samples with different saturation ratios

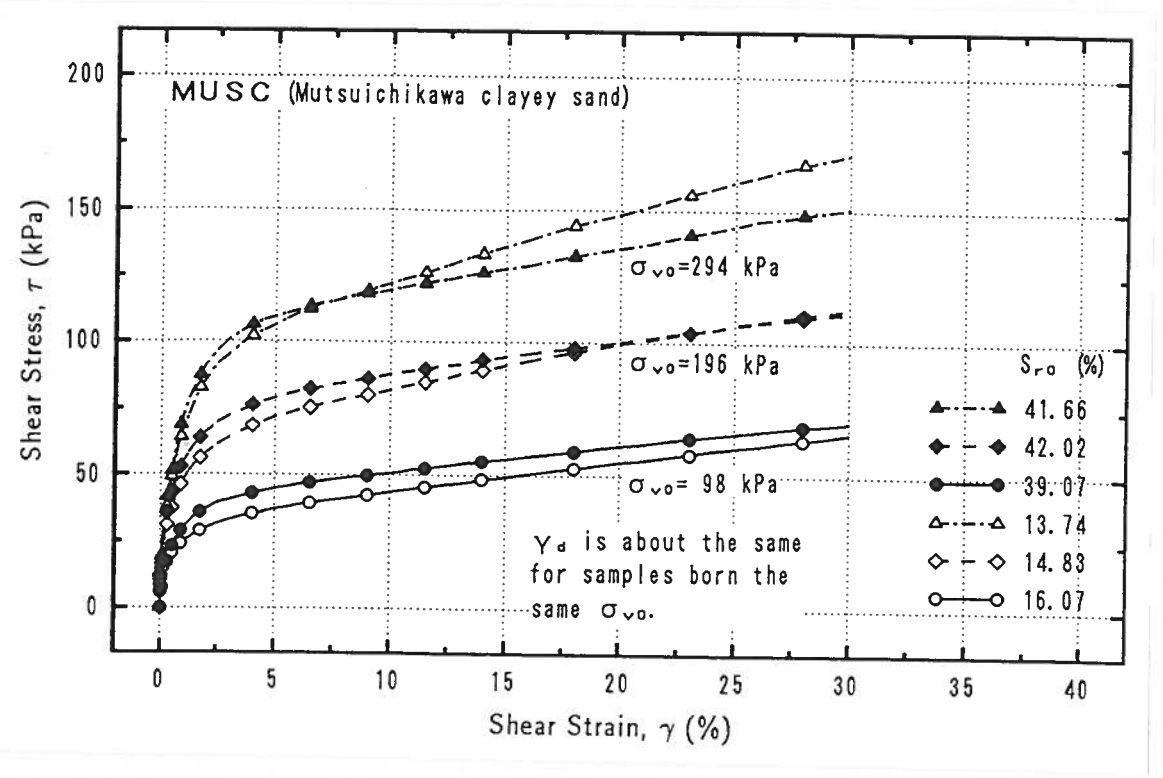

Figure 8.16: Stress-strain curves of samples with different saturation ratios

properties, *i.e.*:

$$C_s = \frac{G_{S_r}}{G_{S_r10}} \tag{8.4}$$

or

$$C_s = \frac{G_{S_r}}{G_{S_r10}} = \frac{\tau_{S_r}/\gamma}{\tau_{S_r10}/\gamma} = \frac{\tau_{S_r}}{\tau_{S_r10}} = \frac{(\tau_{S_r}/\sigma_{v0})}{(\tau_{S_r10}/\sigma_{v0})} \tag{8.5}$$

where the subscript $_{S_r}$ corresponds to any degree of saturation and the subscript $_{S_r10}$ means saturation ratio of 10%. The results obtained in such a way are presented in Figs. 8.17 to 8.20. Similar to the changes of collapse factor and wetting factor, the saturation factor decreases as the shear strain increases. It is noticeable that, unlike in the case of wetting factor or collapse factor, the saturation factors intersect the axis of $C_s = 1$ at points of shear strain unequal to 0. At saturation ratios less than about 50% (except for material *TKSC*), the saturation factors are larger than 1 at low shear strain level and decrease to less than 1 when the shear strain increases and becomes larger than a critical value. At high saturation ratio, C_s is less than 1 even at low strain level. The results for material *TKSC* (Mixture of Toyoura sand and 15% kaolinite, Fig. 8.17) show that the saturation factor is less than 1 even at relatively small degree of saturation. This phenomenon may be due to by suction action (contribution of suction to effective stress). As described in Chapter 5, at a critical value of saturation ratio, suction action is maximum. Because of this suction action (suction induced effective stress), the strength of soils at this critical degree of saturation is maximum. Therefore, the saturation factors are larger than 1. In Chapter 5, it has been found that the critical saturation ratio decreases as the overburden pressure increases. Similar tendency is also shown in the results of saturation factor. In Figs. 8.18, 8.19 and 8.20, it can be seen that the saturation factors decrease as the stress level increases. This is reasonable because suction should be constant at any stress level if the dry density does not change much. As the confining stress level increases, the proportion of suction to effective stress decreases. If the confining stress level is so high that the proportion of suction to effective stress is about zero, the effect of suction action on deformation and strength properties of soils would be negligible.

The excess pore pressures developed during shearing for the four materials are illustrated in Figs. 8.21 to 8.26. The excess pore pressure increases as the degree of saturation increases. It is noticeable that negative excess pore pressure occurs in material *TKSC* (Mixture of Toyoura sand and 15% kaolinite) when the saturation ratio and the applied load are low. This means that shear dilation occurs during shearing. Due to dilatancy, effective stress increases during shearing and soils show relatively high strength.

The above results and those given in Chapters 5 and 7 indicate that both the

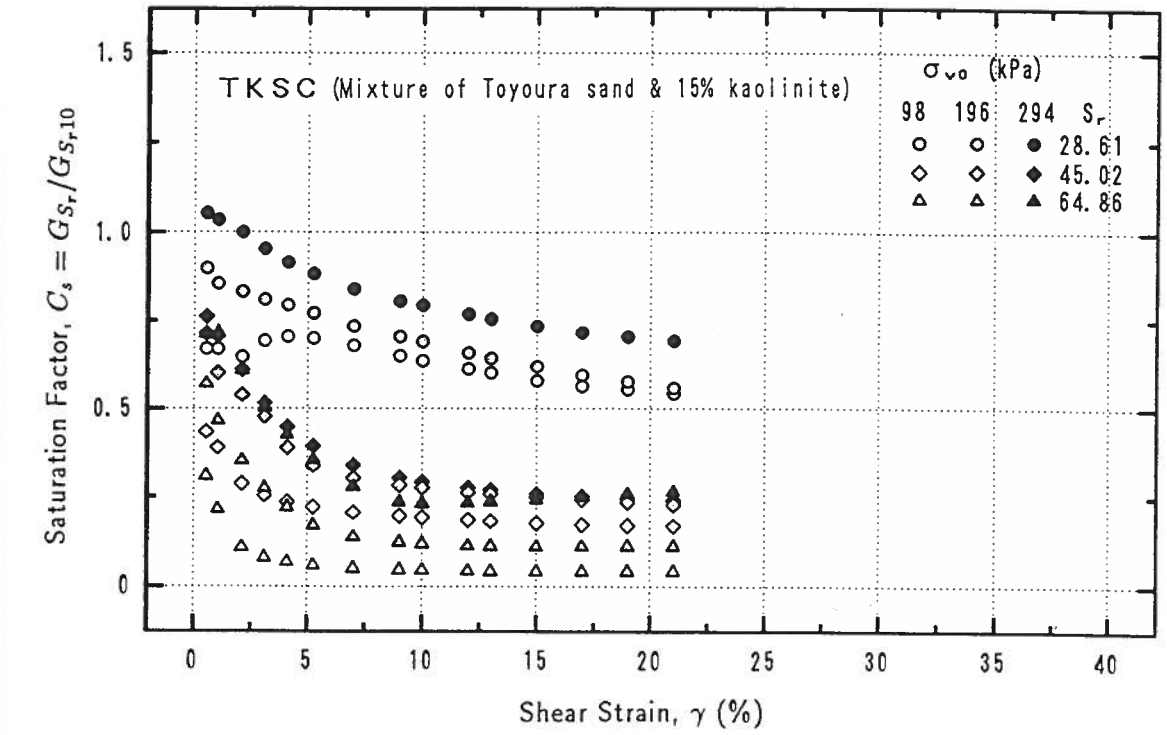

Figure 8.17: Saturation factor versus shear strain

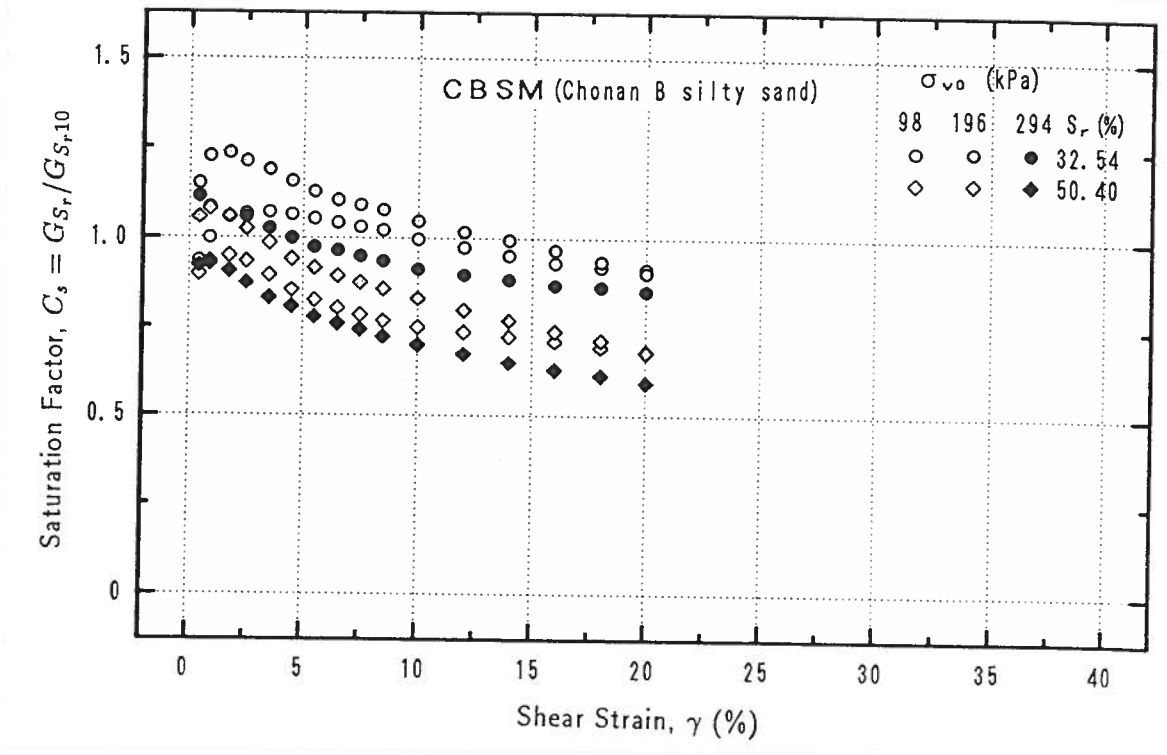

Figure 8.18: Saturation factor versus shear strain

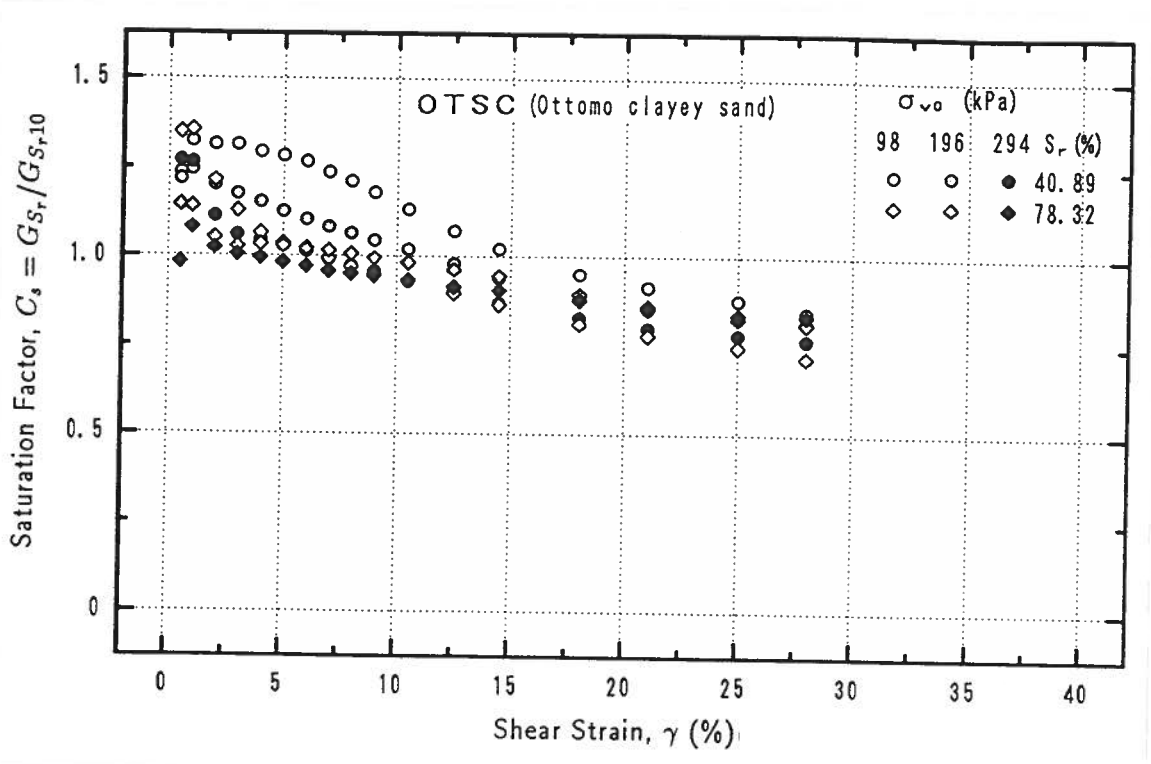

Figure 8.19: Saturation factor versus shear strain

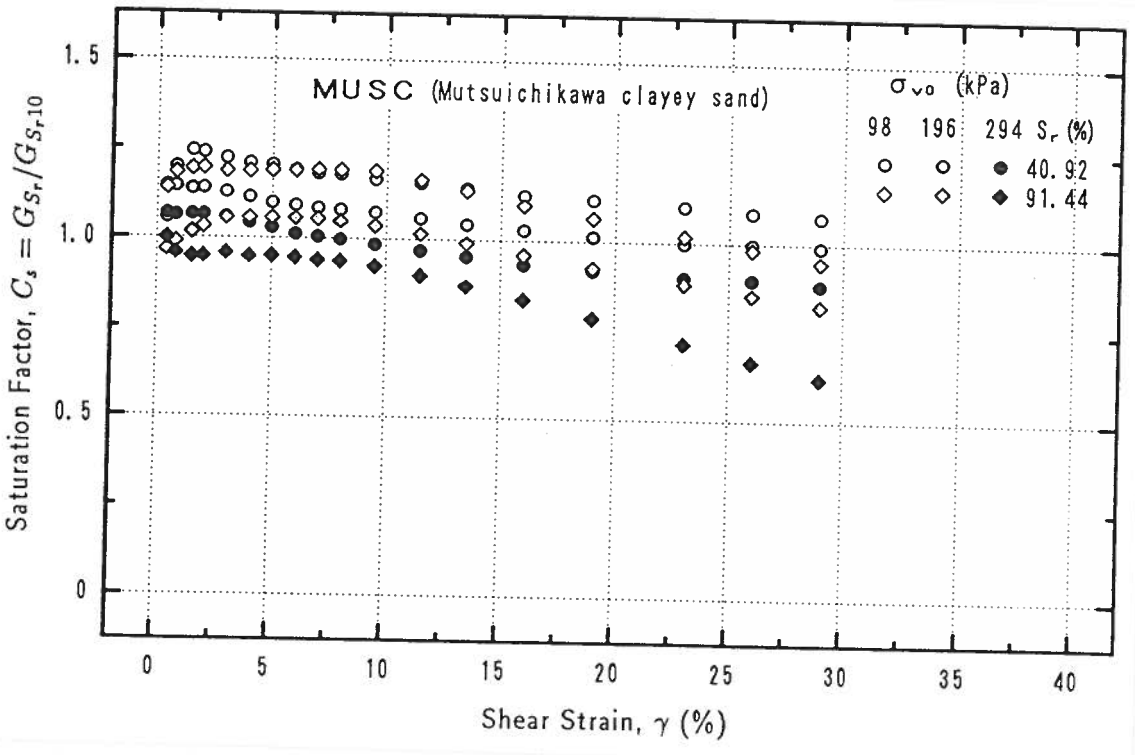

Figure 8.20: Saturation factor versus shear strain

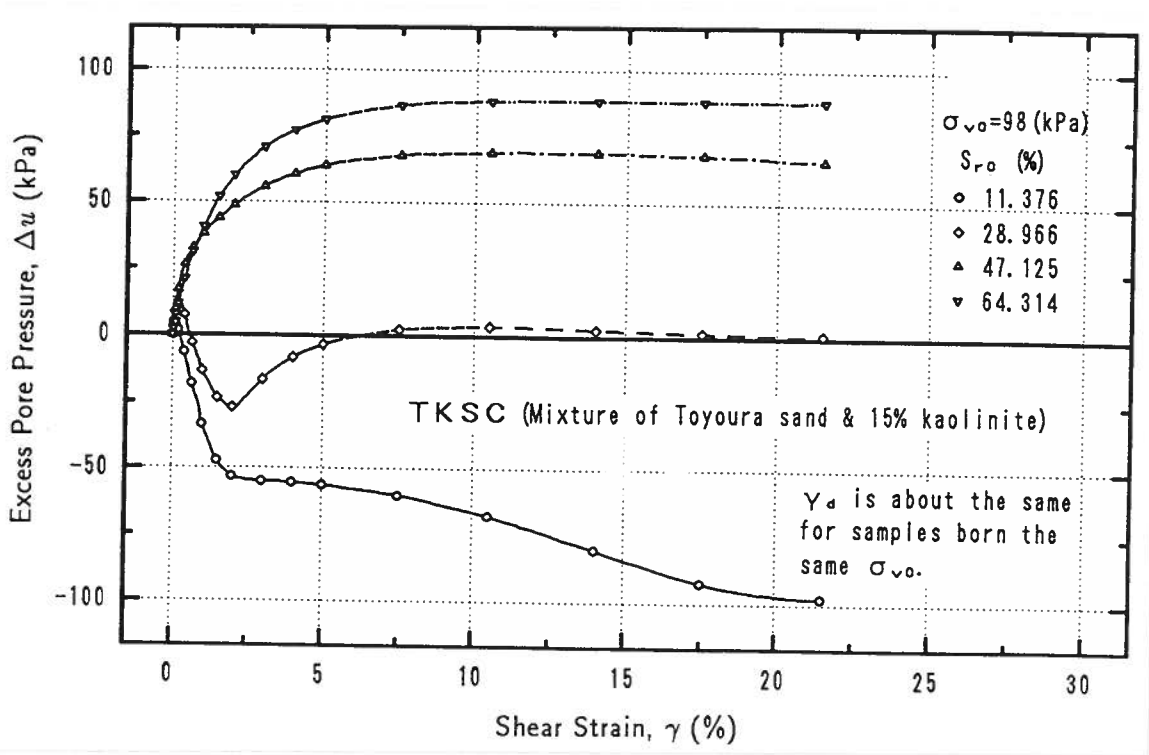

Figure 8.21: Excess pore pressure developed in samples of different saturation ratios

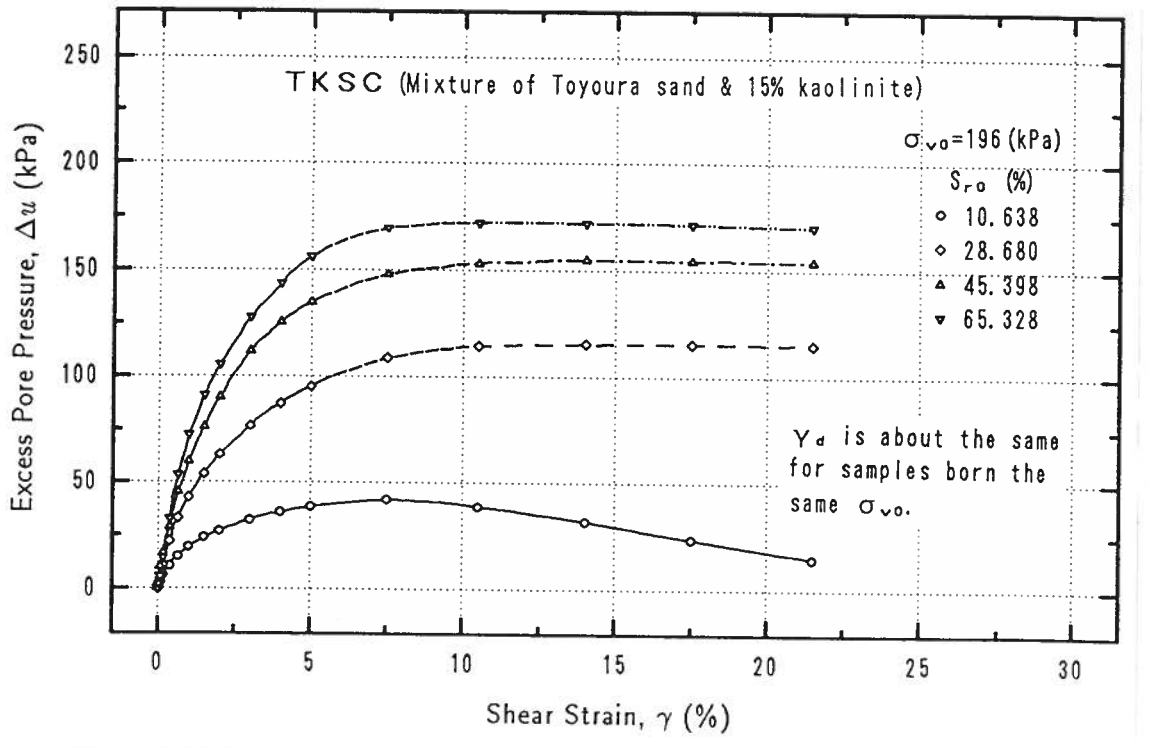

Figure 8.22: Excess pore pressure developed in samples of different saturation ratios

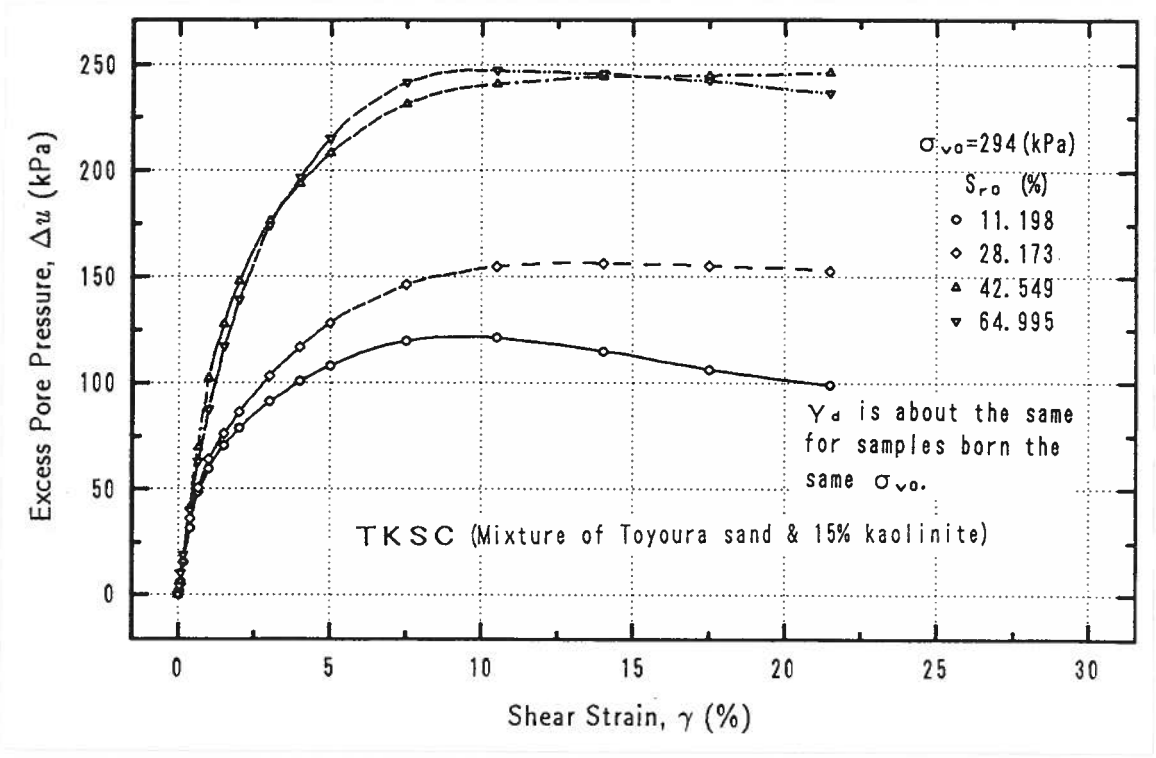

Figure 8.23: Excess pore pressure developed in samples of different saturation ratios

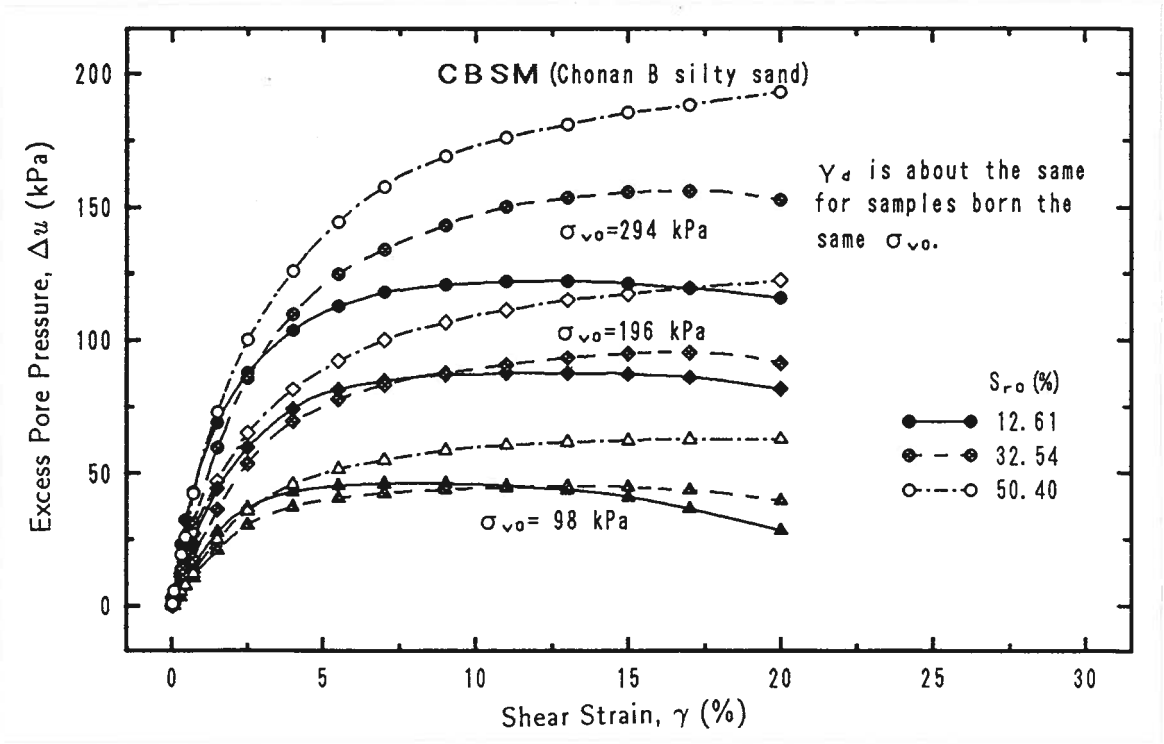

Figure 8.24: Excess pore pressure developed in samples of different saturation ratios

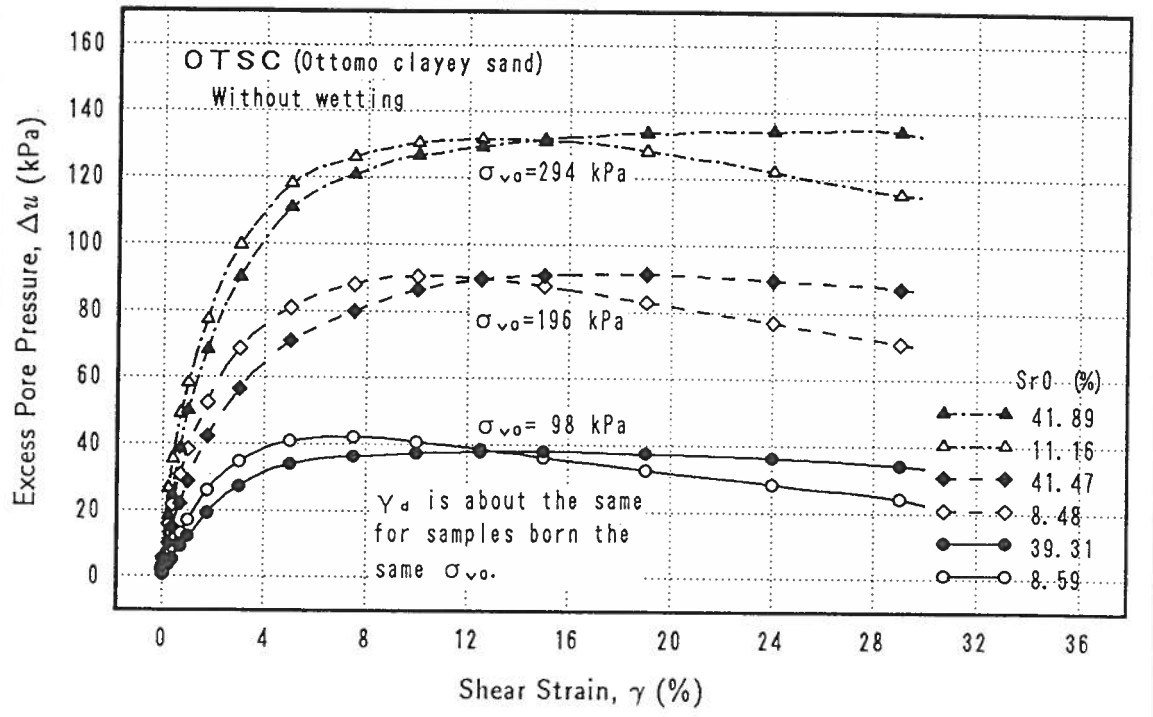

Figure 8.25: Excess pore pressure developed in samples of different saturation ratios

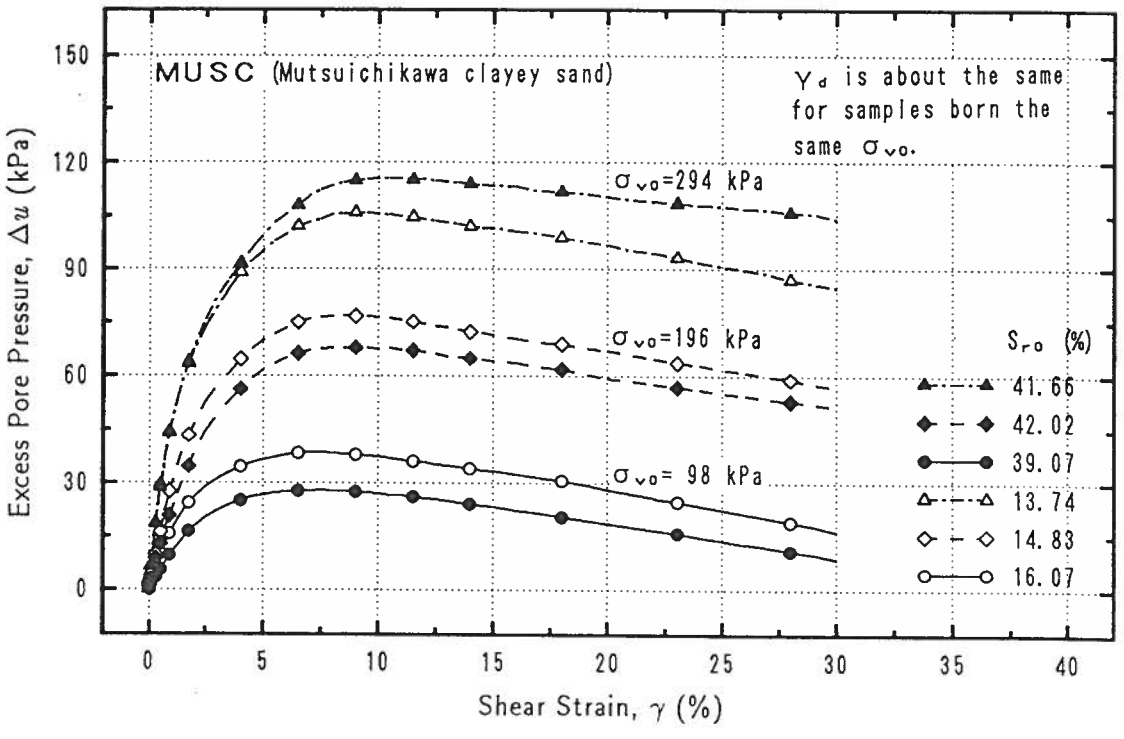

Figure 8.26: Excess pore pressure developed in samples of different saturation ratios

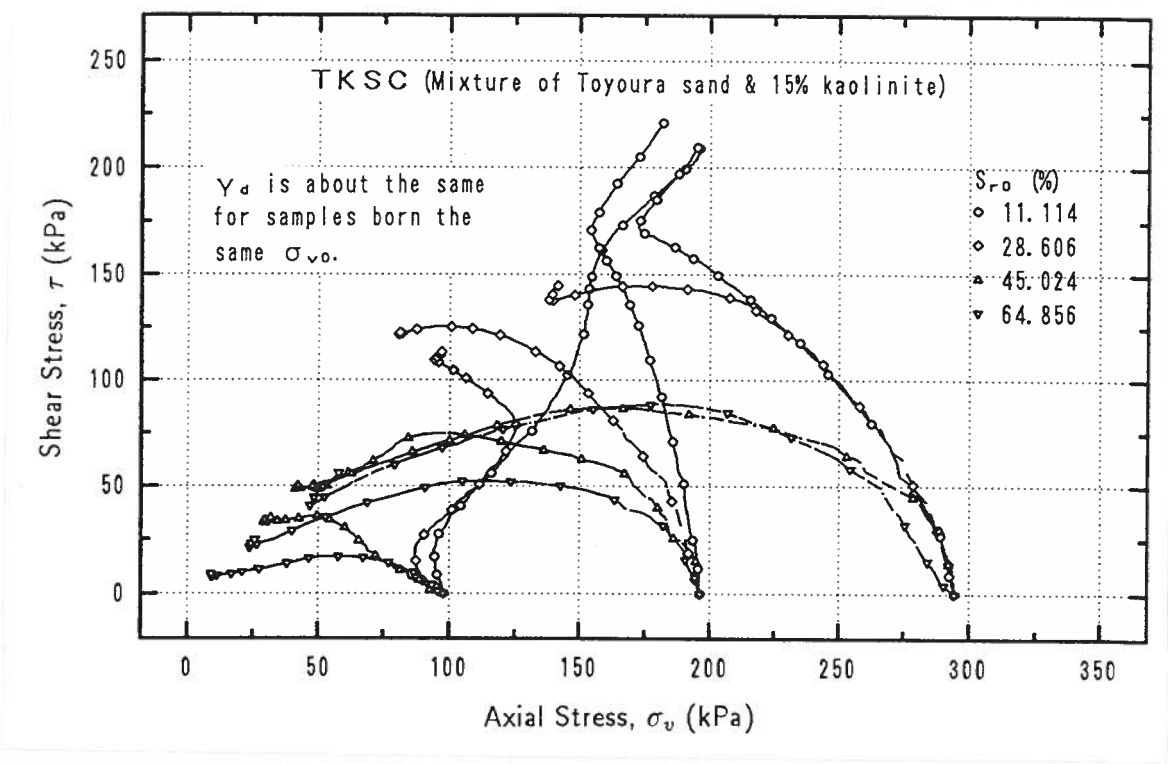

Figure 8.27: Relationships between shear stress and measured axial stress of samples with different saturation ratios

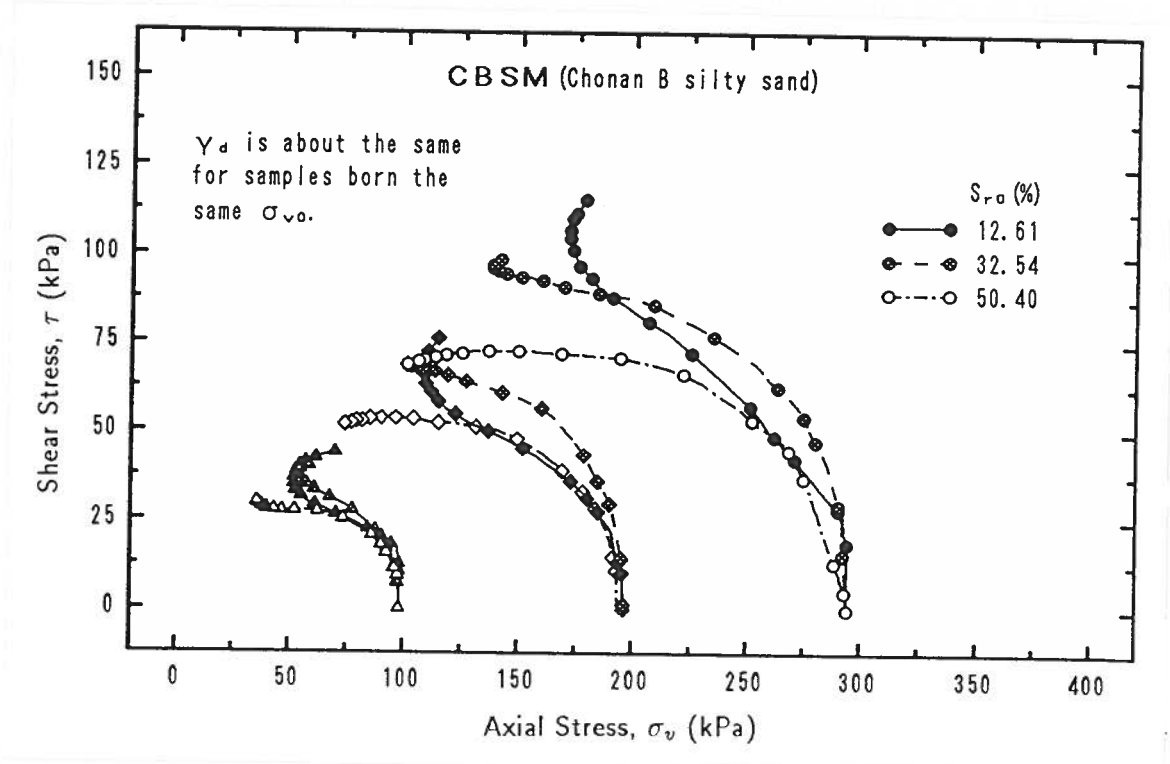

Figure 8.28: Relationships between shear stress and measured axial stress of samples with different saturation ratios

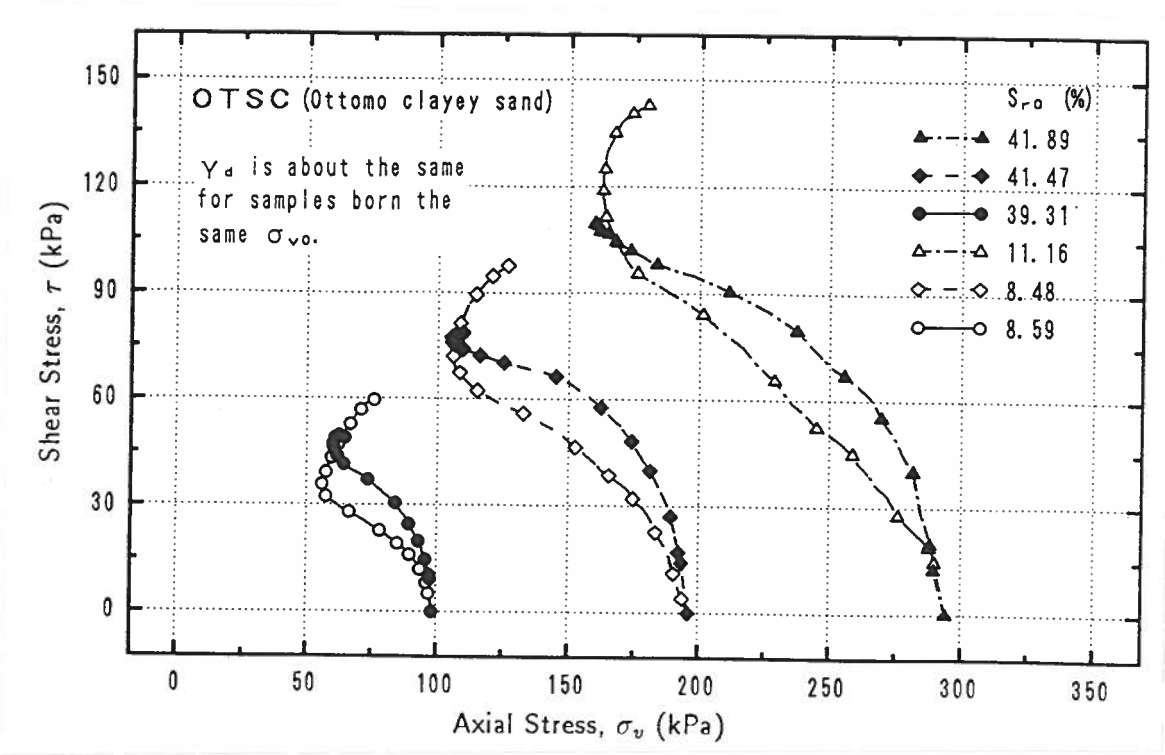

Figure 8.29: Relationships between shear stress and measured axial stress of samples with different saturation ratios

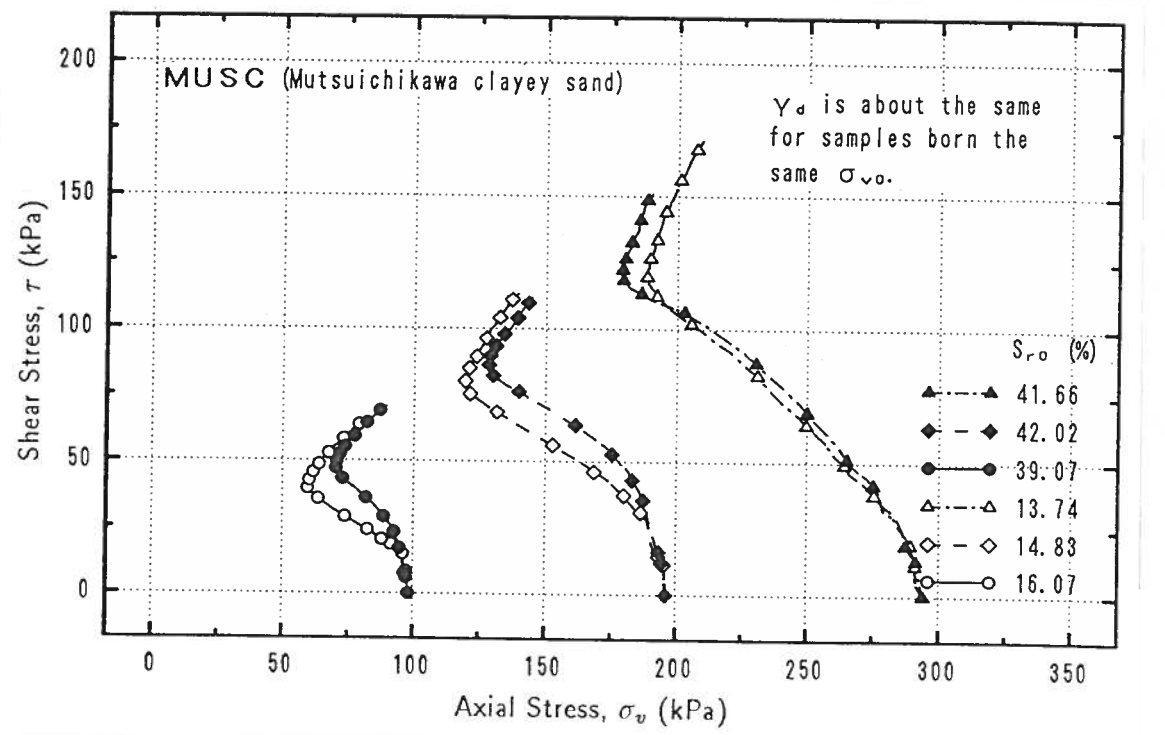

Figure 8.30: Relationships between shear stress and measured axial stress of samples with different saturation ratios

parameters of strength (cohesive intercept d and angle of shearing resistance β) and stiffness (volumetric compressibility, shear modulus, $\cdots$) change with the increase in saturation ratio of soils. The volumetric compressibility and secant shear modulus usually decrease as the degree of saturation increases. The cohesive intercept d also decreases with saturation ratio. The angle of shearing resistance β does not always decrease with degree of saturation but the total shear strength does. All aforementioned test results prove that the parameters of strength and stiffness in partly saturated soils are not constant. They depend on the condition of saturation. If other conditions, such as initial void ratio, initial structure, stress history, *etc.*, are identical for a given soil, these parameters are unique functions of saturation ratio.

8.4 THE GENERAL PRINCIPLE OF EFFECTIVE STRESS

The validity of classical *effective stress principle* in partly saturated soils, especially in explaining the wetting-induced *collapse* phenomenon, has been questioned by many researchers (Jennings and Burland, 1962; Jennings, 1963; Burland, 1965; Newland, 1965; Brackley, 1971; and Sridharan, *et al.*, 1973). Newland (1965) and Burland (1965) have proposed the concepts of two kinds of effective stress and of grain contact stability (see Chapter 2), respectively, to try to explain the collapse phenomenon. Their theories are not new theories of principle of effective stress. In fact, they explained the mechanism of the change of strength and deformation characteristics with saturation ratio. The divergence of Terzaghi's classical principle of effective stress from the fact of wetting-induced collapse proves in no way the invalidity of this principle but the misapplication of it. The test results given in the above section indicate that the strength and deformation characteristics are, for a given soil, by no means constant in partly saturated soils but are the functions of the degree of saturation.

By considering the fact that strength and deformation characteristics of partly saturated soil change with saturation ratio, a *General Principle of Effective Stress* can be described as follows:

1. Soil is a three phase medium: solid, air and water.

2. All measurable effects of the change of stress and/or of saturation ratio, such as compression, distortion, and change in the shearing strength of soil, are due exclusively to changes in the effective stress and/or saturation ratio.

3. The effective stress is defined as the stress transmitted by the skeleton of soil which consists of two components, exogenous effective stress, σ'_E, and endogenetic effective stress, σ'_I.

$$\sigma' = \sigma'_E + \sigma'_I \tag{8.6}$$

The endogenetic effective stress includes various attractive and repulsive forces (electrical, osmotic, Van der Waals, *etc.*) and the menisci forces (or suction).

4. For a given soil (having identical initial condition of void ratio, fabric structure, stress history, *etc.*), the stiffness and strength parameters are the exclusive functions of the degree of saturation. They approach the limits at a degree of saturation of 100%. In the deformation problem, the stiffness of a soil is shown as volumetric compressibility (m_v), Young's modulus (E), Poisson's ratio (ν), rebounding modulus (E_r), initial shear modulus, G_0, *etc.* In the strength problem, the parameters are cohesive strength, c', and inter-particle friction angle, ϕ'.

For granular material, the expression of effective stresses can be derived in following way. Consider a plane through a partially saturated granular mass as shown in Fig. 8.31(a). This plane will pass through mineral grains, water and air. A simplified

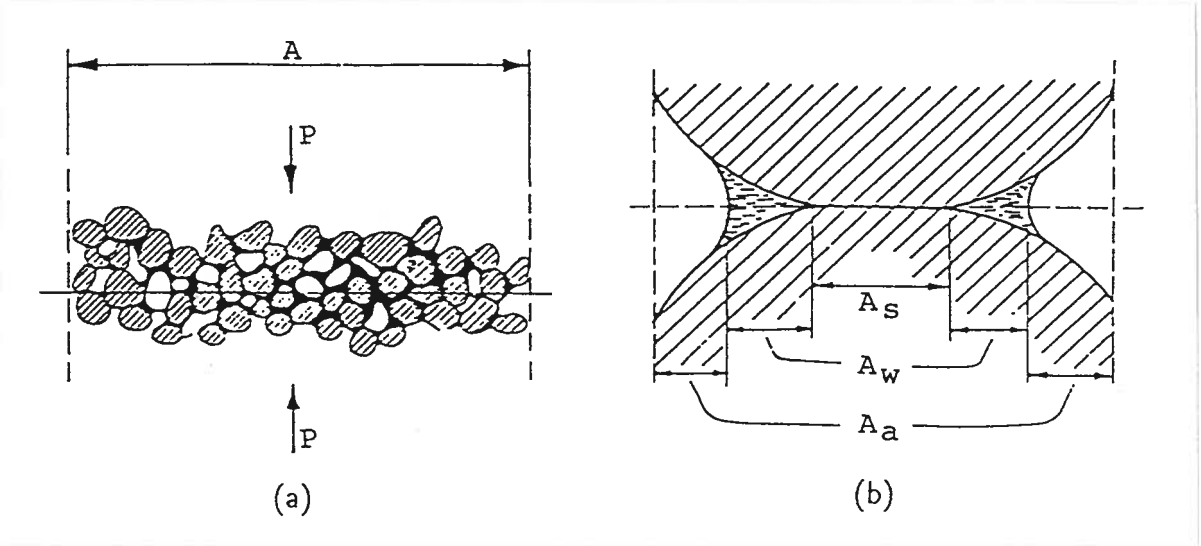

Figure 8.31: (a). Section in granular medium; (b). Stresses in the different components of soil

picture is given in Fig. 8.31(b) in which the minute contact surfaces are combined into

a single contact area A_s and the assemblage of solid particles is fused into two grains. Likewise, the water present in the soil is depicted as contact moisture and the rest of the pore space is occupied by air. The two grains in contact are pressed together by force P which acts in normal direction. Let the total area upon which the load P acts be denoted by A. Then,

$$A = A_s + A_w + A_a \tag{8.7}$$

where A_s is the contact area of solid and A_w and A_a are surfaces of water and air passed by the plane, respectively. Let the respective portions of the stresses carried by the separate phases be noted by σ_s, u_w and u_a. Equilibrium requires that

$$P = \sigma_s A_s + u_w A_w + u_a A_a \tag{8.8}$$

Introducing the following ratios

$$a_s = A_s/A, \quad a_w = A_w/A \quad and \quad a_a = 1 - [a_s + a_w] \tag{8.9}$$

the total stress acting across the section can be written as

$$\sigma = \frac{P}{A} = a_s\sigma_s + a_w u_w + [1 - (a_s + a_w)]u_a \tag{8.10}$$

or

$$\sigma = a_s\sigma_s + (1 - a_s)u_w + [1 - (a_s + a_w)](u_a - u_w) \tag{8.11}$$

In practical cases the contact area ratio is usually very small and therefore it can be considered with enough accuracy that $(1 - a_s) \to 1$. The contact stress σ_s, on the other hand, is very high and may even reach the yield limit of mineral grains; therefore, the product $a_s\sigma_s$ cannot be zero but have a finite value, and is denoted by σ'. Eq. 8.11 becomes

$$\sigma = \sigma' + u_w + (1 - a_w)(u_a - u_w) \tag{8.12}$$

or

$$\sigma' = \sigma - u_a + a_w(u_a - u_w) \tag{8.13}$$

Eq. 8.13 is the same as Bishop's equation. Comparison of the two equations results in $a_w = \chi$.

From Eq. 8.9, there is

$$a_w = \frac{A_w}{A} = \frac{A_w}{A_s + A_w + A_a} \cong \frac{A_w}{A_w + A_a} \tag{8.14}$$

The definition of degree of saturation gives

$$S_r = \frac{V_w}{V_v} = \frac{V_w}{V_w + V_a} \tag{8.15}$$

Assuming that the phases have average heights $\overline{h}_w$ and $\overline{h}_a$, the volumes are expressed as

$$V_w = \overline{h}_w A_w \quad and \quad V_a = \overline{h}_a A_a \tag{8.16}$$

Substituting Eq. 8.16 into Eq. 8.15, results in

$$S_r = \frac{V_w}{V_w + V_a} = \frac{A_w \overline{h}_w}{A_w \overline{h}_w + A_a \overline{h}_a} \tag{8.17}$$

If the saturation ratio is less than a certain critical value, air will form continuous channels. The soil and the pore water will be concentrated in the region around the interparticle contacts. The average height of water will be less than that of air, *i.e.*, $\overline{h}_w < \overline{h}_a$. Therefore, by comparing the right term of Eq. 8.14 with Eq. 8.17, the following is obtained

$$a_w > S_r \tag{8.18}$$

If the saturation ratio of the soil is close to unity, it is likely that pore air will exist in the form of bubbles within the pore water and the surface of pore air passed by the plane will be negligible. Eq. 8.14 will give the value of a_w close to unity. If the soil is oven dried, the water content will be zero and a_w will also be zero. The value of a_w will mainly depend on the saturation ratio and the shape of the grains of soil.

8.5 THE MECHANISM OF HYDRAULIC COLLAPSE

The mechanism of hydraulic collapse has been studied by many individuals (see Chapter 2). Several mechanisms have been reported by researchers. However, nobody was able to explain the phenomenon on the basis of the classical principle of effective stress. In this section, it is intended to give an explanation based on the *general principle of effective stress* described above.

The mechanics of one dimensional collapse process can be represented by means of a simple analogy as in Fig. 8.32. Fig. 8.32(a) shows a spring inside a cylinder filled with water and air and a piston, fitted with a valve, on top of the spring. It is assumed that there is no friction between the piston and the cylinder. The spring represents the compressible soil skeleton, the water and air in the cylinder the pore water and pore air, respectively. The ratio of the volume of water to the total volume (water and air) represents the initial degree of saturation. The compressibility of the spring is a function of the degree of saturation. The cylinder itself simulates the condition of no lateral strain in the soil. Because of the tension on the water surface, there is an effective stress $\Delta p'_0$ acting on the spring, which is the contribution of the initial suction in the system.

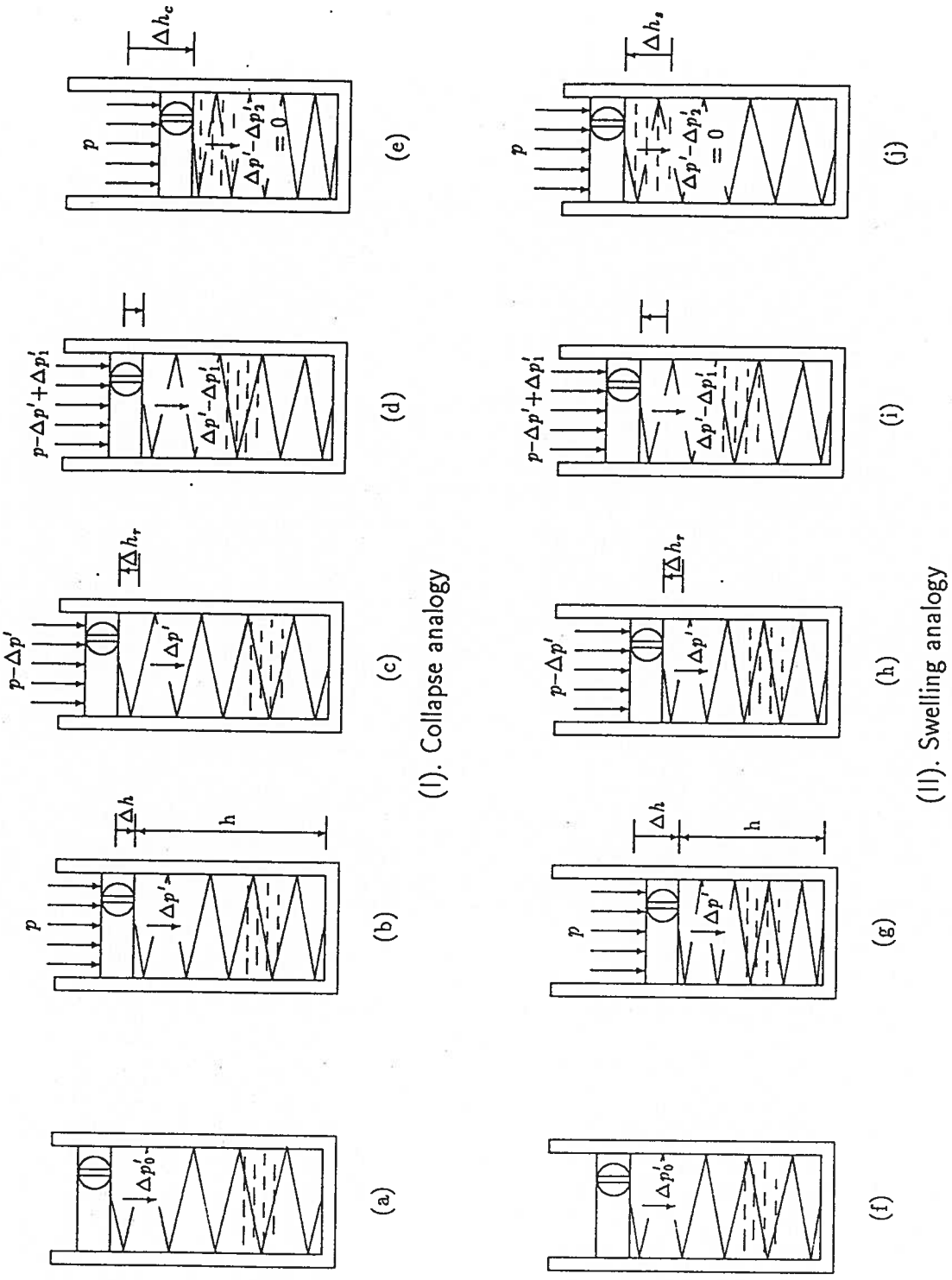

Figure 8.32: Analogy of collapse and swelling

Suppose a load p is now applied on the piston with the valve open (air pressure is equal to atmosphere). Assuming air to be compressible and water incompressible, the piston will move downward. The amount of movement depends on the compressibility of spring at the initial degree of saturation. The whole system will come to an equilibrium at load p, as in Fig. 8.32(b). After the piston comes to an equilibrium of deformation, the saturation ratio becomes S_r due to settlement deformation and suction changes to $\Delta p'$ because of the change in saturation ratio. The total effective stress acting on the spring is equal to $p + \Delta p'$. This situation corresponds to the consolidation of the soil at plane strain condition.

If the load is now decreased, and because unloading is not accompanied by large change of saturation ratio, the spring will rebound. The amount of rebound depends on the rebounding ability at saturation ratio S_r. When the decrease of external load is equal to the contribution of suction $\Delta p'$, the amount of rebound is Δh_r. The system arrives at new equilibrium of stress and deformation as shown in Fig. 8.32(c). The effective stress acting on the spring is equal to the initial external load p.

Next, water is introduced into the cylinder. During this process, saturation ratio will increase and suction will decrease. Assume at time t that the reduction of suction-induced effective stress is $\Delta p'_1$. In order to maintain the effective stress being constant, the external load is increased simultaneously an increment of $\Delta p'_1$. The change of degree of saturation will result in the change of compressibility of the spring. For collapsible soil, the compressibility usually increases with saturation ratio. Therefore, a new settlement occurs (Fig. 8.32(d)). As water is continuously added into the cylinder, the compressibility of the spring continuously increases and so with the settlement. This corresponds to the process of wetting. Eventually, as shown in Fig. 8.32(e), the cylinder is fully filled with water, suction becomes zero and external load becomes p again. All the external load is carried by the spring and the piston comes to rest. The system comes to a new equilibrium, with a deformation Δh_c and air being replaced by water, which corresponds to the end of hydraulic collapse. Because one part of collapse deformation has been eliminated by rebounding, the total collapse deformation is $\Delta h_c - \Delta h_r$. It is evident, in the above analogy, that the collapse of soil is caused by the increase in the compressibility of spring which is the results of increasing the saturation ratio. The above analogy can also be described in a more general way in e–$\log p$ and e–$\log p'$ planes as follows.

Assume a set of samples to have identical initial void ratio, structure and stress history but different water contents. The typical compression curves of these samples are as shown in Fig. 8.33(a) with water content $w_5 > w_4 > w_3 > w_2 > w_1$. The curve with

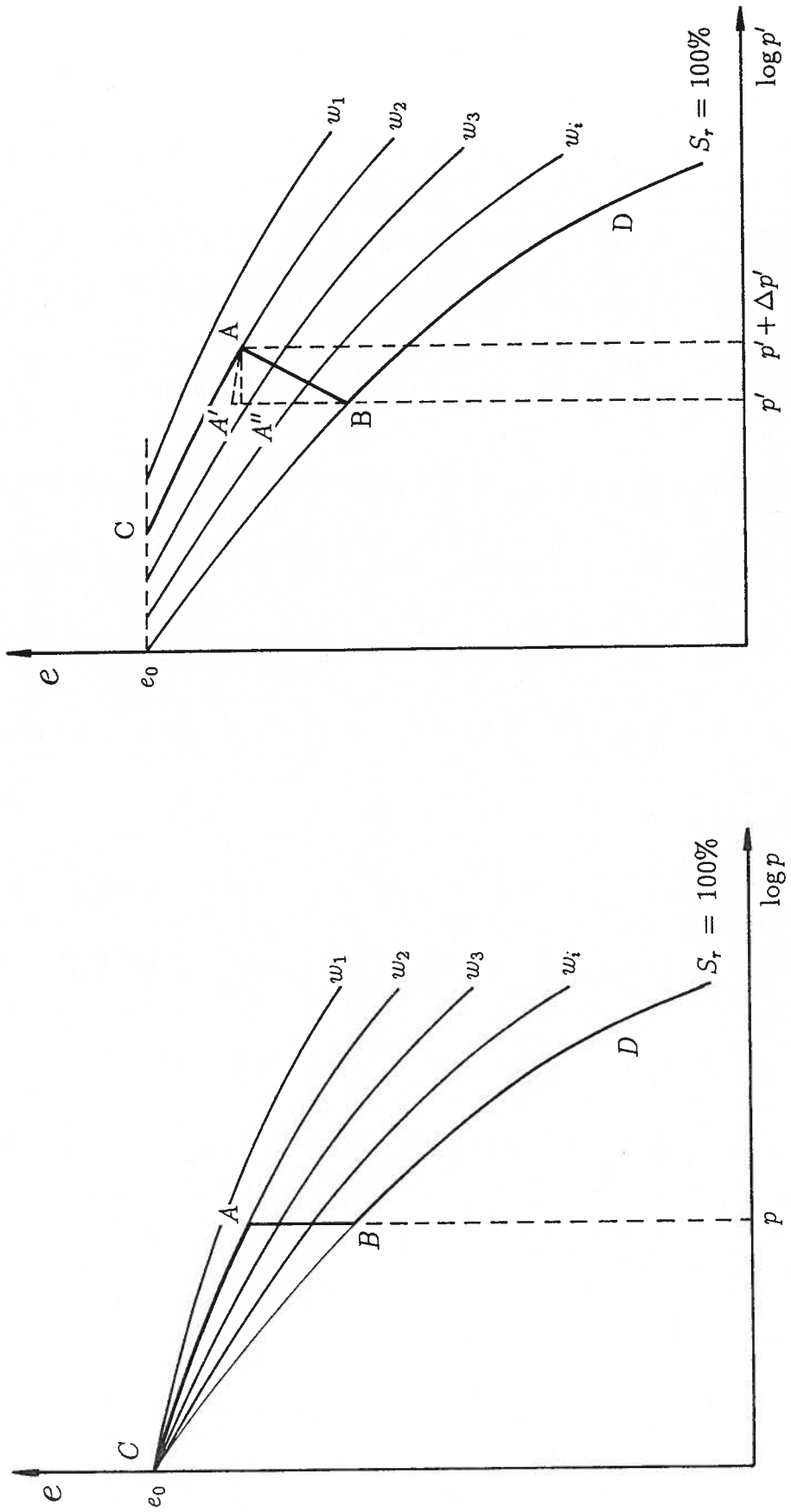

(a). Compression curves in total pressure

(b). Compression curves in effective pressure

Figure 8.33: Compression curves of the same soil at different water content

initial water content w_5 represents the curve when the soil is in a soaked or saturated state. From test results, it is known that the drier the soil, the less is the compression. If a sample of initial water content w_2 is consolidated to a pressure p and wetted at this pressure and then consolidated again, the locus of consolidation and wetting will follow the line $C \rightarrow A \rightarrow B \rightarrow D$. $A \rightarrow B$ is the collapse of soil caused by wetting at a constant external load p. Re-plotting the compression curves in terms of effective stress results in Fig. 8.33(b). Because of suction in partly saturated samples, the compression curves in e–$\log p$ plane move towards the right in e–$\log p'$ plane. The distance of movement is equal to the decrease in effective stress caused by suction action. Consider the collapse in state A. The last state after collapse is B. Because collapse occurred at a constant external pressure p, A and B fall in a vertical line in e–$\log p$ plane with the pressure equal to p. Assume the soil is fully saturated after wetting. Then, the effective stress at B is equal to the external stress (test is performed in drained condition), *i.e.*, $p_B = p = p'$. However, at point A, soil is partly saturated. The tension in the menisci causes negative pressure in pore water. The effective stress is larger than that at point B, *i.e.*, $p'_A = p' + \Delta p'$. Therefore, point A moves to the right of point B in Fig. 8.33(b). During soaking, the effective stress $\Delta p'$ disappears due to the increase in saturation ratio and volume decrease occurs.

Assume that the sample is unloaded from A, the water content is kept constant, and the change in saturation ratio is negligible during unloading. The deformation characteristics will not change at constant degree of saturation. Therefore, soil will rebound with a rebounding index κ_A because of the reduction in effective stress. This can be expressed by A' in Fig. 8.33(b). The amplified figure is given in Fig. 8.34. The void ratio at A and A' can be expressed as follows,

$$e_A = e_{1A} - C_{cA} \log\left(\frac{p' + \Delta p'}{p'_1}\right) \tag{8.19}$$

$$e_{A'} = e_A + \overline{A''A'} \tag{8.20}$$

where e_{1A} is the void ratio at p'_1 on compression curve w_2, and C_{cA} is the compression index at A.

Now, let the water get into the soil at a constant effective stress p'. Because the compressibility of soil is a function of the degree of saturation and it increases as the saturation ratio increases, e_{1A} and the compression index will change. As the soil becomes fully saturated due to wetting, e_{1A} will change to e_{1B} and compression index will change to C_{cB}. The void ratio at B is

$$e_B = e_{1B} - C_{cB} \log\left(\frac{p'}{p'_1}\right) \tag{8.21}$$

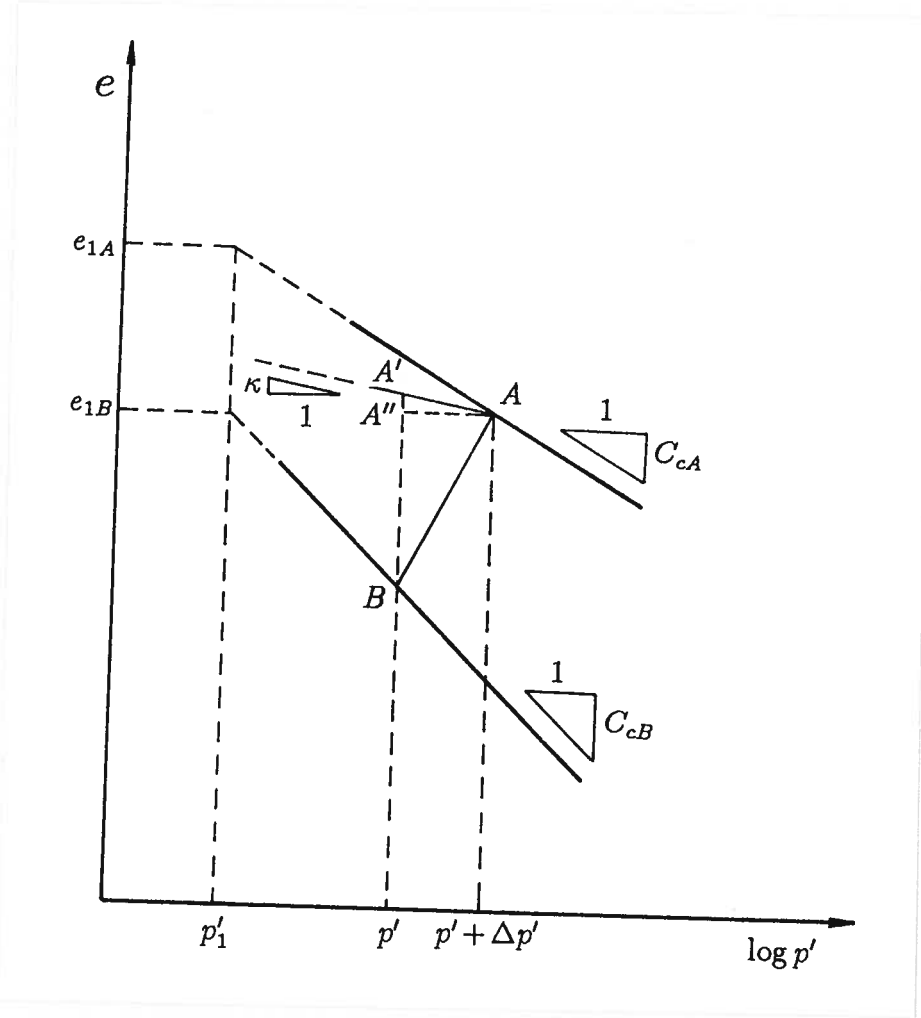

Figure 8.34: Change of effective stress and void ratio during wetting

The deformation induced by the change in compressibility which is caused by the increase in degree of saturation is $\overline{A'B}$ and

$$\overline{A'B} = e_{A'} - e_B \tag{8.22}$$

or

$$\overline{A'B} = e_{A'} - e_B = (e_{1A} - e_{1B}) - C_{cA}\log(\frac{p' + \Delta p'}{p'_1}) + C_{cB}\log\frac{p'}{p'_1} + \overline{A''A'} \tag{8.23}$$

It is evident that the collapse is caused by the saturation induced change of soil properties. It is noted that the magnitude of collapse calculated by Eq. 8.23 is larger than the measured value $\overline{A''B}$. This is because in the measured value, one part of the collapse deformation $\overline{A'A''}$ has been offset by the rebounding deformation $\overline{A''A'}$. The net collapse deformation should be

$$\overline{A''B} = \overline{A'B} - \overline{A''A'} = e_A - e_B = \Delta e \tag{8.24}$$

or

$$\Delta e = (e_{1A} - e_{1B}) - C_{cA}\log(\frac{p' + \Delta p'}{p'_1}) + C_{cB}\log\frac{p'}{p'_1} \tag{8.25}$$

Because for a given water content (or degree of saturation), the compression index is a function of the effective stress p', the void ratio on the compression curve can be expressed as

$$e = -0.434\int_{p'_0}^{p'}\frac{C_{c(w_i)}}{p'}dp' \tag{8.26}$$

and Eq. 8.25 becomes

$$\Delta e = -0.434\int_{p'_0}^{p'+\Delta p'}\frac{C_{c(w_2)}}{p'}dp' + 0.434\int_{0}^{p'}\frac{C_{c(w_5)}}{p'}dp' \tag{8.27}$$

where p'_0 is the initial suction-induced effective stress.

Based on the *general principle of effective stress*, not only collapse but also swelling can be explained reasonably. In the case of swelling, the first three steps (Fig. 8.32(f), (g) and (h)) are the same as (a), (b) and (c). Now, introduce water into the cylinder. Suction will decrease as the saturation ratio increases. In order to maintain constant effective stress, increase the external load by an increment equal to the reduction in effective stress caused by suction. Because of the hydration between water and expansive clay, the compressibility of the spring decreases with the increase in the degree of saturation, and, therefore the spring rebounds and the piston moves further upward (Fig. 8.32(i)). Eventually, the system will come to an equilibrium of saturation ratio, deformation and stress. Air is replaced by water, suction becomes zero, the effective stress acting on the spring is equal to the external load p, and the piston moves by an amount equal to Δh_s during the replacement of air with water (Fig. 8.32(j)). The total deformation caused by the reduction of effective stress and the increase in saturation ratio will be $\Delta h_r + \Delta h_s$.

8.6 SUMMARY

The classical principle of effective stress is established based on saturated soils and can only be applied in fully saturated soil. The extension of this principle to partly saturated soil has been attempted by many individuals. However, because of the misconception of unity of strength and deformation characteristics of soil, the extension is unable to explain satisfactorily the phenomenon occurring in partly saturated soil. In this chapter, based on the observation of test results, a *General Principle of Effective Stress* has been proposed. The phenomenon of wetting-induced collapse as well as swelling in soil can be satisfactorily explained based on this general principle. According to this general principle of effective stress, the hydraulic collapse is caused by the change of strength and deformation characteristics with degree of saturation.

Chapter 9

THE MECHANISM OF SOFTENING CAUSED BY COLLAPSE HISTORY

The variation of strength and deformation characteristics of soil which experienced different hydraulic collapse has been reported in Sections 6.4.2, 6.5.2, 7.2.2, 7.3.2. When investigating the effect of collapse history, samples have been brought to an approximately identical state of dry density and degree of saturation before the application of monotonic or cyclic shearing. It is to be noted that there are a little differences in the degree of saturation. However, the degrees of saturation after wetting are usually larger than 80%. In addition, tests are performed under constant volume condition. It is considered that under these conditions, the effect of suction is negligible. In order to understand the mechanism of the effect of collapse history on strength and deformation characteristics, *Scanning Electronic Microscope (SEM)* tests are performed on samples which have undergone different magnitude of collapse. The results are demonstrated in Photos 9.1 to 9.5. In each pair of micrograph, the dry density is approximately the same.

Photo. 9.1(a) shows the micrograph of *TKSC* (Mixture of Toyoura sand and 15% kaolinite) soil which had undergone high collapse. The soil is found to have its sand particles mostly coated by clay with a few clay bridges. The distribution of soil particle is relatively homogeneous. In Photo. 9.1(b), the soil almost experienced no collapse in its collapse history. Besides the existence of a number of macro-pores which can be seen with naked eye, the sand particles are more bridged by clay than in soil which had undergone high collapse in collapse history. The macro-pores are formed at the time of sample preparation. Because these samples are of relatively high molding water content, soil particles have the tendency to glue together and form numerous visible macro-pores. Although the sample has deformed during consolidation, the pores are still visible to the naked eye even at the end of the test. It is interesting to note that no collapse has occurred when additional water is introduced into sample even though these macro-pores exist. In fact, water is drained out in the process of consolidation. Although water is passed through the sample, no additional water is absorbed by the soil during soaking. This

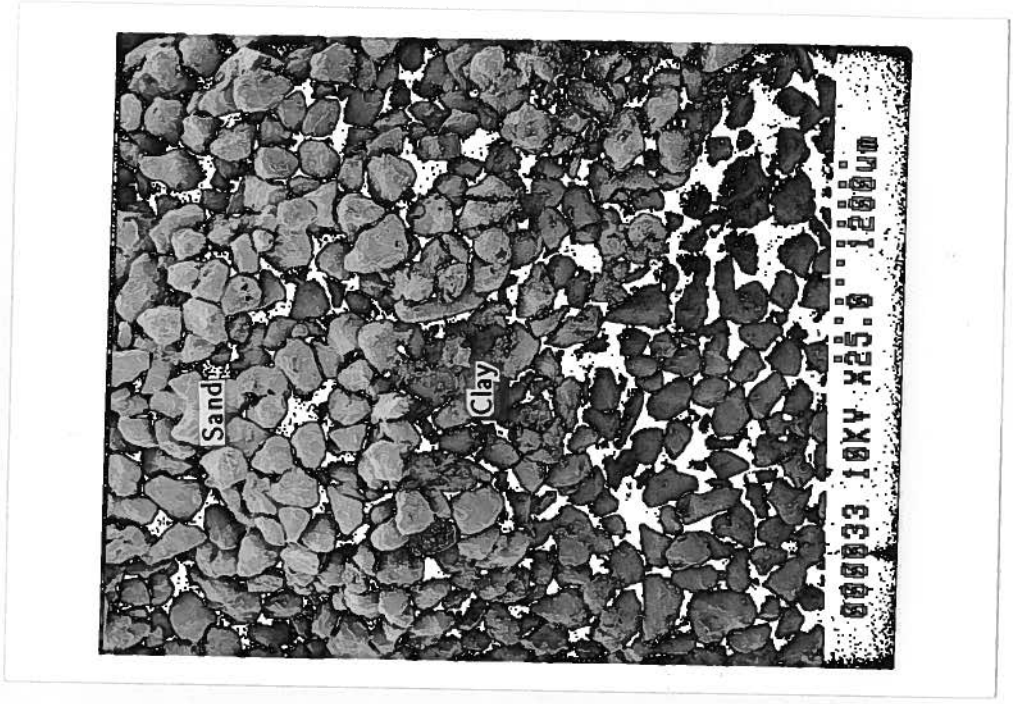

(a). SEM micrograph for soil which has undergone high collapse

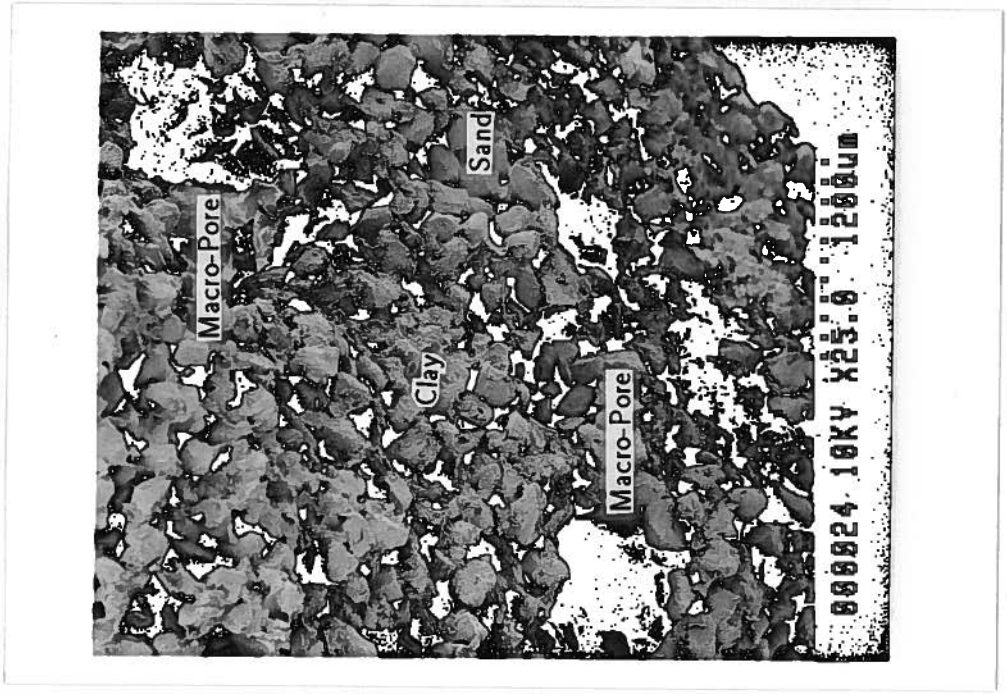

(b). SEM micrograph for soil which has undergone low collapse

Photo. 9.1: SEM micrograph for TKSC soil which has undergone different collapse (×25)

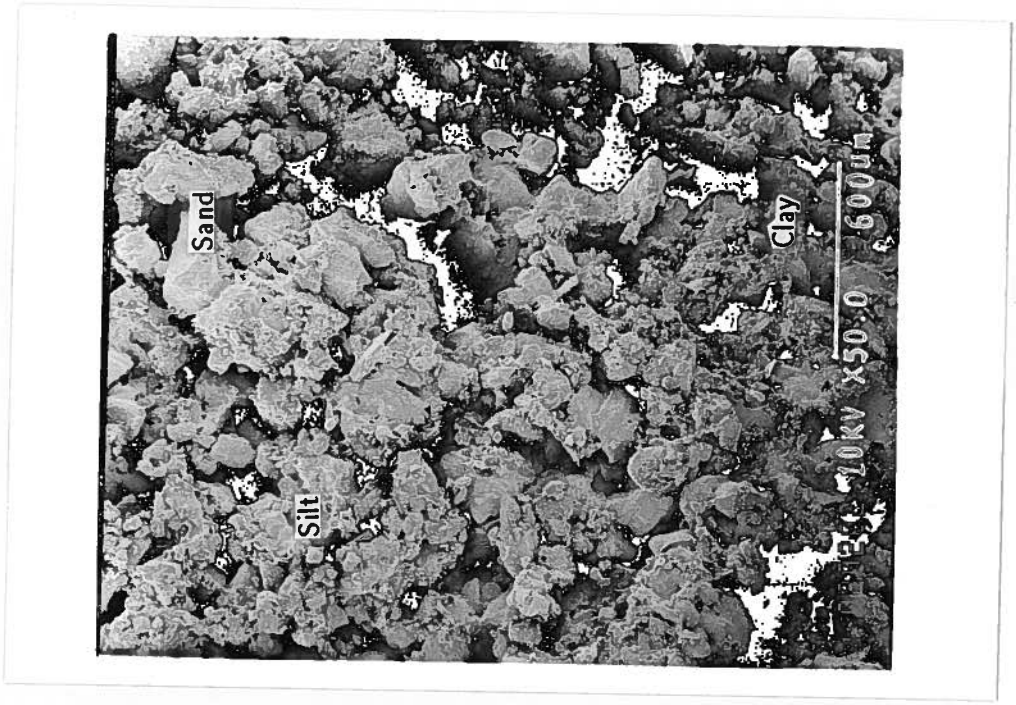

(a). SEM micrograph for soil which has undergone high collapse

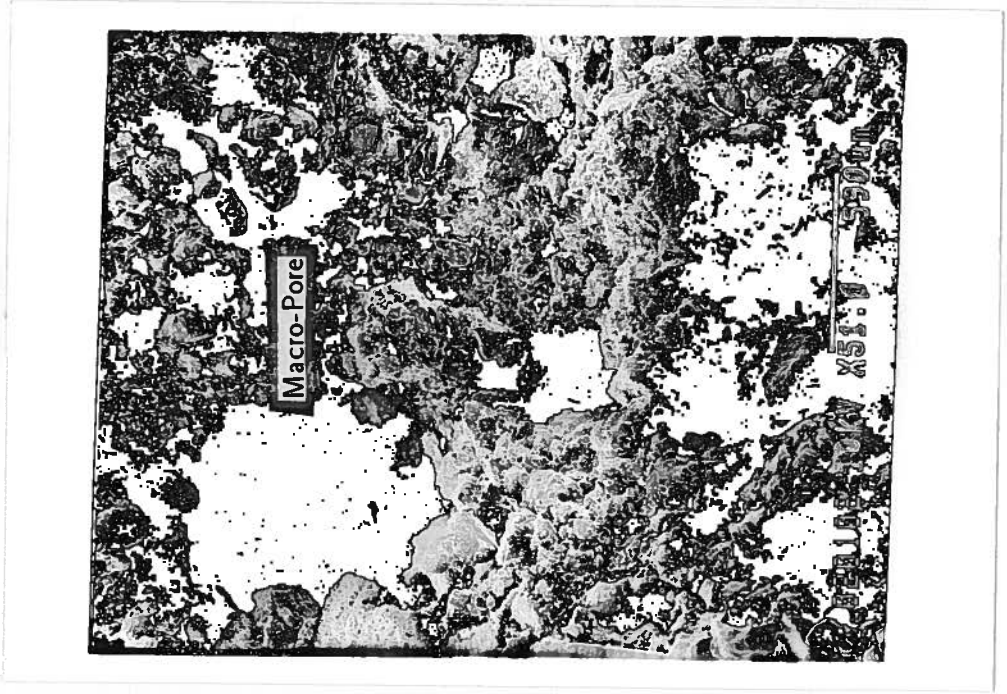

(b). SEM micrograph for soil which has undergone low collapse

Photo. 9.2: SEM micrograph for CBSM soil which has undergone different collapse (×50)

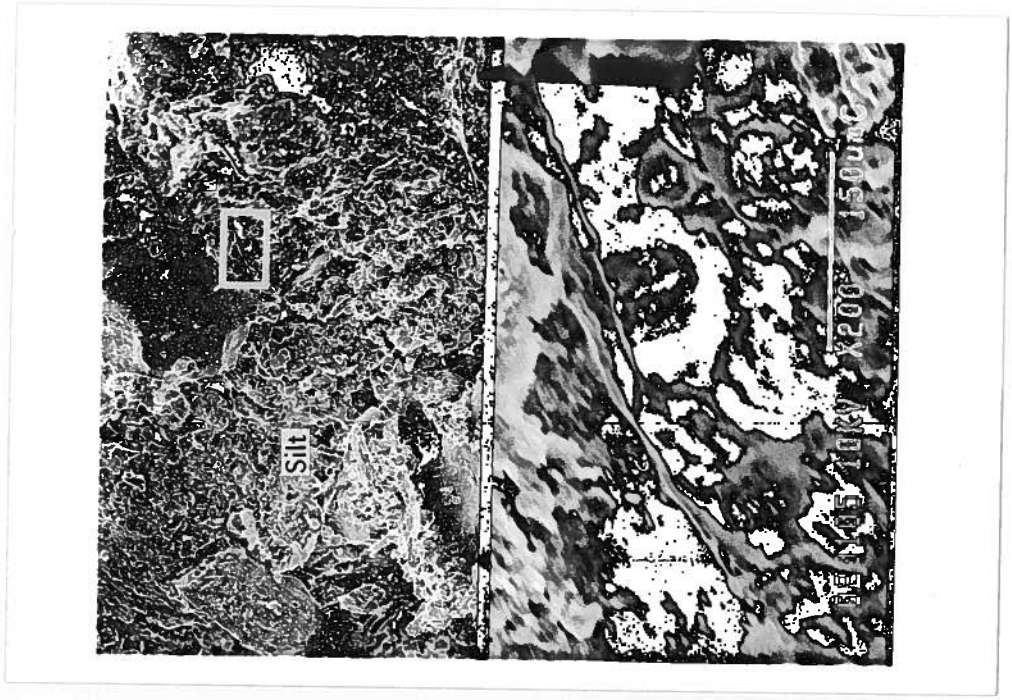

(a). SEM micrograph for soil which has undergone high collapse

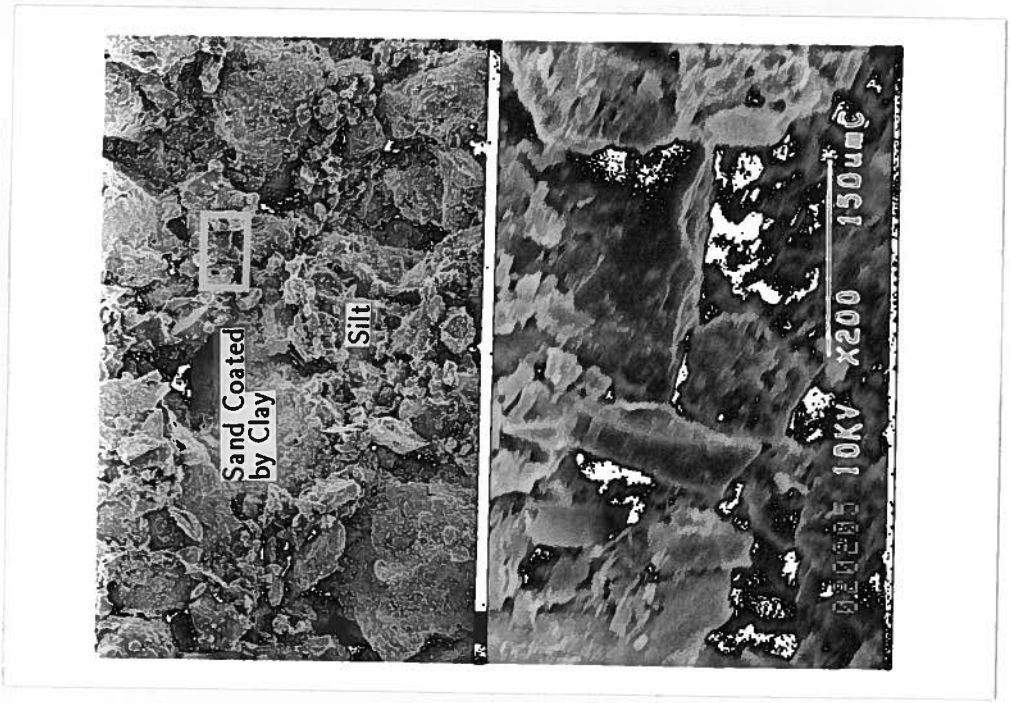

(b). SEM micrograph for soil which has undergone low collapse

Photo. 9.3: SEM micrograph for CBSM soil which has undergone different collapse (×200)

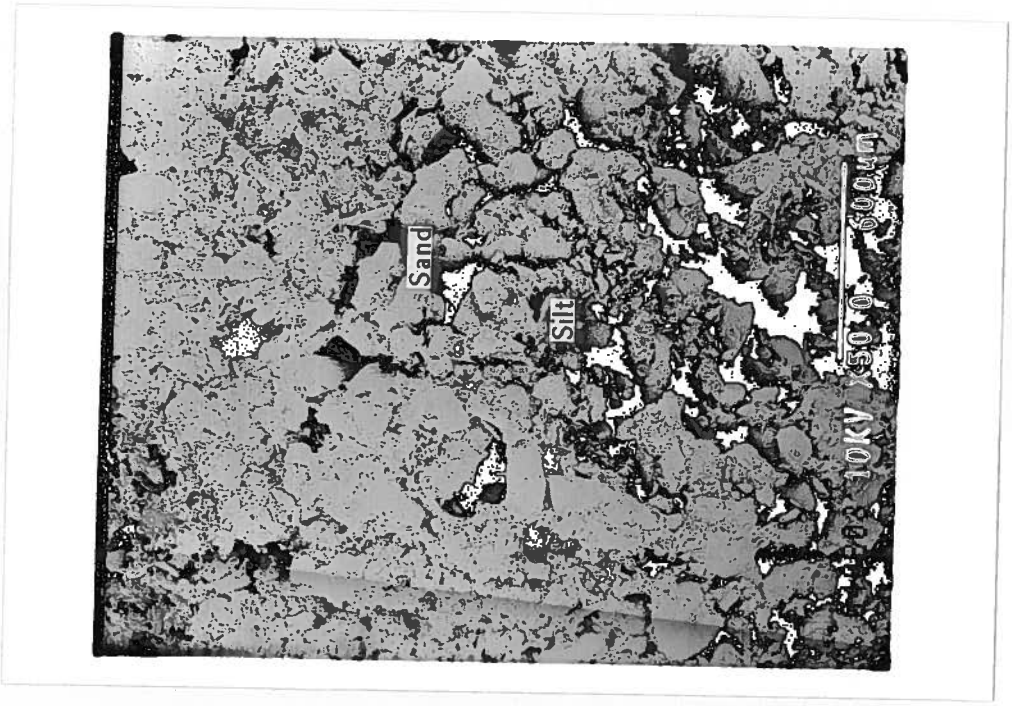

(a). SEM micrograph for soil which has undergone high collapse

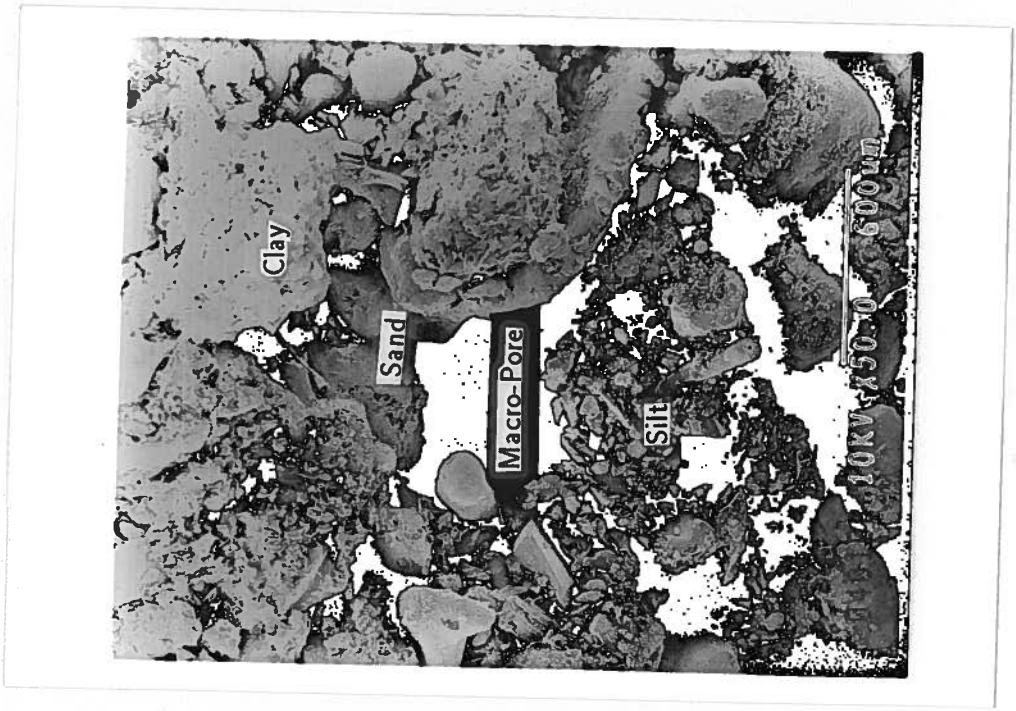

(b). SEM micrograph for soil which has undergone low collapse

Photo. 9.4: SEM micrograph for OTSC soil which has undergone different collapse (×50)

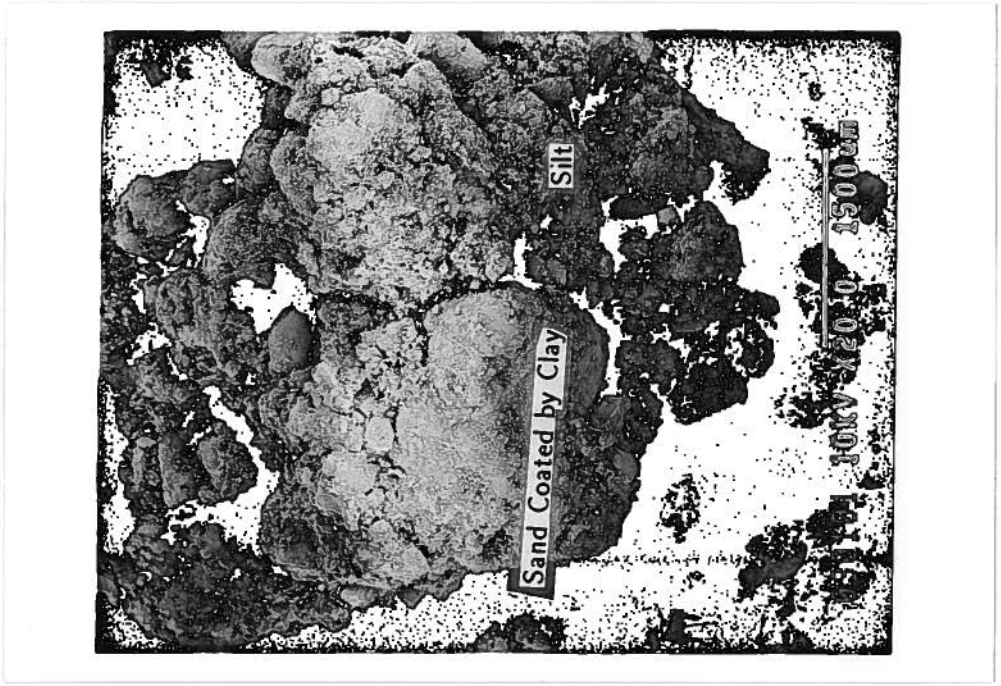

(a). SEM micrograph for soil which has undergone high collapse

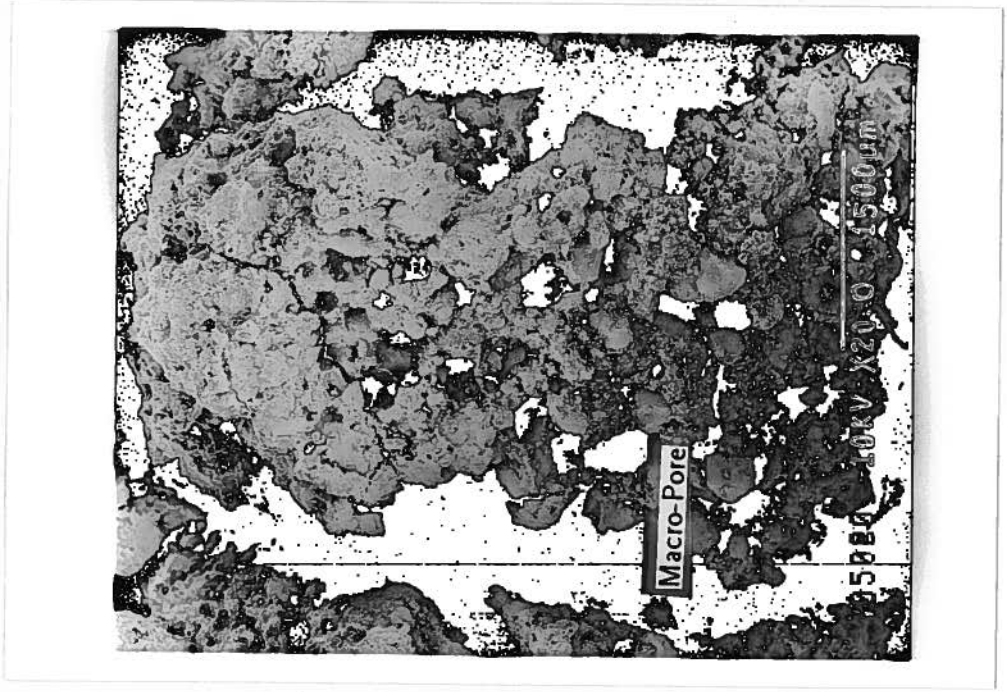

(b). SEM micrograph for soil which has undergone low collapse

Photo. 9.5: SEM micrograph for MUSC soil which has undergone different collapse (×20)

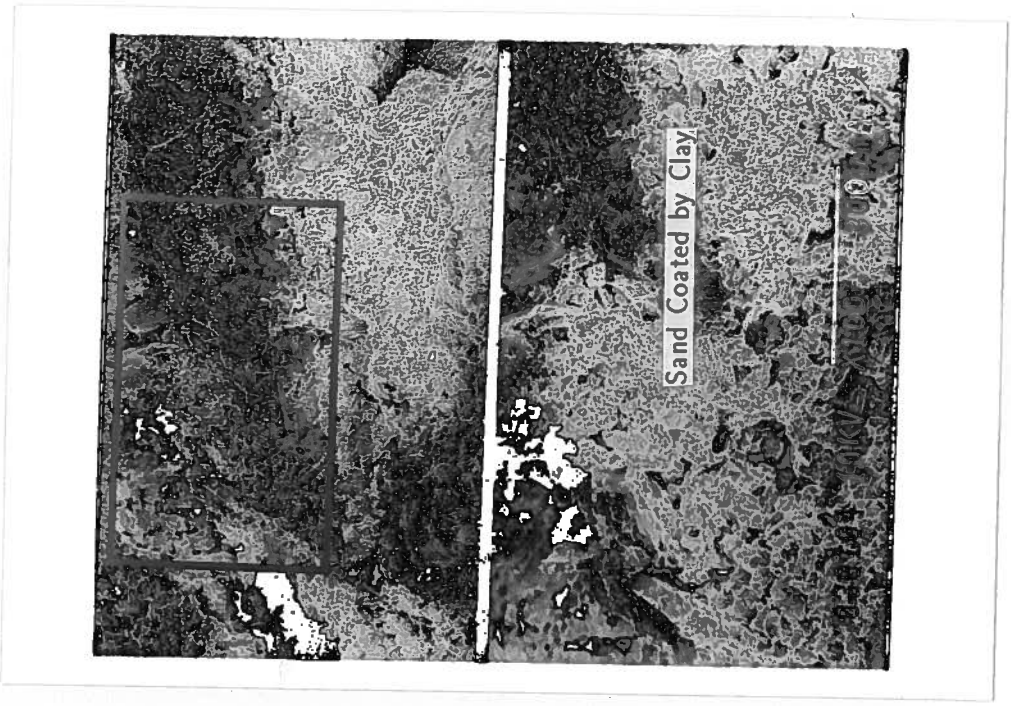

(a). SEM micrograph for soil which has undergone high collapse

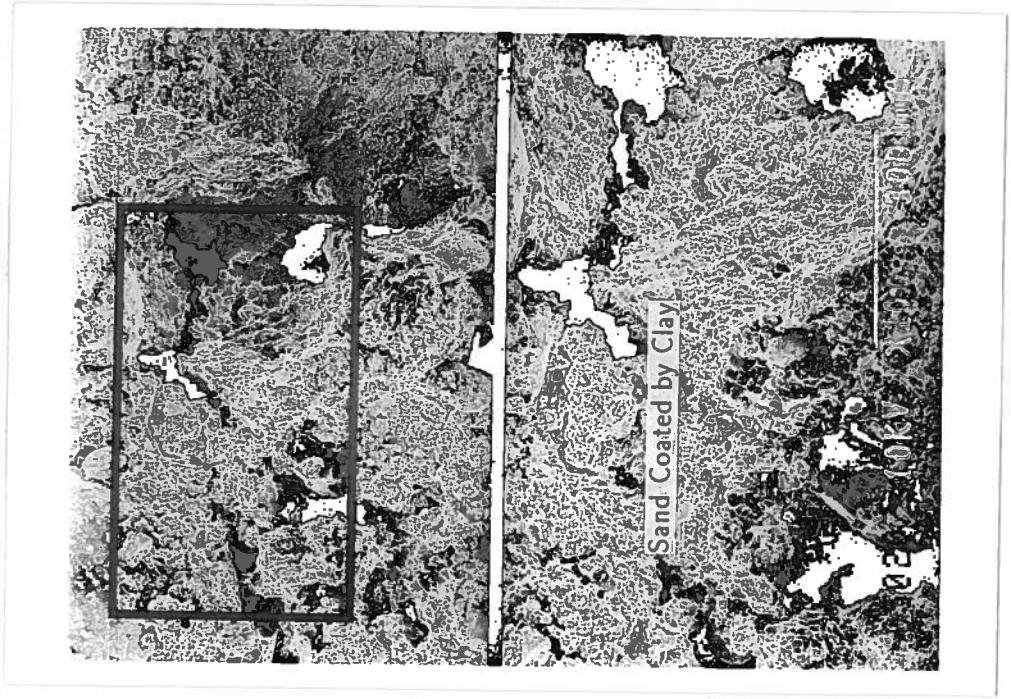

(b). SEM micrograph for soil which has undergone low collapse

Photo. 9.6: SEM micrograph for MUSC soil which has undergone different collapse (×100)

means that the governing factors which influence collapse are the removal of the capillary force and the solution of cemented agent upon inundation rather than the amount of clay and the shape of silt grains as proposed by Alwail (1990), although the shape of soil particles is also very important in controlling the amount of hydraulic collapse.

Photo 9.2 is the micrograph of *CBSM* (Chonan B silty sand) soil. This is a silty sand according to the Unified Classification System. The silt content is 31.9%. Similarly, the microstructure of the sample which experienced high collapse is shown in Photo 9.2(a). It is obvious that silt grains and clay aggregate to form bridges between sand particles. In addition, the sand particles are coated by clay. These bridges have been destroyed by water infiltration (Photo 9.3(a)). In Photo 9.2(b), macro-pores also appear. Silt grains and clay also blend and fill the micro-voids between sand particles(Photo 9.3(b)).

The micrograph of materials *OTSC* and *MUSC*, which are clayey sands according to the Unified Classification System, are illustrated in Photos 9.4 and 9.5. The macro-pores are still present in the sample of low collapse history. *MUSC* (Mutsuichikawa clayey sand) has relatively high fine content (23.7% silt, 16.0% clay). The voids between sand particles are fully filled with fine grains after collapse (Photo 9.5(a)). No big difference in the arrangement of soil particles can be seen except for the macro-pores (Photo 9.6). *OTSC* has less clay content (7.5%) than *MUSC*. In fact it may be classified as silty sand because it is in the borderline in the classification chart. Due to the less cohesiveness and, therefore, the difficulty in preparing the sample for *SEM* purpose, the quality of micrograph is not good enough. However, the existence of macro-pores is obvious. These macro-pores are visible with the naked eye during the removal of the sample after the test.

It can be seen from these microscopes that there exists difference in the micro-structure of the samples having different magnitudes of collapse. There is a common feature of the micro-structure, *i.e.*, macro-pores exist in the structure of the samples having low magnitude of hydraulic collapse while these macro-pores do not appear in the structure of the samples having high magnitude of hydraulic collapse. In other words, the samples wherein the hydraulic collapse is high is more homogeneous than that wherein the hydraulic collapse is low. Because the samples having different collapse history have the same void ratios, the macro-pores make a denser arrangement of soil particles around themselves. It is this denser arrangement of soil particles and the different bounding structures of silt and clay grains that make the samples of macro-pore structure possess higher shear resistance.

The fact that samples which experienced low hydraulic collapse are of higher shear-

ing resistance is of engineering significance in construction with compacted soils. It means that soil compacted at high water content not only shows low hydraulic induced deformation but also possesses higher shearing resistance. In practice, it might be easier to compact soil at lower water content. However, earth structure compacted at low water content will bear high collapse deformation when its moisture content, for any external reason, say heavy rain, rise in ground water level, first time storage in reservoir *etc.*, increases, and the shearing resistance after collapse is lower. Therefore, it is suggested that soil be always compacted at a moisture content high than the line of optimum.

The existence of macro-pores in the micro-structure of the soil which has low collapsibility further verifies that the governing factors of hydraulic collapse are the *low degree of saturation* and the *loose structure.* The two factors are inseparable. Collapse may not occur if any one of the two factors does not hold, *e.g.*, even though there exists macro-pore in the micro-structure of the soil, no collapse will occur if the degree of saturation is high. On the other hand, if the dry density is very high (dense structure), collapse will also not occur even though the degree of saturation is very low. The attempt to try to separate the two factors is meaningless.

Chapter 10

SUMMARY, CONCLUSIONS AND RECOMMENDATIONS

The phenomenon of hydraulic-induced collapse of some partly saturated soils has been noted decades ago. A number of papers and reports can be found dealing with the problem. In recent years, most of the work has been concentrated on the additional settlement caused by collapse and the mechanism of hydraulic collapse of soil. However, a series of catastrophic landslides which occurred recently in loessial deposits has warned geotechnical engineers to pay attention to the strength and deformation behaviors of collapsible soils. In this study, an attempt has been made to understand the strength and deformation characteristics, as well as the additional subsidence, of collapsible soils whether subjected to water infiltration or not. The degree to which the aim of the present investigation has been accomplished will be discussed in the following.

The study started with the state-of-the-art of the work on collapsible soils. The research on both natural and compacted soils has been reviewed. The lack of test data to understand the behavior of collapsible soils under monotonic and cyclic loading conditions is emphasized. Because wetting-induced collapse of soil structure is the fundamental problem of the soil, it has been decided to start the research from collapse tests and further extended to include the behavior under monotonic and cyclic loading conditions. In order to illustrate the importance of the study on strength and deformation behavior, twenty two failure cases which occurred in loessial and other collapsible soil deposits have been summarized. These case history can be traced back to the beginning of this century. These failure cases indicate that although there are several types of failure, the sliding failure, which is caused mostly by earthquakes as well as other reasons (*e.g.*, heavy rain, breakage of pipe lines, first time store of the reservoir, rise in ground water level, *etc.*), is the most dangerous and the loss is the largest. Some of the failures have been reviewed in detail.

The experimental work has been performed on five different materials: one artificial mixture of Toyoura sand and 15% commercial available kaolinite and four other materials

sampled from manufactured fills where failures have occurred during earthquakes. Detailed discussions of the test materials, apparatus and experimental procedures are given in Chapter 4.

The experimental investigation starts with the study of one-dimensional hydraulic collapse by the use of conventional consolidmeter. Factors influencing the magnitude of collapse, such as as-compacted dry density, molding water content, and overburden pressure, have been investigated in detail. It is to be noted that for compacted soils, there exists a certain range of molding water content and as-compacted dry density within which hydraulic collapse can most possibly occur. This range is estimated based on a series of compaction tests of different compacting energies. The initial state of dry density and water content of samples is within this estimated range. Two methods, *wetting tests* and *double-oedometer tests*, have been used to investigate the effect of different factors. The former, which follow the real stress path in-situ, are used to study the effect of initial conditions of dry density and water content, and the latter, which do not follow the real stress path in-situ, are conducted to study the effect of overburden pressure. Several comparable tests are performed to test and verify the comparability of the two methods. Test results show that they are comparable.

Chapter 6 is devoted mainly on the effect of collapsibility on strength and deformation behaviors of collapsible soils under cyclic loading condition. Tests are conducted on simple shear test apparatus. For partly saturated collapsible soil under seismic load action, the test conditions change depending on the wetting. In case that the soil is unwetted, soil is usually relatively dry and is in drained or partly drained condition even under seismic load action. In this case, liquefaction will never occur. On the other hand, if the soil is wetted, soil usually possesses relatively high degree of saturation and even fully saturated after being subjected to water infiltration. Therefore, an undrained condition is possible under seismic loading. If the soil is fully saturated, the undrained tests can be equivalent by undrained constant volume tests. Therefore, only the seismic behavior of wetted samples are investigated in this chapter, and all the tests are performed under plane strain and constant volume condition during the application of cyclic shearing. A detailed discussion has been devoted to the stress state and stress changes under constant volume condition and during shear. It has been found that the measured vertical load during shearing is equal to the algebraic difference of effective stress and the proportion of soil suction that contributes to the effective stress; in other words, the measured vertical stress during shearing is the intergranular stress caused by external load. In order to separate the effects of dry density and collapsibility on seismic strength of soil, samples are prepared such that the states of dry densities and saturation ratios of samples before the

application of cyclic loading are identical. The discussions on the state history of samples before shearing are also given. Test results show that cyclic shear strength decreases as the magnitude of collapse increases.

The third category of tests are concerned with the behavior of collapsible soils under monotonic loading condition. Two series of tests are performed: wetted and unwetted, and wetted and of high or low magnitude of collapse. Similar to the investigation of seismic behavior of collapsible soil, the test conditions are determined according to wetting condition. In case that the soil is unwetted, the drained and volume changeable conditions are considered to be suitable. Tests are conducted under these conditions. On the other hand, if the soil is wetted, the undrained condition is considered to be possible. The undrained and constant volume tests are performed to imitate the situation that soil is fully saturated and failure occurs relatively fast. For comparison, undrained and constant volume tests are also conducted on unwetted samples. All the tests mentioned above belong to the first series and are used to investigate the wetting-induced strength decrease. In order to study the effect of collapsibility on strength and deformation properties of collapsible soils under monotonic loading condition, similar to the cases of cyclic tests, samples are prepared such that they experience different collapse history but reach an identical state of dry density and saturation ratio before the application of monotonic loading. The test results demonstrate that wetting changes the degree of saturation and drainage condition and results in tremendous loss in shear strength, and shear strength decreases as the increase in the value of hydraulic collapse.

The classical principle of effective stress has been proven to be invaluable to the engineer who is concerned with the prediction of soil behavior, and, in fact, has come to be regarded by many foundation engineers as axiom. The value of Terzaghi's effective stress principle lies on the fact that it enables the behavior of soil undergoing changes in σ and u to be related to a single variable. The fundamental role played by Terzaghi's principle of effective stress in the prediction of the behavior of fully saturated soils has led workers in attempting to extend the concept to cover partly saturated soils. However, the extensions come up against the difficulties in explaining the phenomenon of wetting-induced collapse. In Chapter 8, a detailed review of Terzaghi's principle of effective stress and the prerequisite for application have been given. The reason for the failure of these extensions to explain the phenomenon of wetting-induced collapse has been found to be the misconception of the unity of strength and deformation characteristics of soil under fully saturated and partly saturated conditions. A series monotonic shear tests have been conducted on samples of different molding saturation ratios but the same dry densities to demonstrate further the change of strength and deformation properties of collapsible

soil with degree of saturation. Based on the test results and the results presented in the previous chapters, and those of other individuals on partly saturated soils, a *General Principle of Effective Stress* has been proposed, which indicates that all the measurable variation of strength and deformation are due exclusively to the changes in effective stress and/or degree of saturation; the effective stress is regarded as the stress transmitted by the skeleton of soil which is equal to algebraical sum of exogenous effective stress and endogenetic effective stress; for a given soil, the stiffness and strength parameters are the exclusive functions of degree of saturation and reach the limits at degree of saturation of 100%. Upon reaching full saturation, the *General Principle* becomes the classical principle.

Based on the *General Principle of Effective Stress*, an explanation of the phenomenon of wetting-induced collapse as well as swelling has been given, which prove that the said principle can explain both the phenomena well.

Detailed discussions on the mechanism of the effect of collapse history on strength and deformation characteristics of collapsible soils are given Chapter 9. The difference in strength and deformation behaviors of samples which have experienced different collapse history is caused by the microstructure difference of the samples. The presence of a large number of macro-pores on samples which have undergone little collapse accounts for the denser soil structure around the macro-pores, and this further makes the sample possess higher shearing resistance. The existence of macro-pores in samples which have experienced little collapse further verifies that the low saturation ratio and the loose structure are the governing factors of the occurrence of hydraulic collapse. The two factors are inseparable.

From this study, the following main conclusions can be made:

- Wetting changes the degree of saturation and drainage condition, and this makes that the occurrence of liquefaction is possible in collapsible soil which used to possess relatively high strength and will never liquefy if no water infiltration occurs.
- The shear strength of collapsible soil decreases tremendously upon the soil being subjected to water permeation and collapsed.
- Both the static and seismic strength decreases as the magnitude of collapsibility increases.
- The strength and deformation behaviors of partly saturated soil are exclusively functions of effective stress and degree of saturation.

Based on this study, it is suggested that:

1. For partly saturated collapsible soil deposits, it should investigate *any* possibility of hydraulic collapse. If this hydraulic collapse is possible, both the static and seismic strength and deformation properties of the soil should be studied at *wetted condition* to examine the stability of the deposits.

2. Collapsible soils should be always compacted at a moisture content higher than the *line of optimum*.

Bibliography

[1] Abelev, I. M. (1968). "Principles of Planning and Execution in Collapsible Loess Soils," *Gosstroiizdat*, Moscow.

[2] Aitchison, G. D. (1960), "Relationships of Moisture Stress and Effective Stress Functions in Unsaturated Soils," *Proc. Conference Pore Pressures*, Butterworths, London.

[3] Aitchison, G. D. (1973), "Problems of Soil Mechanics and Construction on Soft Clays and Structurally Unstable Soils (Collapsible, Expansive and Others)," *Proc. 8th International Conference on Soil Mechanics and Foundation Engineering*, 3, Moscow, pp.161–190.

[4] Aitchison, G. D. and Donald, I. B. (1956), "Effective Stresses in Unsaturated Soils," *Proc. 2nd Australia-New Zealand Conference on Soil Mechanics and Foundation Engineering*, Christchurch, N.Z., pp. 192–199.

[5] Akinmusuru, J. O. (1987), "The Effect of Cementation on the Stress–Strain Behavior of a Sand," *Proc. 9th Regional Conference for Africa on Soil Mechanics and Foundation Engineering*, 1, Lagos, pp. 435–442.

[6] Allam, M. M. and Sridharan, A. (1981), "Effect of Wetting and Drying on Shear Strength," *Journal of Geotechnical Engineering*, ASCE, 107(4), pp. 421–438.

[7] Al Mohammadi, N. M. and Nashaat, I. H. (1987), "Compressibility and Collapse of Gypseous Soils," *Proc. 8th Asian Regional Conference on Soil Mechanics and Foundation Engineering*, 1(2/1), Kyoto, pp. 151-154.

[8] Alonso, E. E., Gens, A. and Josa, A. (1990), "A Constitutive Model for Partially Saturated Soils," *Géotechnique*, 40(3), pp. 405–430.

[9] Alwail, T. A. (1990), "Mechanism and Effect of Fines on the Collapse of Compacted Sandy Soils," dissertation presented to Washington State University, Pullman, Washington, in partial fulfillment of the requirements for the degree of Doctor of Philosophy.

[10] Alwail, T., Ho, C. L. and Fragaszy, R. J. (1991), "Collapse Mechanisms of Low Cohesion Compacted Soils," *Proc. 9th Pan-American Conference on Soil Mechanics and Foundation Engineering*, 1, Vinadelmar, Chile.

[11] Amirsoleymani, T. (1989), "Mathematical Approach to Evaluate the Behavior of Collapsible Soils," *Proc. 12th International Conference on Soil Mechanics and Foundation Engineering*, 1, Rio de Janeiro, pp. 575–582.

[12] Austerlitz, G., Ishai, I. and Komornik, A. (1983), "Prediction of Collapse Potential in Israeli Loess Subgrades," *Proc. 7th Asian Regional Conference on Soil Mechanics and Foundation Engineering*, 1, Israel, pp. 106–111.

[13] Bara, J. P. (1976), "Collapsible Soils," *presented at the September 1976, ASCE Annual Convention and Exposition, held at Philadelphia, Pa.*

[14] Barden, L., Madedor, A.O. and Sides, G. R. (1969), "Volume Change Characteristics of Unsaturated Clay," *Journal of Soil Mechanics and Foundations Division*, ASCE, 95(1), pp.33–53.

[15] Barden, L., McGown, A. and Collins, K. (1973), "The Collapse Mechanism in Partly Saturated Soil," *Engineering Geology*, 7, pp. 49–60.

[16] Barden, L. and Sides, G. R. (1970), "Engineering Behavior and Structure of Compacted Clay," *Journal of Soil Mechanics and Foundations Division*, ASCE, 96(4), pp. 1171–1200.

[17] Barden, L. and Sides, G. R. (1971), "Sample Disturbance in the Investigation of Clay Structure," *Géotechnique*, 21(3), pp. 211–222.

[18] Berezantzev, V. G., Mustafayev, A. A., Sidorov, N. N., Kovalyov, I. V. and Aliev, S. K. (1969), "On the Strength of Some Soils," *Proc. 7th International Conference on Soil Mechanics and Foundation Engineering*, 1, Mexico, pp. 11–19.

[19] Bhatia, S. K. and Quast, D. (1984), "The Behavior of Collapsible Soil Under Cyclic Loading," *Fourth Australia – New Zealand Conference on Geomechanics*, Perth, pp. 73–77.

[20] Bishop, A. W. (1959), "The Principle of Effective Stress," *Teknisk Ukeblad*, 106(39), pp. 859–863.

[21] Bishop, A. W. and Blight, G. E. (1963), "Some Aspects of Effective Stress in Saturated and Partly Saturated Soils," *Géotechnique*, 13, pp. 177–197.

[22] Bishop, A. W. and Donald, I. B. (1961), "The Experimental Study of Partly Saturated Soil in the Triaxial Apparatus," Proc. 5th International Conference on Soil Mechanics and Foundation Engineering, 1, Dunod, Paris, pp. 13–21.

[23] Bishop, A. W. and Eldin, G. (1950), "Undrained Triaxial Tests on Saturated Sands and Their Significance in The General Theory of Shear Strength," *Géotechnique*, 2(1), 13–32.

[24] Bjerrum, L. (1954), "*Theoretical and Experimental Investigations on the Shear Strength of Soils*," *Norwegian Geotechnical Institute Publication 5*, Oslo, 113pp.

[25] Bjerrum, L. and Landva, A. (1966), "Direct Simple-Shear Tests on A Norwegian Quick Clay," *Géotechnique*, 16(1), pp. 1–20.

[26] Blight, G. E. (1965), "A Study of Effective Stresses for Volume Change," *Proc. International Research Conference on Expansive Clay Soil*, Texas, 1, pp. 259–269.

[27] Blight, G. E. (1967), "Effective Stress Evaluation For Unsaturated Soils," *Journal Soil Mechanics and Foundations Division*, ASCE, 93(2), pp. 125–148.

[28] Booth, A. R. (1975), "Factors Influencing Collapse Settlement in Compacted Soils," *Proc. 6th Regional Conference for Africa on Soil Mechanics and Foundation Engineering*, 1, Durban, South Africa, pp. 57–66.

[29] Booth, A. R. (1977), "Collapse Settlement in Compacted Soils," *CSIR Research Report 324*, NITRR Bulletin 13, Pretoria, South Africa.

[30] Brackley, I. J. A. (1971), "Partial Collapse in Unsaturated Expansive Clay," *Proc. 5th Regional Conference for Africa on Soil Mechanics and Foundation Engineering*," 1, pp. 23–30.

[31] Brandon, T. L., Duncan, J. M. and Gardner, W. S. (1990), "Hydrocompression Settlement of Deep Fills," *Journal of Geotechnical Engineering*, ASCE, 116(10), pp. 1536–1548.

[32] Brink, A. S. A., Partridge, T. C. and Williams, A. A. B. (1982), "Engineering Soil Problems," *Soil Survey for Engineering*, Clarendon Press Oxford, pp. 118–124.

[33] Bull, W. D. (1964), "Alluvial Fans and Near-surface Subsidence in Western Fresno County," *Geological Survey Professional Paper 437–A*, Washington, pp71.

[34] Burland, J. B. (1961), Discussion, Section 1, *Proc. 5th International Conference on Soil Mechanics and Foundation Engineering*, Donud, Paris, 3, pp. 120.

[35] Burland, J. B. (1965), "Some Aspects of the Mechanical Behavior of Partly Saturated Soils," *Moisture Equilibria and Moisture Changes in Soils Beneath Covered Areas*, Butter Worths, Australia, pp. 270–278.

[36] Casagrande, A. (1932), "The Structure of Clay and its Importance in Foundation Engineering," *J. Boston Soc. of Civil Engineers*, 19(4), pp. 168–209.

[37] Chen, Z. Y., Qian, H.J. and Bao, C.G. (1987), "Problems of Regional Soils," *Proc. 8th Asian Regional Conference on Soil Mechanics and Foundation Engineering*, 2, Kyoto, Japan, pp. 167–190.

[38] Clemence, S. P. and Finbarr, A. O. (1981), "Design Consideration for Collapsible Soils," *Journal of Geotechnical Engineering*, ASCE, 107(3), pp. 305–317.

[39] Close, U. and McCormick, E. (1922), "Where the Mountains Walked," *The National Geographic Magazine*, XLI(5).

[40] Cooling, L. F. and Smith, D. B. (1936), "The Shearing Resistance of Soils," *Proc. 1st International Conference on Soil Mechanics and Foundation Engineering*, Harvard University, Cambridge, Mass., 1, pp. 37–41.

[41] Cox, D. W. (1978), "Volume Change of Compacted Clay Fill," *Proc. Conference on Clay Fills*, Institute of Civil Engineers, London, pp. 79–87.

[42] Craig, R. F. (1987), "Soil Mechanics,", Van Nostran Reinhold (UK) Co. Ltd, 4th edition.

[43] Croney, D., Coleman, J. D. and Black, W. P. M. (1958), "Movement and Distribution of Water in Soil in Relation to Highway Design and the Performance," *Highway Research Bd, Special Report No. 4.*

[44] Das, B. J. (1983), "Fundamentals of Soil Dynamics,", Elsevier Science Publishing Co., Inc.

[45] Day, R. W. (1990), "Sample Disturbance of Collapsible Soil," *Journal of Geotechnical Engineering*, ASCE, 116(1), pp. 158–161.

[46] Day, R. W. and Axten, G. W. (1991), "Softening of Fill Slopes due to Moisture Infiltration," *Journal of Geotechnical Engineering*, ASCE, 116(9), pp. 1424–1427.

[47] Denisov, N. J. (1946), "Settlement Properties of Loessial Soils," *Soviet Science*, U.S.S.R. Government Publishing Office, Moscow.

[48] Denisov, N.Y. (1951), "The Engineering Properties of Loess and Loess Loams," *Gosstroiizdat*, Moscow, 136 pp.

[49] Derbyshire, E. and Mellors, T. W. (1988), "Geological and Geotechnical Characteristics of Some Loess and Loessic Soils from China and Britain: A Comparison," *Engineering Geology*, 25(2-4), pp.135–176.

[50] DiBernardo, A. and Lovell, C.W. (1979), "The Effect of Laboratory Compaction on the Compressibility of a Compacted Highly Plastic Clay," Purdue University, West Lafayette, IN, Joint Highway Research Project Report 79-3.

[51] DiBernardo, A. and Lovell, C.W. (1984), "COMPACTIVE PRESTRESS EFFECTS IN CLAYS," *Transportation Research Record 945*, Washington, D. C. pp. 51–58.

[52] Donald, I. B. (1965), "SHEAR STRENGTH MEASUREMENTS IN UNSATURATED NON-COHESIVE SOILS WITH NEGATIVE PORE PRESSURE," *Proc. 2nd Australia-New Zealand Conference on Soil Mechanics and Foundation Engineering*, Christchurch, N.Z., pp. 200–204.

[53] Dudley, J. H. (1970), "REVIEW OF COLLAPSING SOILS," *Journal of Soil Mechanics and Foundations Division*, ASCE, 96(3), pp925–947.

[54] ECIWC (Eastern China Institute of Water Conservancy), (1982), "GEOTECHNICAL PRINCIPLES AND CALCULATIONS," (華東水利学院土力学教研室, 土工原理与計算, 水利電力出版社) (in Chinese).

[55] El-Sohby, M. A. and Elleboudy, A.M. (1987), "SWELLING AND COLLAPSIBLE BEHAVIOR OF UNSATURATED CEMENTED SAND UPON WETTING," *Groundwater Effects in Geotechnical Engineering, Proc. 9th European Conference on Soil Mechanics and Foundation Engineering*, 2, Boston, pp.553–556.

[56] El-Sohby, M.A., Sherif, M.M. and Elleboudy, A.M. (1989), "CRITICAL EVALUATION OF COLLAPSIBILITY MEASUREMENTS FOR CEMENTED SAND," *Proc. 12th International Conference on Soil Mechanics and Foundation Engineering*, 1, Rio de Janeiro, pp.593–596.

[57] El-Sohby, M.A. and Rabbaa, S.A. (1984), "DEFORMATIONAL BEHAVIOR OF UNSATURATED SOILS UPON WETTING," *Proc. 8th Regional Conference for Africa on Soil Mechanics and Foundation Engineering*, 1, Harare, pp. 129–137.

[58] El-Sohby, M.A., Rabbaa, S.A. El-Khoraibi, M.C. and El-Saadany, M.M. (1987), "INFLUENCE OF SOIL CONSTITUENTS ON COLLAPSIBLE SOILS," *Proc. 9th Regional Conference for Africa on Soil Mechanics and Foundation Engineering*, 1, Lagos, pp. 147–153.

[59] Feda, J. (1966), "STRUCTURAL STABILITY OF SUBSIDENT LOESS SOIL FROM PRAHA-DEJVICE," *Engineering Geology*, 1(3), pp. 201–219.

[60] Feda, J. (1971), "CONSTANT VOLUME SHEAR TESTS OF SATURATED SAND," *Archiv. Hydrot.*, 18(3), pp. 349–367.

[61] Finn, W. D. L. (1985). "ASPECTS OF CONSTANT VOLUME CYCLIC SIMPLE SHEAR," *Advances in the Art of Testing Soils Under Cyclic Conditions*, Edited by Vijay Khosla, New York. pp. 74–98.

[62] Fukuda, M. (1978), "DECREASE OF SHEAR-RESISTANCE OF SOIL DUE TO SUBMERGENCE AND STABILITY ANALYSIS OF EMBANKMENT SLOPE — WITH SPECIAL REFERENCE TO WEATHERING SANDY SOIL LIKE DECOMPOSED GRANITE SOIL

— ," *Soils and Foundations*, 18(3), pp. 75–83. (福田　護, 浸水に伴う土のせん断抵抗の低下と盛土斜面の一安定解析 — まさ土のような風化砂質土を対象として —, 土質工学会論文報告集) (in Japanese).

[63] Gao, G. (1988), "Formation and Development of the Structure of Collapsing Loess in China," *Engineering Geology*, 25(2-4), pp.235–246.

[64] Gibbs, H.J. (1961), "Properties Which Divide Loose and Dense Uncemented Soils," *U.S. Bureau of Reclamation, Report No. EM-608.* Denver, Colorado.

[65] Gibbs, H. J. and Bara, J.P. (1962), "Predicting Surface Subsidence from Basic Soil Tests," *Special Technical Publication No. 322*, American Society for Testing and Materials, pp. 231–247.

[66] Gibbs, H. J. and Bara, J.P. (1967), "Stability Problems of Collapsing Soils," *Journal of Soil Mechanics and Foundation Engineering Division*, ASCE, 93(4), pp. 577–594.

[67] Gibbs, H. J. and Holland, W. Y. (1960), "Petrographic and Engineering Properties of Loess," *Engineering Monograph No. 28*, U.S. Bureau of Reclamation.

[68] Grabowska-Olszewska, B. (1988), "Engineering-Geological Problems of Loess in Poland," *Engineering Geology*, 25(2-4), pp.177–200.

[69] Gubin, I. E., (1960), "Regime of Seismicity on the Territory of Tadjikistan," *Academy of Sciences Press*, U.S.S.R.

[70] Gulhati, S. K. and Satija, B. S. (1981). "Shear Strength of Partially Saturated Soils," *Proc. 10th International Conference on Soil Mechanics and Foundation Engineering*, 1, Stockholm, pp.609–612.

[71] Hardin, B. O. and Drnevich, V. P. (1972a), "Shear Modulus and Damping in Soils: Measurement and Parameter Effect," *Journal of the Soil Mechanics and Foundations Division*, ASCE, 98(6), pp. 603–624.

[72] Hardin, B. O. and Drnevich, V. P. (1972b), "Shear Modulus and Damping in Soils: Design Equations and Curves," *Journal of the Soil Mechanics and Foundations Division*, ASCE, 98(7), pp. 667–692.

[73] Henkel, D. J. (1959), "The Relationship Between The Strength, Pore-Water Pressure and Volume Change Characteristics of Saturated Clays," *Géotechnique*, 9(1), 119–135.

[74] Henkel, D. J. (1960), "The Relationship Between The Effective Stresses and Water Content in Saturated Clays," *Géotechnique*, 10(1), 41–54.

[75] Holtz, W. G. (1948), "The Determination of Limits for the Control of Placement Moisture in High Rolled Earth Dams," *Proc. ASTM*, Philadelphia, pp. 1240–1248.

[76] Holtz, W. G. and Hilf, J. W. (1961), "Settlement of Soil Foundations Due to Saturation," *Proc. 5th International Conference on Soil Mechanics and Foundation Engineering*, 1(3A/20), Dunod, Paris, pp. 673–679.

[77] Houston, S. L. (1988), "Pavement Problems Caused by Collapsible Subgrades," *Journal of Transportation Engineering*, ASCE 114(6), pp. 673–683.

[78] Houston, S. L., El-Ehwany, M. (1991), "Sample Disturbance of Cemented Collapse of Soils," *Journal of Geotechnical Engineering*, ASCE, 117(5), pp. 731–752.

[79] Houston, S. L., Houston, W. N. and Spadola, D. J. (1988), "Prediction of Field Collapse of Soils due to Wetting," *Journal of Geotechnical Engineering*, ASCE, 114(1), pp. 40–58.

[80] Huang, D. (1989), "A Laboratory Investigation on the Behavior of Collapsible Soil," *thesis presented to Colorado State University, Fort Collins, Colorado, in partial fulfillment of the requirement for the Master of Science.*

[81] Huang, W. X. (1983), "Engineering Properties of Soil," (黄文　，土的工程性質，水利電力出版社), (in Chinese).

[82] Huret, C., Cojean, R. and Devueghele, M. (1988), "Temperature Effects on Engineering Properties of Loess: Application to a Loess of the Parisian Basin from 5° to 80°C," *Engineering Geology*, 25(2-4), pp.209–228.

[83] Ishihara, K. (1976), "Fundamentals of Soil Dynamics," (石原研而，土質動的力学の基礎，鹿島出版社)。(in Japanese).

[84] Ishihara, K. (1982), "Evaluation of Soil Properties for Use in Earthquake Response Analysis," *International Symposium on Numerical Models in Geomechanics*, Zurich.

[85] Ishihara, K. (1988), "Soil Mechanics," (石原研而，土質力学，丸善株式出版社)。(in Japanese).

[86] Ishihara, K. and Nagase, H. (1988), "Multi-Directional Irregular Loading Tests on Sand," *Soil Dynamics and Earthquake Engineering*, 7(4), pp. 201–212.

[87] Ishihara, K., Okusa, S., Oyagi, N. and Ischuk, A. (1990), "Liquefaction-Induced Flow Slide in the Collapsible Loess Deposit in Soviet Tajik," *Soils and Foundations*, 30(4), pp.73–89.

[88] Ishihara, K. and Yamazaki, F. (1980), "Cyclic Simple Shear Tests on Saturated Sand in Multi-Directional Loading," *Soils and Foundations*, 20(1), pp. 45–59.

[89] Ishihara, K., Yasuda, S. and Yoshida, Y. (1990), "Liquefaction-Induced Flow Failure of Embankments and Residual Strength of Silty Sand," *Soils and Foundations*, 30(3), pp. 69–90.

[90] Ishihara, K., Yoshida, Y., Yi, F. and Murata, M. (1990), "Seismic Behavior of Collapsible Soils Subjected to Water Permeation," *Proc. the 1st International Seminar on Soil Mechanics and Foundation Engineering of Iran*, 2, pp. 60–72.

[91] Ismael, N.F. (1989). Discussion on "Prediction of Field Collapse of Soils Due to Wetting," *Journal of Geotechnical Engineering*, ASCE, 115(12), 1806–1808.

[92] JASM, (1979). "Testing Methods of Soils," (土質工学会，土質試験法)。(in Japanese).

[93] Jennings, J.E. (1957), *Discussion* on M. S. Youssef's Paper, *Proc. 4th International Conference on Soil Mechanics and Foundation Engineering*, 3, pp.168.

[94] Jennings, J.E. (1963), *Discussion* on "Expansive and Collapsing Soils and Soil Moisture," *Proc. 3rd Regional Conference for Africa on Soil Mechanics and Foundation Engineering*, 2, pp. 22–23.

[95] Jennings, J.E. and Burland, J. B. (1962), "Limitations to the Use of Effective Stress in Partly Saturated Soils," *Géotechnique*, 12(2), pp.125–144.

[96] Jennings, J. E. and Knight, K. (1957), "The Additional Settlement of Foundations due to a Collapse of Structure of Sandy Subsoils on Wetting," *Proc. 4th International Conference on Soil Mechanics and Foundation Engineering*, 1, London, pp316–319.

[97] Jennings, J. E. and Knight, K. (1975), "A Guide to Construction on or with Materials Exhibiting Additional Settlement due to Collapse of Grain Structure," *Proc. 6th Regional Conference for Africa on Soil Mechanics and Foundation Engineering*, 1, Duban, South Africa, pp99–105.

[98] Kantey, B. A. et al (1963), "Expansive and Collapsing Soils and Soil Moisture," *Proc. 3rd Regional Conference for Africa on Soil Mechanics and Foundation Engineering*, 2, University College of Rhodesia and Nyasalan, Salisbury, South Rhodesia, pp. 19–40.

[99] Karube, D. (1987), "Constitutive Equations of Unsaturated Clay," *Proc. Symposium on Unsaturated Soils*, Osaka, Japan, pp. 59–68. (軽部大蔵，不飽和土の構成式，不飽和土の工学的性質研究の現状シンポジウム。) (in Japanese).

[100] Karube, D. and Kato, S. (1989), "YIELD FUNCTIONS OF UNSATURATED SOIL," *Proc. 12th International Conference on Soil Mechanics and Foundation Engineering*, 1, Rio de Janeiro, pp. 615–618.

[101] Kassif, G. (1956), "THE ENGINEERING PROPERTIES OF NEGEV LOESS AS APPLIED TO EMBANKMENTS," Department of Civil Engineering, Technion, Haifa.

[102] Kézdi, A. (1969), "LANDSLIDE IN LOESS ALONG THE BANK OF THE DANUBE," *Proc. 7th International Conference on Soil Mechanics and Foundation Engrg*, 2, Mexico, pp617–626.

[103] Kézdi, A. (1974), "HANDBOOK OF SOIL MECHANICS, Volume 1, *Soil Physics*," Elsevier Scientific Publishing Company.

[104] Kiso-Jiban Consultants Co., Ltd., (1987). "REPORT ON DAMAGES IN CHIBA TOHO-OKI EARTHQUAKE ON DEC. 17, 1987," (基礎地盤コンサルタンツ株式会社，１９８７年１２月１７日千葉県東方沖の地震による被害状況（速報））。(in Japanese).

[105] Knight, K. (1961), "THE COLLAPSE OF SANDY SUB-SOILS ON WETTING," *M.S. thesis*, University of Witwatersrand.

[106] Knight, K. and Dehlen, G. L. (1963), "THE FAILURE OF A ROAD CONSTRUCTED ON A COLLAPSING SOIL," *Proc. 3rd Regional Conference for Africa on Soil Mechanics and Foundation Engineering*, 1, University College of Rhodesia and Nyasalan, Salisbury, Southern Rhodesia, pp. 31–34.

[107] Knodel, P. C. (1981), "CONSTRUCTION OF LARGE CANAL ON COLLAPSING SOILS," *Journal of Geotechnical Engineering*, ASCE, 107(1), pp. 79–94.

[108] Kondner, R. L. and Zelasko, J. S. (1963), "A HYPERBOLIC STRESS-STRAIN FORMULATION OF SANDS," *Proc. 2nd Pan American Conference on Soil Mechanics and Foundation Engineering*, pp. 289–324.

[109] Lambe, T.W. (1958), "THE STRUCTURE OF COMPACTED CLAY," *Journal of Soil Mechanics and Foundations Division*, ASCE, 84(2), pp. 1654-1–33.

[110] Lambe, T.W. (1960a), "A MECHANISTIC PICTURE OF SHEAR STRENGTH IN CLAY," *Proc. Research Conference on Shear Strength of Cohesive Soils*, ASCE, Boulder, Colorado, pp. 555–580.

[111] Lambe, T.W. (1960b), Discussion on "FACTORS CONTROLLING THE STRENGTH OF PARTLY SATURATED COHESIVE SOILS," *Proc. Research Conference on Shear Strength of Cohesive Soils*, ASCE, Boulder, Colorado, pp. 1094–1095.

[112] Lawton, E. C. (1986), "WETTING-INDUCED COLLAPSE IN COMPACTED SOIL,", *thesis presented to Washington State University, Pullman, Washington, in partial fulfillment of the requirements for the degree of Doctor of Philosophy.*

[113] Lawton, E. C., Fragaszy, R. J. and Hardcastle, J. H. (1989), "Collapse of Compacted Clayey Sand," *Journal of Geotechnical Engineering*, ASCE, 115(9), pp. 1252–1264.

[114] Lawton, E. C., Fragaszy, R. J. and Hardcastle, J. H. (1991), "Stress Ratio Effect on Collapse of Compacted Clayey Sand," *Journal of Geotechnical Engineering*, ASCE, 117(5), pp. 715–730.

[115] Leonards, G. A. and Narain, J. (1963), "Flexibility of Clay and Cracking of Earth Dams," *Journal of Soil Mechanics and Foundations Division*, ASCE, 89(2), pp47–98.

[116] Lin, P.S. and Lovell, C.W. (1983), "Compressibility of Field-Compacted Clay," *Transportation Research Record 897*, Washington, D.C., pp. 51–60.

[117] Liu, Z. D., Gue, Z. Y. and Cheng, Z. H. (1985), "The Deformation Characteristics of Shaanxi Loess," *Selected Works of Geotechnical Engineering*, China Building Industry Press, Peking, pp. 29-33.

[118] Lodbell, G. T. (1981), "Hydroconsolidation Potential of Palouse Loess," *Journal of Geotechnical Engineering*, ASCE, 107(6), pp733–742.

[119] Mackechine, W. R. (1967), "Summery of Specialty Session on Collapse Soils," *Proc. 4th Regional Conference for Africa on Soil Mechanics and Foundation Engineering*, 2, Cape Town, Amsterdam, pp. 294–296.

[120] Machechnie, W. R. (1989), "General Report on Collapsible Soils," *Proc. 12th International Conference on Soil Mechanics and Foundation Engineering*, Brazil, pp. 1–6.

[121] Marin, (1969), "Properties of the Collapsible Soils of Ecuador," *Proc. 7th International Conference on Soil Mechanics and Foundation Engineering*, specialty session 5, Mexico.

[122] Martin, G. R., Finn, W. D. L., and Seed H., B., (1973), "Fundamentals of Liquefaction under Cyclic Loading," *Journal of Geotechnical Engineering*, ASCE, 101(5), pp. 423–438.

[123] Martin, G. R., Finn, W. D. L., and Seed H., B., (1978), "Effects of System Compliance on Liquefaction Tests," *Journal of Geotechnical Engineering*, ASCE, 104(4), pp. 463–479.

[124] Milovic, D. (1988), "Stress Deformation Properties of Macroporous Loess Soils," *Engineering Geology*, 25(2-4), pp. 283–302.

[125] Miranda, A. N. and Van Zyl, D. (1989), "Finite Element Method Approach for Collapsing Soils," *Proc. 12th International Conference on Soil Mechanics and Foundation Engineering*, 1, Rio de Janeiro, pp. 625–628.

[126] Milovic, (1969), "SOME ENGINEERING PROPERTIES OF LOESS," *Proc. 7th International Conference on Soil Mechanics and Foundation Engineering*, specialty session 5, Mexico.

[127] Mogami, T. (1969), "SOIL MECHANICS," (最上武雄，土質力学，技報堂）。(in Japanese).

[128] Moore, P. J. and Millar, D. V. (1971), "THE COLLAPSE OF SANDS UPON SATURATION," *Proc. 1st Australia-New Zealand Conference on Geomechanics*, 1, Melbourne, pp. 54–60.

[129] Morland, L. W. and Hastings, C. R. (1973), "A VOID-COLLAPSE MODEL FOR DRY POROUS TUFFS," *Engineering Geology*, Amsterdam, The Netherlands, 7(2), pp. 81-97.

[130] Moussa, A. A. (1975), "EQUIVALENT DRAINED-UNDRAINED SHEARING RESISTANCE OF SAND TO CYCLIC SIMPLE SHEAR LOADING," *Géotechnique*, 25(3), pp. 485–494.

[131] Nagase, H. (1981), "二方向単純せん断装置を用いた飽和密詰め砂の繰り返しせん断特性", 修士論文, *thesis presented to University of Tokyo, Tokyo, in partial fulfillment of the requirements for the degree of Master of Engineering.* (in Japanese).

[132] Nagase, H. (1984), "多方向の不規則荷重を受ける砂の変形強度特性", 博士論文, *thesis presented to University of Tokyo, Tokyo, in partial fulfillment of the requirements for the degree of Doctor of Engineering.* (in Japanese).

[133] Nagase, H. and Ishihara, K. (1987), "EFFECTS OF LOAD IRREGULARITY ON THE CYCLIC BEHAVIOR OF SAND," *Soil Dynamics and Earthquake Engineering*, 6(4), pp. 239–249.

[134] Newland, P. L. (1965), "THE BEHAVIOR OF SOILS IN TERMS OF TWO KINDS OF EFFECTIVE STRESS," *Engineering Effects of Moisture Changes in Soils—Concluding Proc. International Research and Engineering Conference on Expansive Clay Soils*, Texas A& M Press, Collage Station, Texas, pp. 78–92.

[135] Nishida, K. and Aoyama, C. (1987), "FAILURE MECHANISM OF A WEATHERED RESIDUAL SOIL SLOPE," *Proc. 8th Regional Conference on Soil Mechanics and Foundation Engineering*, (2/1), Kyoto, Japan, pp. 197–200.

[136] Northey, R. D. (1969), "ENGINEERING PROPERTIES OF LOESS AND OTHER COLLAPSIBLE SOILS," *Proc. 7th International Conference on Soil Mechanics and Foundation Engineering*, 3, Mexico, pp. 445–452.

[137] Novais-Ferreira, H. and Meireles, M. F. (1967), "ON THE DRAINAGE OF MUCEQUE—A COLLAPSING SOIL," *Proc. 4th Regional Conference for Africa on Soil Mechanics and Foundation Engineering*, 1, Cape Town, South Africa, pp. 151–155.

[138] Nowatzki, E. A. (1980), "Settlement Estimates in Collapsible-Susceptible Soils," *Journal of Civil Engineering Design*, 2(2), pp. 121–147.

[139] Ohta, H. and Hata, S. (1977), "Strength of Dynamically Compacted Soils," *Proc. 9th International Conference on Soil Mechanics and Foundation Engineering*, 1, pp. 2339–242.

[140] Pickering, D. J. (1973), "Drained Liquefaction Testing in Simple Shear," *Journal of the Soil Mechanics and Foundations Division*, ASCE, 99(12), pp. 1179–1184.

[141] Pientong, T. (1989), "Engineering Properties of Loessial Soils in Khon Kaen City," *thesis presented to Asian Institute of Technology, Bangkok, Thailand, in partial fulfillment of the requirements for the degree of Master of Engineering.*

[142] Prakash, S. and Puri, V. K. (1982), "Liquefaction of Loessial Soils," *Third International Earthquake Microzonation Conference Proceedings*, (2), Seattle, USA, pp. 1101–1107.

[143] Priklonskij, V. A. (1952), "Mechanical and Physical Properties of Loess and Other Soils Susceptible to Sudden Failure," *Gruntovedenie (Grounting)*, Chapter 2, Gosgeolizdat.

[144] Proctor, R. R. (1933), "Fundamental Principles of Soil Compaction," *Engineering News-Record*, 111(9), pp. 245–248.

[145] Qian, J. H. (1987), "Dynamic Consolidation, from Practice to Theory," *Proc. 8th Asian Regional Conference on Soil Mechanics and Foundation Engineering*, 2, Kyoto, Japan, pp. 201–204.

[146] Reginatto, A.R. (1989). Discussion on "Prediction of Field Collapse of Soils Due to Wetting," *Journal of Geotechnical Engineering*, ASCE, 115(12), pp.1810–1812.

[147] Reginatto, A.R. and Ferreto, J. C. (1973), "Collapse Potential of Soils and Soil-Water Chemistry," *Proc. 8th International Conference on Soil Mechanics and Foundation Engineering*, Vol. 2.2, Mockba, pp.177–183.

[148] Robinson, L. (1989). Discussion on "Prediction of Field Collapse of Soils Due to Wetting," *Journal of Geotechnical Engineering*, ASCE, 115(12), pp.1812–1814.

[149] Seed, H. B. (1968), "Landslides during Earthquakes due to Soil Liquefaction," *Journal of Soil Mechanics and Foundations Division*, ASCE, 94(5), pp. 1053–1122.

[150] Seed, H. B. and Peacock, W. H. (1971), "Test Procedures for Measuring Soil Liquefaction Characteristics," *Journal of the Soil Mechanics and Foundations Division*, ASCE, 97(8), pp. 1099-1119.

[151] Skempton, A. W. (1960), "Effective Stress in Soils, Concrete, and Rocks," *Proc. Conference Pore Pressure*, Butterworths, London.

[152] Skempton, A. W. and Bishop, A. W. (1950), "The Measurement of the Shear Strength of Soils," *Proceedings of the Conference on the Measurement of the Shear Strength of Soils in Relation to Practice, Géotechnique*, 2, pp. 90–108.

[153] Sokolovich,V. E. (1971), "New Developments in the Chemical Strengthening of Ground," *Osnonaniya, Fundamenty i Mekhanika Gruntov*, No. 2, pp. 23–25.

[154] Sowers, G. F. (1962), "Shallow Foundations," *Foundation Engineering*, G. A. Leonards, ed., McGraw-Hill Book Co., Inc., New York, N. Y.

[155] Sridharan, A. (1968), "Some Studies on the Strength of Partly Saturated Soils," *Ph.D. Thesis presented to the Purdue University, Lafayette, Indiana.*

[156] Sridharan, A., Rao, G. V. and Pandian, R. S. (1973), "Volume Change Behavior of Partly Saturated Clays During Soaking and The Role of Effective Stress Concept," *Soils and Foundations*, 13(3), pp. 1–15.

[157] Stark, T. D. and Duncan, J. M. (1991), "Mechanisms of Strength Loss in Stiff Clays," *Journal of Geotechnical Engineering*, ASCE, 117(1), pp. 1339–154.

[158] Sultan, H. A. (1969), "Collapsing Soils, State-of-the-Art," *Proc. 7th International Conference on Soil Mechanics and Foundation Engineering*, Specialty sessions, No. 5.

[159] Taylor, D. W. (1953), "A Direct Shear Test with Drainage Control," *American Society for Testing Materials. Special Technical Publication 131*, pp. 63–74.

[160] Terzaghi, K. (1923), "Die Berechnungder Durchlassigkeitsziffer des Tones aus dem Verlauf der hydrodynamischen Spannungserscheinungen," ("Calculation of the Porosity Index of Clay From Hydrodynamic Tension Condition"), *Sitzbericht (Abt. IIa) Akademie der Wissenschaften*, Vienna, 132.

[161] Terzaghi, K. (1932), "Tragfahigkeit der Hachgrundungen" ("Bearing Capacity of Shallow Foundations"), *Prelim. Pub., 1st Congr. Int. Ass. Bridge Struct. Eng.*, pp. 659–672.

[162] Terzaghi, K. (1936), "The Shearing Resistance of Saturated Soils and The Angle Between The Planes of Shear," *Proc. 1st International Conference on Soil Mechanics and Foundation Engineering*, Harvard University, Cambridge, Mass., 1, pp. 54–56.

[163] Terzaghi, K. and Peck, R. B. (1967), "Soil Mechanics in Engineering Practice," 107, 2nd edition, New York, John Wiley.

[164] Toll, D. G. (1990), "A Framework on Unsaturated Soil Behavior," *Géotechnique*, 40(1), pp. 31–44.

[165] Toulemont, M. (1970), "Geological Observation of the Dissolution of Gypsum in the Paris Area," *Proc. 1st International Congress*, International Association of Engineering Geology, 1, pp. 62-73.

[166] Uchida, I., Matsumoto, R. and Onitsuka, K. (1968), "Shear Characteristics of Compacted Partially Saturated Soils," *Soils and Foundations*, 8(3), pp. 32–45.

[167] Uriel, S. and Serrano, A. A. (197), "Geotechnical Properties of Two Collapsible Volcanic Soils of Low Bulk Density at the Site of Two Dams in Canary Islands (Spain)," *Proc. 8th International Conference on Soil Mechanics and Foundation Engineering*, 2.2, Moscow, pp. 257–264.

[168] Vucetic, M. and Lacasse, S. (1982), "Specimen Size Effect in Simple Shear Test," *J. of Geotechnical Engineering*, ASCE, 108(12), pp. 1568–1585.

[169] Williams, A. A. B. (1957), "Studies of Shear Strength and Bearing Capacity of some Partially Saturated Sands," *Proc. 4th International Conference on Soil Mechanics and Foundation Engineering*, 1, London, pp. 453–456.

[170] Wu, S., Gary, D. H. and Richard, F. E. (1984), "Capillary Effects on Dynamic Modulus of Sands and Silts," *Journal of Geotechnical Engineering*, ASCE, 110(9), pp. 1188–1203.

[171] Wu, S., Gary, D. H. and Richard, F. E. (1985), "Capillary Effects on Shear Modulus at High Strains," *Proc. 11th International Conference on Soil Mechanics and Foundation Engineering*, 2, pp. 1091–1094.

[172] Xie, D. Y., Zhi, H. W. and Guo, Y. T. (1980), "*Preliminary Research on Undisturbed Loessial Soil under Dynamic Conditions*," Hydraulic Department of West North Agriculture College, Xian, (in Chinese, after Bhatia and Quast, 1984).

[173] Yamada, G., Takayama, T., Muromachi, T., Fujiwara, T., Sato, Y. and Kobayashi, Y. (1968), "Report on the Tokachioki Earthquake on May 16, 1968," *Railway Technical Research Report, No. 650*, The railway Technical Research Institute, Japanese National Railways. (in Japanese).

[174] Yamazaki, F. (1978), "二方向に繰り返しせん断した時の砂の挙動", 修士論文, *thesis presented to University of Tokyo , Tokyo, in partial fulfillment of the requirements for the degree of Master of Engineering.* (in Japanese).

[175] Yi, F., Ishihara, K., Towhata, I. and Murata, M. (1990), "DYNAMIC PROPERTIES OF COLLAPSIBLE SOILS," *25th Japan National Conference on Soil Mechanics and Foundation Engineering*, 1(D7), Okayama, pp. 833-836.

[176] Yi, F., Ishihara, K., Harada, K., Towhata, I. and Miura, H. (1991), "WETTING-INDUCED COLLAPSE AND THE EFFECT ON STATIC SHEAR STRENGTH," *26th Japan National Conference on Soil Mechanics and Foundation Engineering*, 1(D6), Nagano, pp. 673-676.

[177] Yoshinaka, R. and Kazama, H. (1973), "MICRO-STRUCTURE OF COMPACTED KAOLIN CLAY," *Soils and Foundations*, 13(2), pp.19–34.

[178] Zur, A. and Wiseman, G. (1973), "A STUDY OF COLLAPSE PHENOMENA OF AN UNDISTURBED LOESS," *Proc. 8th International Conference on Soil Mechanics and Foundation Engineering*, Specialty session No. 4, Moscow.

APPENDIX A

MINERALOGY OF MATERIALS

Photo. 0.1: SEM micrograph of the mixture of Toyoura sand and 15% kaolinite (dry mixed)

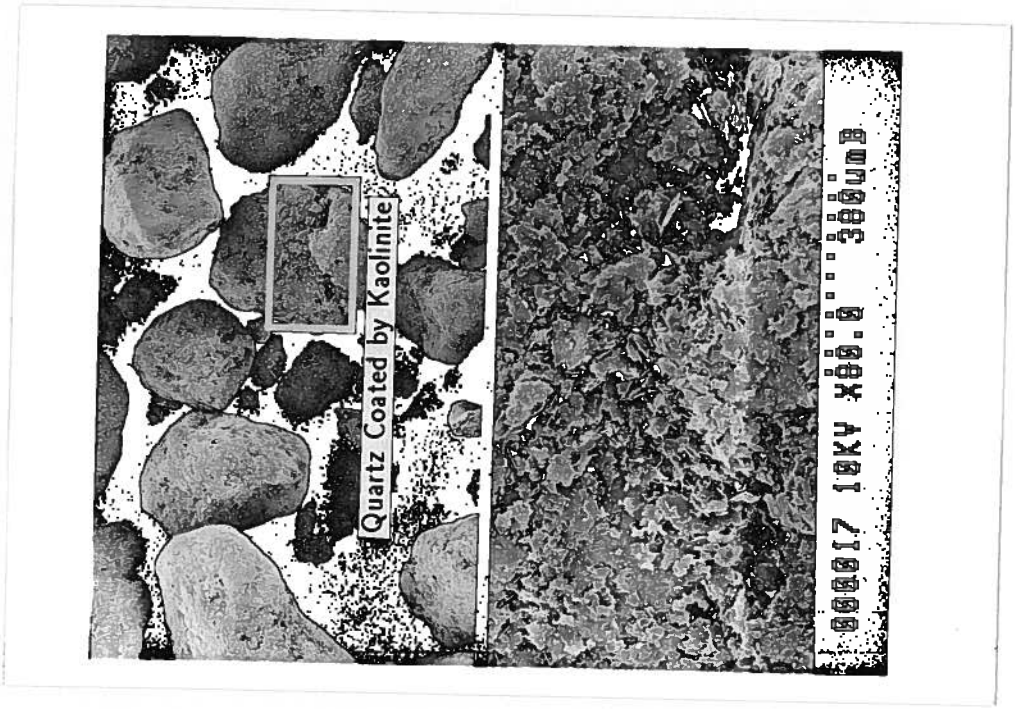

Photo. 0.2: SEM micrograph of the mixture of Toyoura sand and 15% kaolinite (wet mixed)

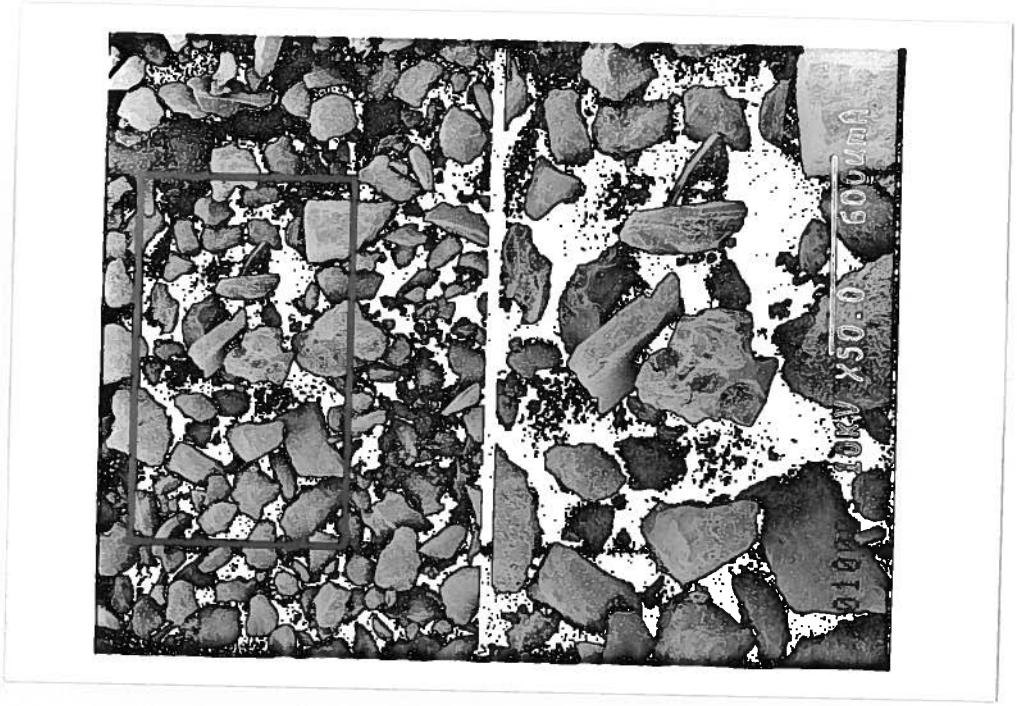

Photo. 0.3: SEM micrograph of Chonan A silty sand

Photo. 0.4: SEM micrograph of Chonan A silty sand

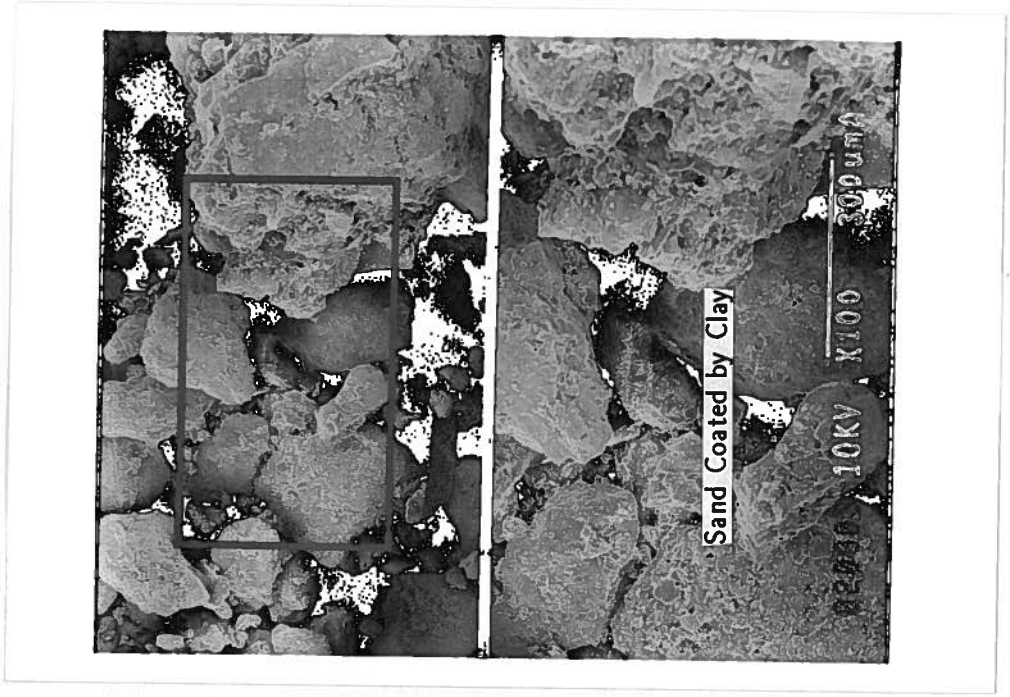

Photo. 0.5: SEM micrograph of Chonan B silty sand

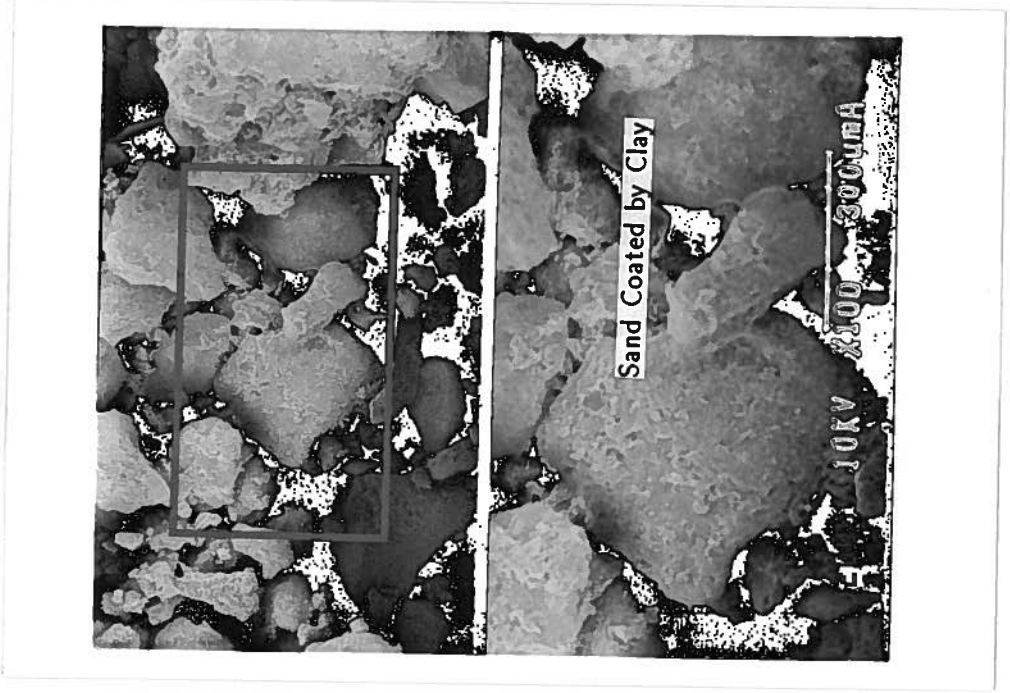

Photo. 0.6: SEM micrograph of Chonan B silty sand

Photo. 0.7: SEM micrograph of Ottomo clayey sand

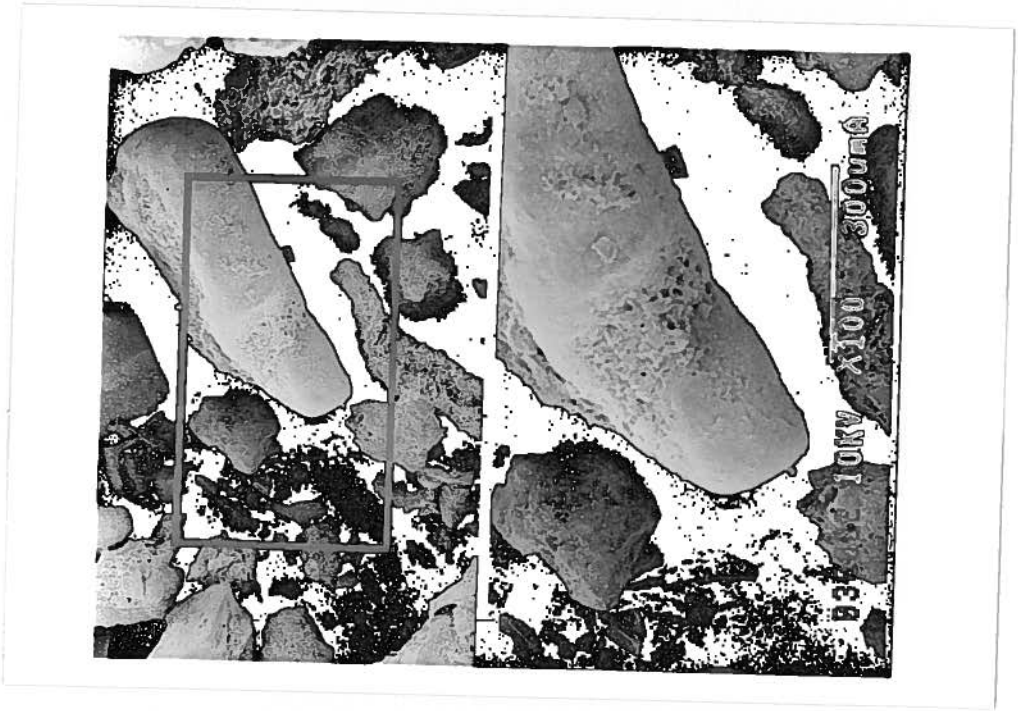

Photo. 0.8: SEM micrograph of Ottomo clayey sand

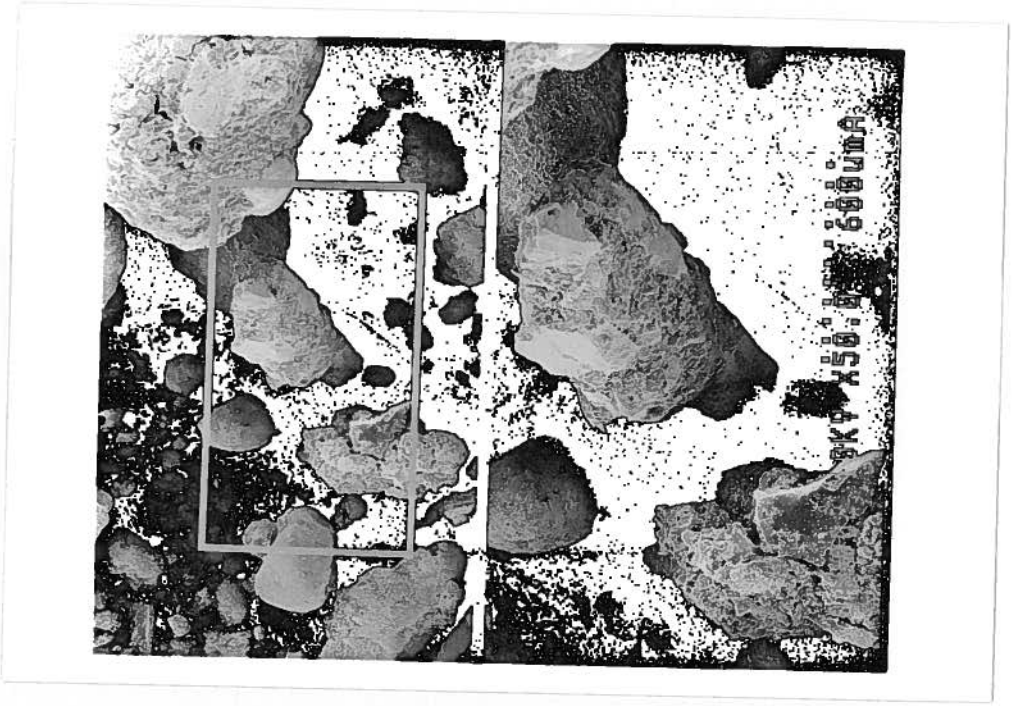

Photo. 0.9: SEM micrograph of Mutsuichikawa clayey sand

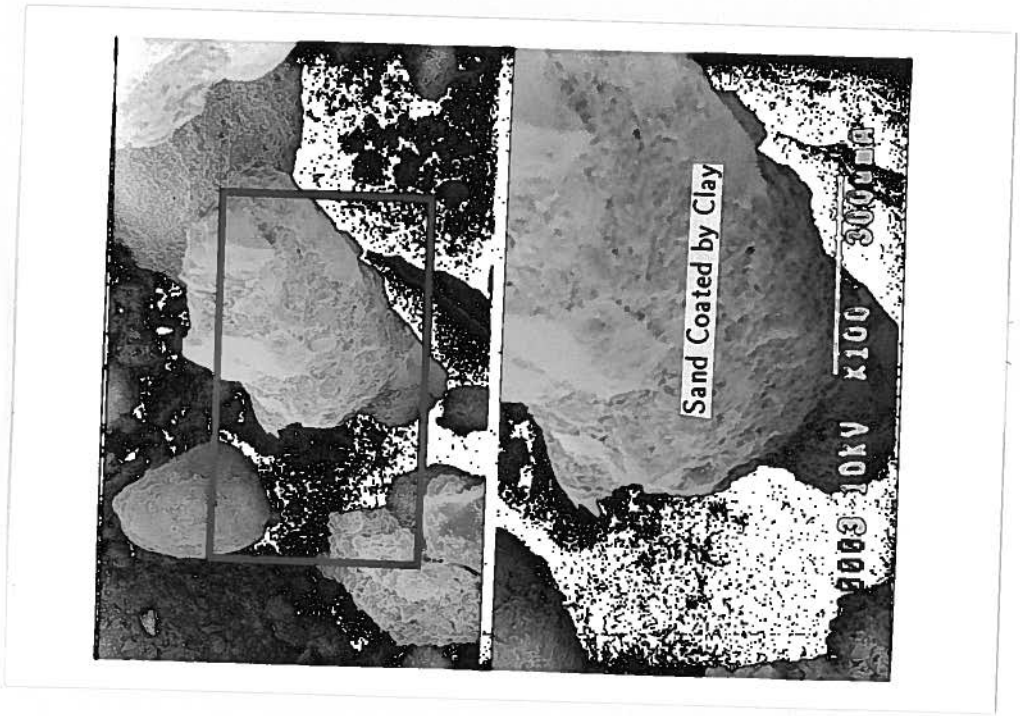

Photo. 0.10: SEM micrograph of Mutsuichikawa clayey sand

Photo. 0.11: Mineralogy of mixture of Toyoura sand

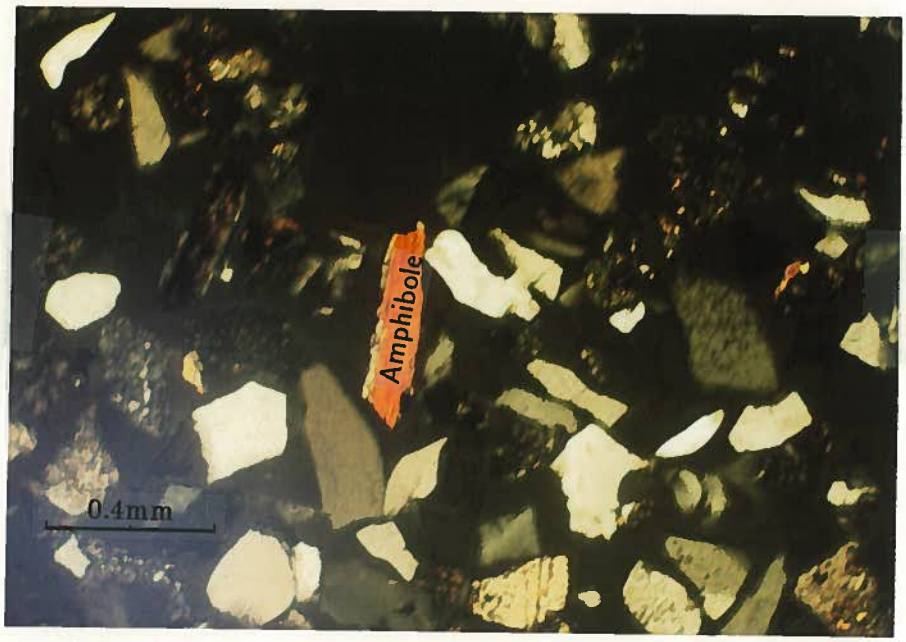

Photo. 0.12: Mineralogy of Chonan A silty sand

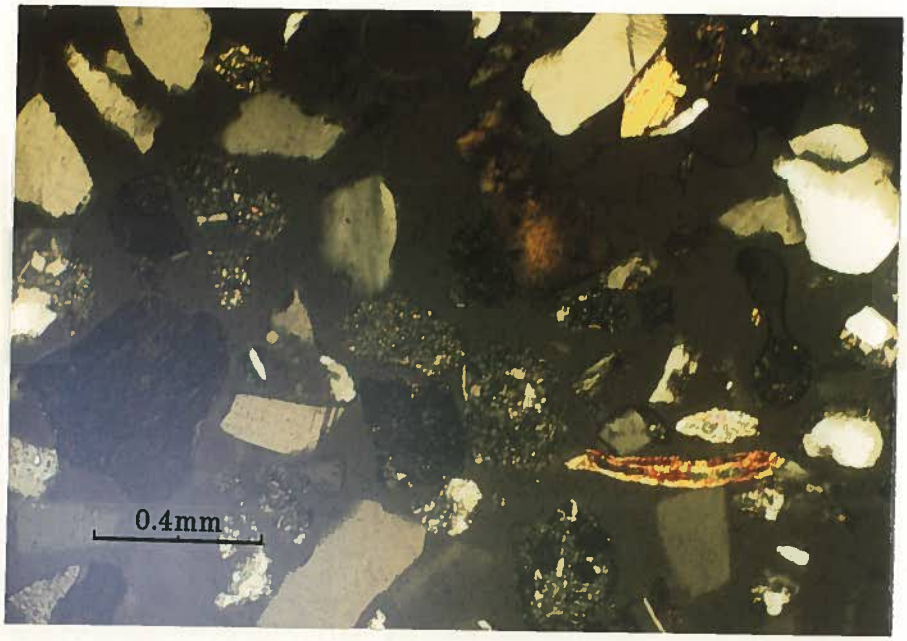

Photo. 0.13: Mineralogy of Chonan B silty sand

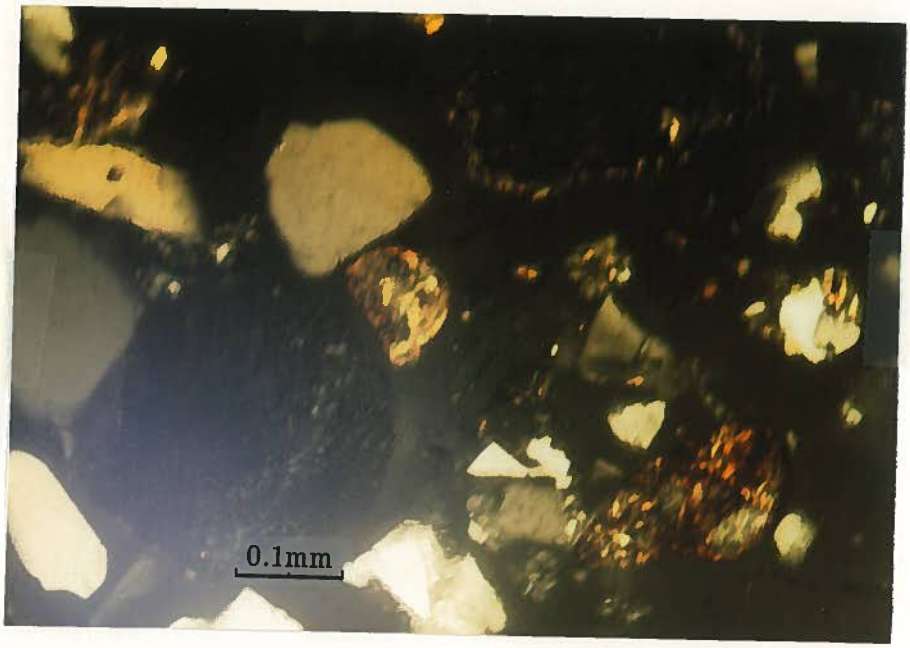

Photo. 0.14: Mineralogy of Chonan B silty sand

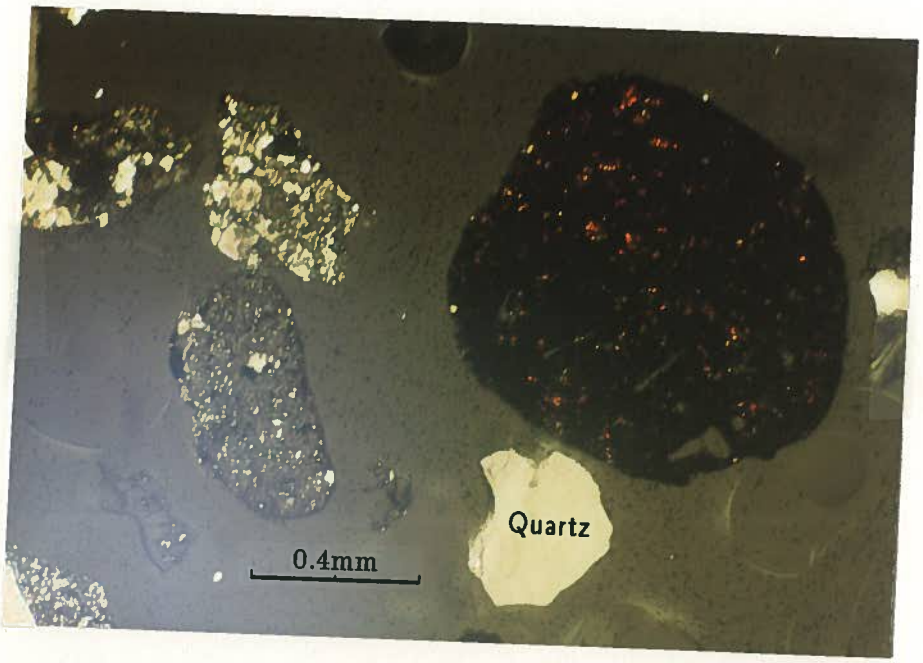

Photo. 0.15: Mineralogy of Ottomo clayey sand

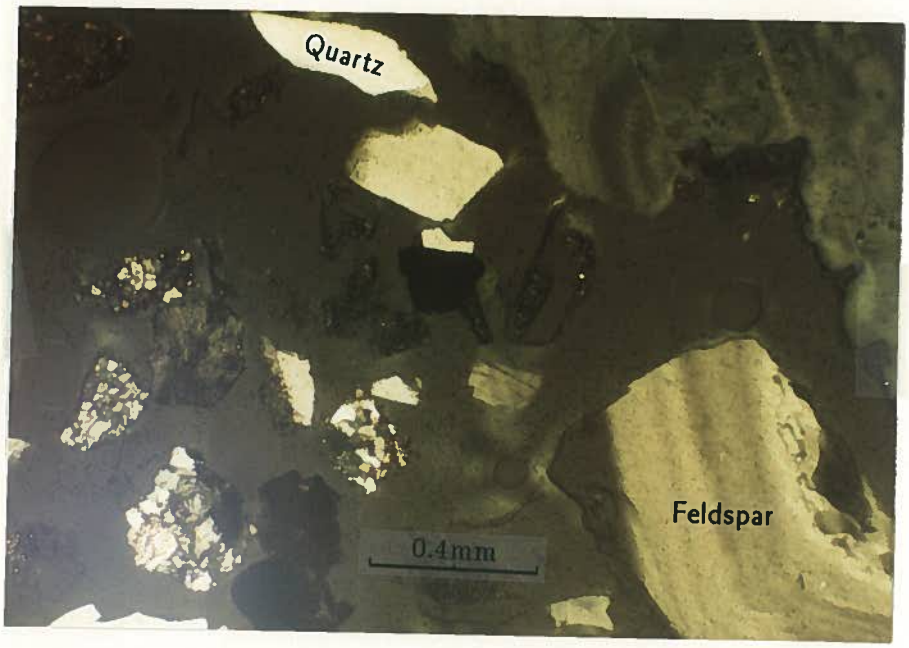

Photo. 0.16: Mineralogy of Ottomo clayey sand

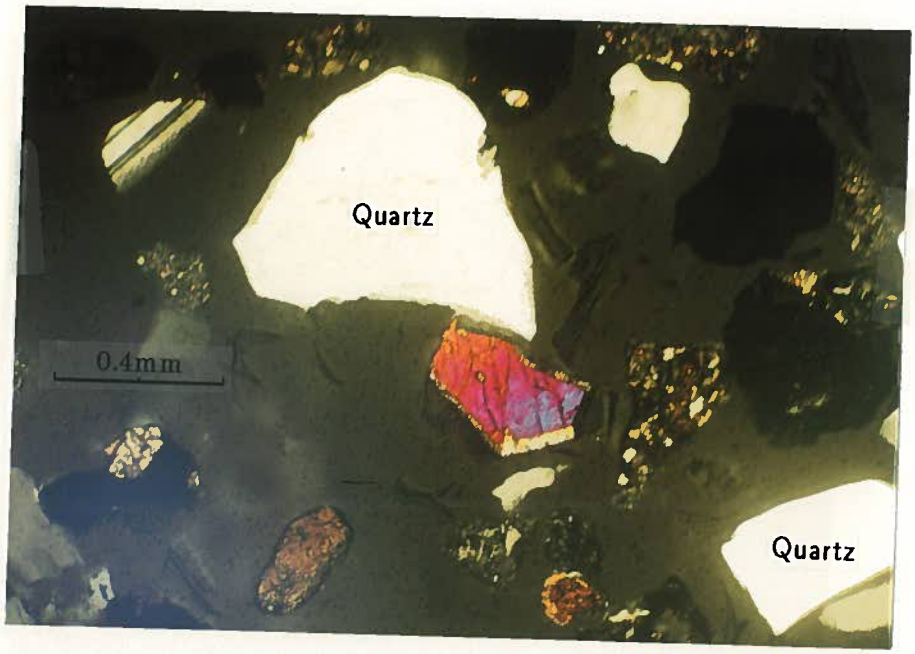

Photo. 0.17: Mineralogy of Ottomo clayey sand

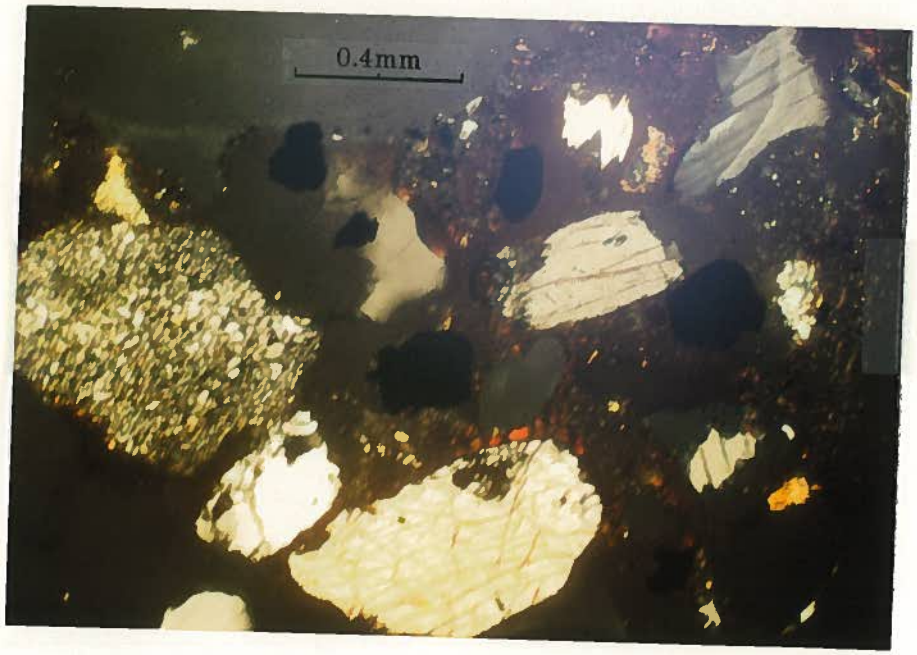

Photo. 0.18: Mineralogy of Mutsuichikawa clayey sand

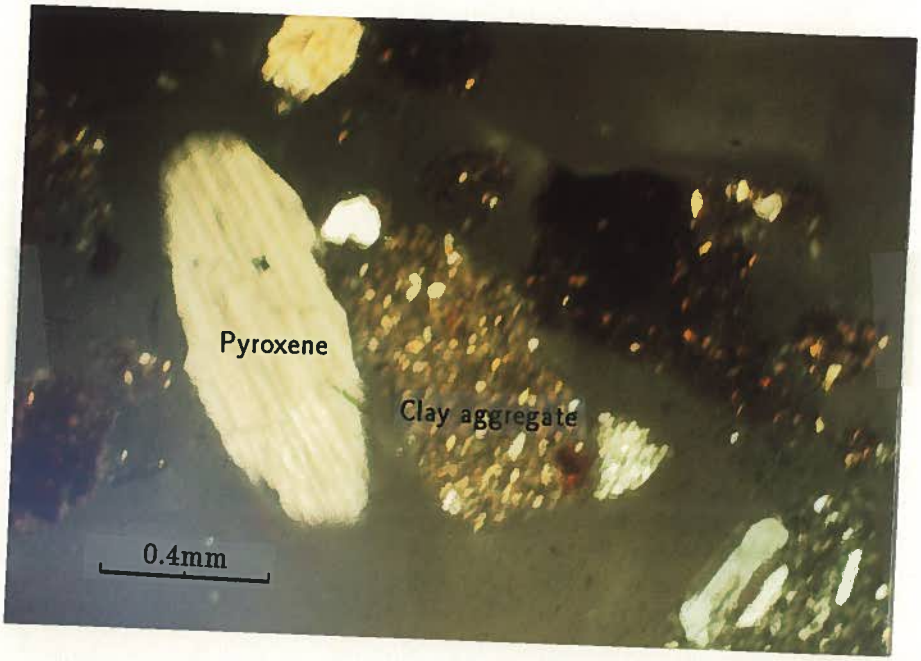

Photo. 0.19: Mineralogy of Mutsuichikawa clayey sand

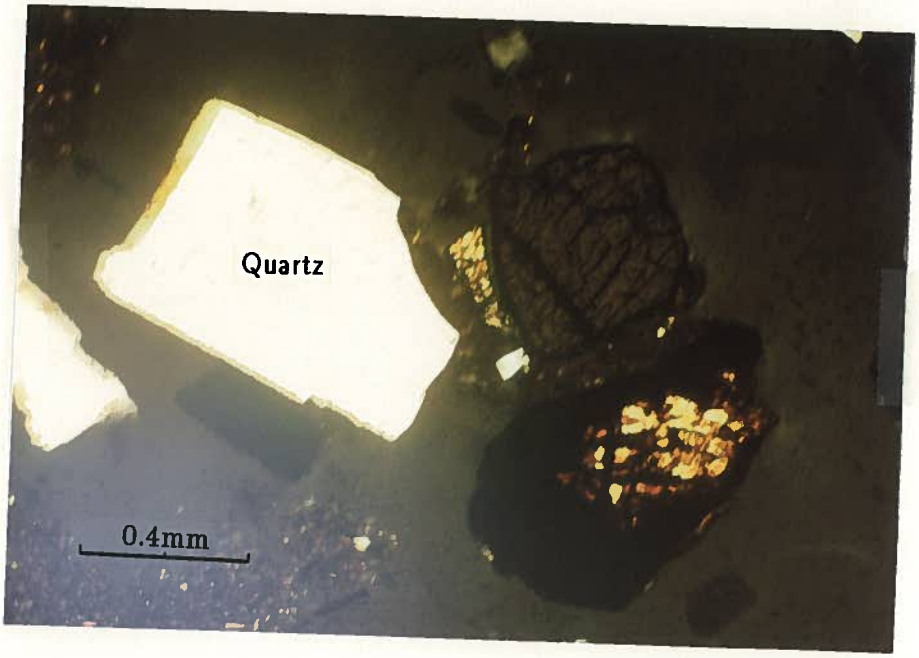

Photo. 0.20: Mineralogy of Mutsuichikawa clayey sand

Photo. 0.21: Mineralogy of Mutsuichikawa clayey sand

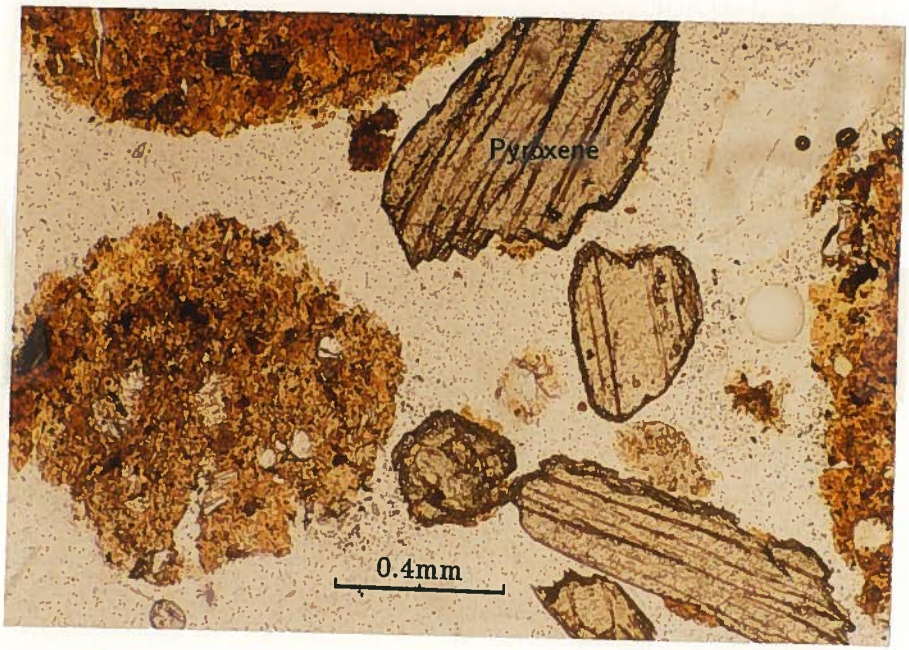

Photo. 0.22: Mineralogy of Mutsuichikawa clayey sand